

The Essence of Solid-State Transformers

Fundamentals, Design Challenges, R&D Overview, Comparative Evaluation, Outlook

Johann W. Kolar & Jonas Huber

Power Electronic Systems Laboratory
ETH Zurich

September 8, 2023



Agenda

1. Introduction & Intended SST Applications
2. SST Concepts & Key Design Aspects



3. Selected Results of Recent University / Industry SST R&D Activities
4. Comparative Evaluation of SSTs for Datacenters and EV Charging
5. Summary & Research Vectors

Acknowledgment

Dr. T. Guillod
Dr. P. Czyz
Dr. D. Rothmund
Dr. G. Ortiz

PDF Download



<https://u.ethz.ch/Y6nxX>

Part I

Introduction & Intended SST Applications

- Transformer Basics and Key SST Motivations
- Global Megatrends and Intended SST Applications
- Terminology



Transformer History

1800 ● **1830 Henry / Faraday**
Property of Induction

1810 ●

1820 ● **1880 Ferranti**
Early Transformer

1830 ● **1882 Gaulard & Gibbs**
Linear-Shape Xfmr (1994, 2 kV, 40 km)

1840 ● **1884 Bláthy / Zipernowksi / Déri**
Toroidal Core Xfmr

1850 ●

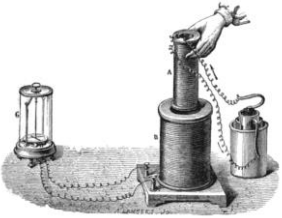


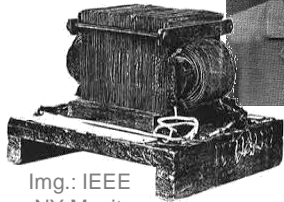

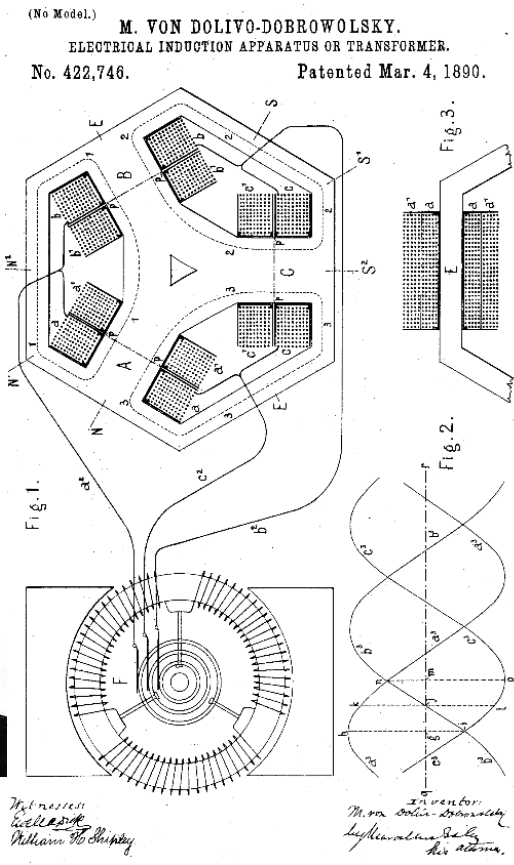
1860 ●

1870 ● **1885 Stanley (& Westinghouse)**
Easily Manufact. Xfmr
(1st Full AC Distr. System)

1880 ●

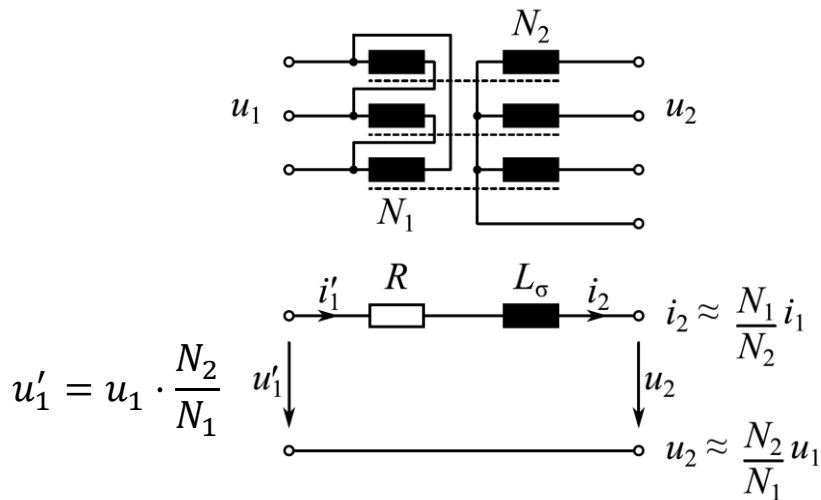
1890 ● **1889 Dolivo-Dobrowolsky**
→ **Three-Phase Transformer**

1900 ● **1891 1st Complete AC System**
(Gen. + Xfmr + Transm. + El. Motor+ Lamps, 40 Hz, 25 kV, 175 km)

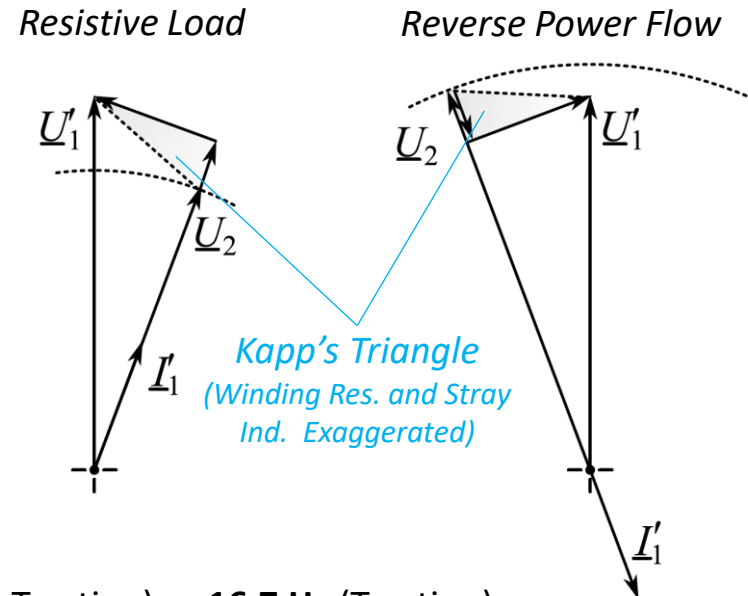







Transformer Basics (1)

- Voltage Transfer Ratio **Fixed**
- Current Transfer Ratio **Fixed**
- Active Power Transfer **Fixed ($P_1 \approx P_2$)**
- Reactive Power Transfer **Fixed ($Q_1 \approx Q_2$)**
- Frequency Ratio **Fixed ($f_1 = f_2$)**



- Typ. Operating Frequency **50/60 Hz (Power Grid, Traction) or 16.7 Hz (Traction)**
- Typ. Operating Voltages **6...35 kV (Power Grid)**
400 V (Power Grid)
15 kV or 25 kV (Traction)



Transformer Basics (2)

Construction Equations

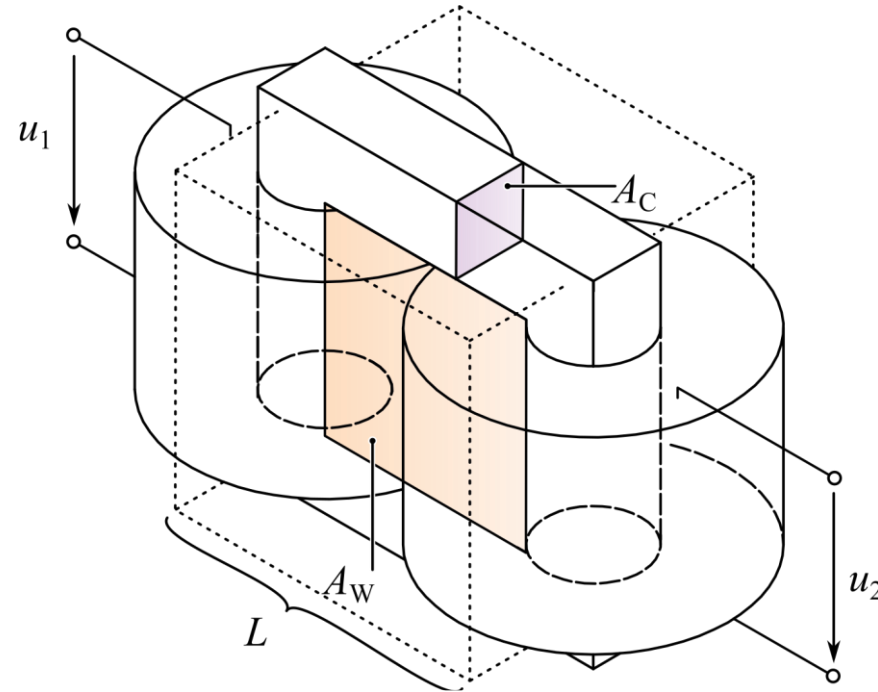
● Core Area $A_C = \frac{U_1}{\sqrt{2}\pi B_{\max} f N_1}$

● Window Area $A_W = \frac{2I_1}{k_W J_{\text{rms}}} N_1$

■ Area Product $A_C A_W \propto \frac{S}{k_W J_{\text{rms}} B_{\max} f}$

- S Rated Power ($S = U_1 I_1$)
- k_W Window Utilization Factor
- B_{\max} Flux Density Amplitude
- J_{rms} Winding Current Density
- f Frequency

■ Construction Volume $A_C A_W \propto L^4 \propto \frac{S}{f} \Rightarrow V \propto L^3 \propto \frac{S^{3/4}}{f^{3/4}}$
 for given $B_{\max}, J_{\text{rms}}, k_W$



Transformer Basics (3)

■ Advantages

- Relatively Inexpensive
- Highly Robust / Reliable
- Highly Efficient (98.5%...99.5% Dep. on Power Rating)
- Short Circuit Current Limitation (Stray Ind.)

■ Weaknesses

- Voltage Drop Under Load
- Losses at No Load
- Not Directly Controllable
- Sensitivity to DC Offset & Load Imbalances
- Sensitivity to Harmonics
- Low Frequency → Large Volume and Weight

*Vacuum Cast Coil Dry-Type
Distribution Transformer*

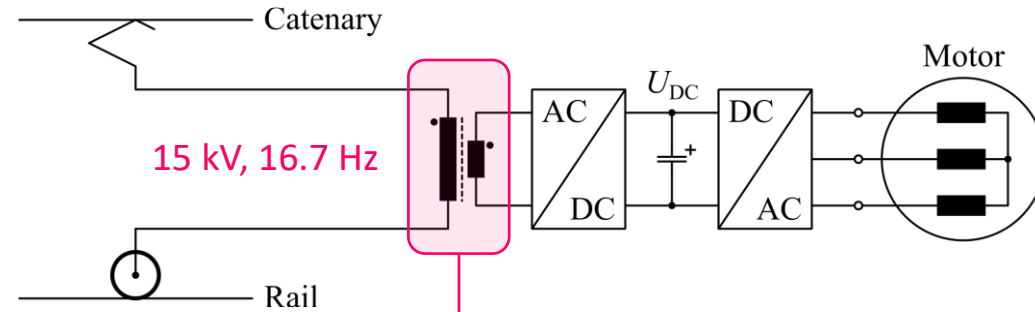


*1 MVA – 12 kV / 400 V @ 2600 kg
0.2%/1% Losses @ No/Rated Load*

Classical Traction Vehicles

■ Isolated AC-DC Conversion

- Catenary AC Voltage 15 kV or 25 kV
- Frequency 16.7 Hz or 50 Hz
- Power Level 1...10 MW typ.



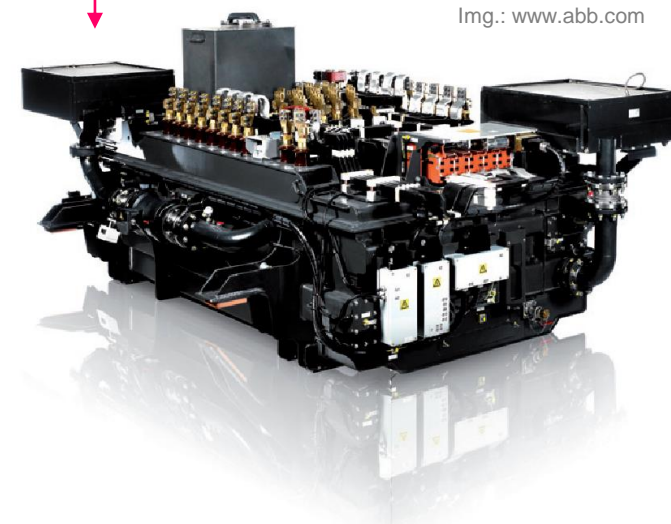
■ Volume & Weight Constraints

$$A_C A_W \propto \frac{S}{k_W J_{rms} B_{max} f}$$

- $k_W < 1$
- J_{rms} "Soft" Limit: Losses / Cooling
- B_{max} Hard Limit: Saturation
- f Fixed

→ Volume & Weight Reduction by Increasing J_{rms} (the Only DoF!)

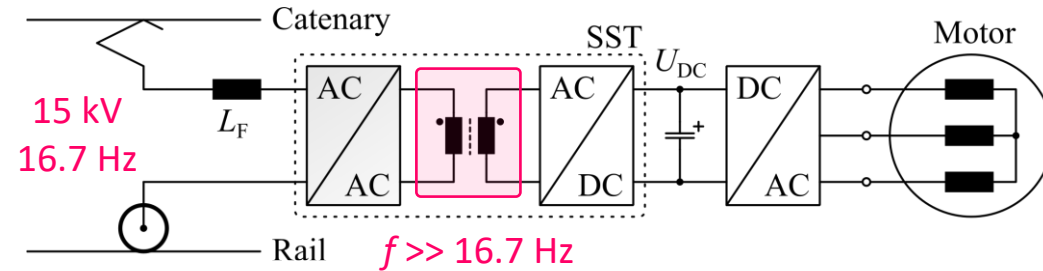
- Current Density 6 A/mm² (2 A/mm² Typ. for Distr. Transf.)
- Efficiency 90...95 % (99+ % Typ. for Distr. Transf.)
- Power Density 2...4 kg/kVA



Next-Generation Traction Vehicles (1)

Isolated AC-DC Conversion

- Catenary AC Voltage 15 kV or 25 kV
- Frequency 16.7 Hz or 50 Hz
- Power Level 1...10 MW typ.



Power Electronic Converter Stages Unlock f as DoF

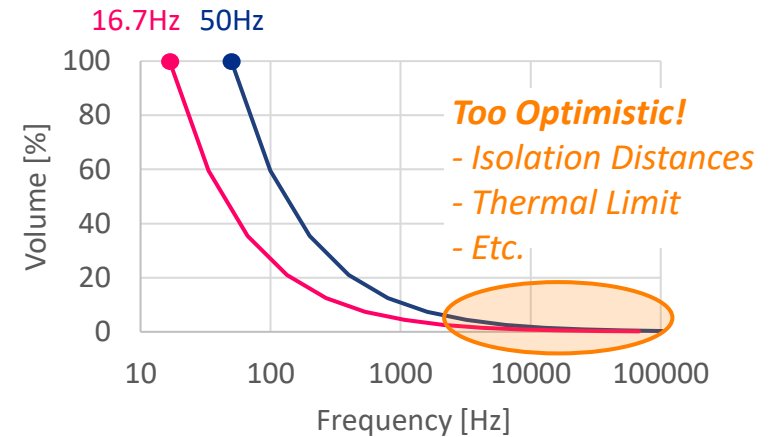
- LF Transformer → Medium-Frequency Transformer (MFT)

$$A_C A_W \propto \frac{S}{k_W J_{rms} B_{max} f}$$

→ Volume & Weight Reduction by Increasing f

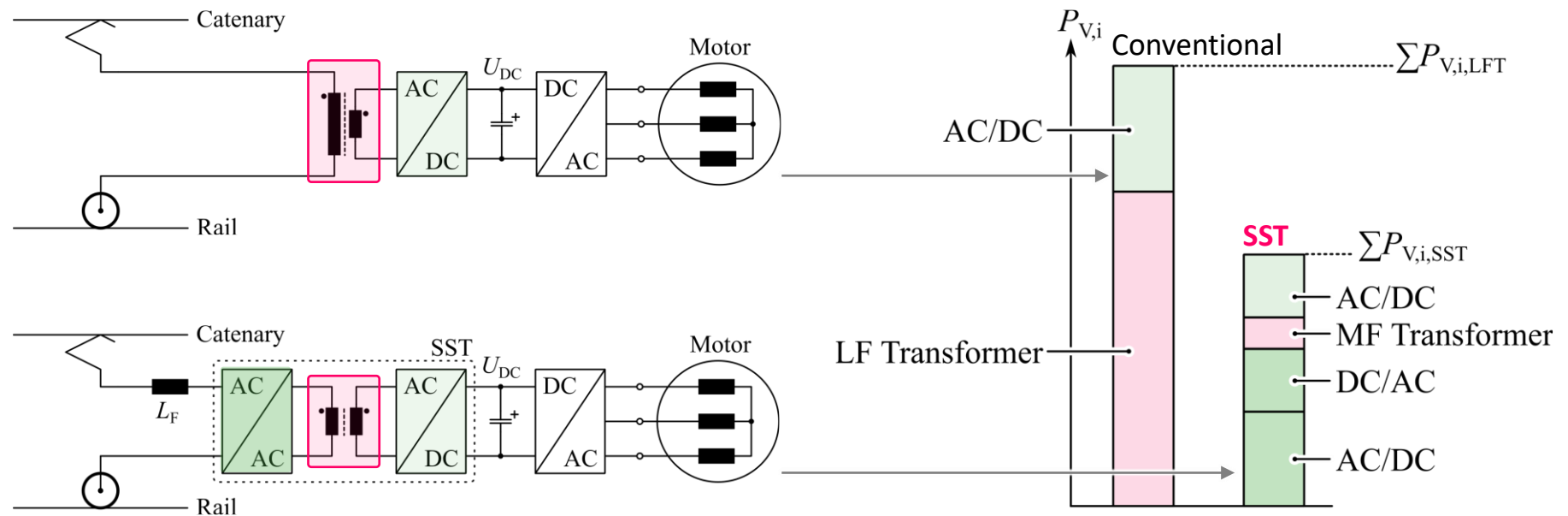
AC-DC SST with MFT and AC-AC and AC-DC Conversion Stages

- Volume/Weight Contribution?
- Overall MVAC-LVDC Efficiency?



Next-Generation Traction Vehicles (2)

■ Drivetrain Loss Distribution of Conventional & Next-Generation Traction Vehicles



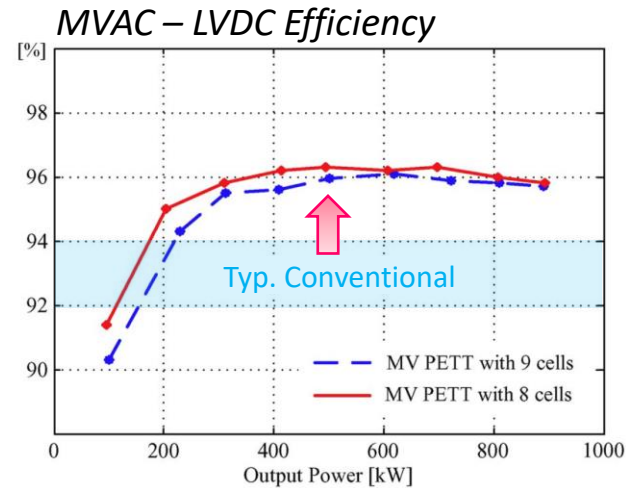
■ Key Motivation for SSTs: Space/Weight-Limited Applications

- Medium Frequency Provides Degree of Freedom → Allows Loss Reduction AND Volume Reduction



Example: 1.2 MVA AC-DC Power Electron. Traction Transf.

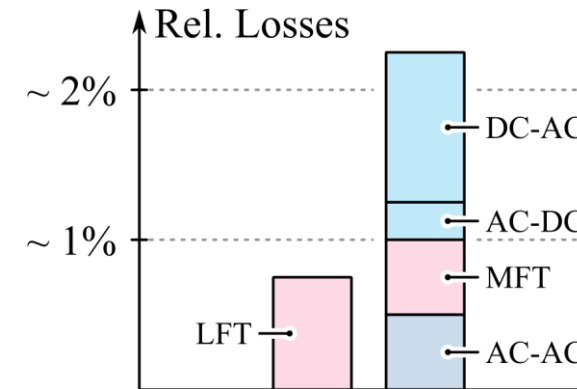
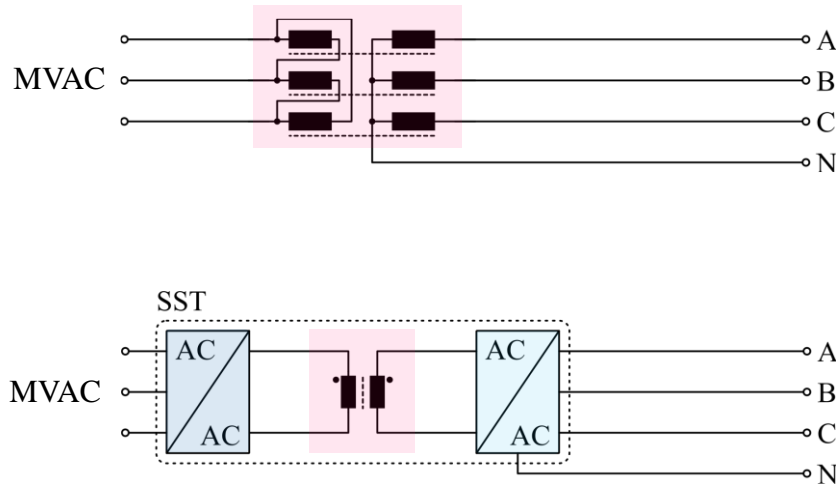
- 15 kV, 16.7 Hz AC Input to 1.5 kV DC Output / Silicon IGBT Technology / Modular Topology
- Significant Efficiency Improvement (+2...4 %)
- Significant Weight Reduction (0.5...0.75 kVA/kg vs. 0.2...0.35 kVA/kg for Conventional Traction AC-DC Conv.)



- World's First Locomotive with an SST (2012) / Field Test on Swiss Railway System > 13'000 km

Traditional AC-AC Grid Applications

- Power Transformers Typ. w/o Volume/Weight Constraint → High Efficiency of 99+ %

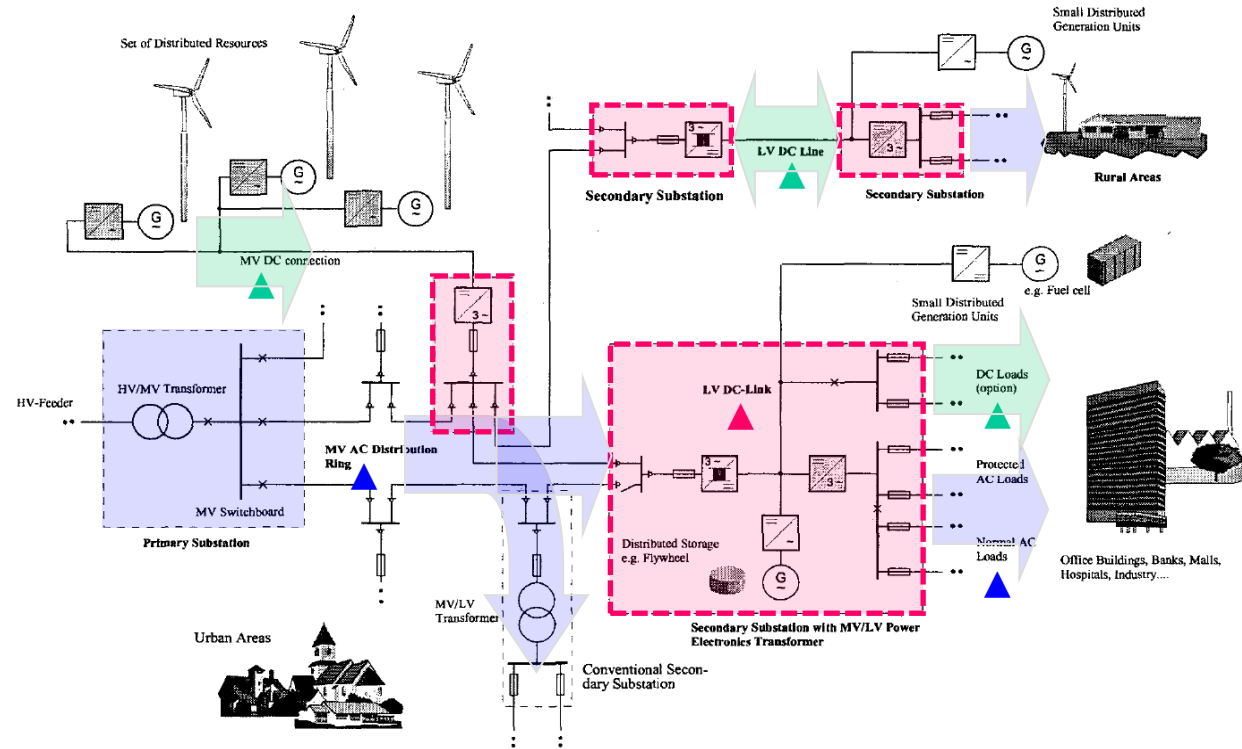


- SST Efficiency Significantly Worse (Two Power Electronic Conversion Stages!)
- SST Functionality Significantly Higher → Not a 1:1 Replacement!



Advanced (High Power Quality) Grid Concept

■ Heinemann / ABB (2001)



- MV AC Distribution with DC Subsystems (LV and MV) and Large Number of Distributed Resources
- MF AC-AC Conv. with DC-Link Coupled to Energy Storage provide High Power Qual. for Spec. Customers



FREEDM System

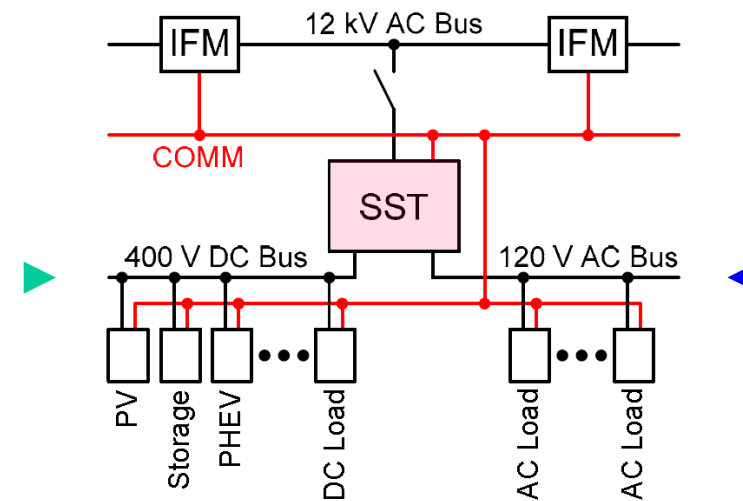
■ Future Ren. Electric Energy Delivery & Management System (Huang et al., 2008)

■ SST as Enabling Technology for the “Energy Internet”

- Full Control of the Power Flow
- Integr. of DER (Distr. Energy Res.)
- Integr. of DES (Distr. E-Storage) + Intellig. Loads
- Protects Power System From Load Disturbances
- Protects Loads from Power System Disturbances
- Enables Distrib. Intellig. through COMM
- Ensure Stability & Opt. Operation
- etc.
- etc.



IFM = Intellig. Fault Management

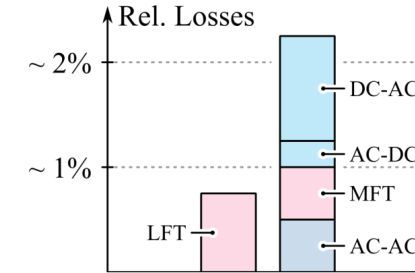
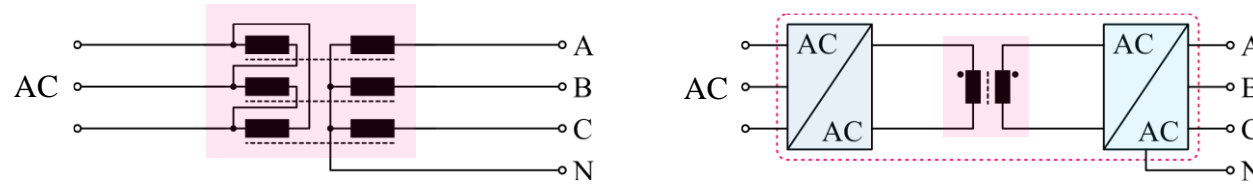


■ Bidirectional Flow of Power & Information / High Bandw. Comm. → Distrib. / Local Autonom. Ctrl.

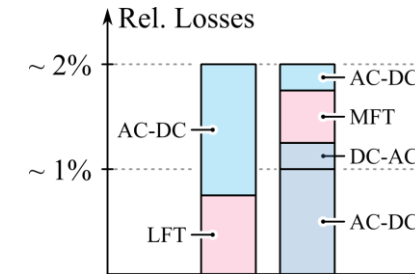
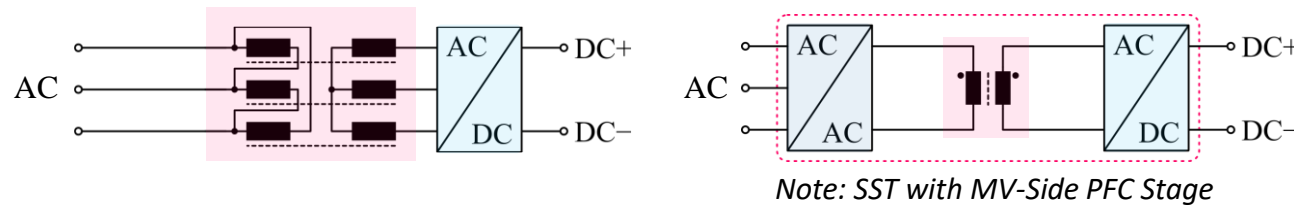


Functionality for Future Grids

- MVAC-LVAC | Note SST with Add. Functionality!

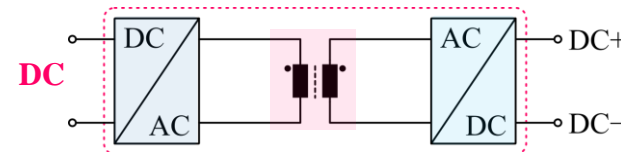


- MVAC-LVDC (Energy Storage, LVDC Grids)



- MVDC-LVDC for Future MVDC Grids

LFT-Based: n/a (!)

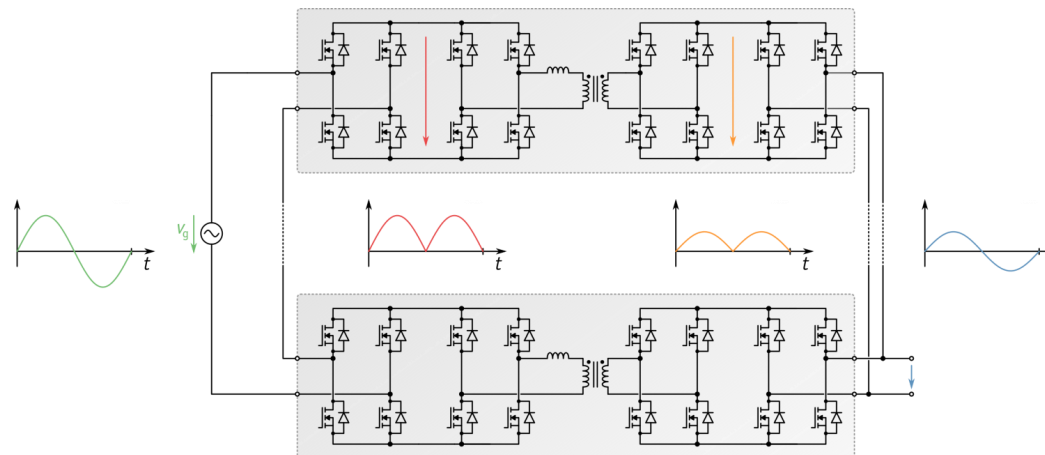


- Key Motivation for SSTs: Functionality & Enabler for DC Grids



Example: 1 MVA, 20 kHz Solid-State Power Substation

- 1 MVA, 13.8 kV to 270 V Single-Phase Demonstrator / One Phase-Module of a Three-Phase System
- Indirect Matrix Converter Modules ($f_1 = f_2$)
- DCX Isolation Stages w. ZVS → 20 kHz Transformers
- 4 Modules w. 10 kV SiC MOSFETS / Input Series & Output Parallel



- 97% Efficiency at 855 kVA / 3 x Losses of LFT w. 99+% Efficiency
- -70% Weight & -50% Volume Compared to LFT / Limited Gain Despite 400 x Higher Transformer Freq.

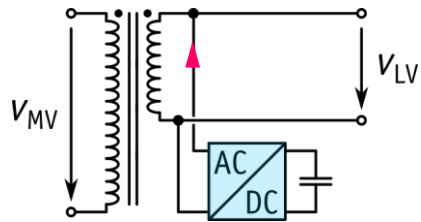


Remark: Hybrid Transformers

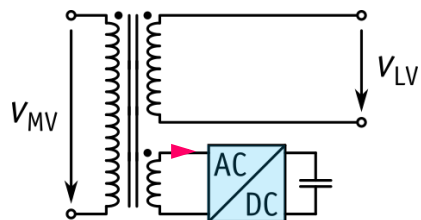
■ Shunt

Reactive Current Injection

- Power Factor Correction
- Harmonic Filtering
- Flicker Control



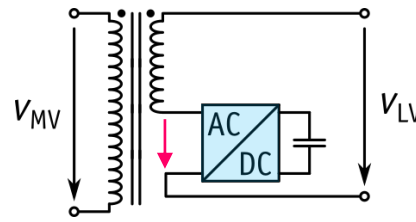
- Shunt Conv. Volt. Indep. of V_{LV}



■ Series

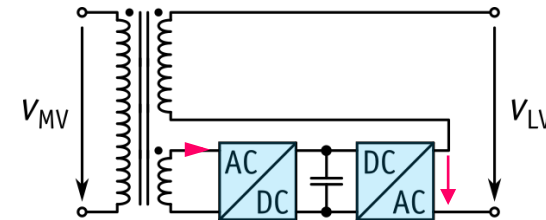
Reactive Voltage Injection

- Phase Shifting
- Voltage injection



■ Combined

- Power Factor Correction
- Harmonic Filtering
- Flicker Control
- AC Regulation
- Phase Shifting



- **Fractional Power Processing** → Power Electronic Stage Processes Only a Fraction of the Power/Voltage



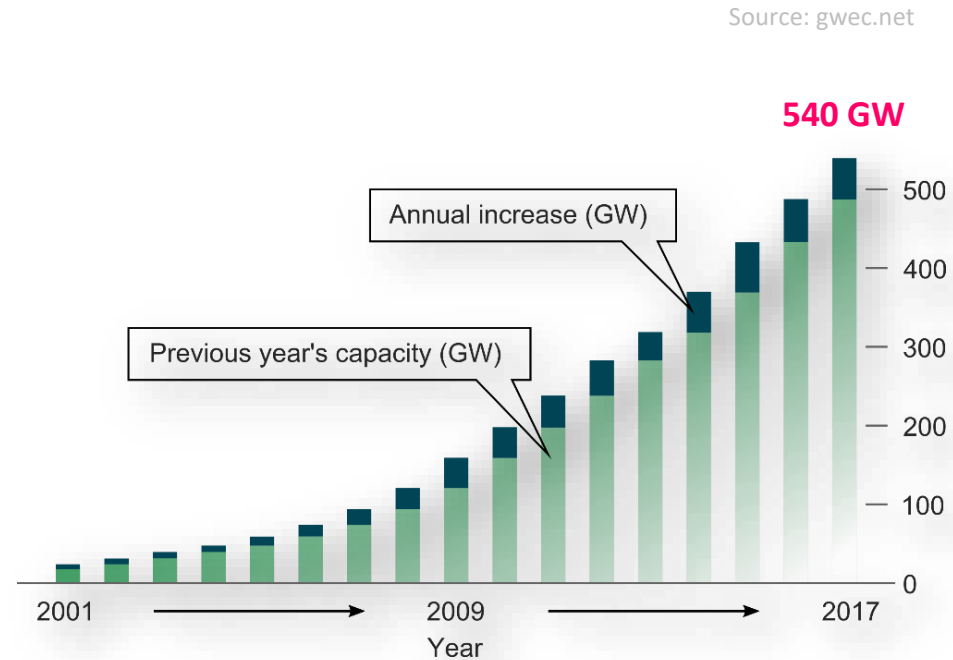
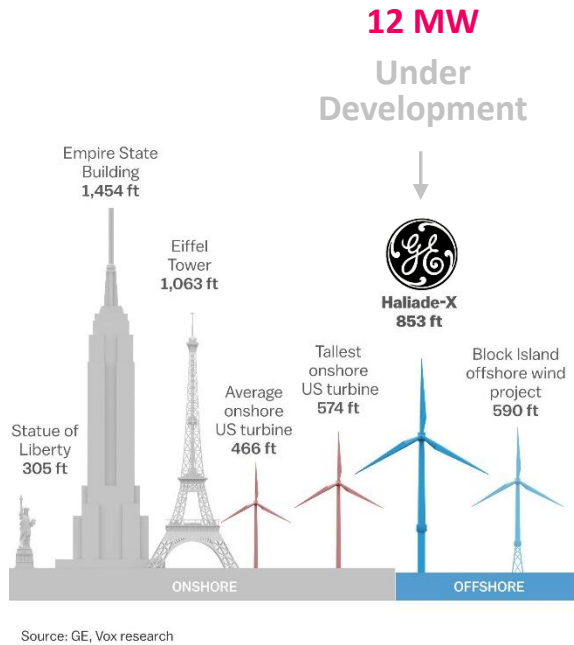
Global Megatrends & Intended SST Applications

- **Renewable Energy**
- Digitalization
- Sustainable Mobility
- Urbanization



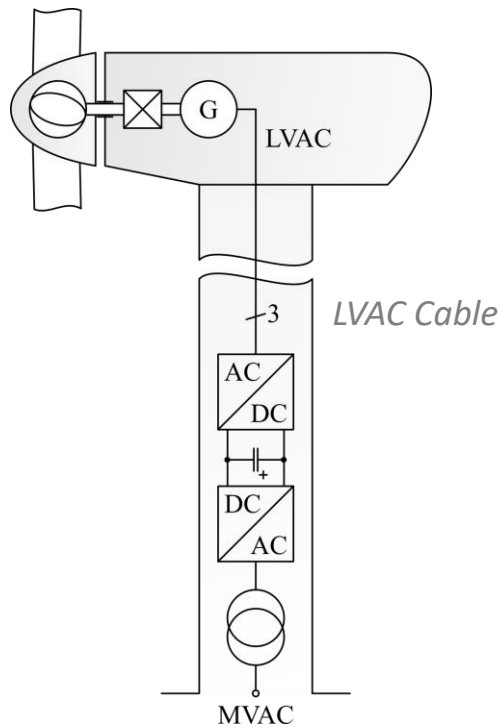
Wind Energy

- Power prop. to D^2 → “Bigger is Better” / Lower Relative Costs
- 50 kW ($D = 15$ m) in 1980 → Up to 20 MW ($D = 250$ m) in Future

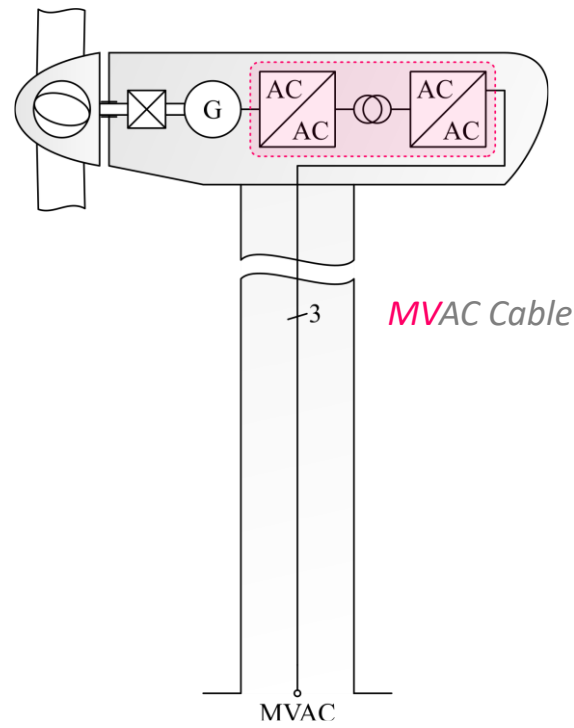


Wind Turbine Electrical Systems

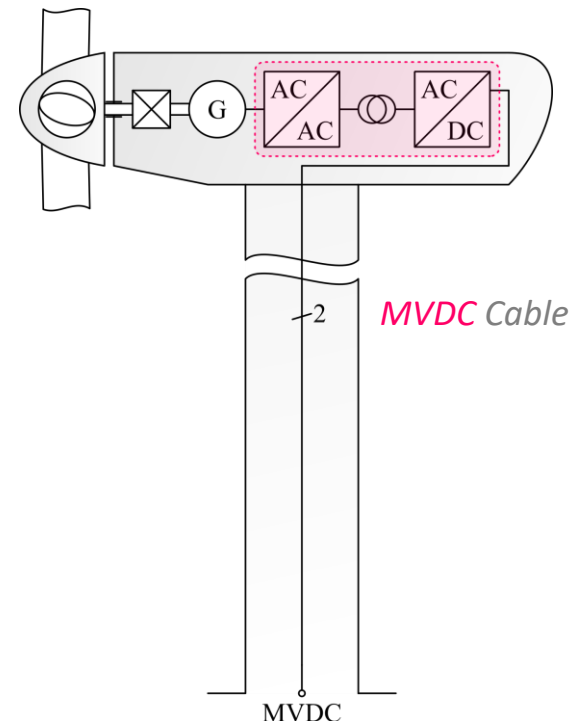
- 690 V Electrical System → Cabling Weight/Costs & Space Requirement
- Future Local Medium-Frequency Conversion to **Medium-Voltage AC or DC**



Convention / On-Shore



Future MVAC / Off-Shore



Future **MVDC** / Off-Shore

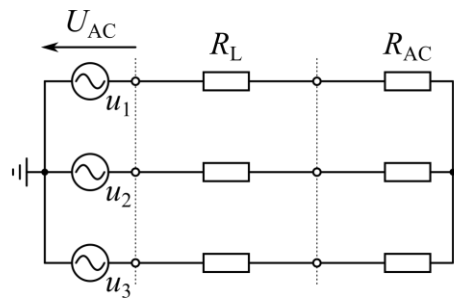
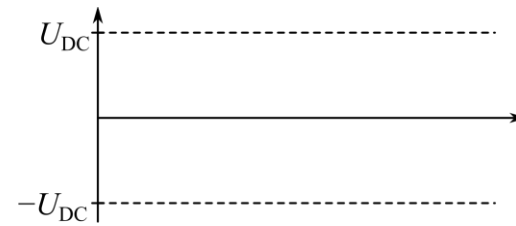
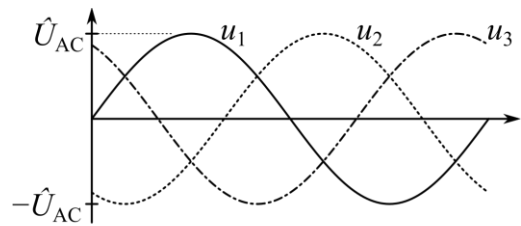


AC vs. DC Power Transmission (1)

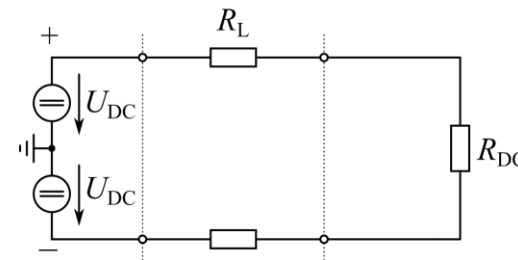
■ DC Voltage Ensures Max. Utilization of Isolation Volt.

→ Highest Voltage RMS Value / Lowest Current (!)

→ Lower Losses & Less Conductor Material!



$$P_{V,AC} = 3 \left(\frac{P/3}{U_{AC}} \right)^2 R_L$$



$$P_{V,DC} = 2 \left(\frac{P}{2U_{DC}} \right)^2 R_L$$

$$\frac{P_{V,DC}}{P_{V,AC}} = \frac{3}{2} \cdot \left(\frac{U_{AC}}{U_{DC}} \right)^2 = 0.75 \text{ with } U_{DC} = \hat{U}_{AC} = \sqrt{2}U_{AC}$$

Note: Only 2 (!) Cables with Same Cross Section / Lower Realization Effort for DC!

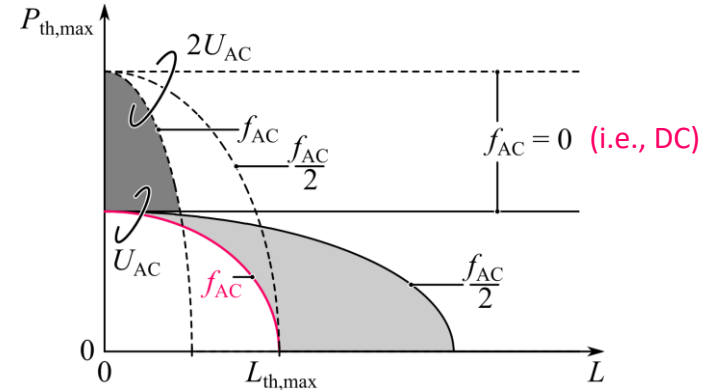
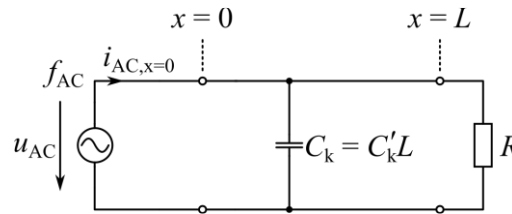
■ DC Voltage Level Transformation Requires Power Electronics Interface

■ DC Fault Current Clearing is Challenging (Missing Regular Current Zero Crossing)

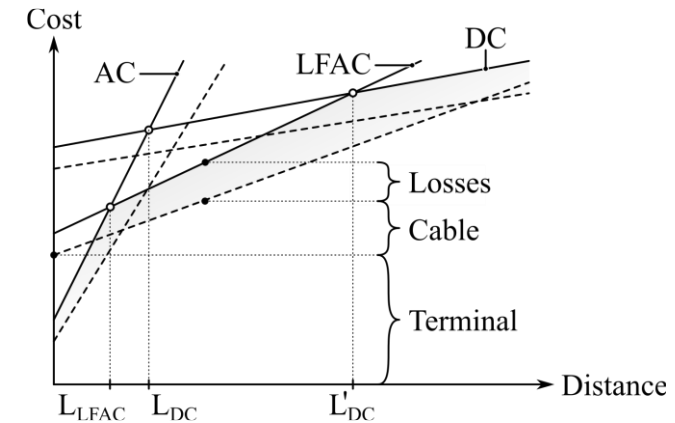
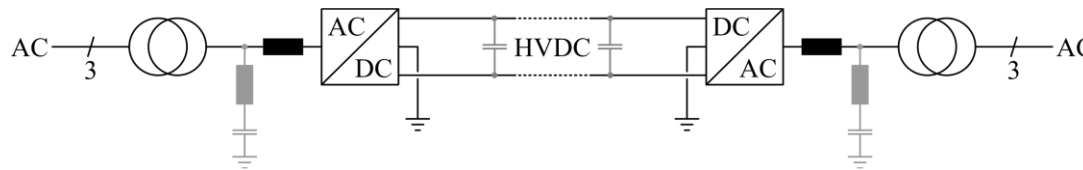


AC vs. DC Power Transmission (2)

AC Cable – Thermal Limit Due to Capacitive current @ $L = 0$



HVDC Transmission – Advantageous for Longer Distances

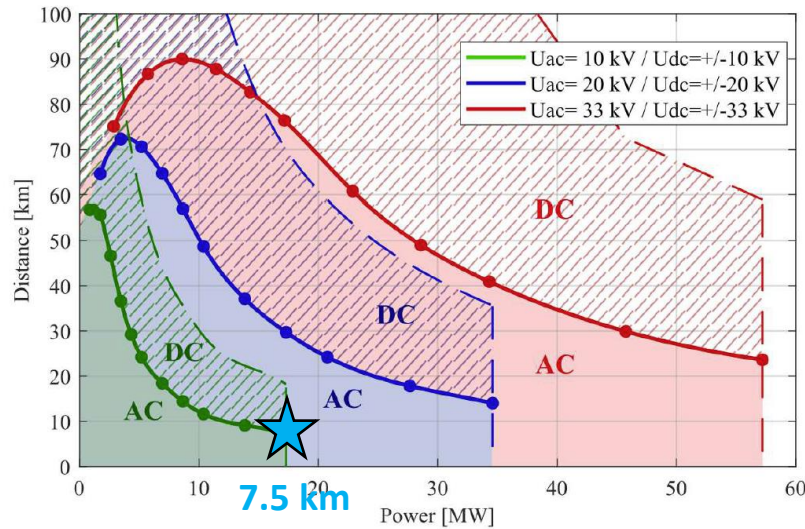


Low-Frequency AC (LFAC) as Possible (Purely Passive) Solution for Medium Transmission Distances

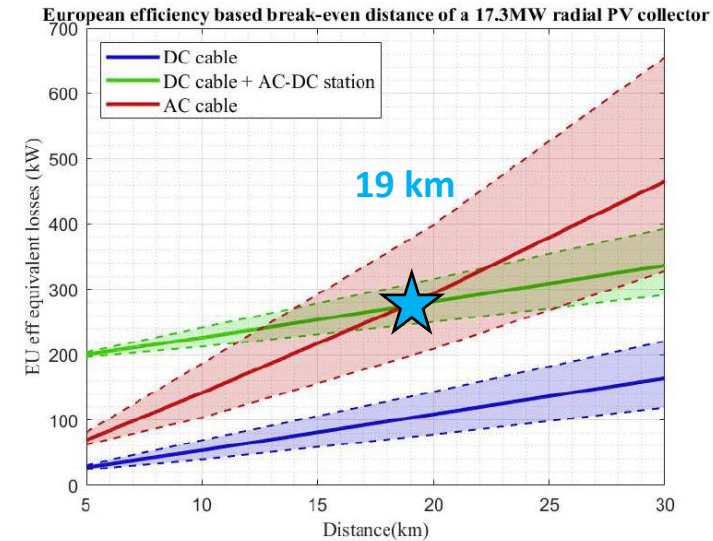


MVDC Break-Even Distances

- MVDC Break-Even Distance is Shorter than for HVDC (typ. 50 km, Submarine Cable)
- Criteria: Efficiency/Losses (not Cost) / Identical Cable Cross Sections Considered



- Point-to-Point Connections
 - Power Limit: 1 kA Cable Current
 - Distance Limit. 5% Losses
 - 2 Converter Stations



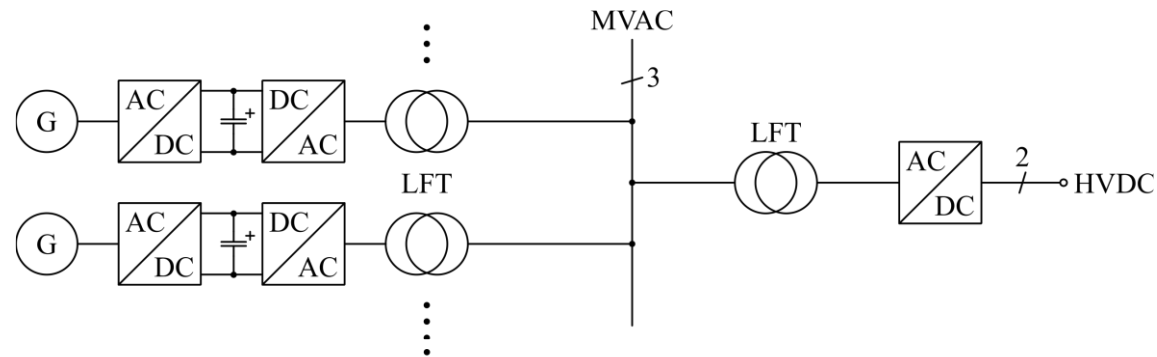
- Radial PV Collecting Grid (10 kV, 17.3 MW)
 - EU Weighted Efficiency / Losses
 - Stochastic Distribution of Sources in Grid
 - 1 Converter Station

- Break-Even Distance Increases with Voltage & Decreases with Power (Except for Low Power: Cap. Current)
- Low-Output Conditions of Renewables (e.g., PV) Increase the Break-Even Distance

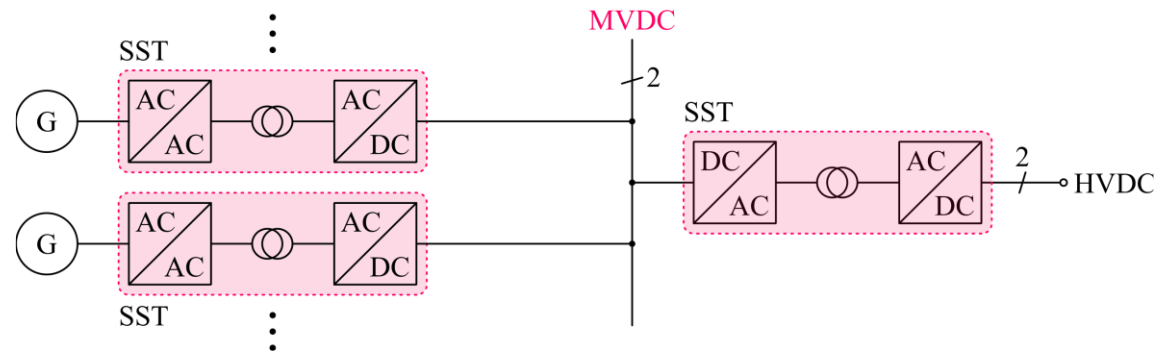


Off-Shore DC Collector Grid

■ Conventional AC Collector-Grid



■ MVDC Collector-Grid



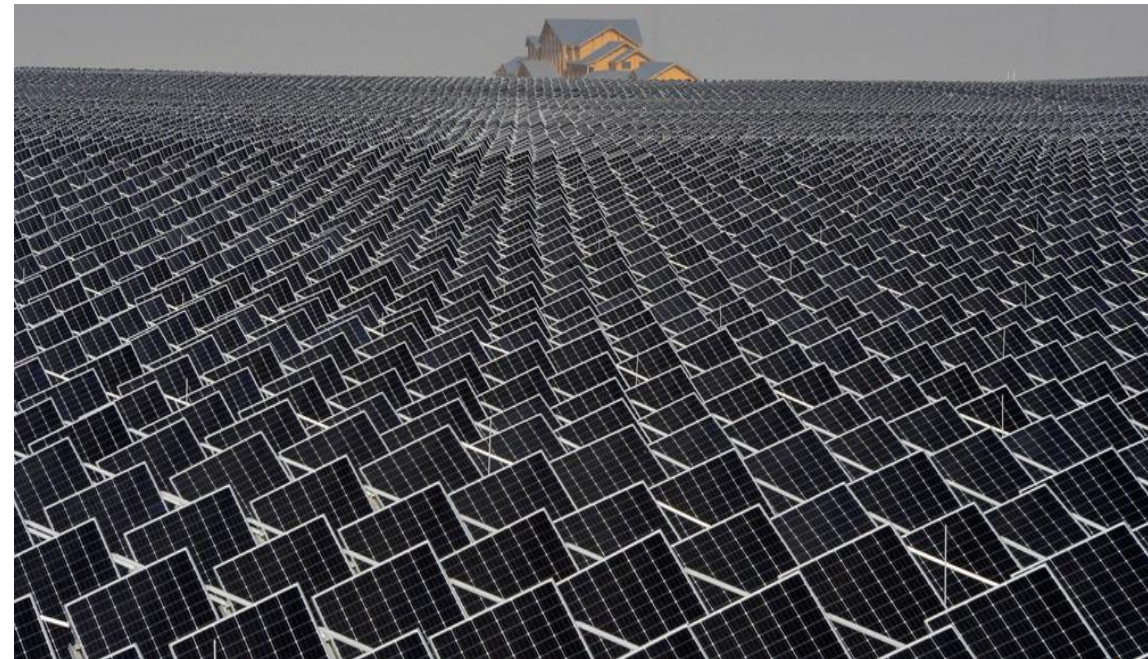
- DC-DC SST — Wind Turbine DC-Link to MVDC Collector Grid → Lower Losses (1%) & Volume
- DC-DC SST — MVDC Grid to HVDC Transmission → Lower Losses (1%) & Volume



Utility-Scale Solar Power Plants

■ Medium-Voltage Power Collection and Transmission

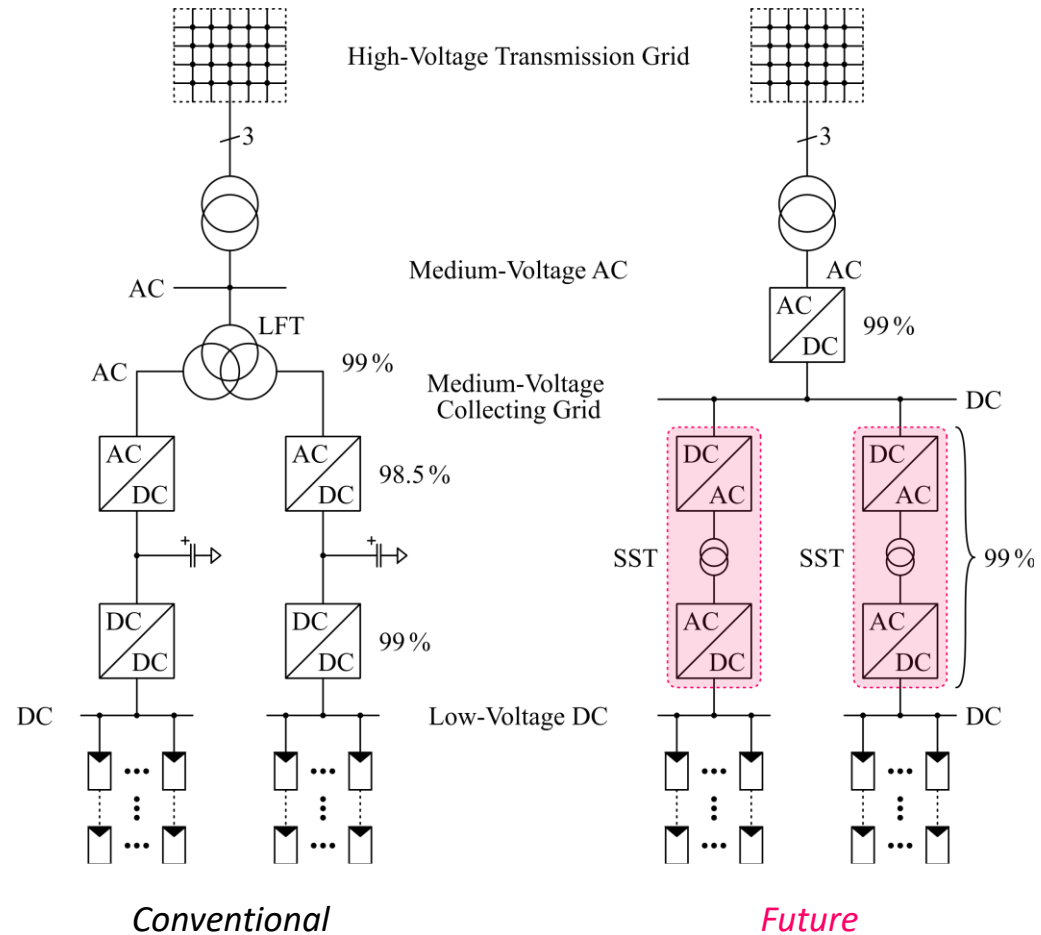
Source: REUTERS/Stringer



- Globally Installed PV Capacity Forecasted to **2.7 TW by 2030** (IEA)

Future DC Collector Grid

- DC-DC SST for MPPT & Direct Interfacing to MV Collector Grid
- 1.5% Efficiency Gain Compared to Conv. AC Technology



Global Megatrends & Intended SST Applications

- Renewable Energy
- **Digitalization**
- Sustainable Mobility
- Urbanization



Hyper-Scale Datacenters

- MV (kV) → Power-Supplies-on-Chip (< 1 V) Power Conversion
- Short Innovation Cycles
- Modularity / Scalability

Server-Farms
up to **450 MW**
99.9999%, i.e., < 30 s/a
\$1.0 Mio./Outage

Since 2006
Running Costs > Initial Costs

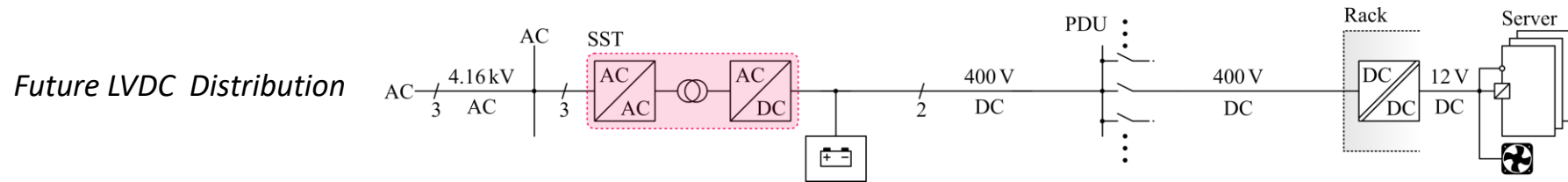
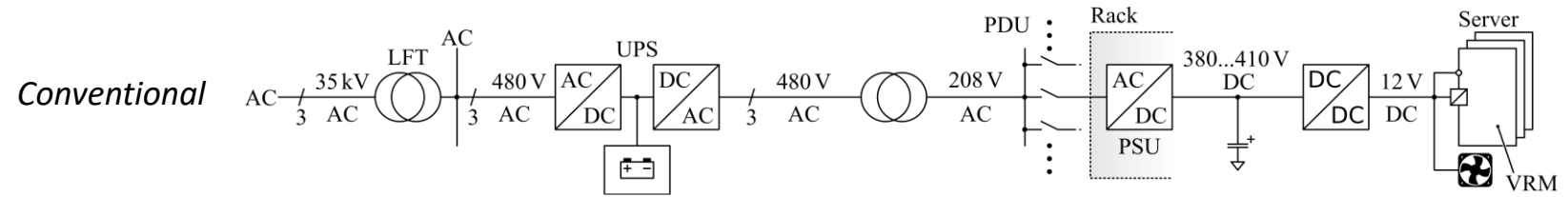
Source: Facebook



- Higher Availability
- Higher Efficiency
- Higher Power Density
- Lower Costs

Future Modular SST-Based Power Distribution

- Reduction in Losses & Smaller Footprint / Improves Reliability & Power Quality



- MV → 48 V → 1.0 V – Only 2 Conversion Stages from MV to CPU-Level (!)

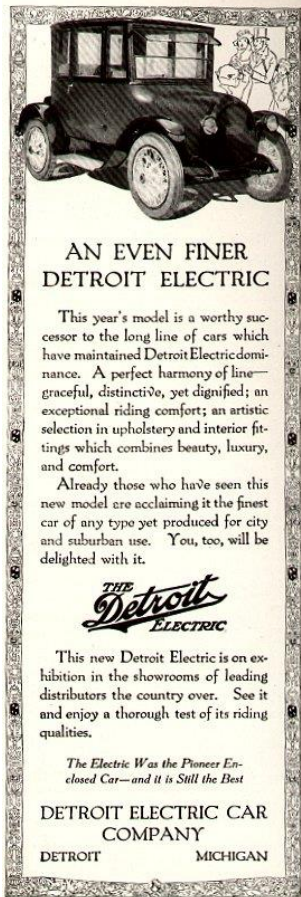


Global Megatrends & Intended SST Applications

- Renewable Energy
- Digitalization
- **Sustainable Mobility**
- Urbanization



The *THE Detroit* ELECTRIC



**AN EVEN FINER
DETROIT ELECTRIC**

This year's model is a worthy successor to the long line of cars which have maintained Detroit Electric dominance. A perfect harmony of line—graceful, distinctive, yet dignified; an exceptional riding comfort; an artistic selection in upholstery and interior fittings which combines beauty, luxury, and comfort.

Already those who have seen this new model are acclaiming it the finest car of any type yet produced for city and suburban use. You, too, will be delighted with it.

THE Detroit
ELECTRIC

This new Detroit Electric is on exhibition in the showrooms of leading distributors the country over. See it and enjoy a thorough test of its riding qualities.

The Electric Was the Pioneer Enclosed Car—and it is Still the Best

DETROIT ELECTRIC CAR COMPANY
DETROIT MICHIGAN

1920
Advertisement



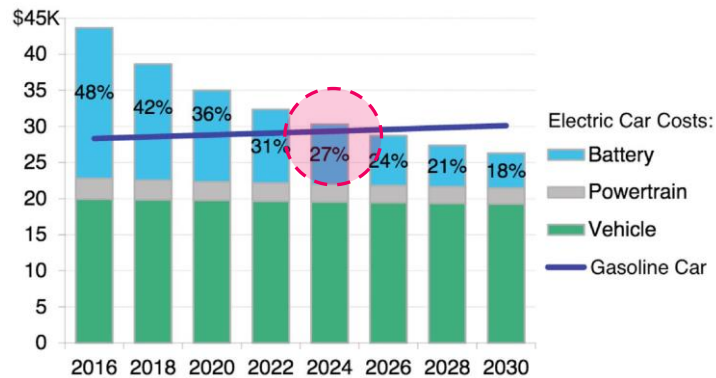
- Anderson Electric Car Company
- 1907...1939 / 13'000 Cars
- 80 mi (130 km) per Charge
- 20 mph (32 km/h) Top Speed

Electric Vehicle Outlook

- Bloomberg NEF — **By 2040 — 57% of All Passenger Vehicle Sales**
30% of Global Passenger Vehicle Fleet

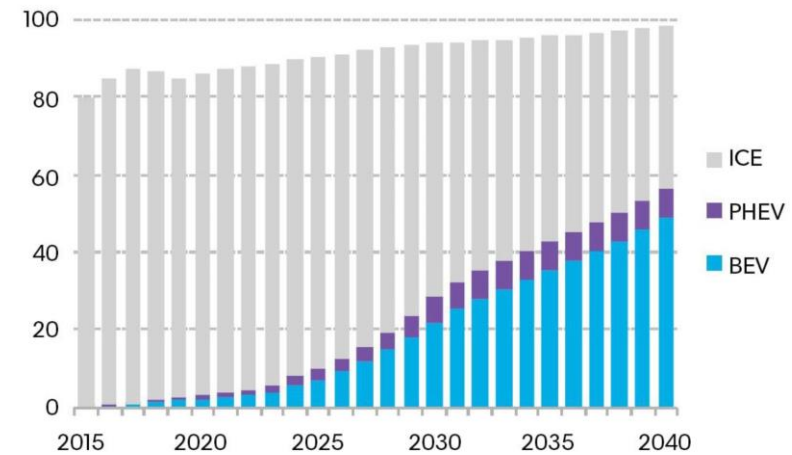
Electric Cars Will Win on Price

Falling battery prices undercut gasoline cars by mid-2020s



Global long-term passenger vehicle sales by drivetrain

Million vehicles



Source: BloombergNEF

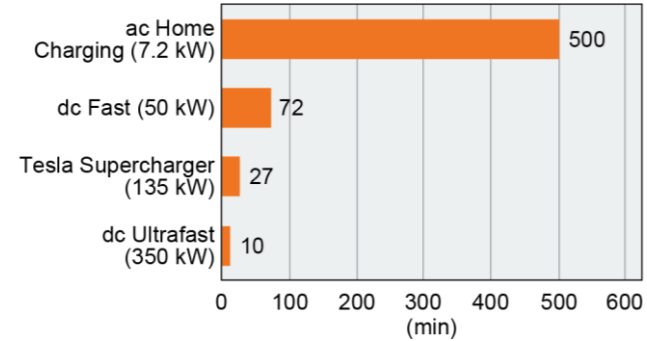
- Falling Battery Costs → **Price Parity of EVs and ICE-V by Mid-2020s** → Tipping Point for EV Industry



EV Charging Anxiety

■ 200+ Miles EV → 50+ kWh

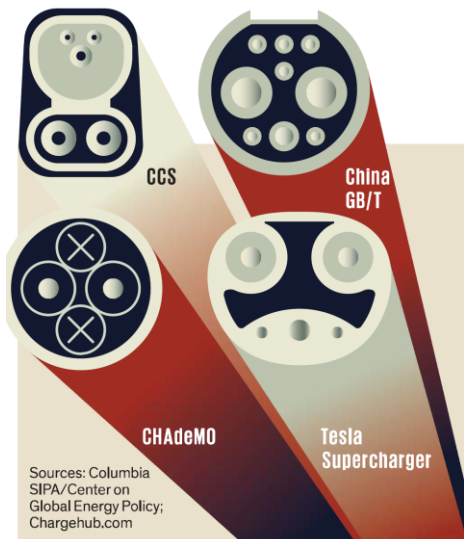
Source: S. Srdic et al., IEEE Electr. Mag., 2019



ChargePoint stations (projected growth)



- 350 kW Extreme Fast Charging (XFC) → Only 10 min Charg. Time



Sources: Columbia SIPA/Center on Global Energy Policy; Chargehub.com

DUELING CHARGERS

Source: J. Voelcker, IEEE Spectrum, 2019

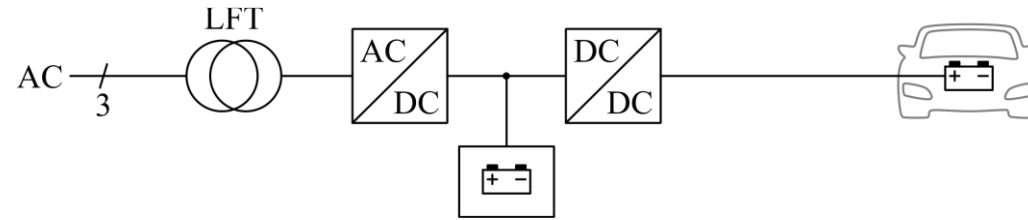
System	Public chargers worldwide	Kilowatts	Availability
Combined Charging System (CCS)*	22,000	50–350	United States, European Union, Australia, Korea
China GB/T	330,000	237.5	China, India
Tesla Supercharger	13,000	135	Global
CHAdeMO	25,300	50–100	Global

* North American and European versions are not compatible.

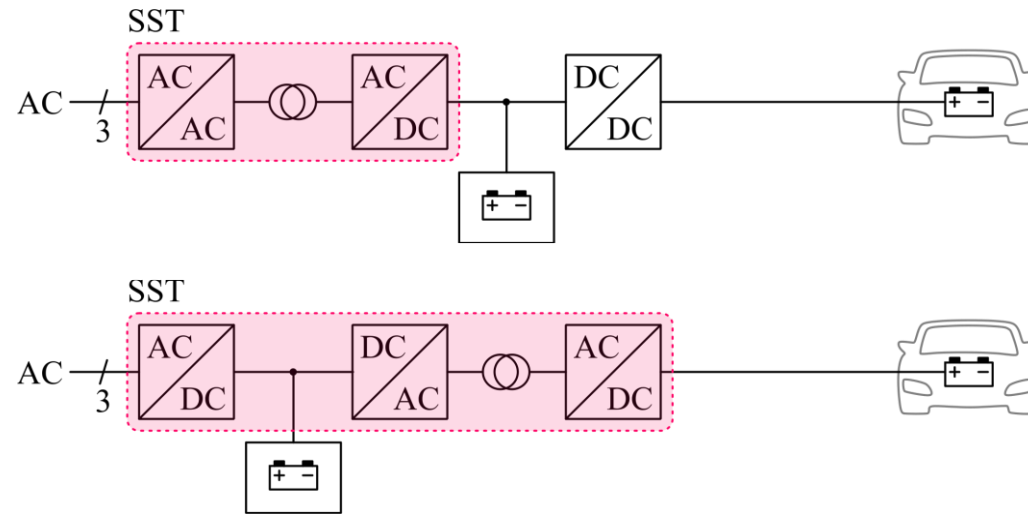


Bidirectional MV Interface for Ultrafast EV Charging

■ Conventional



■ Future



- On-Site Power / Energy Buffer → „Energy-Hub“
- Power / Energy Management → Peak Load Shaving & Grid Support / Stabilization

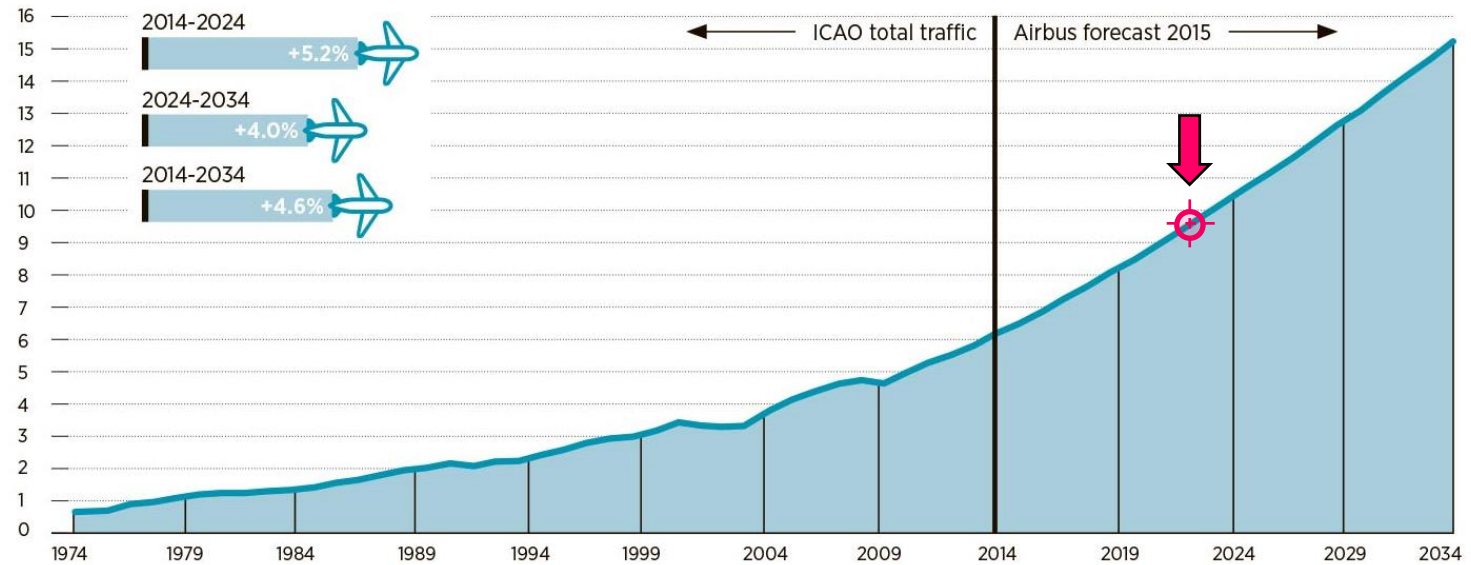


Air Transportation

- **Massive Steady Increase of Global Air Traffic Over the Next Decades**
 - Need for **70'000 New Airliners** over the **Next 20 Years** (Boeing & Airbus)
 - Stringent **Flightpath 2050 Goals** of ACARE → **Reduction of CO₂/NO_x/Noise Emissions**

GLOBAL AIR TRAFFIC (TRILLION REVENUE PASSENGER KILOMETRES)

Traffic is expected to double in the next 15 years



Source: International Civil Aviation Organization (ICAO)/Airbus 2015



Future Aircraft Concepts

■ Cut Emissions Until 2050

- CO₂ by 75%,
- NO_x by 90%,
- Noise Level by 65%

Source:



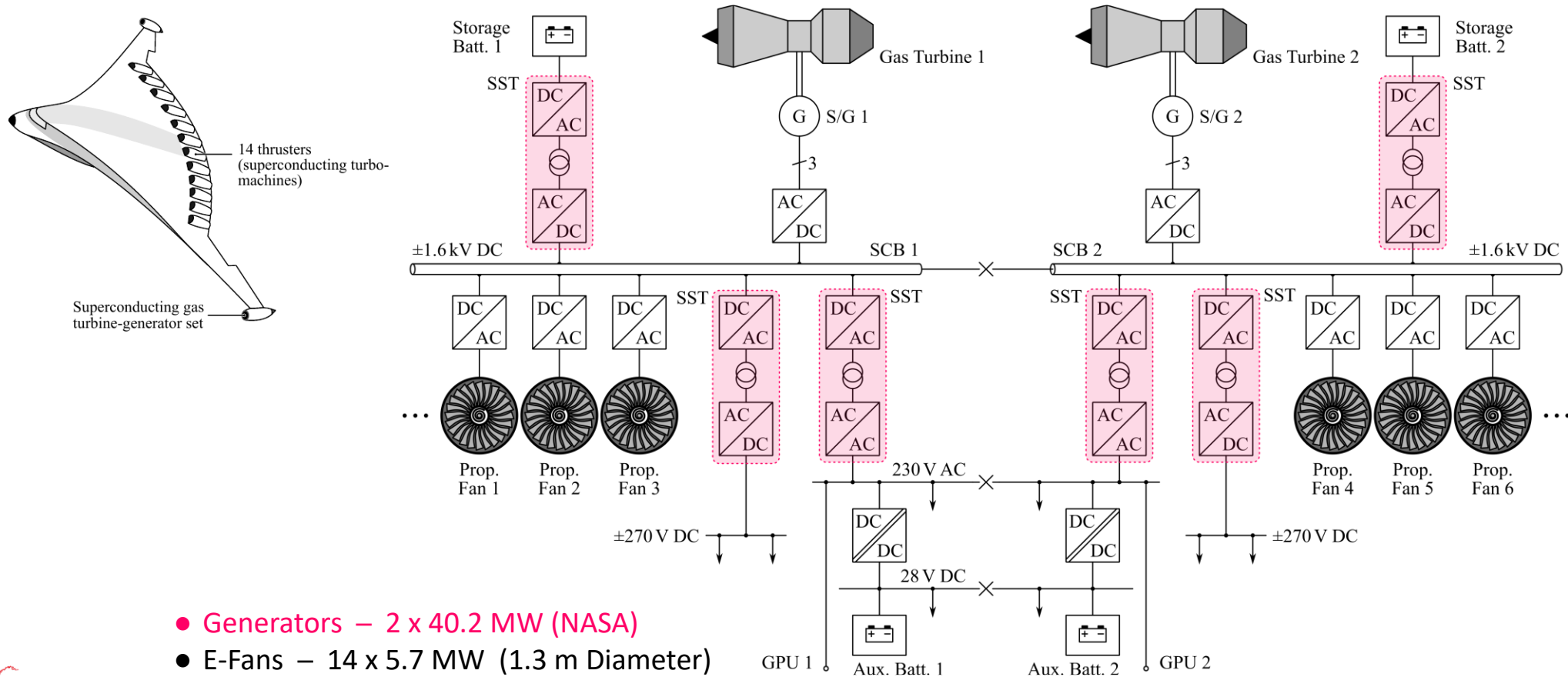
NASA N3-X Vehicle Concept



- Wing-Tip Mounted Efficiency-Optimized Gas Turbines & Distributed E-Fans (“E-Thrust” & Thrust Vectoring)
- MV or Superconducting Power Distribution with Integrated 1000 Wh/kg Batteries (EADS-Concept)

Future Aircraft Electric Power System

■ MV or Superconducting Power Distribution with Integrated 1000 Wh/kg Batteries (EADS-Concept)



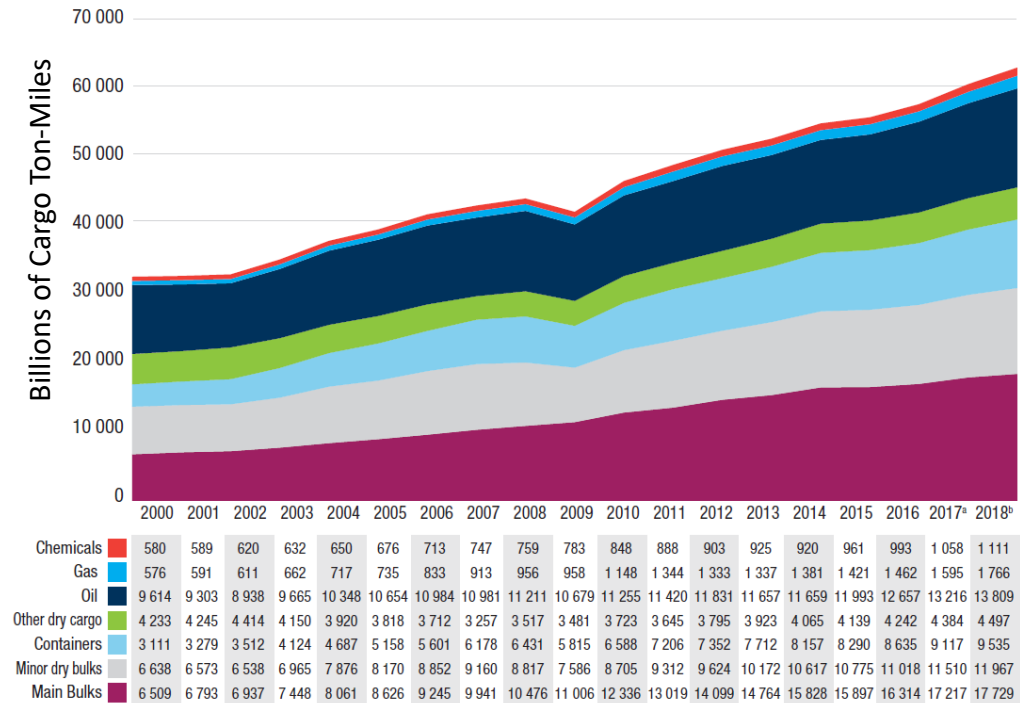
- Generators – 2 x 40.2 MW (NASA)
- E-Fans – 14 x 5.7 MW (1.3 m Diameter)



Sustainable Maritime Transportation

- **80% of All Globally Traded Goods Transported by Ships**
- IMO → **Ship Energy Efficiency Management Plan (SEEMP) & Energy Efficiency Design Index (EEDI)**
- Crude Oil → New Fuel Types (LNG)
- Fully-Electric Port Infrastructure

Source: UNCTAD 2018

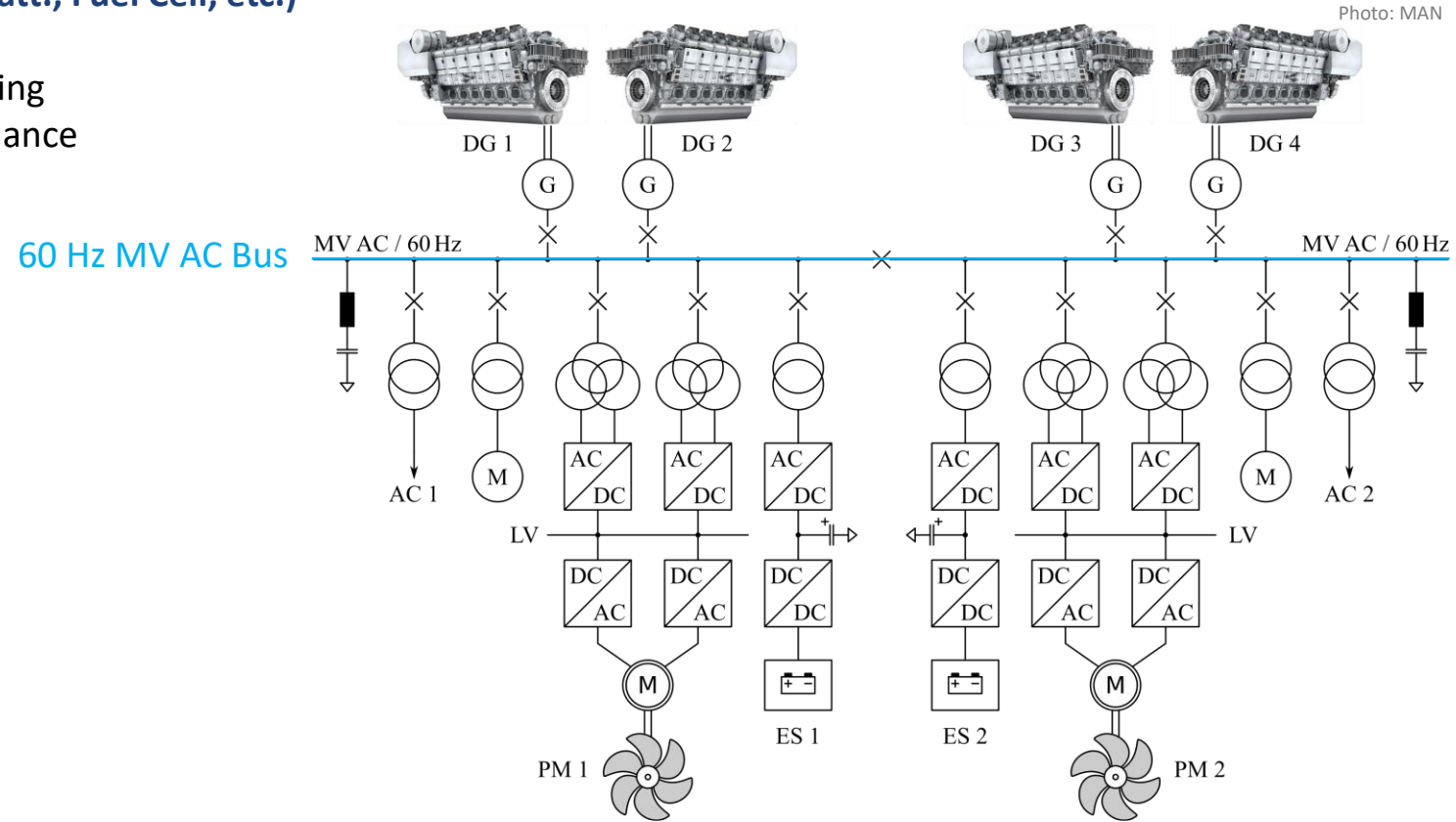


■ **Worldwide Seaborne Trade > 60'000 Billions of Cargo Ton-Miles**



Hybrid Diesel-Electric Propulsion

- No Mech. Coupling of Propulsion & Prime Movers (DGs) → Eff. Optim. Load Distrib. to the DGs
- Energy Storage (Batt., Fuel Cell, etc.)
 - Peak Shaving
 - Opt. Gen. Scheduling
 - High Dyn. Performance

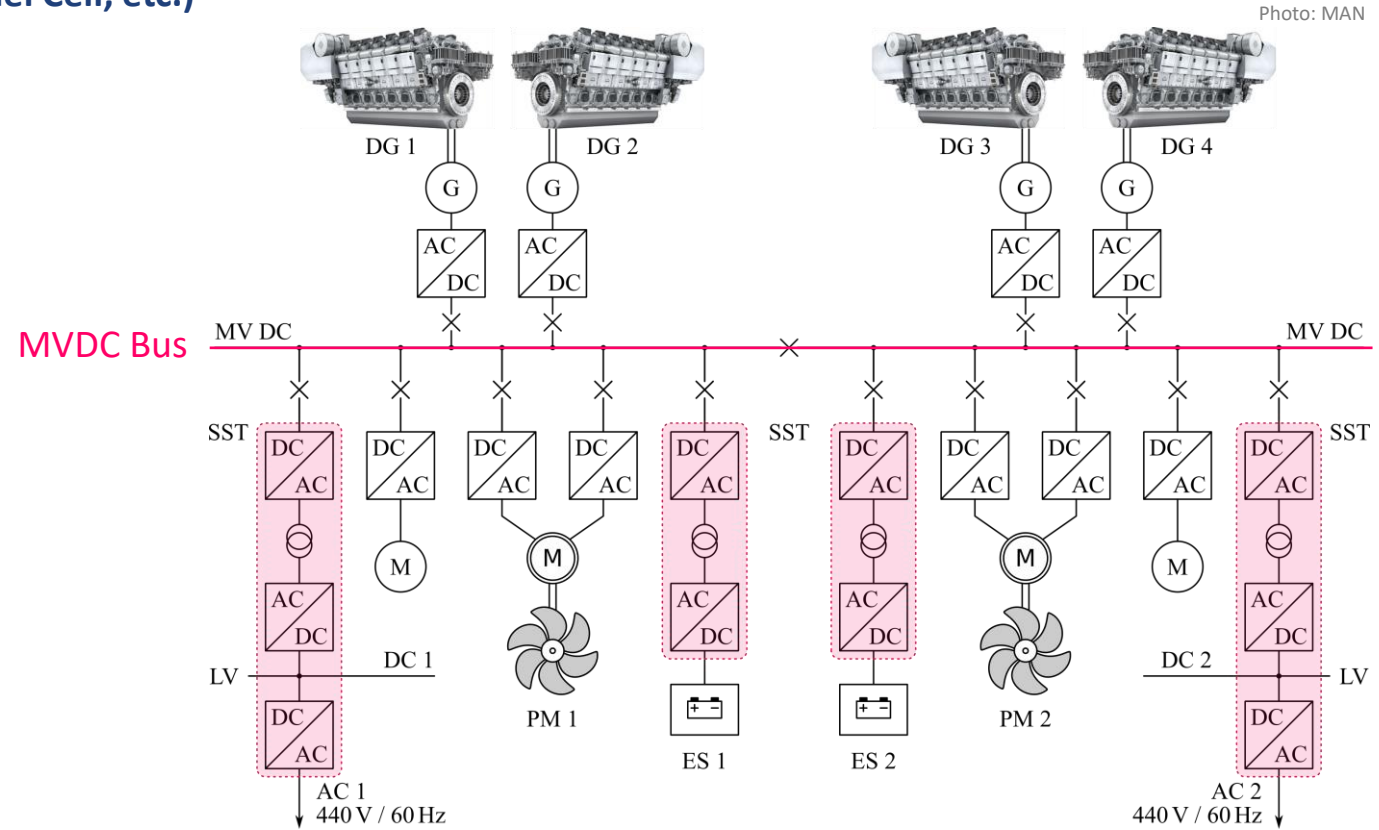


- Conventional AC Power Distribution Network → Disadvantage of Constant Prime Mover / Generator Speed



Shipboard DC Power Distribution

- No Mech. Coupling of Propulsion & Prime Movers (DGs) → Eff. Optim. Load Distrib. to the DGs
- Energy Storage (Batt., Fuel Cell, etc.)
 - Peak Shaving
 - Opt. Gen. Scheduling
 - High Dyn. Performance



- 1 kV, < 20 MW or 1...35 kV, 20...100 MW DC Distribution (Radial or Ring, Central. or Distrib.)

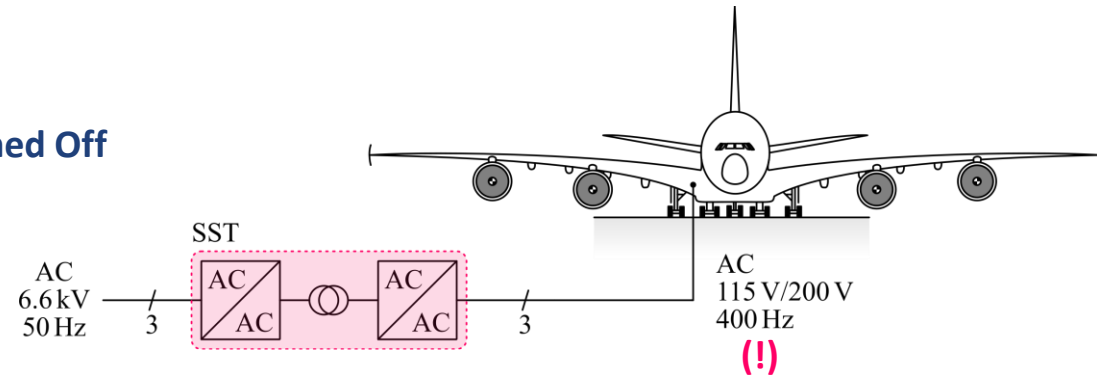


Cutting Emissions & Noise in Airports & Harbors

■ SST Medium-Voltage Interfaces

- Voltage Level / Frequency Adaption
- Low Space Requirement

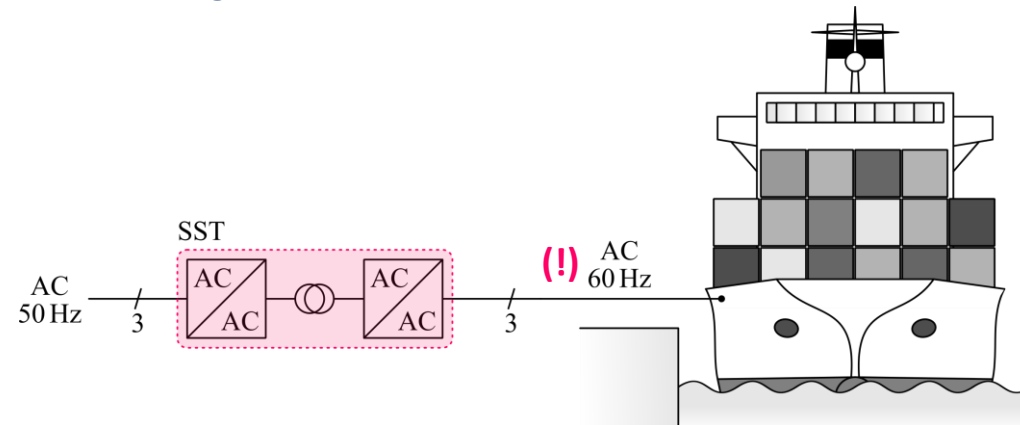
■ Ground Power Supply of Aircraft → APU Turned Off



■ MV-Level Shore-Side Power to Docked Ships (“Cold-Ironing”) → Diesel Aux. Engines Turned Off



Source: iecetech.org



Global Megatrends & Intended SST Applications

- Renewable Energy
- Digitalization
- Sustainable Mobility
- **Urbanization**

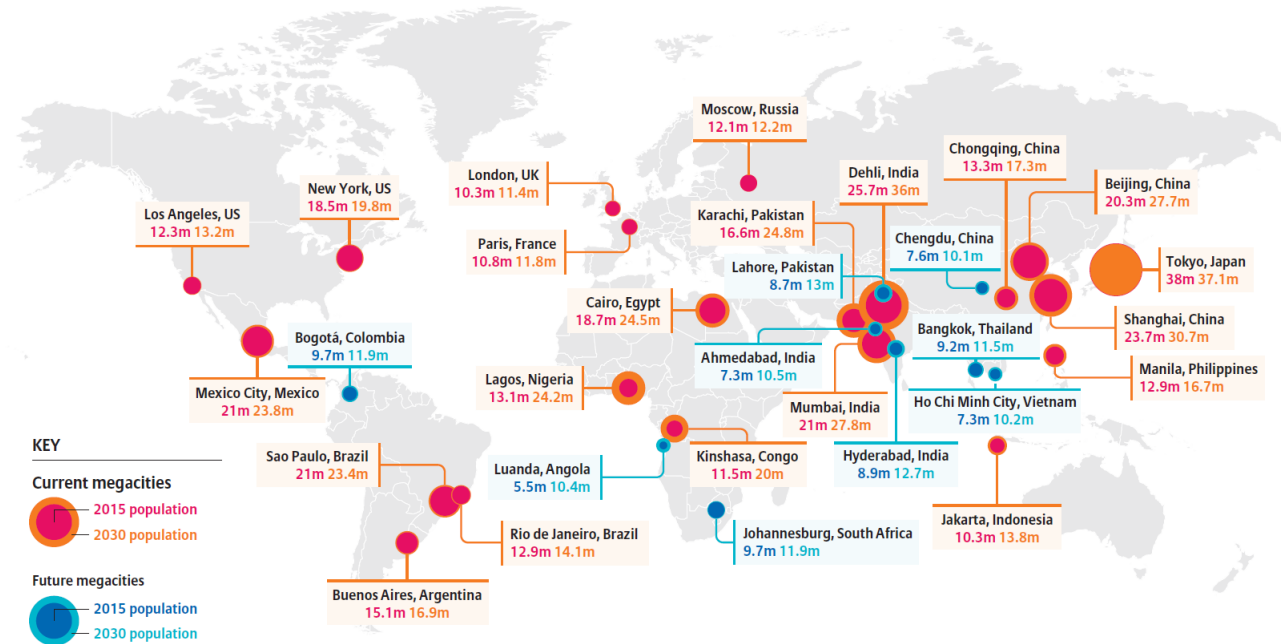


Urbanization

- 60% of World Population Exp. to Live in Urban Cities by 2025
- 30 MEGA Cities Globally by 2023

Source: World Urbanization Prospects: The 2014 Revision

- Smart Buildings
- Smart Mobility
- Smart Energy / Grid
- Smart ICT, etc.

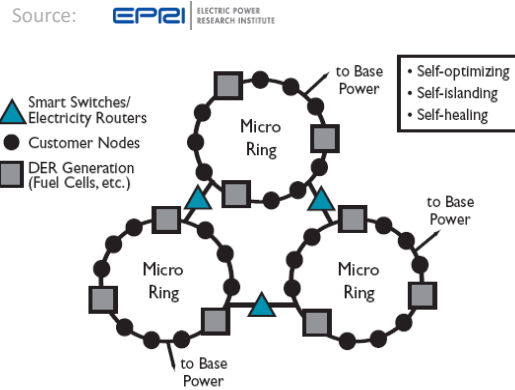


- Selected Current & Future MEGA Cities 2015 → 2030



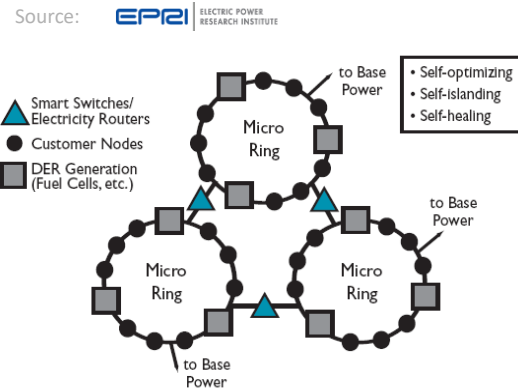
Smart Cities / Grids / Buildings

- Masdar = “Source”
- Fully Sustainable Energy Generation
 - Zero CO₂
 - Zero Waste
- EV Transport / IPT Charging
- to be finished 2025



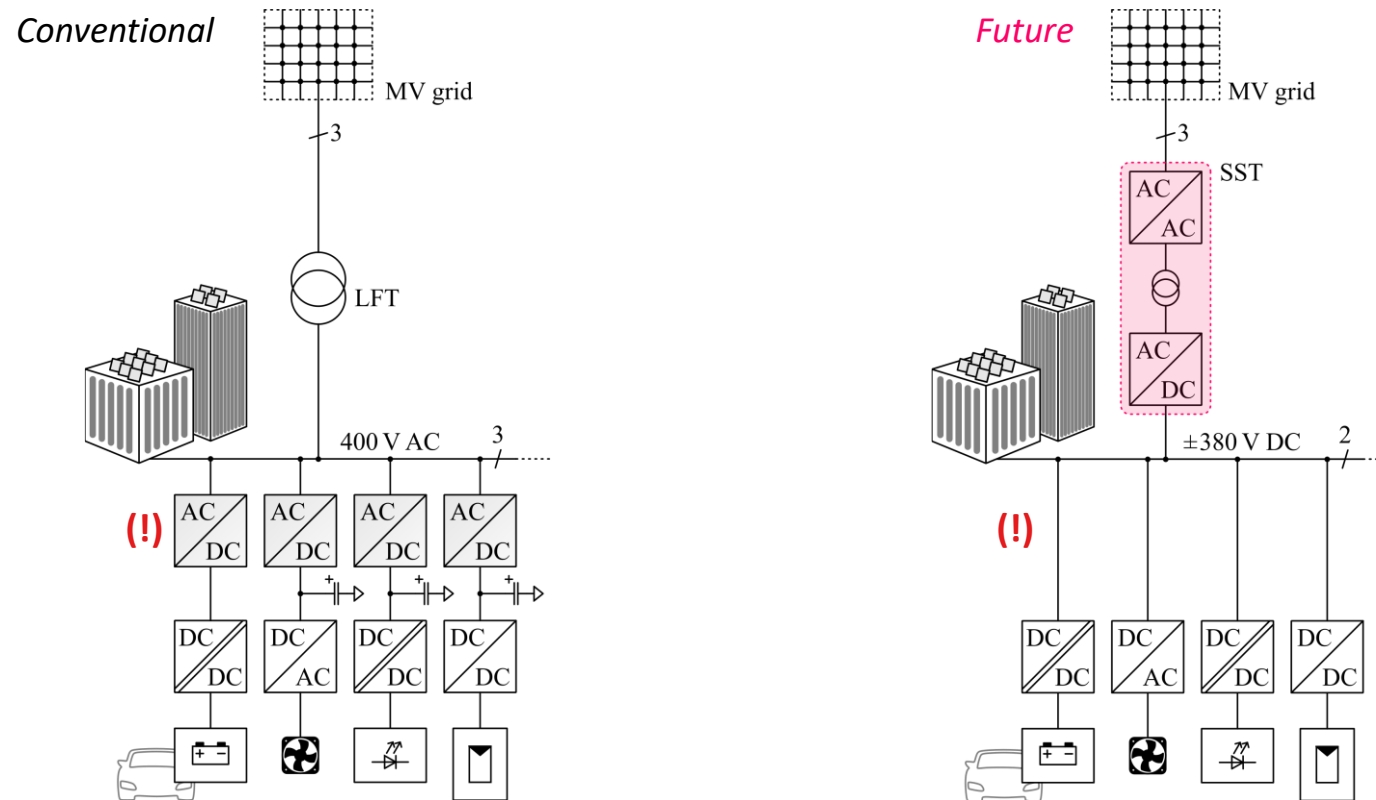
Smart Cities / Grids / Buildings

- Masdar = “Source”
- Fully Sustainable Energy Generation
 - Zero CO₂
 - Zero Waste
- EV Transport / IPT Charging
- to be finished 2025



DC Microgrids

- Local DC Microgrid Integrating Loads/Ren. Sources/Storage
- No Low-Voltage AC-DC Conversion → Higher Efficiency & Lower Realization Effort



Part I

Introduction & Intended SST Applications

- Transformer Basics and Key SST Motivations
- Global Megatrends and Intended SST Applications
- **Terminology**



Terminology (1): Origin of “SST”

United States Patent [19]

Brooks et al.

[11] 4,347,474

[45] Aug. 31, 1982

[54] SOLID STATE REGULATED POWER TRANSFORMER WITH WAVEFORM CONDITIONING CAPABILITY

← “Solid State Regulated Power Transformer ...”

[75] Inventors: James L. Brooks, Oxnard; Roger I. Staab, Camarillo, both of Calif.; James C. Bowers; Harry A. Nienhaus, both of Tampa, Fla.

[73] Assignee: The United States of America as represented by the Secretary of the Navy, Washington, D.C.

[21] Appl. No.: 188,419

[22] Filed: Sep. 18, 1980

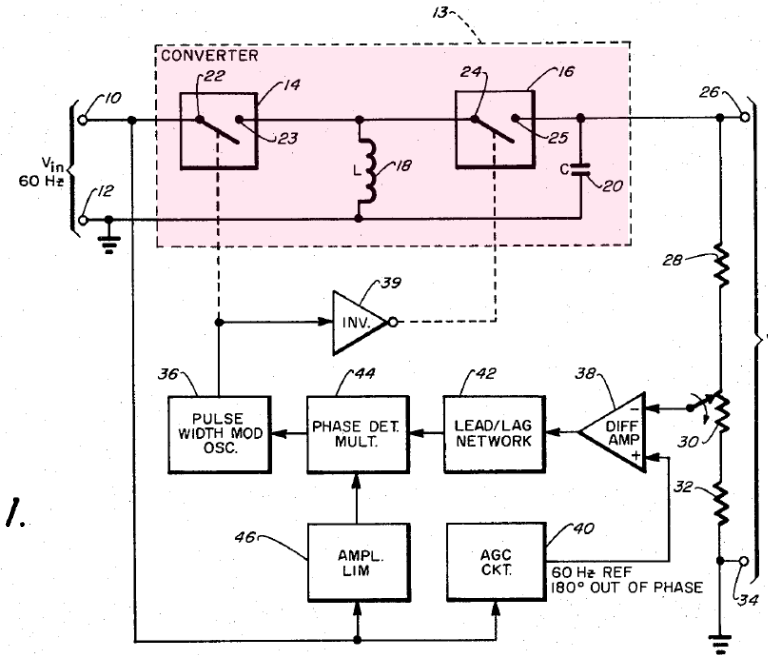


Fig. 1.

- No Isolation (!)
- “Transformer” with Dyn. Adjustable Turns Ratio

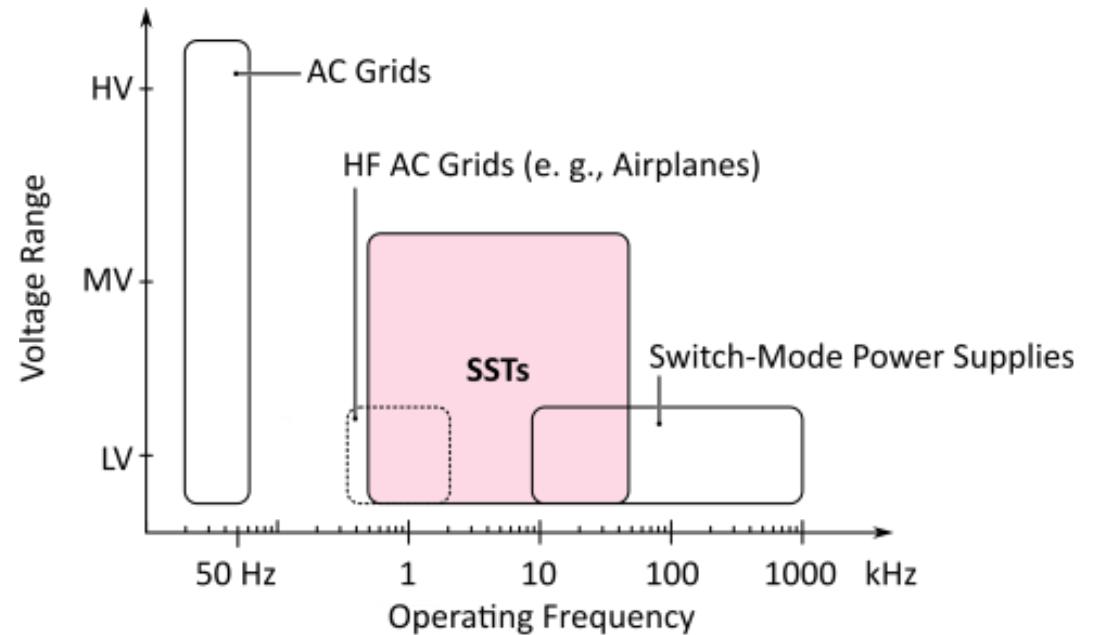


Terminology (2)

- McMurray
- Brooks
- EPRI
- ABB
- Borojevic
- Wang
- ...

- **Electronic Transformer (1968)**
- **Solid-State Transformer (SST, 1980)**
- **Intelligent Universal Transformer (IUT)**
- **Power Electronics Transformer (PET)**
- **Energy Control Center (ECC)**
- **Energy Router**

- **Defining Properties**
- **Interface to Medium-Voltage**
- **Medium-Frequency Isolation**
- **AC or DC Input and/or Output**



Part II

SST Concepts & Key Design Aspects

- Medium-Frequency Power Conversion
- Power Semiconductors
- Key SST Topologies
- Medium-Frequency Transformers
- Isolation Coordination
- Protection
- Reliability
- Standardization & EMC
- Construction & Testing



Part II

SST Concepts & Key Design Aspects

- **Medium-Frequency Power Conversion**
- Power Semiconductors
- Key SST Topologies
- Medium-Frequency Transformers
- Isolation Coordination
- Protection
- Reliability
- Standardization & EMC
- Construction & Testing



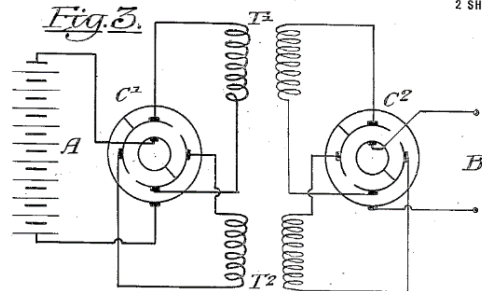
A Brief History of MF Power Conversion

■ Bouchérot (1914)

- DC-DC, Mechanical Switches

1,206,662.

Patented Nov. 28, 1916.
2 SHEETS—SHEET 2.



(!)

■ D. C. Prince (1928)

- “Direct-Current Transformer Circuit”

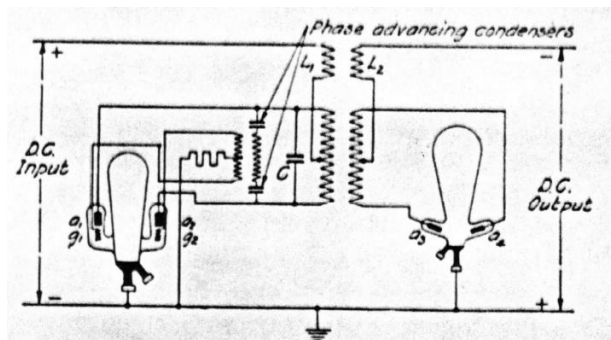
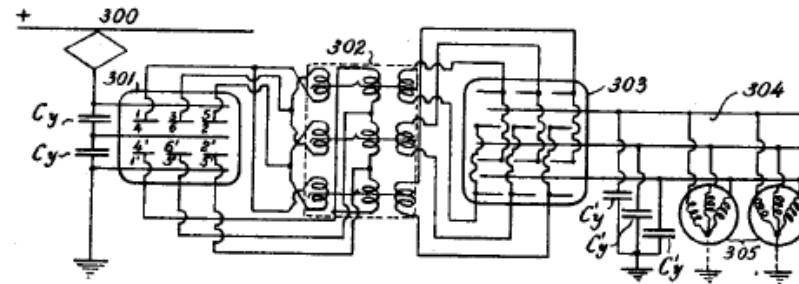


Fig. 7. Direct-current Transformer Circuit, Showing the Combination of Rectifier Circuit (Fig. 5, on right) and Inverter Circuit (Fig. 3, on left)

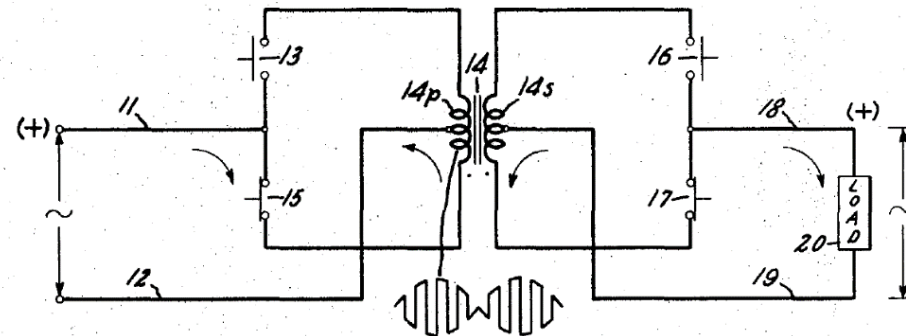
■ Hazeltine (1923)

- DC-AC, Mercury-Arc Valves



■ McMurray (1968)

- Electronic Transformer with Solid-State Switches

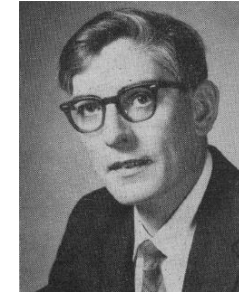


Electronic Transformer (1)

United States Patent Office

3,517,300
Patented June 23, 1970

1
3,517,300
POWER CONVERTER CIRCUITS HAVING A HIGH FREQUENCY LINK
William McMurray, Schenectady, N.Y., assignor to General Electric Company, a corporation of New York
Filed Apr. 16, 1968, Ser. No. 721,817
Int. Cl. H02m 5/16, 5/30
U.S. Cl. 321-60 14 Claims



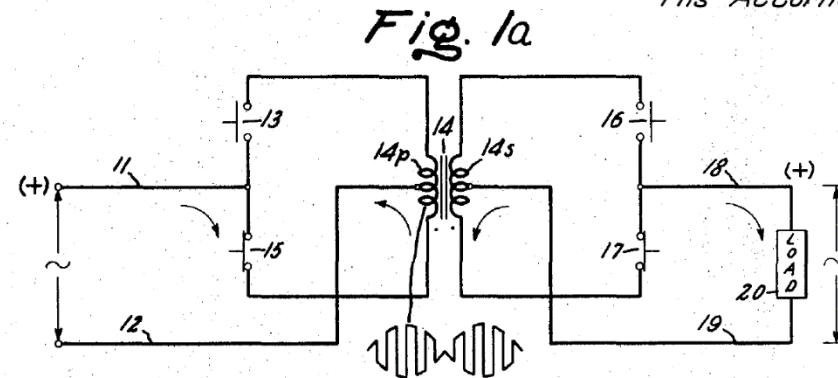
Inventor:
William McMurray,
by Donald R. Campbell
His Attorney.

ABSTRACT OF THE DISCLOSURE

Several single phase solid state power converter circuits have a high frequency transformer link whose windings are connected respectively to the load and to a D-C or low frequency A-C source through inverter configuration switching circuits employing inverse-parallel pairs of controlled turn-off switches (such as transistors or gate turn-off SCR's) as the switching devices. Filter means are connected across the input and output terminals. By synchronously rendering conductive one switching device in each of the primary and secondary side circuits, and alternately rendering conductive another device in each switching circuit, the input potential is converted to a high frequency wave, transformed, and reconstructed at the output terminals. Wide range output voltage control is obtained by phase shifting the turn-on of the switching devices on one side with respect to those on the other side by 0° to 180°, and is used to effect current limiting, current interruption, current regulation, and voltage regulation.

1968

Filed April 16, 1968

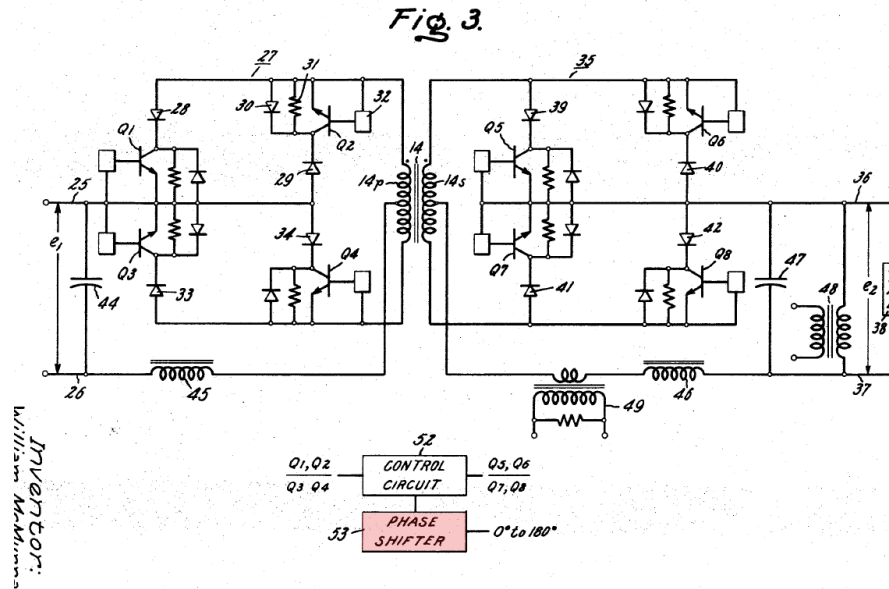


- Electronic Transformer ($f_1 = f_2$)
- AC or DC Voltage Regulation & Current Regulation / Limitation / Interruption

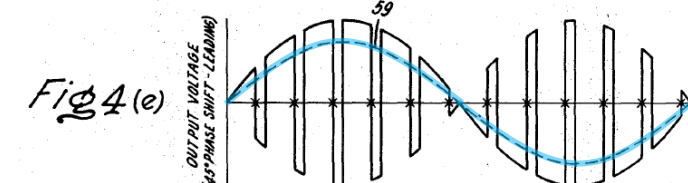
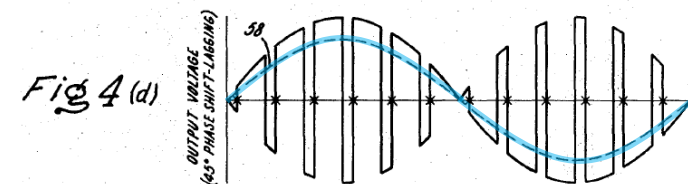
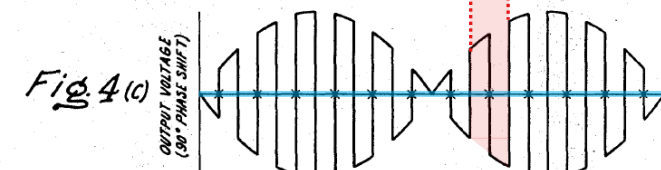
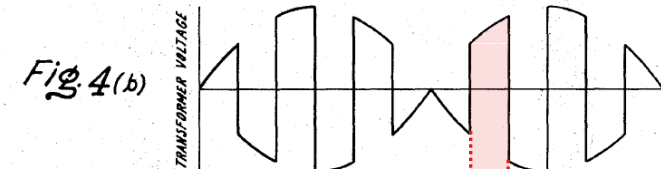
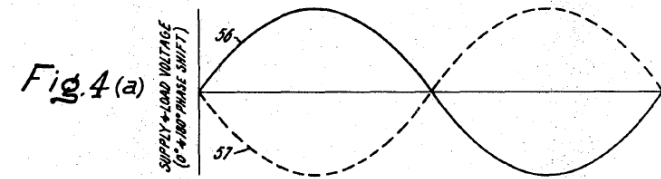


Electronic Transformer (2)

- Inverse-Paralleled Pairs of Turn-off Switches
- 50% Duty Cycle of Input and Output Stage



- $f_1 = f_2 \rightarrow$ Not Controllable (!)
- Voltage Adjustment by Phase Shift Control (!)



Dual Active Bridge (DAB)

Dual Active Bridge

United States Patent [19]
DeDoncker et al.

[11] **Patent Number:** 5,027,264
 [45] **Date of Patent:** Jun. 25, 1991

[54] **POWER CONVERSION APPARATUS FOR DC/DC CONVERSION USING DUAL ACTIVE BRIDGES**

← “... Dual Active Bridges ...”

[75] **Inventors:** Rik W. DeDoncker, Niskayuna, N.Y.;
 Mustansir H. Kheraluwala;
 Deepakraj M. Divan, both of
 Madison, Wis.

[22] **Filed:** Sep. 29, 1989

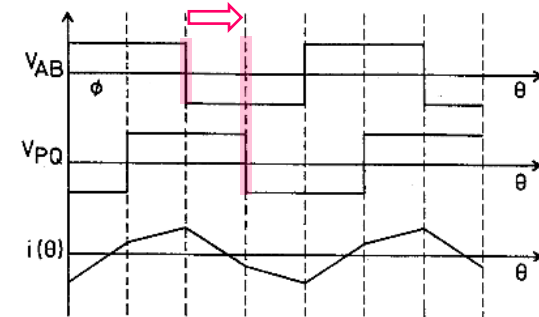
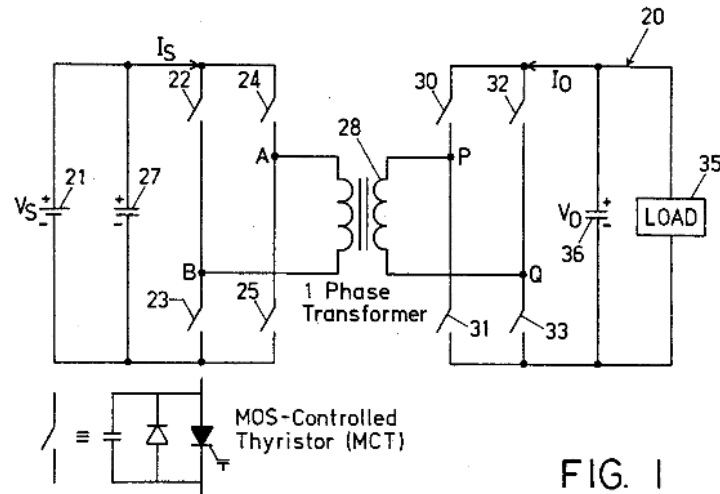


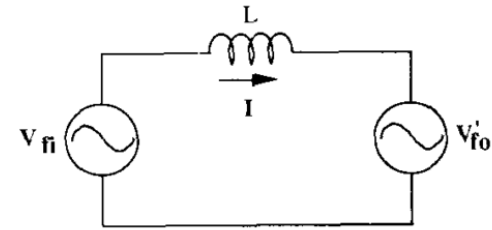
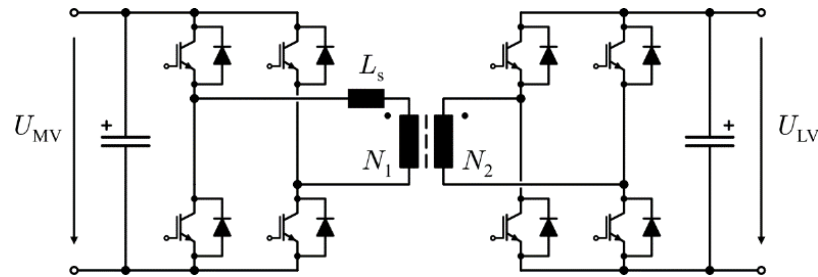
FIG. 2

- Soft-Switching in a Certain Load Range
- Power Flow Control by Phase Shift between Primary & Secondary Voltage

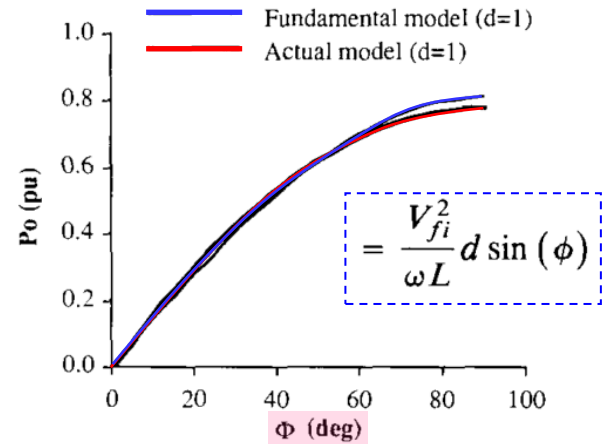
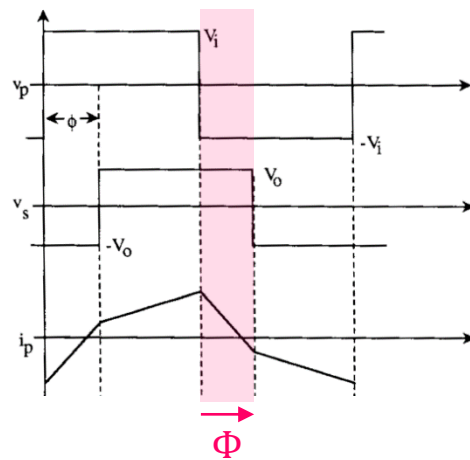


Phase-Shift Modulation (1)

■ Power Transfer Controlled Through Phase Shift Between MV and LV Bridges



Fundamental model of the dual bridge dc/dc converter.

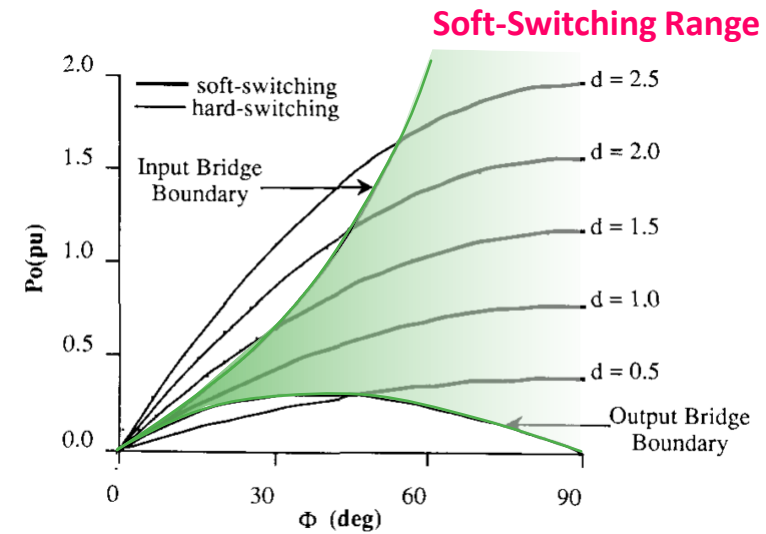
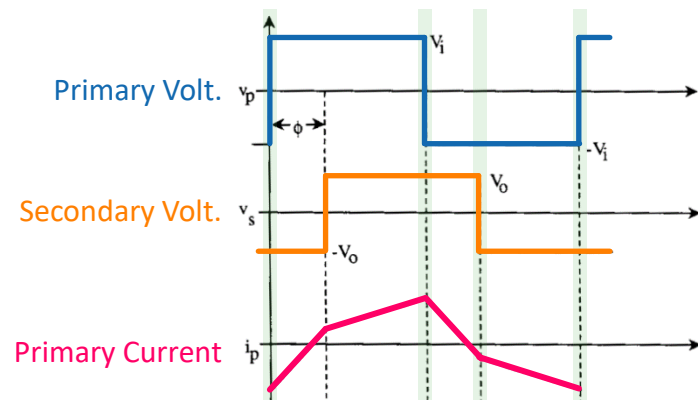
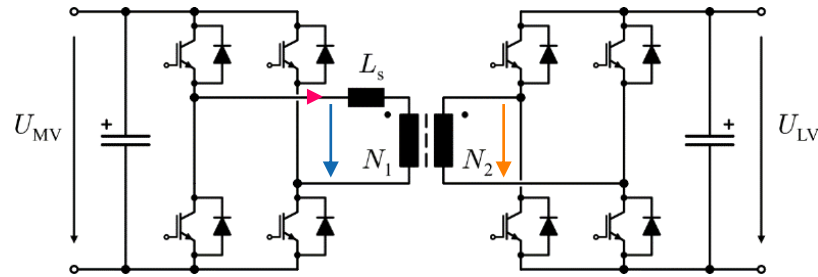


Comparison of the output power versus ϕ , at $d = 1$, from the fundamental model and actual model.



Phase-Shift Modulation (2)

- Zero-Voltage Switching (ZVS) for All Transitions (in a Certain Operating Range)

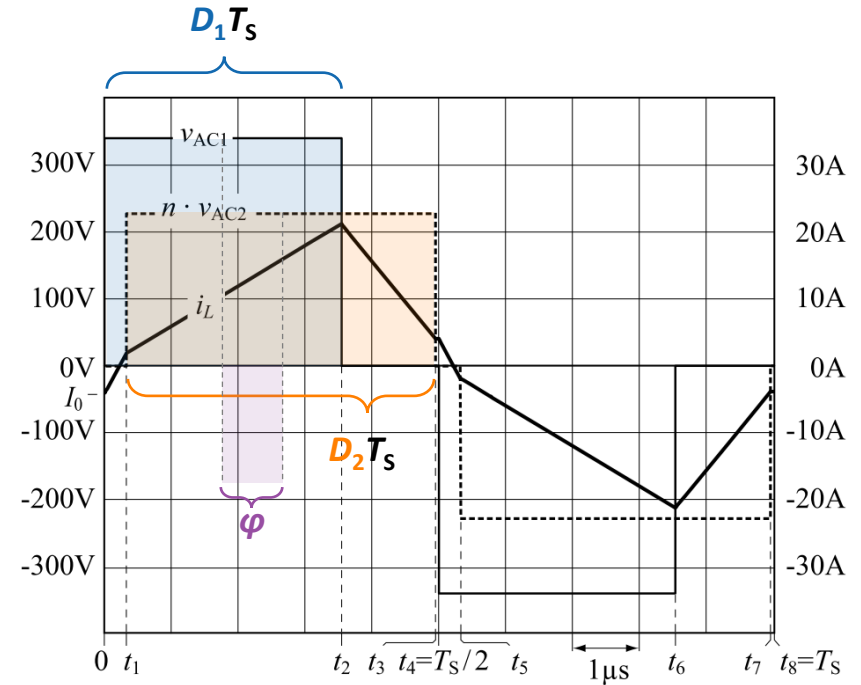
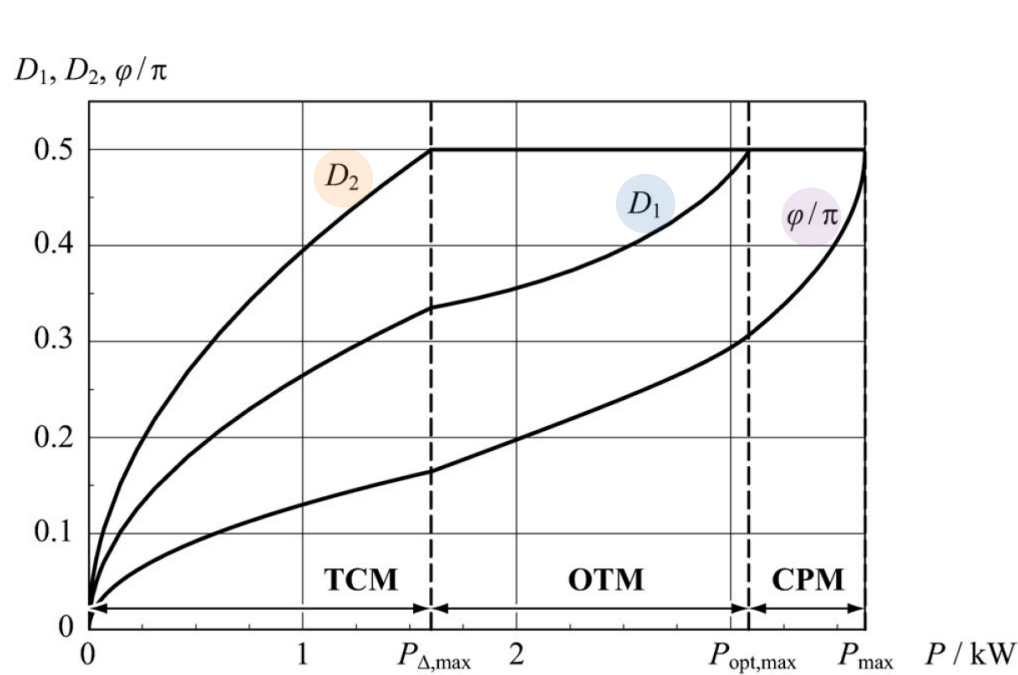


- MV or LV Bridge Loose ZVS Outside of Soft-Switching Range



Phase-Shift / Duty Cycle Modulation

- **Additional Degrees of Freedom** Can Be Utilized for Current Shaping → **Optimization!**
- **For Example: Minimization of the RMS Currents through the Transformer**



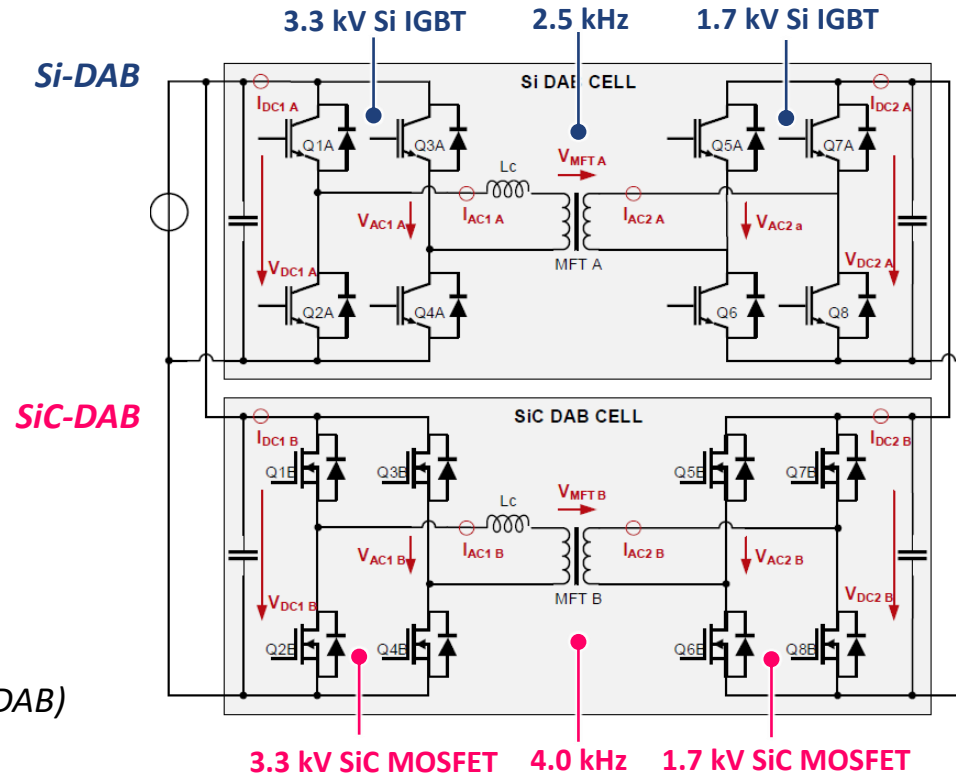
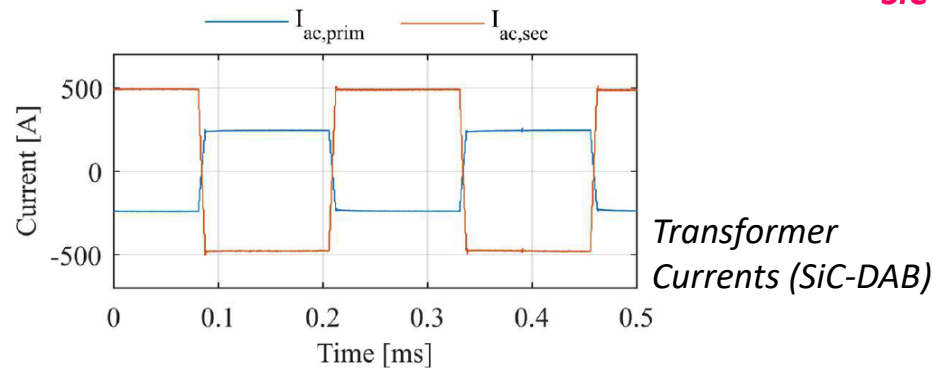
- Note: Not Possible in Half-Bridge Configurations (No Zero Voltage Intervals)



Example: 0.5 MW, 2.5 kV / 1.2 kV DAB

Back-to-Back Testing of Si-Based and SiC-Based DAB Modules

Hitachi Energy



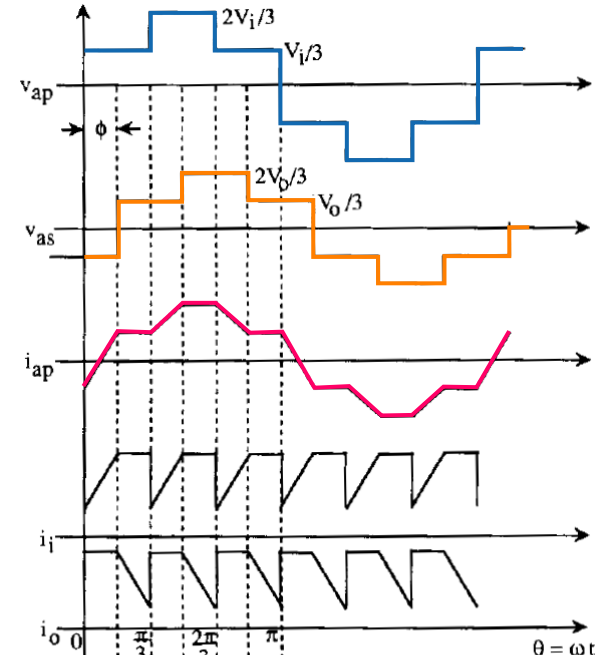
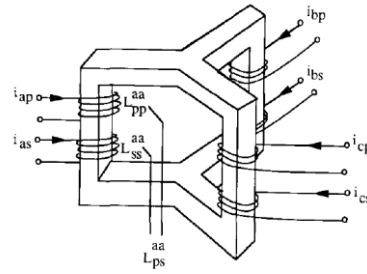
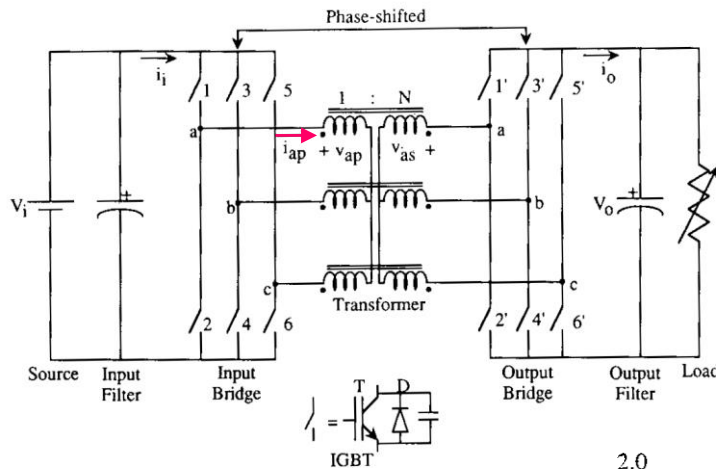
■ Si IGBTs: 98.4% Efficiency @ 360 kW and 2.5 kHz (Calorimetric Measurement)

■ SiC MOSFETs: 99.2% Efficiency @ 360 kW and 4.0 kHz (Calorimetric Measurement)

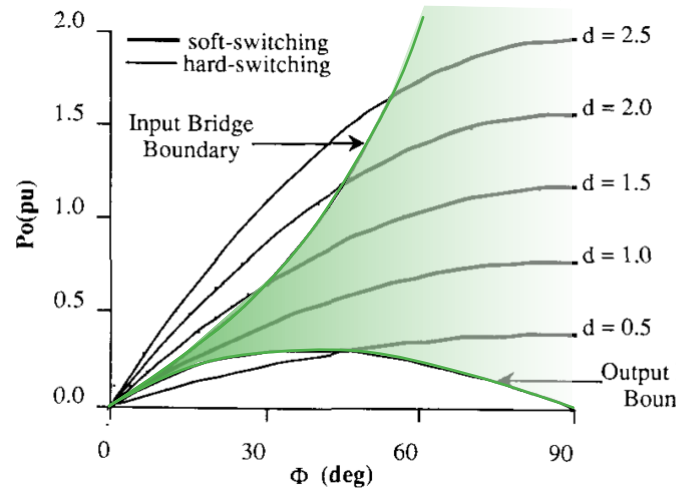


Three-Phase DAB

- Power Flow Control by **Phase Shift** between Primary & Secondary Voltage
- **Zero-Voltage Switching (ZVS) for All Transitions** (in a Certain Operating Range)



Soft-Switching Range



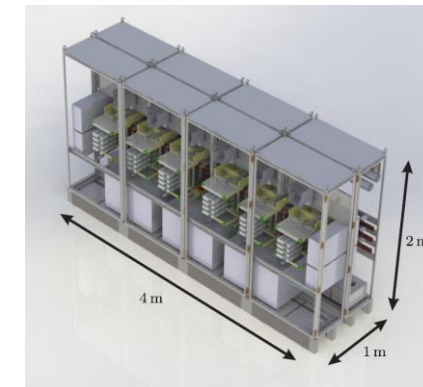
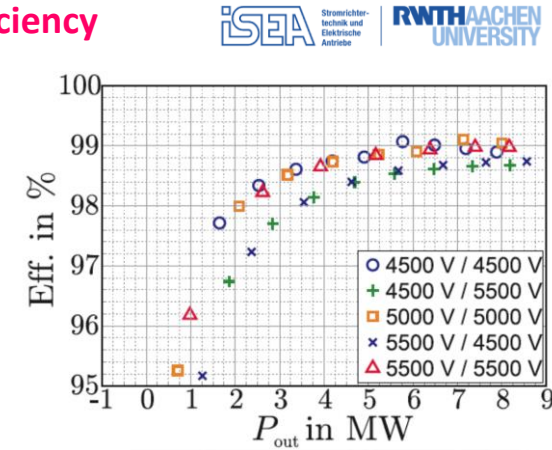
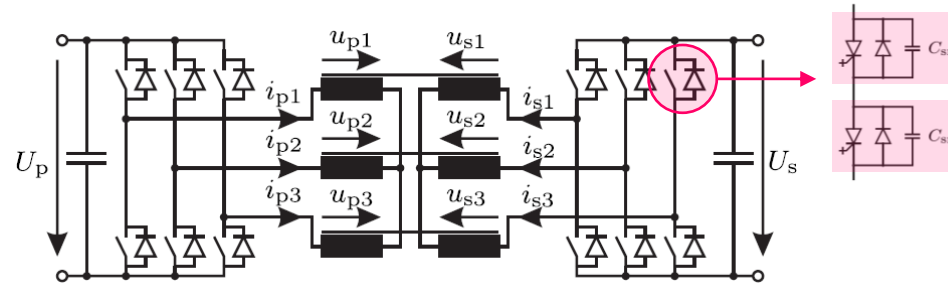
- Full-Range ZVS for $d = 1$ ($V_{in} = V_{out} N_{in}/N_{out}$), i.e., similar input/output voltages

Mode no.						Input Bridge	Output Bridge
1	2	3	4	5	6		
D1, T1	T1	T1	T1	T1	T1	Input Bridge	Output Bridge
T4	T4	T4	T4	D3, T3	T3		
T5	T5	D6, T6	T6	T6	T6		
D2, T2	D1'	D1'	D1'	D1'	D1'	Output Bridge	Output Bridge
D4'	D4'	D4'	D4'	D4', T4'	D3'		
D5'	D5'	D5', T5'	D6'	D6'	D6'		



Example: 7 MW / 5 kV Three-Phase DAB

- 7 MW Power Transfer, 5 kV ± 10% Input & Output Voltages, 99.2 % Pk. Efficiency
- Series-Connection of 2 x 4.5 kV IGCTs / Three MFTs Operating at 1 kHz



- Power Density 0.9 kW/dm³ (14.3 W/in³) with Optimized Arrangement



DC Transformer (DCX)

A Method of Resonant Current Pulse Modulation for Power Converters



FRANCISC C. SCHWARZ, SENIOR MEMBER, IEEE

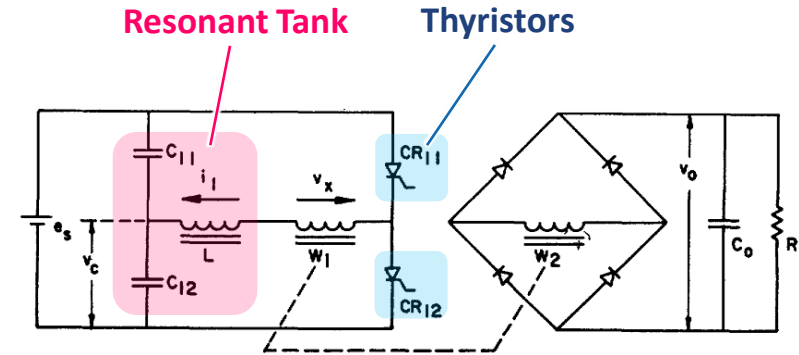
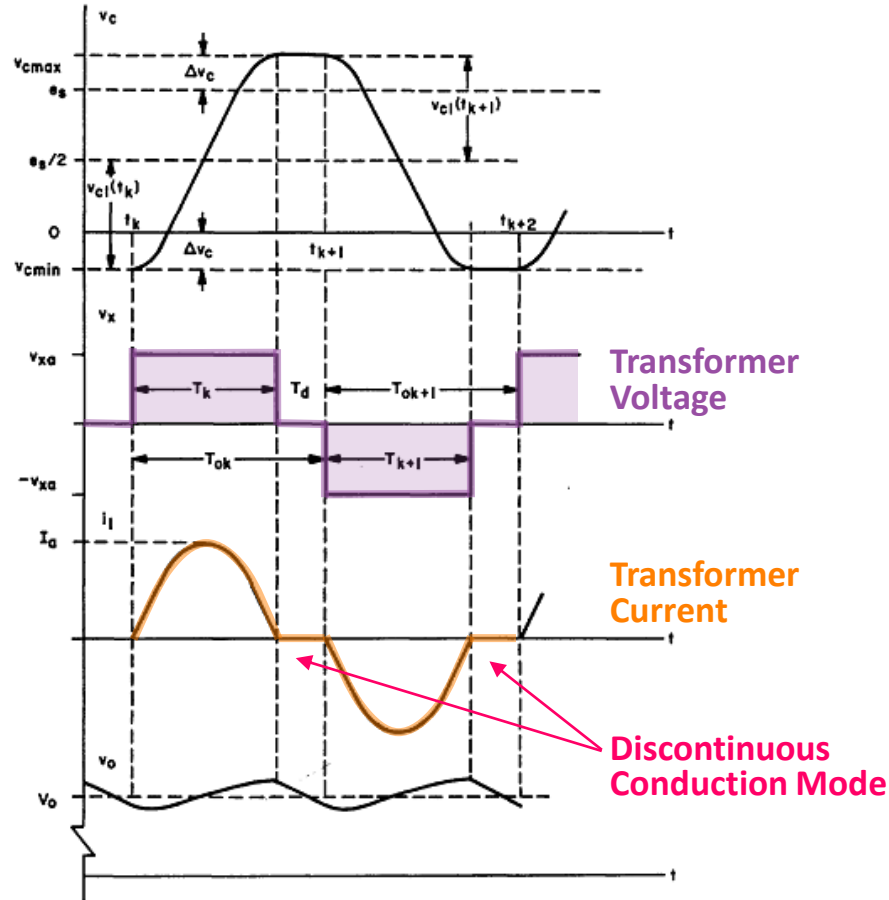


Fig. 4. Alternative simplified schematic of a controllable and load-insensitive series capacitor dc converter with transfer of inductive energy to the load.

“... load-insensitive series capacitor dc converter ...”



Remark: "Electronic Transformer"

United States Patent Office

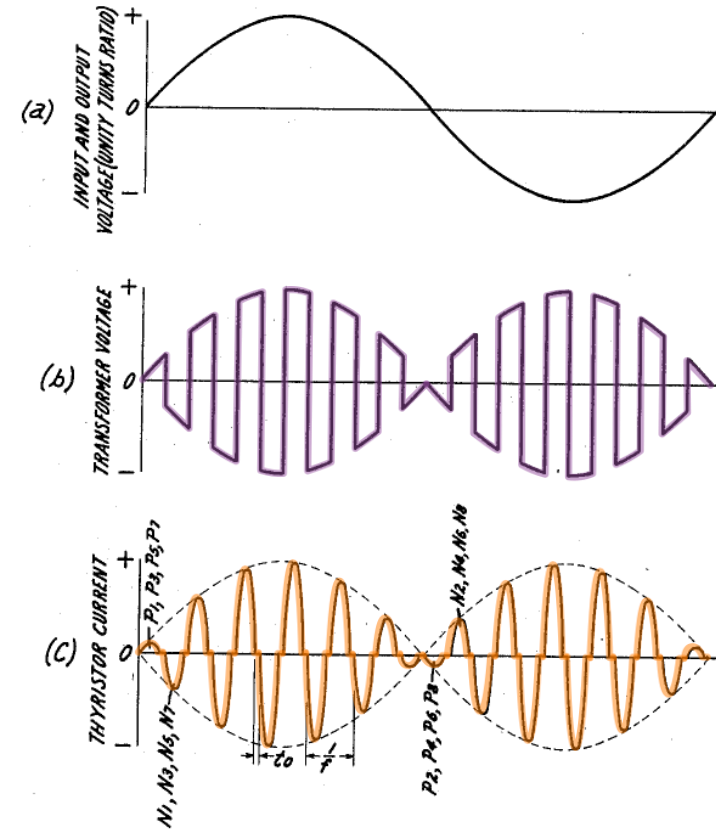
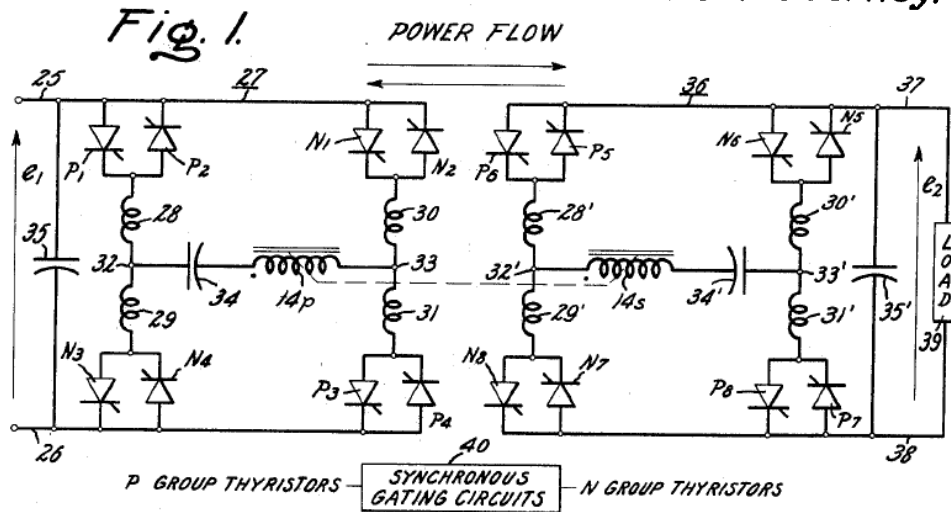
3,487,289
Patented Dec. 30 1969

1969

AC-AC Electronic Transformer

- Resonant Tank with Series Capacitor
- Current Zero Crossing Facilitates Thyristor Turn-Off

Inventor:
William McMurray,
by Donald L. Campbell
His Attorney.



"Initial Use May be Found in Special Applications where Cost and Efficiency are Secondary to Size and Weight."

- W. McMurray, 1971

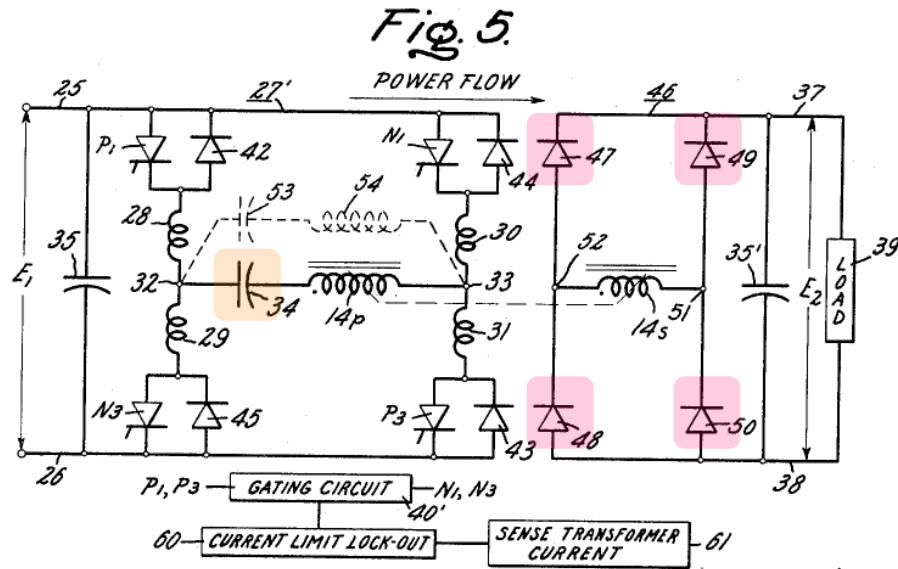


“Electronic DC Transformer”

■ DC-DC Electronic Transformer

- Resonant Tank with Series Capacitor
- Current Zero Crossing Facilitates Thyristor Turn-Off

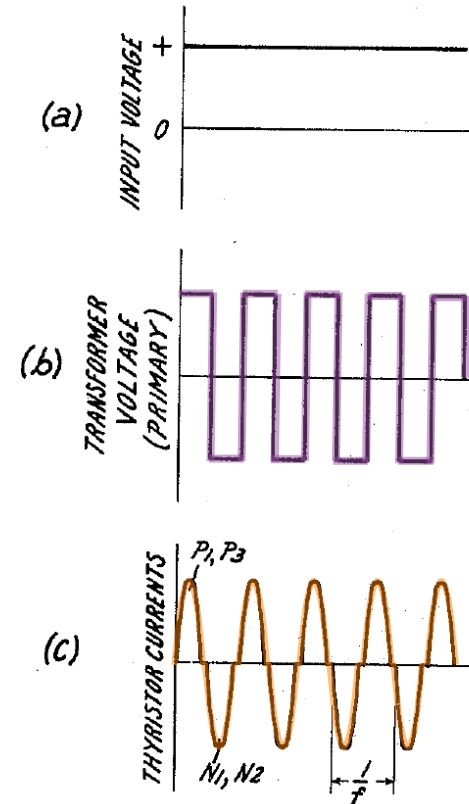
Inventor:
 William McMurray,
 by Ronald L. Campbell
 His Attorney.



United States Patent Office

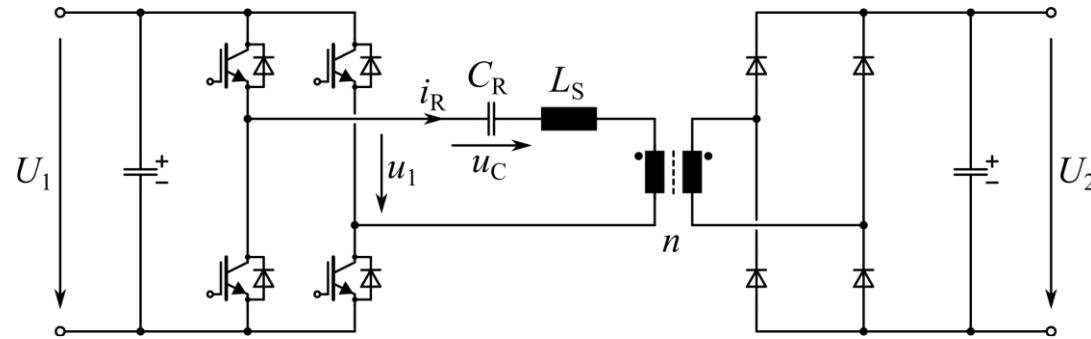
3,487,289
 Patented Dec. 30 1969

1969

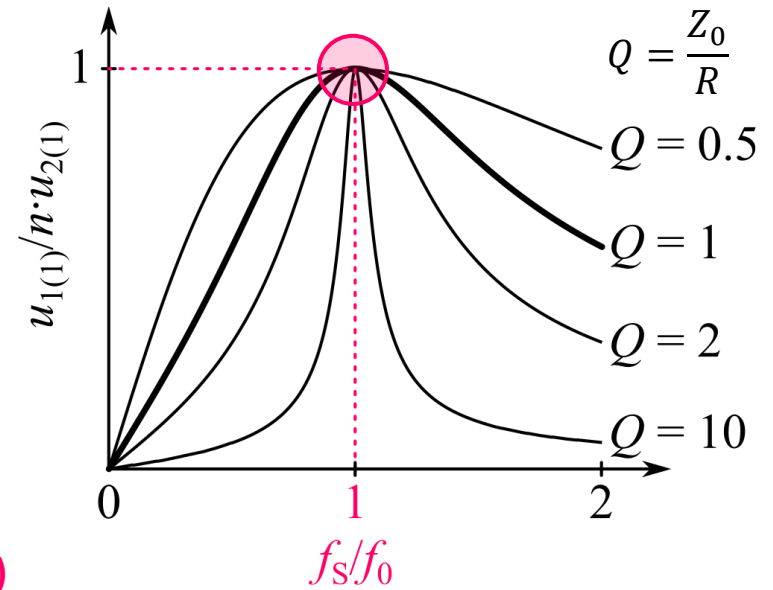
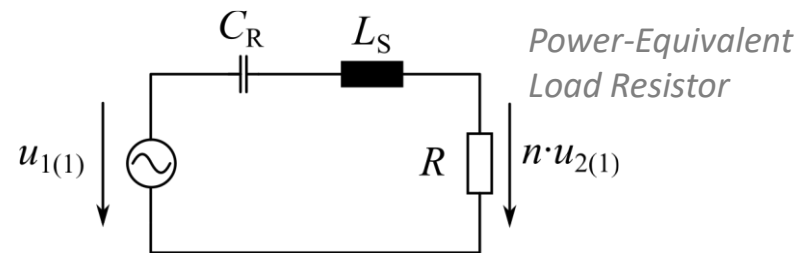


DCX Operating Principle

- Resonance Frequency \approx Switching Frequency \rightarrow Unity Gain



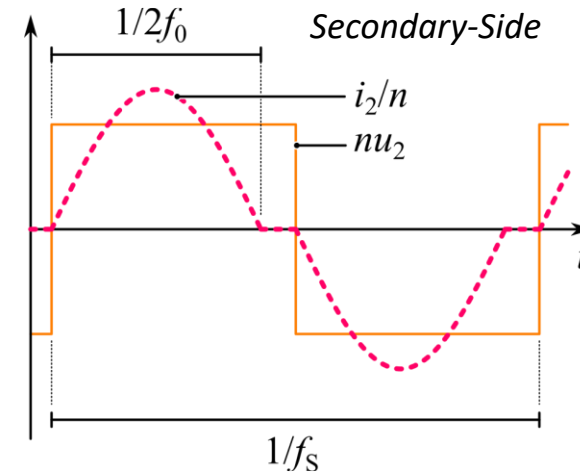
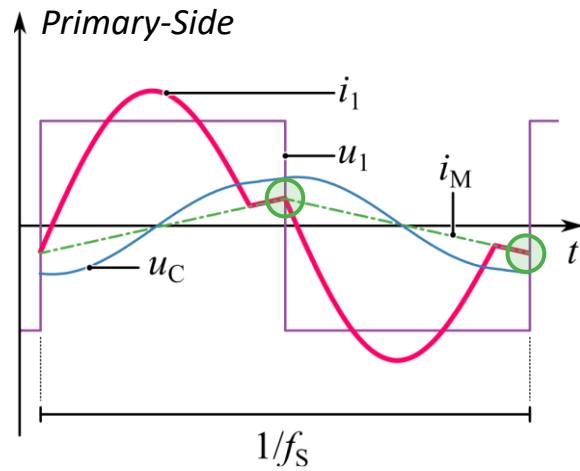
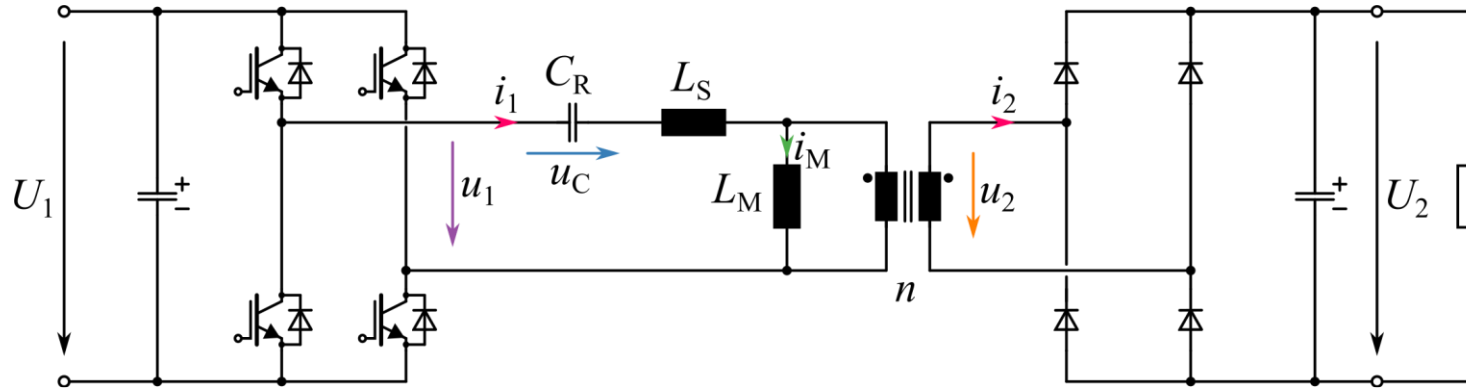
First-Harmonic Equivalent Circuit



- Fixed Voltage Transfer Ratio / Independent of Transferred Power (!)



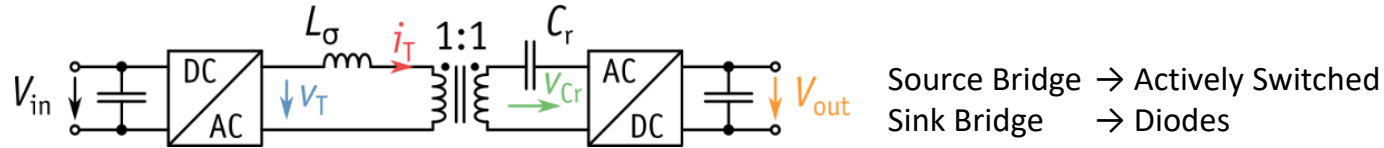
DCX Key Waveforms



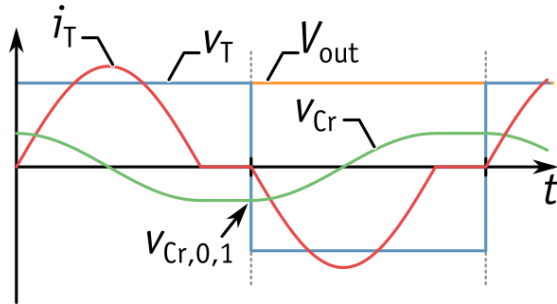
- Magnetizing Current Enables Load-Independent Zero-Voltage Switching / DoF for Optimization (see Later)



DCX “DC Transformer Behavior” Explained

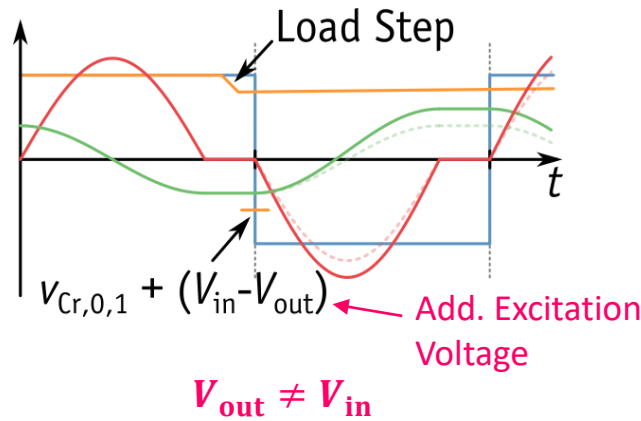


Steady State 1 ($P = P_0$)

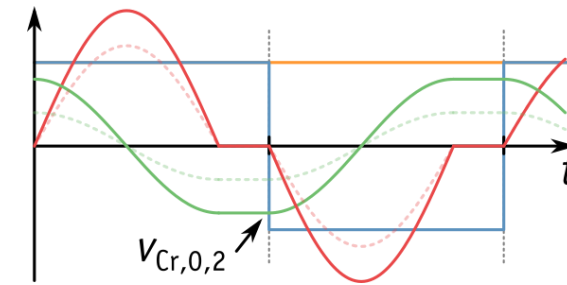


$$\hat{i}_{T,1} = \frac{\hat{v}_{Cr,0,1}}{Z_0} \quad V_{out} = V_{in}$$

Disturbance



Steady State 2 ($P > P_0$)



$$\hat{i}_{T,2} = \frac{\hat{v}_{Cr,0,2}}{Z_0} \quad V_{out} = V_{in}$$

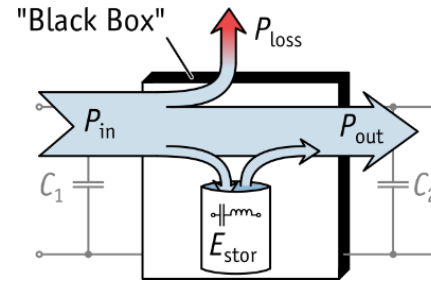
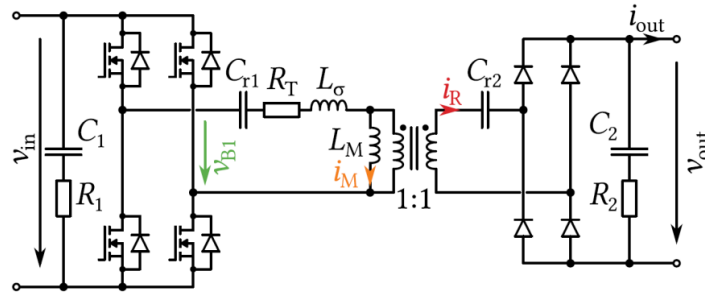
■ Tight Coupling of DC Input and Output Voltages

- Ideal: $V_{out} = V_{in}$ (Lossless Components)
- Real: $V_{out} \approx V_{in}$ (Voltage Drop Due to Losses)

■ No Control Possible/Required – Acts as “DC Transformer” (DCX) with Certain Dynamics!

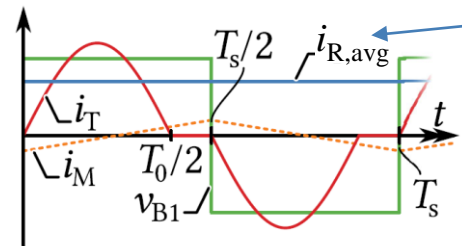


Dynamic Modeling of Terminal Behavior (1)

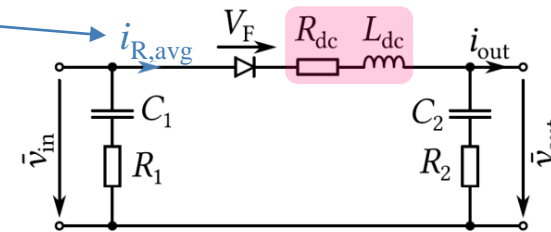


- Capture Load-Dependency of
- Losses
- Stored Energy

Dynamic Equivalent Circuit with Identical Terminal Behavior



Local Average Current



Generic Calculation of Equivalent Circuit Element Values (R_{dc} , L_{dc})

Equal RMS Losses:

$$i_{R,avg}^2 R_{dc} = i_{R,rms}^2 R_{total} \quad R_{dc} = \frac{i_{R,rms}^2}{i_{R,avg}^2} R_{total} = \beta^2 R_{total}$$

Equal Stored Energy:

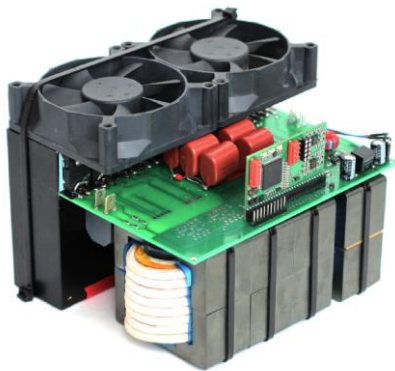
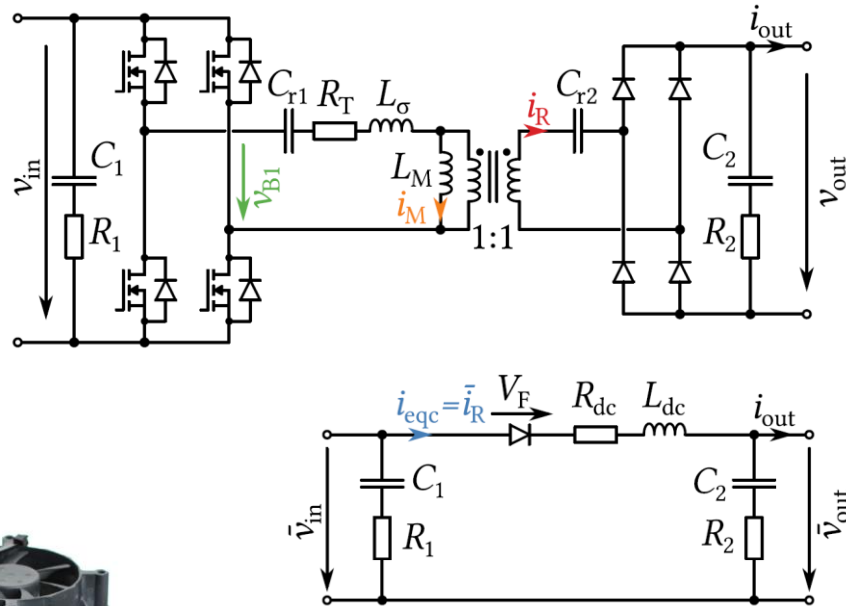
$$i_{R,avg}^2 L_{dc} = i_{R,pk}^2 L_{\sigma} \quad L_{dc} = \frac{i_{R,pk}^2}{i_{R,avg}^2} L_{\sigma} = \alpha^2 L_{\sigma}$$

- Parametrization from Actual Waveforms (Calc., Sim., Meas.) – Not Exactly Sinusoidal (!)

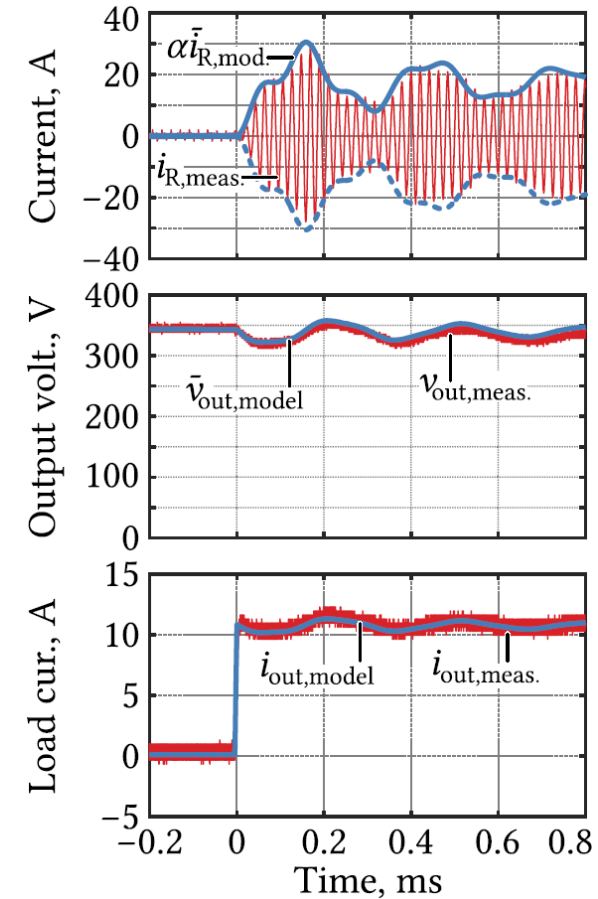


Dynamic Modeling of Terminal Behavior (2)

■ Experimental Verification w. Parametrization from Measured Steady-State Waveforms



10 kW
350 V (in/out)
50 kHz



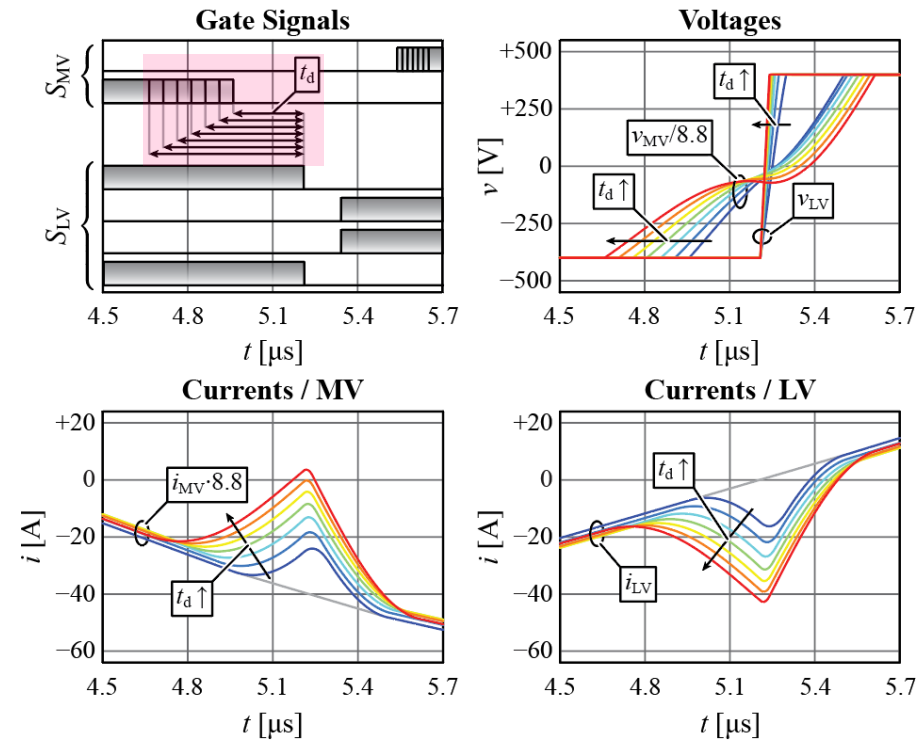
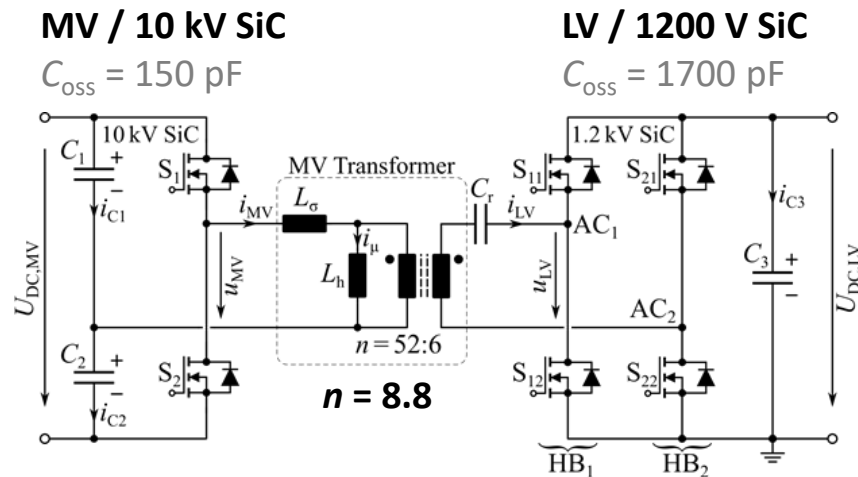
Active Magnetizing Current Splitting (1)

■ Ensure ZVS for Primary and Secondary Bridge (Synchronous Rectification)

- Critical for Very Asymmetric Semiconductor Output Capacitances (Referred to Same Side of Transf.)

■ New Method: Both Bridges are Actively Operated

- Very Small Phase Shift Between the Bridges
- Circulating Current Shifts the Magnetizing Current



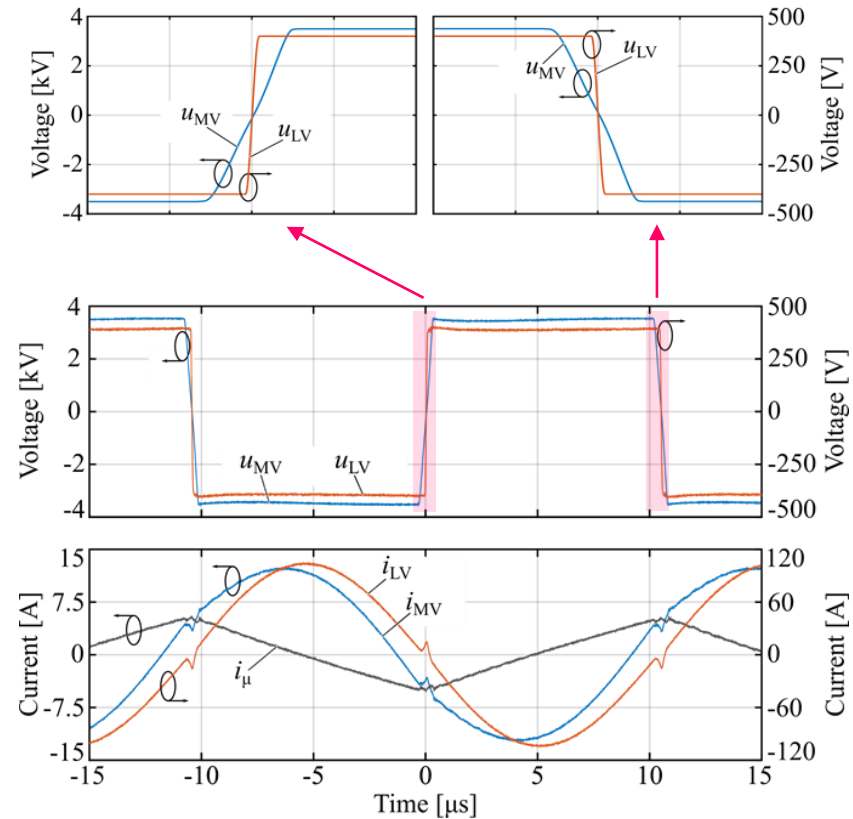
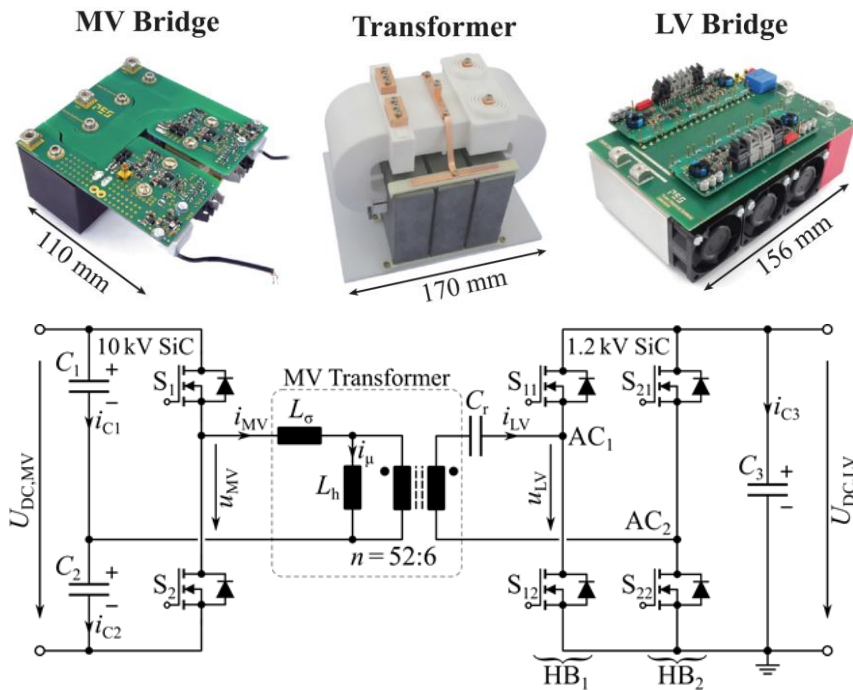
■ Control of the Switching Speed / No Closed-Loop Control Required / Extremely Robust



Active Magnetizing Current Splitting (2)

Experimental Results

- 400 V → 7 kV Operation @ 25 kW / 48 kHz



- ZVS of All MOSFETs Independent of Load

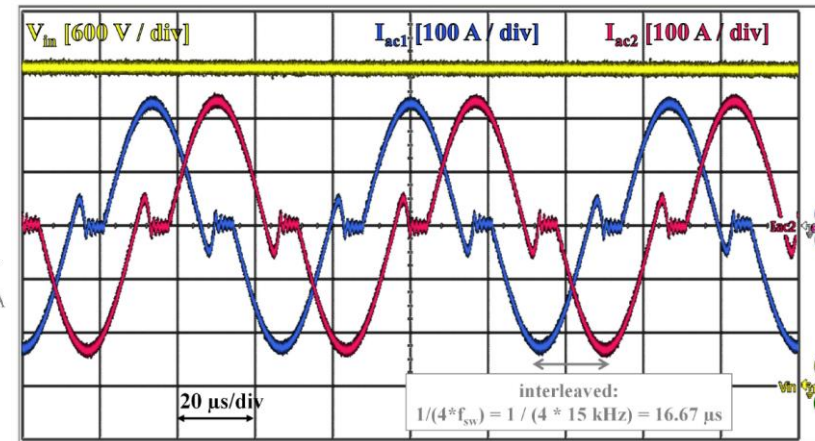
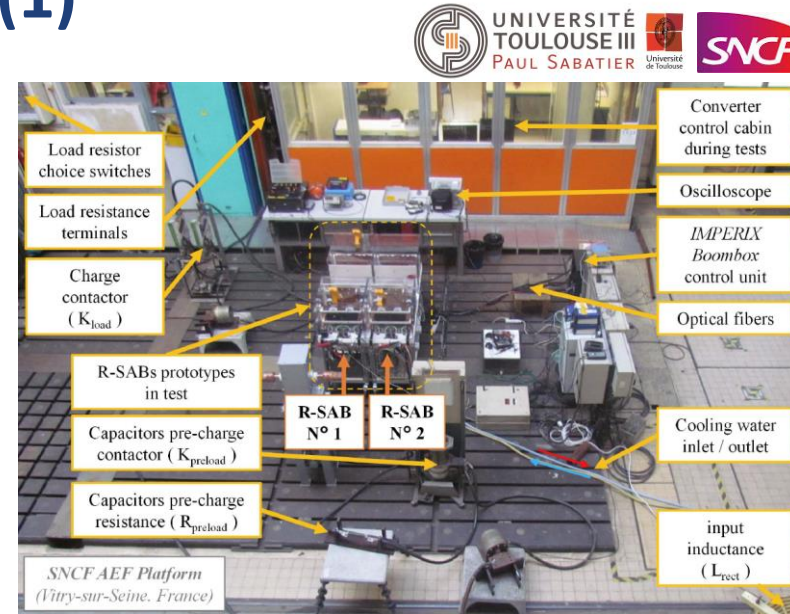
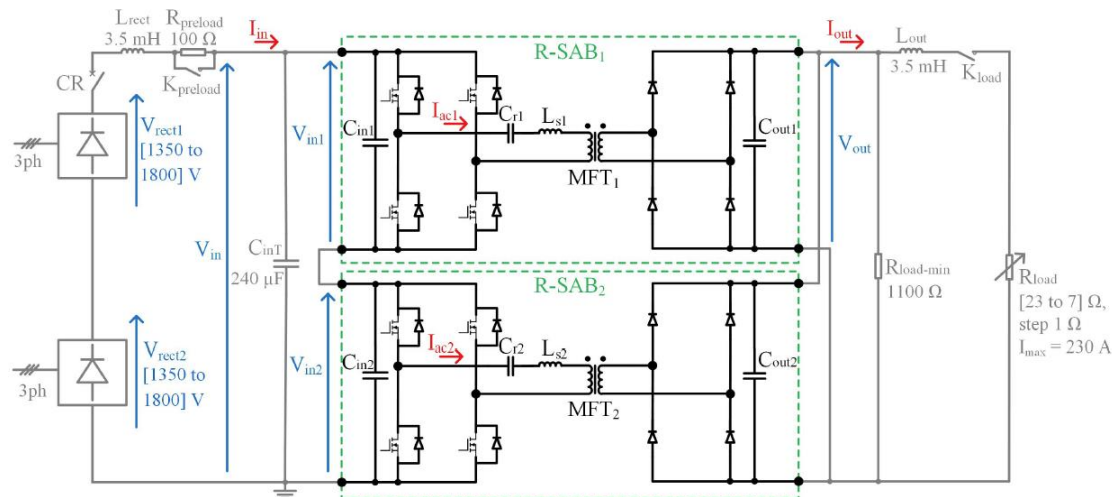
- Load-Independent Voltage Transfer Ratio (< 0.8% Deviation) / 99% DC-DC Efficiency



Example: DC Traction DCX System (1)

- 300 kW DCX Modules / 1.8 kV to 1.8 kV
- 3.3 kV SiC / 15 kHz MFT / 99% Peak Efficiency

- Input-Series Output-Parallel Arrangement of Two DCXs
- Two-Cell ISOP: 3 kV to 1.5 kV DC @ 600 kW
- Natural Input Volt. Balancing & Output Cur. Sharing
- Interleaving Reduced Output Voltage Ripple

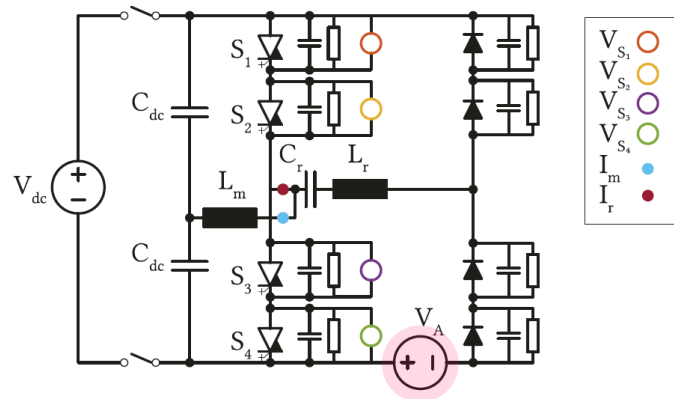


Example: IGCT-Based DCX System (2)

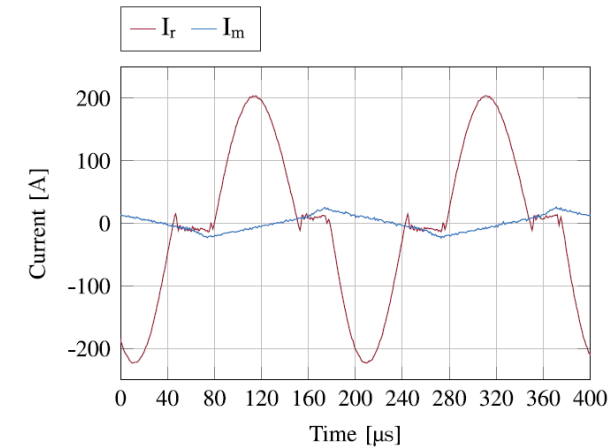
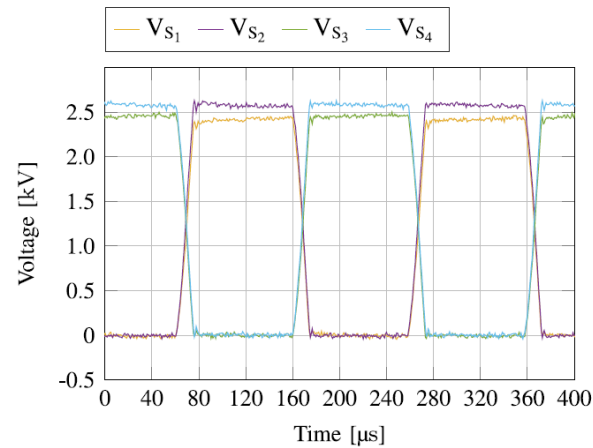
- **Series-Connected 4.5 kV, 68 mm RC-IGCTs** (Reverse-Conducting IGCTs)
- Custom Gate Unit Optimized for ZVS Operation
- Back-to-Back Test @ **5 kV DC** and **500 kW**



SRC Test Bench



Series Voltage to Adjust Power Flow



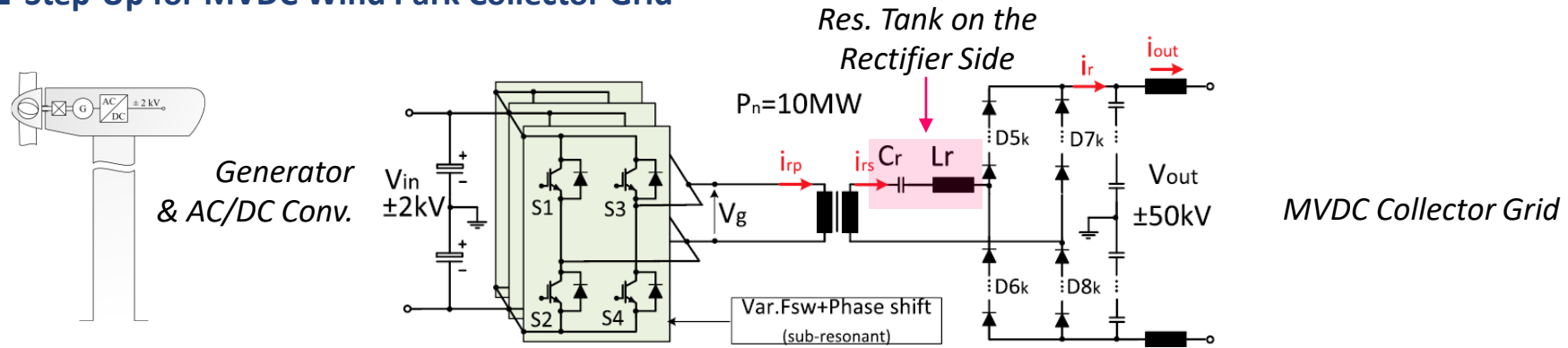
- $f_s = 5 \text{ kHz}$, $f_{res} = 7.4 \text{ kHz} \rightarrow 20 \mu\text{s}$ Dead Time to Ensure IGCT ZVS



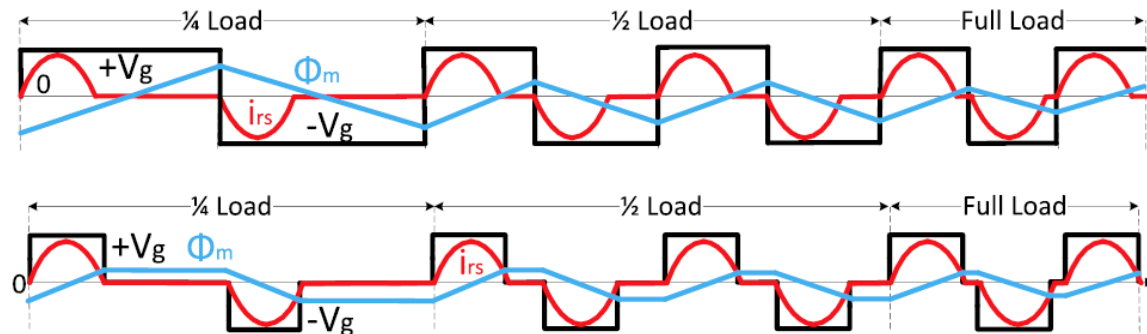
Remark: DCX Power Flow Control

Step-Up for MVDC Wind Park Collector Grid

Vestas



Power Flow Control via Pulse Removal Technique



Frequency Variation Only

Peak Core flux Defined by Lowest Frequency

Frequency & Duty-Cycle

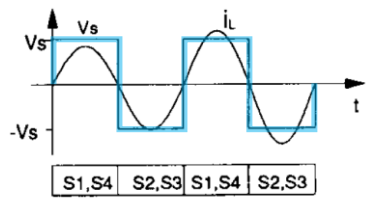
Peak Core Flux Defined by Nominal Frequency

- High Efficiency for $V_{in} \approx nV_{out}$ (Otherwise: High Peak/RMS Currents w.r.t. Average Current/Power)

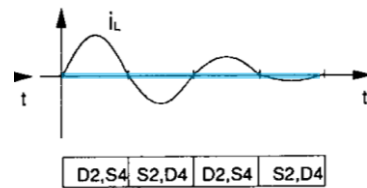


Remark: DCX Quantum Operation

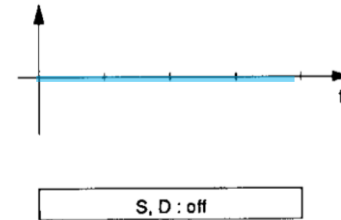
- Output Voltage Control by **Combining Different Operating Modes**
- Mode Transition Only at Current Zero Crossing → **ZCS/ZVS** and **Constant Operating Frequency**



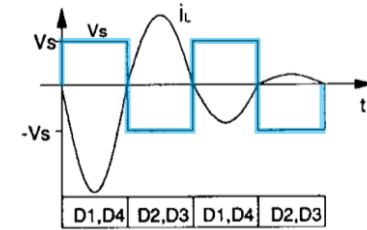
Powering Mode



Free Resonant Mode

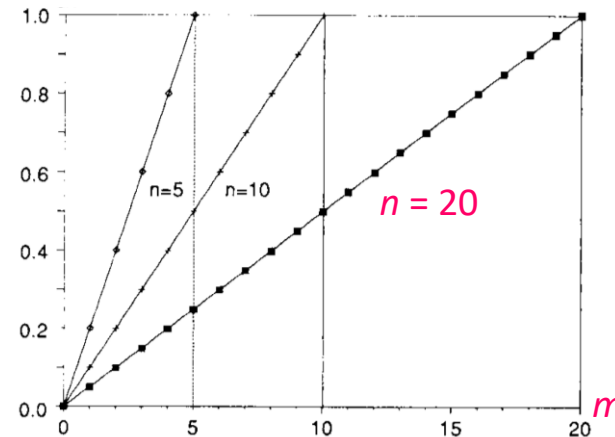
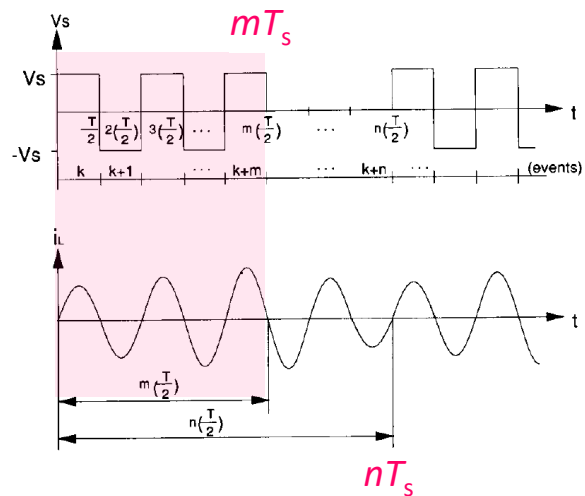


Discontinuous Mode
(Occurs Naturally)



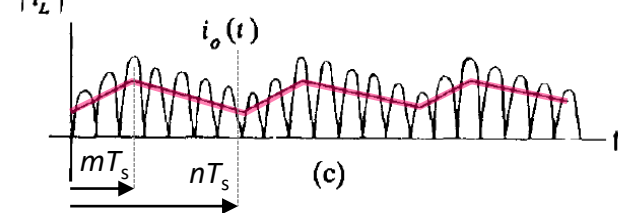
Regeneration Mode
(Low Inp. Power Fact.)

- Powering Mode for **m out of n Cycles** → **Discrete DC Voltage Transfer Ratios**



Rectified Current

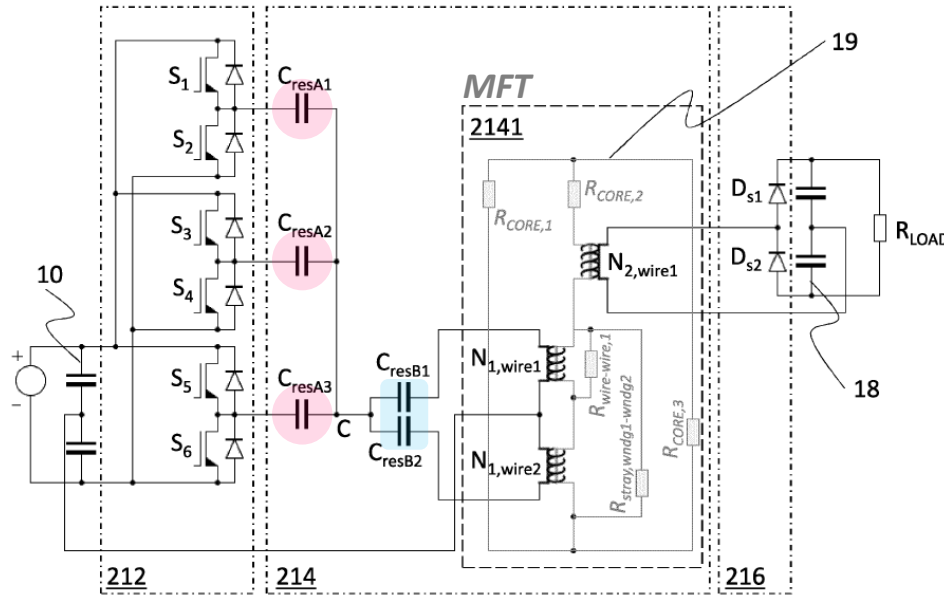
→ **Buck Converter Behavior!**



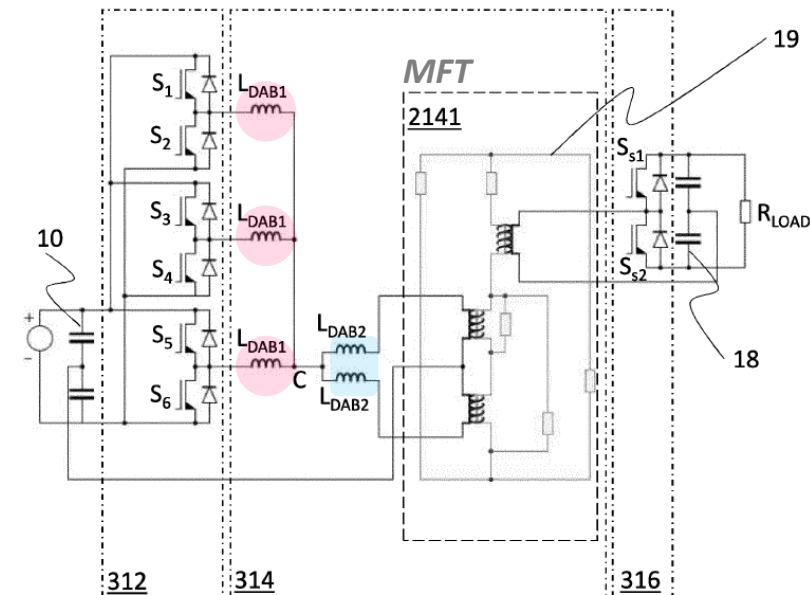
Remark: Paralleling of Bridge-Legs

- Split Series Impedances (Resonant Capacitors or Series Inductors)

DCX / Resonant Topologies



Dual Active Bridges

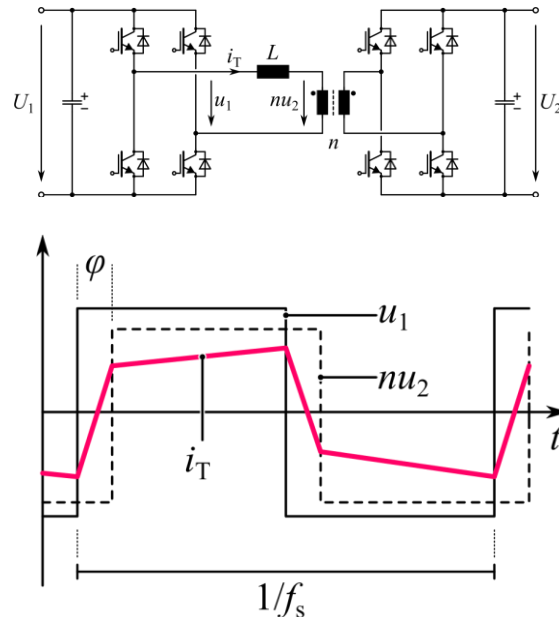


- Ensures Equal Current Sharing Among Bridge-Legs
- Prevents Circulating Currents in Parallel Transformer Windings



Summary: MF Power Conversion for SSTs

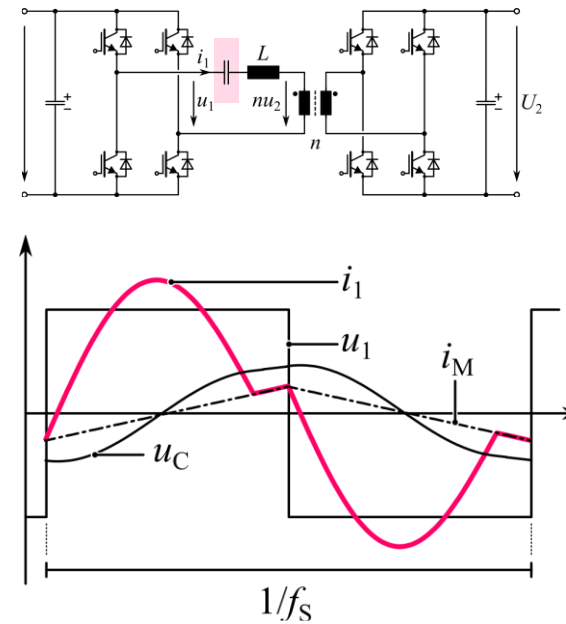
Dual Active Bridge



■ Can (Must!) Be Fully Controlled

- Fully Controllable Power Flows
- Lower RMS Currents for $U_1 \approx nU_2$

DC Transformer ("DCX")



■ Control Not Needed (Not Directly Possible!)

- Reduces Complexity in Multi-Cell Syst. (e.g., Natural MV-Side Volt. Balancing)
- Predominant Solution in Multi-Cell SSTs



Part II

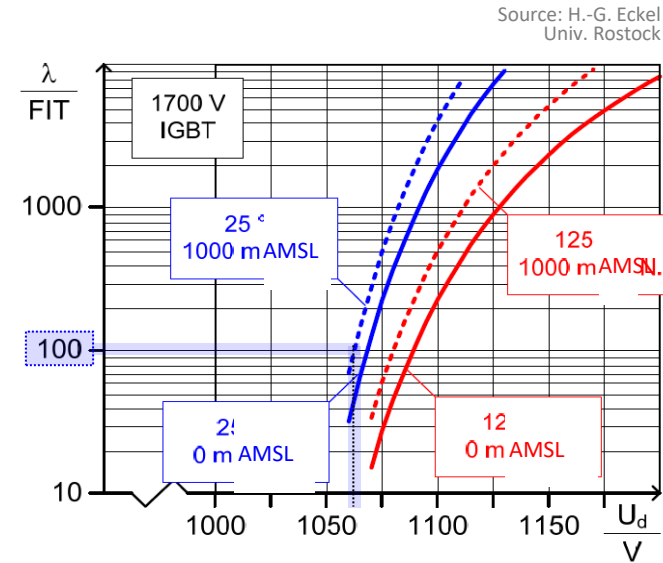
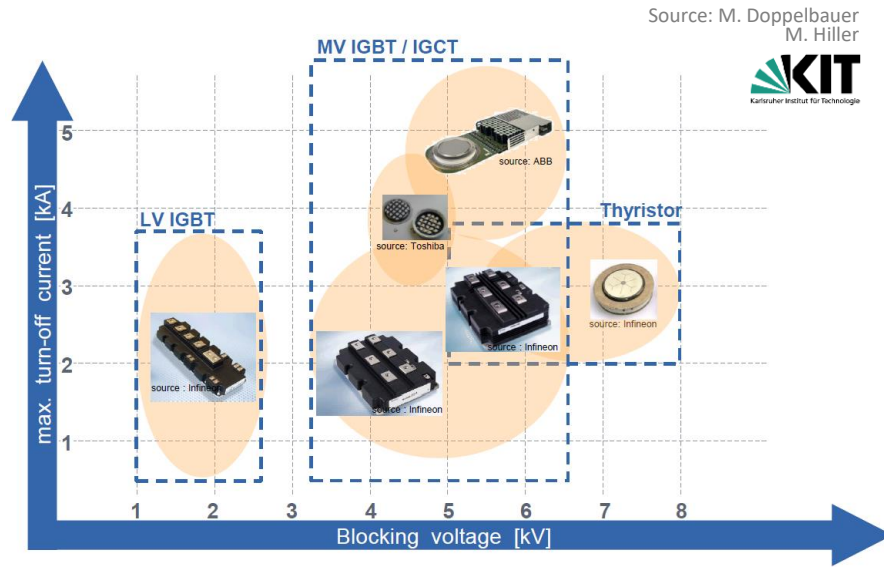
SST Concepts & Key Design Aspects

- Medium-Frequency Power Conversion
- **Power Semiconductors**
- Key SST Topologies
- Medium-Frequency Transformers
- Isolation Coordination
- Protection
- Reliability
- Standardization & EMC
- Construction & Testing



Available Si Power Semiconductors

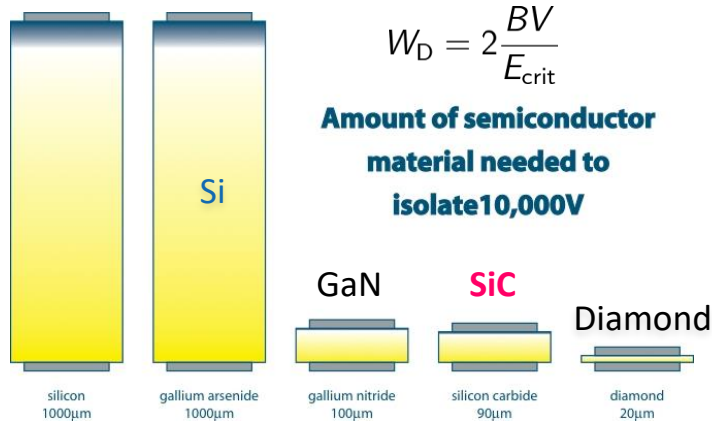
- 1200 V & 1700 V Si IGBTs Most Frequently Used in Industry Applications / Max. 6.5 kV Available
- Derating Requirement due to Cosmic Radiation: **1700 V Si IGBTs** → **ca. 1000 V max. DC Voltage**



- Interfacing to Medium Voltage → Series Connections or Multi-Level Converter Topologies



Si vs. SiC Power Semiconductors (1)



Img.: <http://www.evincetechnology.com/whydiamond.html>

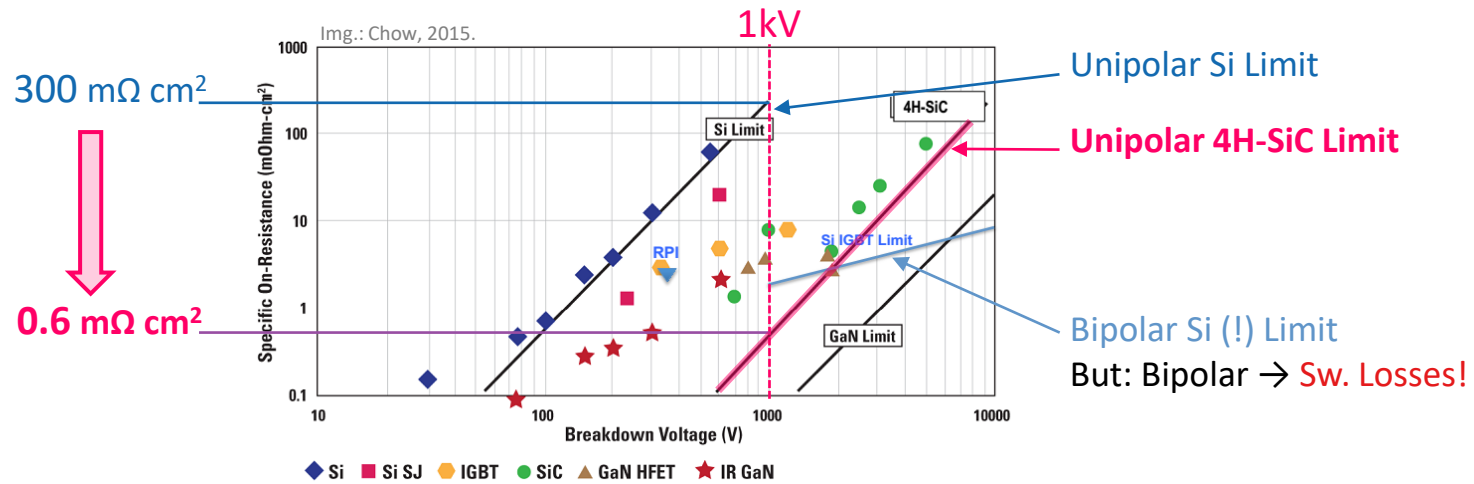
- Specific On-State Resistance

$$R_{on,sp} = \frac{4BV^2}{\epsilon\mu_n E_C^3}$$

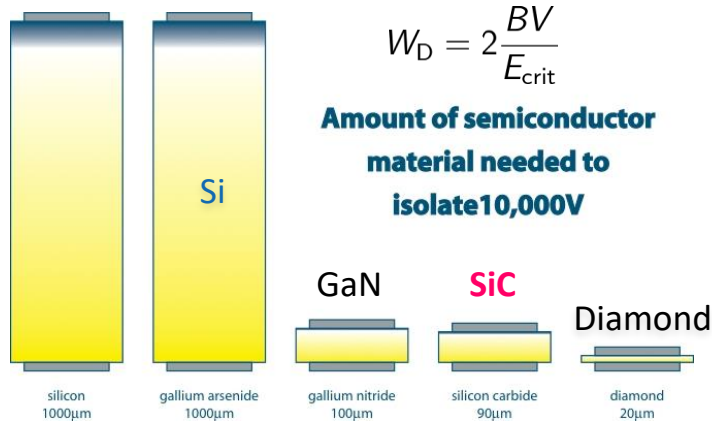
Blocking Voltage
Critical Electric Field

- E_C in SiC ca. 9 x Larger Than in Si

■ Lower $R_{on,sp}$ for Given Blocking Voltage



Si vs. SiC Power Semiconductors (2)



Img.: <http://www.evincetechnology.com/whydiamond.html>

- Specific On-State Resistance

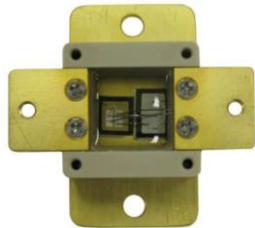
$$R_{on,sp} = \frac{4BV^2}{\epsilon\mu_n E_C^3}$$

Blocking Voltage
Critical Electric Field

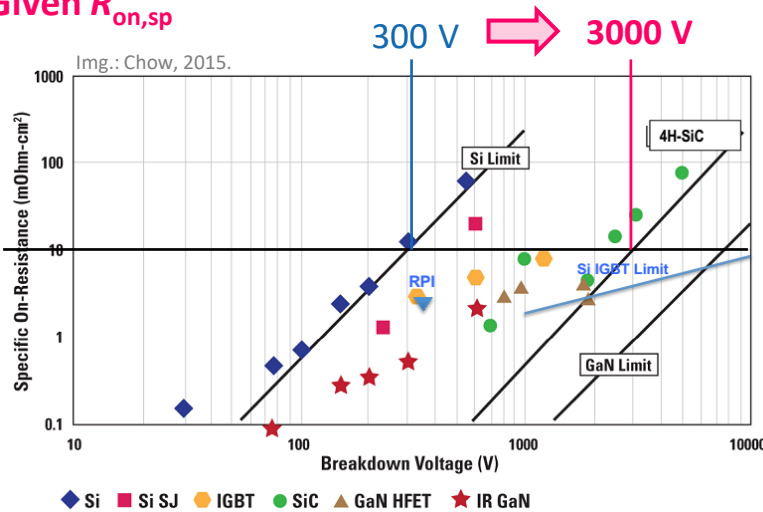
- E_C in SiC ca. 9 x Larger Than in Si

Higher Blocking Voltage for Given $R_{on,sp}$

10 kV SiC MOSFET (Wolfspeed)



10 mΩ cm²

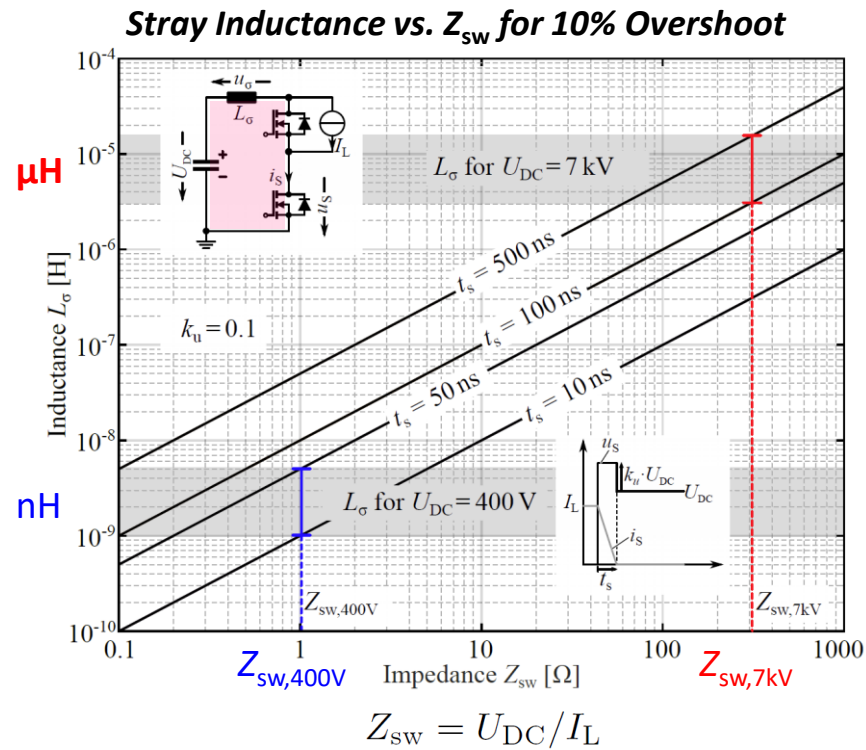


15 kV, 80 A Package (Wolfspeed)

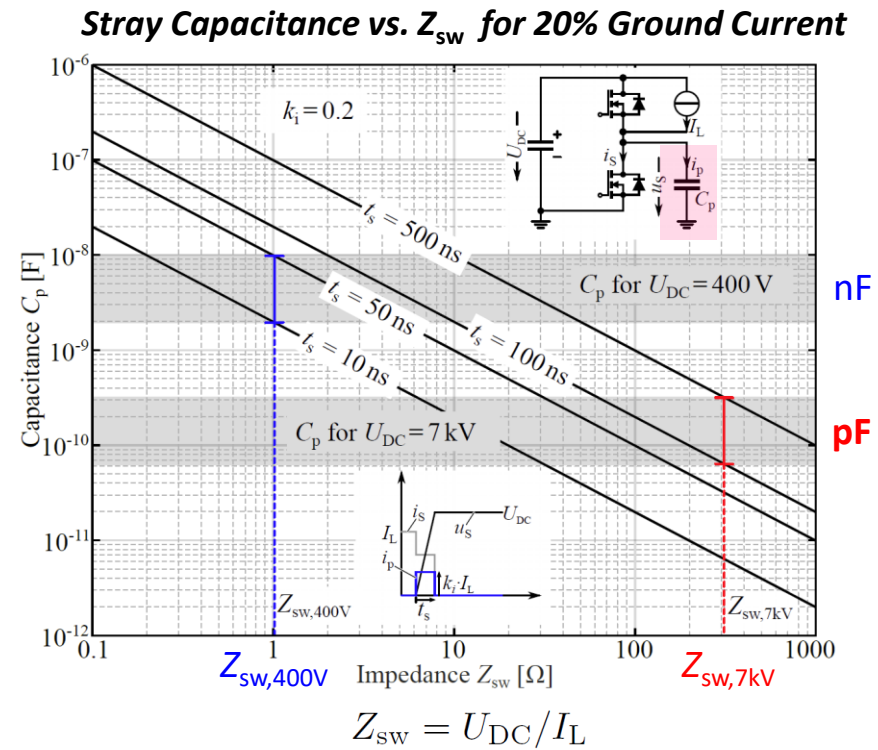


Remark: HV SiC Parasitics

- High di/dt + Stray Inductance → Overvoltages
- High dv/dt + Parasitic Capacitance → Ground Currents
- Exemplary Analysis for a 25 kW, 7 kV to 400 V System



■ LV Devices: Minimize Stray Inductance



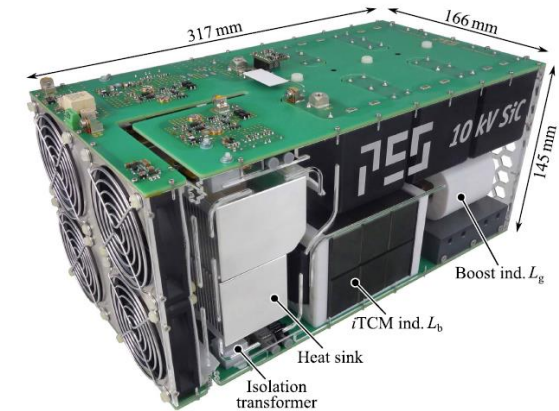
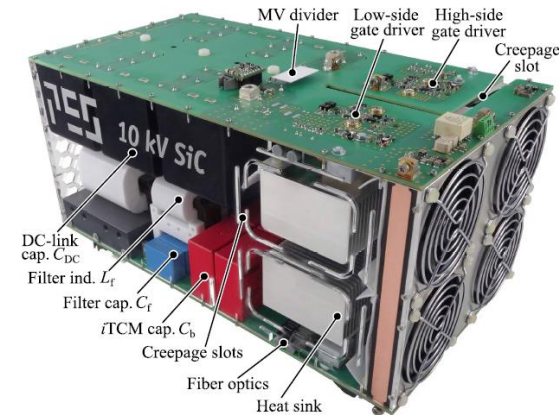
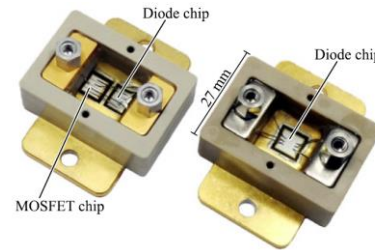
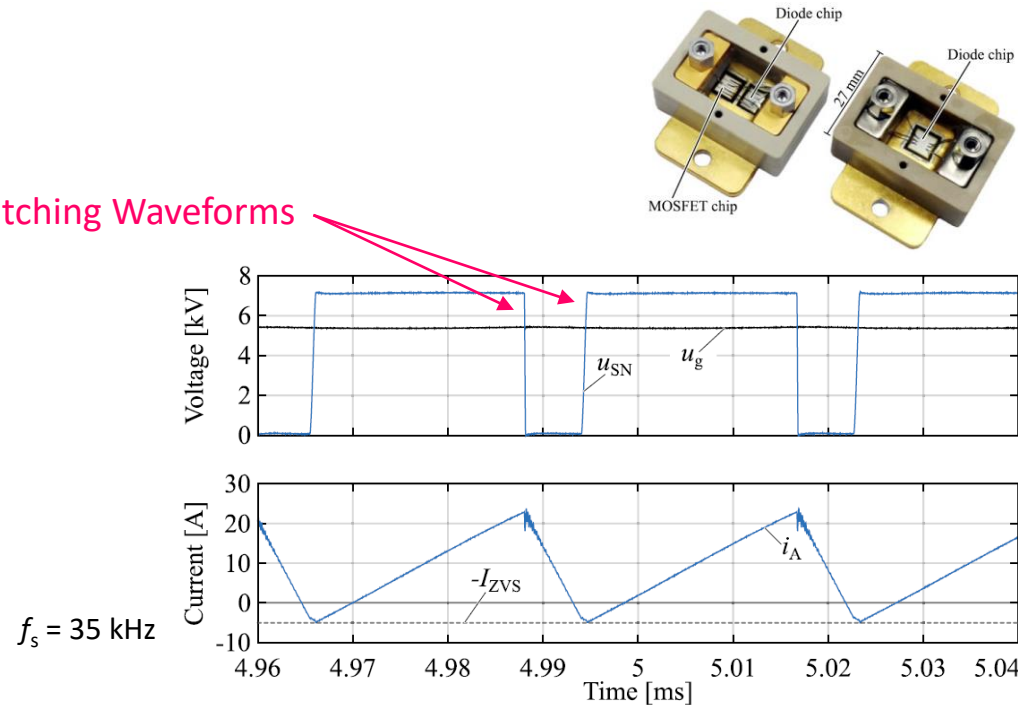
■ HV Devices: Minimize Stray Capacitance



Example: 10 kV SiC AC-DC Converter

- 25 kW / 7 kV DC / iTCM Soft-Switching AC-DC Topology
- 99.1% Efficiency at Rated Load / 3.3 kW/dm³ (54 W/in³) Power Density

Clean 7 kV Switching Waveforms



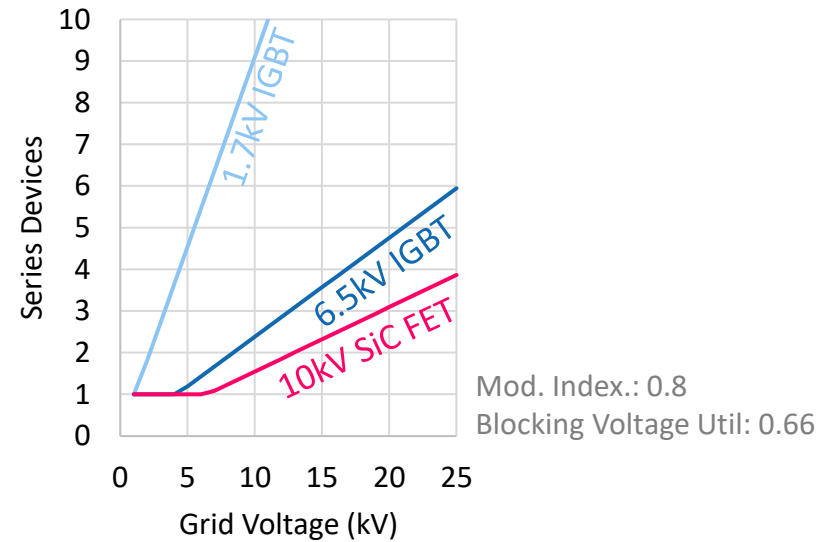
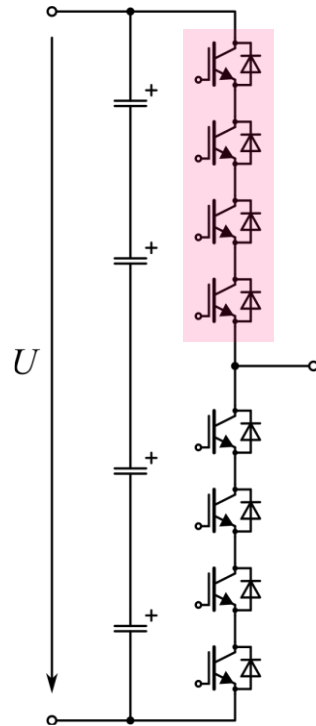
- Converter Systems with 10 kV SiC MOSFETs Can Be Realized (See Also Further Examples Later)



Interfacing to Medium Voltage (1): Direct Series Connection

■ Limited Blocking Voltages of Available Semiconductors & **Max. Utilization Only ca. 50...70%**

- 6.5 kV for Si IGBTs
- 10...15 kV for SiC FETs (Prototype Devices Only)

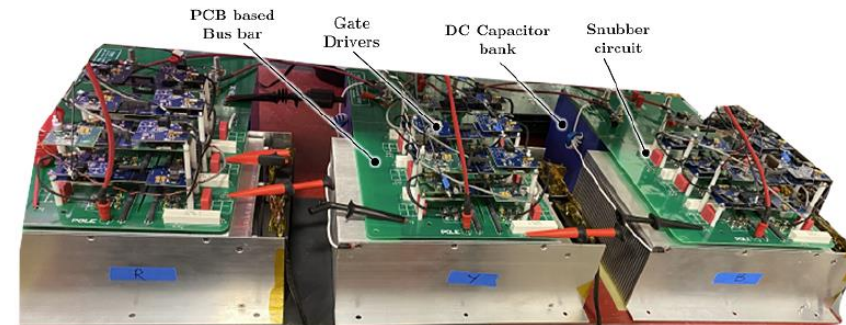
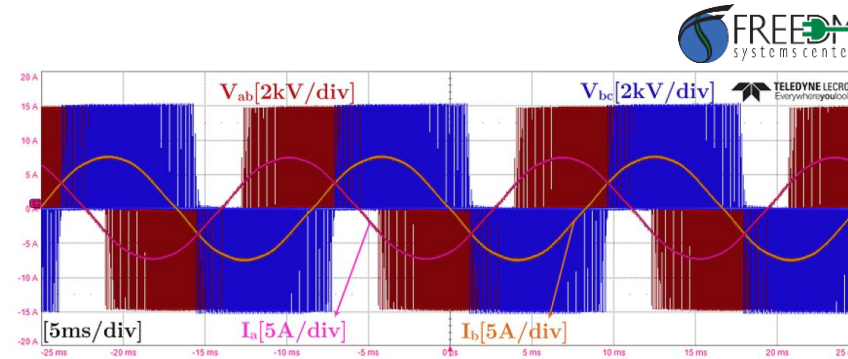
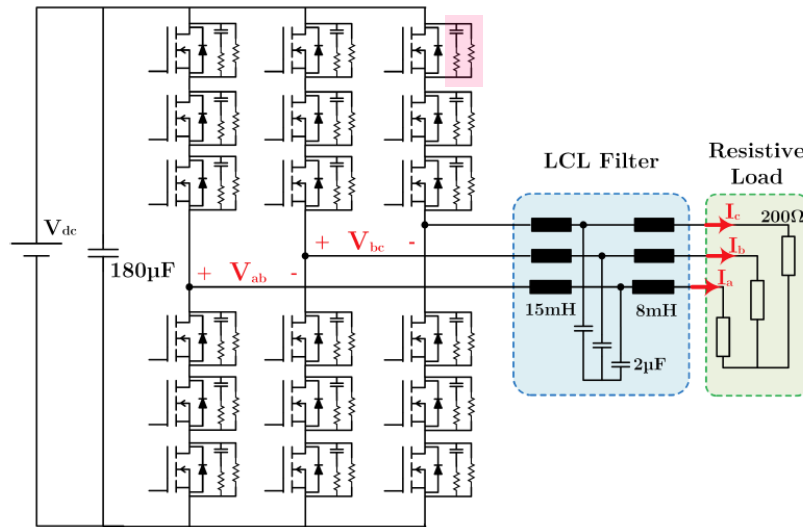


■ Key Challenge: **Static & Dynamic (!) Voltage Sharing**



Example: Direct Series Connection

- 100 kW, 7.2 kV DC Three-Phase Inverter
- Direct Series Connection of 3 x 3.3 kV SiC MOSFETs



- Steady-State Balancing with Parallel Resistors
- Dynamic balancing with RC Snubber

- Advanced Balancing Approaches (e.g., Active Gate Signal Delay Control, ...)

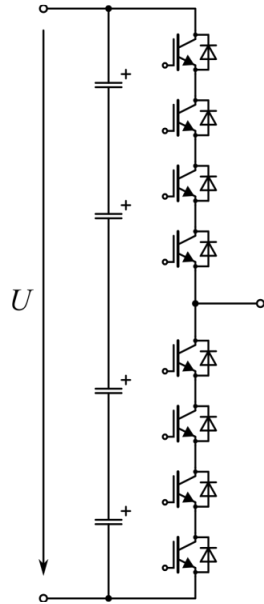
[Lin2022]



Interfacing to MV (2): Multilevel & Multicell Topologies

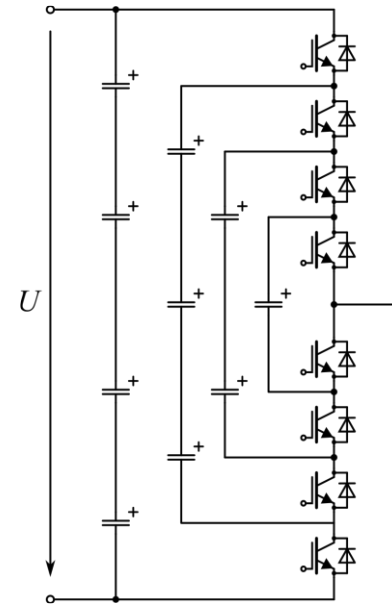
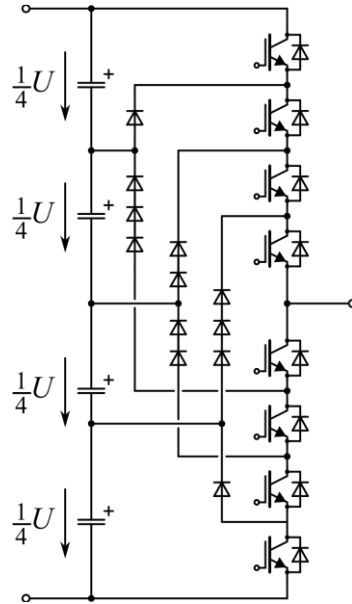
Neutral Point Clamped (NPC)

Baker (1979, Pat. Filed)
Nabae et al. (1981)



Flying-Capacitor Converter (FCC)

Meynard et al. (1992)

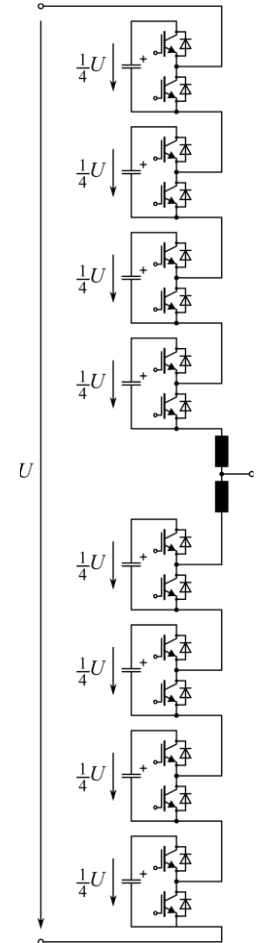
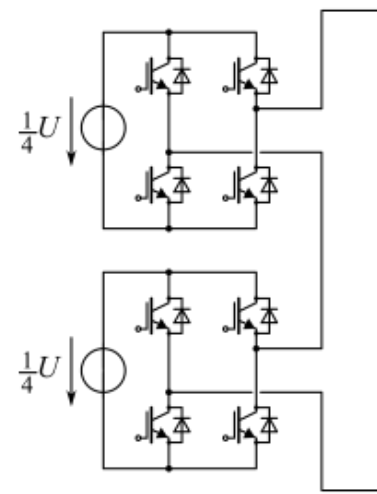


MMC

Marquardt et al. (2002)
See also Baker et al. (1974)

Cascaded H-Bridge

McMurray (1969)



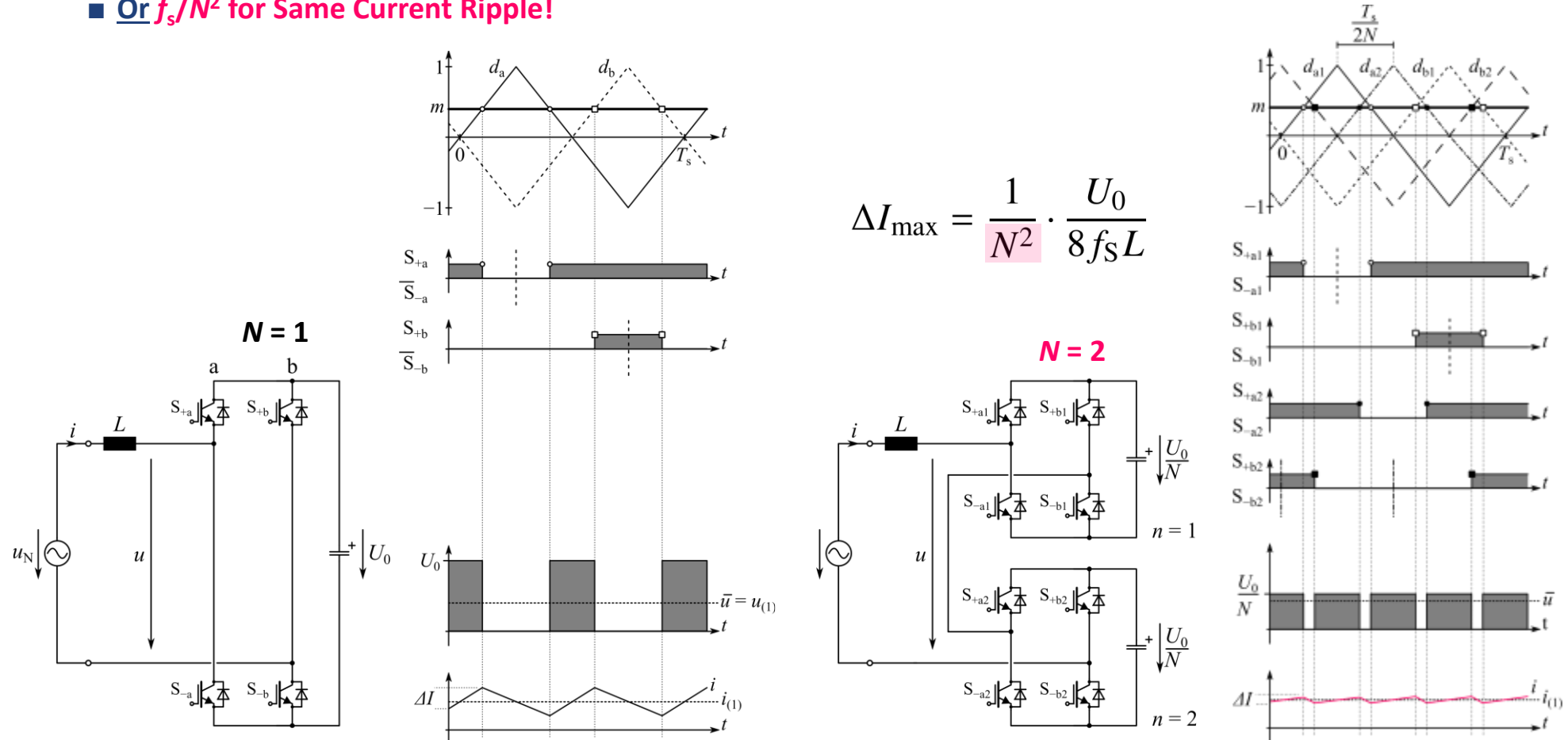
Non-Modular Modular

- Defined Partitioning of Blocking Voltage & Improved Device FoMs for Lower Voltages
- Modular: High Number N of Cells \rightarrow Quadratically Reduces Current Harmonics



Multi-Cell Concept: Interleaving (1)

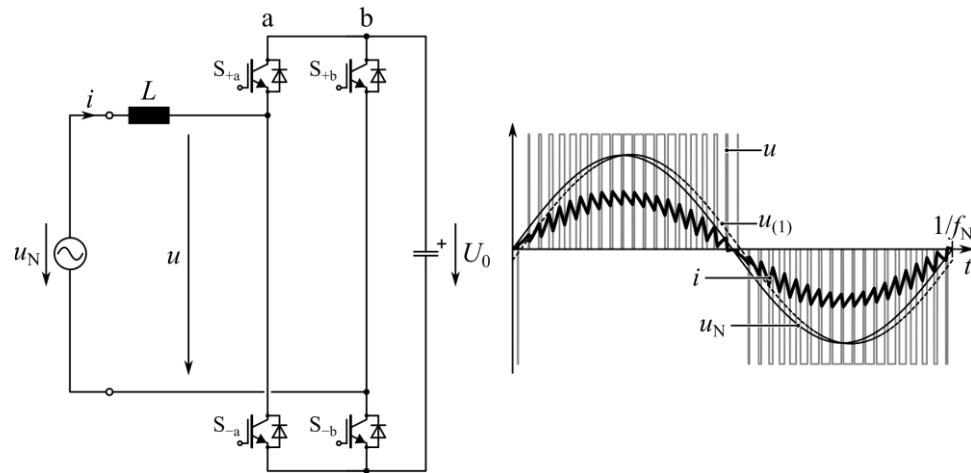
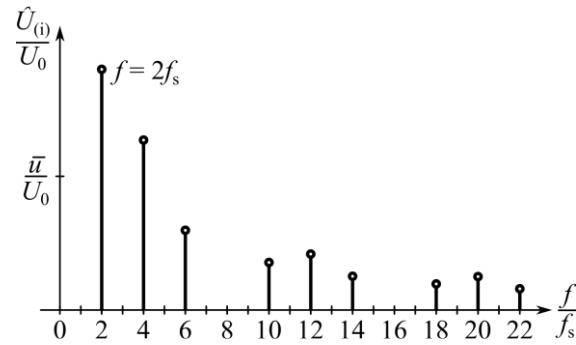
- Example $N = 1 \rightarrow N = 2$: Effective Sw. Frequency $\times 2$ and Voltage Step $\times 0.5 \rightarrow 0.25 \times \Delta I$
- Or f_s/N^2 for Same Current Ripple!



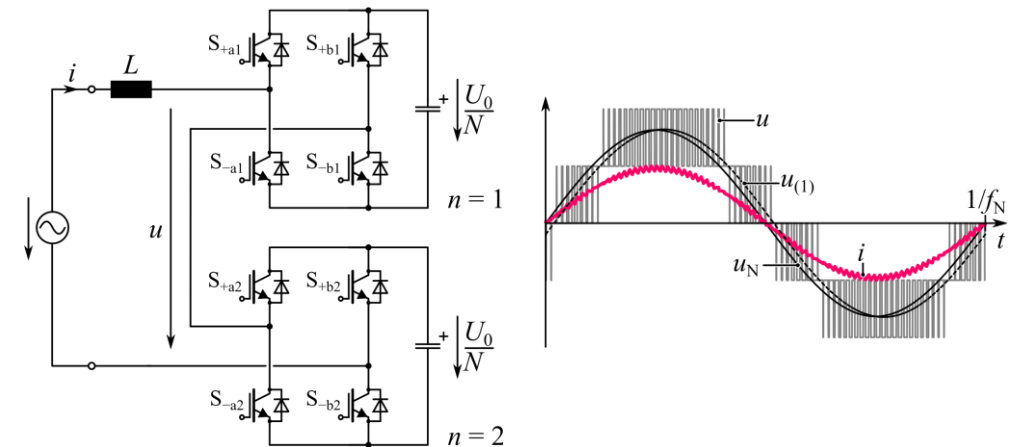
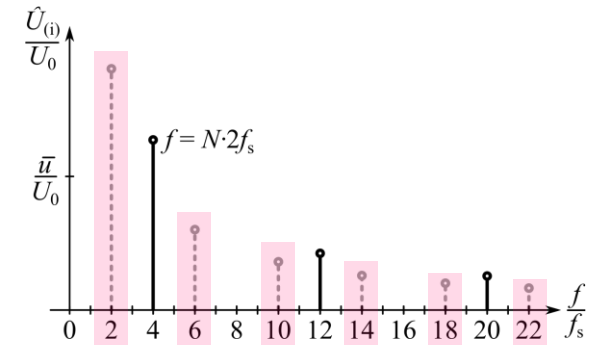
Multi-Cell Concept: Interleaving (2)

■ Example $N = 1 \rightarrow N = 2$: Cancelling of Harmonics at $2 \cdot kf_s$ ($k = 1, 3, 5, 7, \dots$)

$N = 1$

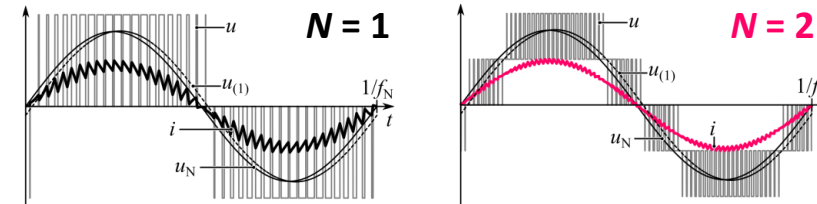


$N = 2$



Multi-Cell Concept: Switching Losses

- Scaling of Switching Losses for Same Ripple Ampl. ΔI
- Same dv/dt and Same di/dt for All Devices (Conservative Assumption!)



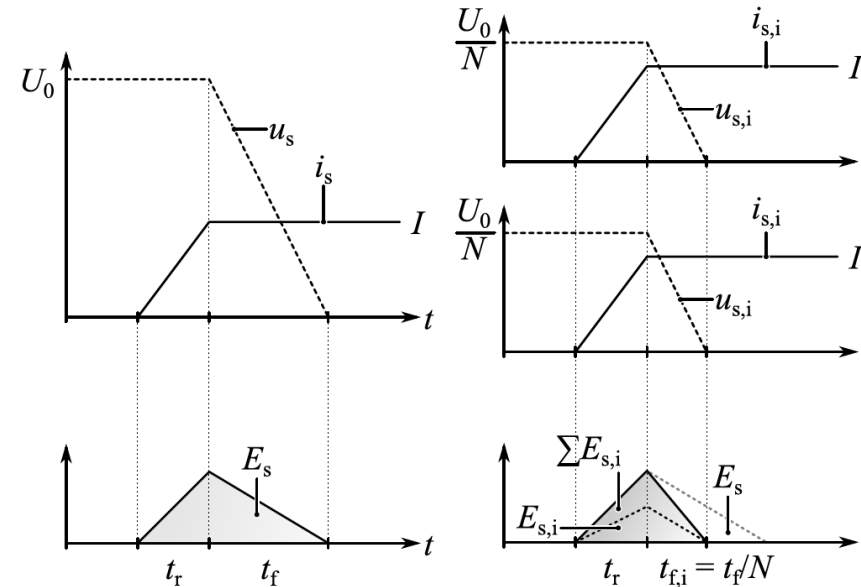
N = 1:

$$P_{sw,N=1} = 2E_{sw,N=1}f_s = 2 \cdot \frac{1}{2} \cdot (t_r + t_f) \cdot U_0 I \cdot f_s$$

N > 1: *Same ΔI*

$$P_{sw,N} = N \cdot 2 \cdot \frac{1}{2} \cdot \left(t_r + \frac{t_f}{N}\right) \cdot \frac{U_0}{N} \cdot I \cdot \frac{f_s}{N^2} = \frac{1}{N^2} \cdot \left(t_r + \frac{t_f}{N}\right) \cdot U_0 I \cdot f_s$$

$$P_{sw,N} \approx \frac{P_{sw,N=1}}{N^2} \dots \frac{P_{sw,N=1}}{N^3}$$



- Series Interleaving Dramatically Reduces Switching Losses (or Harmonics)
- Converter Cells Can Operate at Very Low Switching Frequency
- Minimization of Passives (Filter Components)



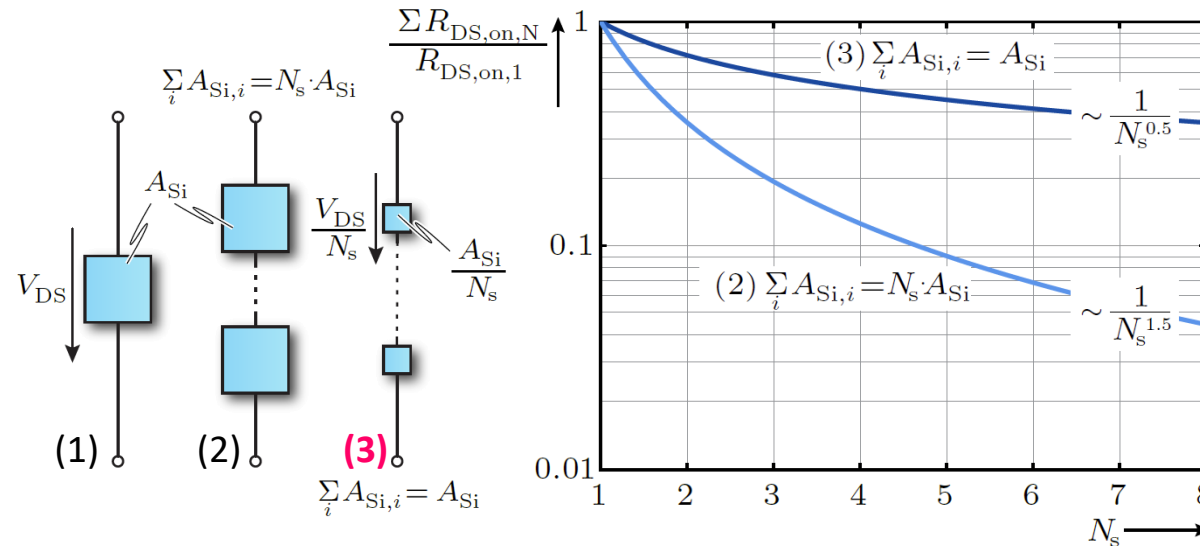
Multi-Cell Concept: Conduction Losses

■ On-State Resistance of MOSFETs Roughly Scales with $BV^{2.5}$ (e.g., Silicon Limit)

(1) $R_{DS,on,N=1} \propto \frac{1}{A_{Si}} (V_{DS})^{2.5}$

(2) $R_{DS,on,N} \propto N \frac{1}{A_{Si}} \left(\frac{V_{DS}}{N}\right)^{2.5}$
 $\Rightarrow R_{DS,on,N} = \frac{R_{DS,on,N=1}}{N^{1.5}}$

(3) $R_{DS,on,N} \propto N \frac{N}{A_{Si}} \left(\frac{V_{DS}}{N}\right)^{2.5}$
 $\Rightarrow R_{DS,on,N} = \frac{R_{DS,on,N=1}}{N^{0.5}}$



■ Even With Constant Total Chip Area, **Conduction Losses Decrease with Increasing N**

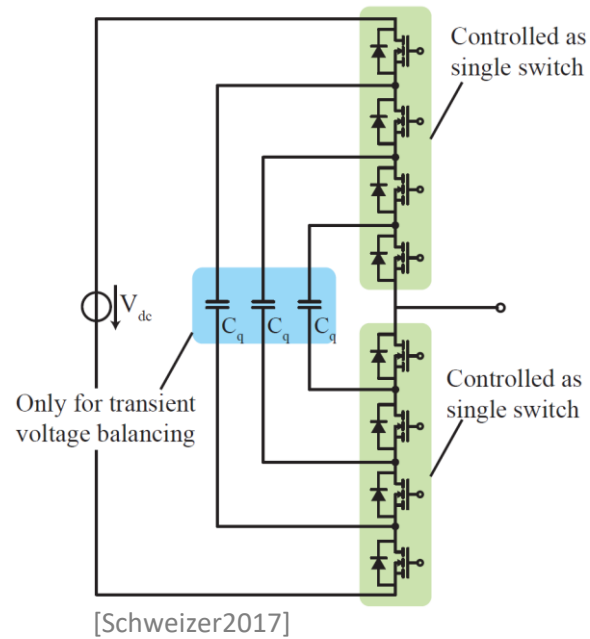
- Beware: Does Not Hold for IGBTs / Bipolar Devices with Approx. Constant Forward Voltage Drop



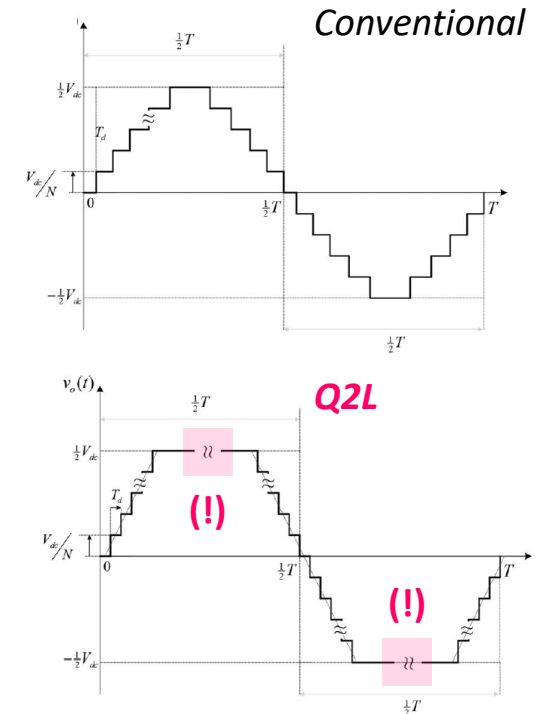
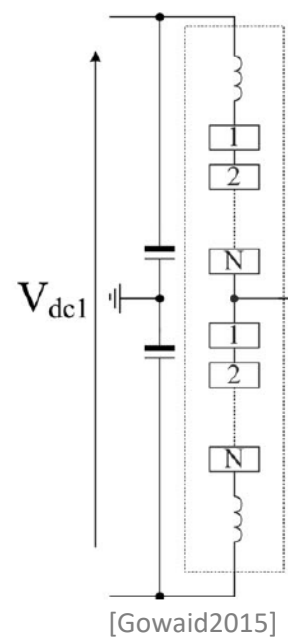
Remark: Quasi-2-Level Operation

- Operation of N -Level Topology in 2-Level Mode
- Intermediate Voltage Levels Only Used During Switching Transients

Flying-Capacitor Bridge-Leg



MMC Bridge-Leg



- Defined Partitioning of Blocking Voltages & Small Flying / Cell Capacitors
- Benefit from Cond. & Sw. Loss Scaling But **Higher Harmonic Content (No Interleaving)**



Part II

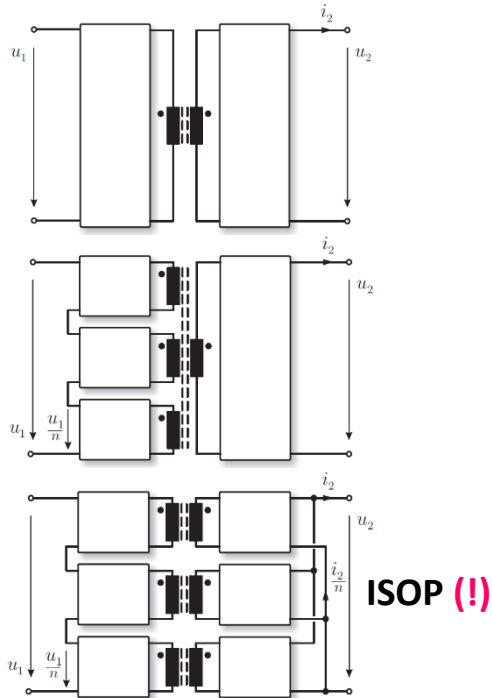
SST Concepts & Key Design Aspects

- Medium-Frequency Power Conversion
- Power Semiconductors
- **Key SST Topologies**
- Medium-Frequency Transformers
- Isolation Coordination
- Protection
- Reliability
- Standardization & EMC
- Construction & Testing

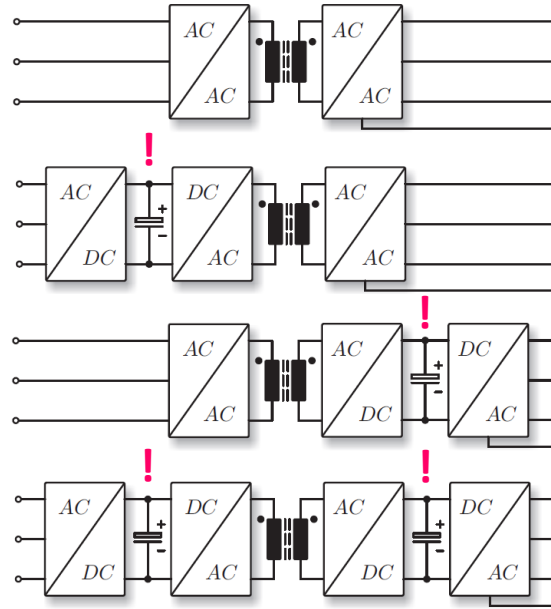


Classification of SST Topologies (1)

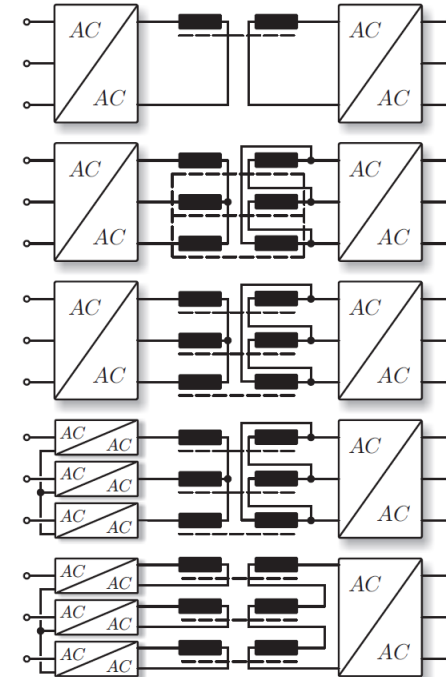
Number of Levels Series/Parallel Cells



Degree of Power Conversion Partitioning



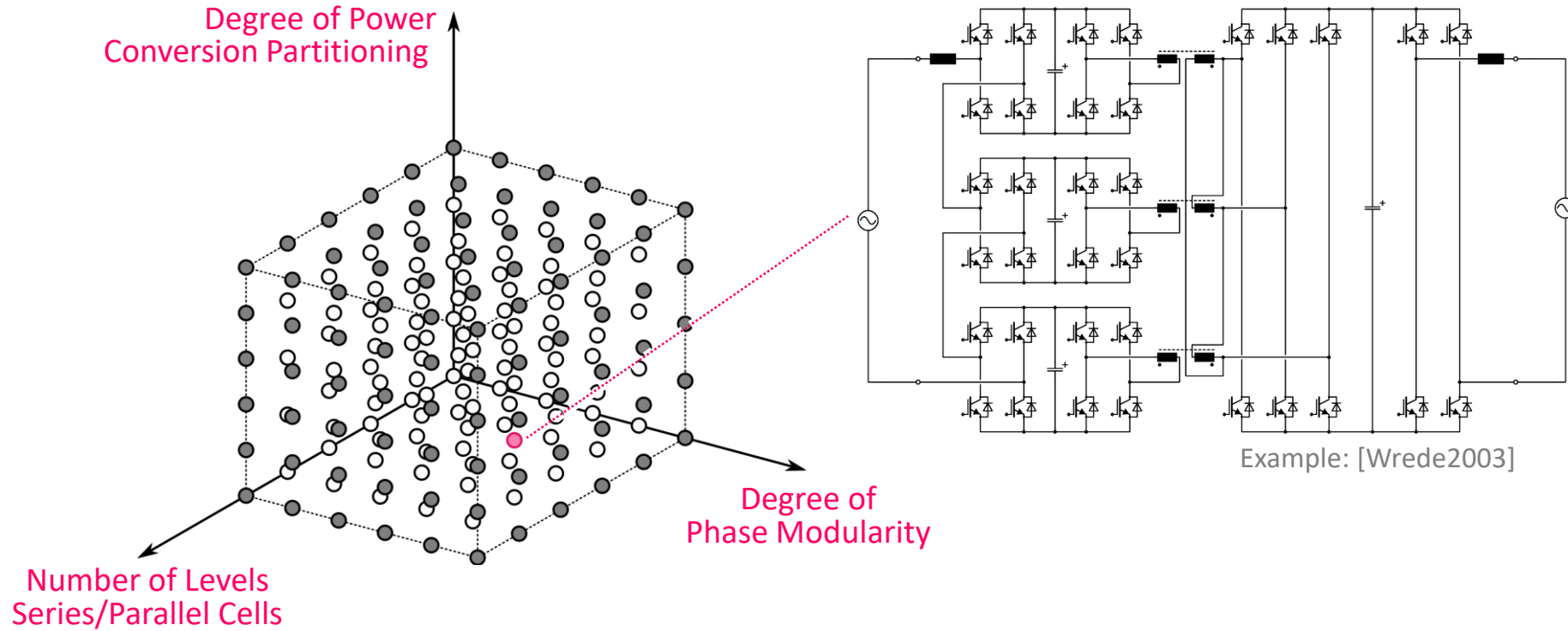
Degree of Phase Modularity



Three-Dimensional Topology Selection Space!



Classification of SST Topologies (2)



■ **Very (!) Large Number of Possible Topologies**

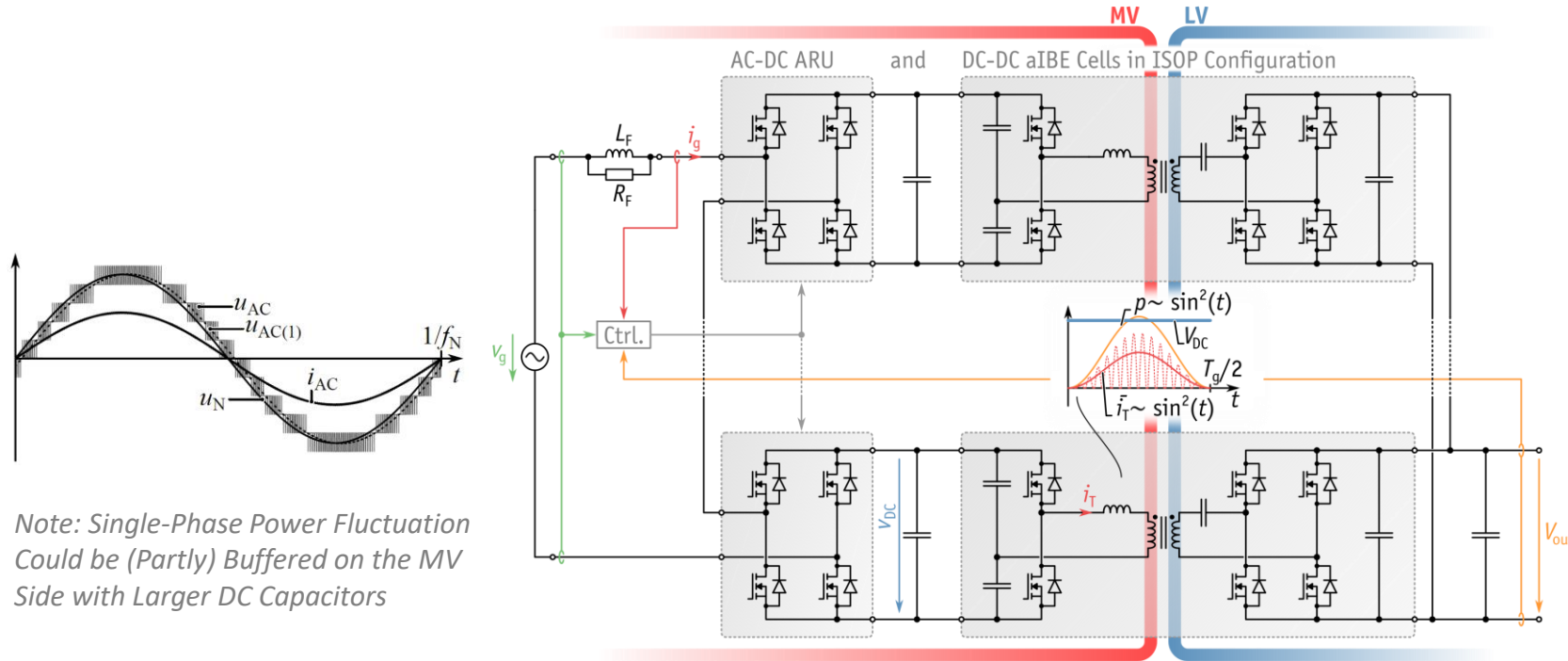
- Partitioning of Power Conversion
 - Splitting of 3ph. System into Individual Phases
 - Splitting of Medium Operating Voltage into Lower Partial Voltages
- Matrix & DC-Link Topologies
 - Phase Modularity
 - Multi-Level/Cell Approaches



Modular Topologies

Isolated Back-End (IBE) AC-DC Conversion

Input-Series Output-Parallel (ISOP) Configuration of AC-DC + DC-DC Converter Cells



Direct Mains Current Control with Cascaded AC-DC Front End

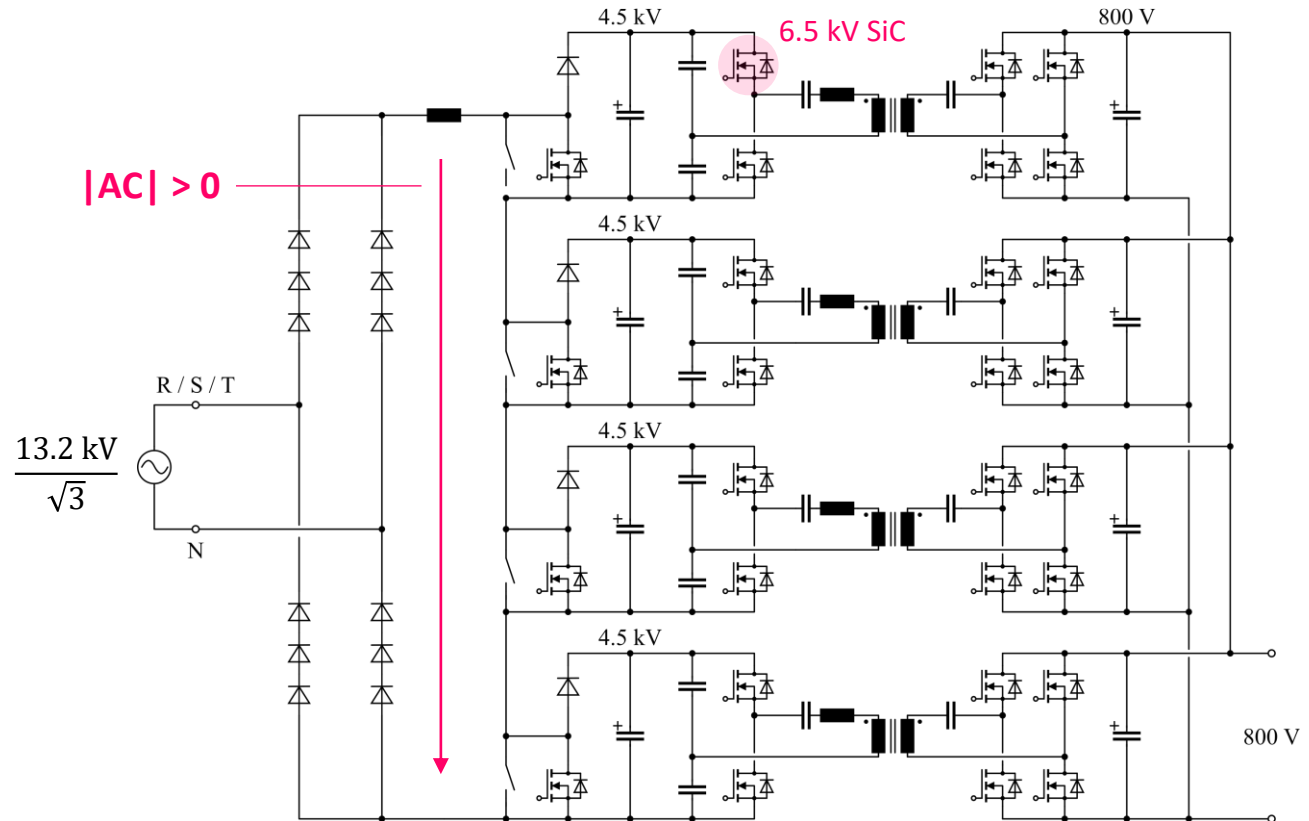
Most Frequently Used Topology Typ. with DCX Isolation Stages

- (Specific Realizations May Vary, e.g., 3-Phase Configurations, Cell Topology, DC-DC Converter Type, etc.)



Remark: Unidirectional Topologies

- Opportunity for Complexity Reduction (# MOSFETs, Gate Drives, ...)



- Example: Multi-Cell Boost ISOP Topology with DCX Isolation Stages

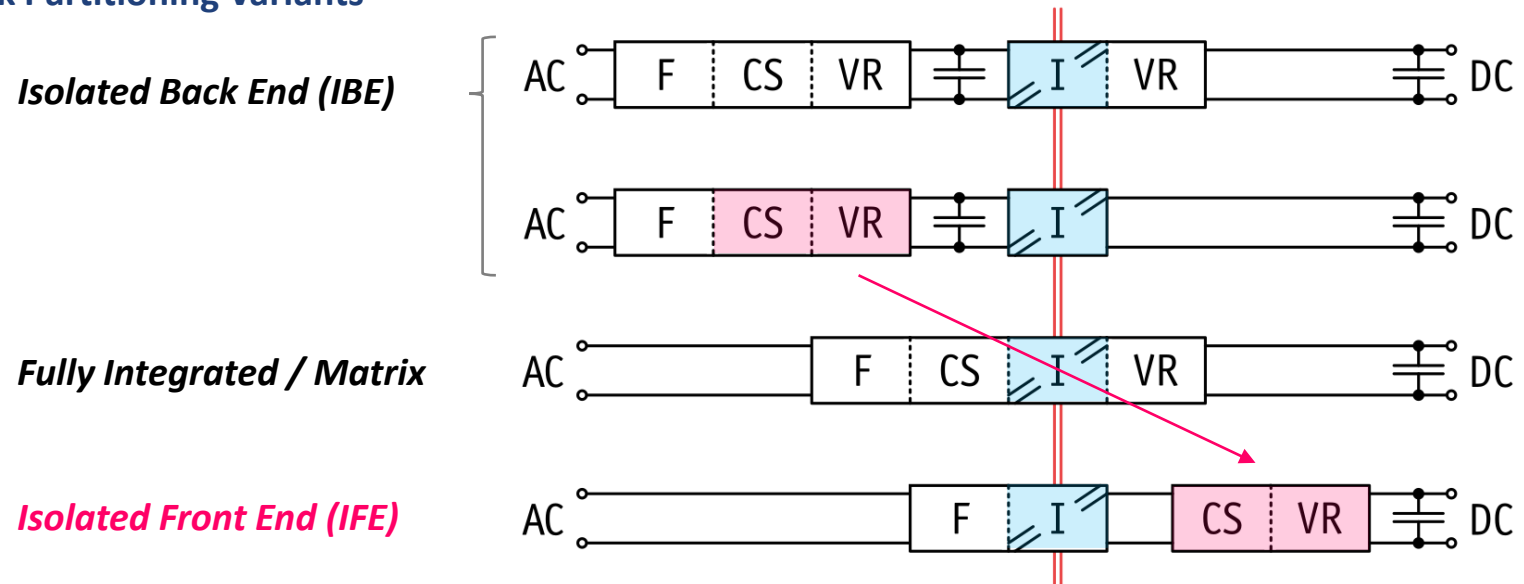


Partitioning of Single-Phase AC-DC PFC Functionality

Required Functionality

- **F** Folding of the AC Voltage Into a $|AC|$ Voltage
- **CS** Input Current Shaping
- **I** Galvanic Isolation & Voltage Scaling (No Regulation Capability)
- **VR** Output Voltage Regulation

Isolated PFC Task Partitioning Variants

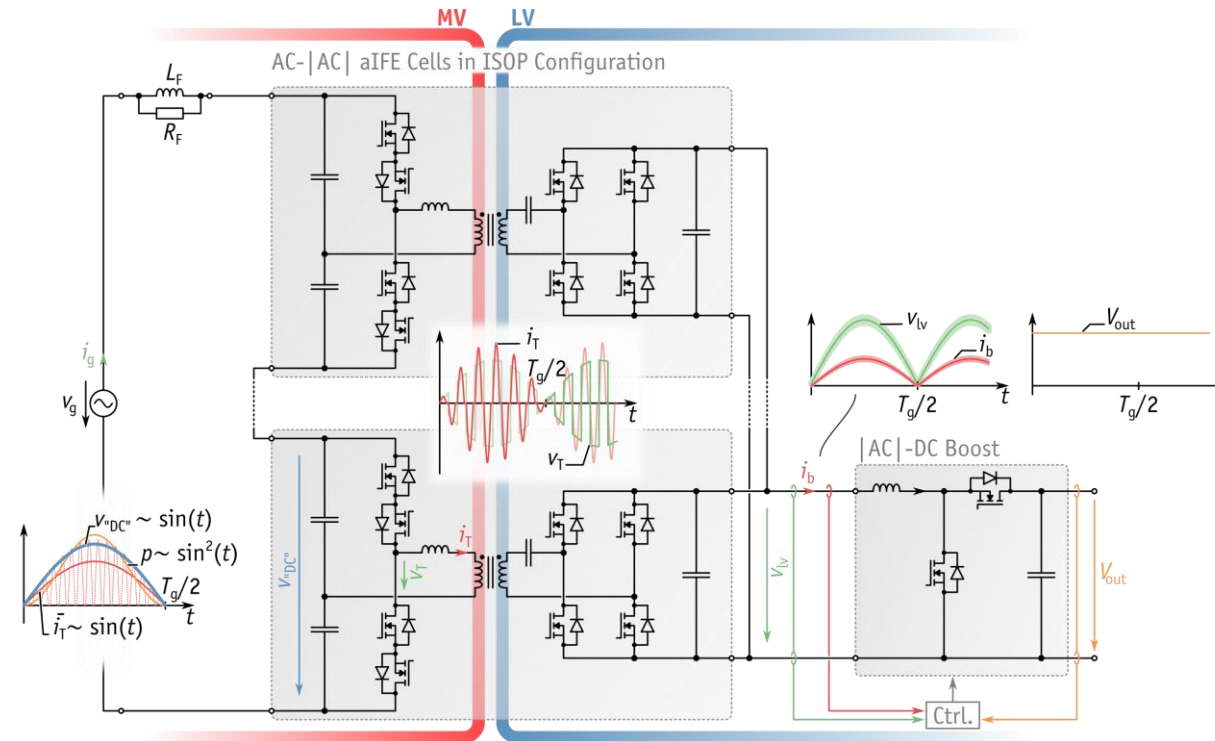


IFE Shifts Input (!) Current Shaping and Output Voltage Regulation to the LV Side



Isolated Front-End (IFE) AC-DC Conversion

- Input-Series Output-Parallel (ISOP) Configuration of Isolated AC-|AC| Stages with LV-Side |AC|-DC Stage
- Minimum MV-Side Complexity with Unregulated AC-|AC| “DCX” Stages

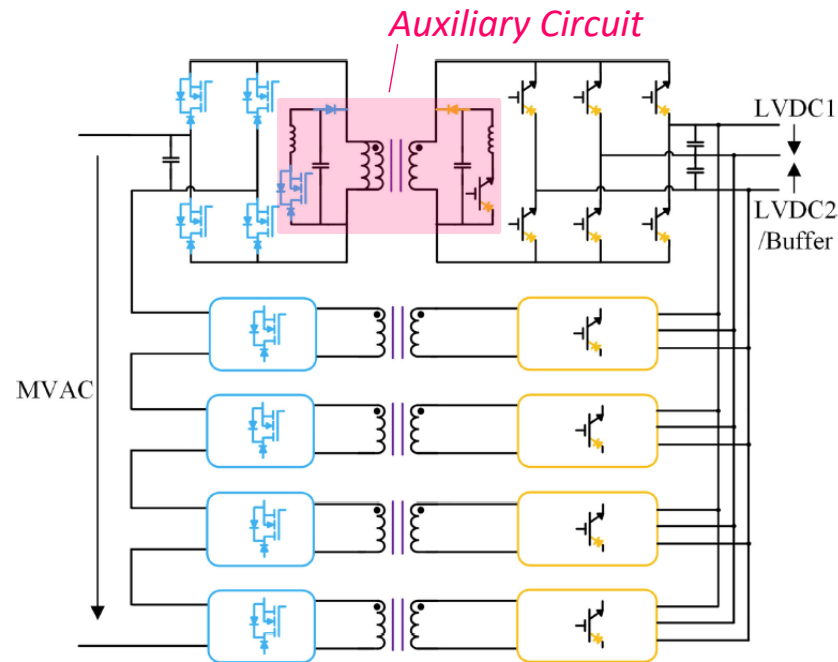


- LV-Side |AC|-DC Operates as in 1-Ph. PFC Rect. | Input Cur. Shaping through Transparent AC-|AC| “DCX”
- Variants: Indirect AC-|AC| Matrix Stages, Parallel-Interleaved |AC|-DC Boost Stages, ...

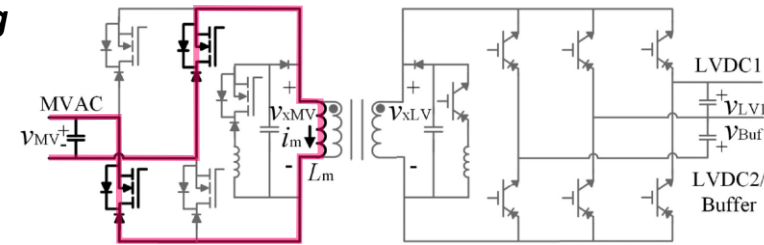


Remark: Current-Source-Type Soft-Switching SST: S4T

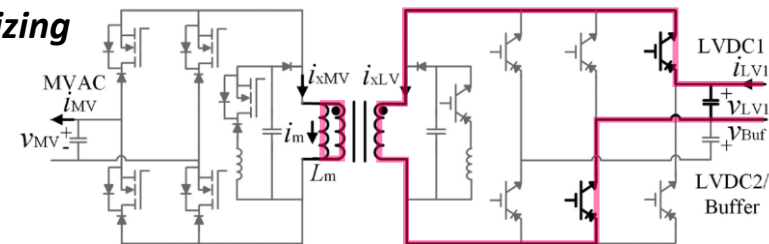
- Magnetizing Inductance as Current DC-Link (Load-Dependent But Constant Current, MFT with Air Gap)
- Flyback-Like Operating Mode – Magnetizing from Side 1 & Demagnetizing to Side 2
- Auxiliary Resonant Circuit Ensures Full-Range ZVS for All Main Devices



Energizing



De-Energizing



- Reverse-Blocking Switches Required (MOSFET + Diode, RB-IGBTs)
- Variants: AC-DC, AC-AC, DC-DC / Bidir. Power Flow & Arbitrary Power Factors

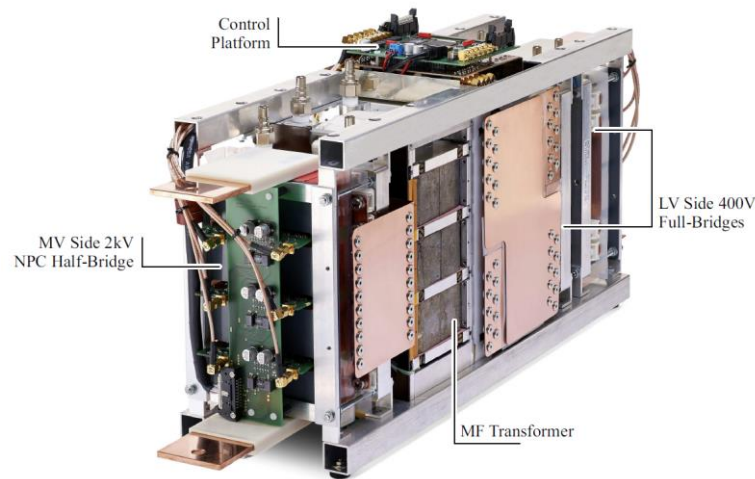


Remark: DC-DC Topologies

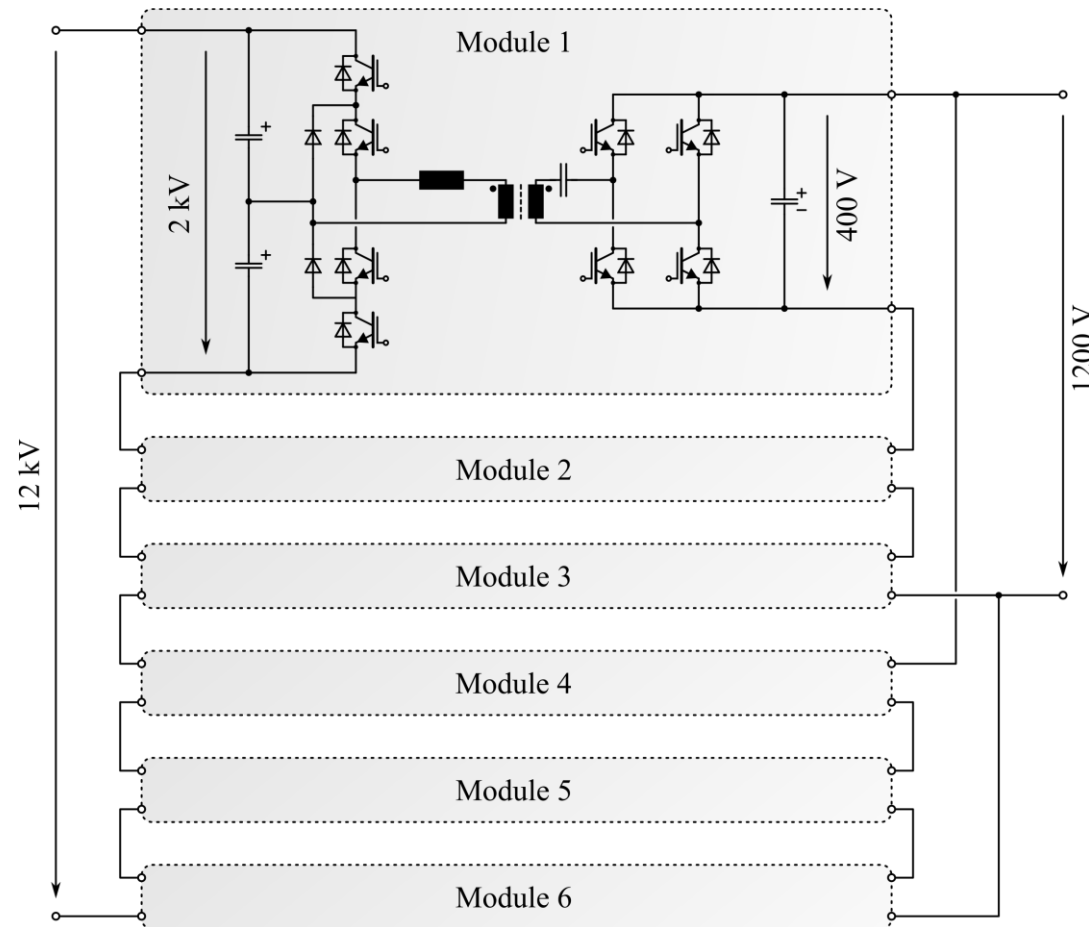
- Fully Modular Approach

- MEGA-Cube @ ETH Zurich

- 1 MW, 2 kV → 1200 V DC-Transformer
- 2 x 3 Connection on LV Side

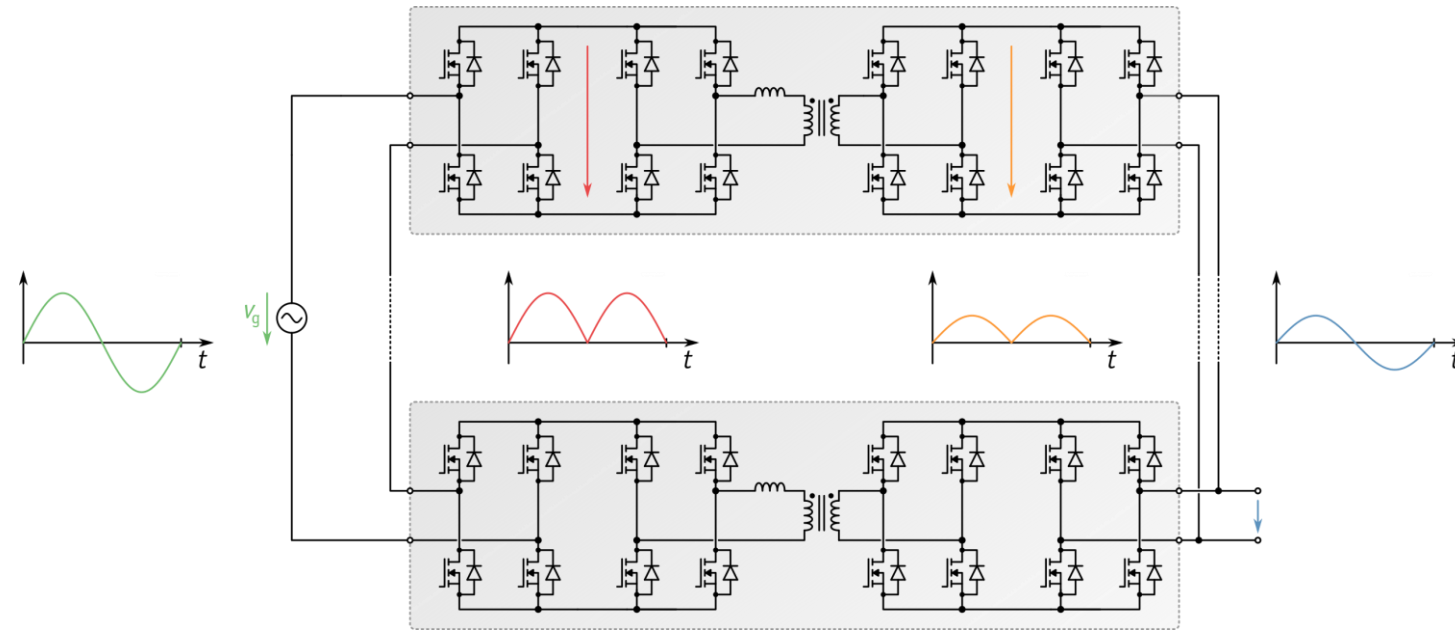


- 166 kW / 20 kHz Si-IGBT DC-DC Converter Module



Remark: AC-AC Topologies

- Fully Modular AC-AC Topology w. Indirect Matrix Converter Modules $\rightarrow f_1 = f_2$



- Specific Realizations May Vary (3-Phase Configurations, Non-Resonant DC-DC Stage, ...)



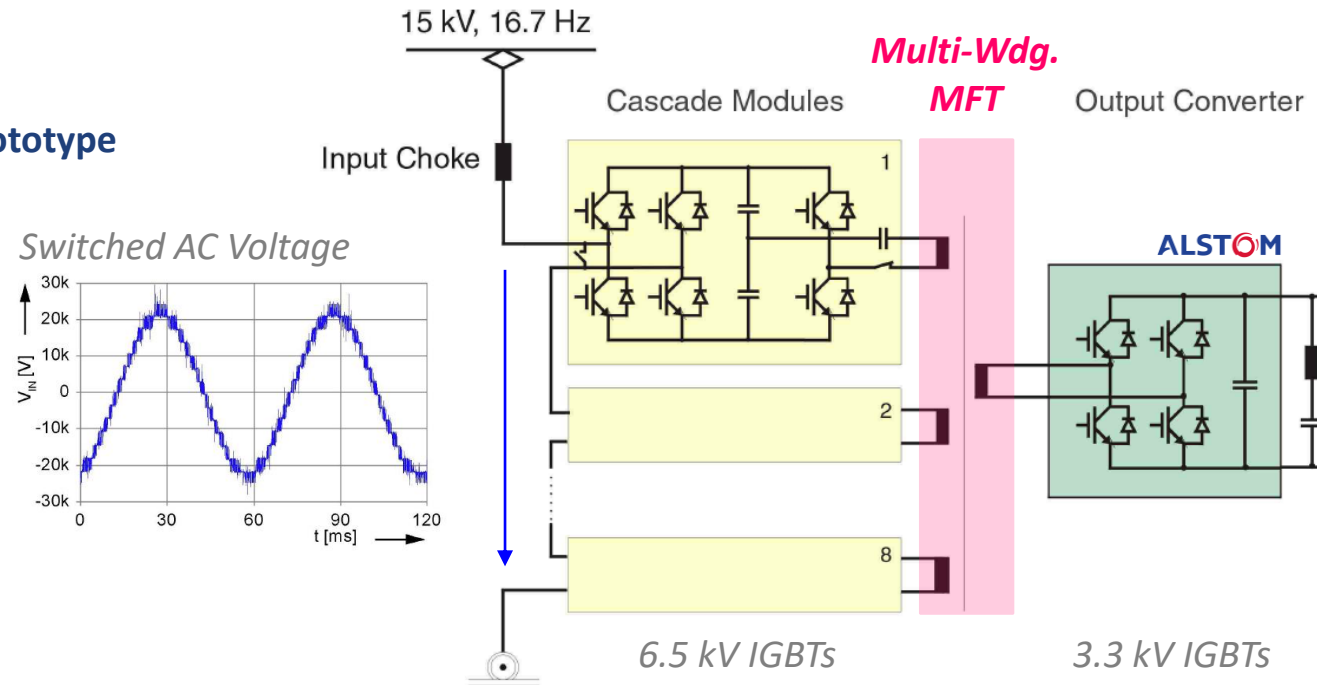
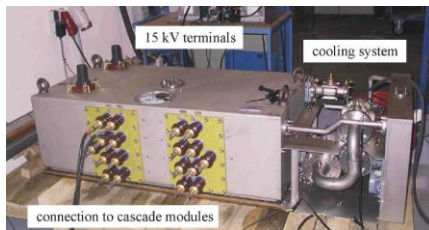
Partly Modular Topologies

IBE AC-DC with Multi-Winding Transformer

- **Single Transformer** w. Full Isolation Voltage Rating / **Modular Power Electronics** (Redundancy)
- **Coupling Between Primary Windings** → **Undesired Current Flows & Oscillations**

■ ALSTOM (2003) Traction Prototype

1.5 MW / 5 kHz
Multi-Winding MFT

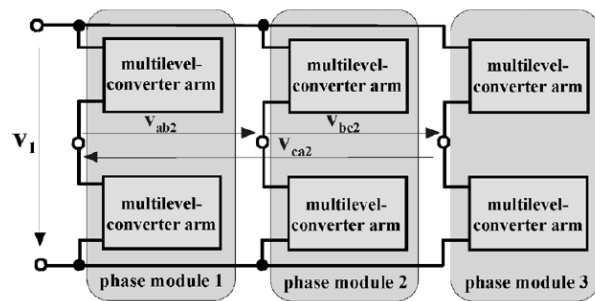


- 15 kV / 16.7 Hz Input, 8 Cascaded Modules (7-out-of-8 Redundancy), 1.5 MW (2.25 MW for 30 s)
- Si-IGBT Technology / 5 kHz MFT / 94 % Efficiency & 0.47 kW/dm³ Power Density

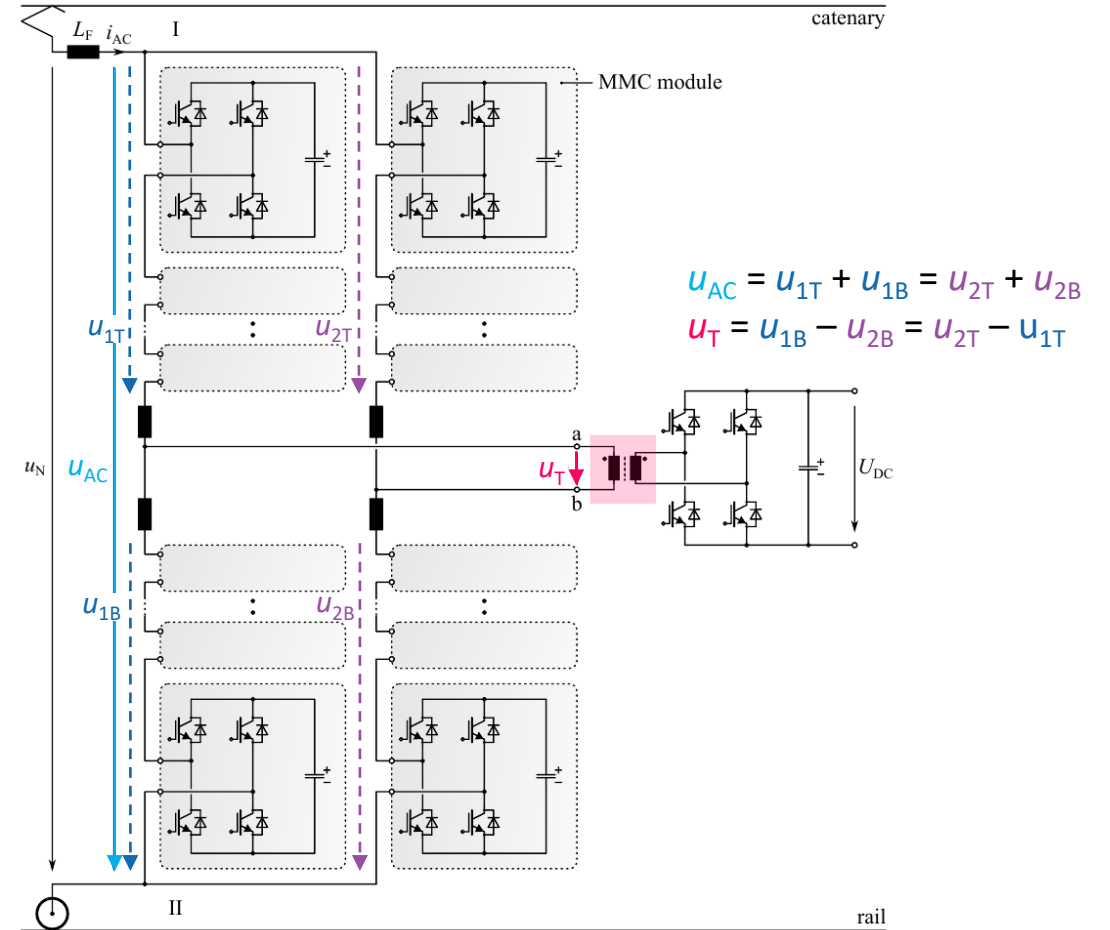


Modular Multilevel Converter (MMC)

- **Single Transformer w. Full Isolation Voltage Rating**
- **Modular Power Electronics (Redundancy)**
- AC-AC Matrix Converter with Fully Independent Generation of u_{AC} and u_T
- High Semicond. Effort (Each Arm Provides Total DC Volt.)
- Active Balancing of Module Cap. Volt. Necessary (Sensing / Control)
- **Variants:**
 - 3-Phase AC \rightarrow 1-Phase HF AC, DC-DC

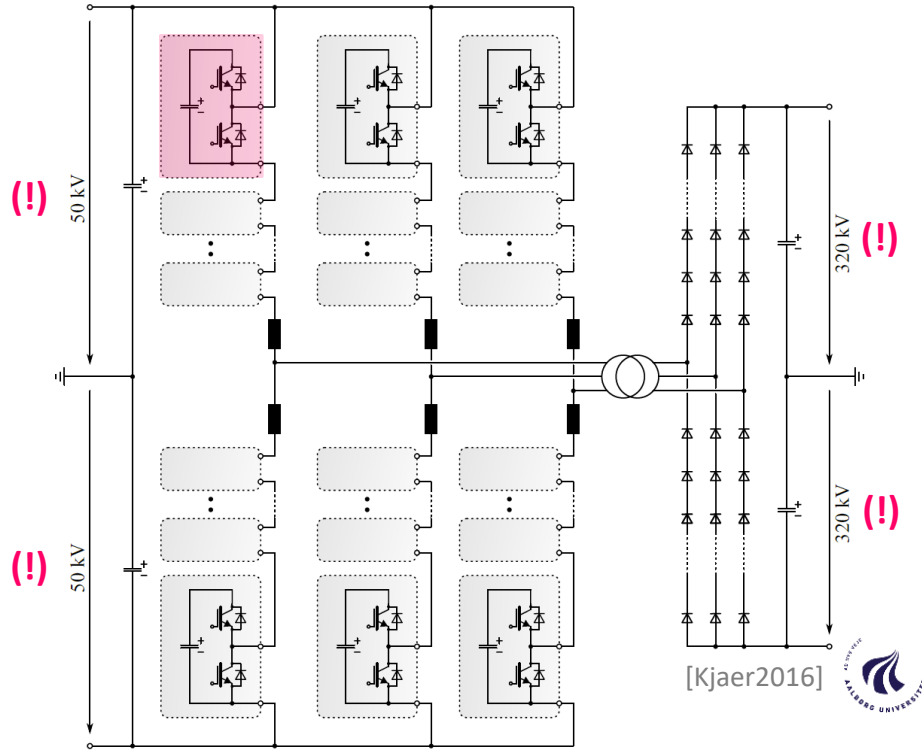


der Bundeswehr
Universität München

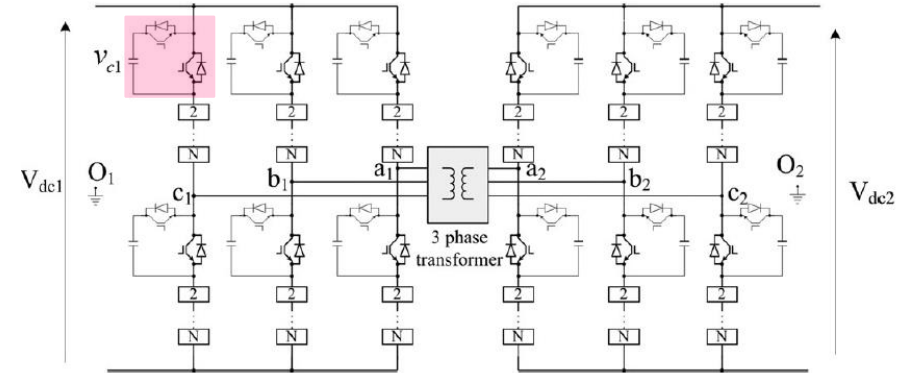


Remark: DC-DC MMC

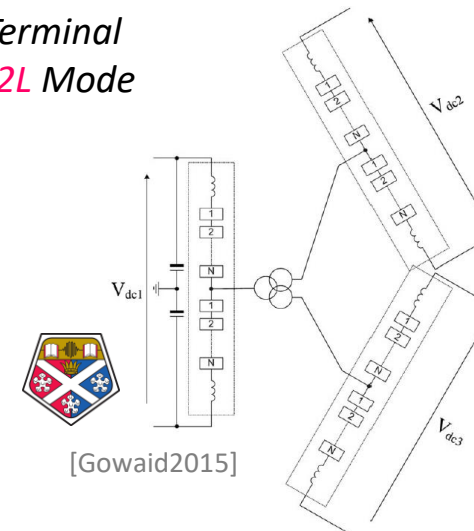
DC Interface with Half-Bridge Converter Cells



Unidirectional ± 50 kV MVDC \rightarrow ± 320 kV HVDC
Step-Up for Offshore Wind Park Collector Grids

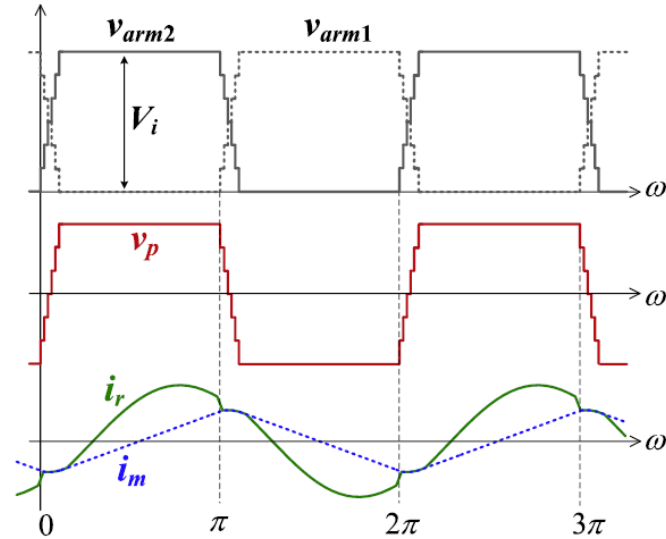
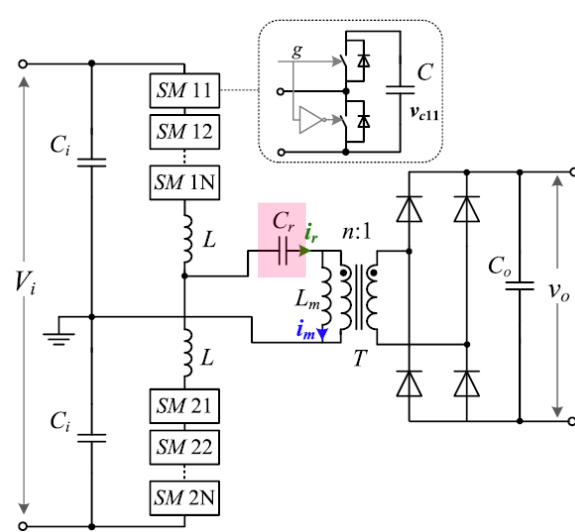


Bidirectional / Multi-Terminal
DC Transformers w. Q2L Mode

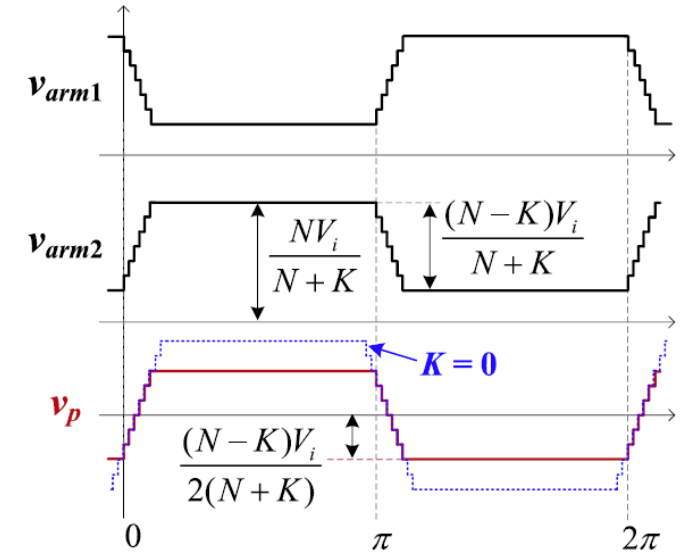


Remark: DC-DC MMC w. Resonant Operation

- DCX with MMC in Q2L Operation
- Output Voltage Regulation: MMC Primary Voltage Amplitude Adaption (Coarse) + Var. Freq. (Fine)



Typ. Operating Waveforms



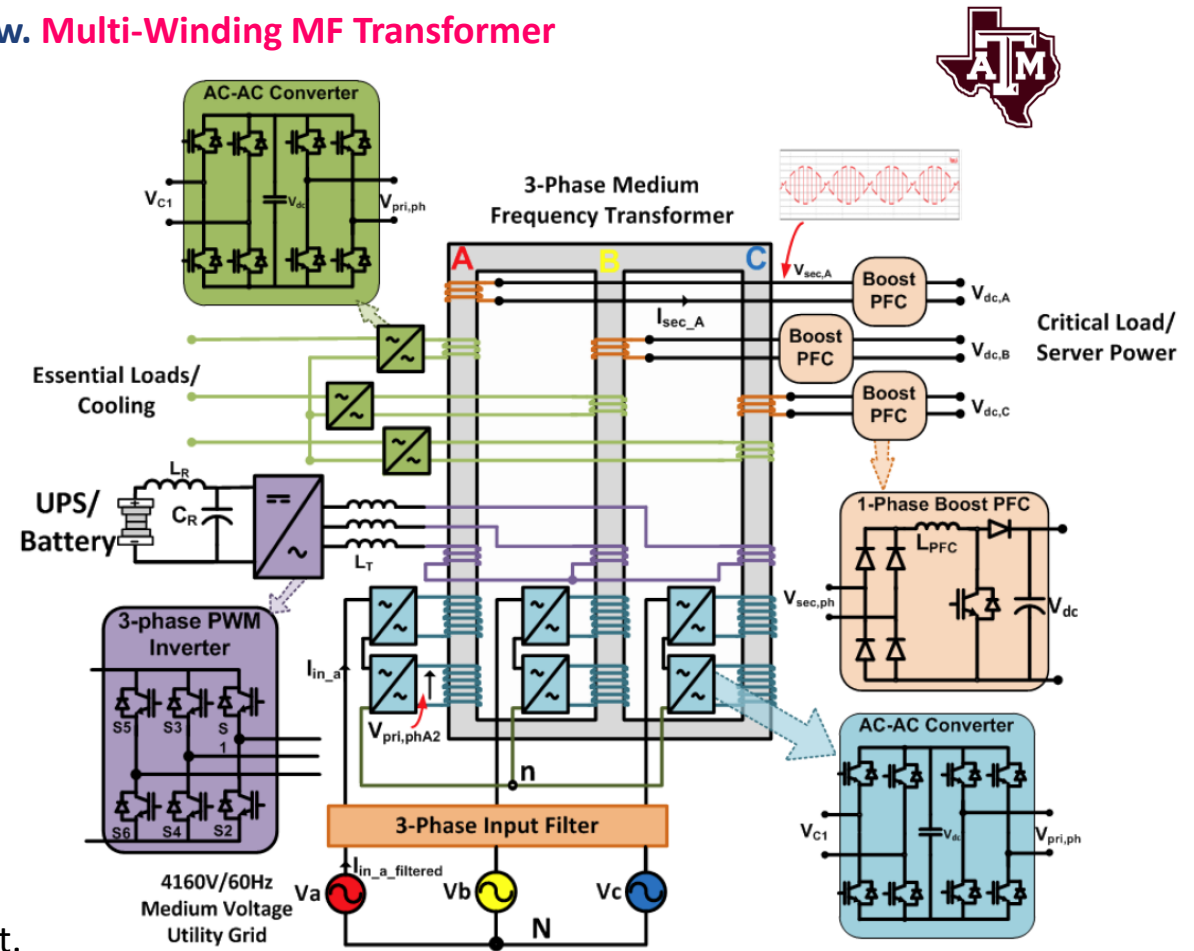
Primary Volt. Ampl. Adaption

- Module Capacitor Voltage Balancing w. Sorting Algorithm
- Not All Devices Achieve ZVS because of DC Circulating Current



Multiport Topologies

- Bidirectional AC-AC (Matrix) Grid Interface w. **Multi-Winding MF Transformer**
- **Hybrid Uni-/Bidirectional:** Unidirectional or Bidirectional Loads



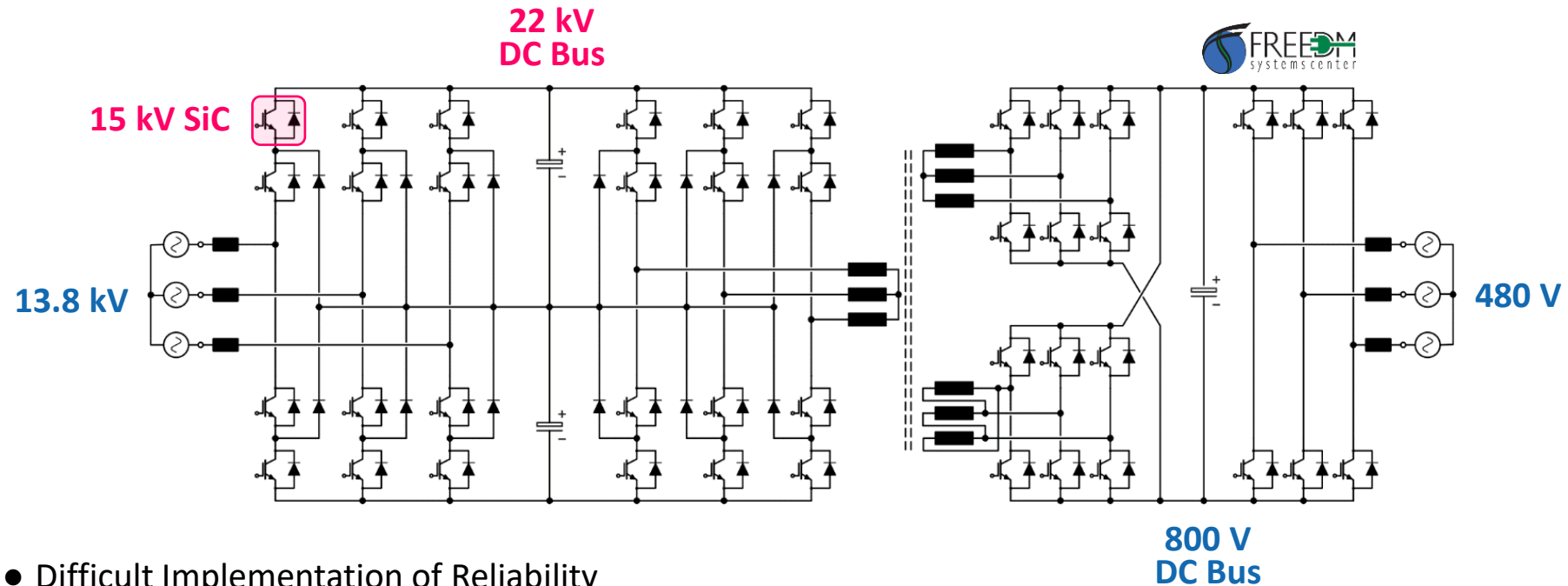
- Target Appl.: Datacenter Power Distribution
- Various Other Configurations Described in Lit.



Non-Modular / Single-Cell Topologies

Single-Cell Topologies Enabled by HV SiC

- Low Complexity / Standard Converter Topologies w. Relatively Few Switches / Single MFT
- HV SiC Devices Needed (10+ kV) / Scarce Availability Outside of R&D



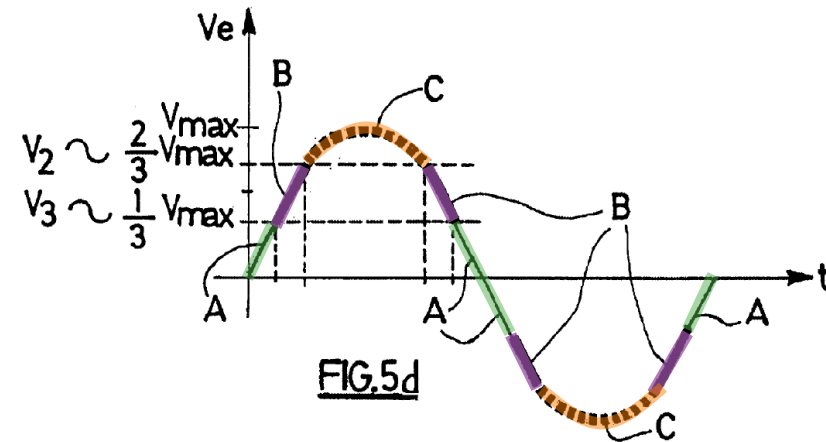
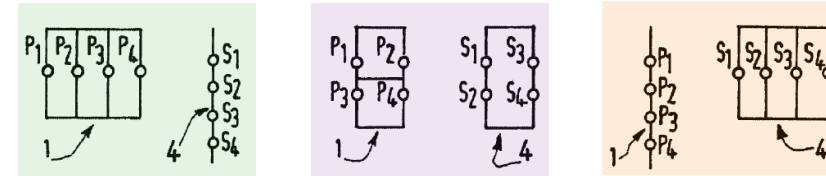
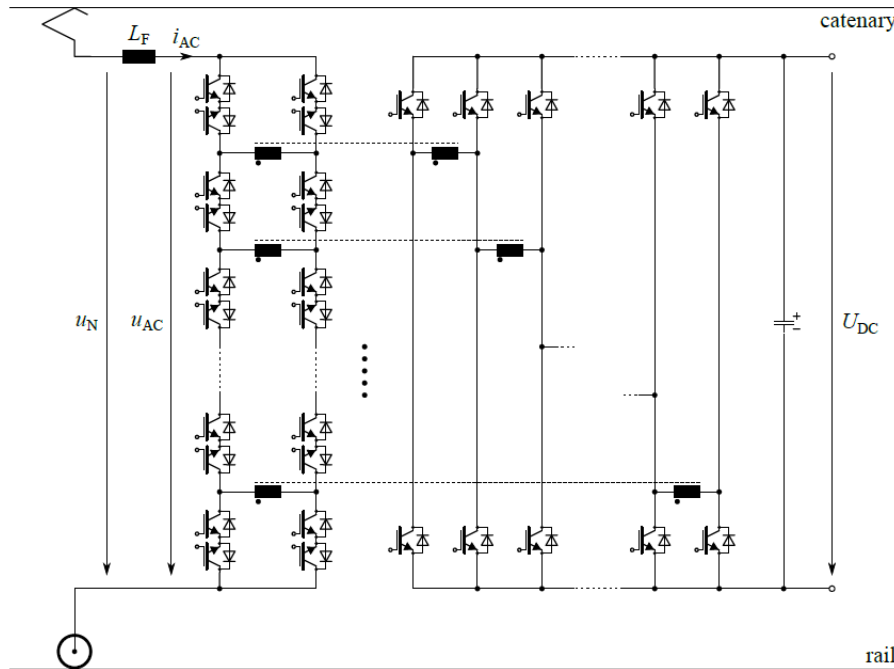
- Difficult Implementation of Reliability
- Not Scalable to Higher Voltages



SPARC Converter

Serial and Parallel Auto Regulated Configuration (SPARC) Converter

- Series/Parallel Connections of Primary/Secondary Transformer Windings
- Input Voltage Distribution & Output Current Sharing as in ISOP

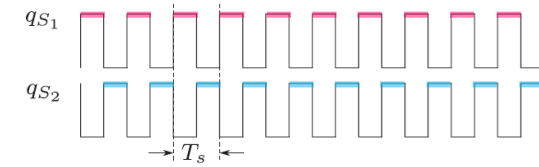
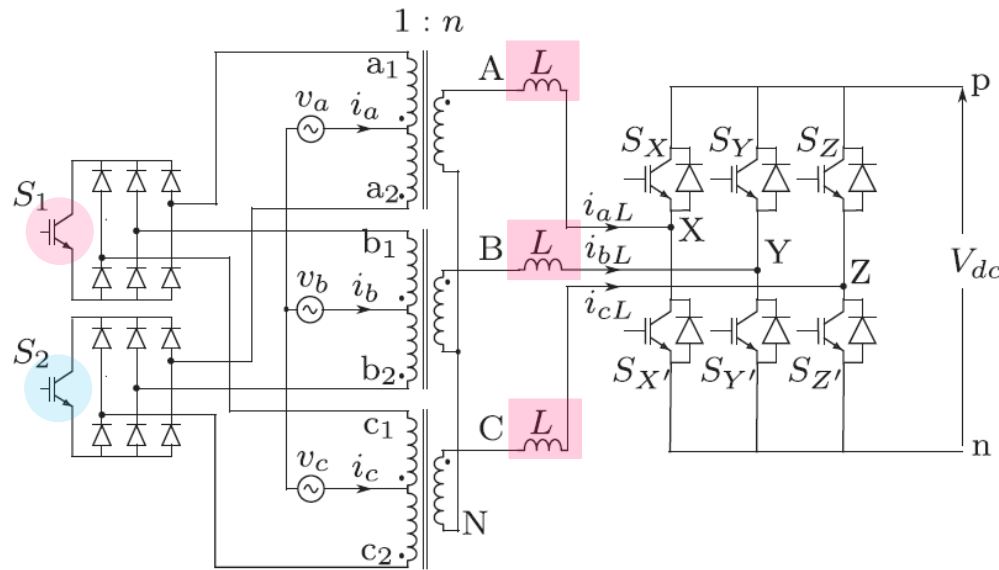


- Input AC Voltage Synthesis from Available Converter Sw. States / # of States Increases with # of Transformers
- Soft-Switching Modulation Possible (Primary CSI with ZCS, VSI with ZVS)

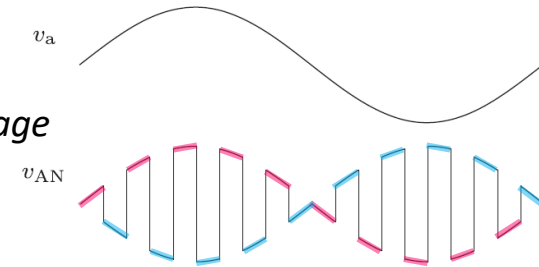


Single-Stage 3-Phase AC-DC Conversion (1)

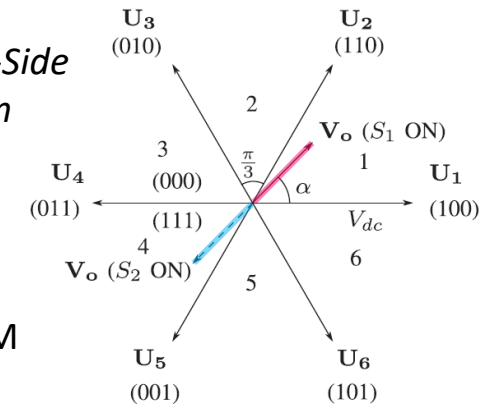
- Single-Stage Power Conversion with Minimum Complexity on the MV Side
- S_1 & S_2 Sync. Switching w. 50% Duty → Amplitude-Modulated HF Transf. Volt.



Transf. Voltage (Phase a)



Secondary-Side SV Diagram



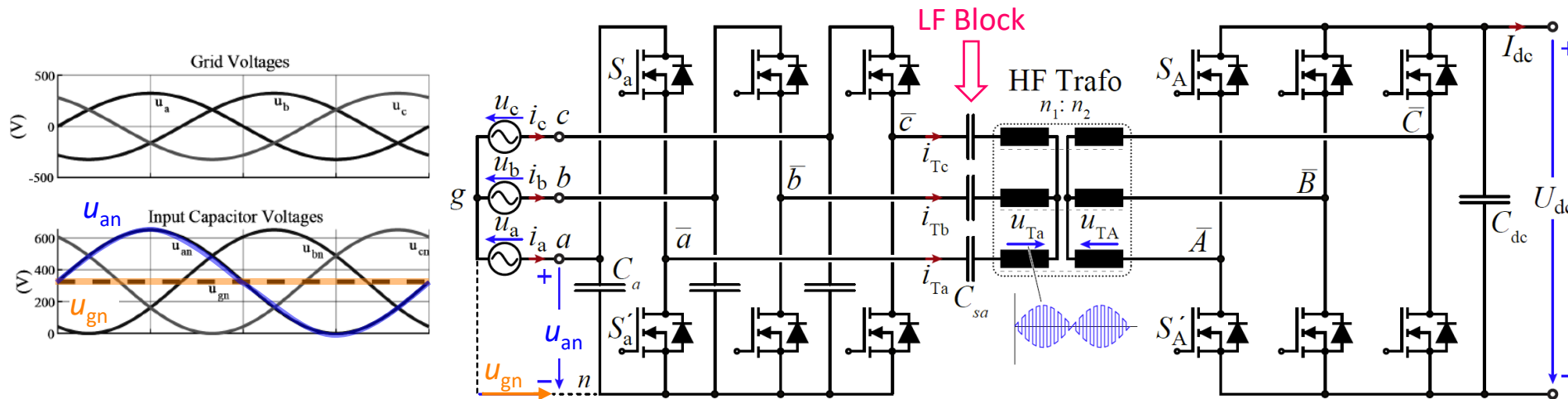
- Three-Phase Voltage-Source Inverter Output Stage
 - DAB-Like Operating Mode / Inductor Current Shaping Using Space-Vector PWM
 - Integrated IFE Approach: LV-Side Stage Shapes the Grid Currents
- AC-AC Version with 3x3 Direct Matrix Converter Output Stage



Single-Stage 3-Phase AC-DC Conversion (2)

Y-Rectifier with Standard Half-Bridge Modules

- Common-Mode Offset Voltage u_{gn} for Strictly Positive Input Capacitor Voltages
- Sync. Switching with 50% Duty ($[000] \leftrightarrow [111]$) / Low-Frequency-Blocking Series Capacitors
- Amplitude-Modulated Three-Phase HF Transformer Voltages



Three-Phase Voltage-Source Inverter Output Stage Operated as on Previous Slide (!)

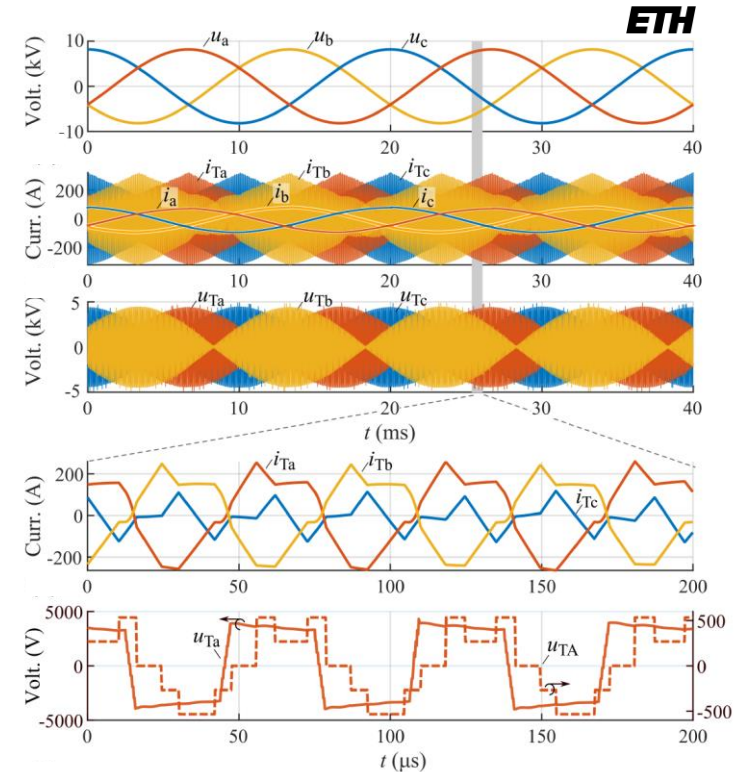
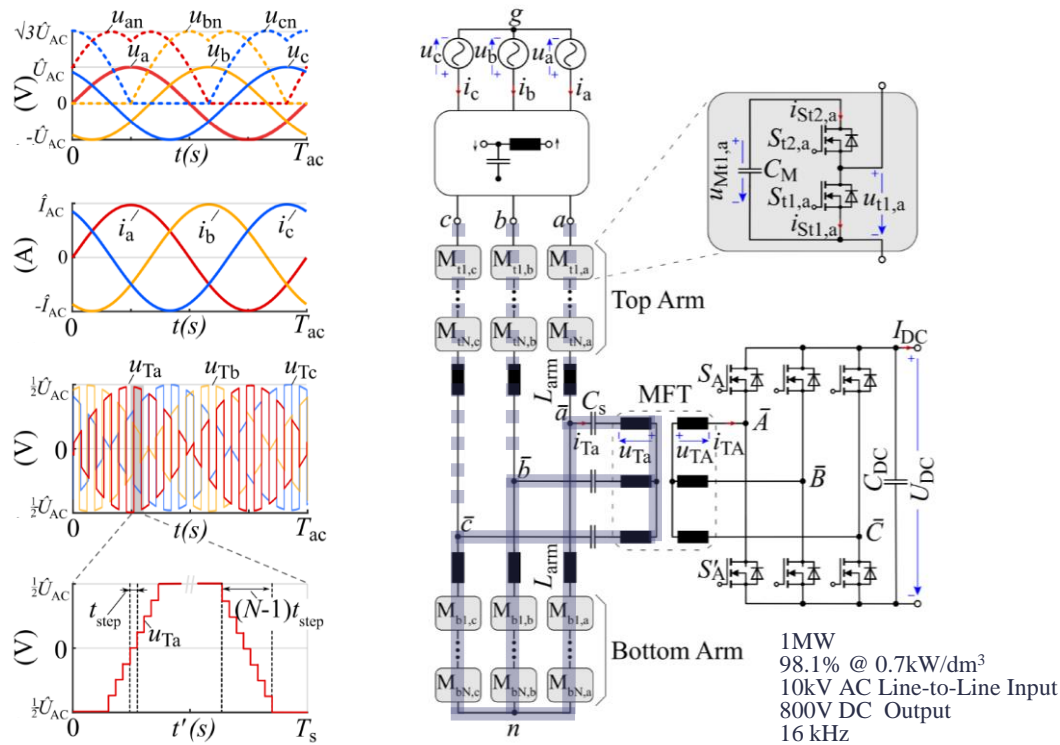
- DAB-Like Operating Mode / Inductor Current Shaping Using Space-Vector PWM
- Integrated IFE Approach: LV-Side Stage Shapes the Grid Currents

Extension to Higher Input Voltages w. Multilevel Bridge-Legs or MMC / AC-AC Versions Possible



Single-Stage 3-Phase AC-DC Conversion (3)

- **Quasi-Two-Level (Q2L) Controlled Front-End Bridge-Legs | Synchr. Sw. of All Three-Phases w/ 50% Duty Cycle**
- **Sw. Freq. Rectangular Transf. Primary Voltages w/ Line-Freq. Phase-Voltage Envelopes**
- **DAB-Type Transformer Phase Curr. Control Utilizing Sec.-Side LV Full-Bridge**

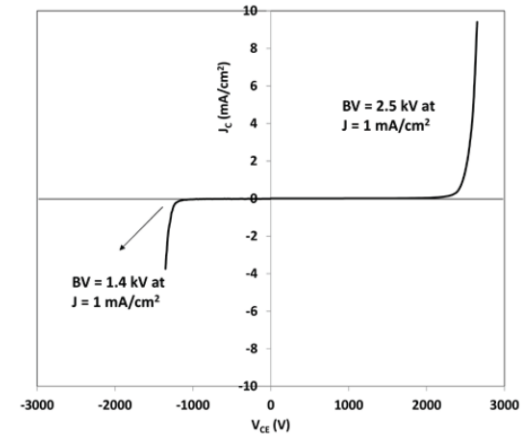
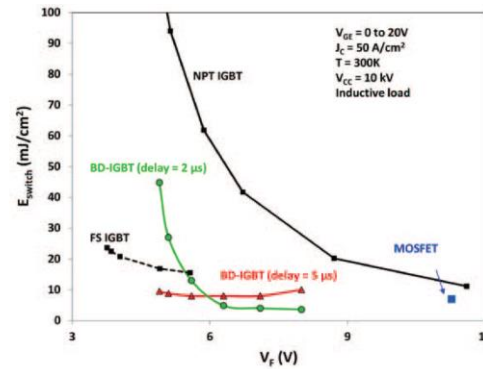
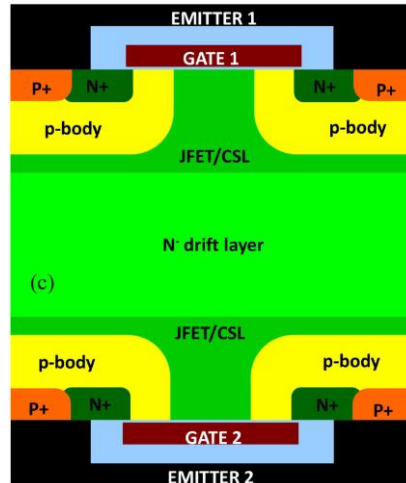


- **Sinusoidal Input Currents | Bidirectional | Buck-Boost Capability | Single MFT**
- **Lower Complexity Comp. to 3-Φ/1-Φ MMC-Matrix-Conv. Front-End | 2x Phase Volt. Ampl. as Max. String Voltages**
- **Rel. High Curr. Stress on Transf. & Switches Due to Input Stage Free-Wheeling and/or 50% Duty-Cycle Operation**



Remark Monolithic Bi-Directional 15 kV SiC IGBT

- Planar-Gate Bi-Direct. IGBT Fabricated w/ Double-Sided Lithography Process
- Conduction & Sw. Loss Influence of Back-Side Gate Voltage Bias
- Challenging Packaging & Cooling

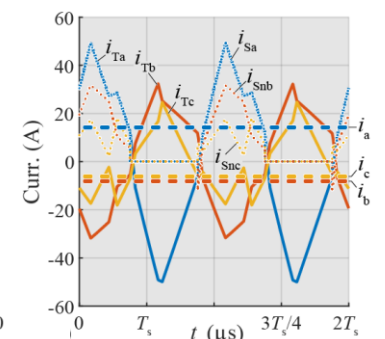
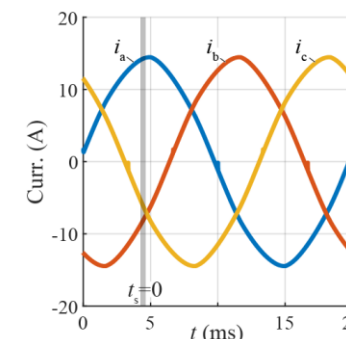
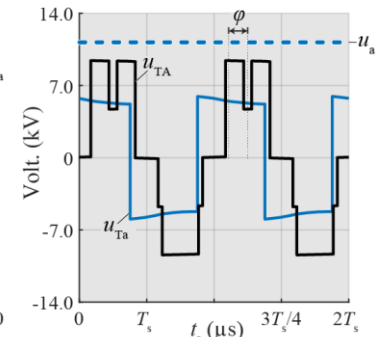
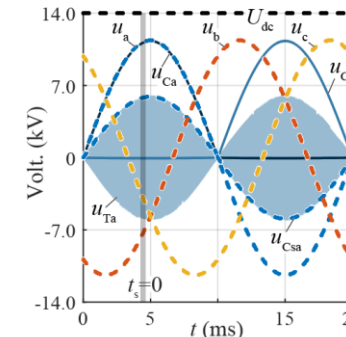
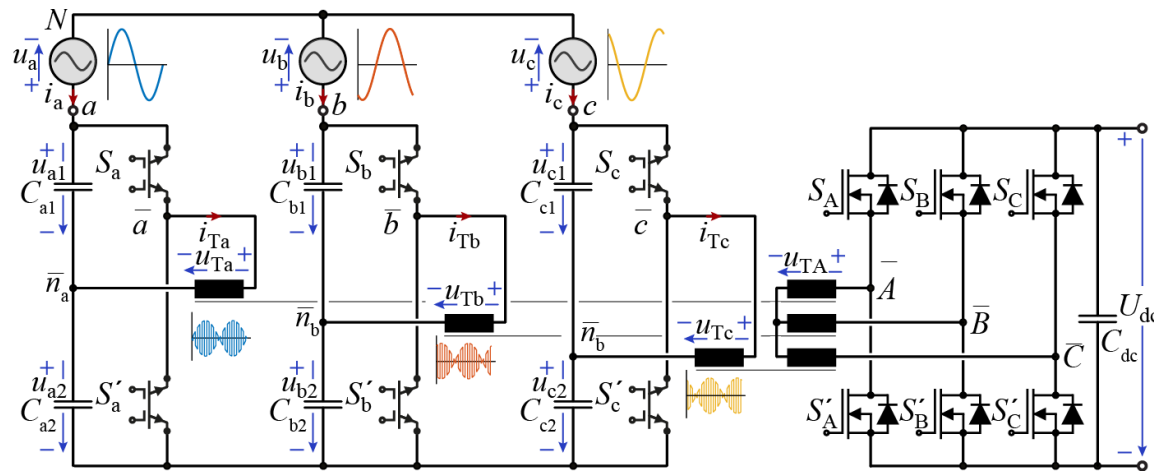


- Simul. Performance of a 15 kV BD-IGBT | Max. 7.2 kV Measured — Epi Layer Defects etc.



MBDS-Based Novel Swiss-SST Concept

- “Isolated Front-End”-Topology — Minimum Complexity of MV Power Electronics & Control Circuit
- 15 kV Monolithic Bidirectional Switch (MBDS, SiC-IGBT) — Direct Connection to 13.2 kV Distrib. Grid
- Unity Power Factor / Bidirectional



- Dual Active Bridge-Type Control
- AC-Side Phase Modularity — Full Rated Power Operation @ 1-Φ Input (!)



Part II

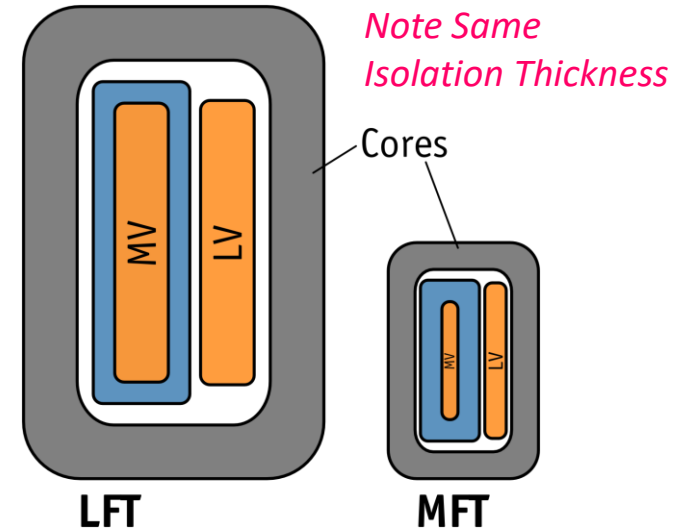
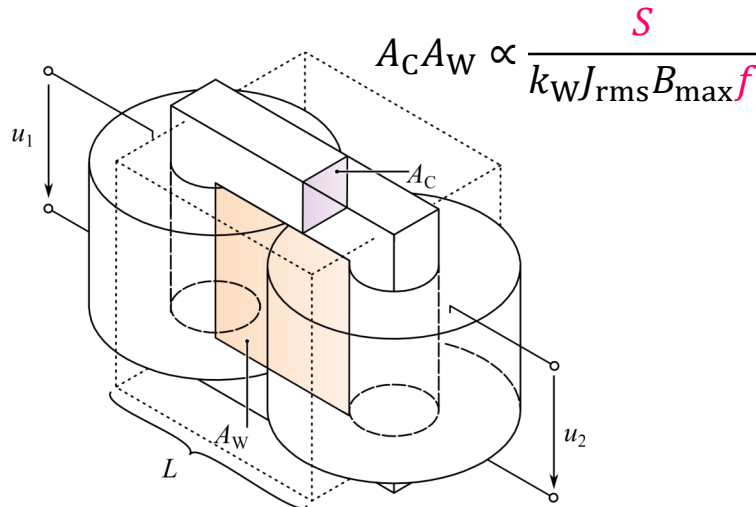
SST Concepts & Key Design Aspects

- Medium-Frequency Power Conversion
- Power Semiconductors
- Key SST Topologies
- **Medium-Frequency Transformers**
- Isolation Coordination
- Protection
- Reliability
- Standardization & EMC
- Construction & Testing



General Challenge of MF Transformers

- Higher Operating Frequency / Lower Unit Power Rating → Smaller Active Volume
- Isolation Requirements/Distances Don't Scale

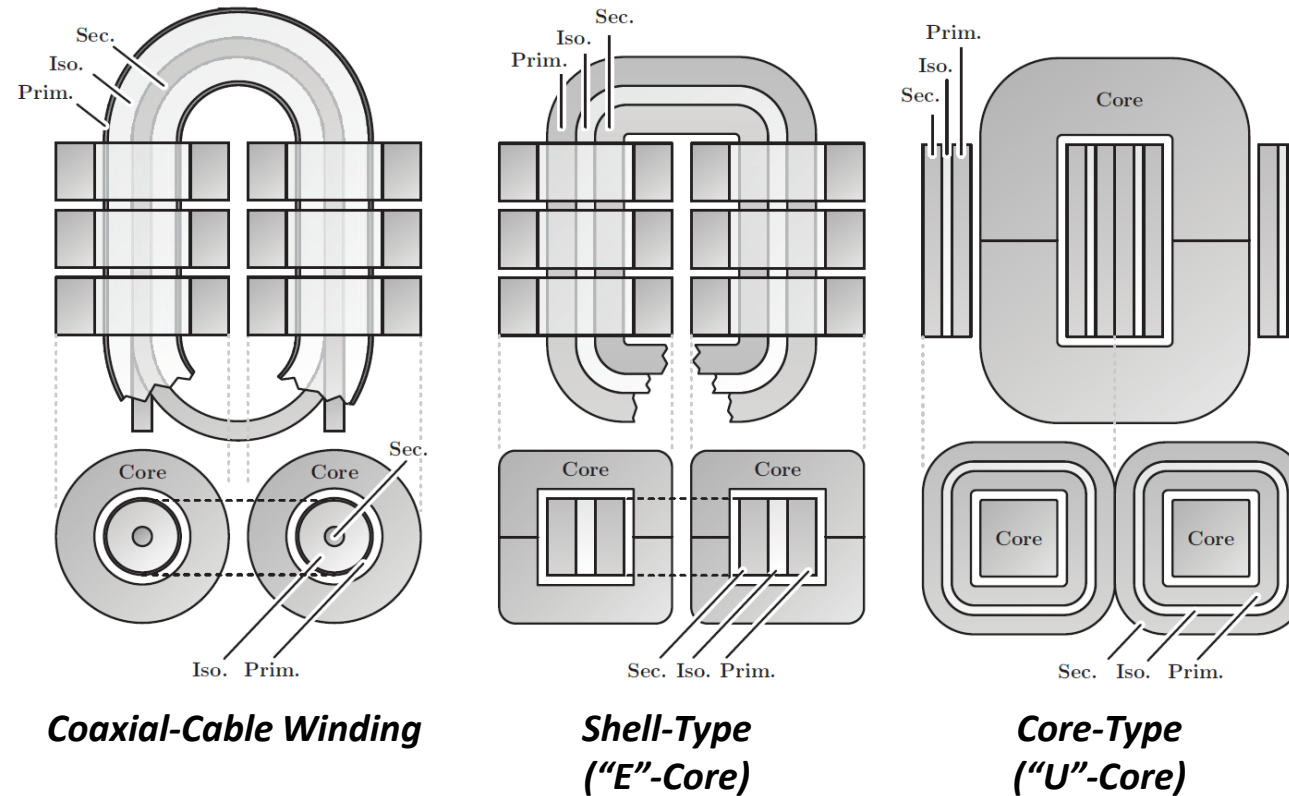


- MV Winding Cooling Through Isolation → Isolation vs. Cooling Trade-Off

- Solid Isolators → Bad Thermal Conductors
- Oil → Coolant And Isolator (!)



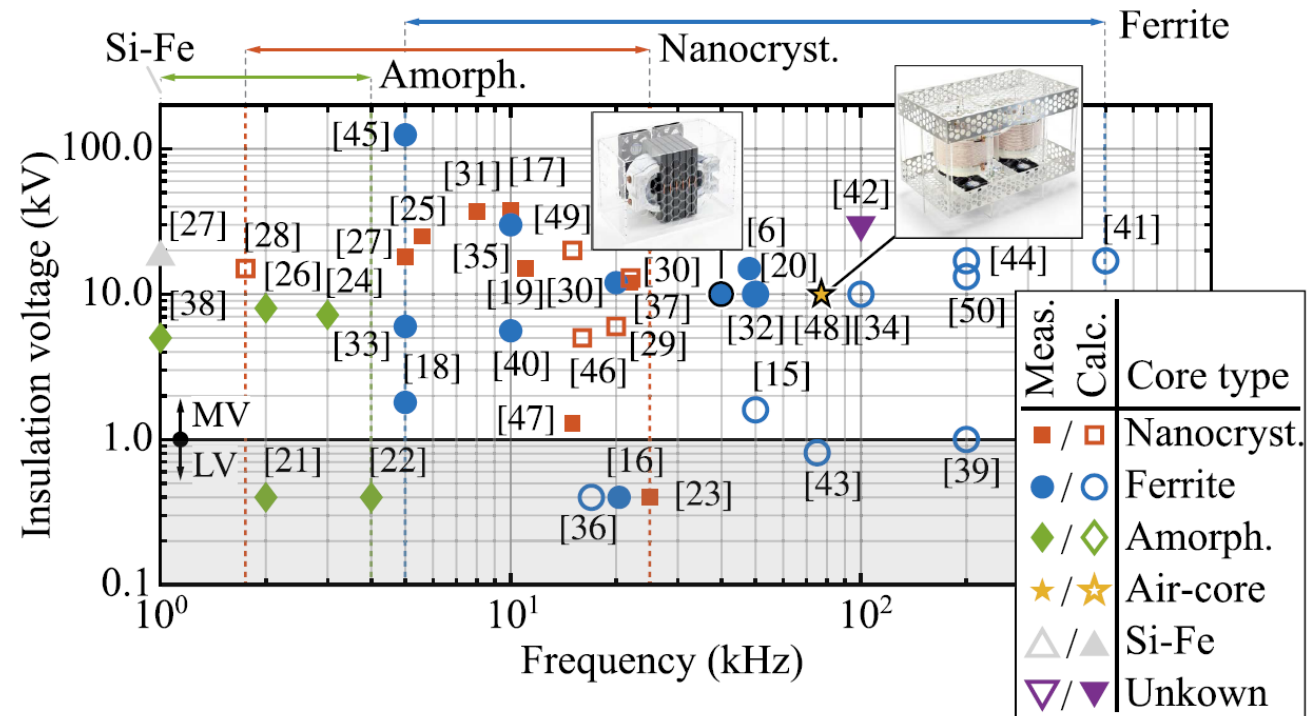
MF Transformer Design – Transformer Types



- Transformer Construction Types Very **Limited by Available Core Shapes** in this Dimension Range
- **Shell-Type has Been Favored** Given Its Construction Flexibility and Reduced Parasitic Components

MFT Core Materials

- Silicon Steel / Amorphous Iron / Nanocrystalline / Ferrite / Air (!)

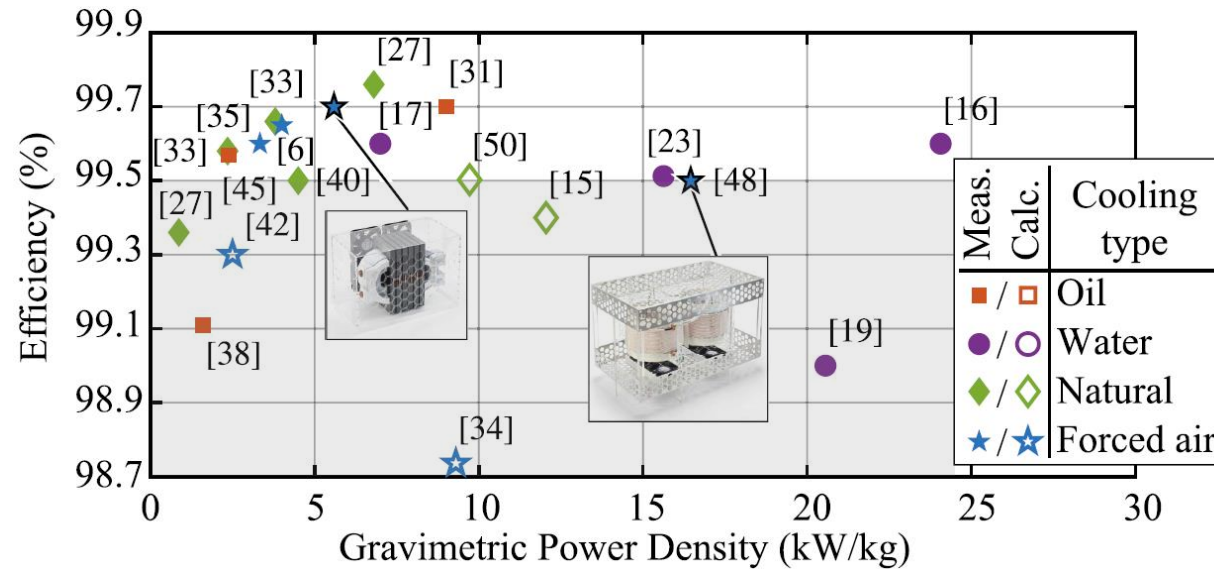


- Frequency-Dependent Choice of Core Materials



MFT Cooling Methods

- Natural Convection / Forced Air / Water / Oil

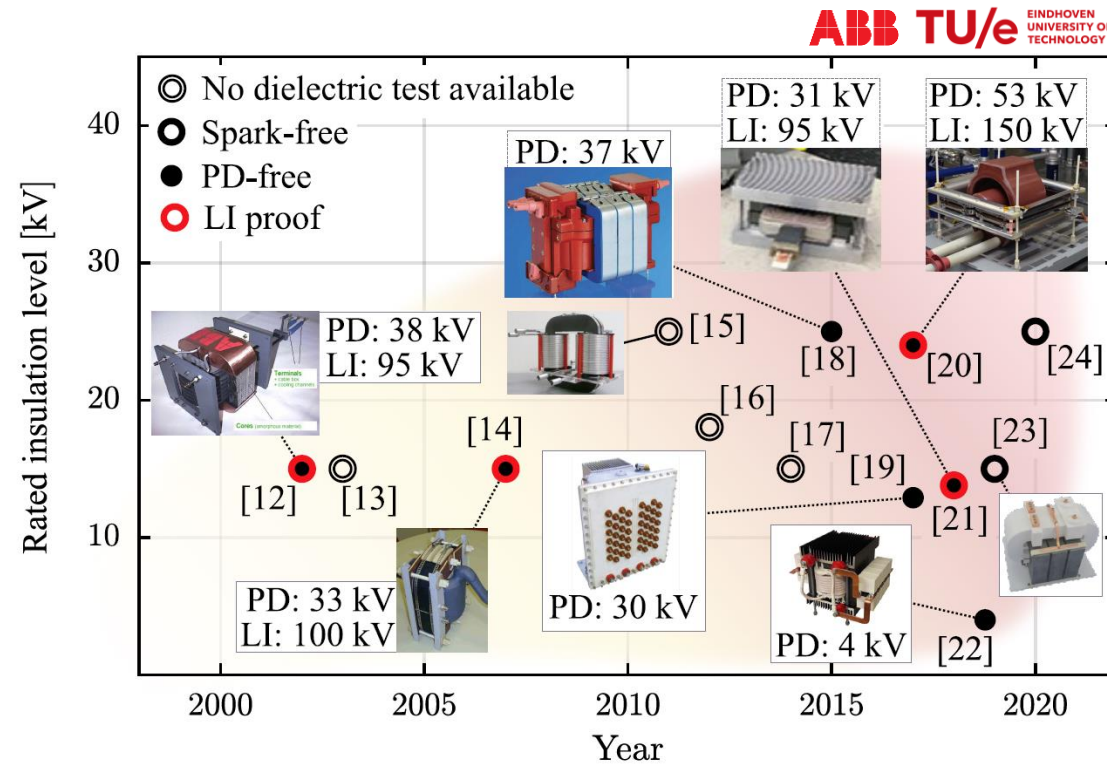


- High Efficiency Facilitates Air Cooling
- Liquid Cooling Facilitates Maximum (Gravimetric) Power Density / Needs External Heat Exchanger



MFT Isolation Systems

- Solids / Air / Oil
- Extreme Lightning-Impulse (LI) Test Voltage Requirements > 100 kV



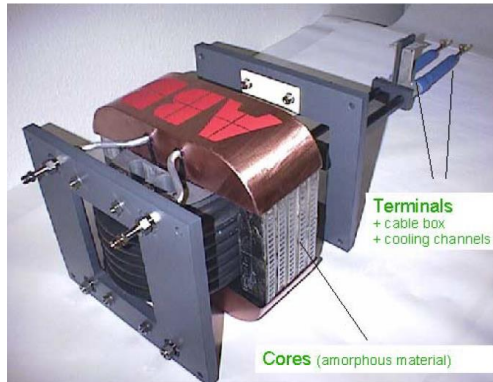
- Wide Variety of Published Designs / Many not Tested at Required LI Levels



MFT Example #1: Early Traction MFT Prototypes

■ Coaxial Cable Winding

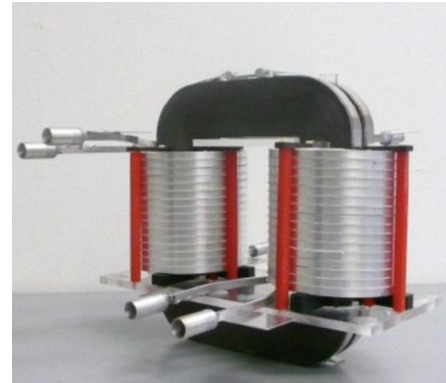
[Heinemann2002]



- 350 kVA / 10 kHz / < 50 kg
- Nanocrystalline Core
- 38 kV PD / 95 kV LI Surge
- Water Cooling w. Hollow Inner Conductor of Coax. Cable
- Unity Turns Ratio (!)

■ Core-Type

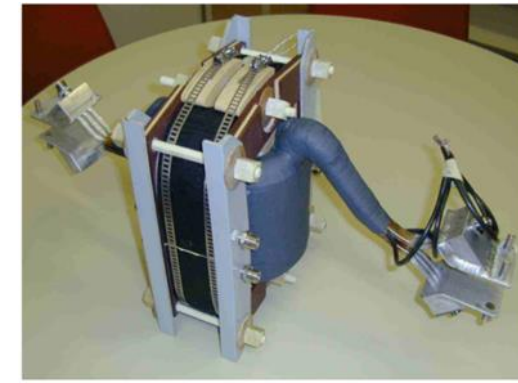
[Hoffmann2011]



- 450 kW / 5.6 kHz
- Nanocrystalline Core
- Oil Isolation / Core Cooling
- Hollow Conductor Water Cooling

■ Shell-Type

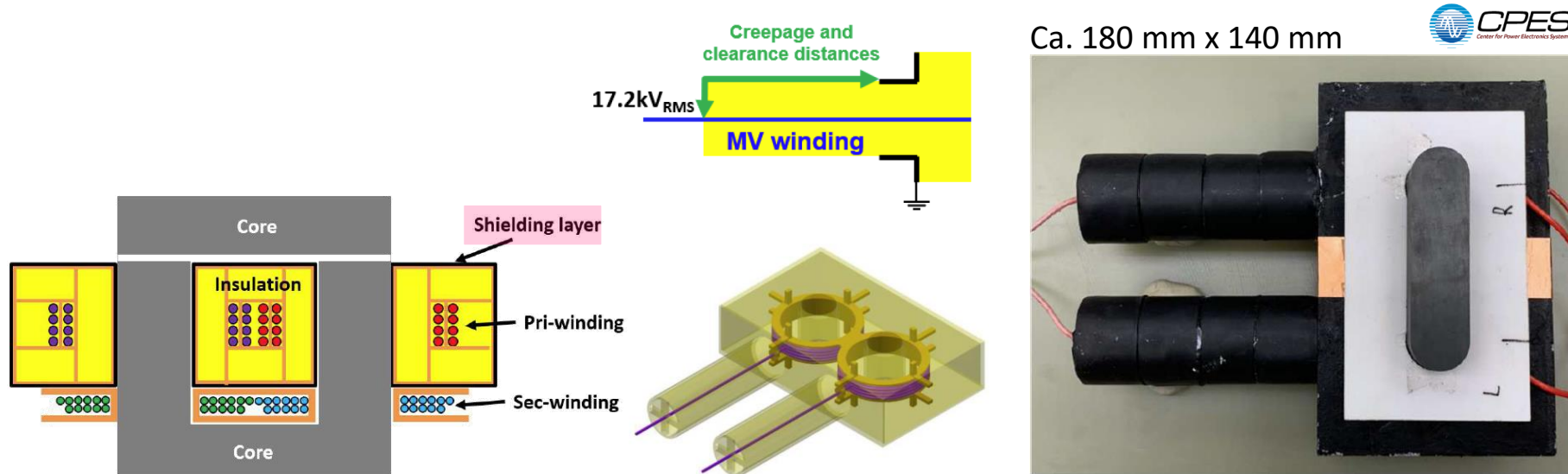
[Steiner2007]



- 500 kW / 8 kHz / 18 kg
- Nanocrystalline Core
- 33 kV PD / 100 kV LI Surge
- Water Cooling w. Hollow Conductors

MFT Example #2: 15 kW / 200 kHz

- Multi-Cell SST Connecting to 13.2 kV MV Grid / CLLC DC-DC Isolation Stages
- 15 kW / 200 kHz / > 99.4% Efficiency / PD Test @ 17.2 kV, HiPot Test 60 s @ 34 kV RMS
- Vacuum-Pressure Impregnation (VPI) with Silicone Gel Material

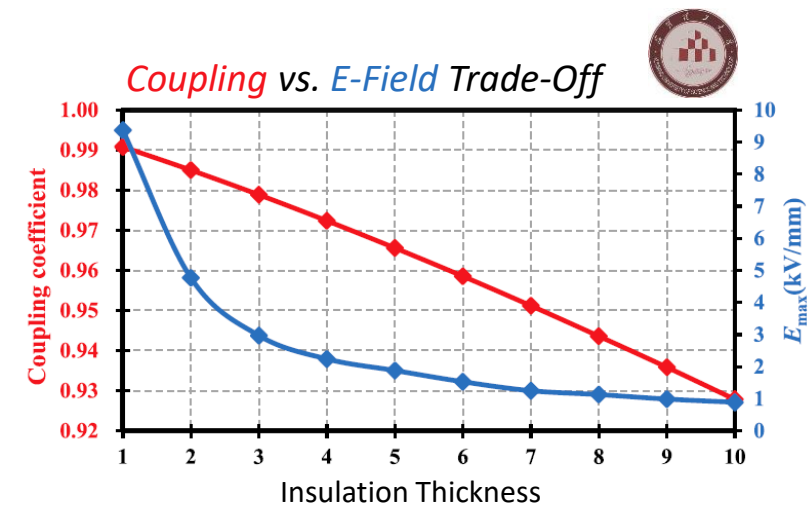
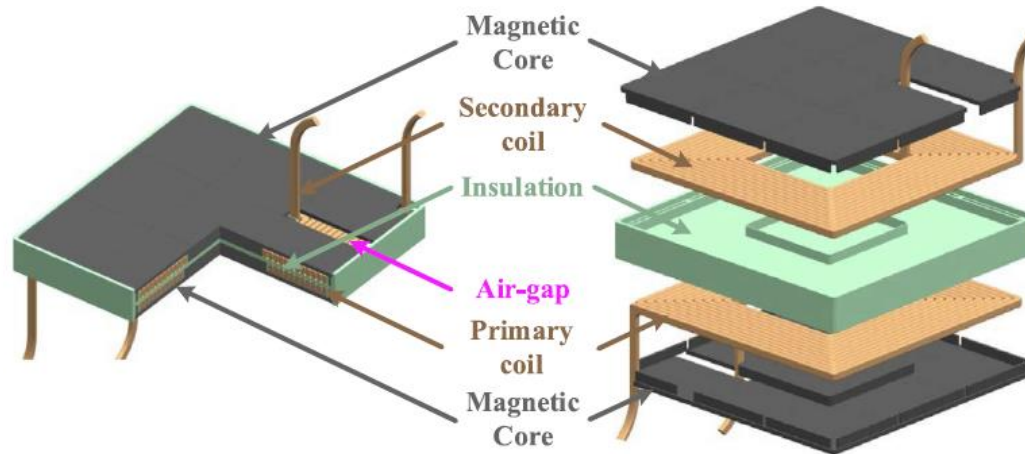


- Isolation System w. Semi-Conductive Shielding & E-Field Stress Grading on Bushings
- Bushing Overhead: > 50% of Total Volume (!)



MFT Example #3: 80 kW / 43 kHz

- Planar Transformer w. Low-Cost Ferrite Core
- Epoxy FR4 Isolation for 10 kV Distribution Grid / Tested at 42 kV RMS for 72 s



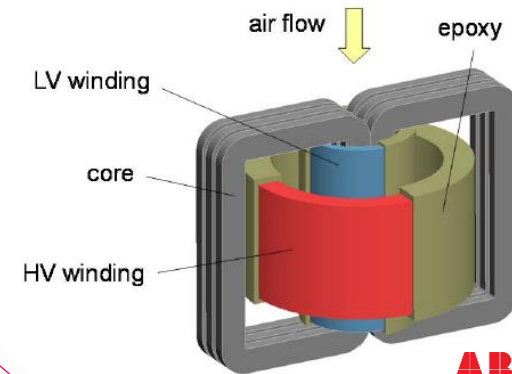
- Compact Design (21.1 kW/dm^3 , 308 mm x 308 mm x 40 mm) w. Large Cooling Surfaces
- Full-Load Efficiency of 99.25% (Calc.) → 850 V DC SiC CLLC DC-DC w. 99.3% @ 24 kW and 98.7% @ 80 kW (Meas.)



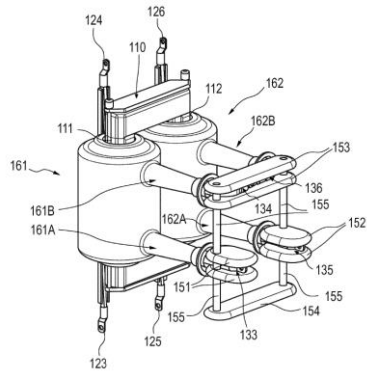
MFT Example #4: 240 kW / 10 kHz

- Hybrid Solid/Air Isolation System Design for 50 kV DC System Voltage
- Air Gap Wide Enough to Avoid PD / Discharges in Air Allowed During LI Tests (Solid Insulation Takes Over)
- Low El. Field in Solid Insulation During Normal Operation & High Surface Area for Cooling

- Full Dielectric Testing of Prototype
 - 70 kV rms / 1 min
 - 150 kV LI (10 Pos., 10 Neg. Pulses)
 - PD Inception at 35 kV rms (Target: 53 kV rms)
 - Improved Field Grading Necessary

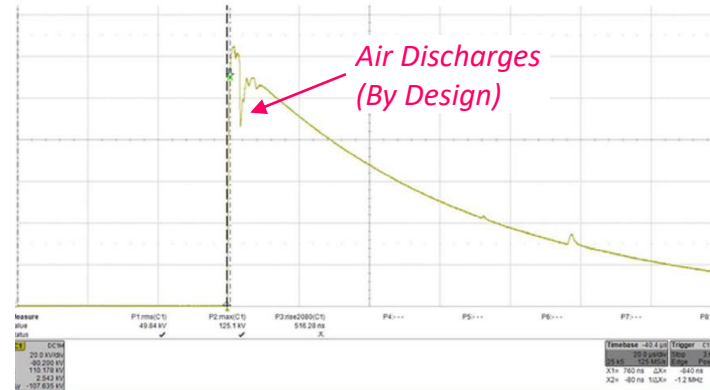


Field Grading Around Core

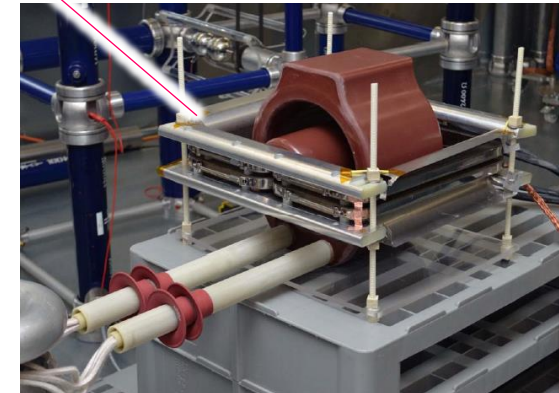


- Alt./Opt. Bushing Arrangement

150 kV LI Test



ABB

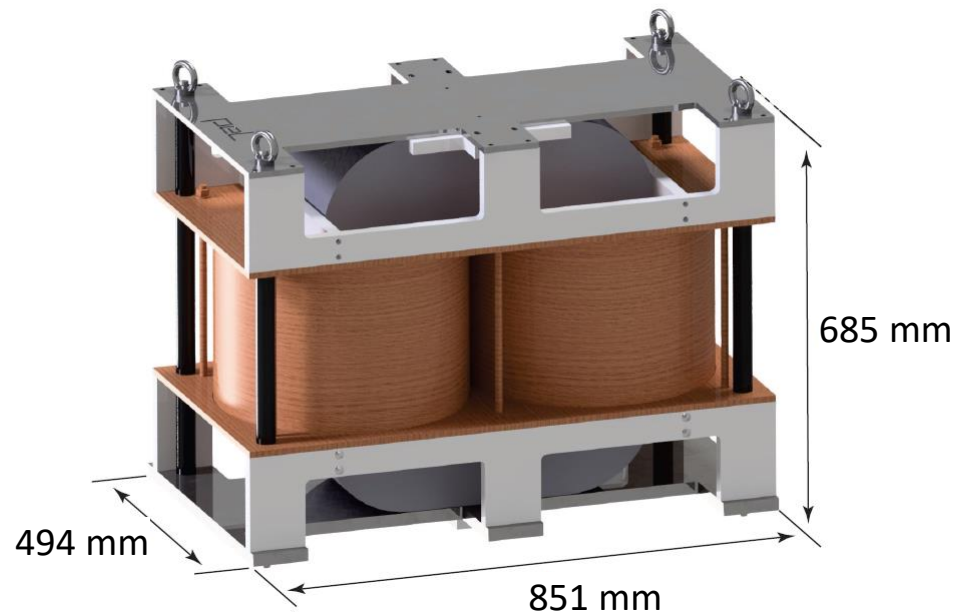


(Bushings Longer than Necessary)



MFT Example #5: 1 MW / 5 kHz

- **Two-Vessel Concept w. 2 x 2 Identical Oil-Immersed Windings** (Biodegradable Synthetic Ester Midel 7131)
- **Hollow Cooper Conductors (Deionized Water Cooling) & Air-Cooled Nanocrystalline Core (400 kg)**
- **2:1 Turns Ratio (Primary: 2 Wdg. in Series, Secondary: 2 Wdg. in Parallel)**

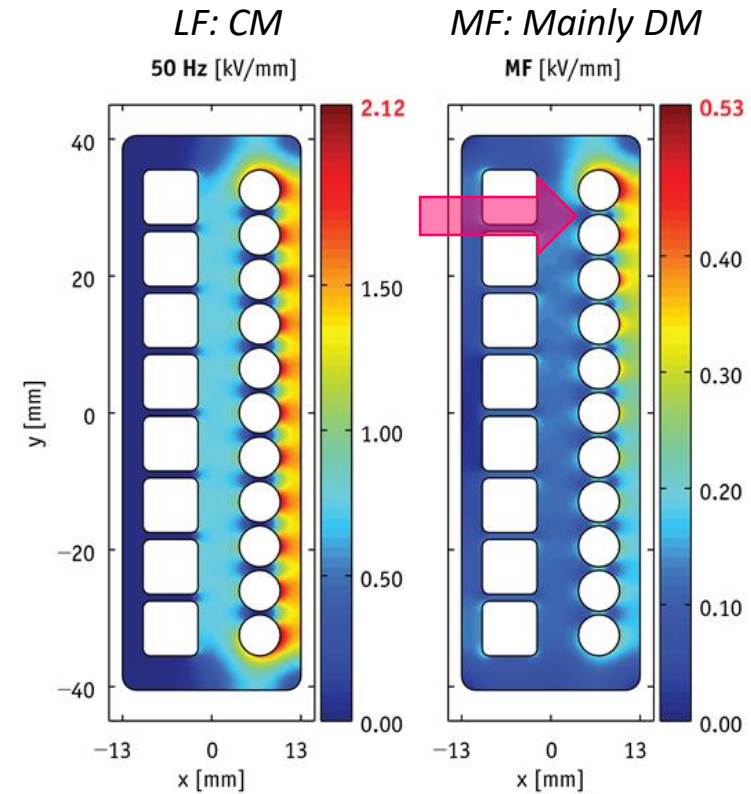
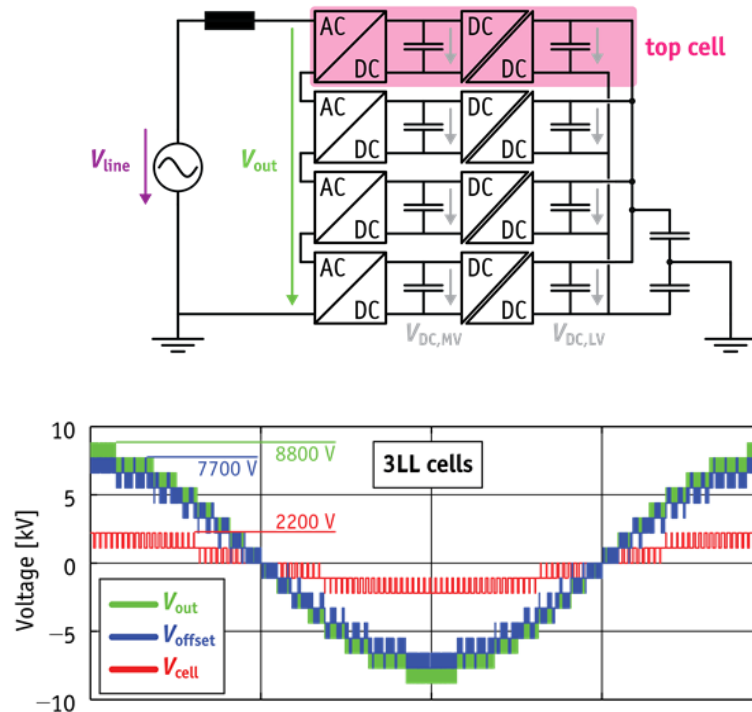


- Calculated MFT Performances: 99.18 % Efficiency, 3.47 kW/dm³ and 2.36 kW/kg Power Density
- Target Application: **IGCT-based 1 MW 10 kV to 5 kV DC Transformer**



Remark: Mixed-Frequency Electric Field Stress

- Combined Electrical Field Stress: **Large DC or Low-Frequency Comp. + Smaller Medium-Frequency Comp.**
- Common-Mode LF Stress + (Mainly) Differential-Mode DM Stress → DoF for Insulation Syst. Optimization



- Known From Electric Machine Insul. Systems / **Physical Breakdown & Ageing Mechanisms To Be Clarified**

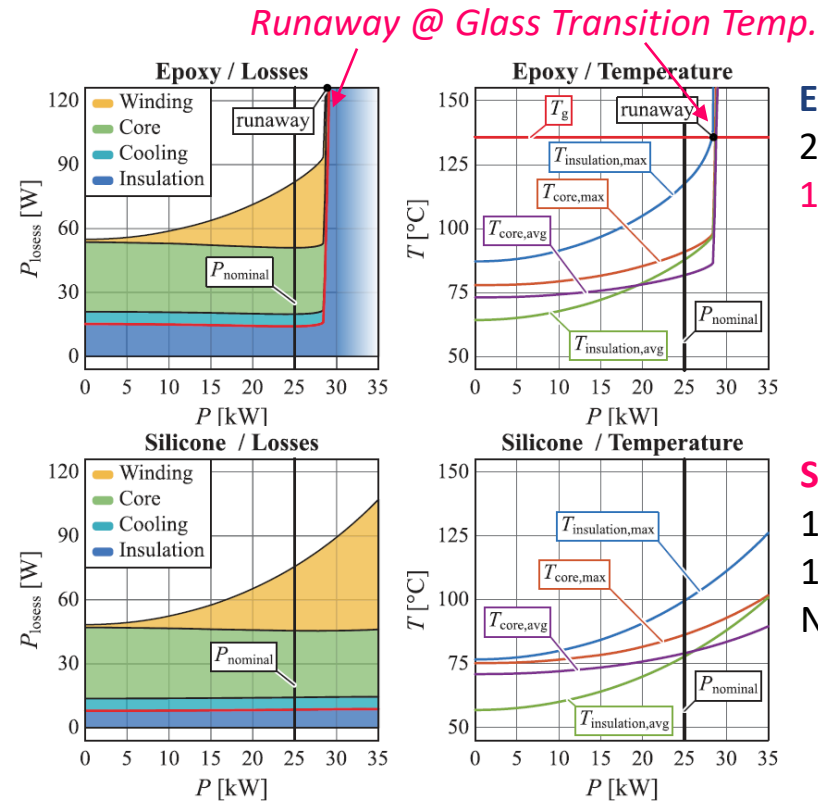
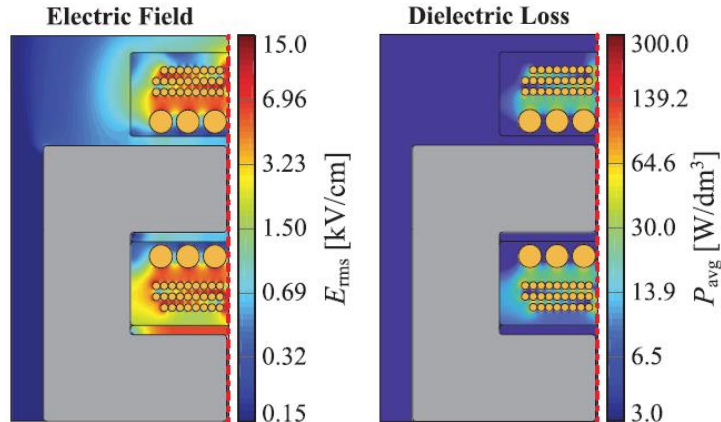


Remark: Dielectric Losses

- Frequency-Dependent Dielectric Losses / Full Description w. Freq.-Dep. & Temp.-Dep. Complex Permittivity
- Case Study w. 25 kW / 48 kHz MFT for 7 kV DC to 400 V DC DCX



$$P_{\text{diel}} \propto f \cdot E_{\text{rms}}^2$$



Epoxy Resin
 27% @ 0 kW
 17% @ 25 kW

Silicone Elastomer
 16% @ 0 kW
 11% @ 25 kW
 No Runaway

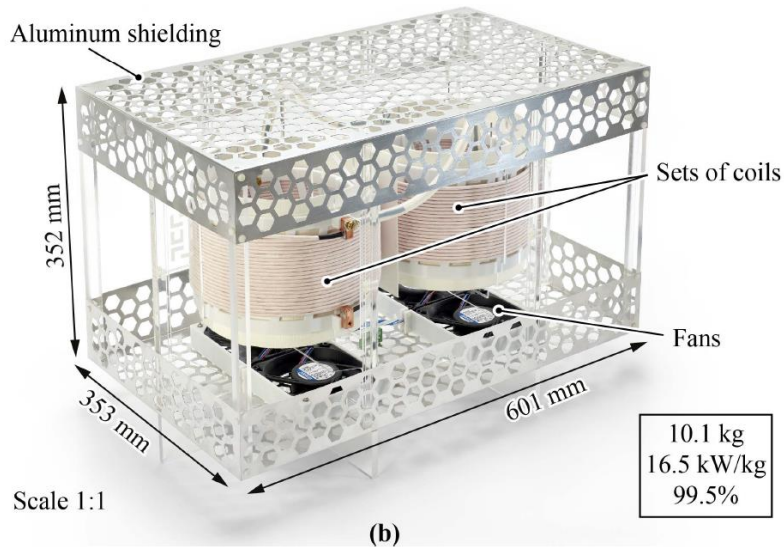
- Experimental Verification w. Small-Signal Diel. Spectroscopy and Calorimetric Meas. at MV Levels
- Careful Choice of Insulation Material is Essential (Field Strength/Thermal Cond./Dielectric Losses)



MFT Example #6: 166 kW / 77 kHz Air-Core Transformer

- MFT for 166 kW DCX (7 kV DC Input/Output) / Clarification of Efficiency vs. Weight Trade-Off
- Full Pareto Optimization / Design Selection $\eta_{DC-DC} \geq 99\%$ & Transf. w. Highest Gravimetric Power Density

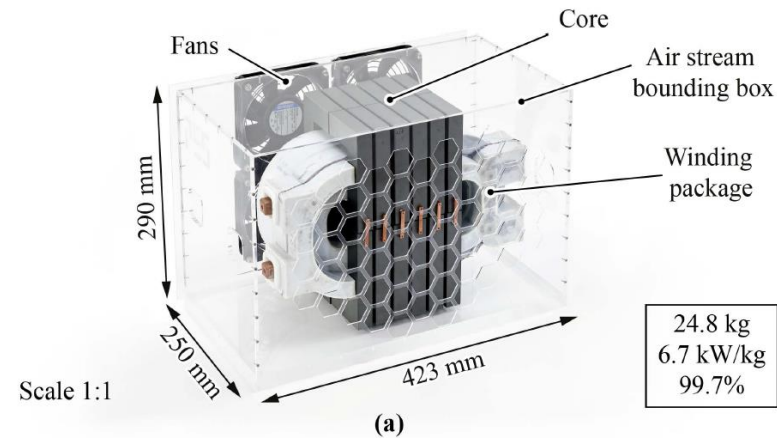
Air-Core Transformer (ACT) @ 77 kHz



$$m_{ACT} = 10.1 \text{ kg} \quad \eta_{ACT} = 99.5\%$$

$$m_{DC-DC} = 17.2 \text{ kg} \quad \eta_{DC-DC} = 99.0\%$$

Magnetic-Core Transf. (MCT) @ 40 kHz



$$m_{MCT} = 24.8 \text{ kg} \quad \eta_{MCT} = 99.7\%$$

$$m_{DC-DC} = 29.7 \text{ kg} \quad \eta_{DC-DC} = 99.2\%$$

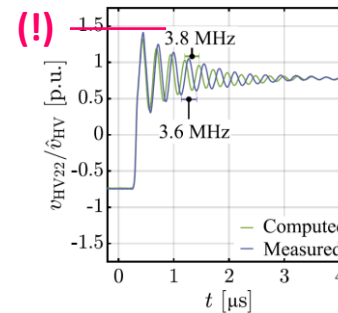
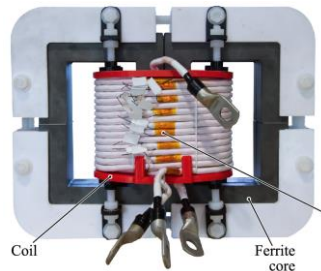
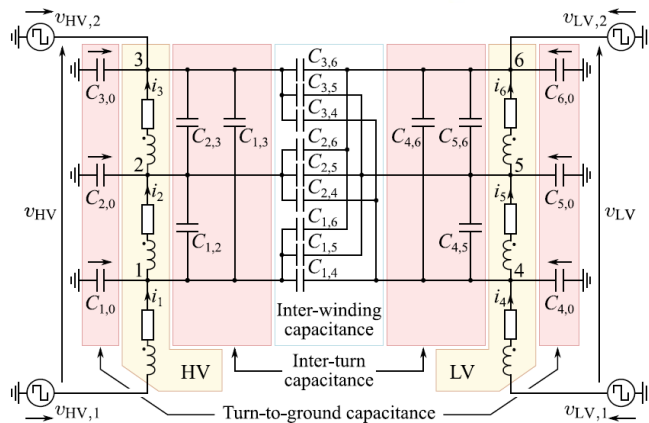
- ACT with Aluminum Shielding → Meets ICNIRP 2010 Guidelines for Exposure to Magn. Fields @ 20 cm
- ACT: A-Posteriori Creepage/Clearance Tuning by Barrier Elements / Isol. Test. $\pm 9.6 \text{ kV DC}$, 6.4 kV AC (1 min)



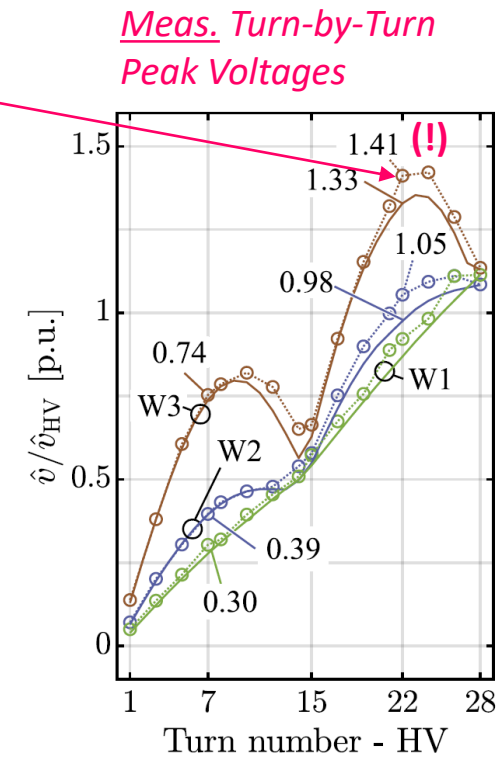
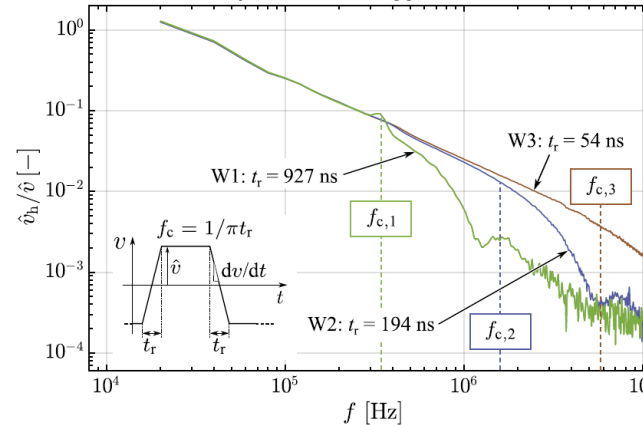
Remark: Parasitic Effects in MFTs

- PWM Excitation with Short Rise Times Non-Uniform Volt. Distr. in Windings (Prop. Delays, Resonances)
- Similar Phenomena Known from PWM Motor Drives

HF Model of a 3:3 MFT



PWM Spectra (Diff. Rise Times)



- Mitigation: Spectrum Corner Frequency < Transformer Series Resonant Frequency
- dv/dt Limitation (cf. Motor Drives!) or Minimizing Transformer Stray Capacitance



Anecdote: Litz Wire Issues

- Unequal Current Sharing in **Imperfectly Twisted Litz Wires**

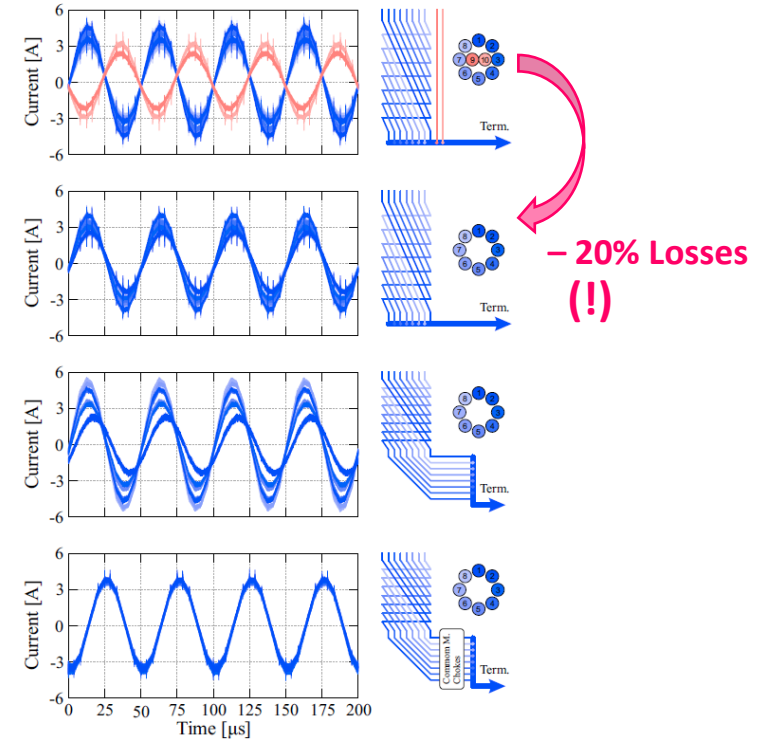


Incorrect Twisting

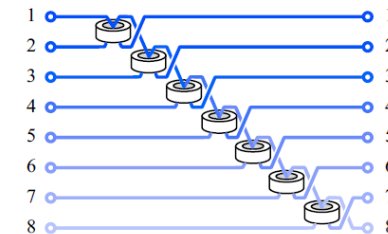
Center Bundles Removed

Impact of Terminations

Common-Mode Chokes

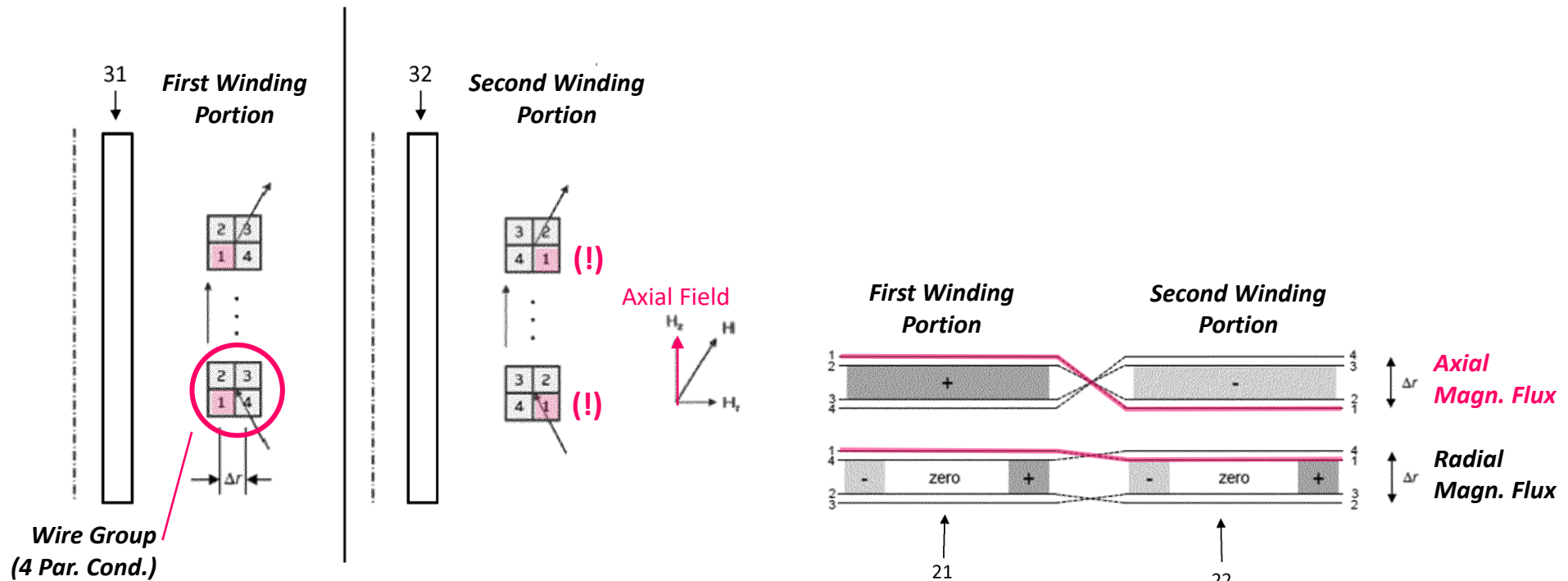


- **Common-Mode Chokes** Force Equal Current Sharing



MFT Windings with Parallel Conductors

- Risk for **Circulating Currents between Parallel Conductors** Due to Unequal Magnetic Flux Exposure
- Interchanging of Conductor Radial Positions Between Series-Connected Windings (on Different Core Limbs)
 - **Complete Flux Cancellation Between all Loops**



- Highly Important for Windings with **Parallel Foils**



Part II

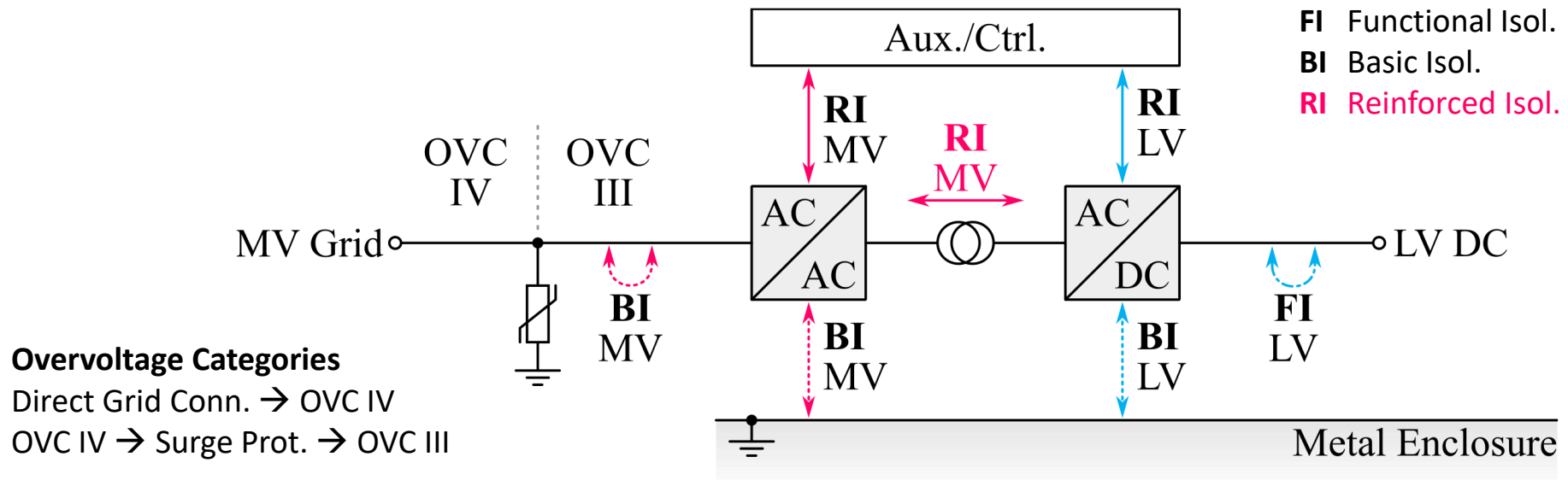
SST Concepts & Key Design Aspects

- Medium-Frequency Power Conversion
- Power Semiconductors
- Key SST Topologies
- Medium-Frequency Transformers
- **Isolation Coordination**
- Protection
- Reliability
- Standardization & EMC
- Construction & Testing



Isolation Coordination

- Decisive Voltage Class (DVC) of MV Side Circuitry: **DVC-D** (> 1 kV AC or > 1.5 kV DC)
- “Safe Isolation” Towards Circuits with Other DVC / Direct Contact → **RI** Required
- **BI** Towards Touchable Grounded Parts Sufficient / **BI** or **FI** Between Circuits with same DVC



- Simplified Example Only
Always Consider Applicable Standards in Full Detail!

SN Schweizer Norm
 Norme Suisse
 Norma Svizzera
EN IEC 62477-2

Safety requirements for power electronic converter systems and equipment - Part 2:
 Power electronic converters from 1 000 V AC or 1 500 V DC up to 36 kV AC or 54 kV DC



Clearance

■ **Example: 13.2 kV MV Grid / Based on IEC 62477-2 (Simplified)**

- **Step 1:** System Voltage 13.2 kV (Phase-to-Phase RMS)

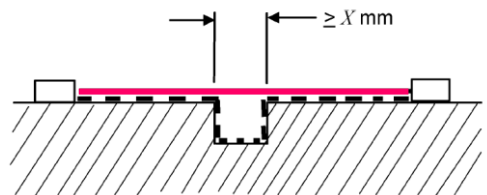
- **Step 2:** Overvoltage Category OVC-III x 1.6 for RI!

↓

- **Step 3:** Basic Impulse Level (BIL) / Lightning Imp. (LI): 63.3 kV (BI) 101.2 kV (RI) Tab. 101 (Linear Interp.)
 Temporary Overvoltage (peak): 42.7 kV (BI) 68.3 kV (RI) Tab. 101 (Linear Interp.)

- **Step 4:** Basic Isolation (BI) BIL 63.3 kV 120 mm Tab. 102 (Grid-Connected Circuit / No Interp.)
 TO 42.7 kV 106 mm Tab. 102 (Linear Interp.)

- **Reinforced Isol. (RI)** BIL 101.2 kV 220 mm Tab. 102 (Grid-Connected Circuit / No Interp.)
 TO 68.3 kV 183 mm Tab. 102 (Linear Interp.)



- Special Considerations Apply for $f > 30$ kHz (Appendix F) and for Altitudes > 2000 m
- Simplified Example Only – Always Consider Applicable Standards in Full Detail!



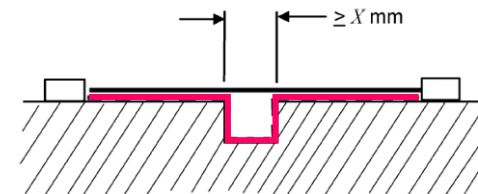
Creepage

■ Example: 13.2 kV MV Grid / Based on IEC 62477-2 (Simplified)

- **Step 1:** Working Voltage 13.2 kV (Exemplary; Depends on Specific Volt. Waveforms, etc.)
- **Step 2:** Pollution Degree PD-2 Typically Only Non-Conductive Pollution
- **Step 3:** Isol. Material Group Group I CTI ≥ 600 (CTI: Comparative Tracking Index)
- **Step 4:** Basic Isolation (BI) 66.4 mm Tab. 103 (Linear Interp..)
- Reinforced Isol. (RI) **132.8 mm** 2 x BI

■ But: Creepage Requirement **Cannot Be Smaller Than Clearance!**

Basic Isolation (BI)	120 mm
Reinforced Isol. (RI)	220 mm



- Special Considerations Apply for for $f > 30 \text{ kHz}$ (Appendix F)
- Simplified Example Only – **Always Consider Applicable Standards in Full Detail!**



Testing Requirements

- Basic Isolation BIL Test + AC or DC Test
- Reinforced Isolation BIL Test + AC or DC Test + PD Test (for Solid Insulation)

■ BIL Test

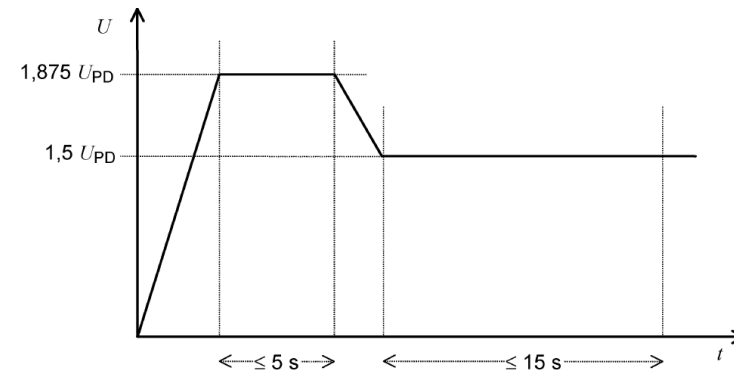
- 1.2/50 μ s Surges: 3 x Positive + 3 x Negative Polarity w. Pauses > 1 s
- Alternative: AC Test w. Peak Voltage = BIL, min. 3 Periods
- Type Test & Random Tests

■ AC or DC Test

- BI: Temporary Overvoltage
- RI: 1.6 x Temporary Overvoltage (Type Test Only)
- Type Test > 60 s / Routine Test > 1 s

■ PD (Partial Discharge) Test

- Test Voltage U_{PD} = Sum of All Repetitive Peak Volt. Sep. by Isol.
- Specific Voltage Profile / PD Discharges < 10 pC During Test
- Type Test & Random Tests



- Simplified Example Only – Always Consider Applicable Standards in Full Detail!

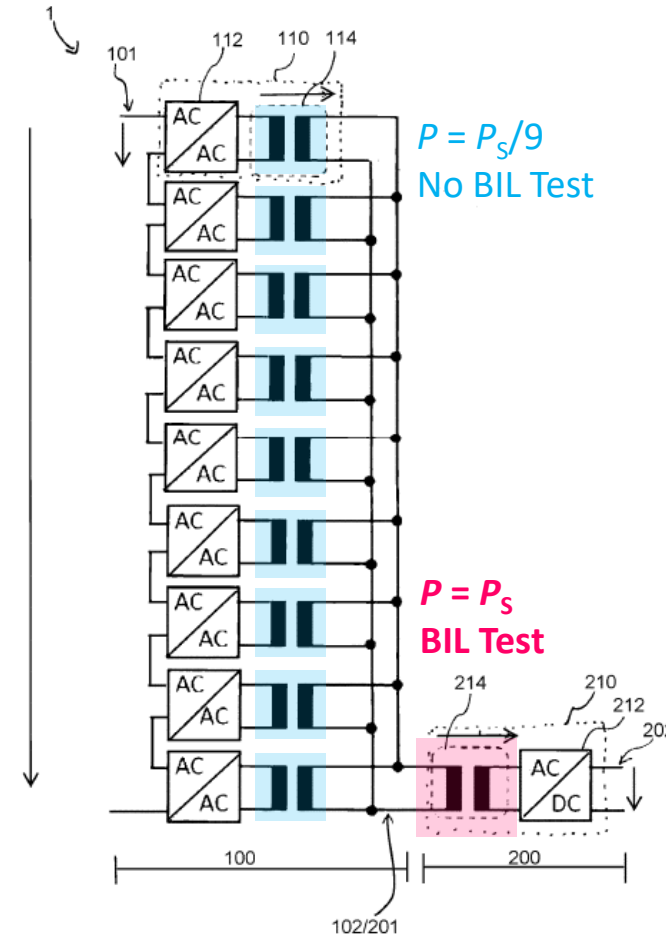
Remark: System-Level Perspective

■ Two-Stage Transformer Approach

First-Stage: Isolation for Nominal Voltage (PD Tests)

Second Stage: Isolation for BIL

■ More Compact Real. of 1st Stage MFTs, e.g., w/o Bushings

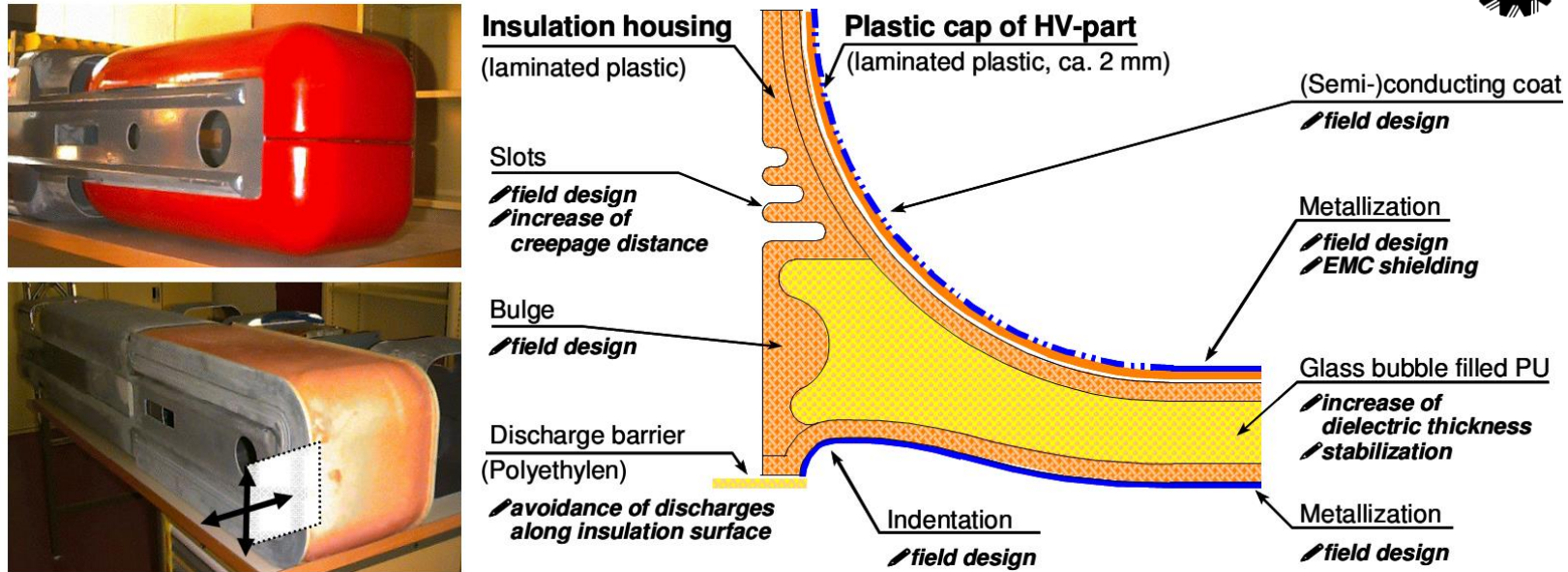


- Design DoF / Separate Optimization
- Especially Interesting for Lower Voltage & Power Ratings (Construction Overhead)



Isolation Design Example #1: Cell Housings

- Isolation Requirements not Limited to MFT
- Components on MV Potential (e.g., Heat Sink) Require Isolation Towards Cabinet/Ground

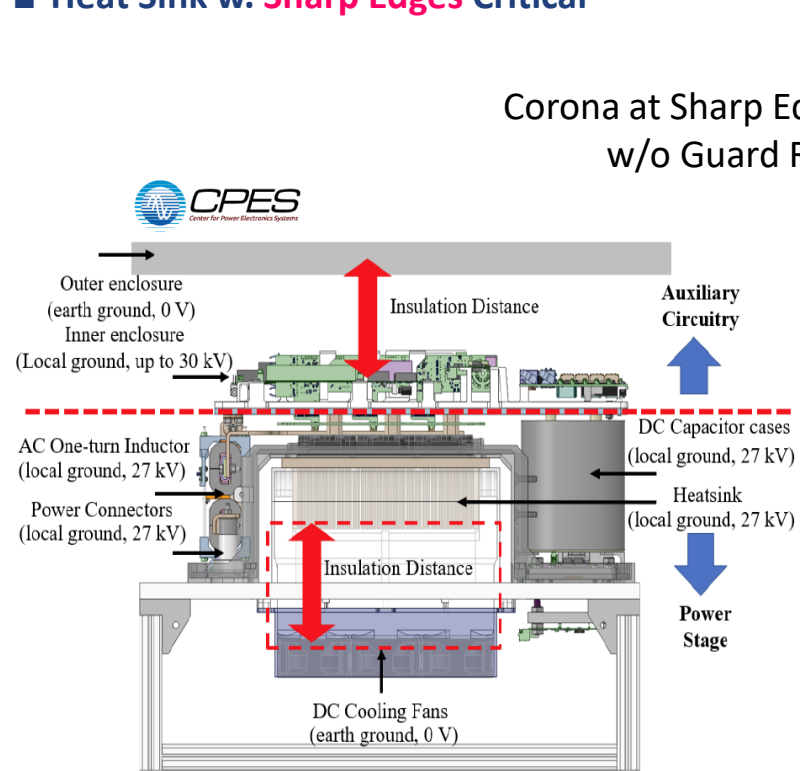


- Field Grading Concepts to Avoid Partial Discharges, etc.

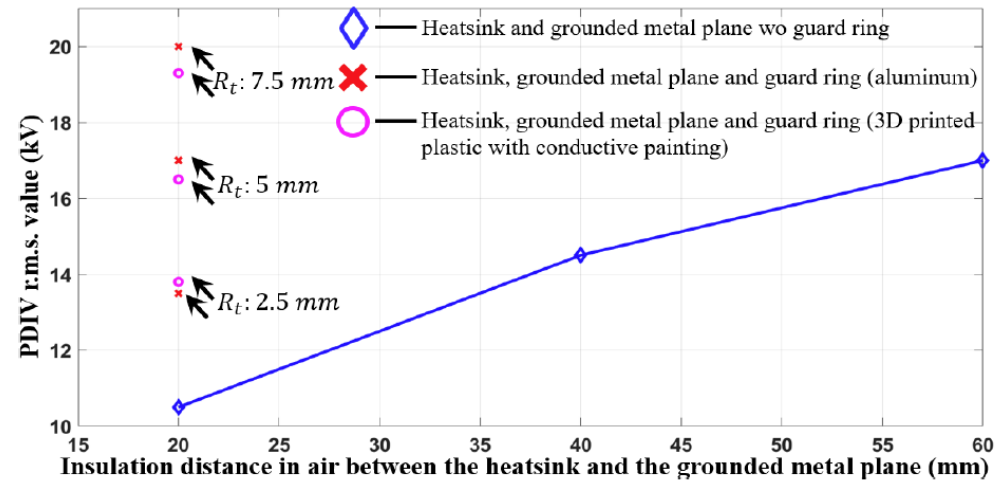
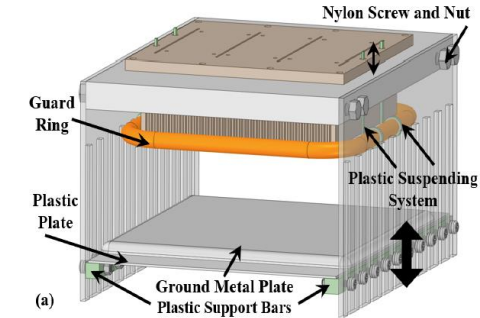
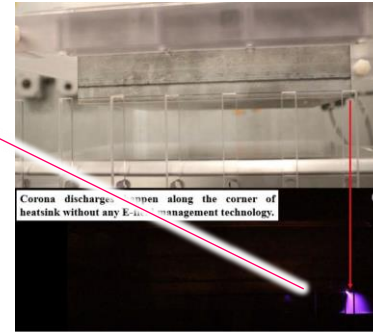


Isolation Design Example #2: Guard Rings

- Electric Field Management in a Stackable 10-kV SiC / 6-kV DC / 1-MW Full-Bridge PEBB
- Heat Sink w. Sharp Edges Critical



Corona at Sharp Edge w/o Guard Ring



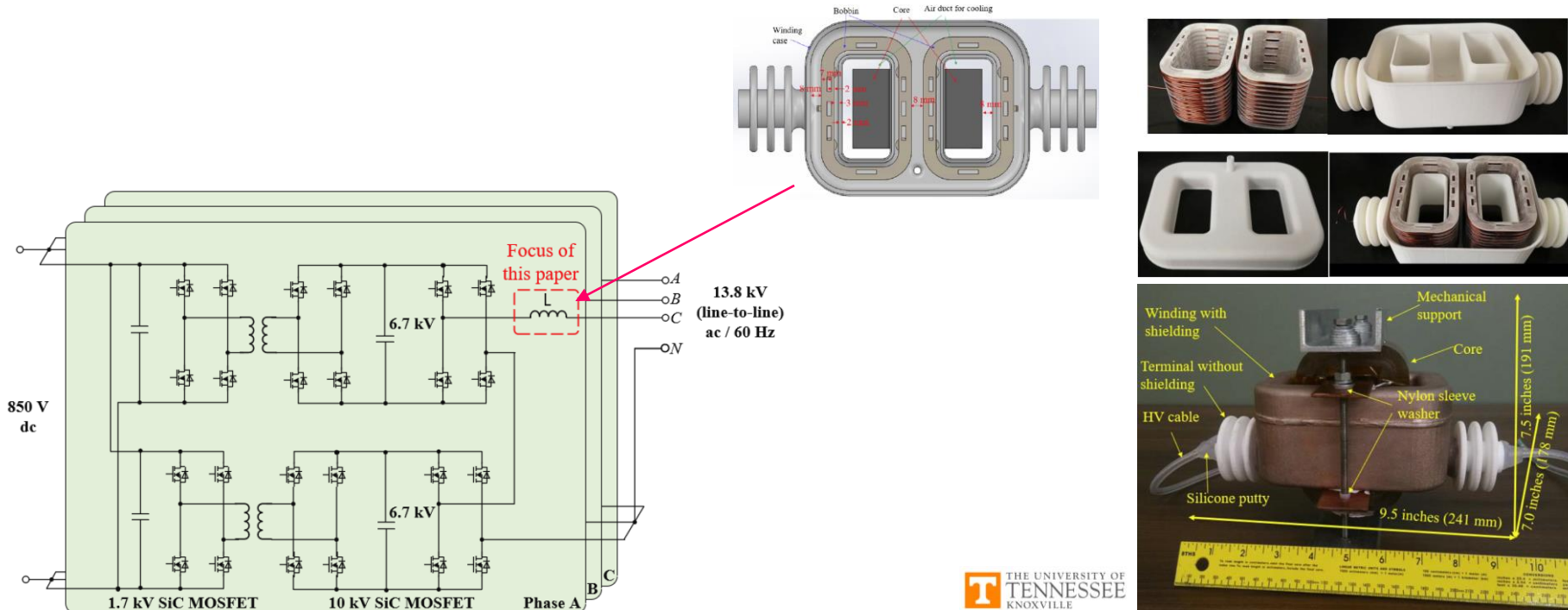
- Guard Rings Reduce Isolation Distance from 80 mm to 20 mm for 20 kV RMS PD Inception Voltage (PDIV)



Isolation Design Example #3: MV Inductor

■ 13.8 kV Grid Filter Inductor for 100 kW, 10-kV-SiC-Based Converter

- Specs.: 44 mH / 4.2 A RMS / 23 A Inrush / 40 kHz Eff. Sw. Freq. / PDIV > 10 kV RMS / BIL 95 kV



THE UNIVERSITY OF TENNESSEE KNOXVILLE

- Compartmentalized Winding to Reduce Max. Layer-Layer Stress
- Silicone Elastomer Insulation / Field Grading w. Shielding Layer on Winding Package Surface
- DC HiPot Test Pass @ 46 kV for 1 min / PD Test Pass @ 12.1 kV RMS



Part II

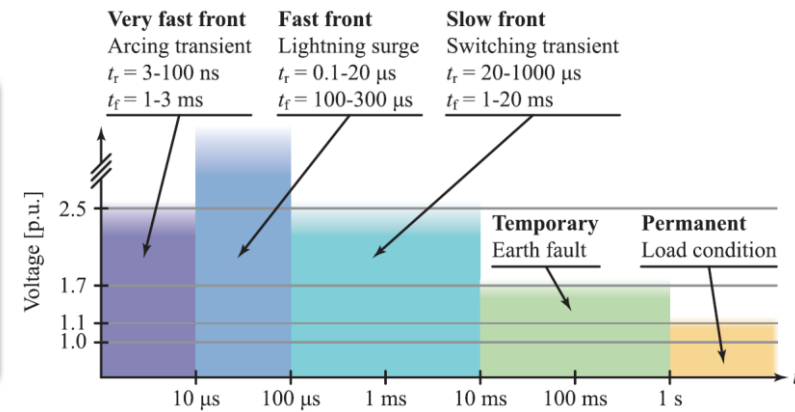
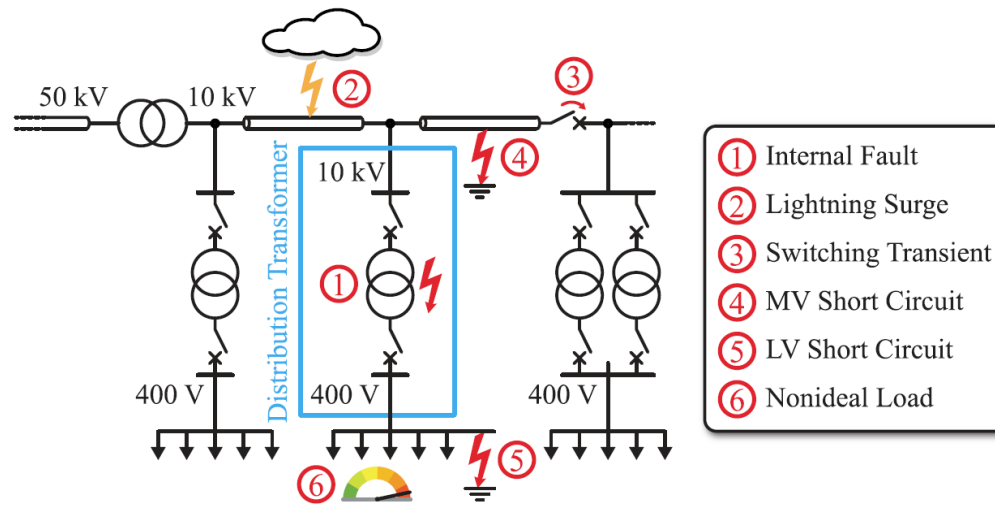
SST Concepts & Key Design Aspects

- Medium-Frequency Power Conversion
- Power Semiconductors
- Key SST Topologies
- Medium-Frequency Transformers
- Isolation Coordination
- **Protection**
- Reliability
- Standardization & EMC
- Construction & Testing



Potential Fault Situations in MV and LV Grids

Extreme Overvoltage Stresses on the MV Side for Conv. Distr. Grids



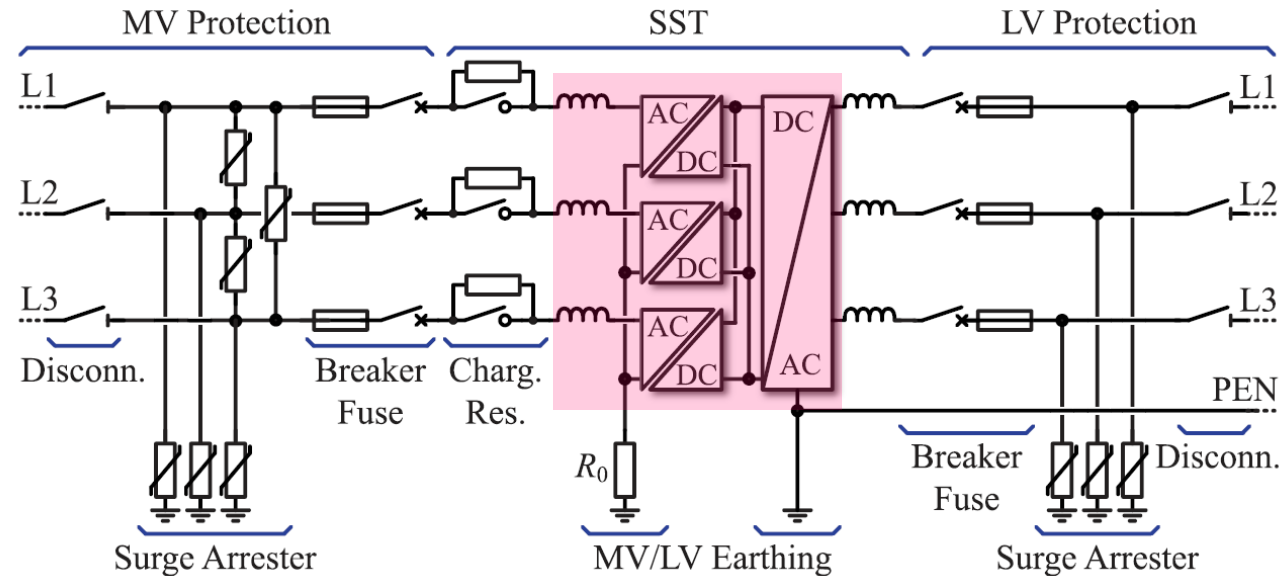
Short-Circuit Events on MV and LV Side

- Protection Scheme Needs to Consider Selectivity / Sensitivity / Speed / Safety / Reliability



Possible SST Protection Concept

■ Extreme Overvoltage Stresses on the MV Side for Conv. Distr. Grids



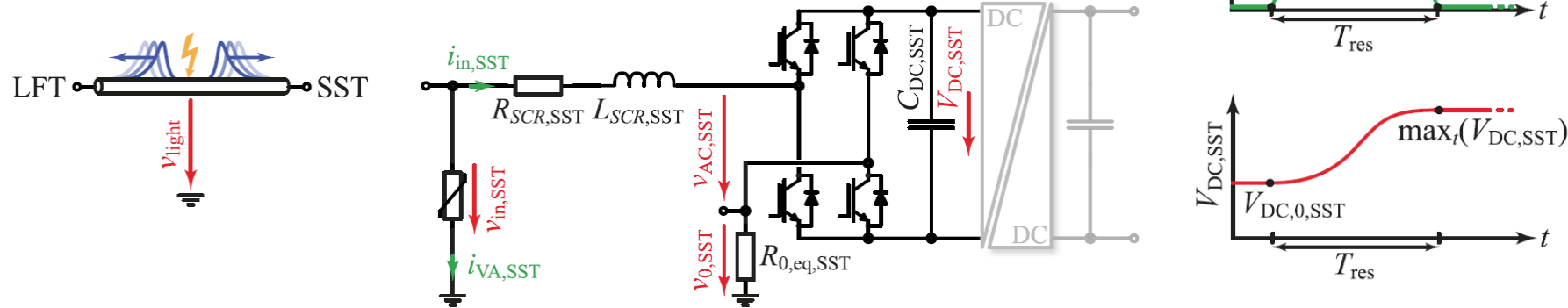
■ Short-Circuit Events on MV and LV Side

- Protection Scheme Needs to Consider Selectivity / Sensitivity / Speed / Safety / Reliability



Example: Surge Protection

- Lightning Impulse Defines Dielectric Strength Requirements (Isol. Coord.)
- But Consider Also **Surge Energy Propagation Inside of the SST**



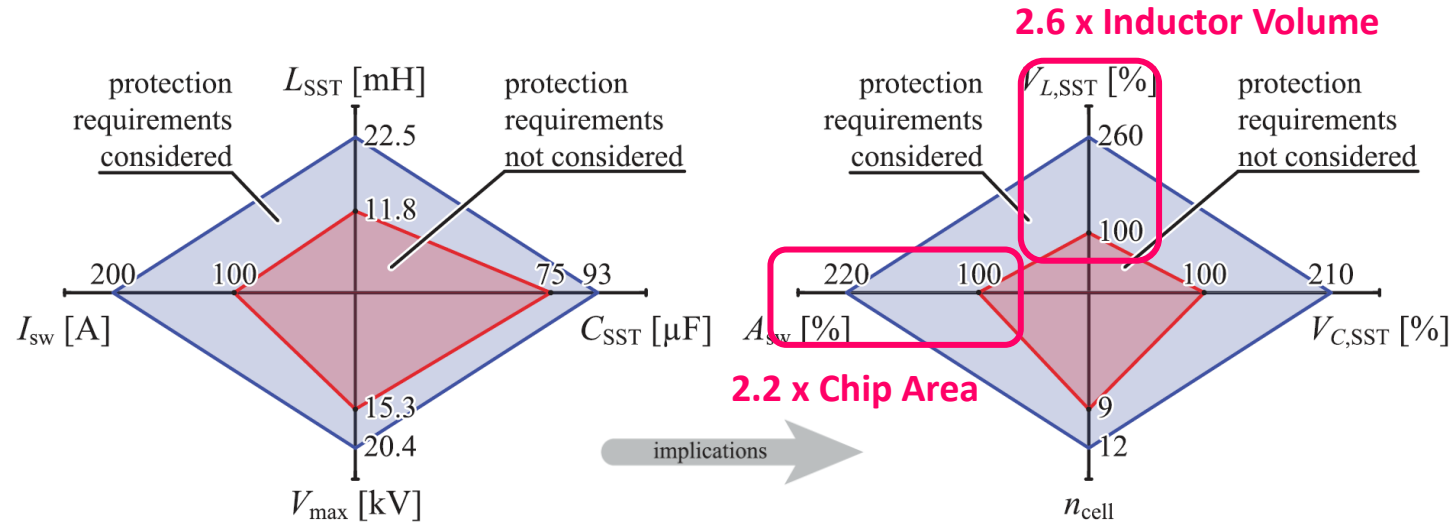
- Depends on Operating State of SST (Active/Passive) & Grounding Scheme
- Defines Minimum Values for Input Ind., DC-Link Cap., Blocking Capability, ... → **Strongly Affects SST Design!**



Protection Impact Case Study

Impact of Protection Requirements on Example SST Design (1 MVA @ 10 kV Grid)

- 9 Cells → 12 Cells
- Si IGBTs 1700 V, 100 A → 1700 V, 200 A
- L_{SST} from IEEE 519 → L_{SST} from SCR = 7%

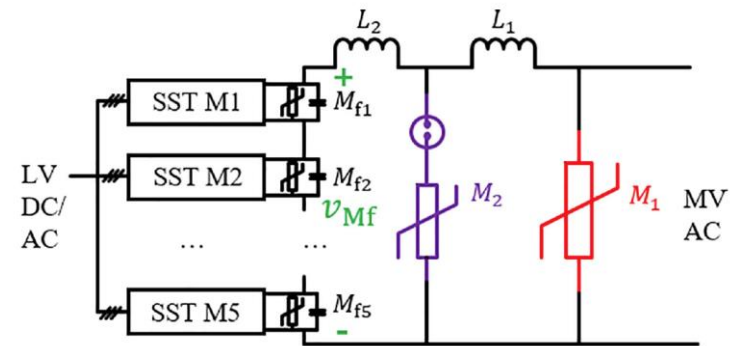


Significant Impact on MV-Side Power Electronics Dimensioning!

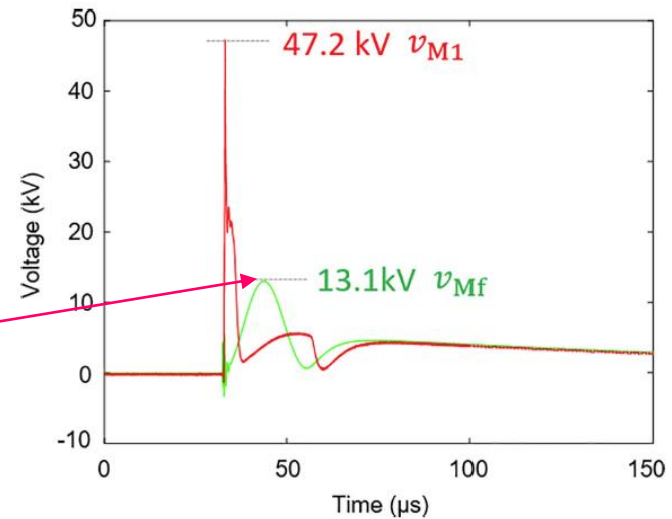


Example: Lightning Protection Scheme

- Two-Stage Lightning Protection Scheme for 7.2 kV / 50 kVA Current-Source SST
- Five Stacked Cells w. 3.3 kV SiC → Max. Total Blocking Volt. 16.5 kV



M1: 15 kV Gapped MOV
 M2: 3 kV Gapped MOV
 (Eff. Sparkover @ 12 kV > Peak Grid Volt.)
 L1, L2: 150 μH Air-Core Inductors

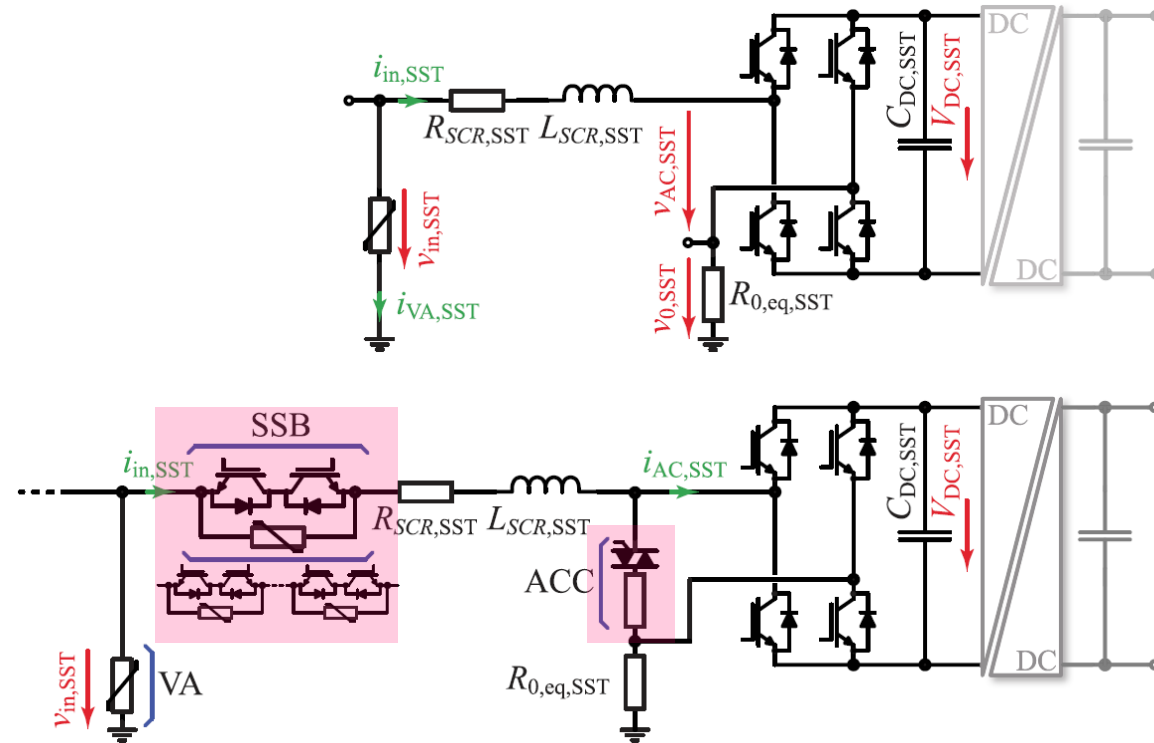


- 90 kV LI Test → Stack Input Voltage < 13.1 kV



Outlook: Advanced Protection Schemes

- Mitigation of High Impact on SST Design: **Solid-State Breakers** / AC Crowbar / ...



- Applications in Industrial Grids / Microgrid w. Central OV Prot. & Coord. SC Protection / Fault Cur. Limit.



Part II

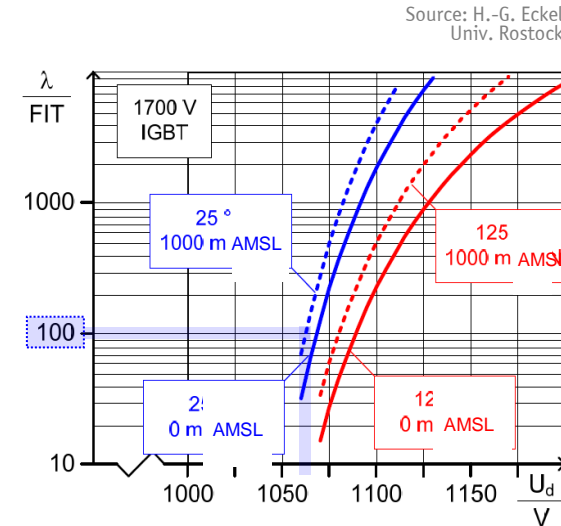
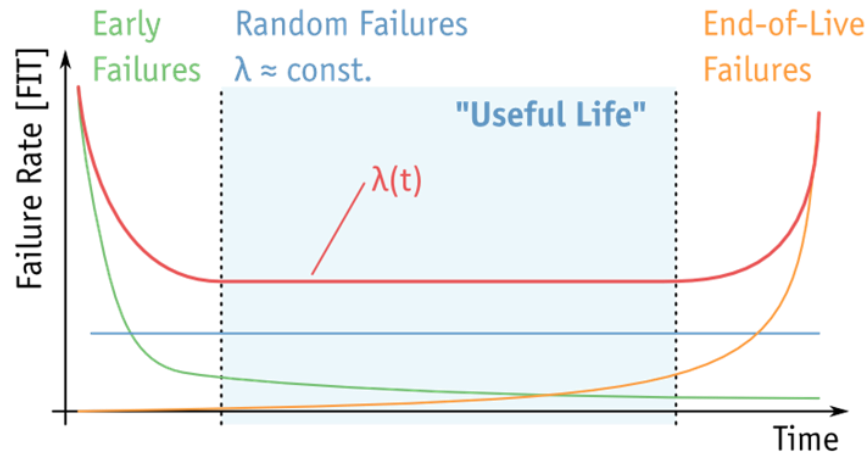
SST Concepts & Key Design Aspects

- Medium-Frequency Power Conversion
- Power Semiconductors
- Key SST Topologies
- Medium-Frequency Transformers
- Isolation Coordination
- Protection
- **Reliability**
- Standardization & EMC
- Construction & Testing



Reliability Modeling (1) – Failure Rate

- Failure Rate $\lambda(t)$ is a Function of Time – “Bathtub Curve”
- Useful Life Dominated by Random Failures $\rightarrow \lambda(t) = \text{const.}$ (Example: Cosmic Rays \rightarrow Semicond. Failures)
- $[\lambda] = 1 \text{ FIT}$ (1 Failure in 10^9 h)



- Sources for Empirical Component Failure Rate Data: MIL-HDBK-217F, IEC Standard 62380, etc.



Reliability Modeling (2) – Reliability Function

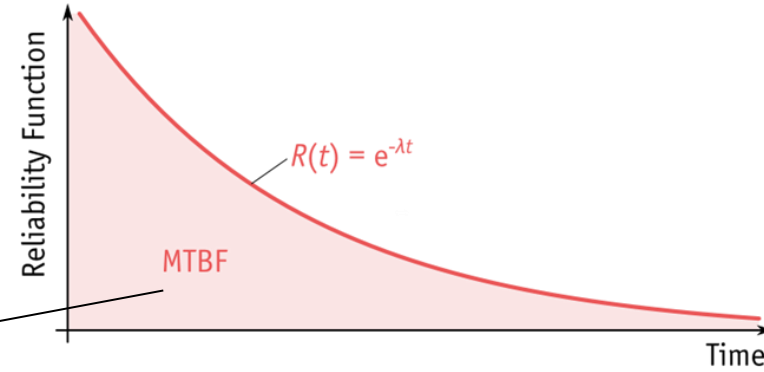
- Reliability Function $R(t)$: Probability of System being Operational after Time t

$$R(t) = e^{-\int_0^t \lambda(x) dx} = e^{-\lambda t}$$

$\lambda(t) = \text{const.}$

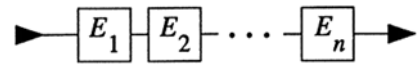
- Mean Time Between Failures (MTBF)

$$\text{MTBF} = \int_0^\infty R(t) dt = \int_0^\infty e^{-\lambda t} dt = \frac{1}{\lambda}$$

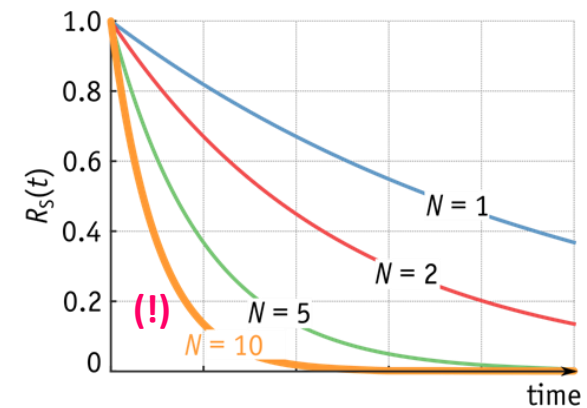


- Multiple Elements: Series Structure

$$\lambda_S = \sum_{i=1}^n \lambda_i$$

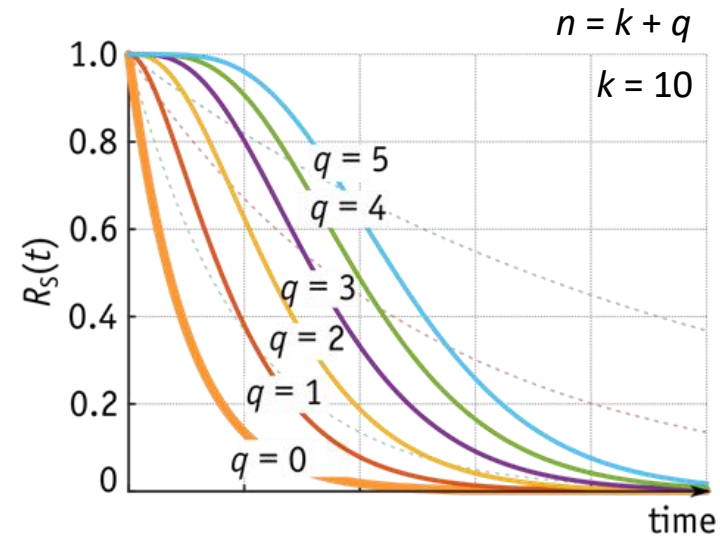
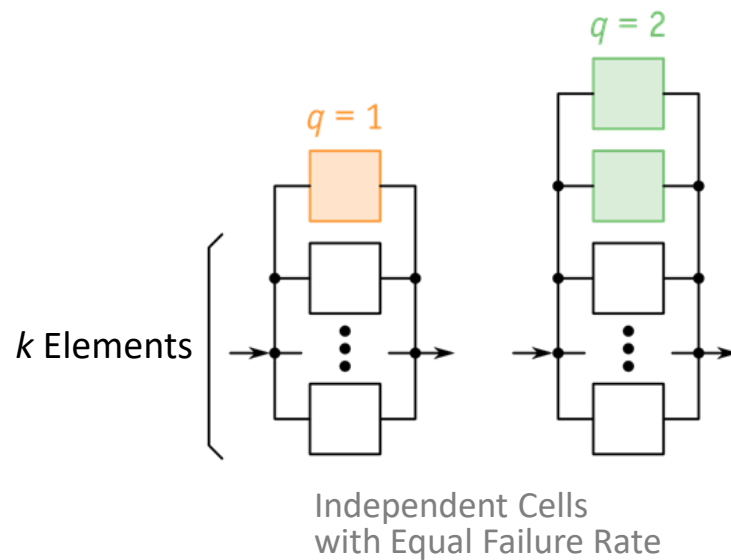


Independent Cells with Equal Failure Rate



Redundancy in Multi-Cell Systems

- **k-out-of-n Redundancy: System is Operational if at Least k-out-of-n Subsystems are OK**
 - Subsystems: Converter cells, etc.

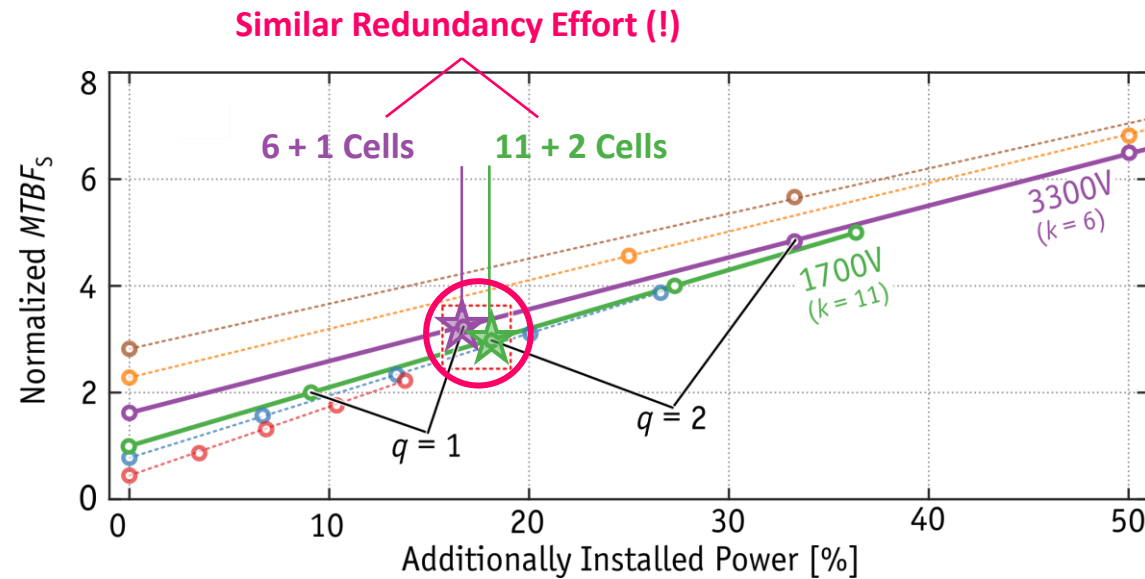


- **Redundancy Significantly Improves System Level Reliability (!)**



Cost of Redundancy

- **Redundant Cells = Additionally Installed But Unused Power Processing Capability**
- **Example: Phase Stacks with Same Total DC Voltage & Different Number of Cells**

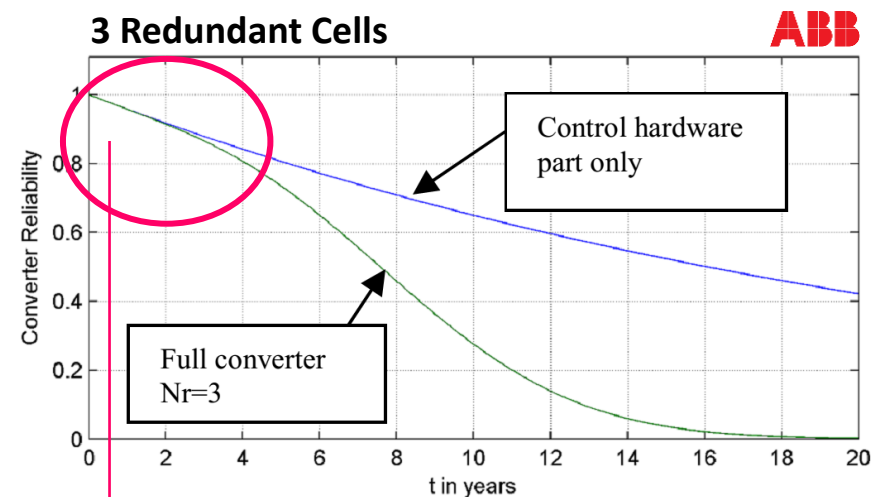
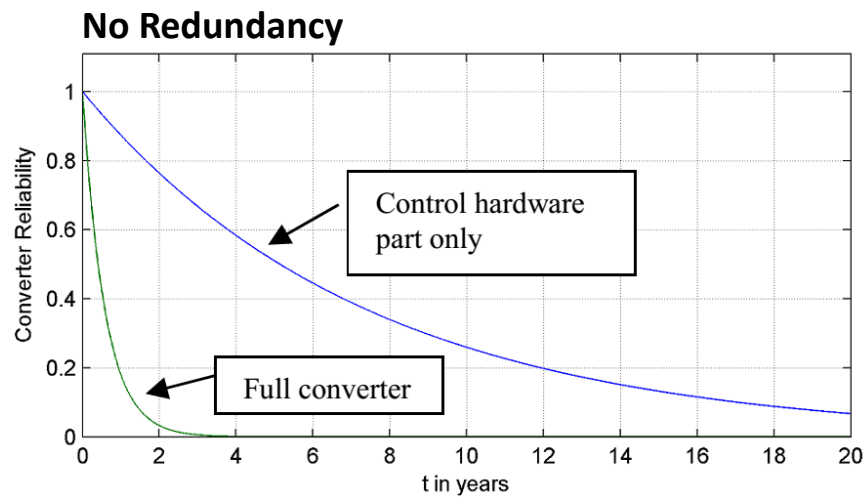


- **Similar Added Power Capability → Similar Normalized MTBFs**
- **Caution: Simplified Consideration / Beware Overheads and Reliability Bottlenecks**



Reliability “Bottlenecks”

- Very Effective Reliability Improvement by Means of Cell-Level Redundancy – Too Good to Be True?



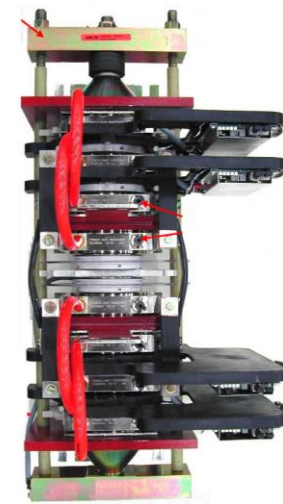
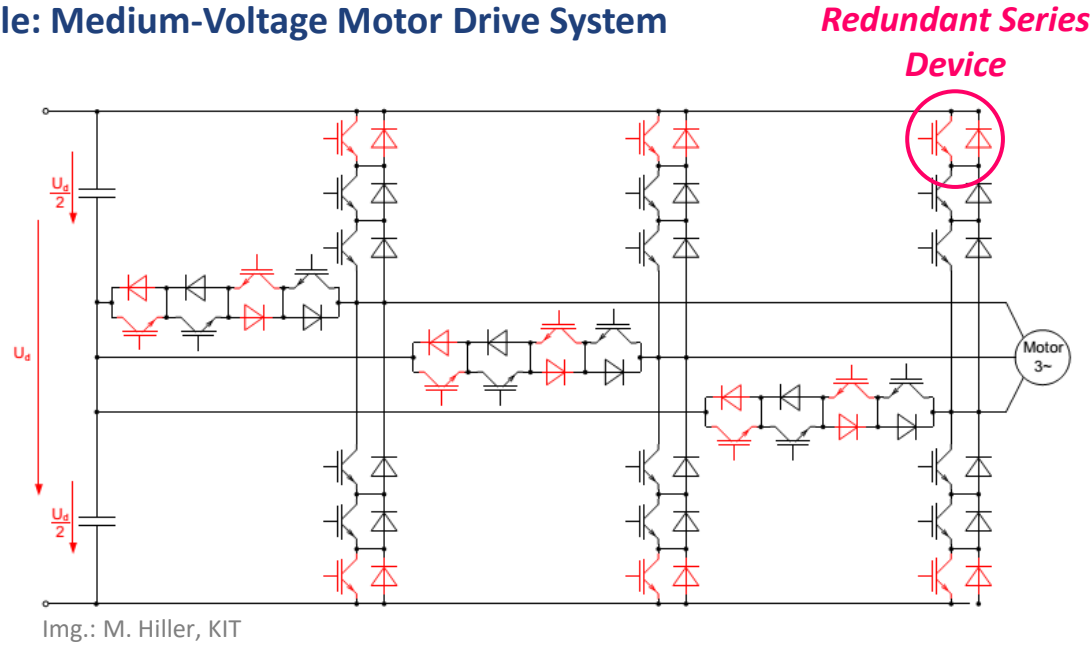
Control Hardware Becomes Limiting Factor!

- Redundancy Effectiveness Limited by Other (Non-Redundant) Parts of the Converter System
 - Control / Auxiliary Supplies / Communication Systems / Bypass Devices / ...



Remark: Redundancy for Single-Cell Systems

■ Example: Medium-Voltage Motor Drive System



Press-Pack NPC Phase Module (Convertteam GmbH)



img: powerguru.org

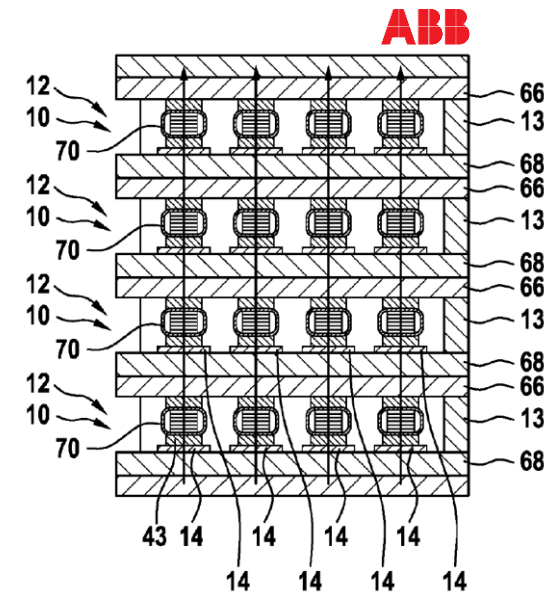
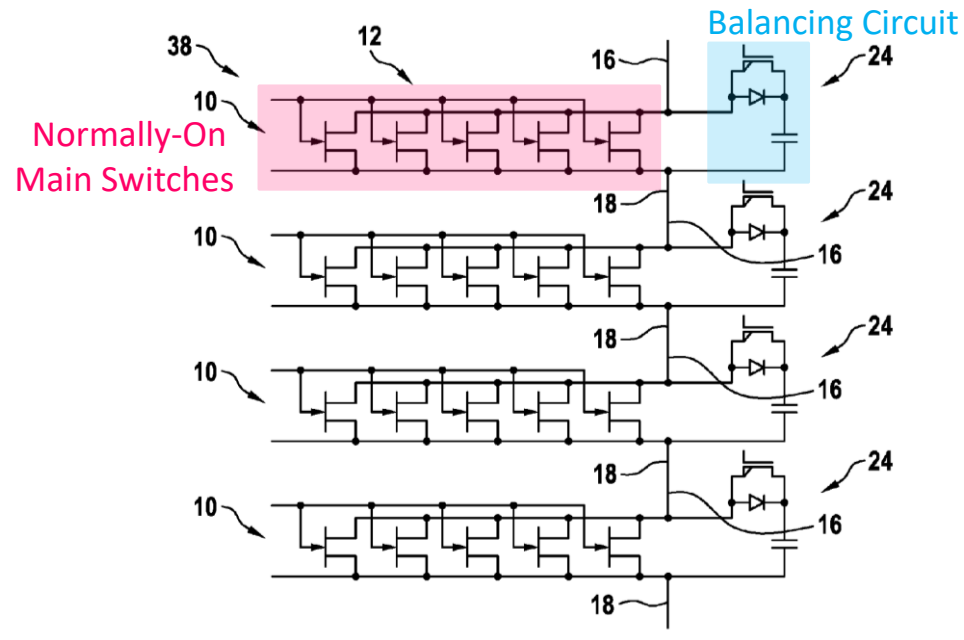
■ Semiconductors with **Fail-To-Short Behavior Required** – Press-Pack IGBTs, etc.



Remark: Fail-To-Short with WBG Devices

■ Normally-On Switches Offer Fail-to-Short w/o Need For Melting Process / Press Packs

- Passive: Short-Circuit Failure Destroys Gate Connection and/or Gate controller
- Active: Sensors & Module-Level Controller Detect Failure and Apply 0 V to the Gate



■ Balancing Circuit Ensures Voltage Sharing / Only Subject to Transient Current Peaks

- Capacitor Connected in Parallel to Main Switch During OFF-State → Defines Voltage Sharing



Part II

SST Concepts & Key Design Aspects

- Medium-Frequency Power Conversion
- Power Semiconductors
- Key SST Topologies
- Medium-Frequency Transformers
- Isolation Coordination
- Protection
- Reliability
- **Standardization & EMC**
- Construction & Testing



Standardization

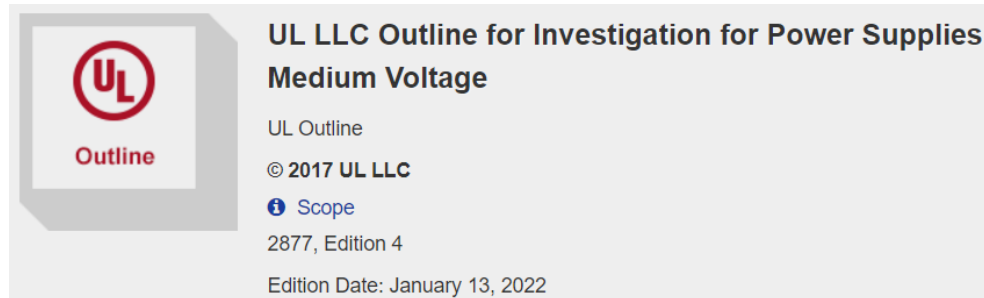
■ Existing (Safety) Standards Such as IEC 62477-2 (Safety) Must Be Considered



EN IEC 62477-2

Safety requirements for power electronic converter systems and equipment - Part 2:
Power electronic converters from 1 000 V AC or 1 500 V DC up to 36 kV AC or 54 kV DC

■ Ongoing SST-Specific Standardization Activities



UL Outline 2877 Ed. 4

“[...] covers requirements for power supplies with input voltage ratings greater than 1000 V, to 38 kV.”

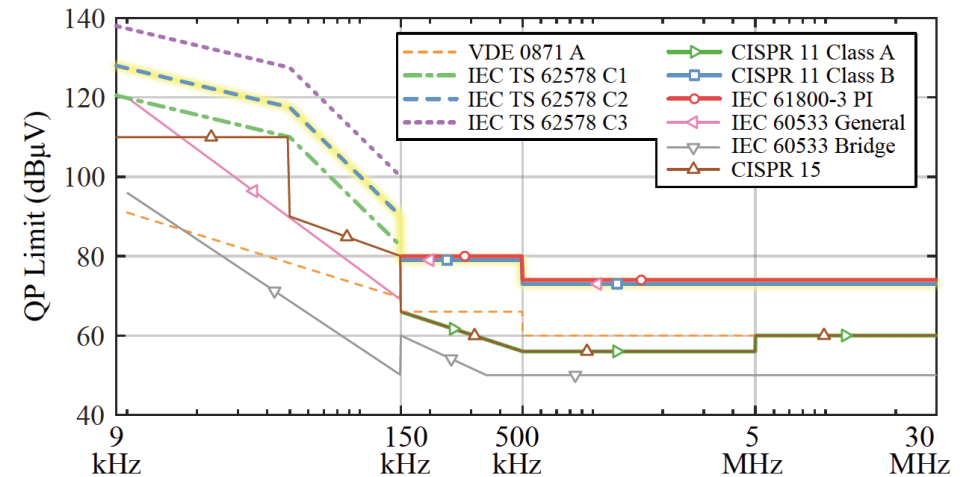
Grid Harmonic and EMI Standards

■ Low-Frequency Grid Current Harmonics (MV and LV Systems)

- IEEE 519, IEEE 1547 up to 50th Harmonic
- BDEW Limits (Germany), ...

■ High-Frequency EMI Limits for LV Systems

- 9...150 kHz Upcoming → IEC TS 62578
- 150 kHz ... 30 MHz CISRP 11



■ EMI Limits for MV Systems TBD!



Part II

SST Concepts & Key Design Aspects

- Medium-Frequency Power Conversion
- Power Semiconductors
- Key SST Topologies
- Medium-Frequency Transformers
- Isolation Coordination
- Protection
- Reliability
- Standardization & EMC
- **Construction & Testing**



From Conceptualization to Realization

- Actual Realization of a Modular MV Converter Systems → Complex / Interdisciplinary Task
- Isolation Coordination / Cooling / Control & Communication / Hot-Swapping / Auxiliary Supply / Mechanical Assembly / ...

PCIM Europe 2015, 19 – 21 May 2015, Nuremberg, Germany

Integration Technologies for a Fully Modular and Hot-Swappable MV Multi-Level Concept Converter

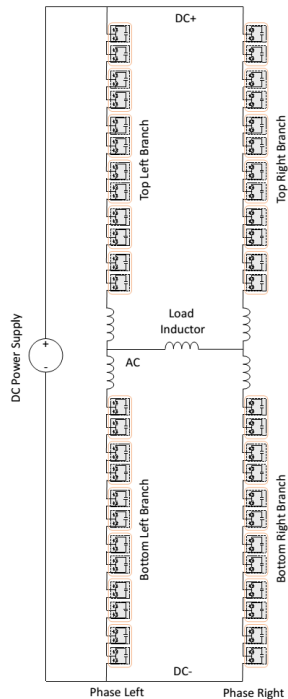
Didier Cottet, Wim van der Merwe, Francesco Agostini, Gernot Riedel, Nikolaos Oikonomou, Andrea Rüetschi, Tobias Geyer, Thomas Gradinger, Rudi Velthuis, Bernhard Wunsch, David Baumann, Willi Gerig, Franz Wildner, Vinoth Sundaramoorthy, Enea Bianda, Franz Zurluh, Richard Bloch, Daniele Angelosante, Dacley Dzung, ABB Switzerland Ltd., Corporate Research, 5405 Baden-Dättwil, Switzerland

Tormod Wien, Anne Elisabeth Vallestad, Dalimir Orfanus, Reidar Indergaard, Harald Vefling, Arne Heggelund, ABB Norway Ltd., Corporate Research, 1375 Billingstad, Norway

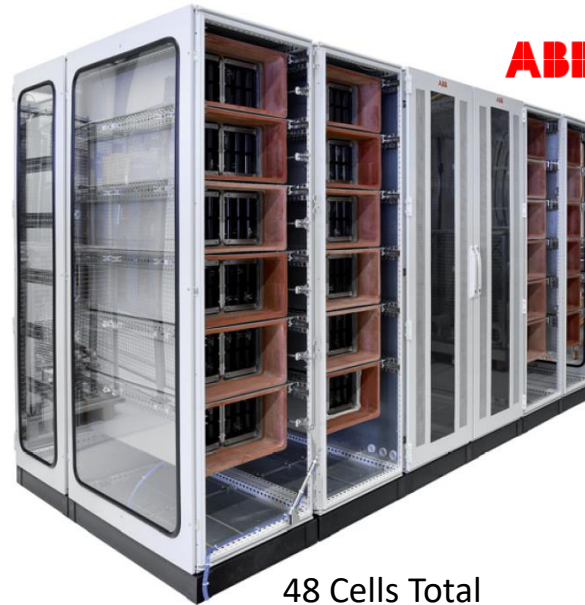
Jonathan Bradshaw, DPS Ltd., Auckland 1010, New Zealand

Contact: didier.cottet@ch.abb.com

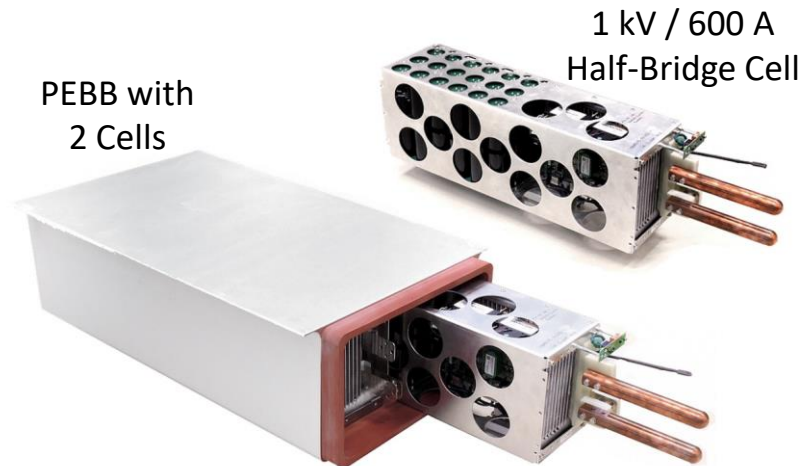
> 25 Authors (!)



Img.: W. van der Merwe



48 Cells Total



PEBC with 2 Cells

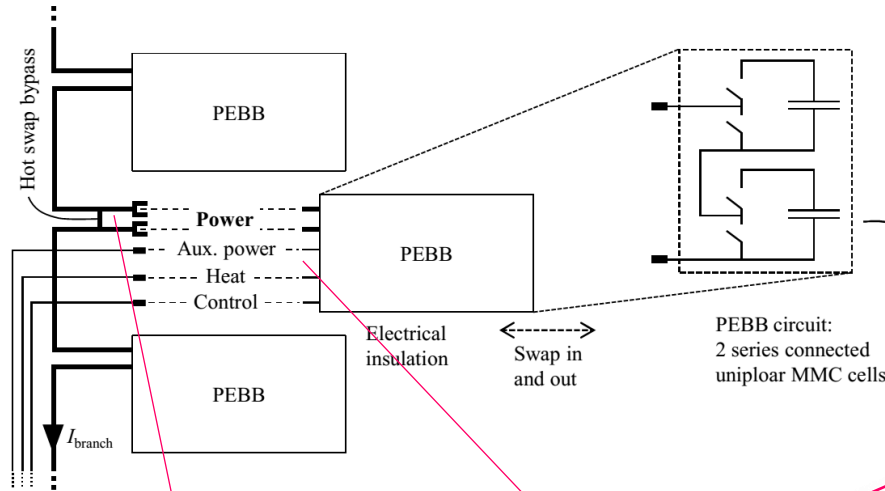
1 kV / 600 A Half-Bridge Cell

- 2 x 1ph MMC in Back-To-Back Conf. | 12 Cells/Arm | 11 kV DC max. | Isol. for 4 kV rms Syst. Volt. / 70 kV BIL



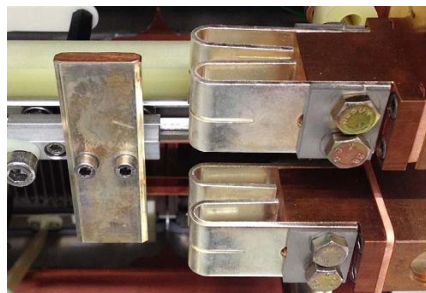
Interfaces & Hot-Swapping

■ All Interfaces Support **Hot-Swapping @ 24 kV rms**

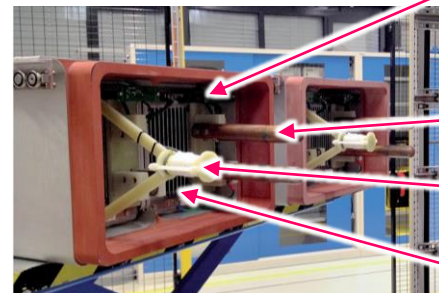


Hot-Swapping Test Setup

ABB



Bypass Switch



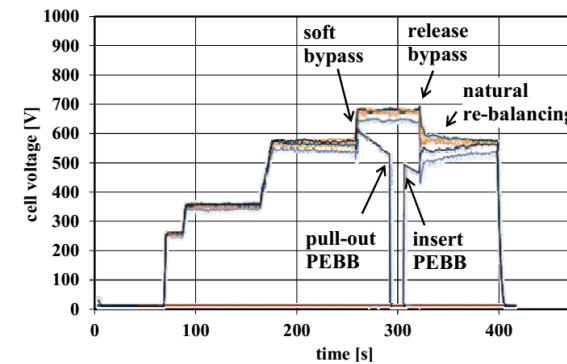
Cell Interface

Communication (Wireless Optical)

Power

Auxiliary (IPT)

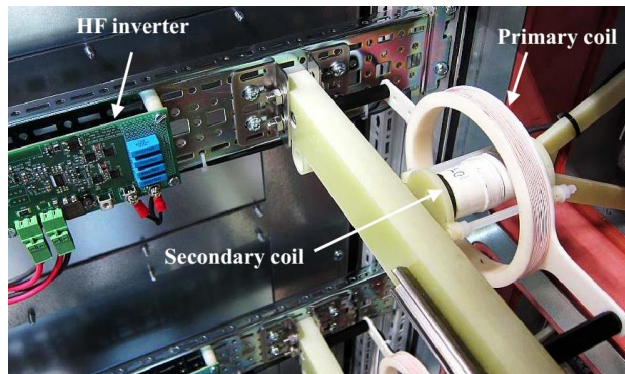
Cooling (Air)



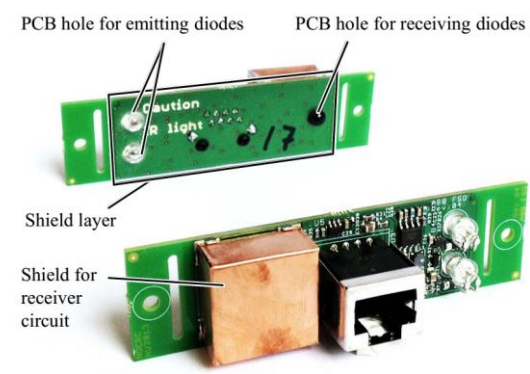
Advanced Integration Technologies

- Building a High-Power/Voltage Demonstrator is a Multi-Disciplinary, Highly Complex Task!

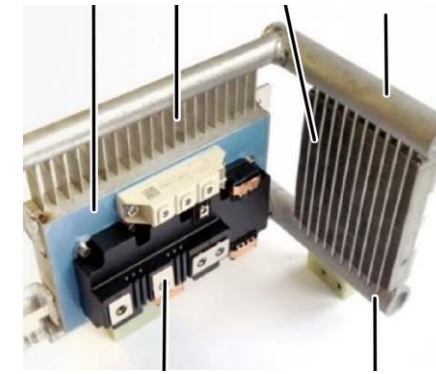
Wireless/Contactless Aux. Power Supply



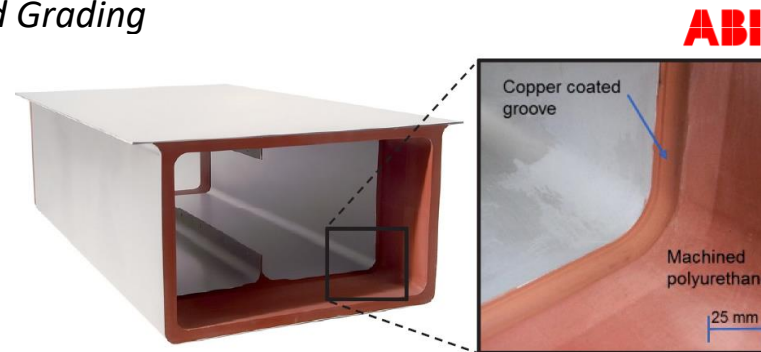
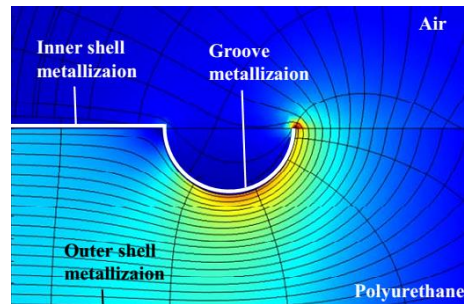
Wireless Optical EtherCAT Comm.



Two-Phase Cooling

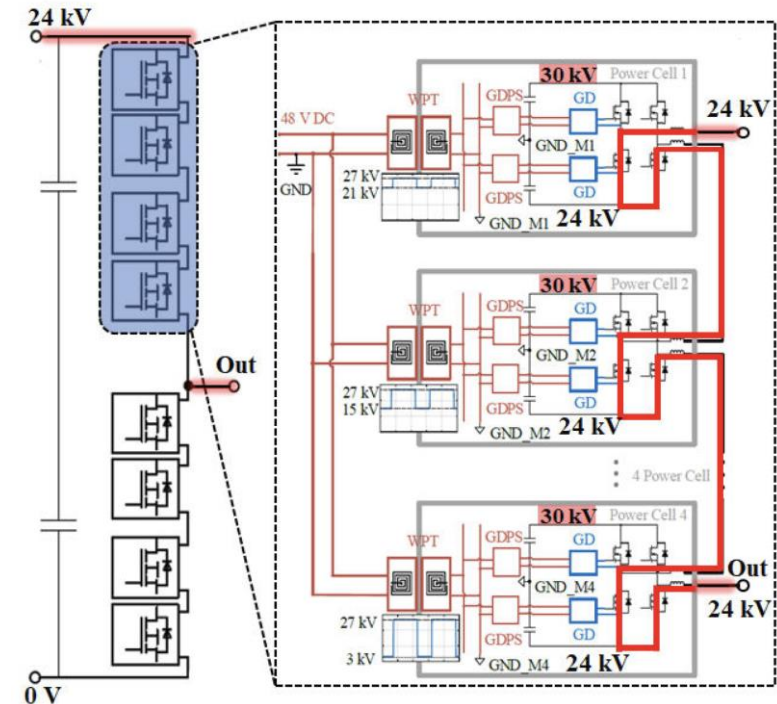
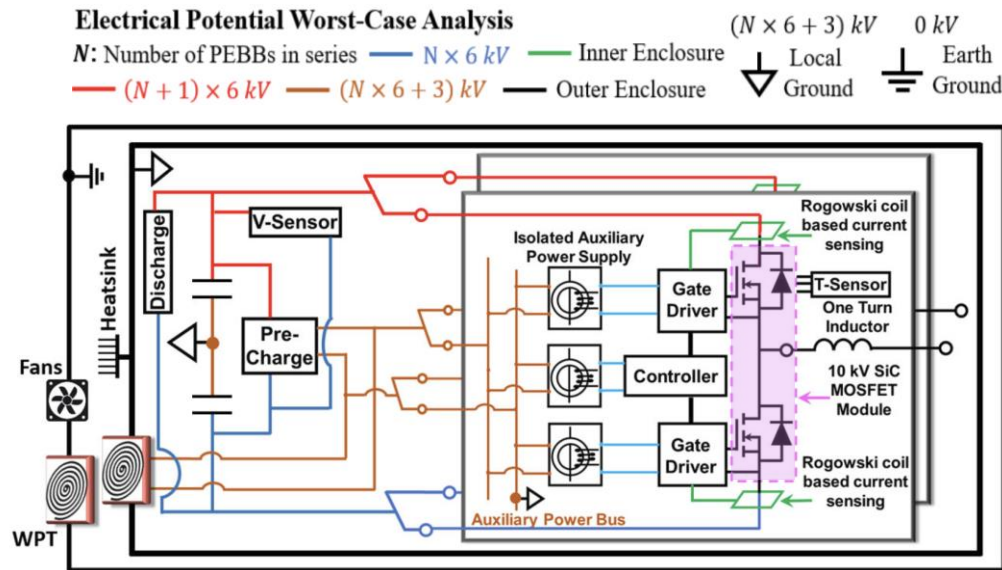


Solid Isolation of PEBBs w. Field Grading



10 kV SiC Ultra-Compact High-Power PEBB

- 1 MW Full-Bridge Power Electronics Building Block (PEBB)
- 10 kV / 240 A XHV-6 Half-Bridge SiC MOSFET Modules | 6 kV DC-Link
- $\rho \approx 15 \text{ kW/dm}^3$

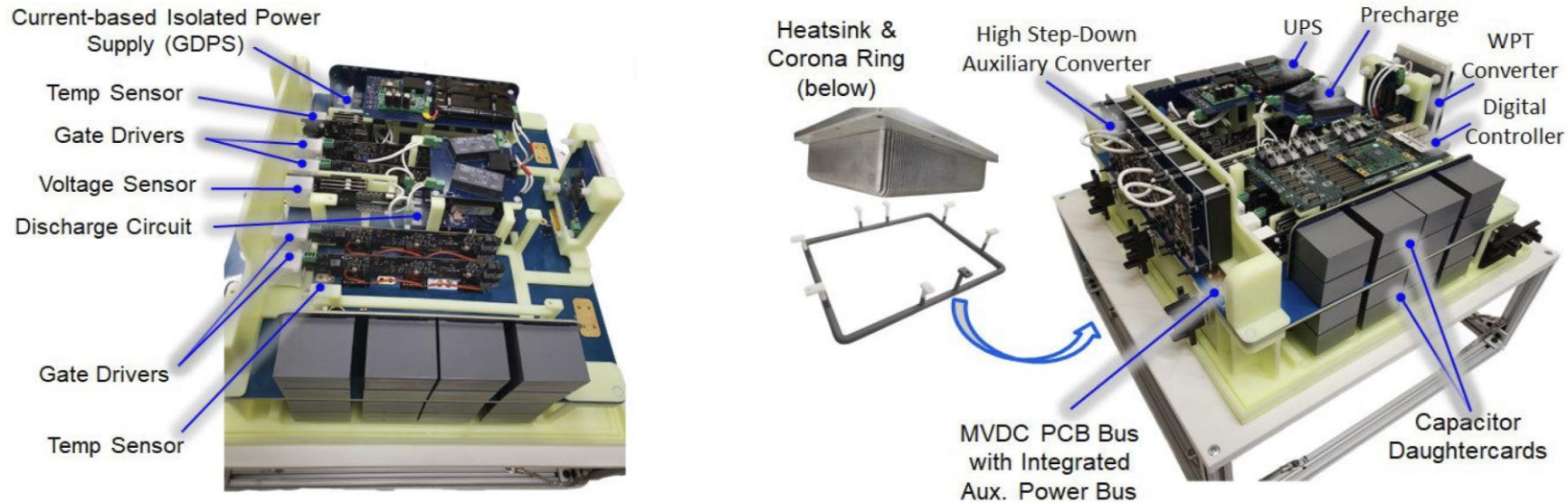


- Multi-Layer PCB MV Power Bus w/ Integr. Aux Power Distribution
- Voltage-Dependent Comp. Grouping / Isol. Coordination for 30 kV CM Voltage w.r.t. Earth
- Wireless or DC-Bus-Derived Aux. Supply / Curr. Loop Gate Drive Supply / Sw. Curr. Sensing / Temp. Sensing etc.



10 kV SiC Ultra-Compact High-Power PEBB

- 1 MW Full-Bridge Power Electronics Building Block (PEBB)
- 10 kV / 240 A XHV-6 Half-Bridge SiC MOSFET Modules | 6 kV DC-Link
- $\rho \approx 15 \text{ kW/dm}^3$

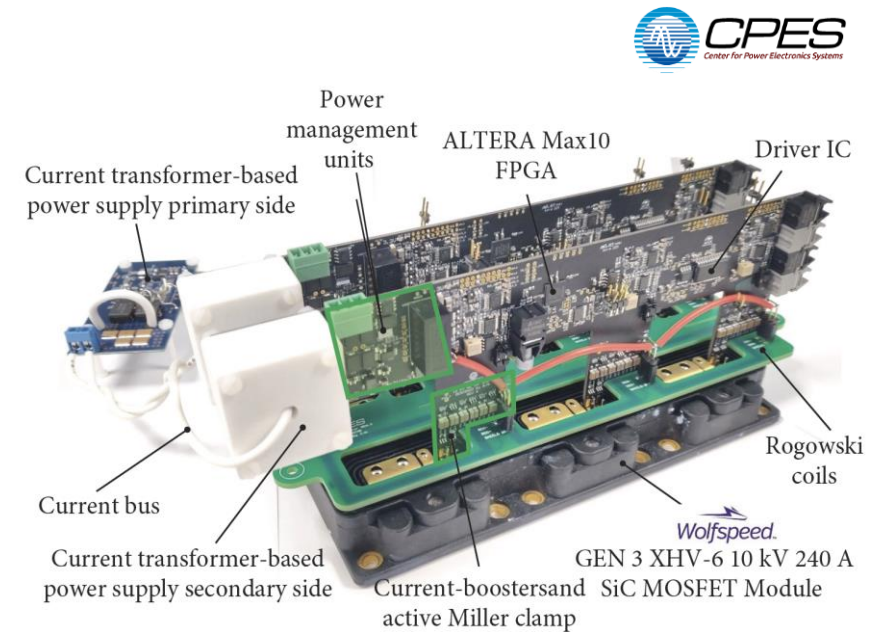
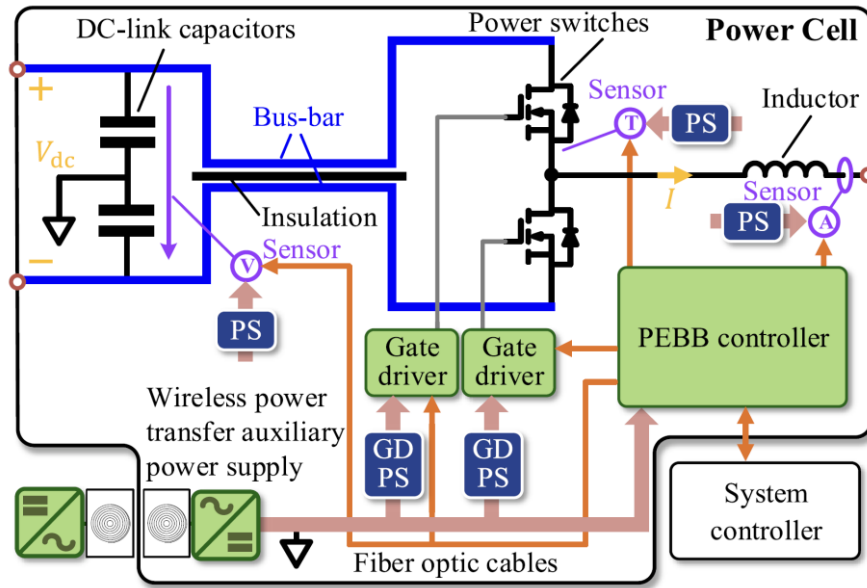


- Multi-Layer PCB MV Power Bus w/ Integr. Aux Power Distribution
- Voltage-Dependent Comp. Grouping / Isol. Coordination for 30 kV CM Voltage w.r.t. Earth
- Wireless or DC-Bus-Derived Aux. Supply / Curr. Loop Gate Drive Supply / Sw. Curr. Sensing / Temp. Sensing etc.



10 kV SiC Power-Cell w/ Integrated Output Inductor (1)

- 250 kW Half-Bridge Power-Cell (HB-PEEB)
- 10 kV / 240 A XHV-6 Half-Bridge SiC MOSFET Modules (4200 kW/dm³) | 6 kV DC-Link
- $\eta \approx 99.6\%$ @ $f_{sw} = 5$ kHz | 99.3% @ 10 kHz for $D = 0.5$ Power Circulation
- $\rho \approx 12$ kW/dm³

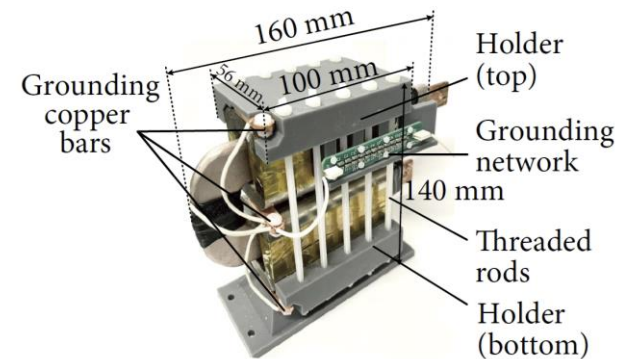
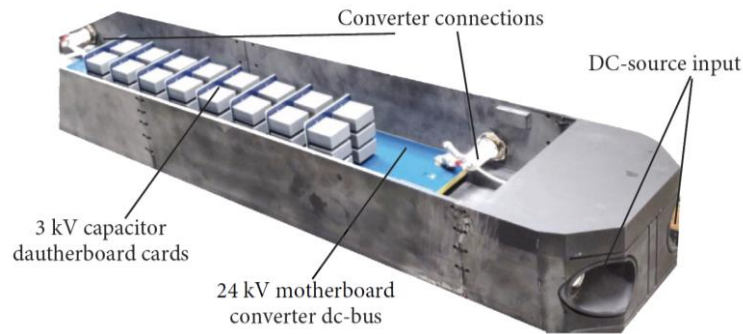


- Multi-Layer PCB DC-Bus | Gate Driver for 100 V/ns Sw. Speed | PCB Rogowski Coil Sw. Curr. Sensing / Protection
- Local Controller & Voltage/Current Sensors | Wireless Aux. Supply | Curr. Loop GD supply | Temp. Sensing etc.



10 kV SiC Power-Cell w/ Integrated Output Inductor (2)

- 250 kW Half-Bridge Power-Cell (HB-PEEB)
- 10 kV / 240 A XHV-6 Half-Bridge SiC MOSFET Modules (4200 kW/dm³) | 6 kV DC-Link
- $\eta \approx 99.6\%$ @ $f_{sw} = 5$ kHz | 99.3% @ 10 kHz for $D = 0.5$ Power Circulation
- $\rho \approx 12$ kW/dm³



- Locally grounded wdg. outer shielding layer
- RC damping network btw shield & DC midpoint
- Double layer dielectric shield termination

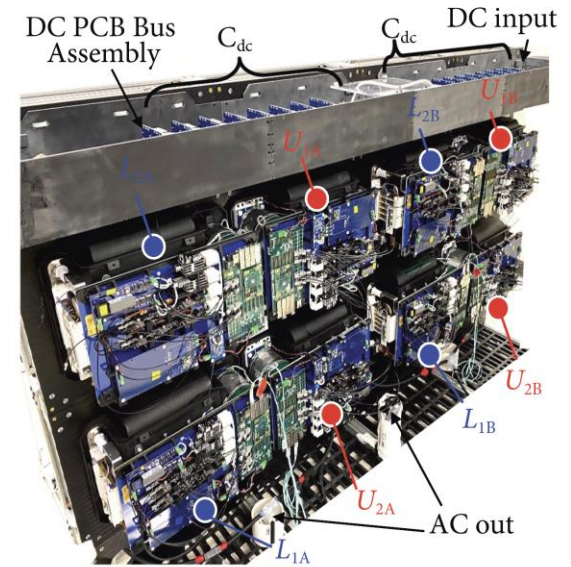
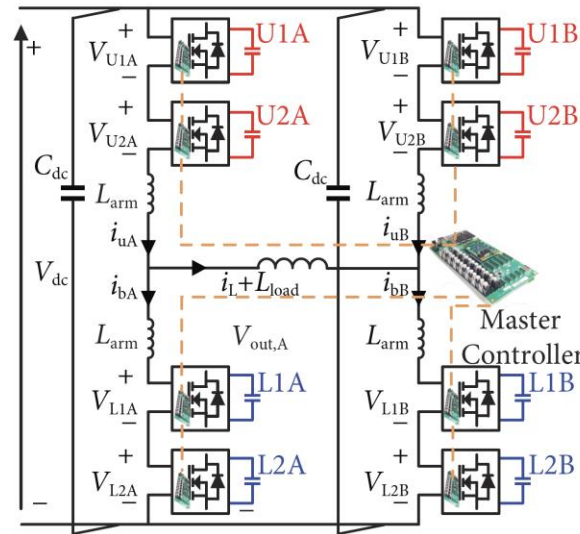
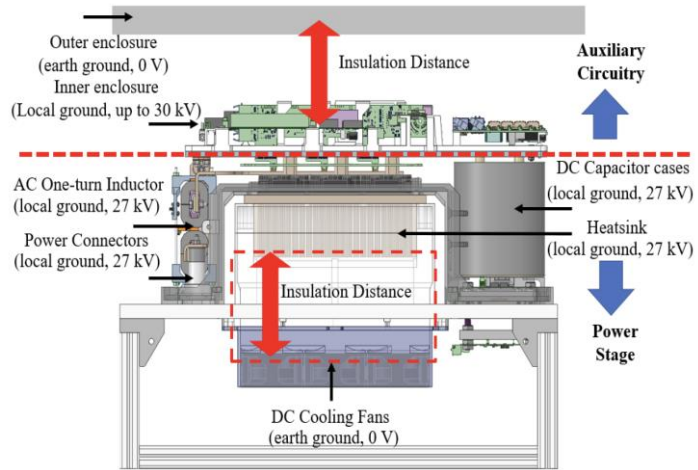
■ Convert-Level PCB-Based DC-Bus Assembly

■ Power-Cell Integrated Output Inductor



10 kV SiC Power-Cell w/ Integrated Output Inductor (3)

- Experimental Analysis in 2-Cell/Arm Converter | 12 kV DC-Link
- $\eta \approx 99.2\%$ @ $f_{sw} = 10$ kHz @ $D = 0.5$ Power Circulation

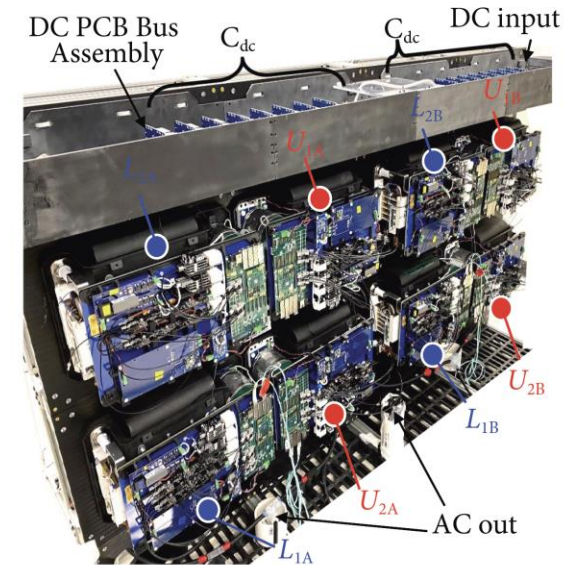
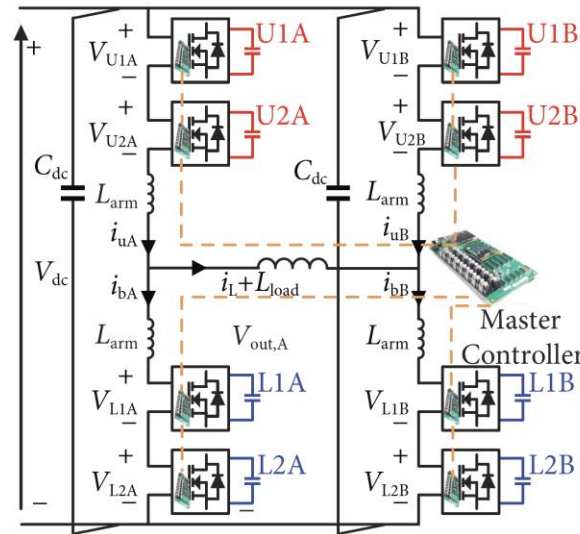
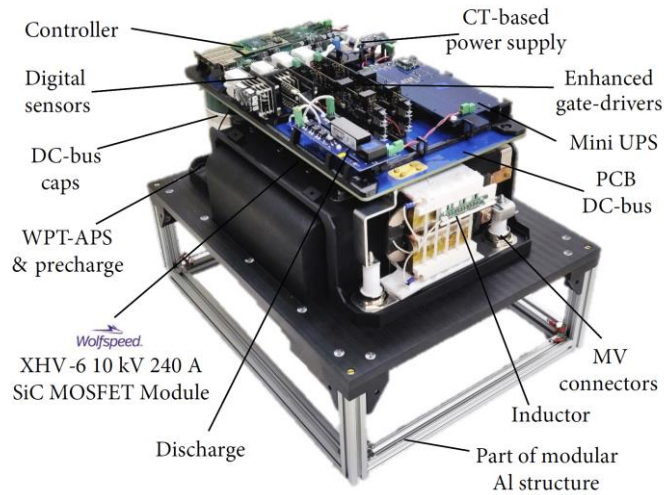


- 10 kV SiC MOSFET-Based Power-Cell | 2-Cell/Arm MMC Bridge-Legs / Q2L-Modulation / Power Circulation



10 kV SiC Power-Cell w/ Integrated Output Inductor (3)

- Experimental Analysis in 2-Cell/Arm Converter | 12 kV DC-Link
- $\eta \approx 99.2\%$ @ $f_{sw} = 10$ kHz @ $D = 0.5$ Power Circulation

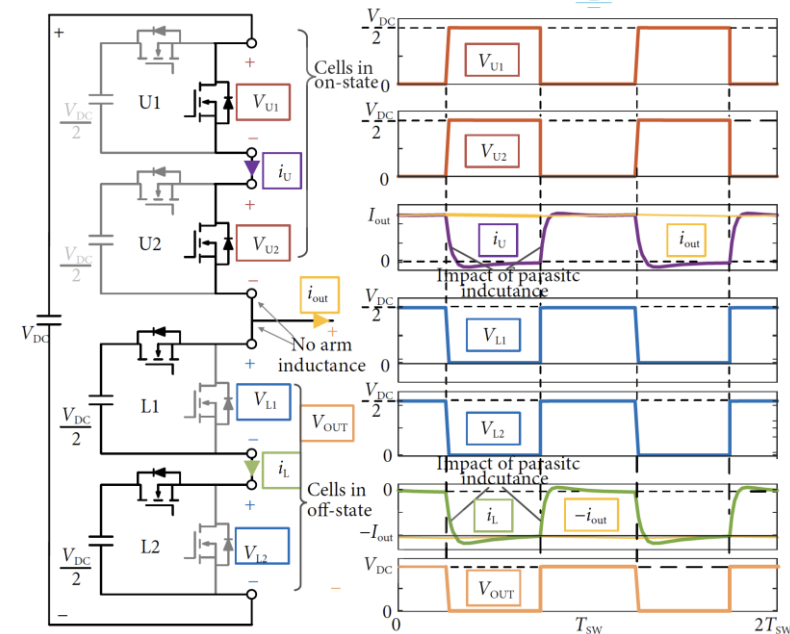
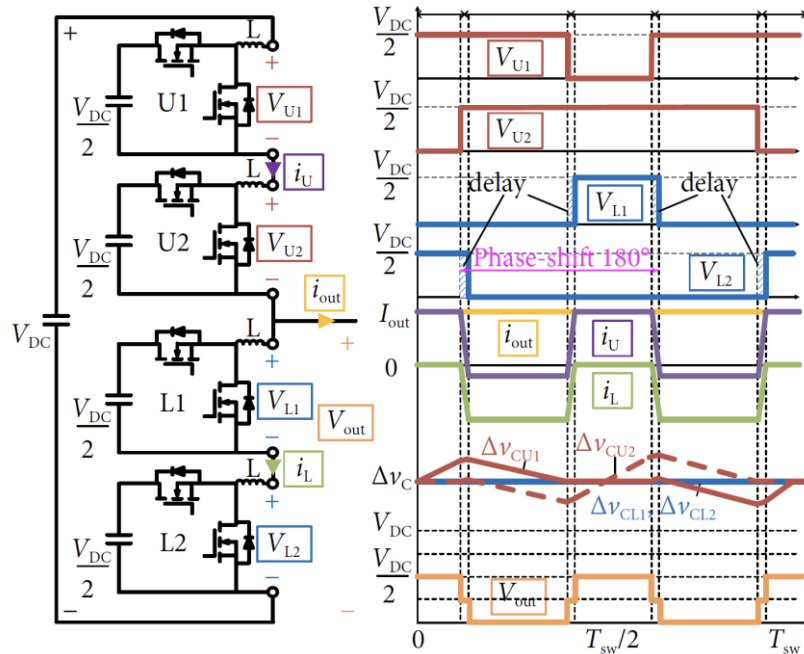


- 10 kV SiC MOSFET-Based Power-Cell | 2-Cell/Arm MMC Bridge-Legs / Q2L-Modulation / Power Circulation



Remark Advanced MMC Modulation Schemes

- Minimization of the Cell Capacitance & Arm Inductance
- Voltage Balancing of Cell Capacitors over Each Switching Cycle (SCC) — Enables DC/DC Operation (!)
- Quasi-2-Level (Q2L) Output Voltage Generation w/o Arm Inductor

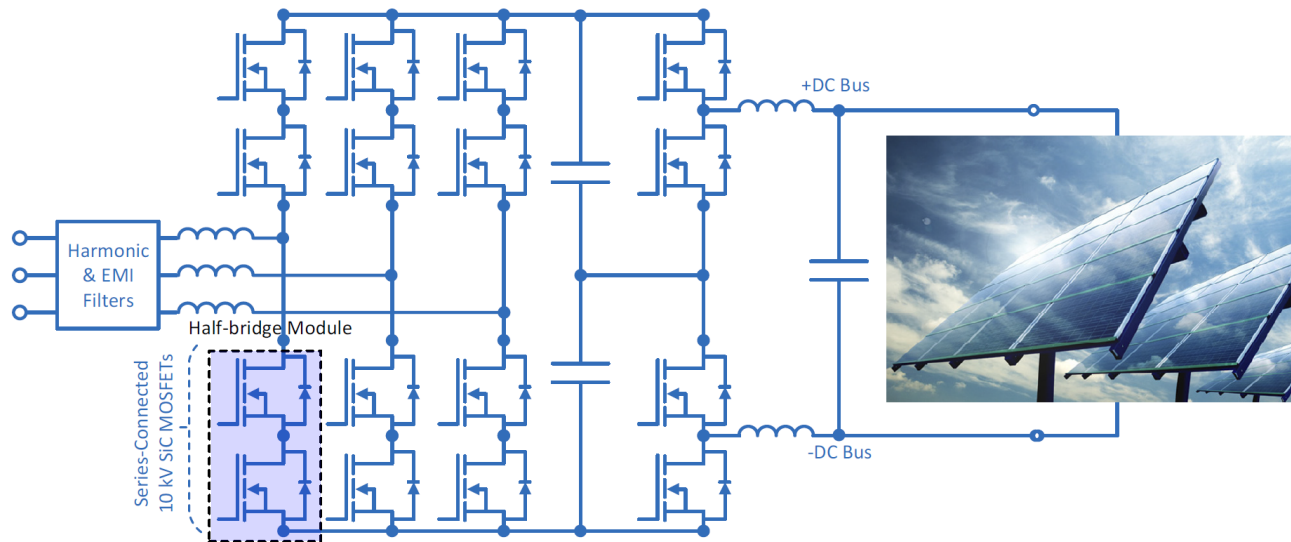


- SCC Cell Volt. Balancing & Shaping of Arm Currents | Q2L — Integr. Cap. Blocked Transistor (ICBT) Concept

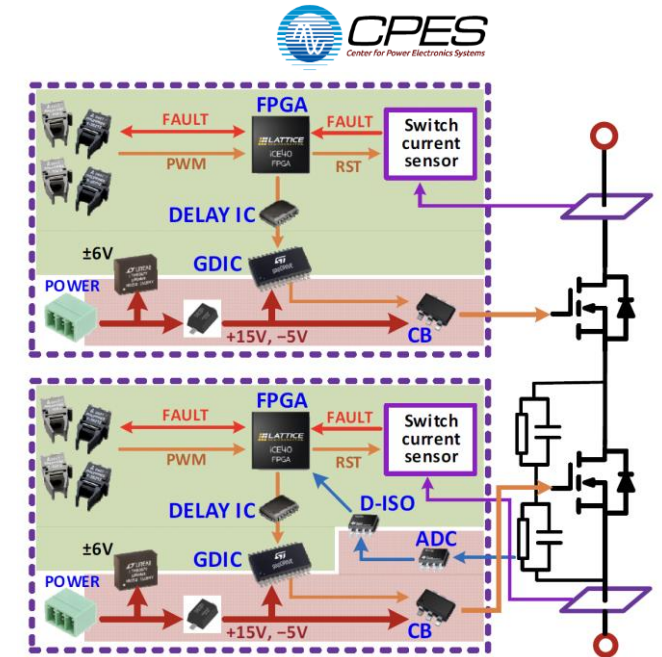


Series-Connected 10 kV SiC 3-Φ AC/DC Converter

- 200 kW | 11 kV 3-Φ AC-Grid / 16 kV DC-link
- 10 kV / 16 A XHV-9 Half-Bridge SiC MOSFET Module | $f_{sw} = 10$ kHz
- $\eta \approx 99\%$ | $\rho \approx 5$ kW/kg

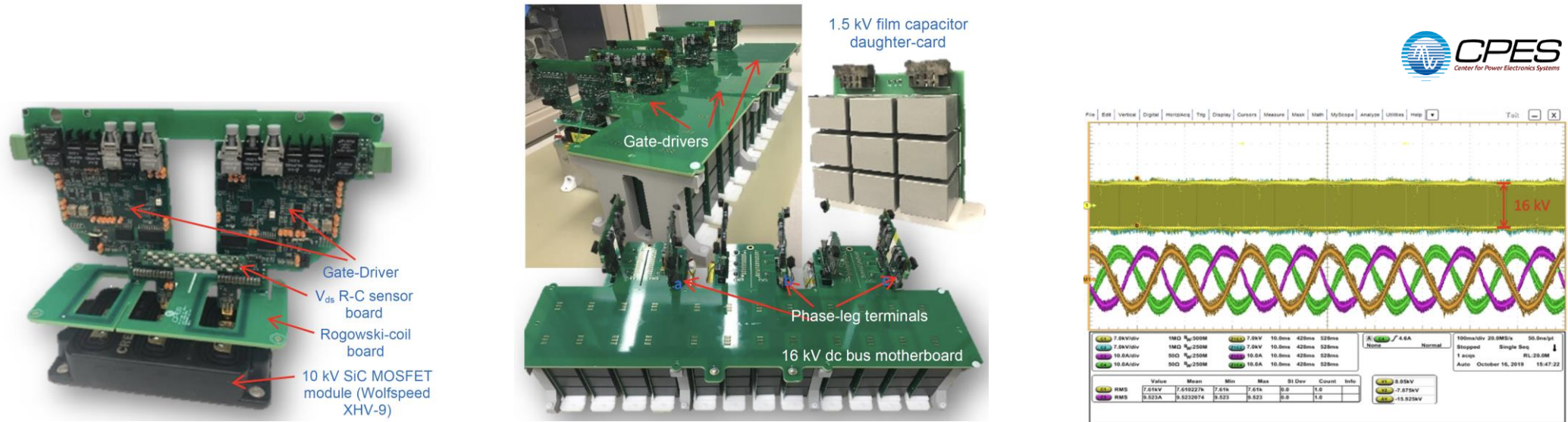


- 16 kV PCB DC-Bus Motherboard w/ E-Field Shaping Layers
- Passive dv/dt Symmetrization & Active GD Delay Voltage Balancing
- PCB Rogowski Coil Sw. Current Sensor / Protection (500 ns Response)



Series-Connected 10 kV SiC 3-Φ AC/DC Converter

- 200 kW | 11 kV 3-Φ AC-Grid / 16 kV DC-link
- 10 kV / 16 A XHV-9 Half-Bridge SiC MOSFET Module | $f_{sw} = 10$ kHz
- $\eta \approx 99\%$ | $\rho \approx 5$ kW/kg



- 16 kV PCB DC-Bus Motherboard w/ E-Field Shaping Layers
- Passive dv/dt Symmetrization & Active GD Delay Voltage Balancing
- PCB Rogowski Coil Sw. Current Sensor / Protection (500 ns Response) | Inverter Operation @ 16 kV / 200 kVA



Testing Infrastructure (1)

- Significant Planning and Realization Effort
- Power Supply / Cooling / Control / Simulation (Integrated)



Img.:Center for Advanced Power Systems / Florida State University

- Large Space & Infrastructure Requirement / Considerable Investment (!)

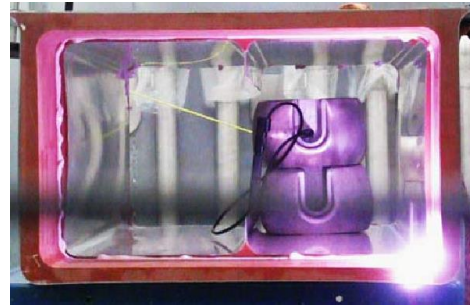


Testing Infrastructure (2)

■ Medium-Voltage and High-Voltage Testing Facilities & Experience



Img.: [Cottet2015b]



Img.: [Cottet2015b]

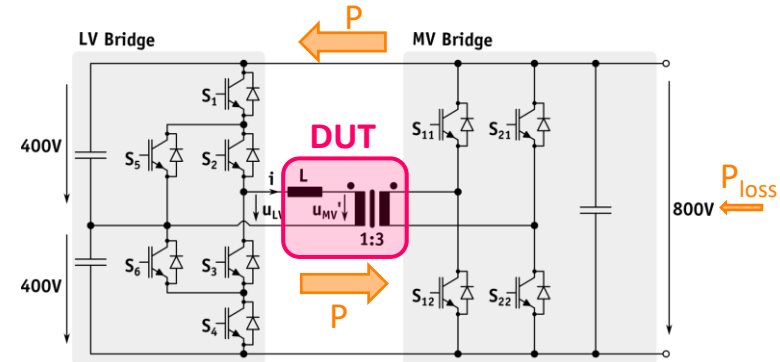


Img.: High Voltage Lab, ETH Zurich

■ Source/Sink 100s of Kilowatts Or Back-To-Back Testing Concepts → Complexity

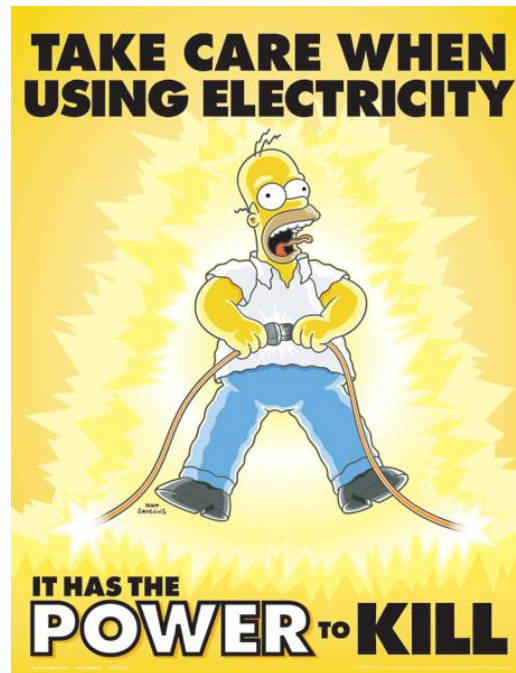


Img.: electrical-engineering-portal.com



Remark: Education and MV Power Electronics

- PhD Students are Missing Practical Experience / Underestimate the Risk
- High-Power-Density Power Electronics Differs from Conventional (Passive) HV Equipment
- **Very Careful Training / Remaining Question of Responsibility**



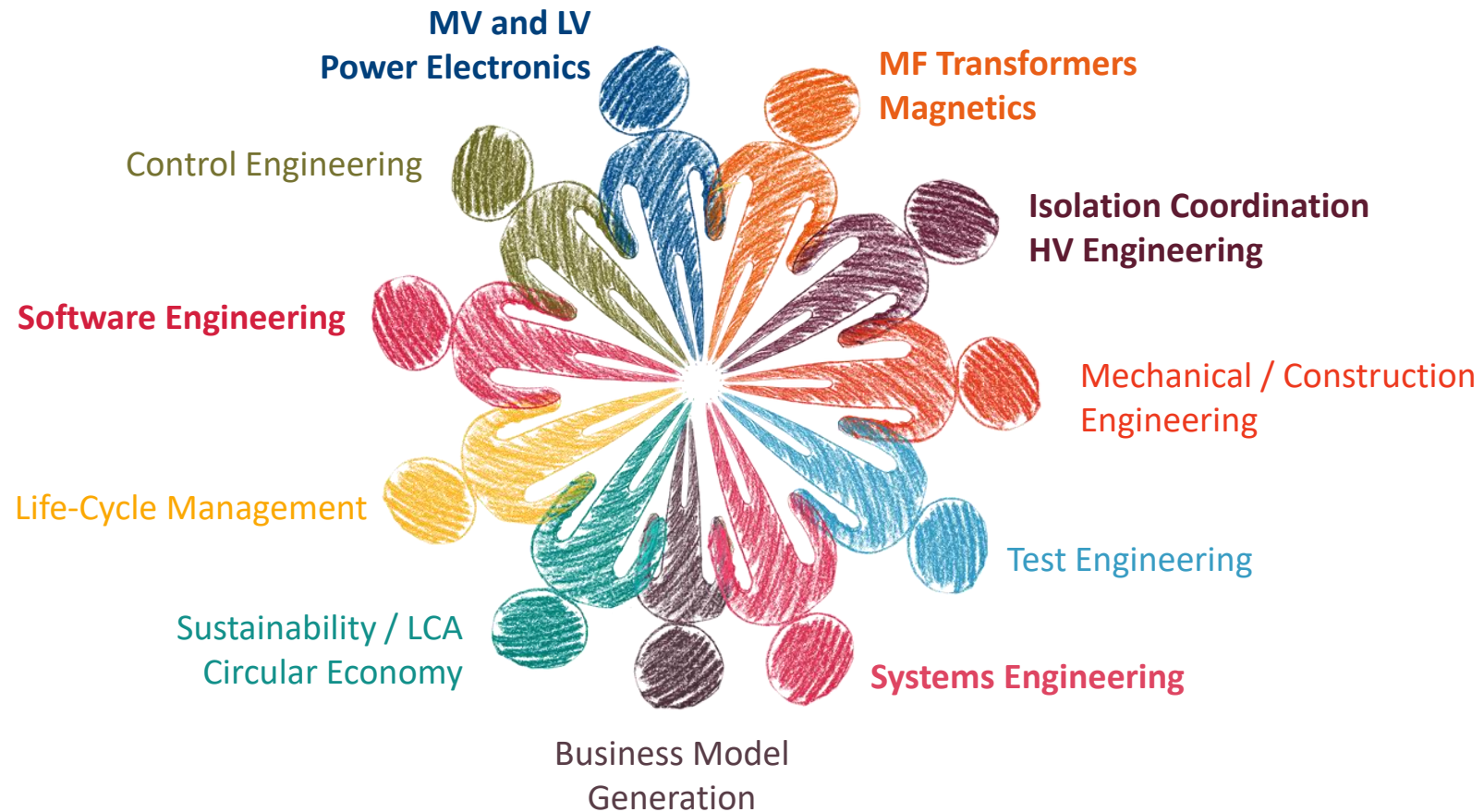
Source: www.safetyposters.com

... ESPECIALLY @ **Medium Voltage (!)**

- **High Costs / Long Manufacturing Time of Test Setups**
- **Complicated Testing Due to Safety Procedures → Lower # of Publications/Time**

Remark: Core Competencies for SST Design

- Developing and Actually Building a High-Power, Std.-Compliant SST is a Complex, **Multi-Disciplinary Task**

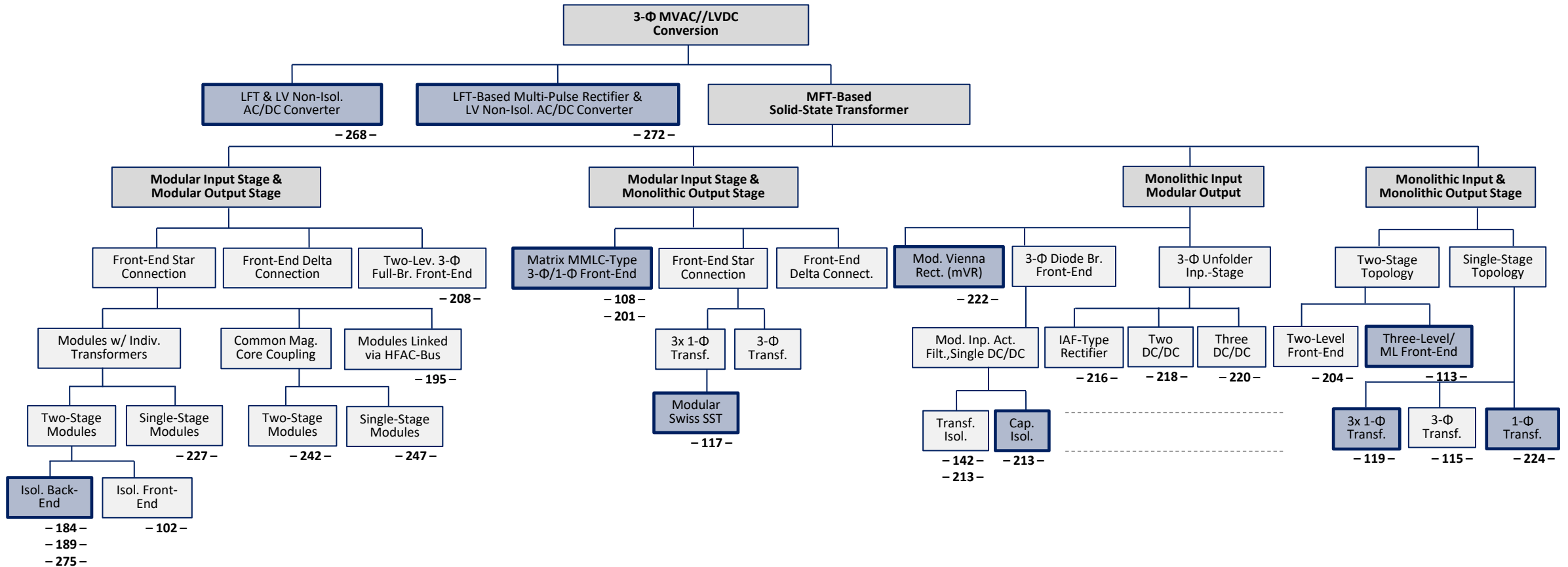




Part III
**Selected Results of Recent
University / Industry SST R&D Activities**



Classification of 3-Φ MVAC/LVDC SST Topologies



- Concepts of High Industry Relevance Highlighted
- Numbers (- xxx -) Refer to Slides Showing the Topology
- Representation Limited to Topologies Described in Literature



— SUNGROW —

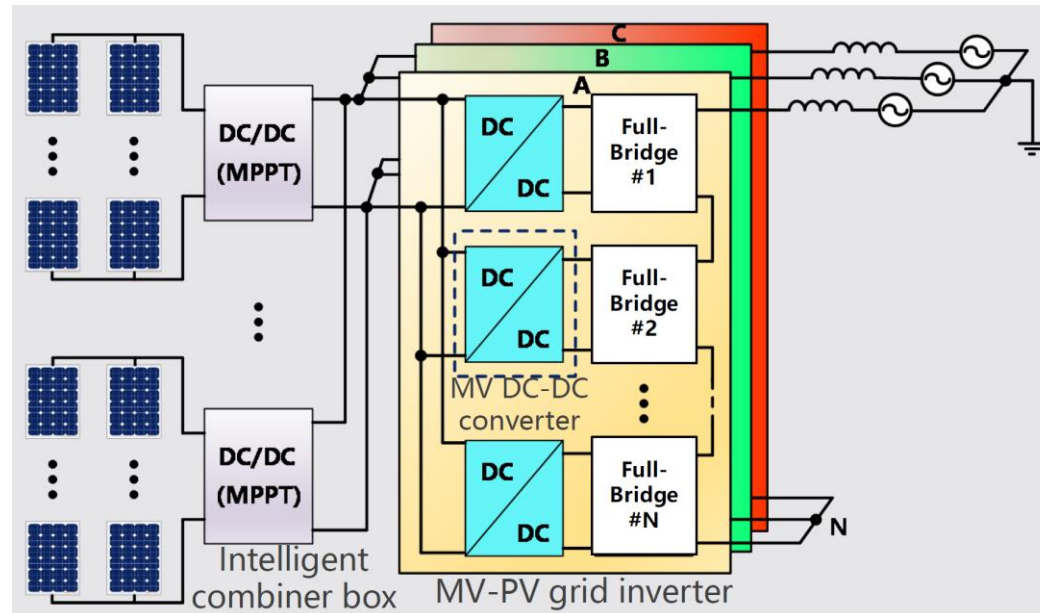
Multi-Partner Industry / University Collaboration

Sungrow Power Supply Co., Ltd
Zhejiang University
Shanghai Jiaotong University
Hefei University of Technology
China Electric Power Research Institute
Xi'an Jiaotong University
Shanghai Electric Power Engineering Co., Ltd
Qingdao Yunlu Energy Technology Co., Ltd



3- Φ Star-Connected Full-Modular AC/DC SST (1)

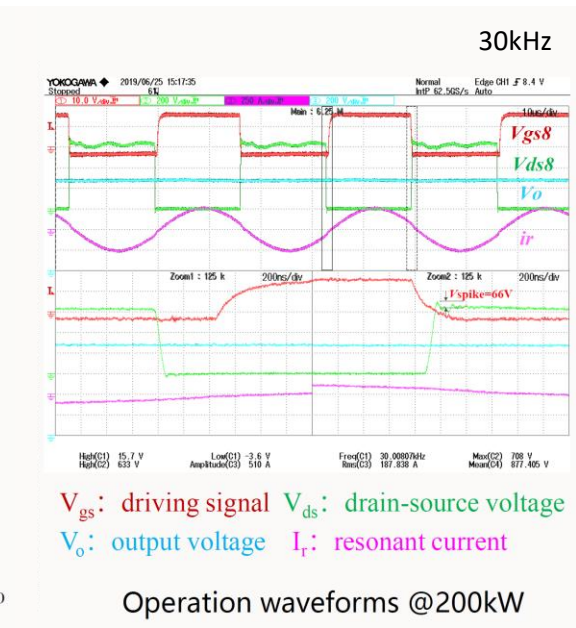
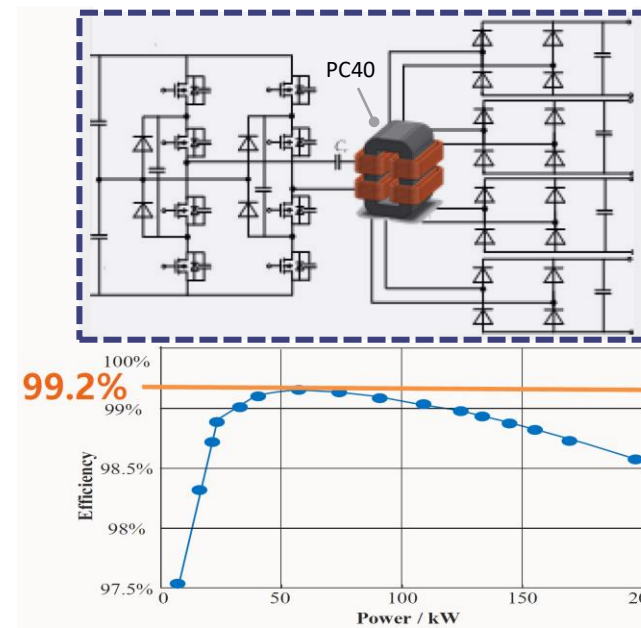
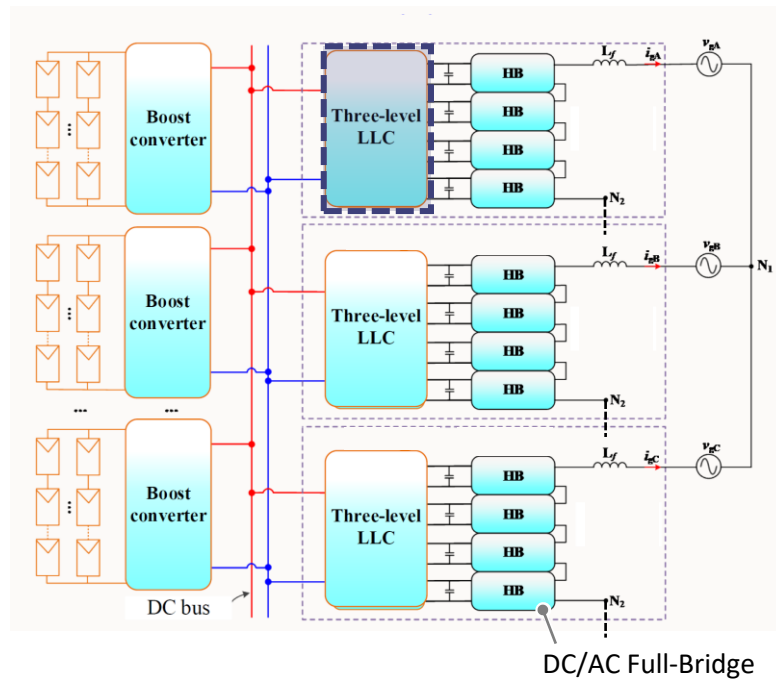
- Utility-Scale PV Medium Voltage Grid Connection — 6 MW @ 35 kV
- Input-Parallel Output-Series (IPOS) Inverter Structure
- 9 Cascaded Full-Bridge DC/DC-DC/AC Modules per Phase



- Grid Following & Grid Forming Operation
- Control Ensures Largely Const. Power Transfer of DC/DC Conv. Despite $2 f_{\text{Mains}}$ Power Pulsation

3-Φ Star-Connected Full-Modular AC/DC SST (2)

- Three-Level Full-Bridge LLC DC/DC Converter Stage / Low Cost 1200 V SiC MOSFETs | 4-in-1 Approach
- 200 kW Modules w/ 35 kV Isolation / Low Total Number of Modules

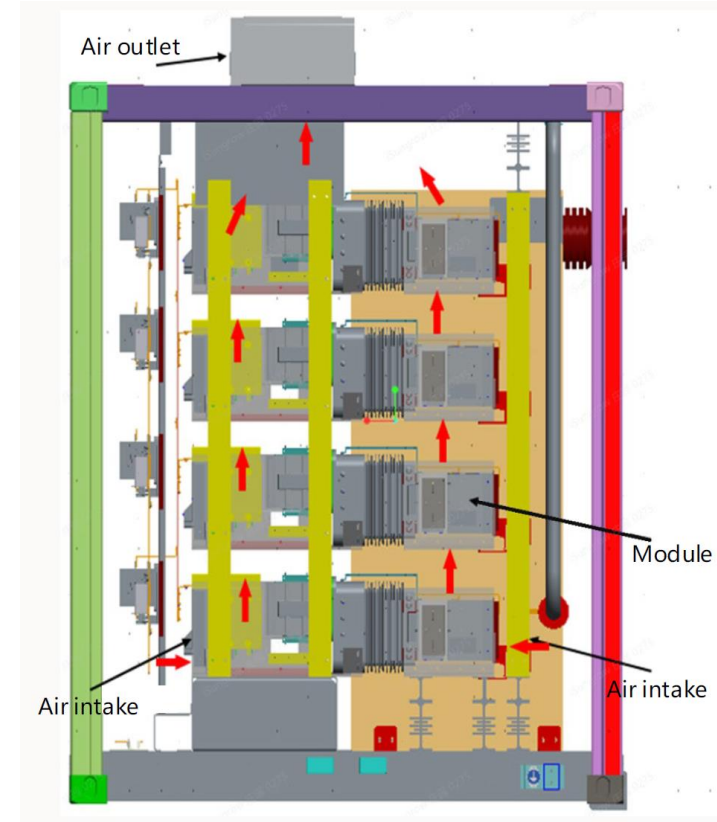
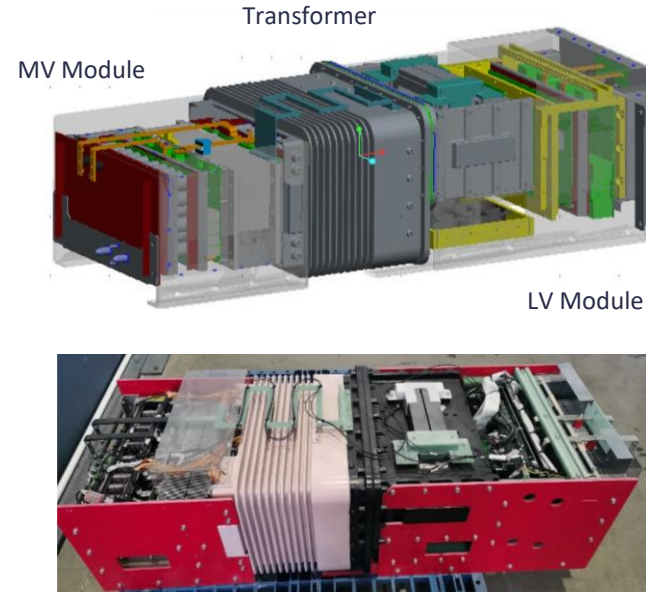
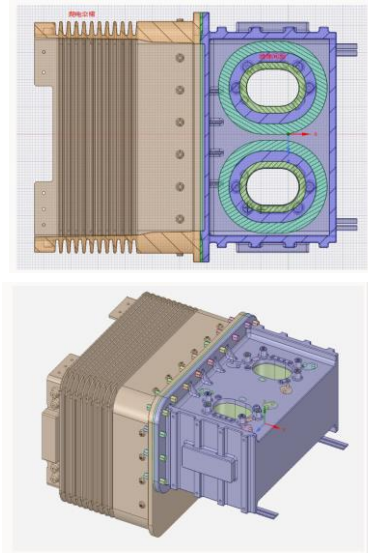


- 1200 V DC Input / 4x 850 V DC Output Supplied to Full-Bridge DC/AC Cells | Max. Efficiency > 99%



3-Φ Star-Connected Full-Modular AC/DC SST (3)

- 200 kW DC/DC Converter | 35 kV / 200 kVA Transformer
- Isol. Test @ 85 kV / 50 Hz / 1 min & PD Test — 44 kV / 3 pC



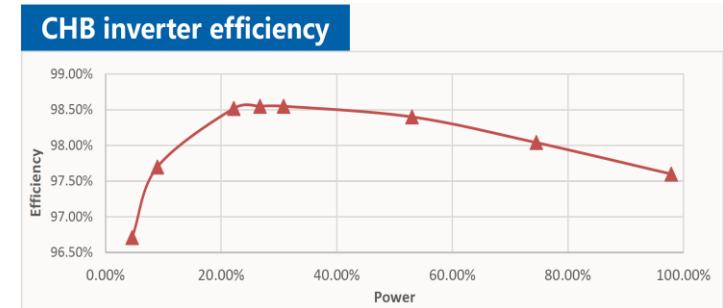
- Construction Details of Transformer | Power Module | Cooling Fans in the Modules & Top of Cabinet
- Specific Epoxy Resin — Compromise Btw El. Strength (20 kV/mm) & Therm. Cond. (1 W/m.K), $\tan \delta < 0.01$
- Shed Design – 350 mm Air Gap / 850 mm Creepage Distance

3- Φ Star-Connected Full-Modular AC/DC SST (4)

- 12 MW (2x 6 MW) @ 35 kV Demonstration | $\approx 0.2 \text{ kW/dm}^3$ Power Density of Inv. Stage w/o L_{input} & Switchgear
- Multi-Scenario Tests & Comprehensive Performance Evaluation Over > 30 Days Runtime



DC/DC-DC/AC Full-Bridge



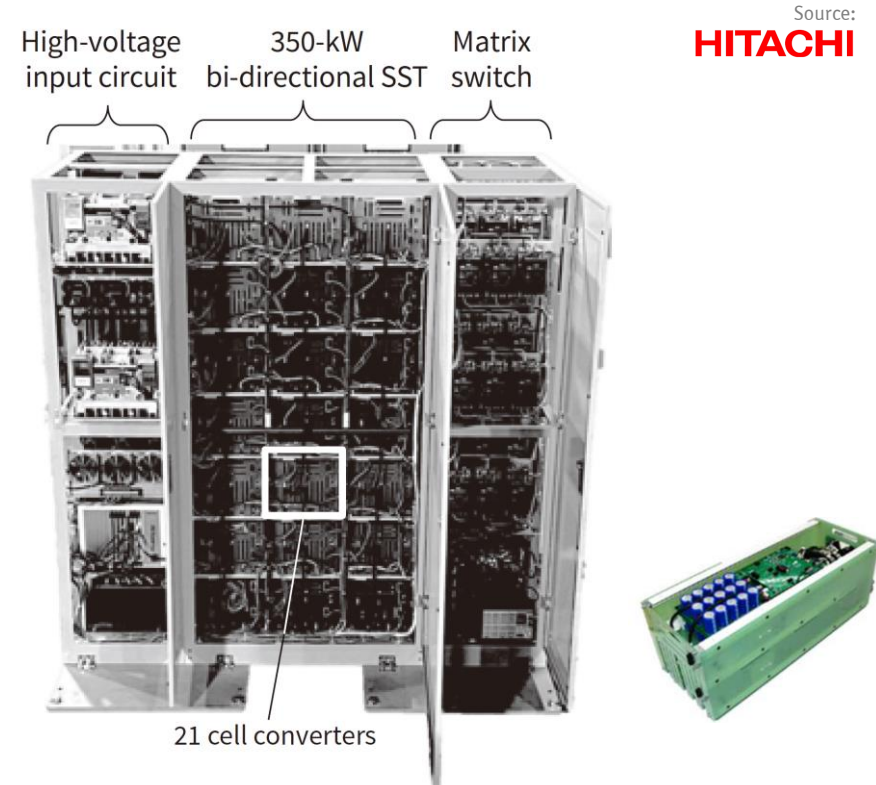
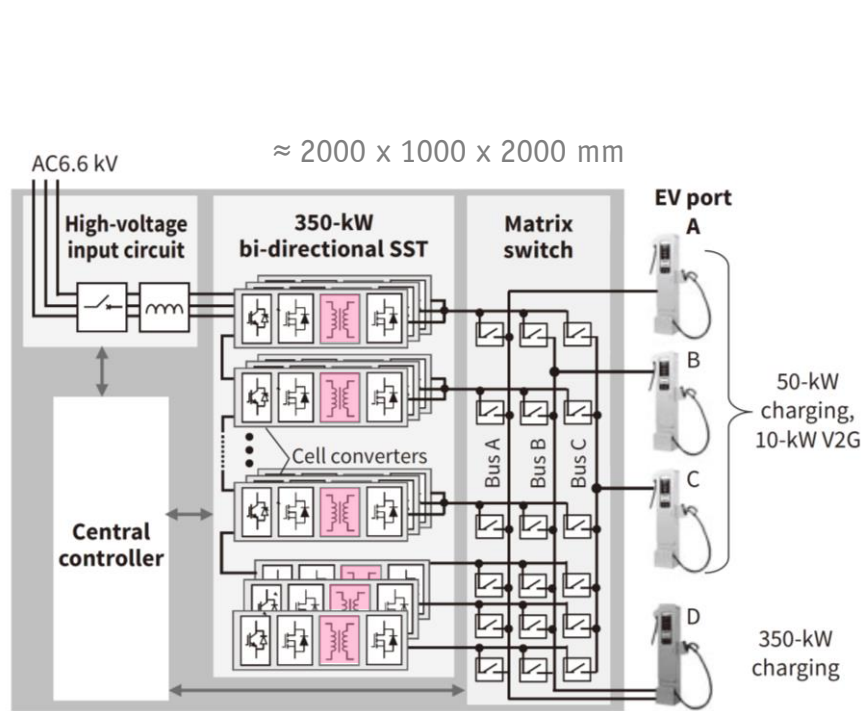
- 54 MW Rated Power Plant
- Max. Overall Efficiency of Max. 96.5% | Grid Inv. Eff. Max. 99.4% | Mains Current THD < 3%



— **HITACHI** —

3-Φ 6.6kV / 350kW SST-Based EV Charger (2)

- 3x7 = 21 Cells | 5 kHz 1.7 kV Si-IGBT AC/DC Stage | 50 kHz 1.7 kV SiC 1050 V/400 V DC/DC Converter
- Matrix Switch Output for 21x 17 kW → 1x 350 kW Charging Port Config. & Cascaded Cell Balancing
- Forced Air Cooling



- Power Density → 0.09 kW/dm³ (System) | ≈ 0.18 kW/dm³ (SST/Cells incl. Isol.)
- -40% Footprint / -70% Weight vs. LFT-Based Solution / 83% Lower Transf. Volume



3- Φ 6.6kV / 350kW SST-Based EV Charger (2)

- 3x7 = 21 Cells | 5 kHz 1.7 kV Si-IGBT AC/DC Stage | 50 kHz 1.7 kV SiC 1050 V/400 V DC/DC Converter
- Matrix Switch Output for 21x 17 kW \rightarrow 1x 350 kW Charging Port Config. & Cascaded Cell Balancing
- Forced Air Cooling



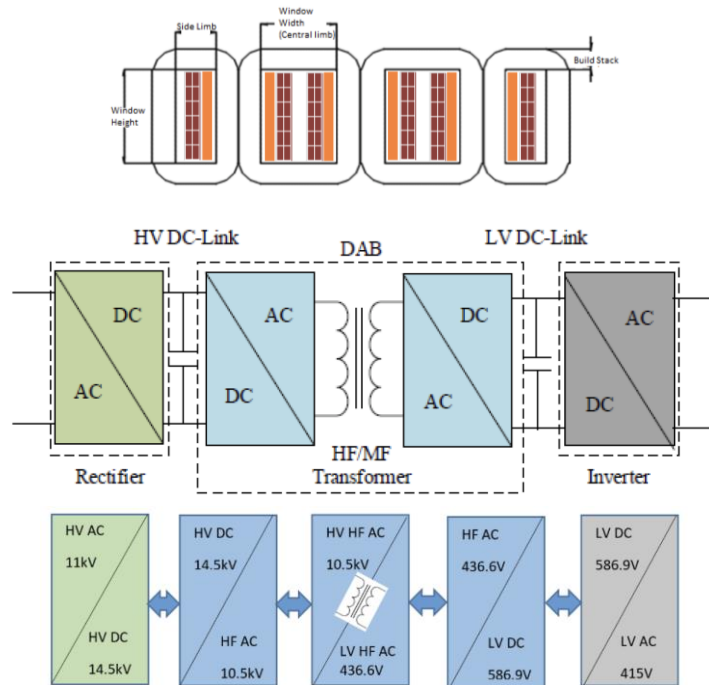
Source:
HITACHI

- Power Density \rightarrow 0.09 kW/dm³ (System) | \approx 0.18 kW/dm³ (SST/Cells incl. Isol.)
- -40% Footprint / -70% Weight vs. LFT-Based Solution / 83% Lower Transf. Volume

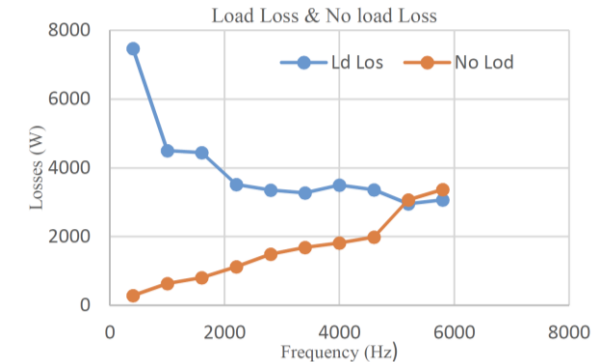
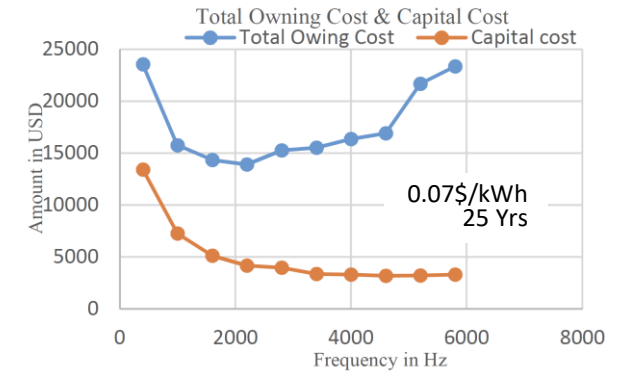


SST Xfrm Cost-Optimal Design

- **Xfrm Design Algorithm for Minimum TOC** (Total Owning Cost = Initial Costs & No-Load & Load Losses)
- **Comprehensive Consideration of Design Parameters** — Operating Frequ., Flux Density, Core Mat., etc.



Design Results		
kVA Rating of Transformer		1000 kVA
Voltage at No Load	HV	11000 V
	LV	415 V
Vector Group		Dyn11
Core Material		Amorphous (2605SA1)
Flux Density		0.199 T
AMPERES	HV	54.99 A
	LV	1327.97 A
Number of Turns	HV	168
	LV	4
Conductor Dimensions	HV	1.1 x 7.5 (mm) - Rectangular Type
	LV	0.8 x 450 (mm) - Foil Type
Core Width		213 mm
Optimum Frequency of Operation		2200 Hz
% Z		4.28 %
No Load Loss		1125 W
Load Loss		3516W
Insulation Class		F
Maximum Winding Temperature rise		100 °C
Type of Cooling		AN-AF
Number of Fans		2
Fault Current Temp rise		262 °C
Weight of Transformer		930 Kg
Total Capital Cost in USD		4100
Total Owning Cost in USD		13900

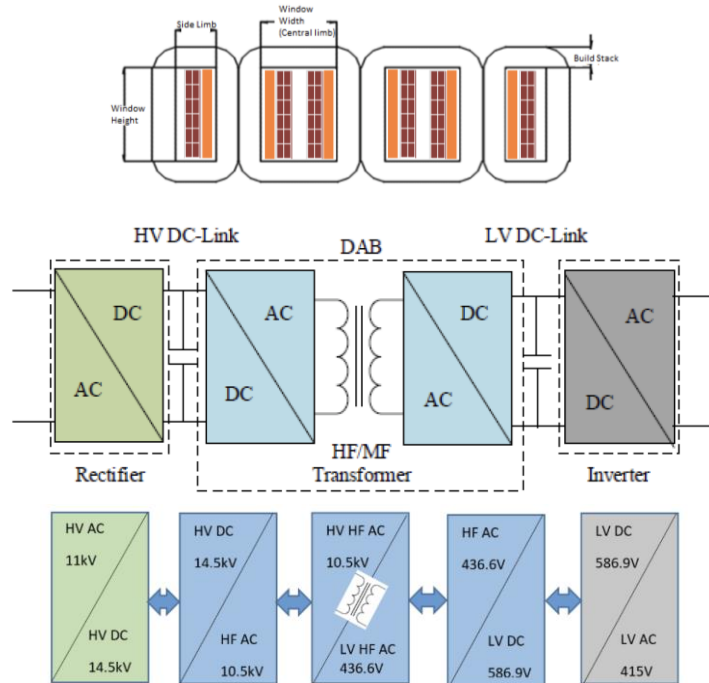


- **Results of 1 MVA | 11 kV / 415 V 3-Φ Wound Core Dry-Type Xfrm**
- **Comparison to LFT — 52% Saving in TOC | 67% in Manufact. Costs | 71% in Weight (Excl. Power Electronics)**



SST Xfrm Cost-Optimal Design

- **Xfrm Design Algorithm for Minimum TOC** (Total Owning Cost = Initial Costs & No-Load & Load Losses)
- **Comprehensive Consideration of Design Parameters** — Operating Frequ., Flux Density, Core Mat., etc.



Design Results		
kVA Rating of Transformer		1000 kVA
Voltage at No Load	HV	11000 V
	LV	415 V
Vector Group		Dyn11
Core Material		Amorphous (2605SA1)
Flux Density		0.199 T
AMPERES	HV	54.99 A
	LV	1327.97 A
Number of Turns	HV	168
	LV	4
Conductor Dimensions	HV	1.1 x 7.5 (mm) - Rectangular Type
	LV	0.8 x 450 (mm) - Foil Type
Core Width		213 mm
Optimum Frequency of Operation		2200 Hz
% Z		4.28 %
No Load Loss		1125 W
Load Loss		3516W
Insulation Class		F
Maximum Winding Temperature rise		100 °C
Type of Cooling		AN-AF
Number of Fans		2
Fault Current Temp rise		262 °C
Weight of Transformer		930 Kg
Total Capital Cost in USD		4100
Total Owning Cost in USD		13900

Comparison Charts of 1000kVA, 11000/415V, dry type transformer.		
Parameters Considered	High frequency Transformer (Amorphous Core material considered)	Power frequency Transformer
Core weight (kg)	725	2024
Conductor weight (kg)	68	423
Insulating material weight (kg)	61	561
Clamp weight(kg)	73	297
Total weight (excluding Tank)	930	3305
Cost of core assembly (\$)	2654	4250
Cost of windings (\$)	515	3189
Cost of insulation system (\$)	478	4391
Cost of accessory arrangements (\$)	364	775
No load losses (W)	1125	1550
Load losses (W)	3516	9000
No load Capitalization (\$/W)	4.809	4.809
Load Capitalization (\$/W)	1.11	1.11
Capital Cost (\$)	4100	12650
TOC (\$)	13900	29000

- **Results of 1 MVA | 11 kV / 415 V 3-Φ Wound Core Dry-Type Xfrm**
- **Comparison to LFT — 52% Saving in TOC | 67% in Manufact. Costs | 71% in Weight (Excl. Power Electronics)**



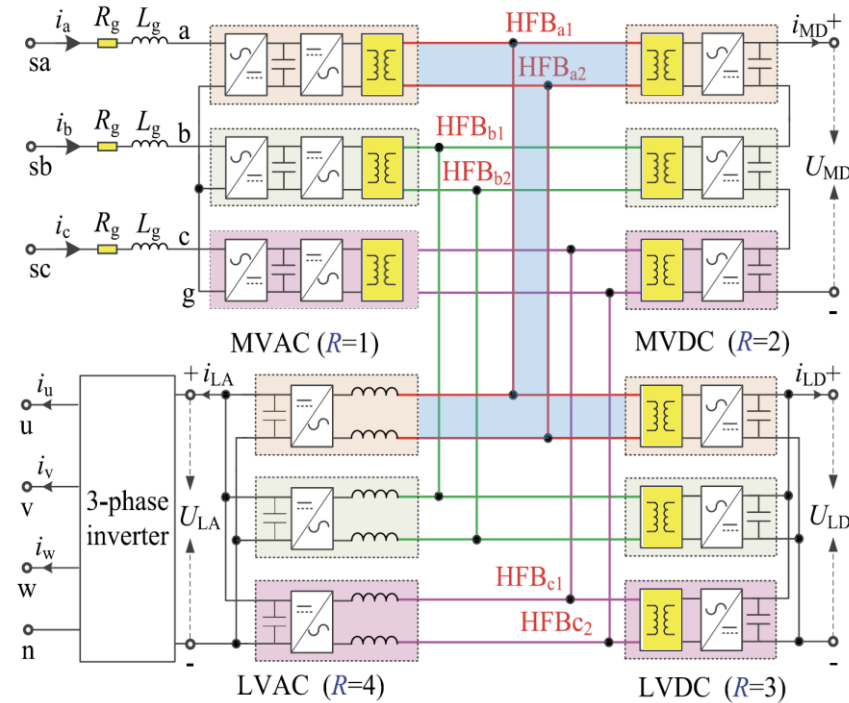
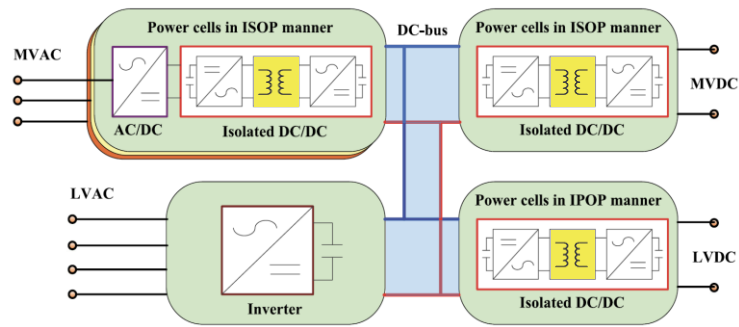


清华大学
Tsinghua University



Medium-Frequency AC-Bus Multi-Port SST (1)

- Highly Modular / Scalable Modular Multi-Active Bridge (MMAB) Topology as Core Element
- MF Isolation / Synchronism of all Ports — Analogy to the 50/60 Hz Grid

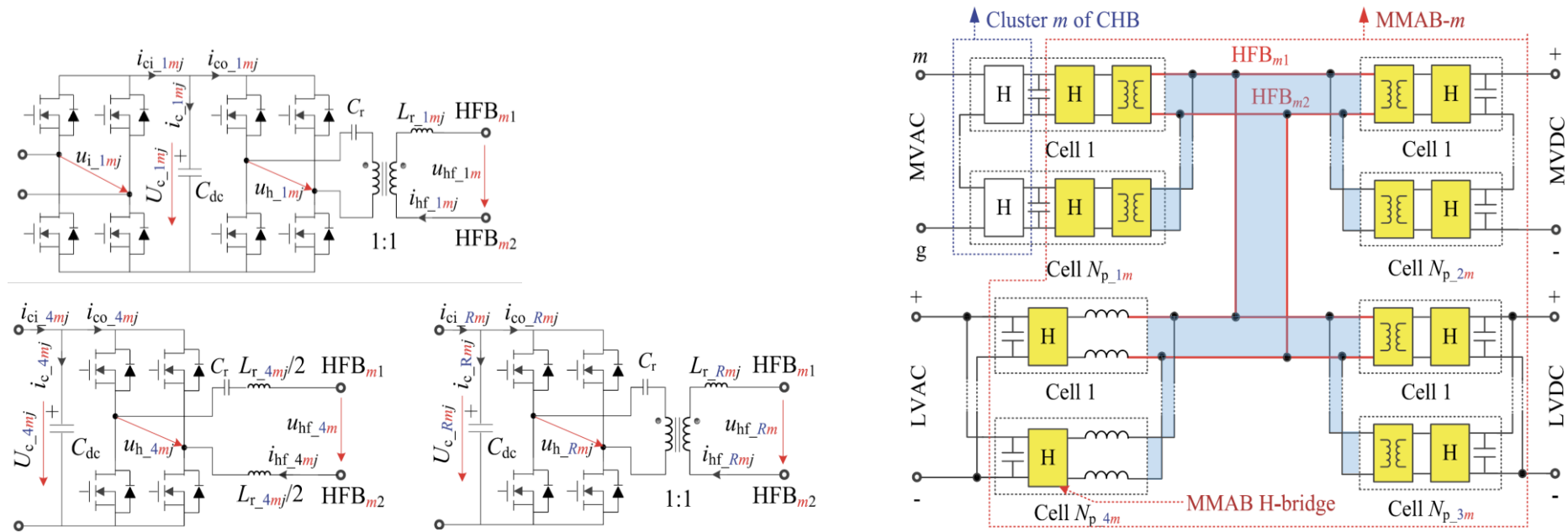


- MF AC-Bus Instead of DC-Bus Coupling of Converter Modules — Lower # of Converter Stages
- Direct Power Cross Coupling of all DC-Ports due to Missing Intermediate Energy Buffer Caps (!)



Medium-Frequency AC-Bus Multi-Port SST (2)

- Individual Xfrms Instead of Single-Core Multi-Wgd Xfrm | Low Complexity Basic Converter Cells
- Large Number of Functional Combinations — ISOP / IPOP etc.



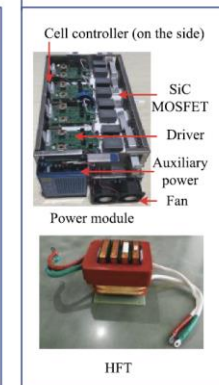
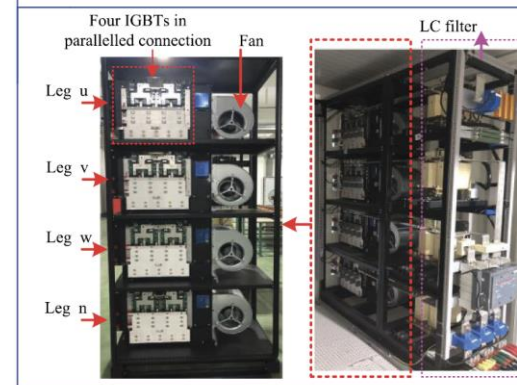
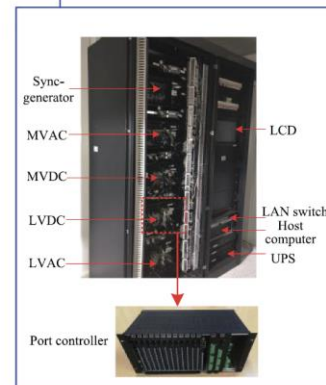
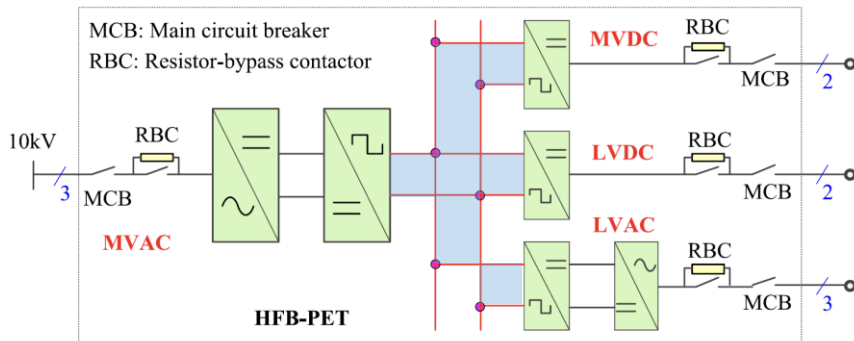
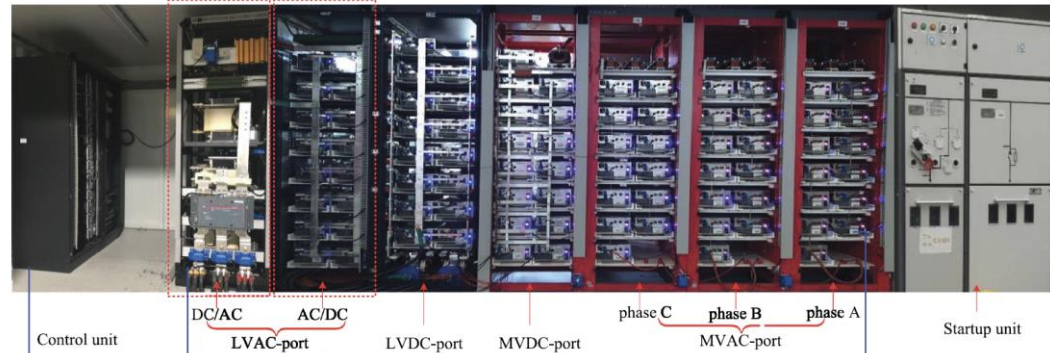
- 4-Port 1- Φ MVAC / MVDC / 1- Φ LVAC / LVDC SST Example
- Rectangular MF Voltages | DAB-Type Phase-Shift-Based Power Flow Control | Cross-Coupling Challenge (!)



Medium-Frequency AC-Bus Multi-Port SST (3)

- 2 MVA 4-Port 3- Φ MVAC / MVDC / 3- Φ LVAC / LVDC Industrial Prototype
- 3 MMAB Units Corresponding to Phases of the 3- Φ AC-Ports / 2 MF AC-Buses per MMAB

10 kV MVAC-Port
 10 kV MVDC-Port
 750 V LVDC-Port
 380 V LVAC-Port

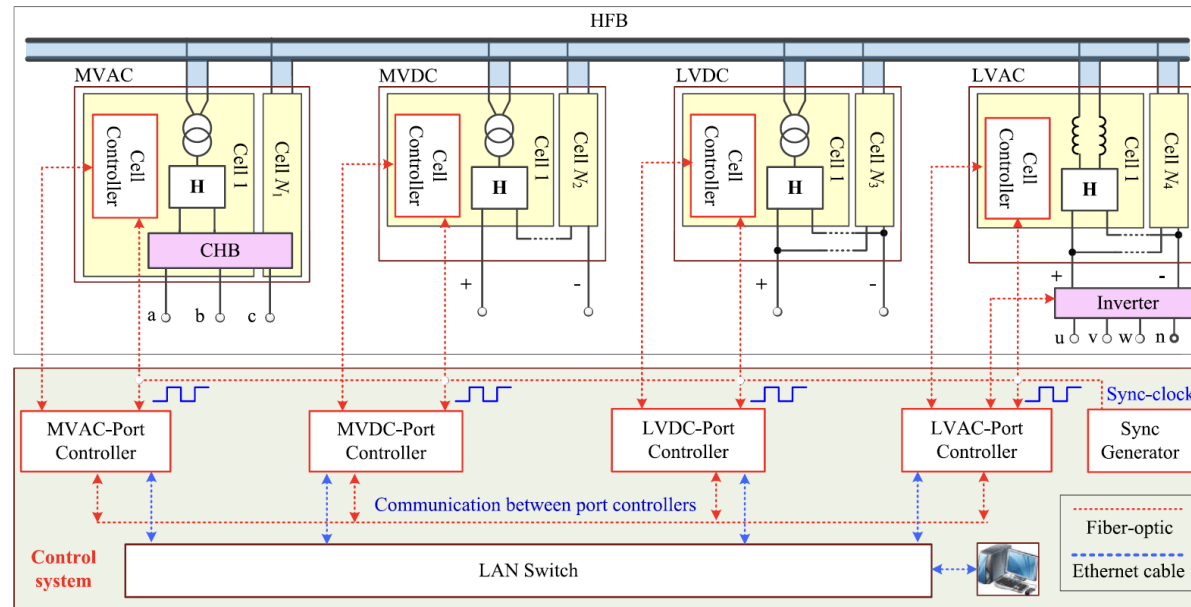


- 1200 V / 120 A SiC MOSFETs | $f_{sw} = 20$ kHz | 1:1 Xfrms / Ferrite UF130 | 850 V_{DC} Cell DC-Link / Output Voltage



Medium-Frequency AC-Bus Multi-Port SST (4)

- **2 MVA 4-Port 3- Φ MVAC / MVDC / 3- Φ LVAC / LVDC Industrial Prototype**
- **Hierarchical — Cell/Port/System — Control Framework with Global Synchronous Clock**

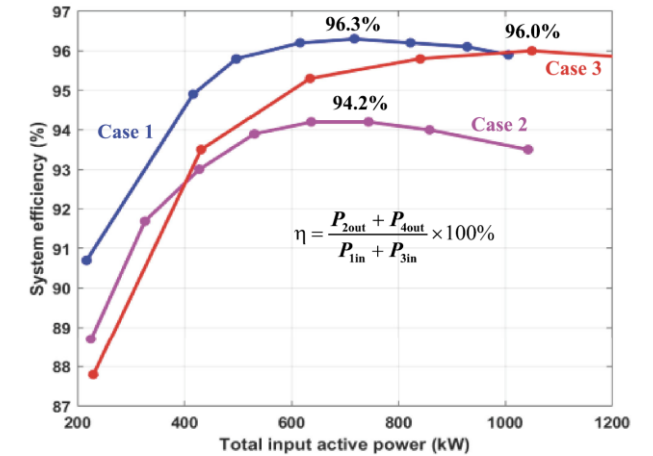
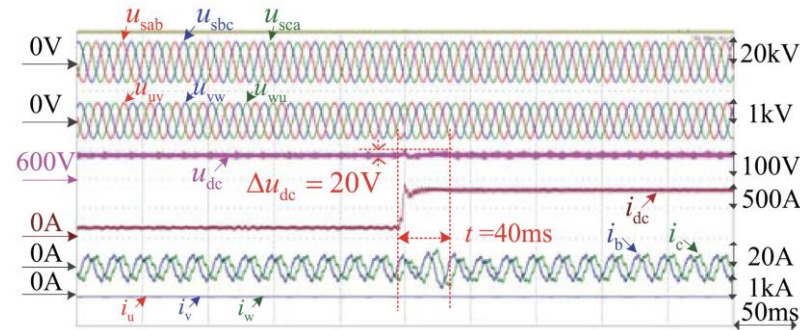
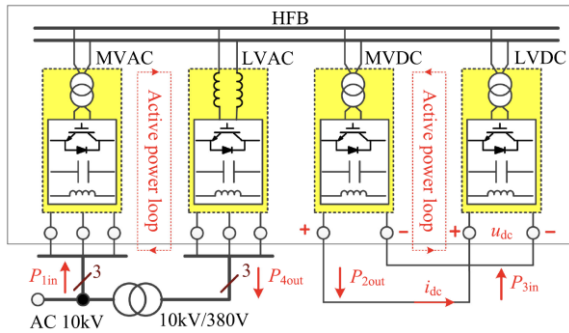


- **Power Cross Coupling Suppression of MMAB Ports by Feedforward Control**
- **Power Decoupling Control of MVAC CHB Converter Enables Unbalanced Grid Operation**
- **Cell-Power Balance Control of the MVDC CHB Cells Ensures Equal DC-Link Voltages**



Medium-Frequency AC-Bus Multi-Port SST (5)

- **Experimental Analysis** of 10 kV / 2 MVA 4-Port MVAC / MVDC / LVAC / LVDC Industrial Prototype
- **Power Circulation Back-to-Back Connection of the Converter Modules**



Case 1: $P_{4out} = 0$. Case 2: P_{2out} is about 90~100 kW.
 Case 3: P_{2out} and P_{4out} increase from ~100kW to ~600kW in steps of 100kW.

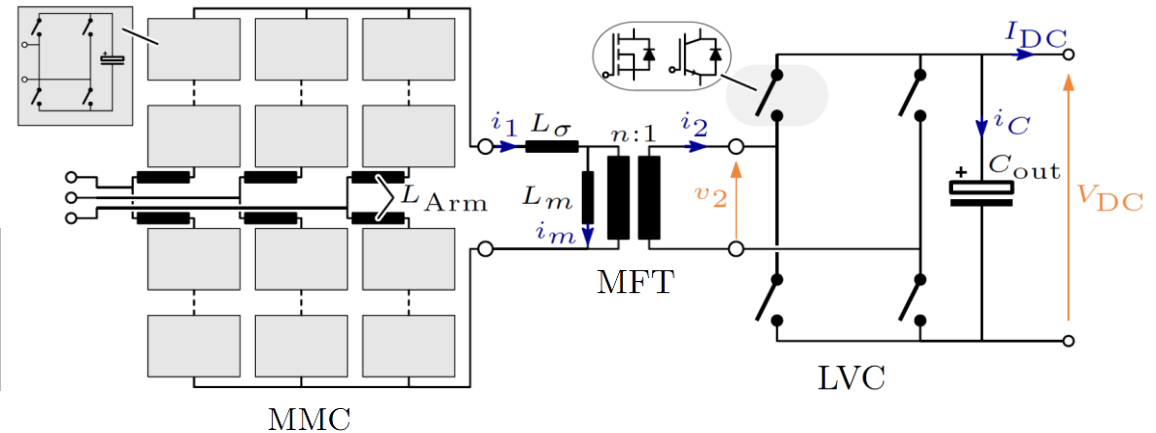
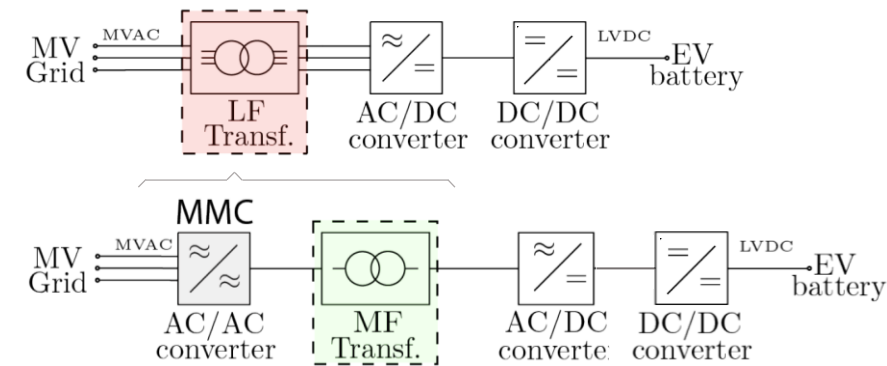
- **Series-to-Parallel Rearrangement of MVDC-Port Cells & Parallel Connection to LVDC-Port**
- **Dynamic Behavior for Load Step of DC-Loop Power Circulation | Power Conversion Efficiency**





3-Φ MMC-Based AC/DC SST (1)

- MV-Connected Compact High Power / Ultra-Fast EV Charging Systems
- 3-Φ LFT Replaced by Matrix-Type 3-Φ 50 Hz / 1-Φ MF AC/AC Conversion & 1-Φ MFT



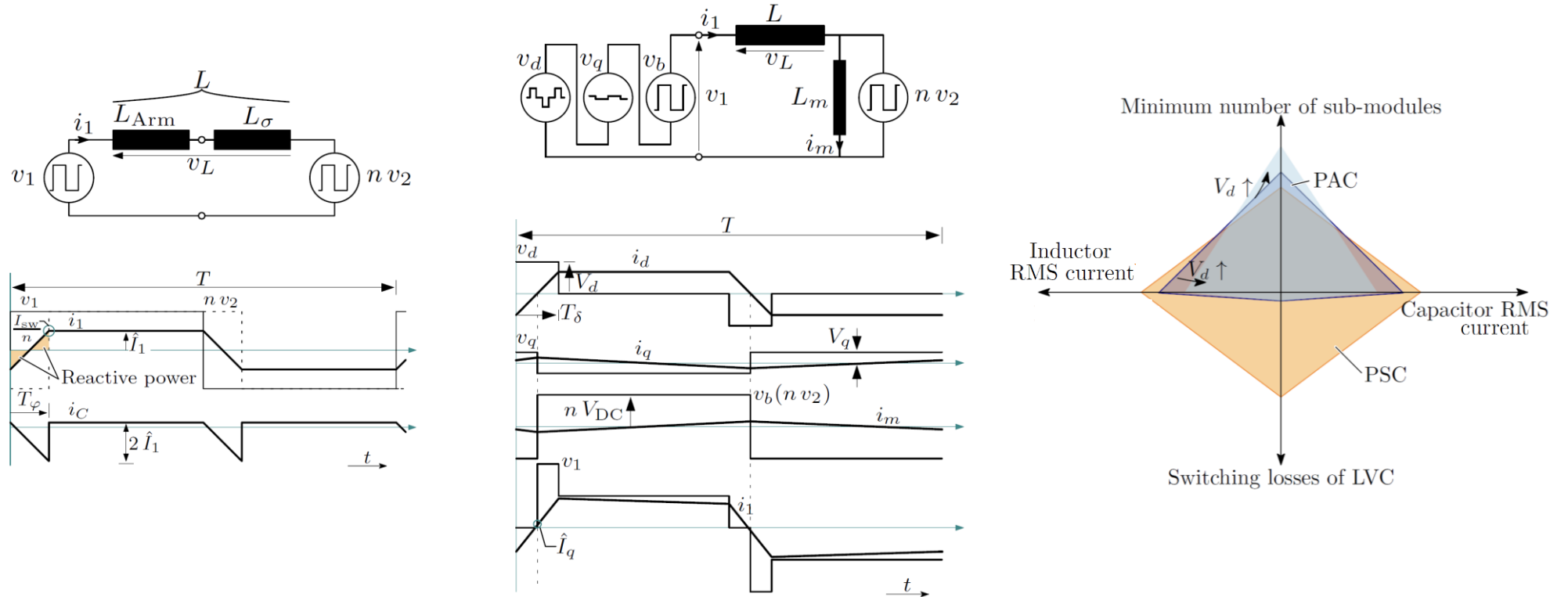
- Advantage of Single MFT Compared to CHB Arrangements
- Scalability | Redundancy Advantageously Limited to Power Semiconductors

1 MW
25 kV_{line-to-line} MVAC-Grid
800 V DC Output
1 kHz Sw. Frequency
10:1 MFT



3-Φ MMC-Based AC/DC SST (2)

- Rectangular MF Voltage for Minimizing $2x f_{sw}$ Power Pulsation
- Phase Shift Control (PSC) or Pulse Amplitude Control (PAC) / Amplitude-Modulated MMC Output Voltage



- PAC — v_d ($\pi/2$ -Shifted) & v_q (π -Shifted) for Decoupled Active & Reactive Power Control
- PAC Reduces Reactive Power & Sw. Losses of the LV Converter (LVC) / Higher # of Modules Comp. to PSC

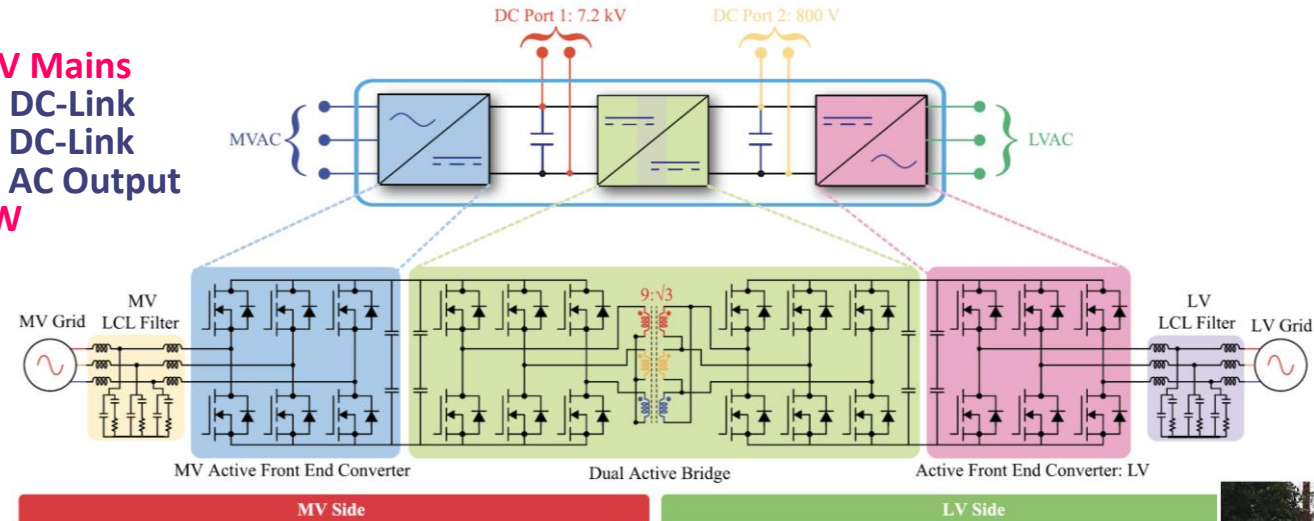




3- Φ 2-Level AC/DC—DC/DC—DC/AC SST (1)

- AC/AC SST for MV Mobile Utility Support Equipment (MUSE-SST) Placed in Mobile Container
- MV and LV DC-Links Facilitate Integration of Renewables / Energy Storage

4.16 kV Mains
7.2 kV DC-Link
800 V DC-Link
480 V AC Output
100 kW



Device used:
 10 kV SiC MOSFET module
 XHV-6/XHV-9 modules



Device used:
 1200 V - 325 A SiC MOSFET
 CAS325M12HM2

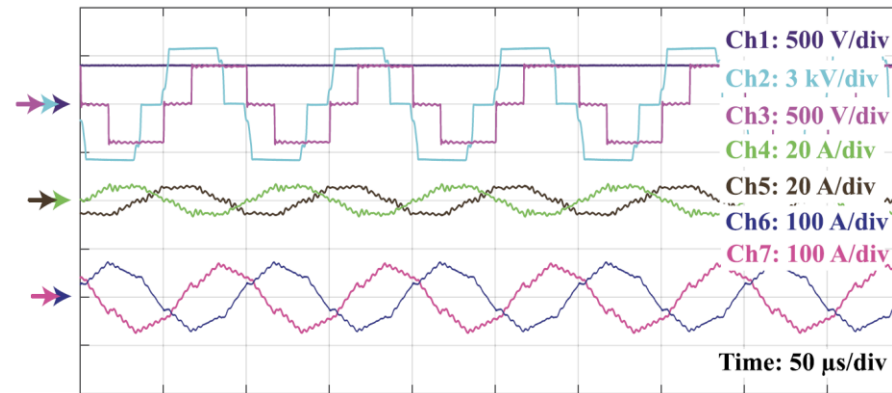
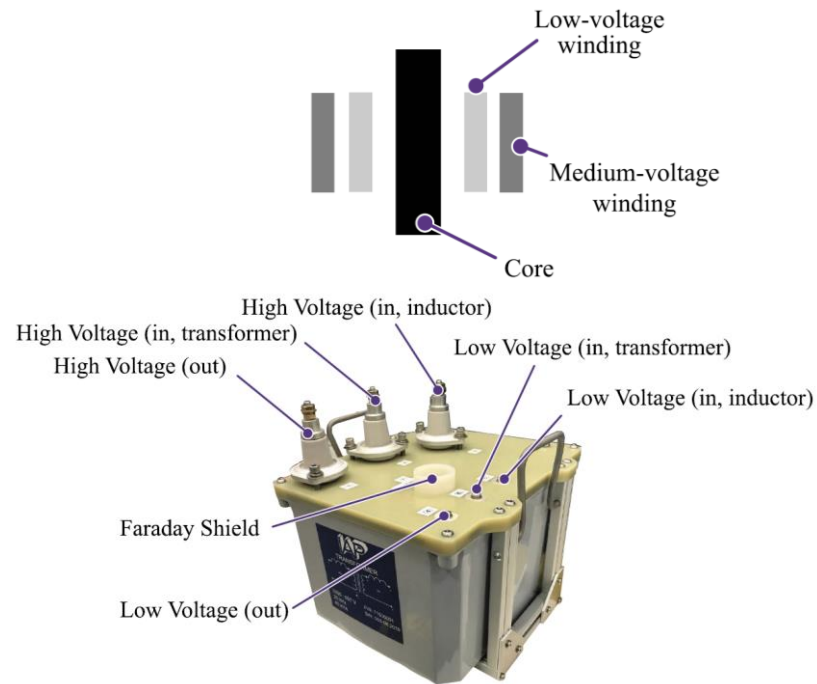


- 10 kV Gen 3 SiC MOSFETs in Extra High Voltage (XHV) Half-Bridge Module | 50 A @ 150 °C | 6 Dies / Switch
- Thermosyphon Air Cooling | Series-Parallel Film Capacitors | Sandwiched Busbar



3-Φ 2-Level AC/DC—DC/DC—DC/AC SST (2)

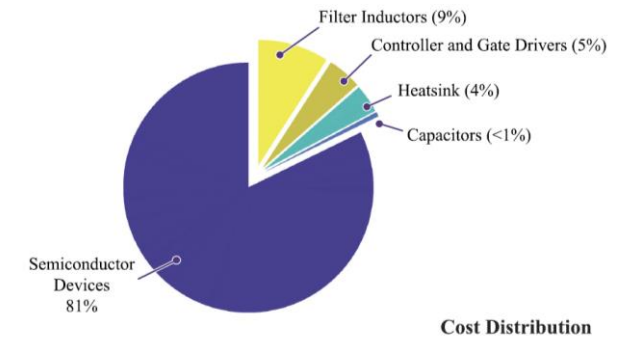
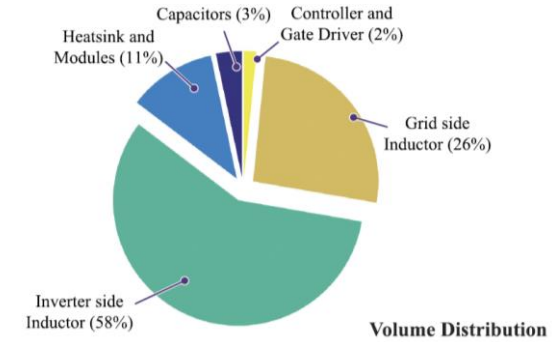
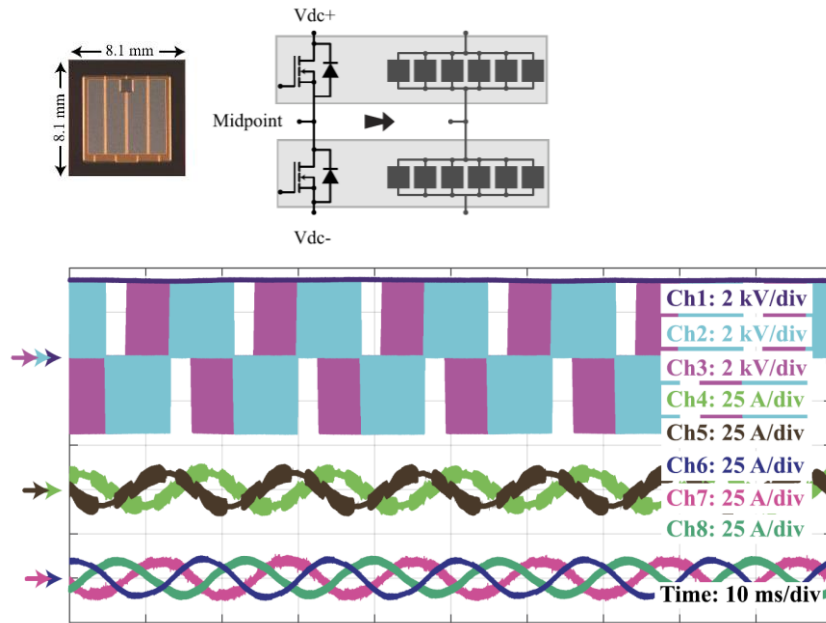
- **3x 1-Φ Xfrm** — Lower Basic Isolation Level (BIL) Voltage Comp. to a 3-Φ Xfrm – 26.7 kV vs. 40 kV
- Oil-Filled Plastic Container | 20 kV Bushings | MV-Side Farady Shield | Nanocryst. C-Cores | Ext. MV & LV Inductors



- Experimental Analysis @ 30 kW | 3.5 kV_{DC} | $f_{sw} = 10$ kHz — Xfrm Primary & Sec. Side Voltages / Currents

3-Φ 2-Level AC/DC—DC/DC—DC/AC SST (3)

- Experimental Analysis of MV Active Front-End Converter
- 30 kW | 3.5 kV_{DC} | f_{sw} = 10 kHz



- Line-line Sw. Stage Voltages | Boost Ind. Currents | Mains Phase Currents — η ≈ 95.5% @ 35 kW
- Volume | Cost Distribution of MV Power Block | 0.2 kW/dm³ | 550 \$/kW | 0.6 kW/kg

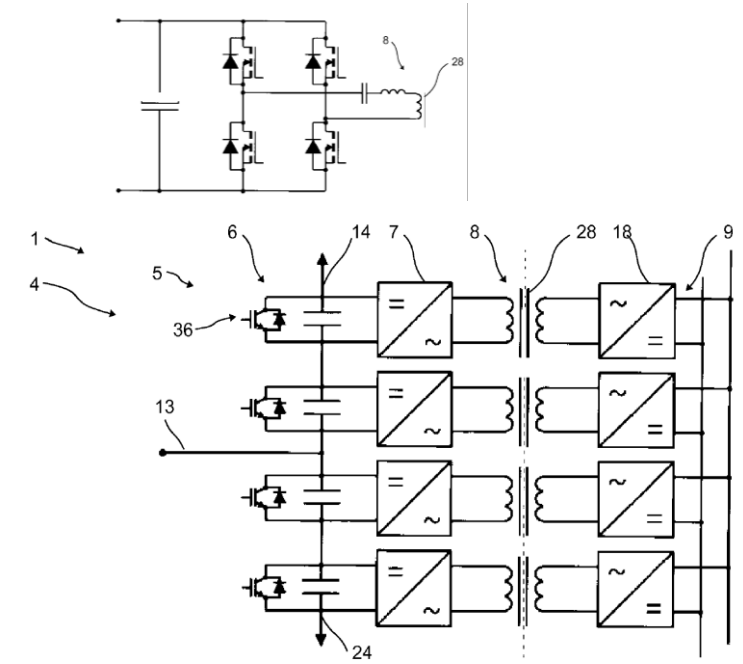
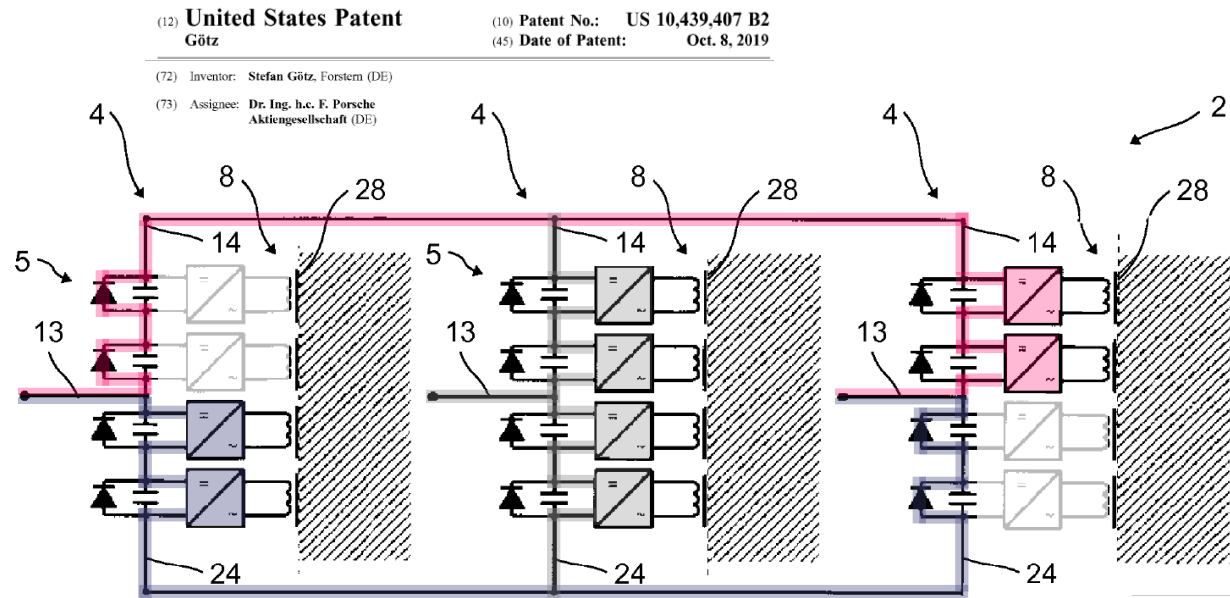




— **PORSCHE** —

3-Φ Full-Bridge-Front-End Modular-Back-End AC/DC SST

- **Diodes Select Active Strings** Dependent on Line-to-Line Mains Voltage & Ensure **Unipolar Mod. Inp. Voltages**
- **Power Consumption of Active Strings Selected for Sinusoidal Mains Current Shaping**
- **Rel. Low Utilization of Overall Installed Module Power**



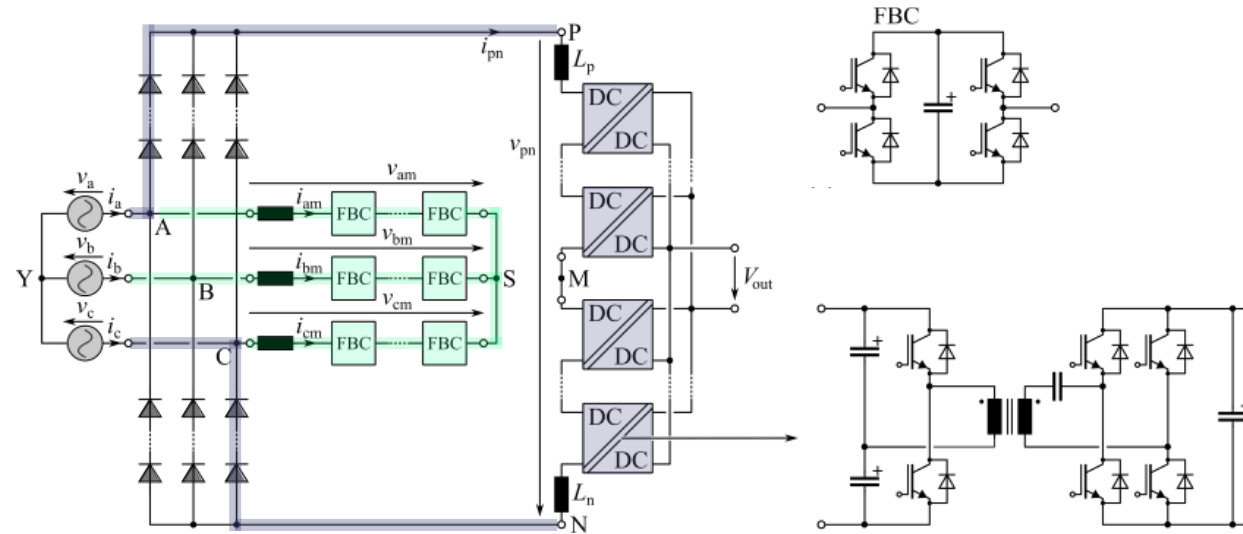
- **Low Complexity Modules w/o AC/DC Input Stages** | High DC Output Interconnection Flexibility
- **Bidir. Power Flow Capability** for Ext. of Diode Branches w/ Antiparallel Transistors
- **Module Input Power Partitioning** Allows Diode Blocking Voltage Balancing





3- Φ Diode-Bridge & Active-Filter Front-End AC/DC SST (1)

- Six-Pulse Shaped Diode-Bridge Output Voltage & Current / Const. Inp. Power of DC/DC Converter String
 - AC-Connected Active Filter (AF) Ensures Sinusoidal Mains Current Consumption
- Addition of AF Current Components to Currents of Conducting Diode Branches / No Avg. Power Flow
- Injection of Current into Not Conducting Diode Branch Phase

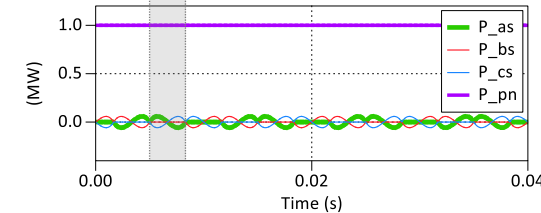
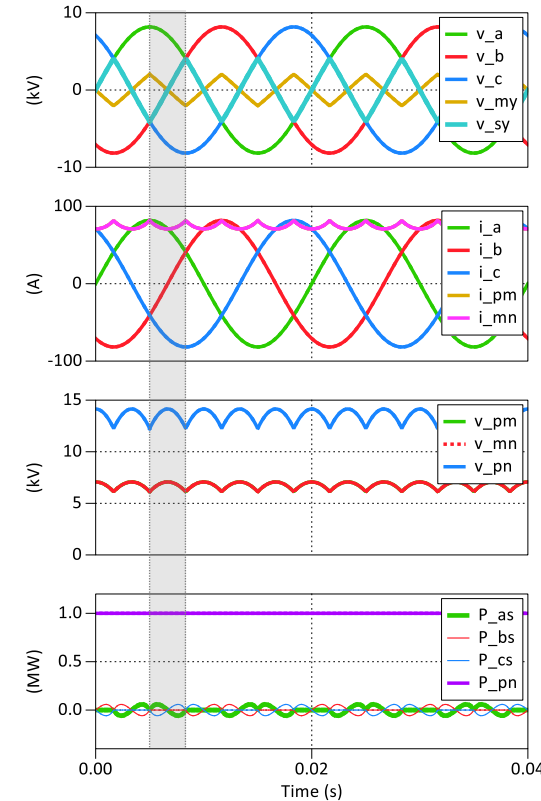
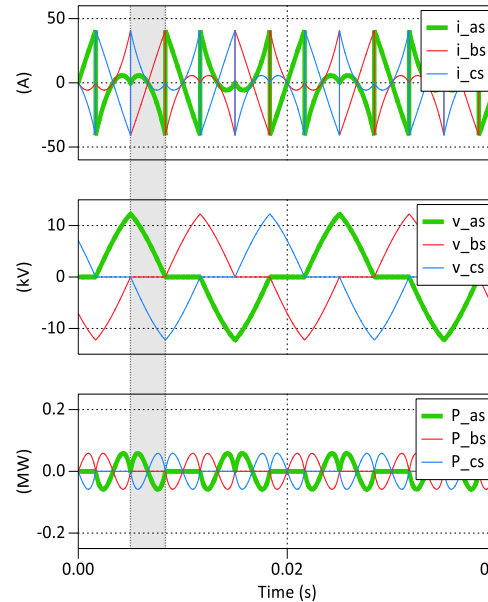
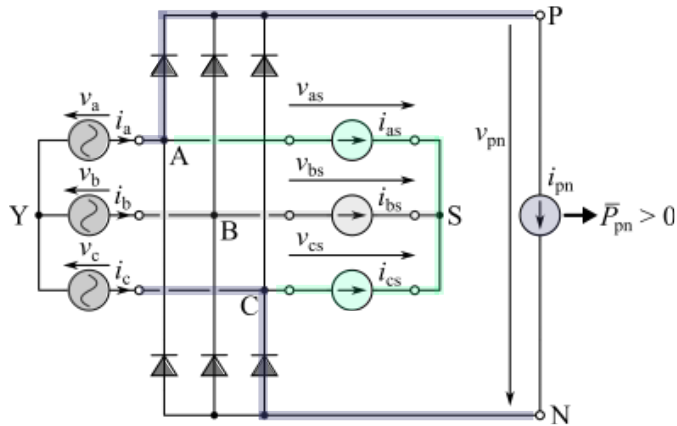


- Lower Complexity Comp. to Three AC-Connected AC/DC Converter Strings
- High Reliability / Load Power Supply Not Dependent on AF Operation



3-Φ Diode-Bridge & Active-Filter Front-End AC/DC SST (2)

- Characteristic Waveforms | m Indicates Virtual Midpoint of P-N
- Operation @ 10 kV_{line-to-line} AC-Mains & 1 MW

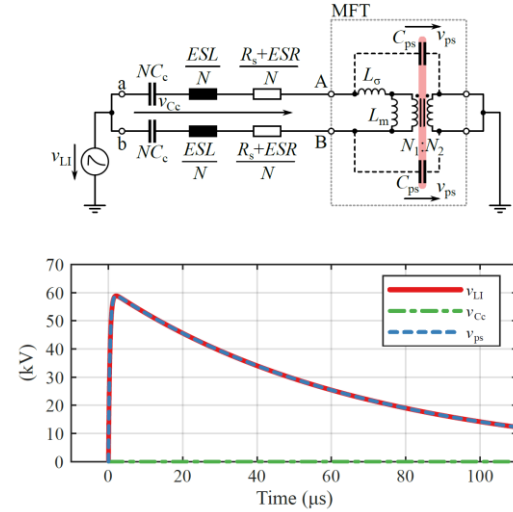
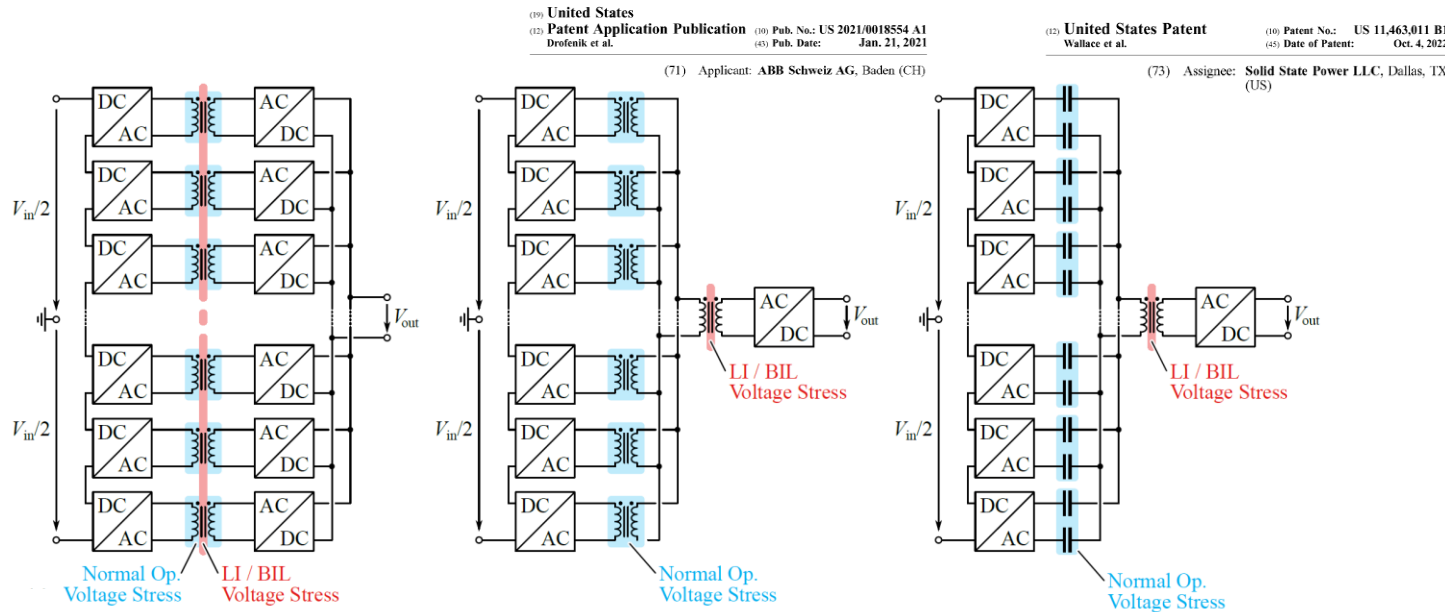


- Possible Limitation of AF Operation to Phases w/ Max. & Min. Voltage / 2-out-of-3 Filter Branches (!)
- Saving of AF Sw. Losses But Higher AF String Voltages



Remark Cascaded Capacitive/Inductive Isolation (1)

- Design of ISOP Module Transformers for LI Test Compliance Results in Large Vol. Overhead
- Splitting of Isolation Requirements — Normal Operation Voltage & LI Test Voltage

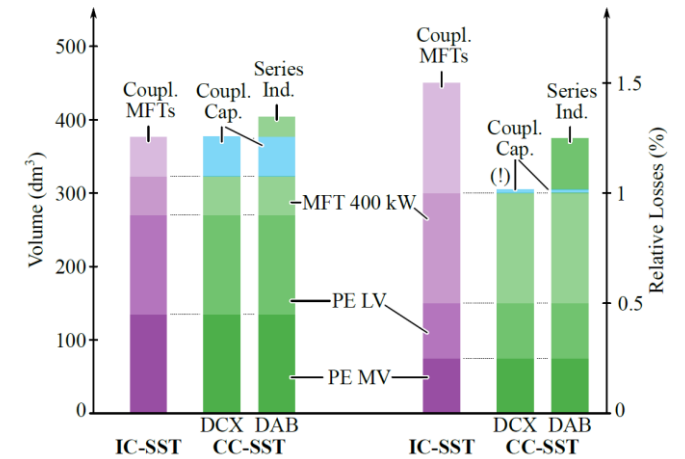
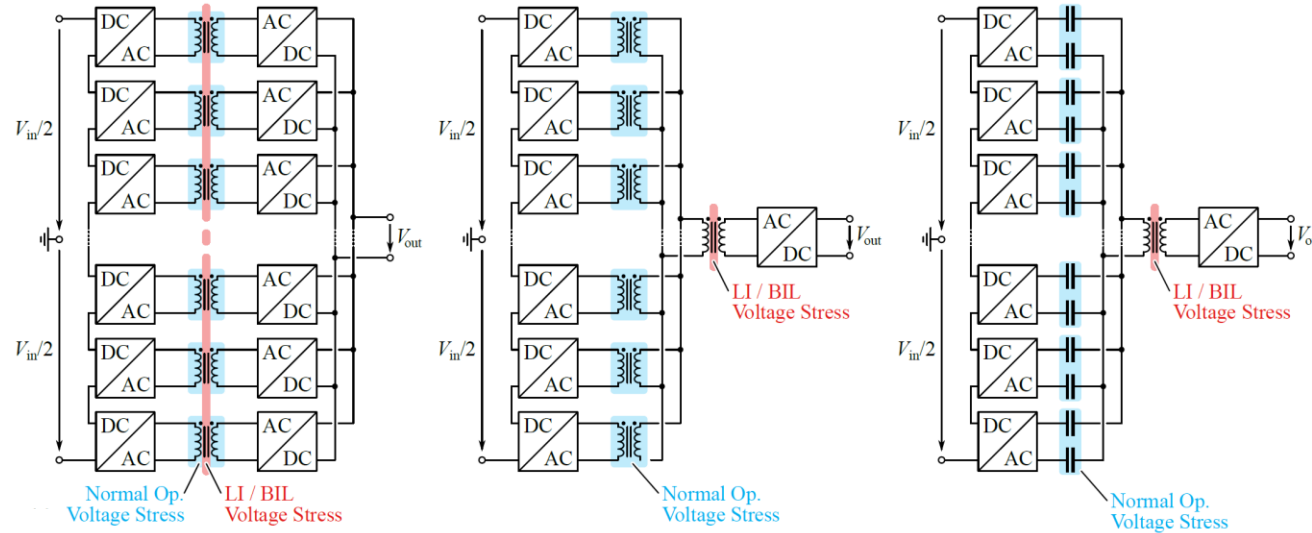


- Module Transformers Designed for Normal Operation Voltage Stress | Alternative Cap. Coupling / Isolation
- Dedicated Add. Transformer for LI Test Compliance / Lower “Modularization Penalty”



Remark Cascaded Capacitive/Inductive Isolation (2)

- Design of ISOP Module Transformers for LI Test Compliance Results in Large Vol. Overhead
- Splitting of Isolation Requirements — Normal Operation Voltage & LI Test Voltage

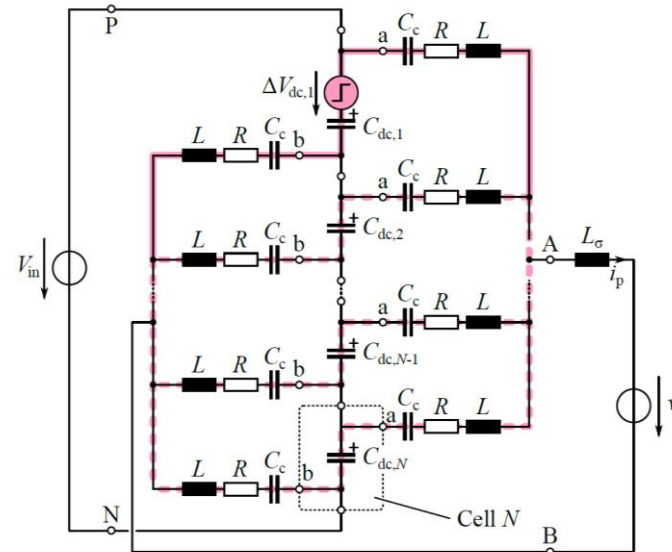
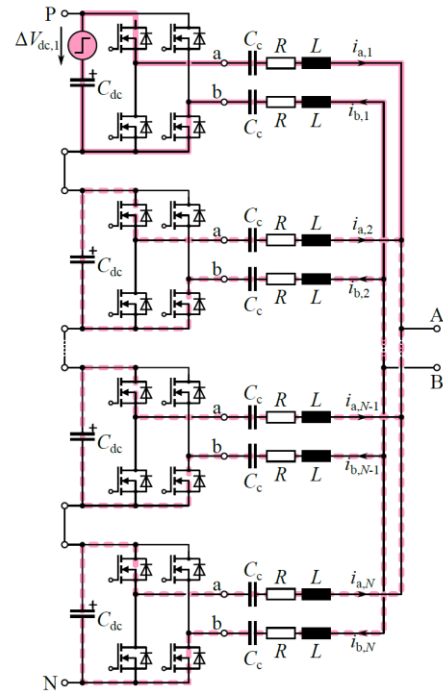


- Cap. Isol. — Lower Losses & Off-the-Shelf Realization / Volume Comparable to Transformer Isolation



Remark Cascaded Capacitive/Inductive Isolation (3)

- Design of ISOP Module Transformers for LI Test Compliance Results in Large Vol. Overhead
- Splitting of Isolation Requirements — Normal Operation Voltage & LI Test Voltage




- DC-Link Voltage Imbalances / Comp. Tolerances / Sw. Time Diff. → Circulating Currents
- Limiting Series Inductors &/or Dual-Active-Bridge-Type Control Instead of DCX Operation

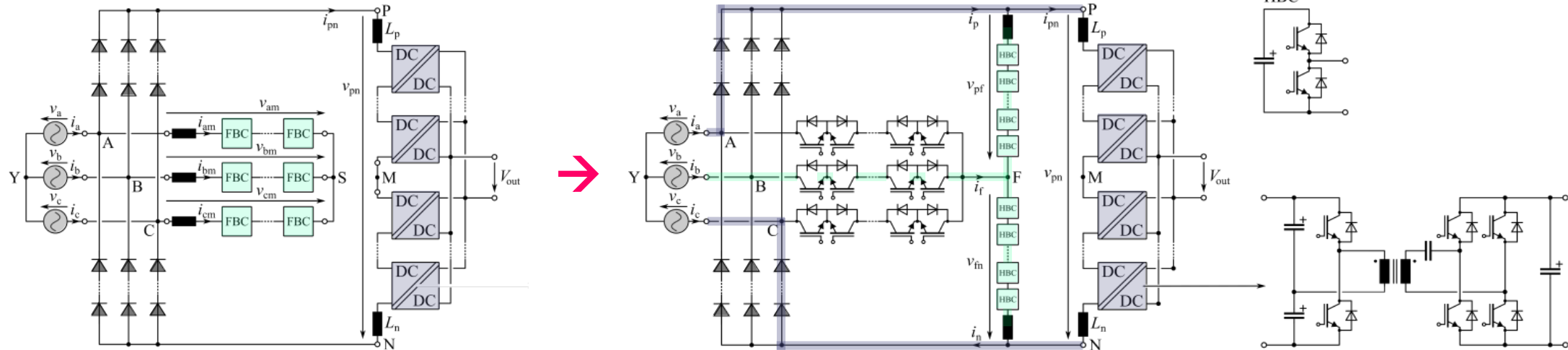


3-Φ Diode-Bridge Front-End & Integr. Act. Filter AC/DC SST (1)

- Six-Pulse Shaped Diode-Bridge Output Voltage & Current / Const. Inp. Power of DC/DC Converter String
- AC-Connected Active Filter (AF) Shifted to Diode-Bridge DC Output / Half-Bridge Cells (!)
- Mains Frequ. Commutated Current Injector Switches

- Injection of Current into Phase w/ Not Conducting Diode Branch
- Currents Drawn from DC+ / DC- Ensure Sin. Diode Bridge Inp. Current

(19)  österreichisches patentamt (10) **AT 516643 B1 2018-02-15**
 (73) Patentinhaber: Schneider Electric Power Drives GmbH 1210 Wien (AT)
 (72) Erfinder: Hartmann Michael 1040 Wien (AT)

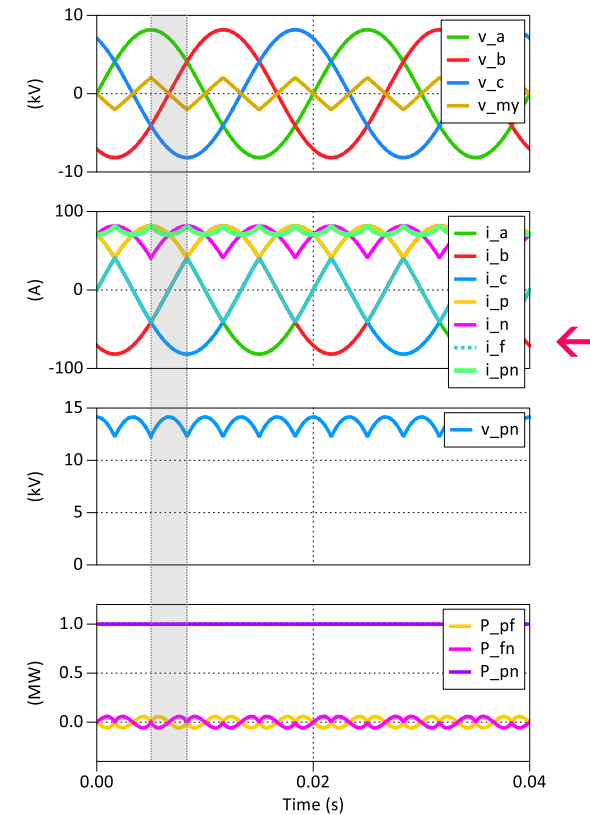
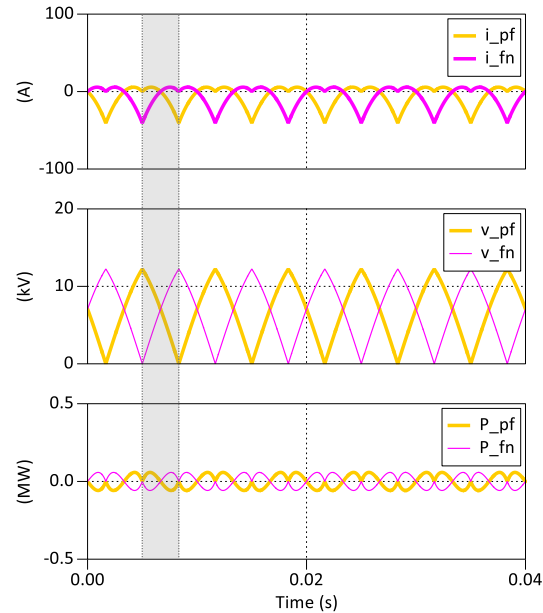
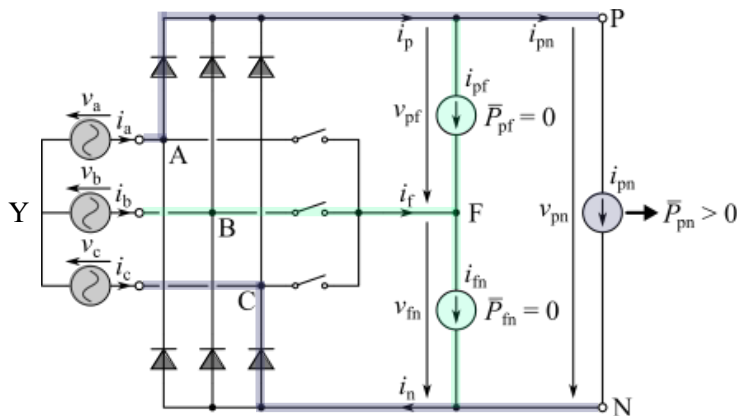


- Lower Complexity Comp. to AC-Side Filter | Voltage Balancing of Series-Connected Injector Switches
- Practical Realization — Full-Bridge Cell Add. to Half-Bridge Filter Cells for Comp. of Inductive Voltage Drops



3-Φ Diode-Bridge Front-End & Integr. Act. Filter AC/DC SST (2)

- Characteristic Waveforms | m Indicates Virtual Midpoint of P-N
- Operation @ 10 kV_{line-to-line} AC-Mains & 1 MW

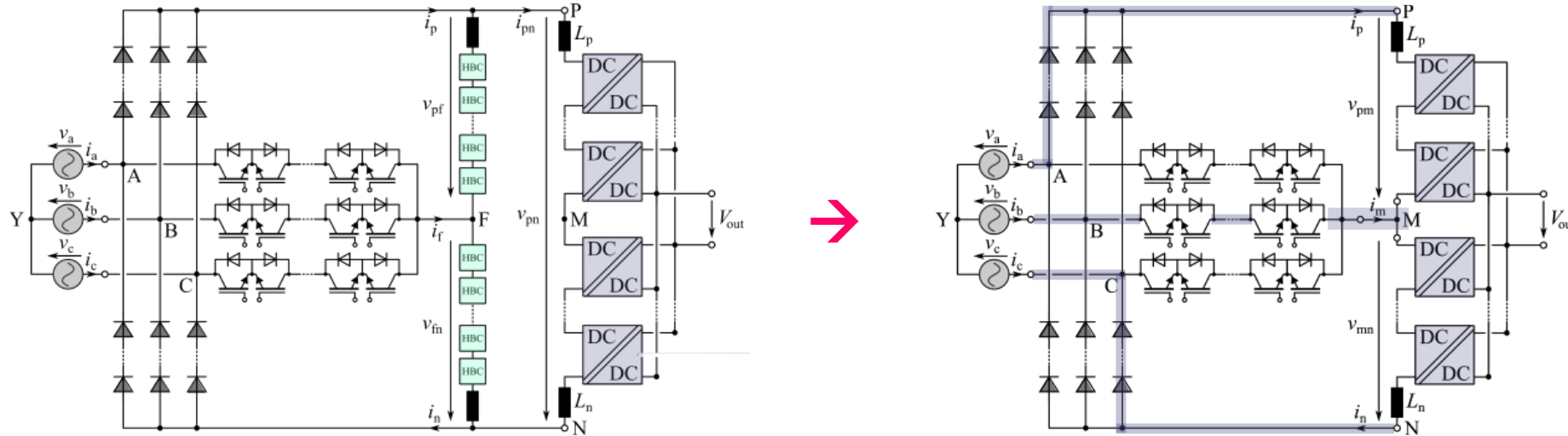


- Low Voltage Values v_{pf} & v_{fn} @ High Values of Currents i_{pf} & i_{fn} — Low Power Rating of Filter Strings
- Rel. High Max. Voltages Across Upper and Lower Filter String



3-Φ Unfolder Front-End AC/DC SST (1)

- **Combination of Active Filter & DC/DC Converter Functionality**
- **String of Bidirectional / Bipolar Blocking Phase Selector Switches**
- **Difference of Upper & Lower DC/DC Conv. String Currents Injected into Phase with Blocking Diode Branch**

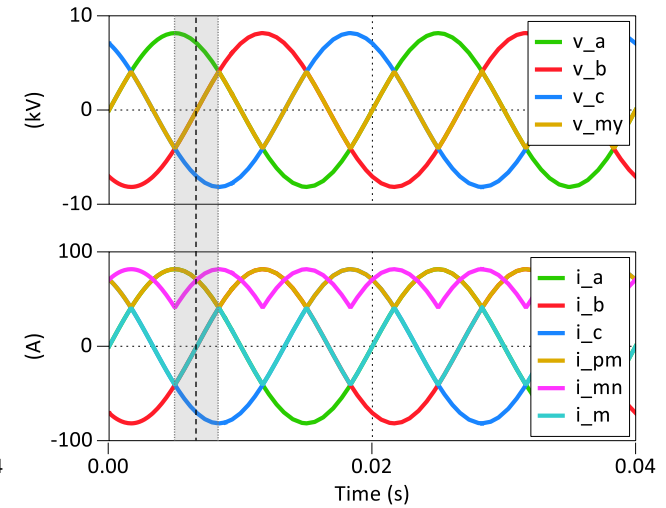
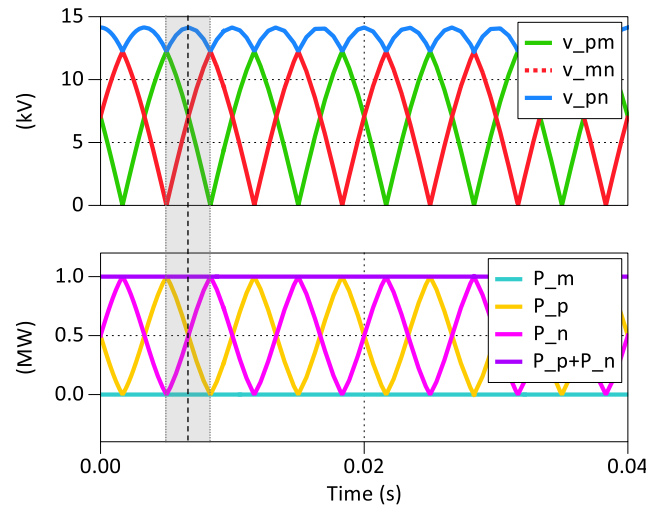
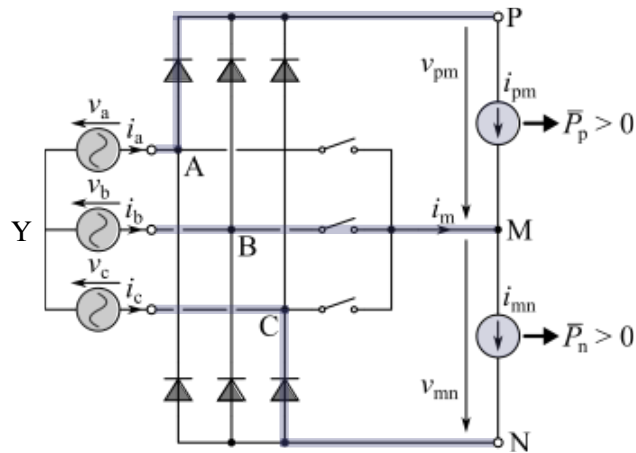


- **Lower Complexity Compared to Integr. Act. Filter Diode-Bridge Rectifier**
- **Large Voltage & Power Fluctuations of the DC/DC Converters Strings / Rel. Low Utilization**



3-Φ Unfolder Front-End AC/DC SST (2)

- Characteristic Waveforms | M Indicates Midpoint of P-N
- Operation @ 10 kV_{line-to-line} AC-Mains & 1 MW

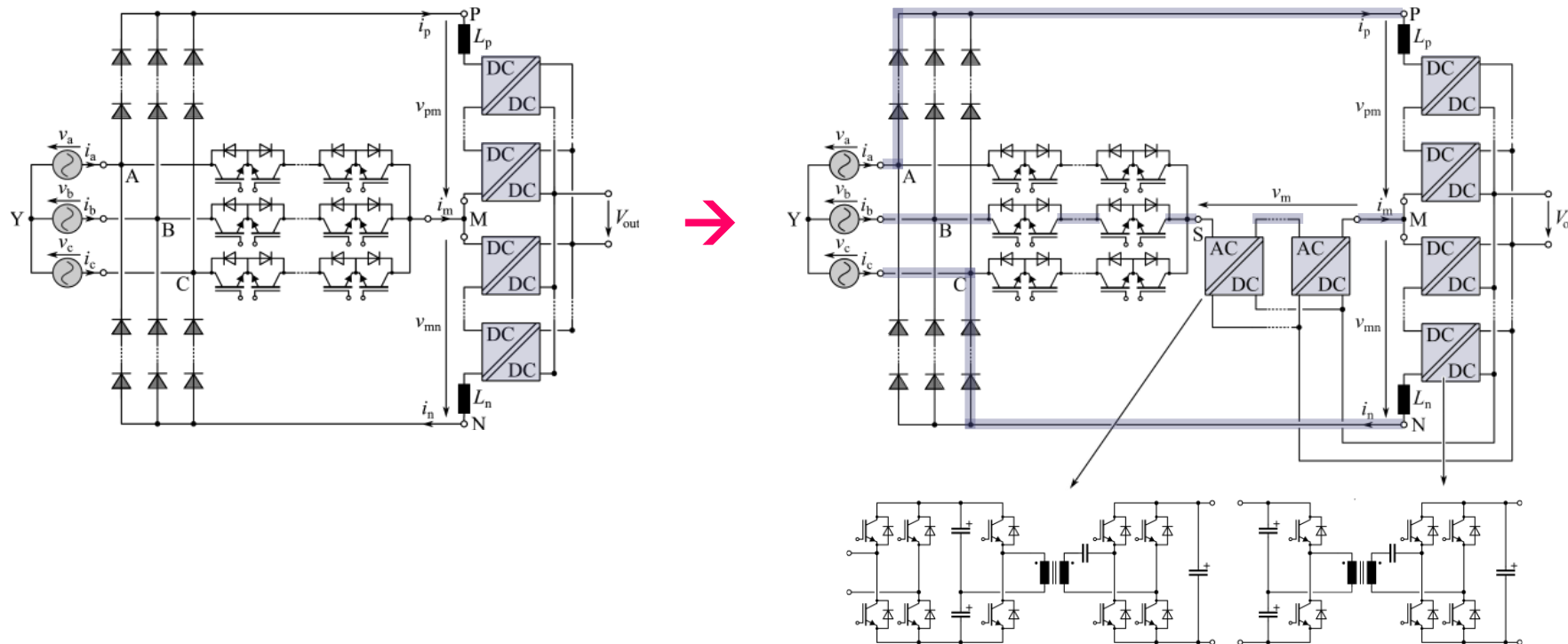


- Voltages v_{pm} & v_{fn} of DC/DC Conv. Strings Varying Btw 0... $\sqrt{3}/2$ Line-to-Line Voltage Amplitude
- Power Processed by DC/DC Conv. Strings Fluctuates Btw 0... $P_{nominal}$



3- Φ Unfolder Front-End Symm. Back-End AC/DC SST (1)

- AC/DC Conv. Cells Inserted Btw Starpoint of Phase Selector Switches & DC/DC Conv. String Midpoint
- Midpoint Curr. Shape Def. by Phase w/ Blocking Diode-Bridge Branch / As for Integr. Act. Filter

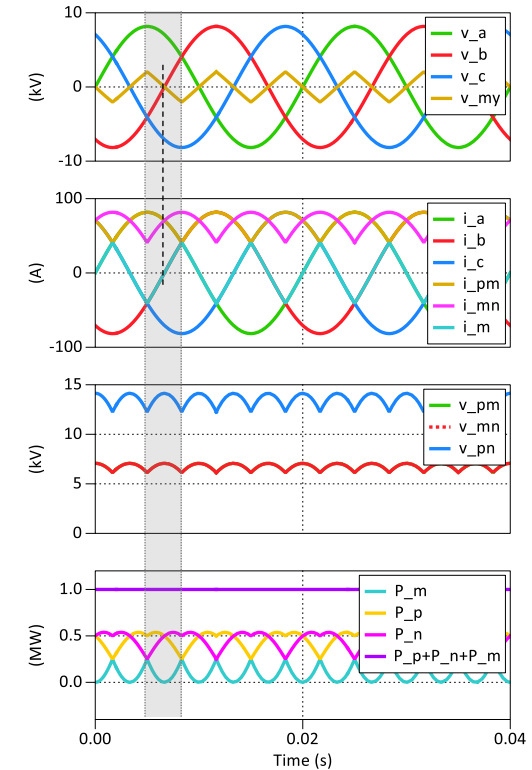
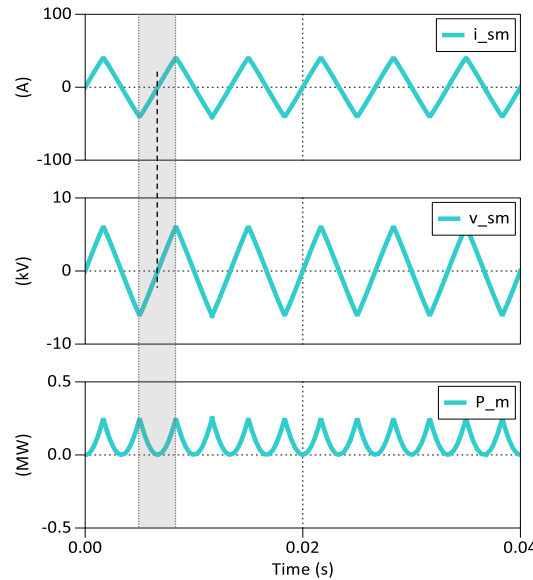
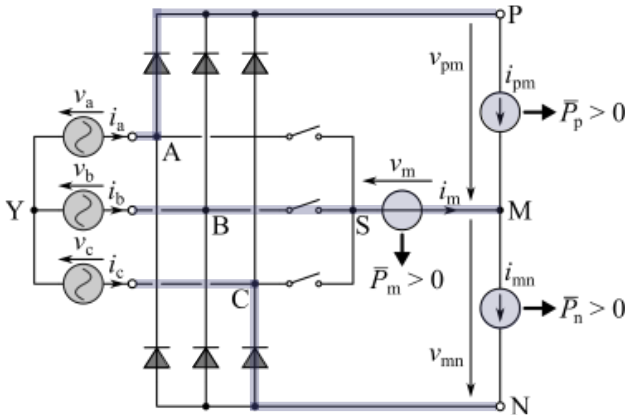


- Largely Const. DC/DC Conv. String Voltages
- Largely Equal Instantaneous Power Delivery of Both DC/DC Conv. Strings



3-Φ Unfolder Front-End Symm. Back-End AC/DC SST (2)

- Characteristic Waveforms
- Operation @ 10 kV_{line-to-line} AC-Mains & 1 MW

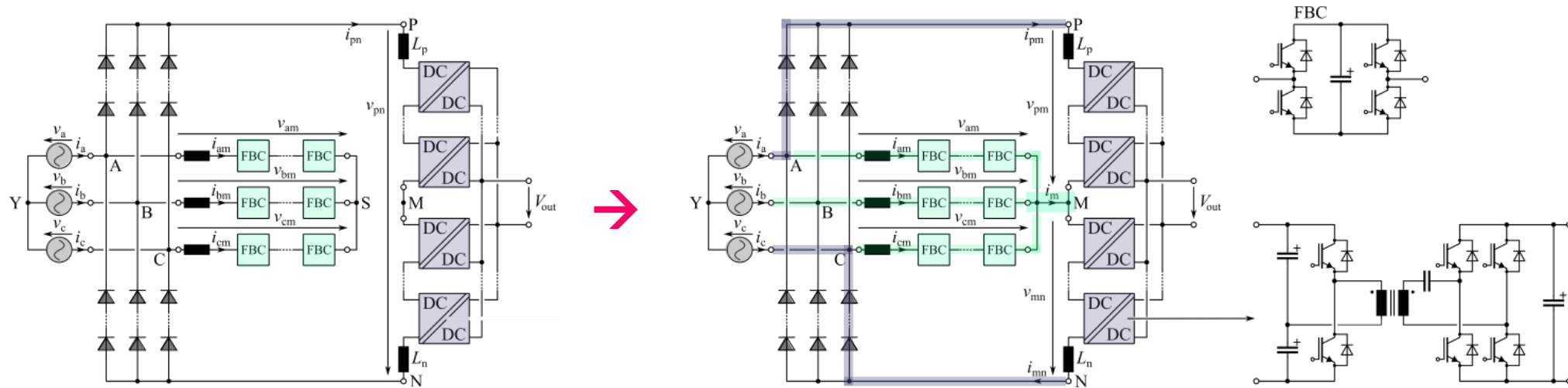


- Largely Const. DC/DC Conv. String Voltages
- Largely Equal Power Delivery of Both DC/DC Conv. Strings / Rel. Low Power Processed by AC/DC Cells



3-Φ Vienna-Rectifier-Type AC/DC SST (1)

- Star-Point of AC-Side Act. Filter Filter Connected to DC-Link Midpoint
- **Active Voltage Balancing** of Upper and Lower DC/DC Converter Strings
- **2/3 Act. Filtering Allows to Limit Sw. Operation to 2 Filter Branches**

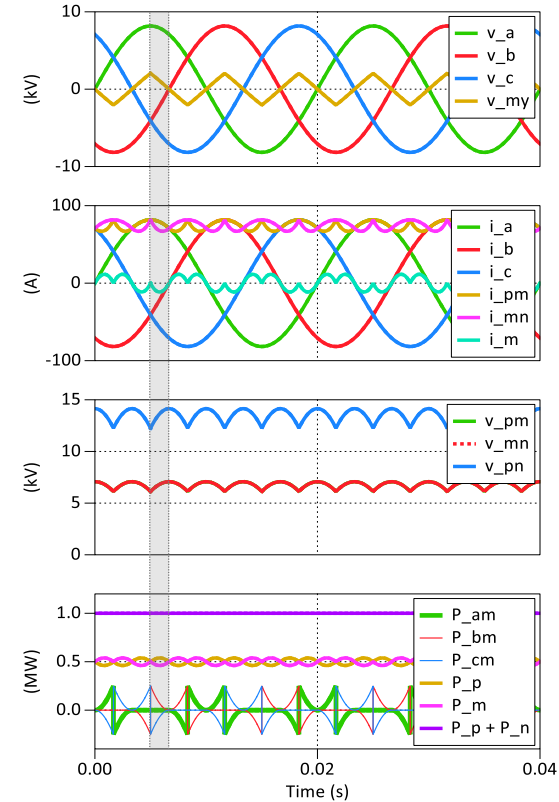
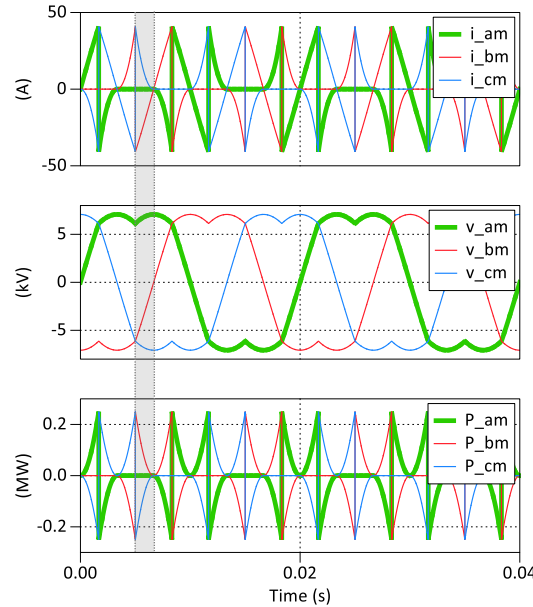
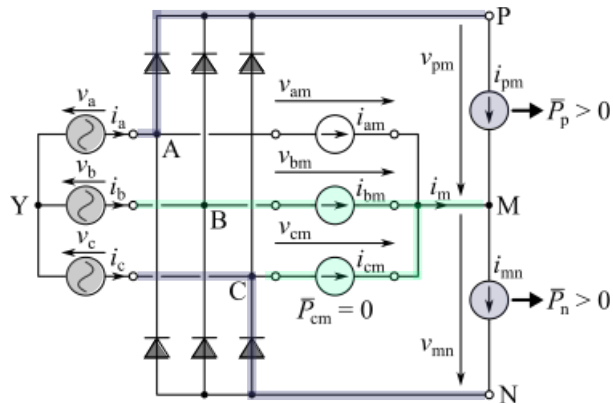


- **Structural Similarity to Vienna Rectifier Topology**
- **String Voltages Def. by 1/2 Instead of $\sqrt{3}/2$ Mains Line-to-Line Voltage Amplitude**
- **Blocking Voltage of All Power Transistors Clamped by Local Cap. &/or Def. by Act. Contr. Voltage Partitioning (!)**



3-Φ Vienna-Rectifier-Type AC/DC SST (2)

- Characteristic Waveforms | M Indicates Midpoint of P-N
- Operation @ 10 kV_{line-to-line} AC-Mains & 1 MW



- 3/3 Act. Filter Operation / All 3 Filter Branches Active / Avg. $i_m = 0$ / $i_{pm} = i_{mn}$ (Not Shown)
- Low Sw. Loss 2/3 Operation Utilizes Midpoint Connection to Allow i_m / Decouple i_{pm} and i_{mn}
- 1-out-of-3 Mains Phase Currents Dir. Controlled by DC/DC String / 2 Other Currents Shaped by 2 Filter Strings

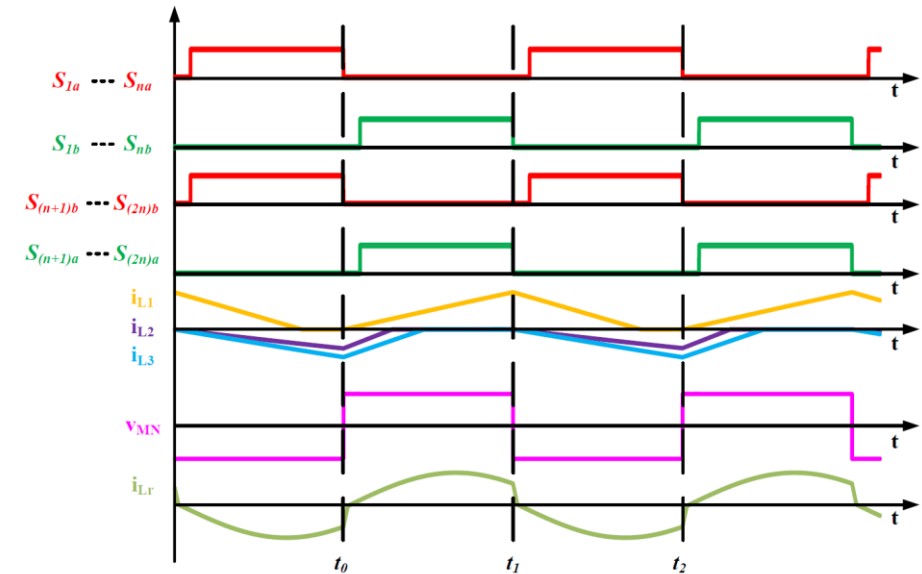
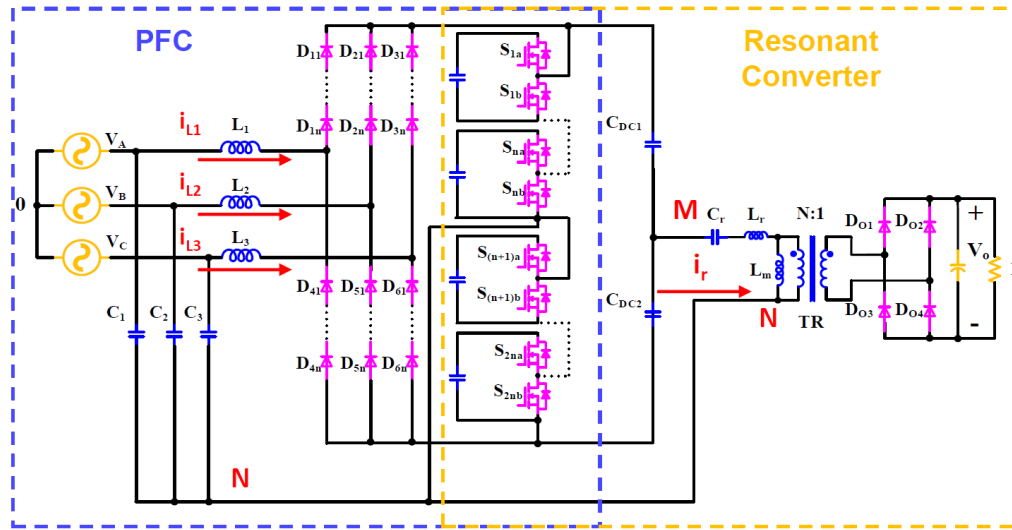




3-Φ Diode-Bridge Front-End TCM Single-Stage Taipei-SST

- Integration of Discont. Current Mode PFC Rectifier & Resonant DC/DC Converter
- Sinusoidal Mains Current | Single Transformer | Single-Stage Power Conversion
- All Switches Operating at Same Frequency

Source:  DELTA
Zhang et al., APEC 2023



$$\begin{aligned} v_{AN} &> 0 \\ v_{BN} &< 0 \\ v_{CN} &< 0 \end{aligned}$$

- Low Complexity Circuit Topology & Control | Unidirectional | $2\hat{U}_{\text{phase}}$ as Min. DC-Link Voltage
- String of Half-Bridges Implementing a Quasi-Two-Level Controlled ZVS Switching-Leg
- MV Input Facilitates High Output Power @ Rel. Low Current Stress Despite DCM Operation



3- Φ Diode-Bridge Front-End TCM Single-Stage Taipei-SST

■ Experimental Verification

12 kW

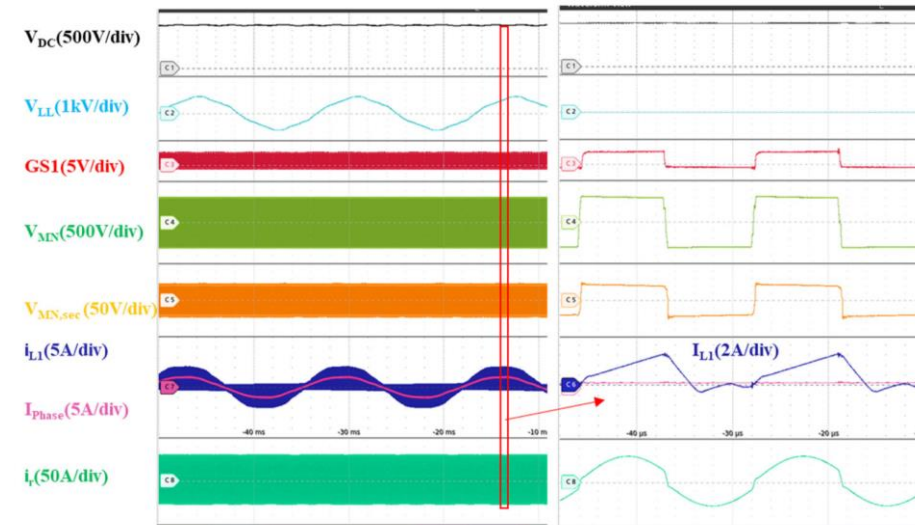
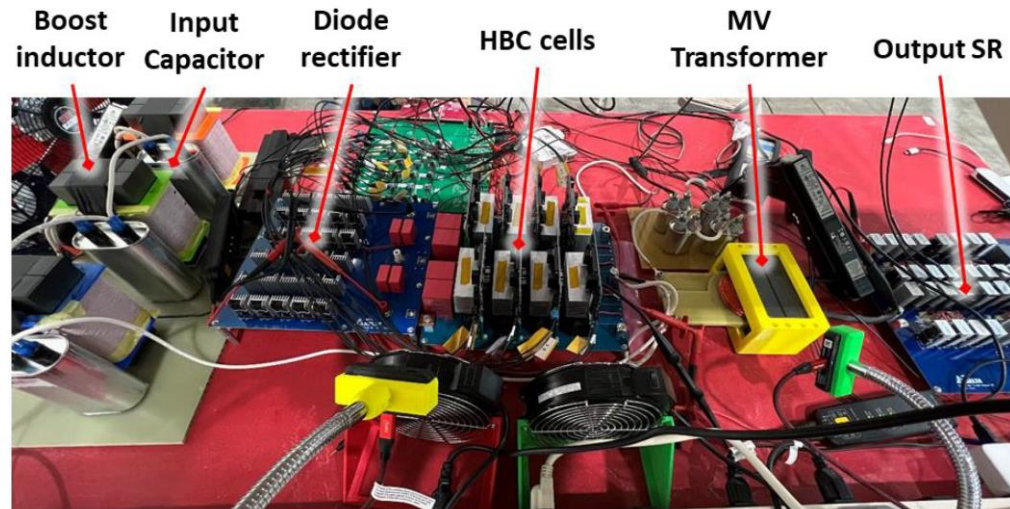
3.4 kV DC-Link ($> 2\hat{U}_{\text{phase}}$)

800 V DC Output

1200 V SiC MOSFETs in 4 Half-Bridge Cells / Arm

1700 V SiC Input Diodes w/ R//C Snubber for Blocking Voltage Symm.

Sw. Freq. 50 ... 200 kHz / 70 kHz Res. Freq.



■ Hardware Demonstrator | Characteristic Waveforms for 1.8 kV Line-to-Line Mains

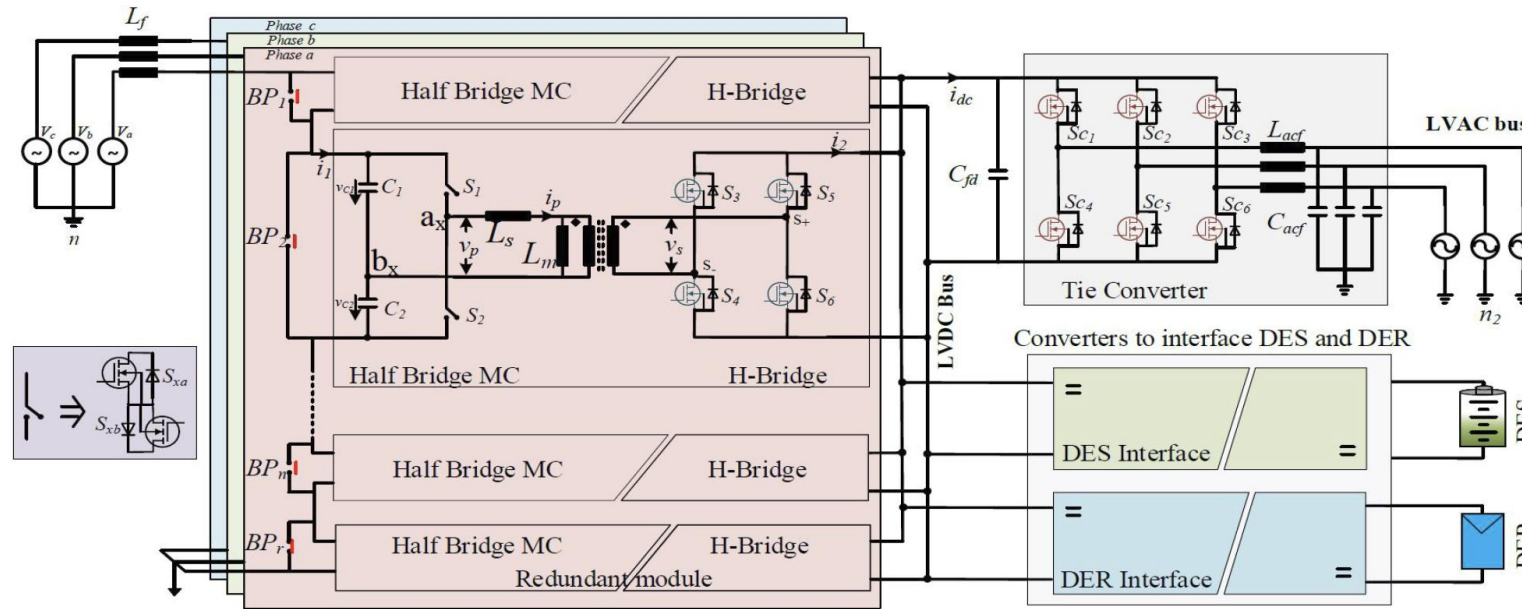
■ Sinusoidal Mains Current, THD < 4% w/o Control





3-Φ Phase-Modular IFE-Type ISOP SST Topology (1)

- Cascaded Single-Stage Dual-Active-Bridge-(DAB)-Based AC/DC Converter Sub-Modules
- Half-Bridge Primary Minimizes Number of MV-Side Power Semiconductors
- Application as Bidirectional 3-Φ Mains Interface of LV DC Nanogrids

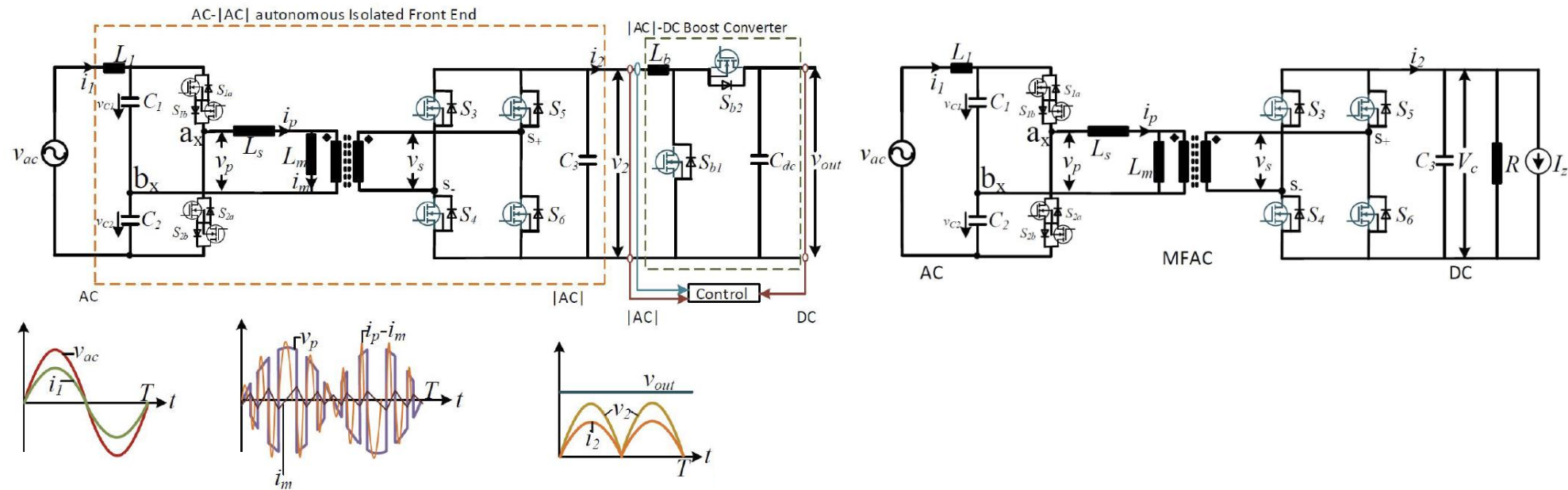


- DAB AC/DC Operation → Single-Stage Power Conversion / High Component Current Stresses



3-Φ Phase-Modular IFE-Type ISOP SST Topology (2)

- Comparison of Two-Stage – Swiss SST – and Single-Stage DAB-Based AC/DC Power Conversion
- Funct. Separation OR Integration of MF AC Generation | Volt. Scaling | Rectification | Sin. Current Shaping

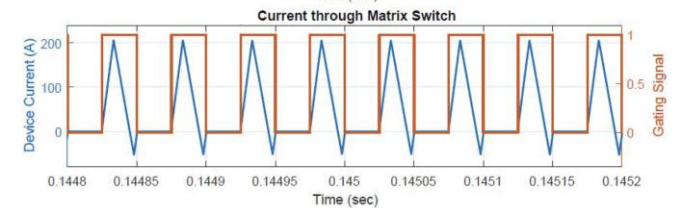
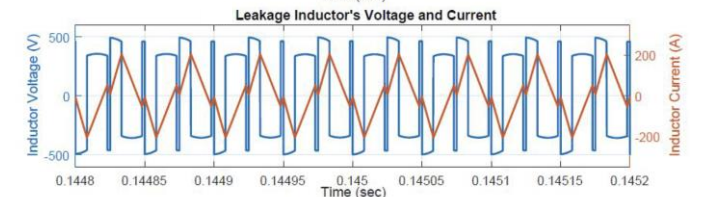
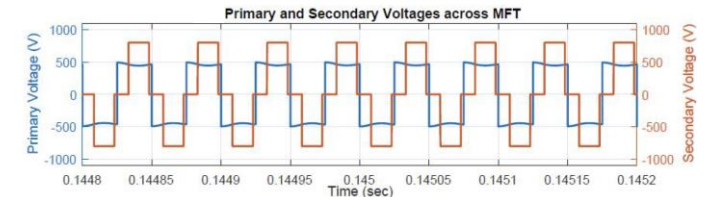
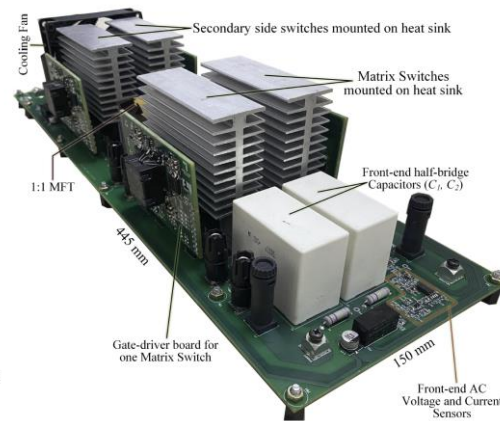
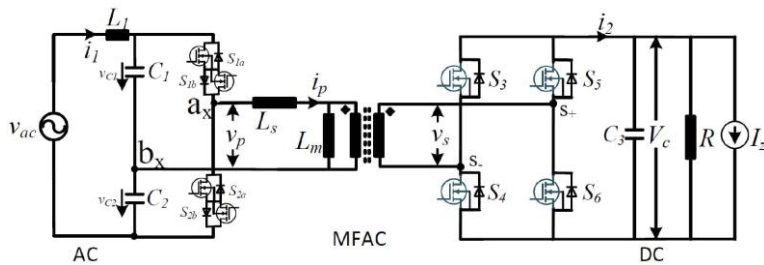
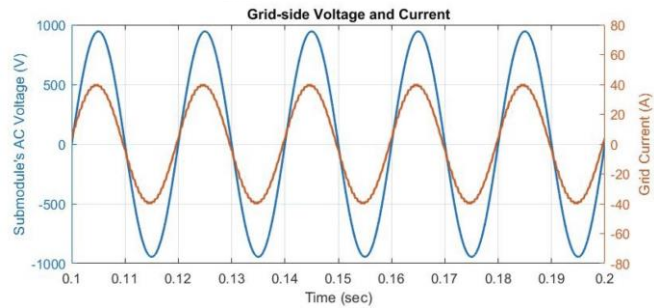


- Swiss SST Input Stage — Autonomous DCX-Type |AC| Voltage / Current Conversion @ Const. Duty Cycle
- Trade-Off Concerning Power Circuit & Control Complexity | Component Stresses



3-Φ Phase-Modular IFE-Type ISOP SST Topology (3)

- Simulation of Sub-Module Operation — $V_{ac} = 545 V_{rms}$, $V_c = 800 V_{DC}$, $P = 17.6 kW$, $f_{sw} = 20 kHz$
- Modulation Ensuring Unity Power Factor Operation & ZCS



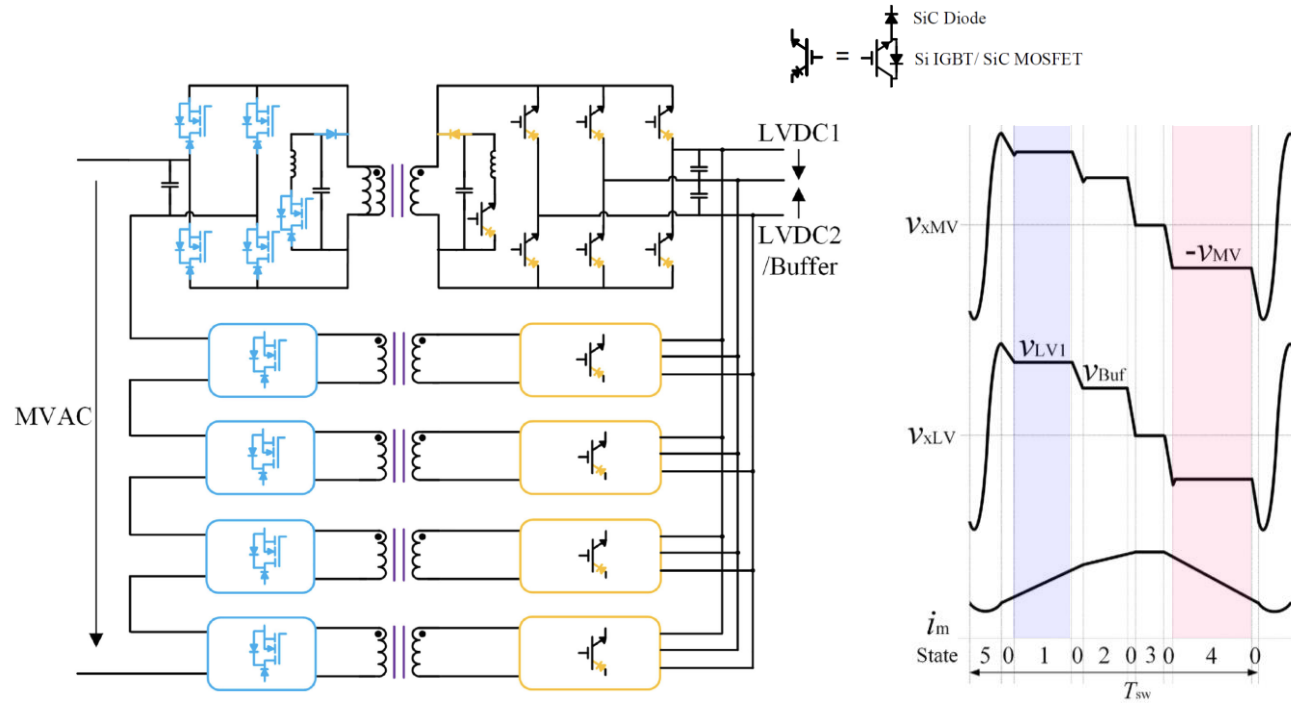
- Mains Frequency Envelope of Square Wave Transformer Primary Voltage
- 3-cell 15 kVA $1.5 kV_{rms} / 450 V_{DC}$ Hardware Demonstrator | $\eta \approx 96\%$ | $\rho \approx 3 kW/dm^3$



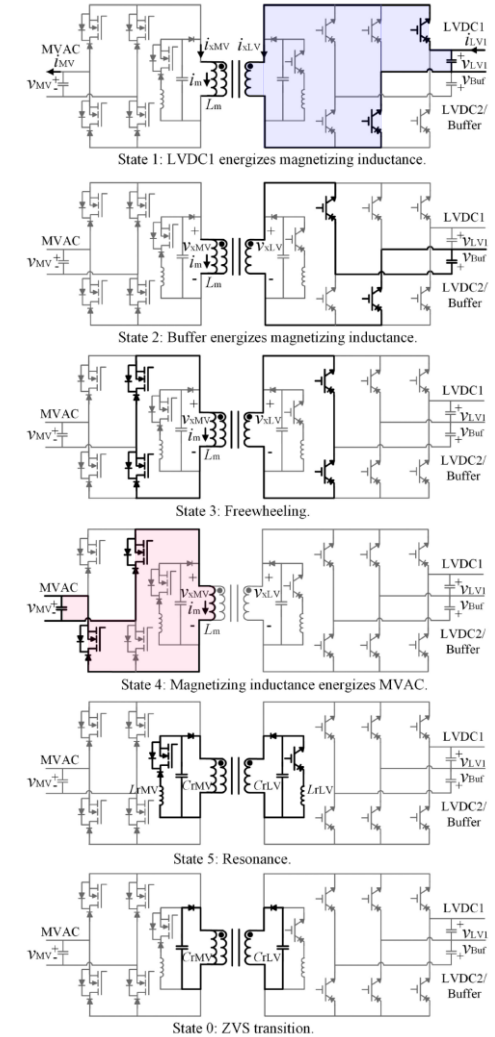


S4T – Soft-Switching Multi-Port SST (1)

- Modular Single-Stage Isol. Current Source Topology — M-S4T
- Cycle-by-Cycle Flyback-Type Power Transfer
- Full-Range ZVS Aux. Commutation Circuit

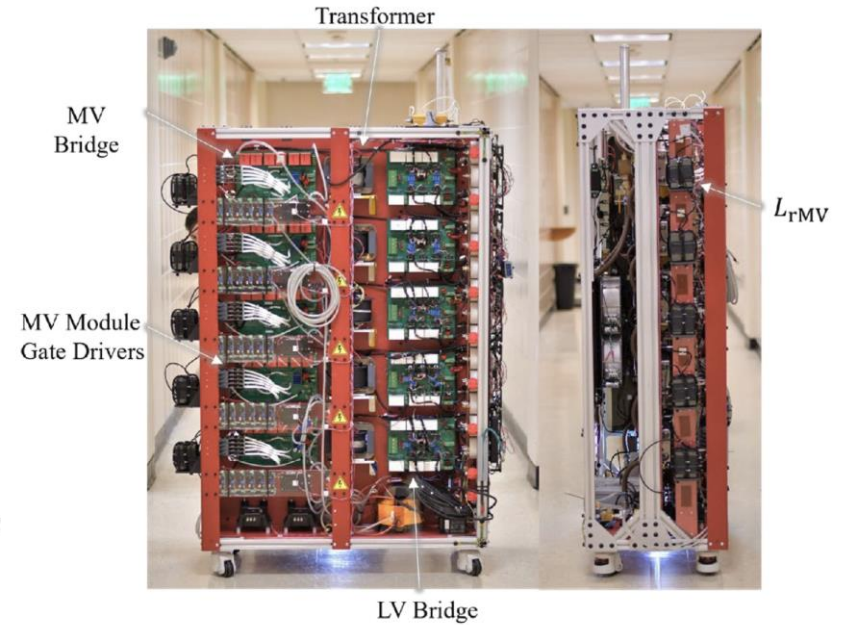
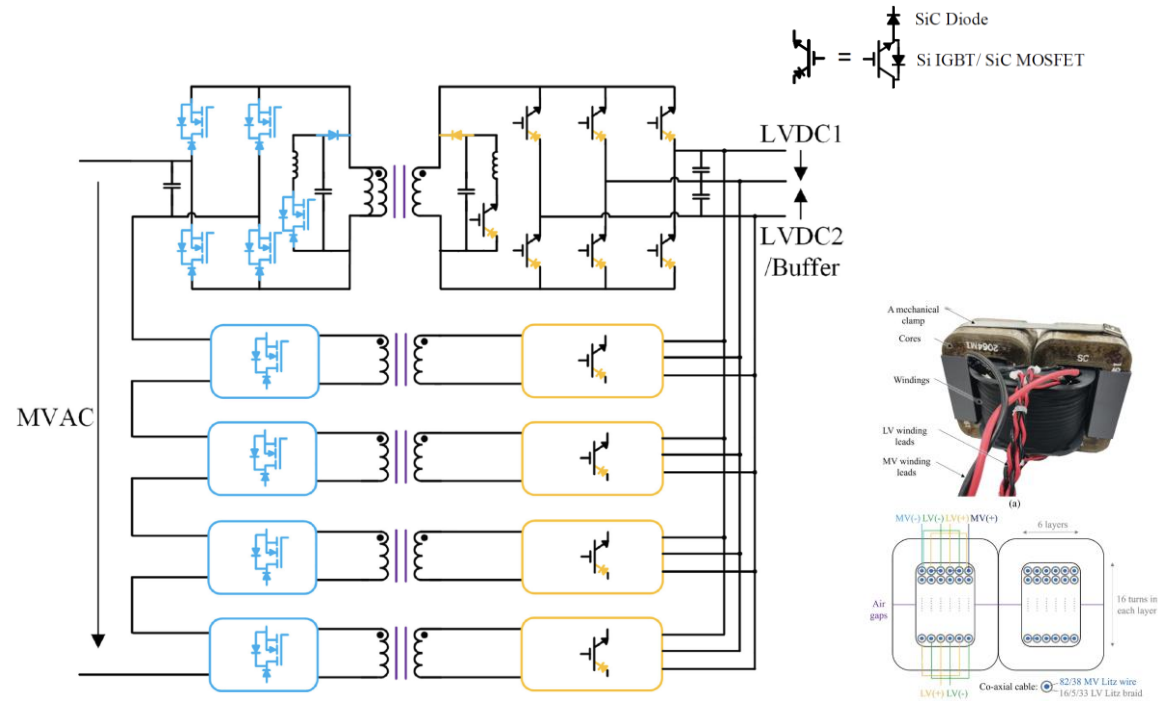


- DC/1-Φ AC System/Integr. Power Pulsation Buffer 3-Port System
- Sw. Cycle Waveforms & Operating States for LV/MV Power Transfer



S4T – Soft-Switching Multi-Port SST (2)

- Modular Single-Stage Isol. Current Source Topology — M-S4T
- Cycle-by-Cycle Flyback-Type Power Transfer
- Full-Range ZVS Aux. Commutation Circuit

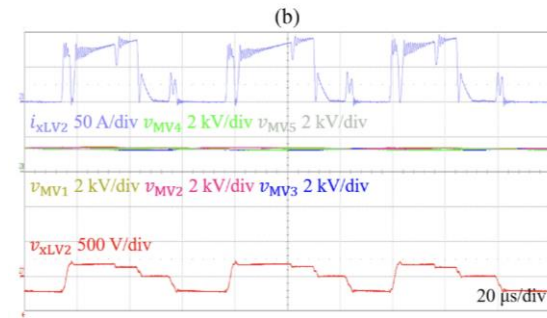
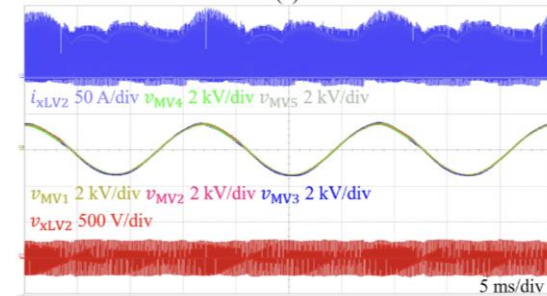
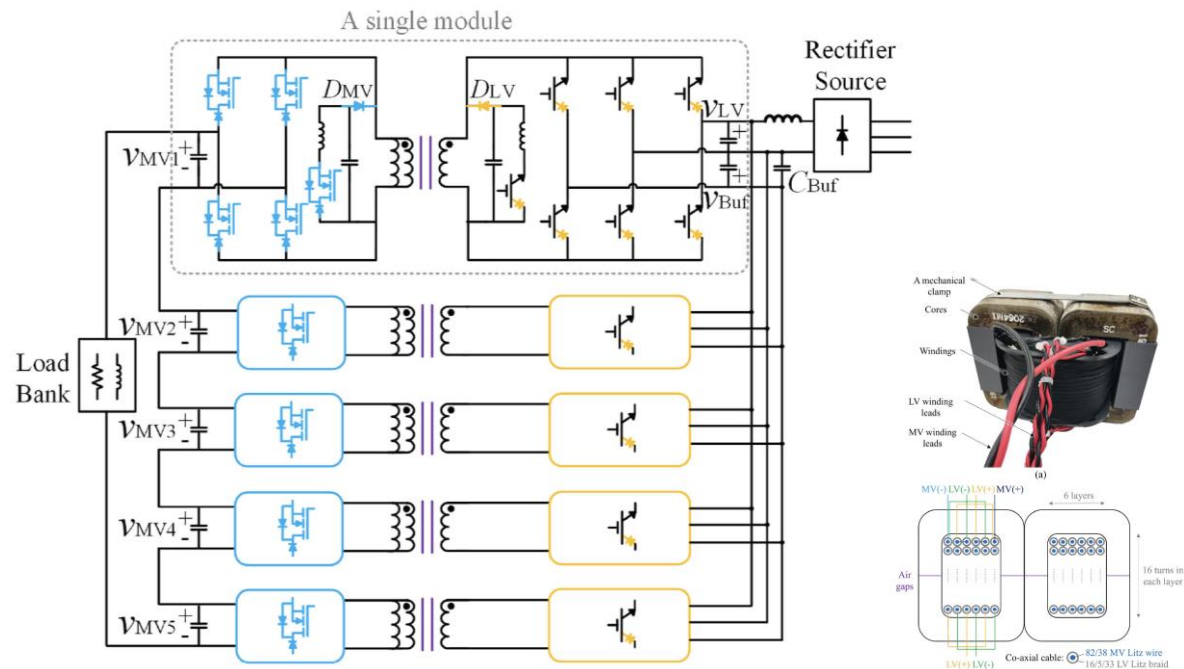


- 1- Φ 7.2 kV 50 kVA 5-Module ISOP Demonstrator | 90 kV BIL | DC/AC Operation | $U_{in} = 350 V_{DC}$
- 3.3 kV SiC MOSFET Module & Series SiC Diode | 650 V Si IGBT & Series SiC Diode | $f_{sw} = 16 \text{ kHz}$
- Low Leakage Inductance 6:1 Xfrm Tested to 55 kV Basic Insul. Level (BIL) | Nanocryst. Core w/ Airgap



S4T – Soft-Switching Multi-Port SST (3)

- Modular Single-Stage Isol. Current Source Topology — M-S4T
- Cycle-by-Cycle Flyback-Type Power Transfer
- Full-Range ZVS Aux. Commutation Circuit

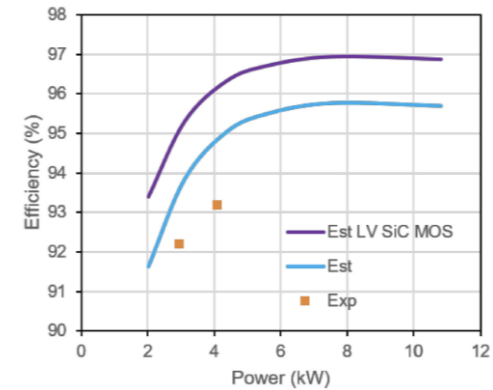
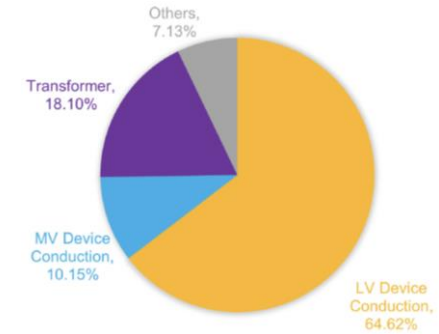
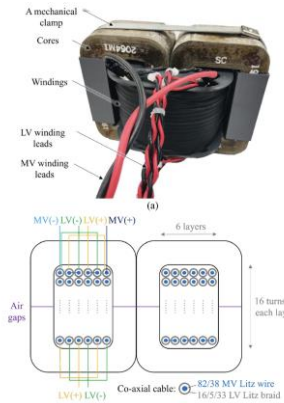
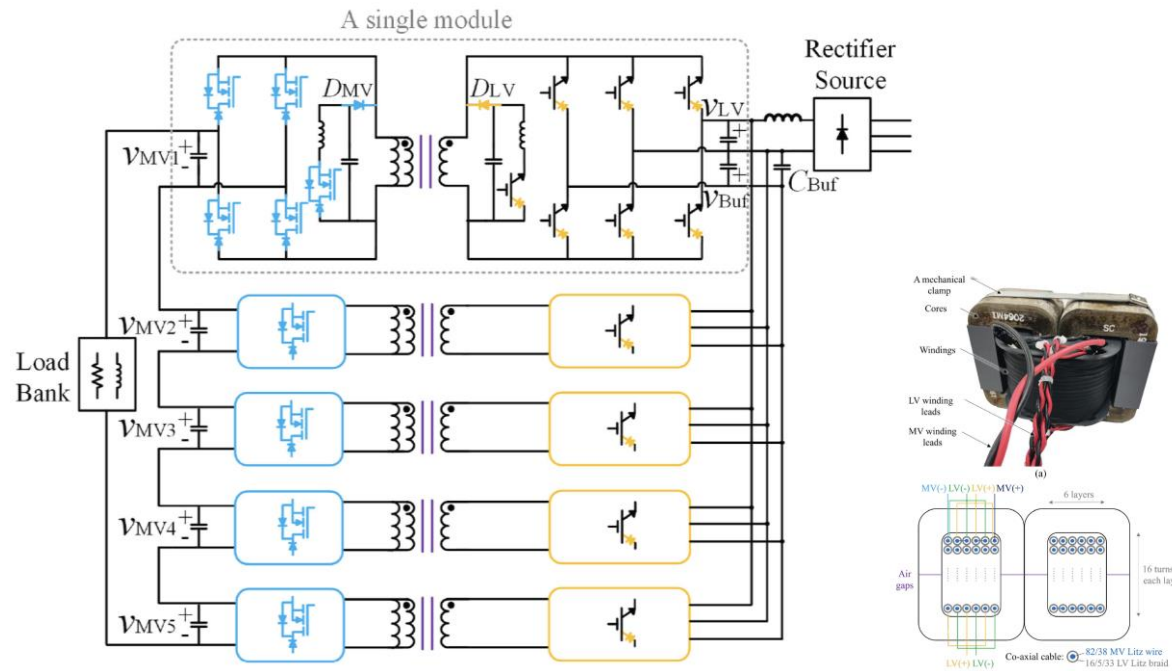


- Exp. Waveforms for 5-Module System | 20 kVA @ 7.5 kV_{pk} | Line Cycle & Sw. Cycles | Low dv/dt of v_{xLV}



S4T – Soft-Switching Multi-Port SST (4)

- Modular Single-Stage Isol. Current Source Topology — M-S4T
- Cycle-by-Cycle Flyback-Type Power Transfer
- Full-Range ZVS Aux. Commutation Circuit



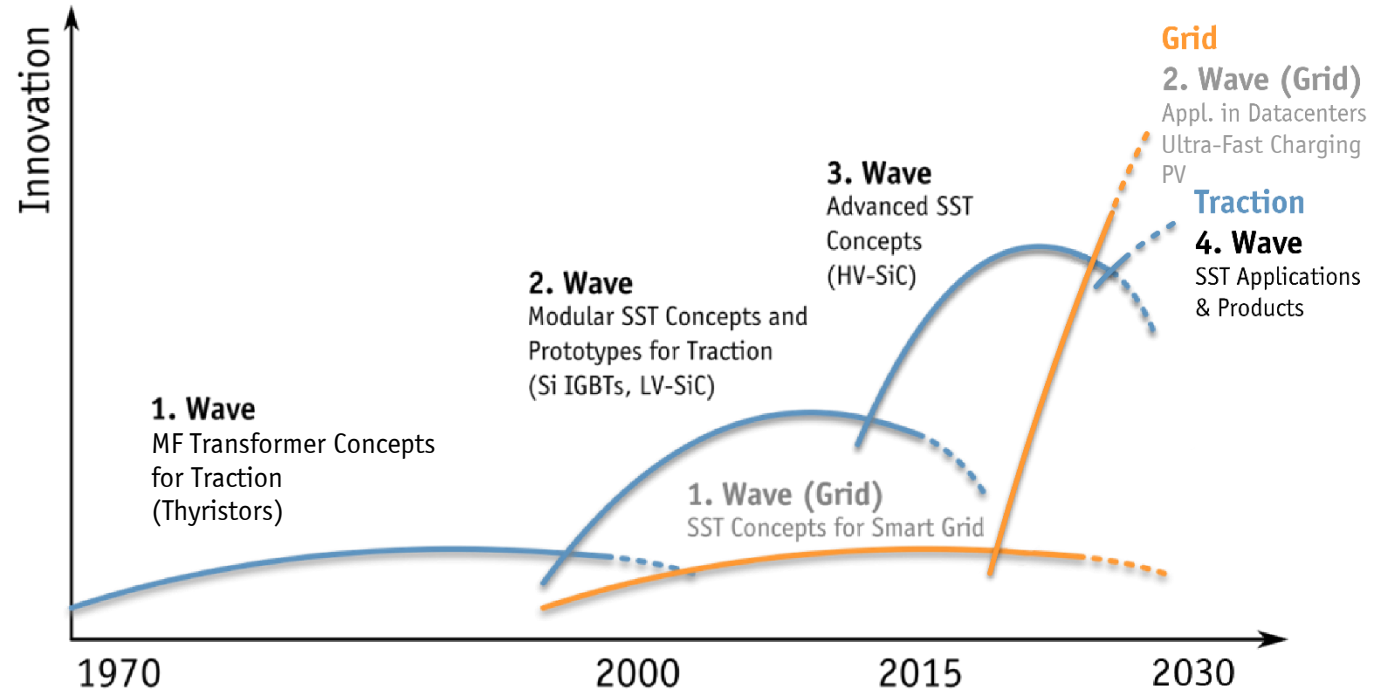
- Efficiency of a 10 kVA 1.4 kV / 350 V SST Module | Estimated Loss Breakdown



— Selected High-Power
EV Charging Research Projects /
Industry Demonstrators



SST Development Cycles

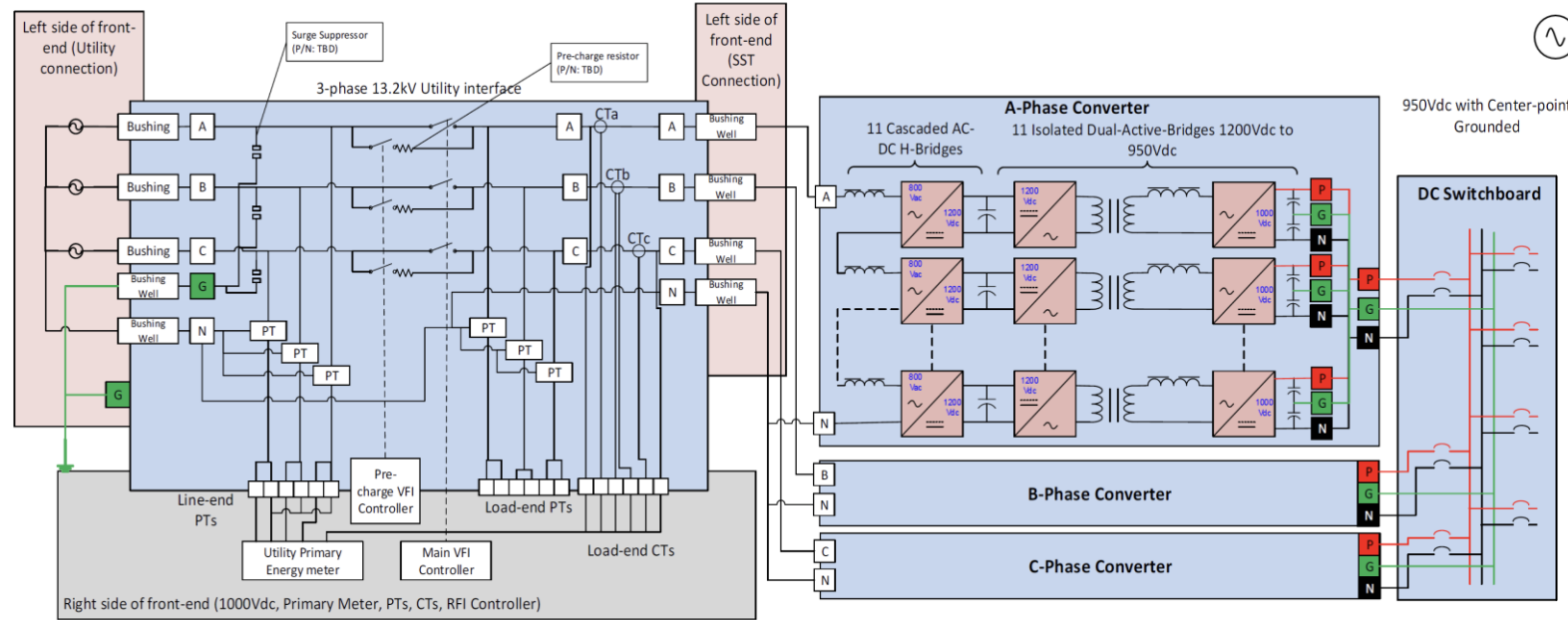


- Development Cycles Reaching Over Decades — Matched to “Product” Life Cycle



1+ MW Multi-Port Charging of Heavy-Duty EVs

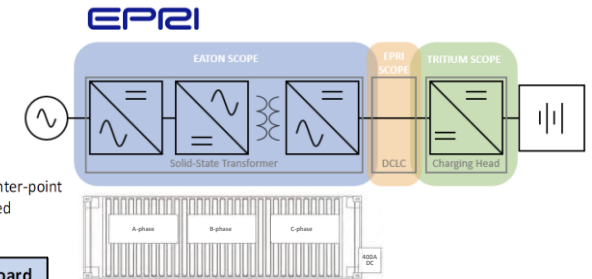
- 3.75 MW — 3000 A @ 1250 V — MW Charging System (MCS) / Charging Interface Initiative (CharIN)
- Aiming for Charging Times of 15...20 min for 200...600 kWh Battery Packs of Trucks



Utility interface box

3- Φ AC/DC SST | 400kW/phase

DC load center



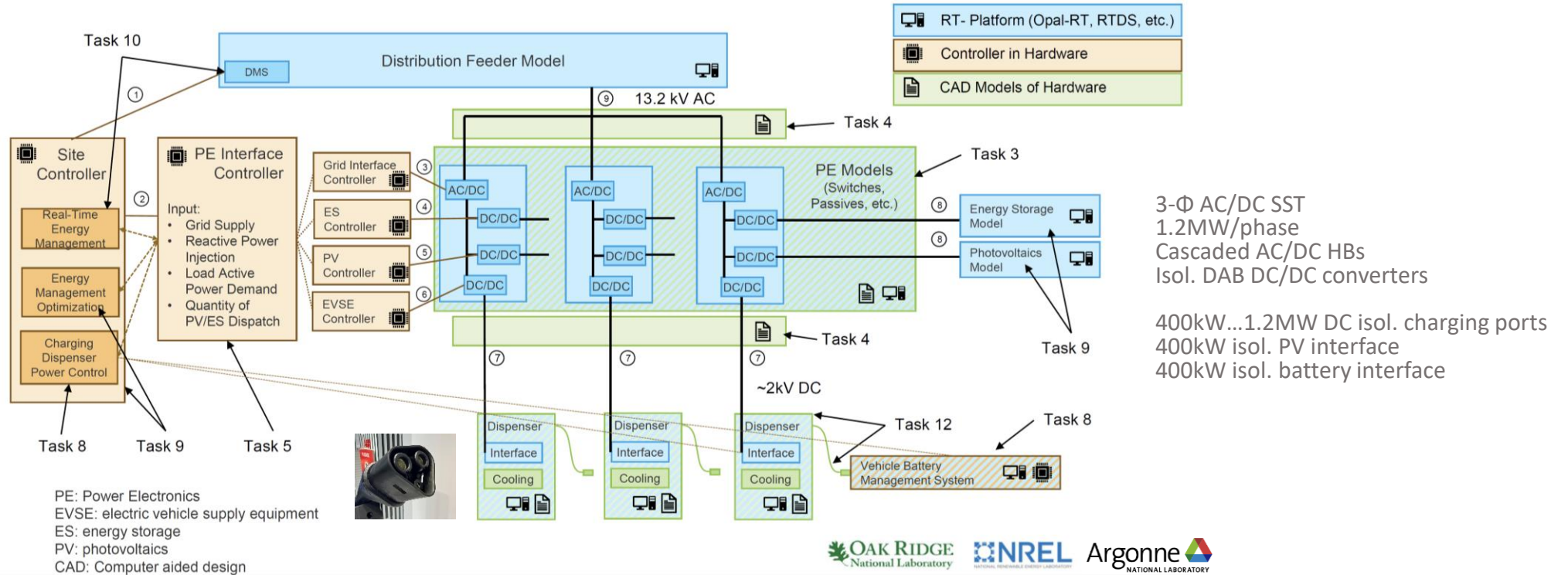
Charger connections
 4x 350kW head-end isolated DC/DC converters

- EPRI Multi-Partner Project “DC as a Service” (DCaaS) for High-Power EV Charging
- 13.2kVAC MV Supply | 7.6kVAC / 1.2V DC-Link / 950VDC (± 475 VDC) Output | 3x 11-Cell SiC-Based SST @ 10kHz
- Potential Extension to DC Microgrid | Integration of (On-Site) PV | Peak Shaving Battery Storage



1+ MW Multi-Port Charging of Heavy-Duty EVs

- 3.75MW — 3000A @ 1250V — MW Charging System (MCS) / Charging Interface Initiative (CharIN)
- Aiming for Charging Times of 15...20min for 200...600kWh Battery Packs of Trucks



- Multi-Partner Project on Key Components of a Multi-Port 1+ MW MV-Connected EV Charging System
- 13.2kVAC MV Supply | 7.6kVAC / 3kV DC-Link / 2kVDC Output | 3x 4-Cell SiC-Based SST @ 10kHz



Up to 3.5 MW Ultra-Charging System

- 20% → 100% **Charging of typ. 200...400 kWh Battery Pack in 15...20 min** — High eVTOL Utilization
- **MegaWatt Charging System (MCS)** — New Charging Std. for Trucks | Buses | eVTOL Aircraft etc.

The composite image illustrates the charging system components and application. On the left, a ChargePoint high-power connector is shown, featuring a yellow handle and a grey plug. In the center, a diagram of a battery pack shows the state of charge (%) from 0 to 100, divided into segments: DO NOT TOUCH (0-10%), RESERVE (10-20%), VERTICAL LANDING (20-30%), CRUISE (30-90%), and VERTICAL TAKE-OFF TRANSITIONS (90-100%). On the right, a rendering shows an eVTOL aircraft docked at a charging station in a modern terminal, with people nearby. The source is cited as NEW ATLAS.

- **ChargePoint High-Power Charge Connector (max. 1.5 kV / 3000 A) incl. Liquid Cooling & Data Transfer**

Remark 480 VAC Supplied Multi-Port Charging Site

- 350 kW max. per Port | 6x 350 kW = 2.1 MW
- Local Battery Storage Coupled @ 480 VAC Panel for Peak Shaving / Demand Management



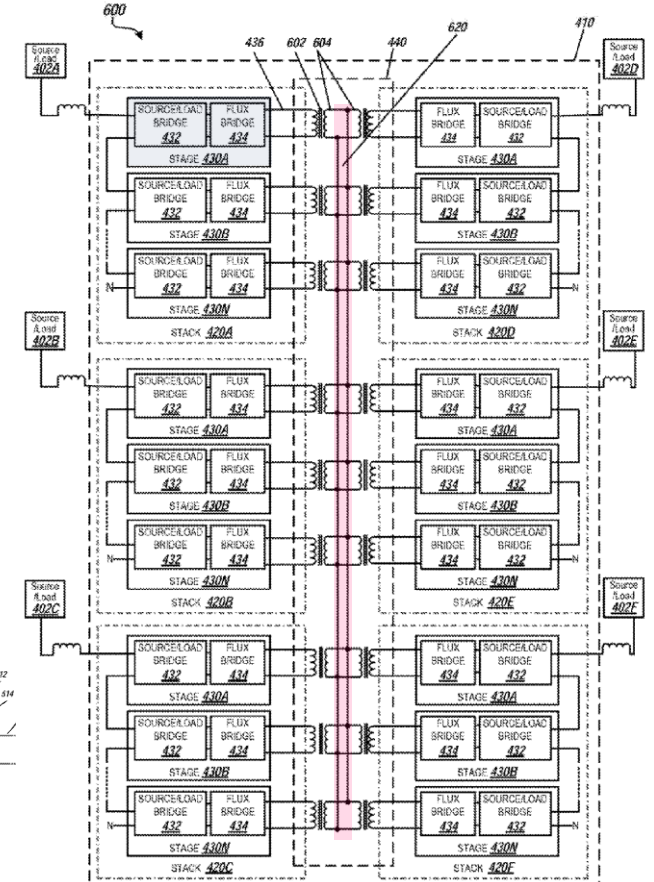
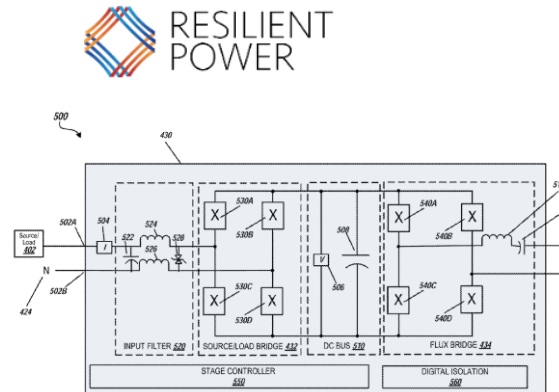
Single & dual output dispensers | 480 VAC/DC conv. cabinets | 480V AC switchgear & 4 battery Powerpacks

- **Somedays All This will Charge 1 Truck (!)** (T. Bohn, ANL)



3-Φ 15 kV / 3.2 MVA SST-Based EV Charger (1)

- “Synchronous Common Coupling” of Converter Cells via MF AC-Bus
- Full Modularity / Low Converter Cell Complexity / 25% Redundancy
- High Scalability / Flexibility — AC or DC Output
- 1.5m x 1.6m x 2.4m Outer Dimensions → 0.5kW/dm³
- Efficiency Not Specified



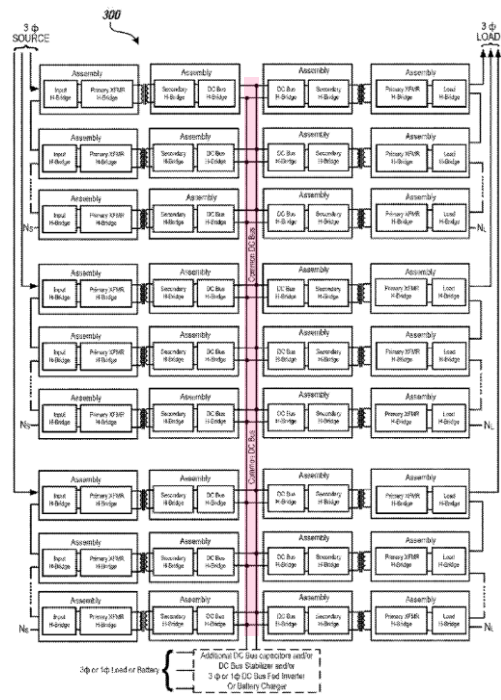
- Insulation Type Not Specified (in Case of Oil → Maintenance / Pot. Environmental Issues & Fire Hazard)



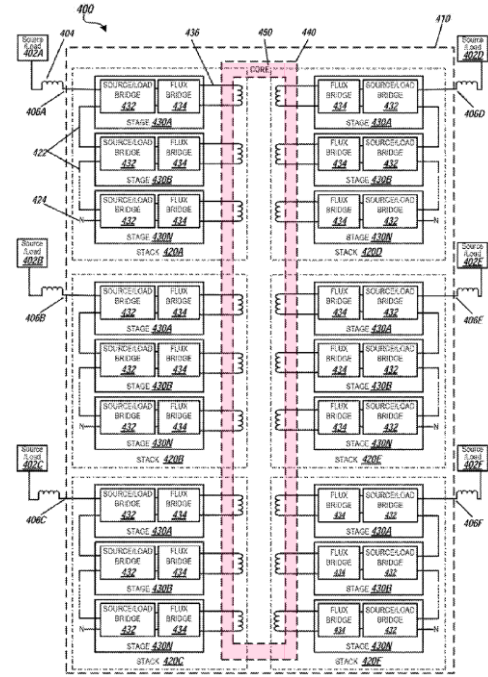


Alternative Multi-Port Coupling Schemes

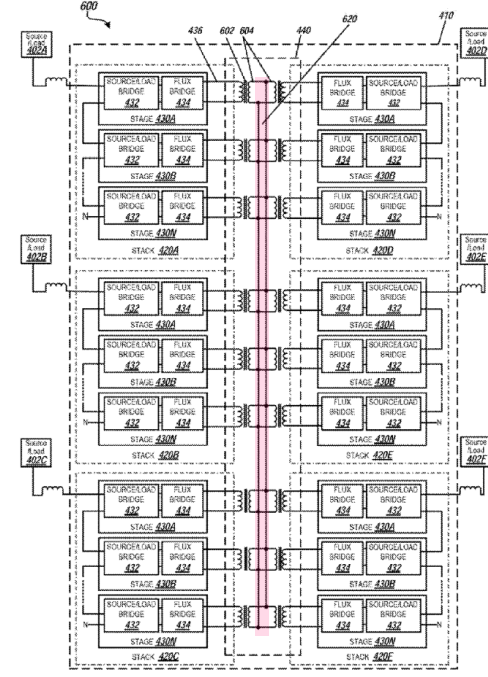
- DC-bus OR AC-bus (Magnetic/Electric) Coupling of Cascaded Cells
- Example of 3-Φ MF Isolated AC/AC Conversion



— DC-Bus Coupling



— Common Magn. Core AC-Coupl.



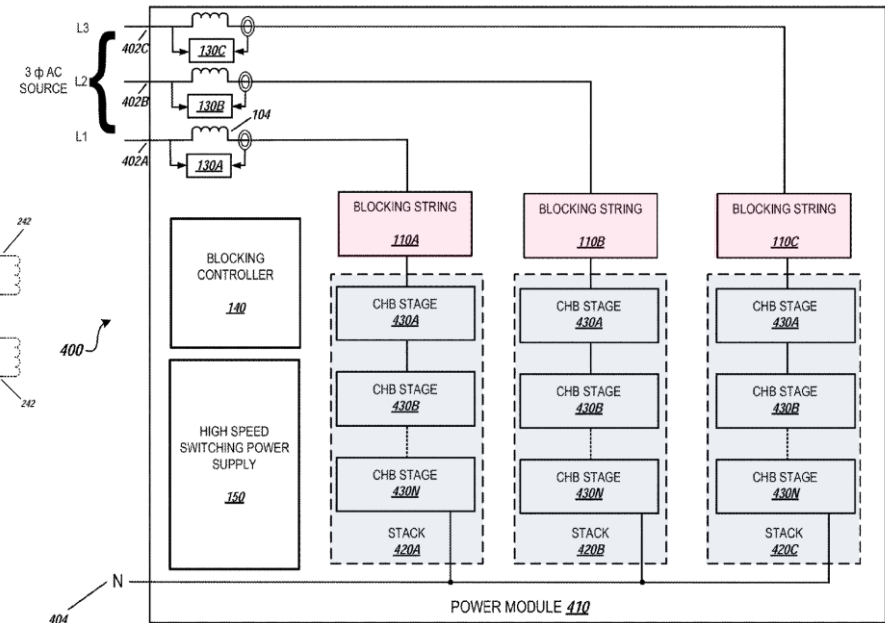
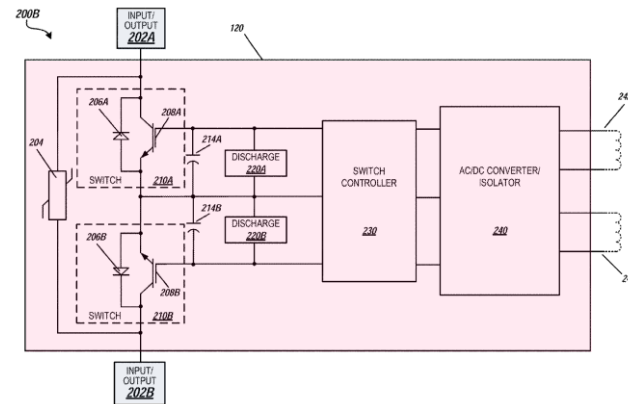
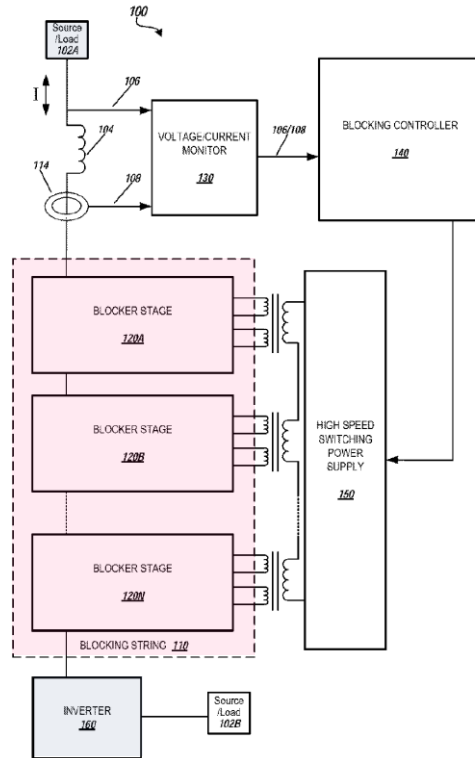
— AC-Bus Coupl. of Indiv. Xfrms

- AC-Bus Coupling Adopt „Synchronous Common Coupling“ of the 50/60Hz Grid
- Low Complexity Converter Cells | Challenge of Power Flow Control / Stability



3-Φ 15kV / 3.2MVA SST-Based EV Charger (2)

- Zero Inrush Current
- Simple Fuse & Disconn. Switch as MV-Grid Interface
- 125 kV Impulse Basic Insulation Level w/o Arresters

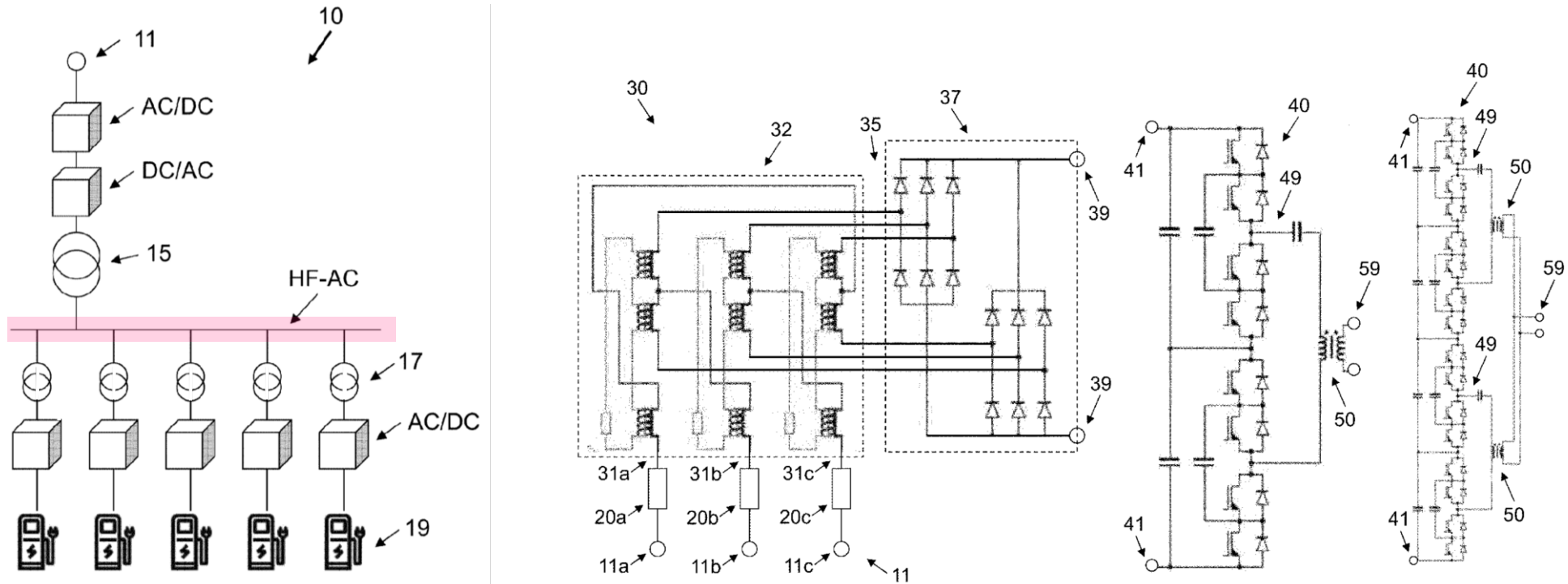


■ Insulation Type Not Specified | In Case of Oil → Maintenance / Pot. Environmental Issues & Fire Hazard)



Medium-Frequency AC Power Distribution

- 400 Hz / 360 ... 800Hz Aviation Systems — Low Vol. of Xfrms & Filter Circuits Comp. to 50/60Hz
- MV-AC/DC Conv. Utilizing PWM OR Multi-Pulse Line-Interphase-Xfrm-Based PFC Rectifiers
- DC/MF-AC Conv. Integrating a MV/LV MF-Xfrm



- LV/LV MF-Xfrms for Galv. Separation of the Charging Ports | Diode or PFC Rectifiers & Non-Isol. DC/DC Converters



———— IFE 3- Φ Transformer SST ————



Matrix-Type 3-Φ MFT-Link Multi-Port SST Topology

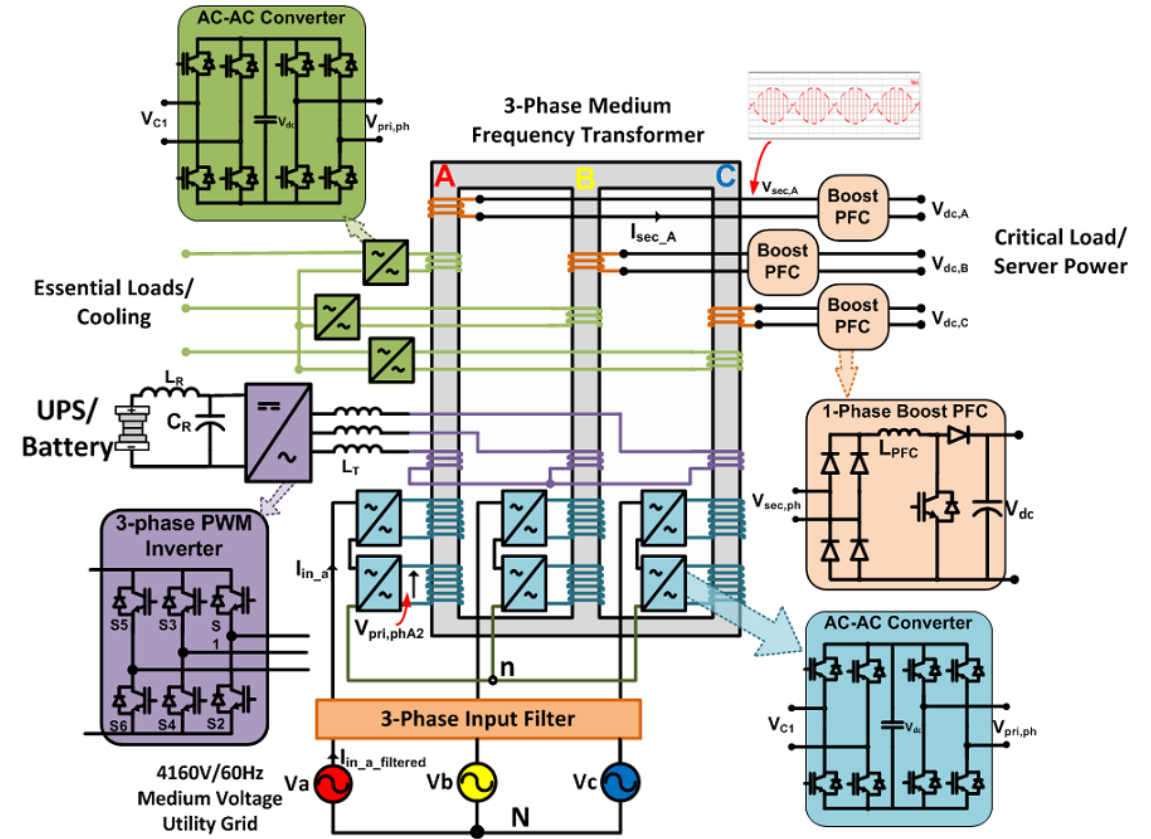
Enjeti, 2014

- Bidirectional LF-AC/|AC|/MF-AC Grid Interfaces
- Input Stage Operates as AC/|AC| Unfolder
- H-Bridge Generates MF-AC Rect. Prim. Voltage
- 50/60Hz Mains Def. MF-AC-Voltage Envelope

- Multi-Wdg Arrangement per Xfrm Leg
- Common Magn. Flux Interconnects All Wdgs
- Prim./Sec. Turns-Ratio Voltage Scaling

- Sec.-Side 3x 1-Φ or 3-Φ Power Conversion
- MF-AC Voltage Folding & LF-|AC|/DC Conv.
- 3-Φ MF-AC/DC PFC Rectifier Systems
- 3x 1-Φ (Star/Delta) MF-AC/DC/AC Conv.

- Proposed as MV Interface of Future Datacenters



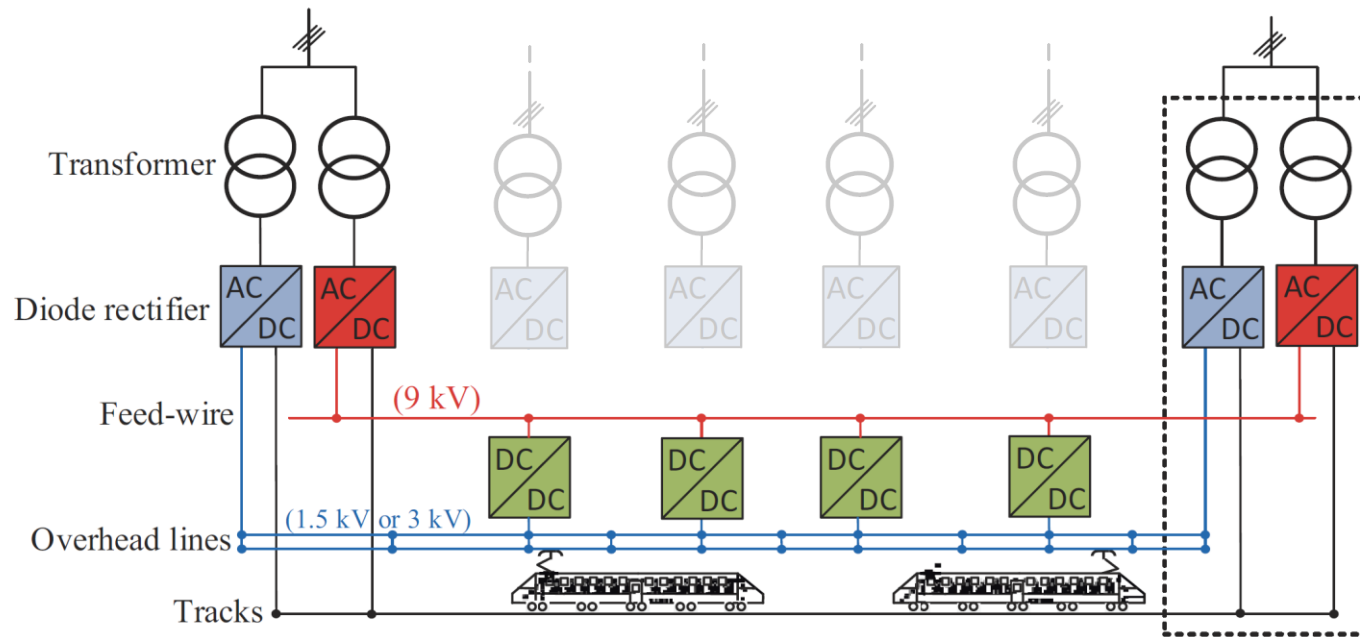


———— Institut National Polytechnique ————
de Toulouse



DC/DC SST for Future MVDC Railway Electrification (1)

- Increase in Regional & Freight Traffic Results in Higher Traction Power Demands
- Extension of Current 1.5 kV | 3 kV SNCF DC System (1000 mm²) with Parallel 9 kV DC-Bus

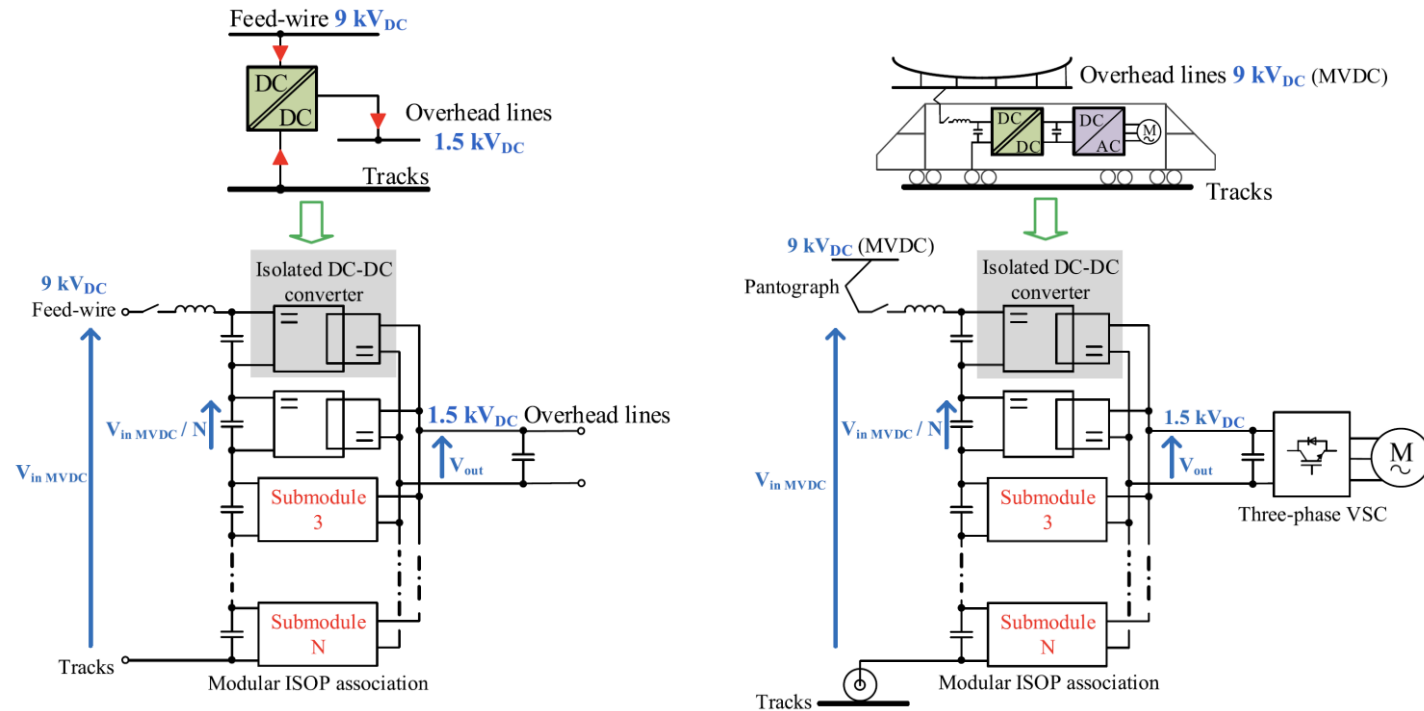


- DC/DC SSTs Instead of New AC/DC Substations — Lower Realization Effort | Higher Eff.
- Potential 9kV DC-Interface to Renewable Energy / Energy Storage / HVDC Lines etc.



DC/DC SST for Future MVDC Railway Electrification (2)

- Increase in Regional & Freight Traffic Results in Higher Traction Power Demands
- Extension of Current 1.5 kV | 3 kV SNCF DC System (1000 mm²) with Parallel 9 kV DC-Bus

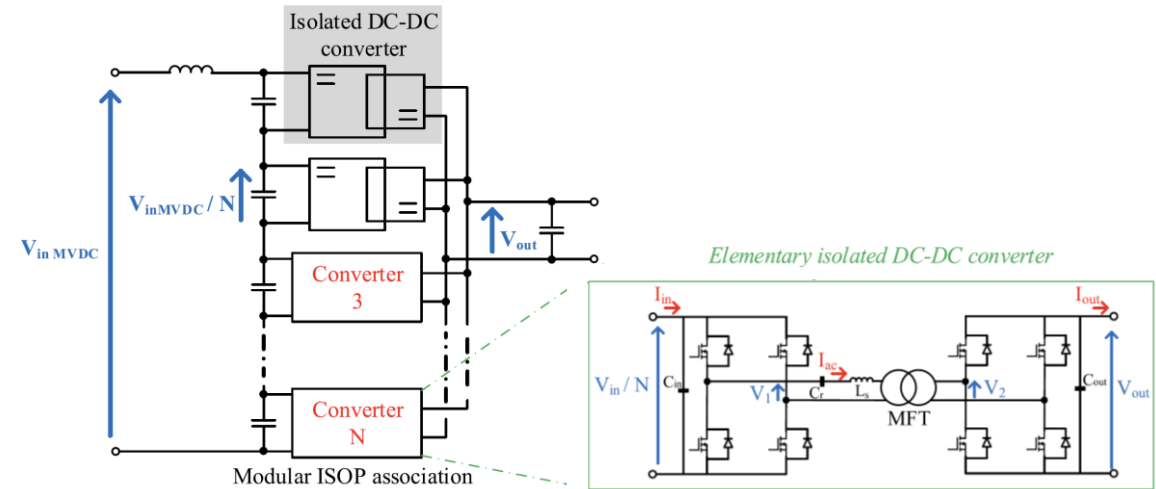
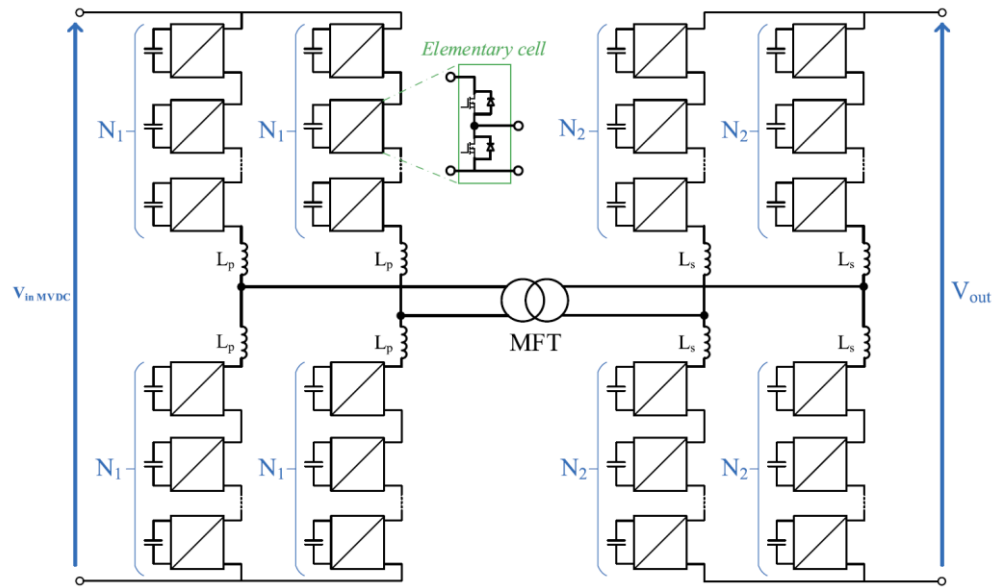


- Future Elimination of 1.5 kV Overhead Lines — Onboard 9 kV / 1.5 kV DC/DC Conversion



DC/DC SST for Future MVDC Railway Electrification (3)

- **CHB Arrangement vs. MMLC — Lower Stored Energy / Lower Losses / Lower Control Complexity**
- **Required 20 kV Isolation Level can be Accommodated in Rel. Low Volume CHB Xfrms**

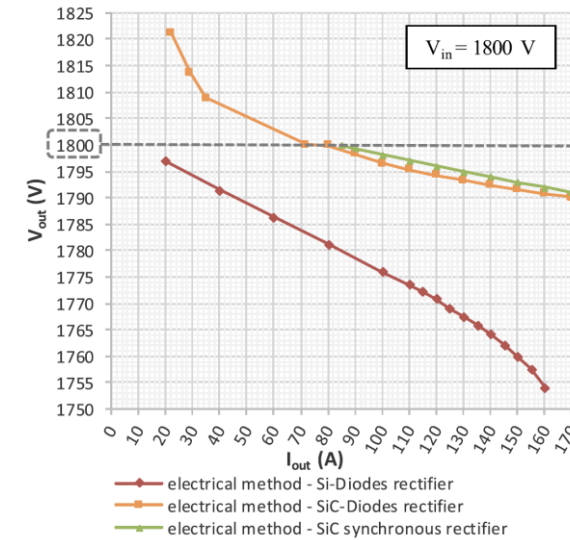
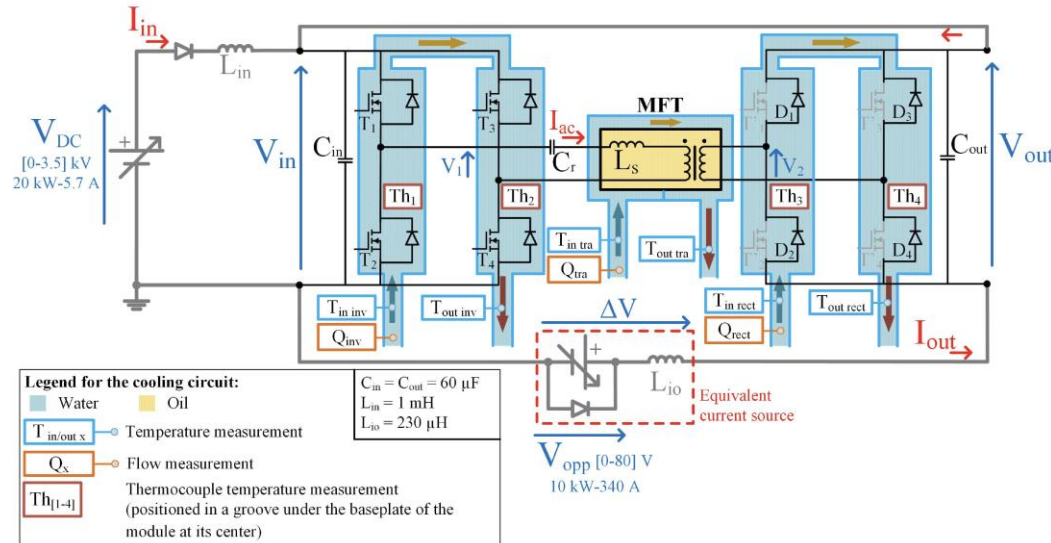


- **Series Res. Soft-Switching DCX-type CHB Conv. Stages | Lower React. Power Compared to DAB Operation**



DC/DC SST for Future MVDC Railway Electrification (4)

- Demonstrator System — 300 kW | $f_{sw} = 15$ kHz | 1.5 kV / 1.5 kV DC/DC Conversion
- 3.3 kV / 750 A SiC MOSFETs | 400 kVA 1:1 Water-Cooled Nanocryst. Core Oil-Tank MFT

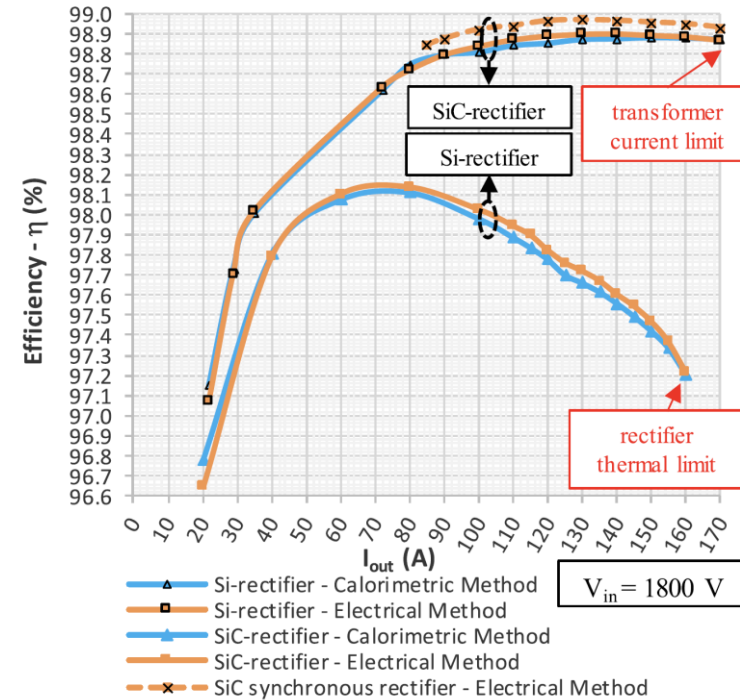
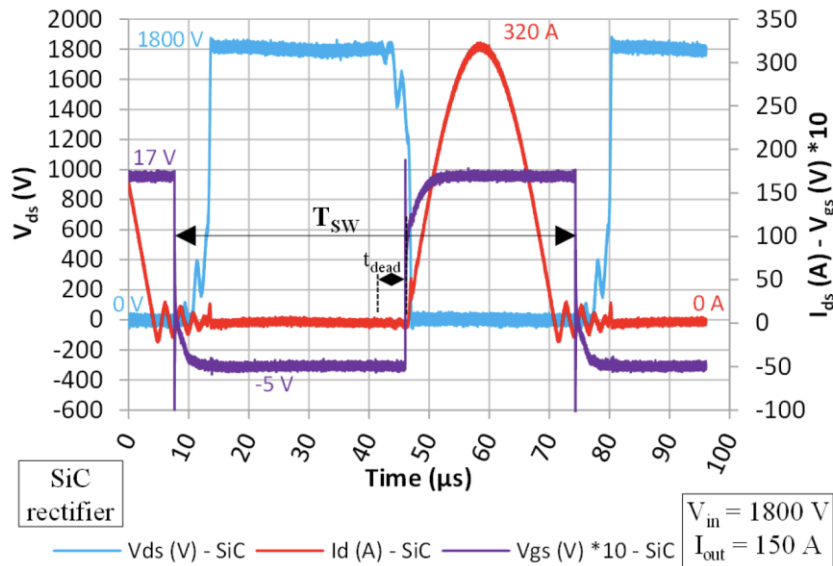


- Direct Connection of Converter Input and Output / Load Power Circulation
- Load Dependence of DCX V_{out} for Synchr. Rect. / SiC Diodes (750 A) / Si Diodes (500 A) – Paras. Cap. V_{out} Increase



DC/DC SST for Future MVDC Railway Electrification (5)

- Demonstrator System — 300 kW | $f_{sw} = 15$ kHz | 1.5 kV / 1.5 kV DC/DC Conversion
- 3.3 kV / 750 A SiC MOSFETs | 400 kVA 1:1 Water-Cooled Nanocryst. Core Oil-Tank MFT

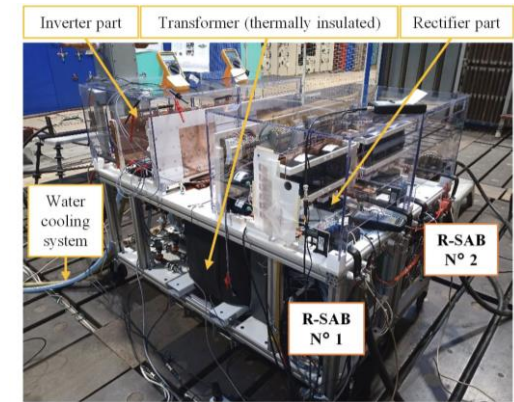
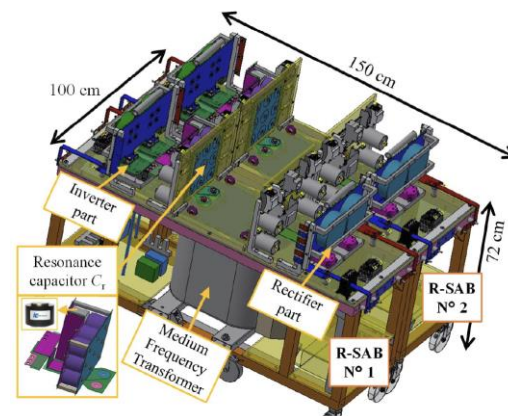
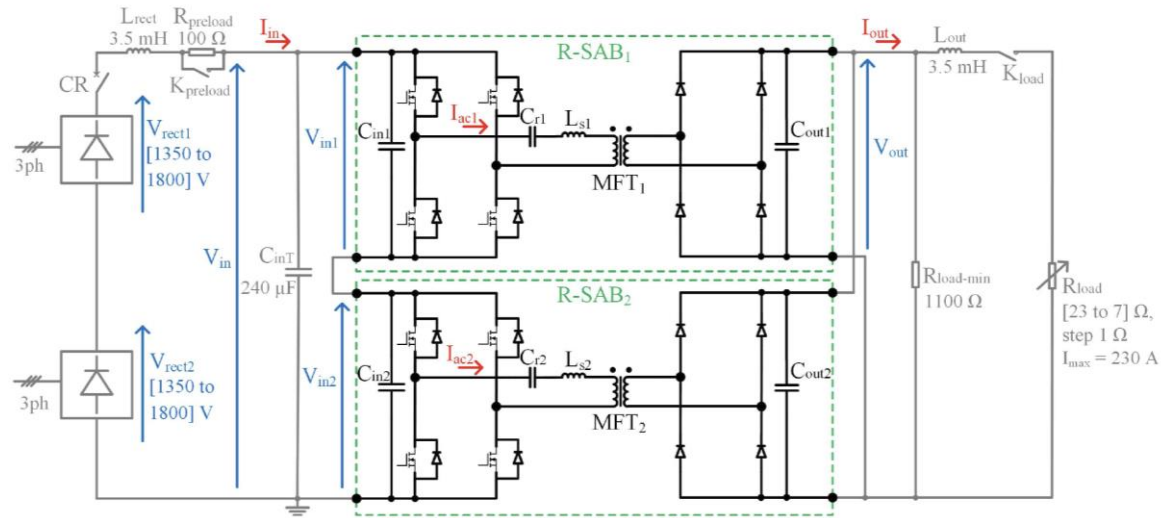


- Characteristic Waveforms for SiC Rect. Diodes
- Load Dependency of Converter Efficiency



DC/DC SST for Future MVDC Railway Electrification (6)

- 2-Stage ISOP Demonstrator System — 600 kW | 3.6 kV / 1.8 kV DC/DC Conversion | $\rho \approx 0.6 \text{ kW/dm}^3$



- Natural Voltage and Current Sharing Exp. Confirmed
- Interleaving of 2 Converter Stages Results in $4 \times 15 \text{ kHz} = 60 \text{ kHz}$ Output Voltage Ripple

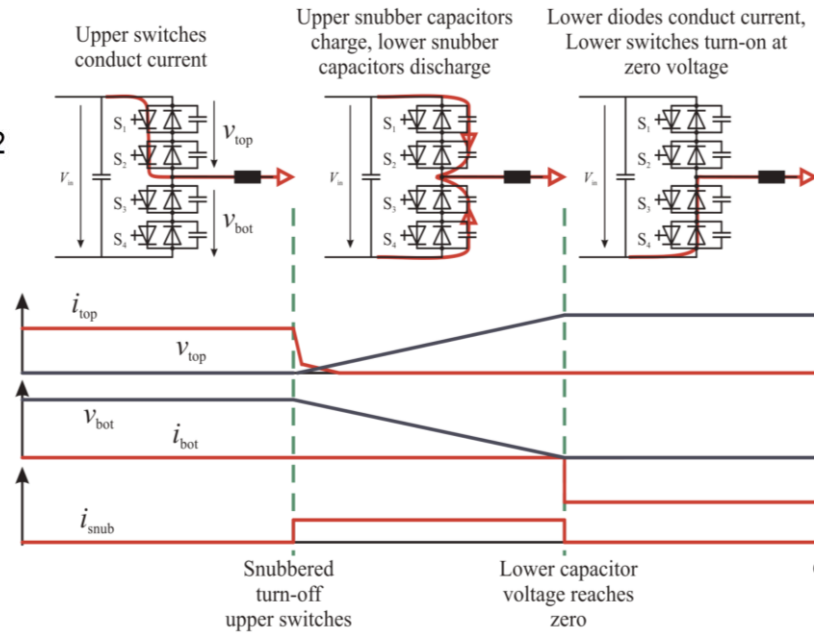
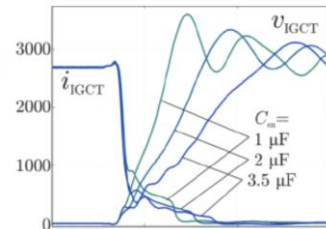
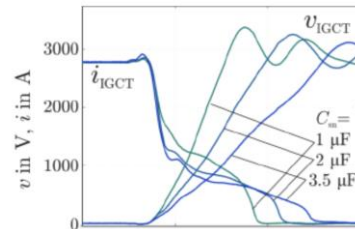
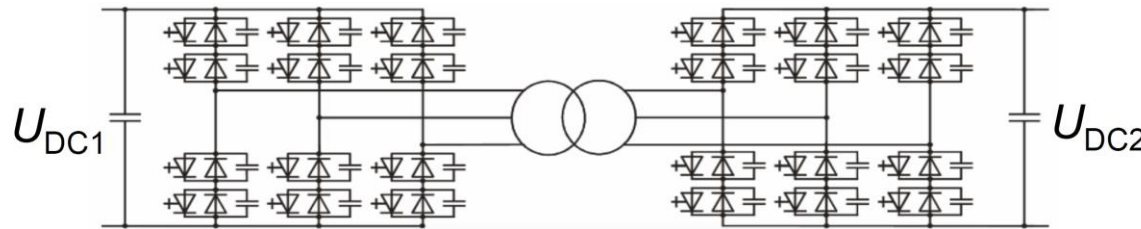


————— **RWTH**AACHEN
UNIVERSITY —————



5 kV DC/DC Dual-Active-Bridge-Based SST (1)

- 3x 1- Φ MFT-Based & 3- Φ MFT-Based Realization
- Series Connection of 2x 4.5 kV IGCTs / Switch | ZVS Snubber Capacitors
- $P = 7 \text{ MW}$ @ $f_{sw} = 1 \text{ kHz}$

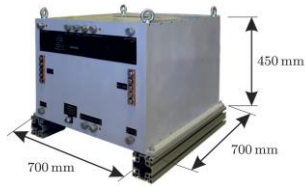
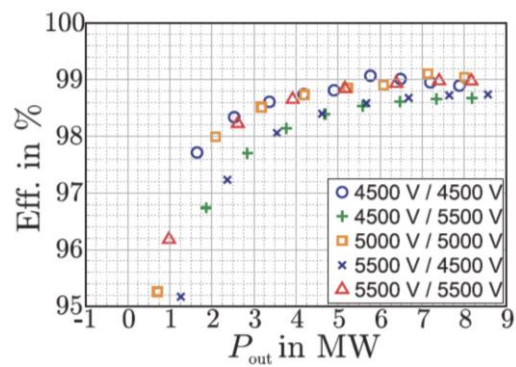
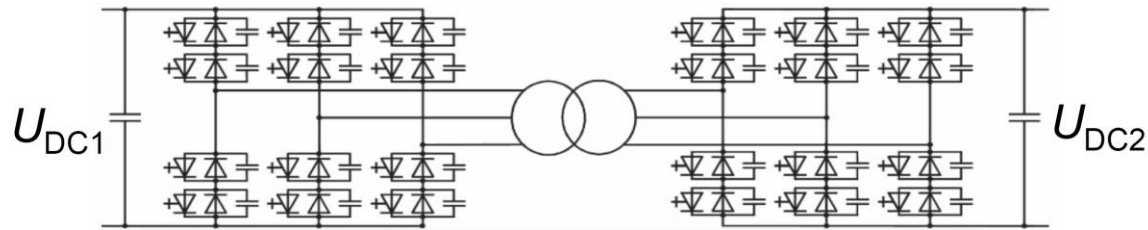


- C-Snubber — Significant Reduction of Sw. Losses | Lower dv/dt Insul. Stress | Voltage Balancing
- Evaluation of Fast-Sw. IGCTs vs. Low Saturation — Up to 80% Red. Sw. Losses @ 1kHz / Highest Overall Eff.

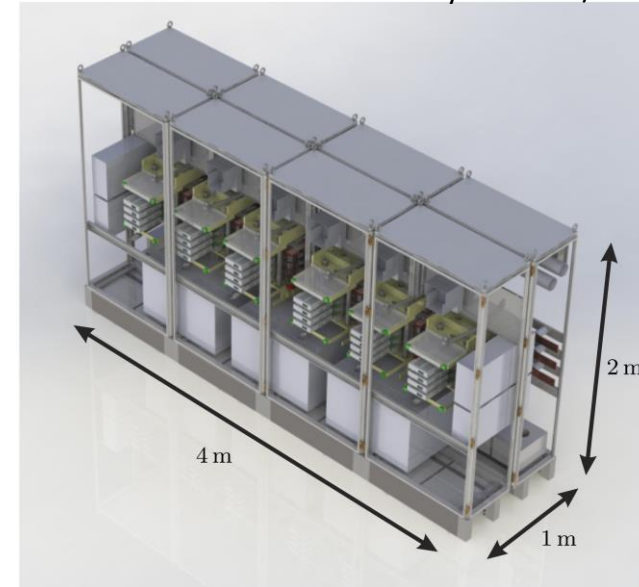


5 kV DC/DC Dual-Active-Bridge-Based SST (2)

- 3x 1-Φ MFT-Based & 3-Φ MFT-Based Realization
- Series Connection of 2x 4.5 kV IGCTs / Switch | ZVS Snubber Capacitors
- $P = 7 \text{ MW} @ f_{sw} = 1 \text{ kHz}$



Power Density: 0.88 kW/dm³

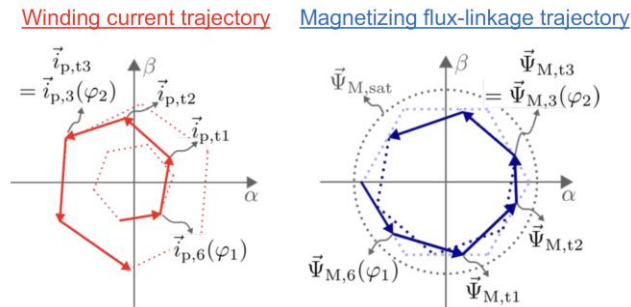
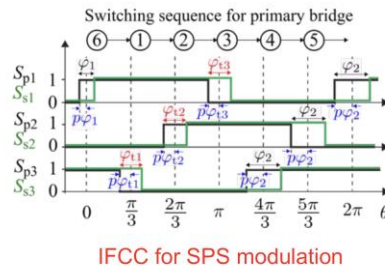
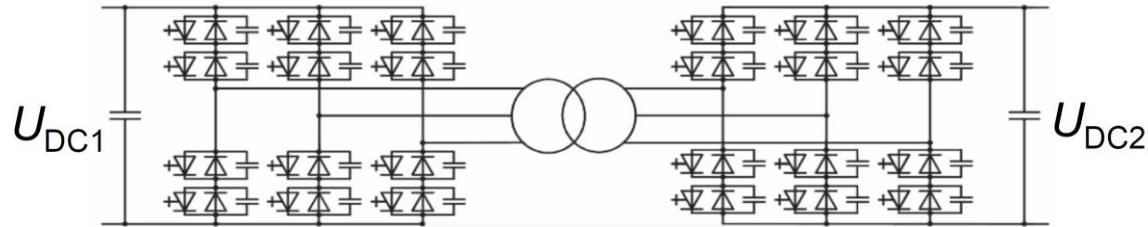


- 1-Φ 2.2 MVA / 1 kHz Xfrm | Silicon Steel Magnetic Core
- Efficiency up to 99.2% — Calcul. Based on Measured Semicond. Losses & Xfrm. Losses



5 kV DC/DC Dual-Active-Bridge-Based SST (3)

- 3x 1- Φ MFT-Based & 3- Φ MFT-Based Realization
- Series Connection of 2x 4.5 kV IGCTs / Switch | ZVS Snubber Capacitors
- $P = 7 \text{ MW} @ f_{sw} = 1 \text{ kHz}$



- 3- Φ 5.0 MVA / 1 kHz Xfrm — 675 kg (0.14 kg/kVA) | 3- Φ 4.6 MVA / 50 Hz Xfrm — 11.500 kg (2.5 kg/kVA)
- Low Hyst. Loss High \$ Amorphous Iron vs. 0.18mm High Sat. Flux Si Steel — Similar Rated Load Efficiencies
- Instantaneous Flux and Current Control (IFCC) During Transients – Fast Dynamics / No Overshoot



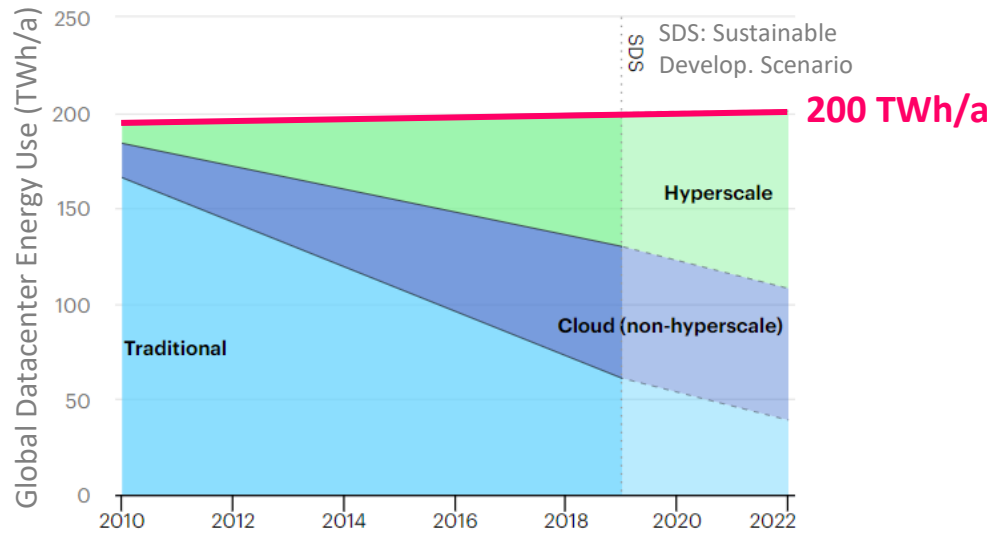
Part IV

Comparative Evaluation of SSTs for Datacenters and EV Charging

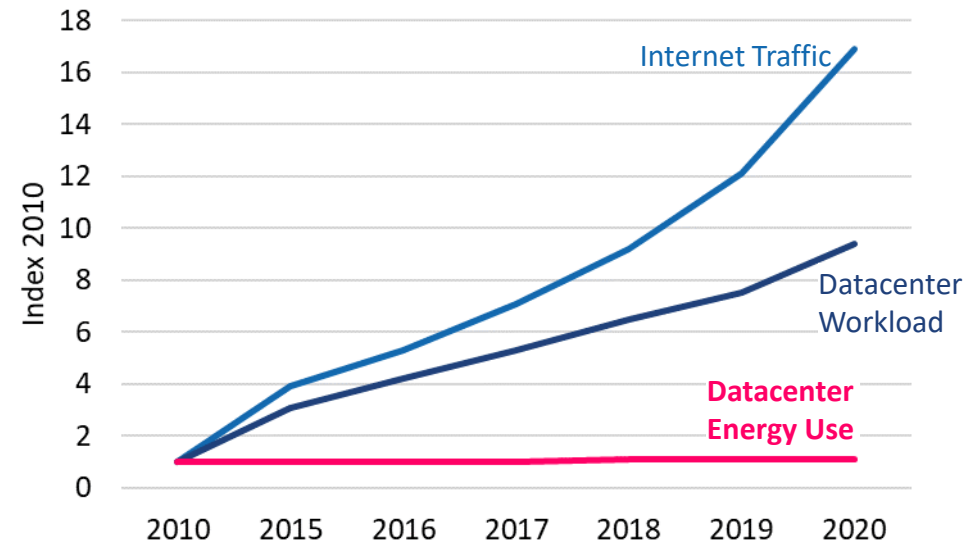


Global Datacenter Electricity Demand

- Datacenters Consume > 200 TWh/a | About 1% of Global Electricity Demand
- Energy Costs Dominate Overall Life-Cycle Costs



Source (Img., Data): <https://www.iea.org/>



- Decoupling of Computing Workload from Energy Use
- Efficiency Improvement on All Levels: Computing Equipment | HVAC | ... | Power Supply System!



AC vs. DC Distribution

THE CURRENT WAR

THE TALE OF AN EARLY TECH RIVALRY

DC

DIRECT CURRENT

The flow of electricity is in one direction only. The system operates at the same voltage level throughout, and is not as efficient for long-distance transmission.

Direct current runs through:

- Battery-Powered Devices
- Fuel and Solar Cells
- Light-Emitting Diodes

"TESLA'S IDEAS ARE SPLENDID, BUT THEY ARE UTTERLY IMPRACTICAL."
- THOMAS EDISON

LATE BLOOMER
Thomas Edison, the youngest in his family, didn't learn to talk until he was almost 4 years old.

FALLING OUT
Edison promised his father a penny reward if he could design and build his direct current system. The young engineer took on the challenge and ended up saving Edison more than \$150,000 (millions of dollars by today's standards). When Tesla asked for his rightful compensation, Edison declined to pay him. Tesla resigned shortly after, and the elder inventor spent the rest of his life campaigning to discredit his counterpart.

EDISON FRIES AN ELEPHANT
In order to prove the dangers of Tesla's alternating current, Thomas Edison staged a highly publicized electrocution of the three-ton elephant known as "Topsy." She died instantly after being shocked with a 6,600-volt AC charge.

AC

ALTERNATING CURRENT

Electric charge periodically reverses direction and is transmitted to customers by a transformer that could handle much higher voltages.

Alternating current runs through:

- Car Motors
- Radio Signals
- Appliances

"IF EDISON HAD A NEEDLE TO FIND IN A HAYSTACK, HE WOULD PROCEED AT ONCE... UNTIL HE FOUND THE OBJECT OF HIS SEARCH. I WAS A SORRY WITNESS OF SUCH DOINGS, KNOWING THAT A LITTLE THEORY AND CALCULATION WOULD HAVE SAVED HIM 90 PERCENT OF HIS LABOR."
- NIKOLA TESLA

You would have never found two geniuses so spiteful of each other beyond turn-of-the-century inventors Nikola Tesla and Thomas Edison. They worked together—and hated each other. Let's compare their life, achievements, and embittered battles.

WAR OF CURRENTS OFFICIALLY SETTLED
In 2007, Con Edison ended 125 years of direct current electricity service that began when Thomas Edison opened his power station in 1882. It changed to one generic alternating current.

NOBEL PRIZE CONTROVERSY
In 1915, both Edison and Tesla were to receive Nobel Prizes for their strides in physics, but ultimately, neither won. It is rumored it has been caused by their animosity towards each other and refusal to share the coveted award.

THOMAS EDISON VS. NIKOLA TESLA

1847 BORN 1858

Milan, Ohio BIRTHPLACE Šteljica, Croatia

Wizard of Menlo Park NICKNAME Wizard of the West

Home schooled and self-taught EDUCATION Studied math, physics, and mechanics at The Polytechnic Institute at Graz

Mass communication and business METHOD Electromagnetism and electromechanical engineering

Pat and error METHOD Getting inspired and having the invention in his mind in detail before fully constructing it

Incandescent light bulb, phonograph, mass production technology, motion picture camera DC motors and electric power DC (Direct Current) WAR OF CURRENTS ELECTRICAL TRANSMISSION IDEA AC (Alternating Current)

NOTABLE INVENTIONS Tesla coil - resonant transformer circuit, radio transmitter, fluorescent light, AC motor, and electric power generation system

1,095 NUMBER OF US PATENTS 112

NUMBER OF NOBEL PRIZES WON 0

1851—Passed away peacefully in his New Jersey home, surrounded by friends and family DEATH 1943—Died lonely and in debt in Boston 3327 at the New Yorker Hotel

SOURCES: SHEPHERD, MARGARET. "TESLA: MAN OUT OF TIME." JOHN ROBERT. "TESLA: MASTER OF ALTERNATING." THOMAS EDISON.COM | P.46, 583 | NER.BIT.EDU | WIKI.ORG

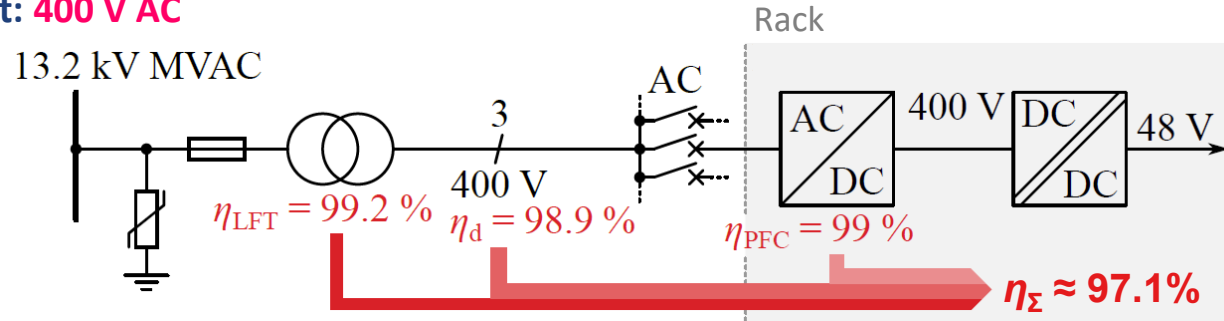
A COLLABORATION BETWEEN GOOD AND COLUMN FIVE

Source: GOOD/Column Five Media (<https://good.is>)

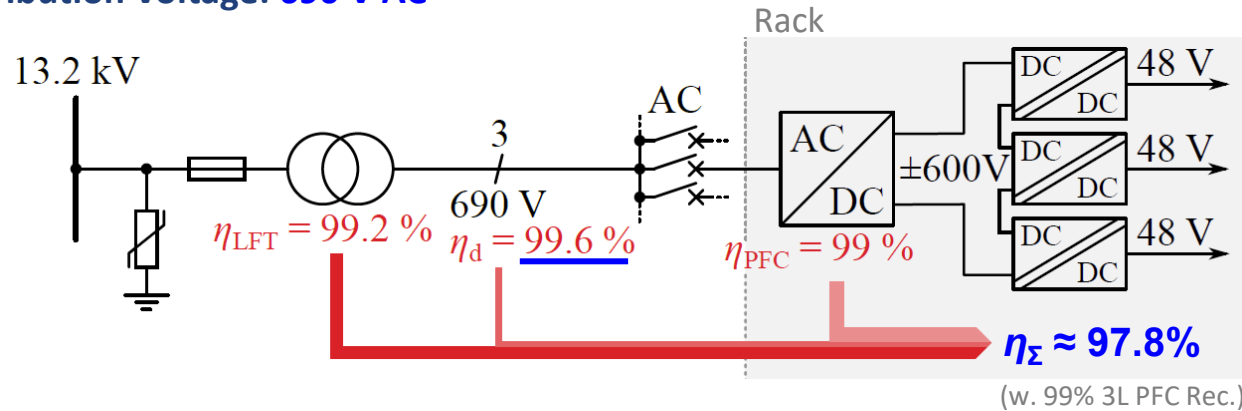


AC Power Distribution

State of the Art: 400 V AC



Increased Distribution Voltage: 690 V AC

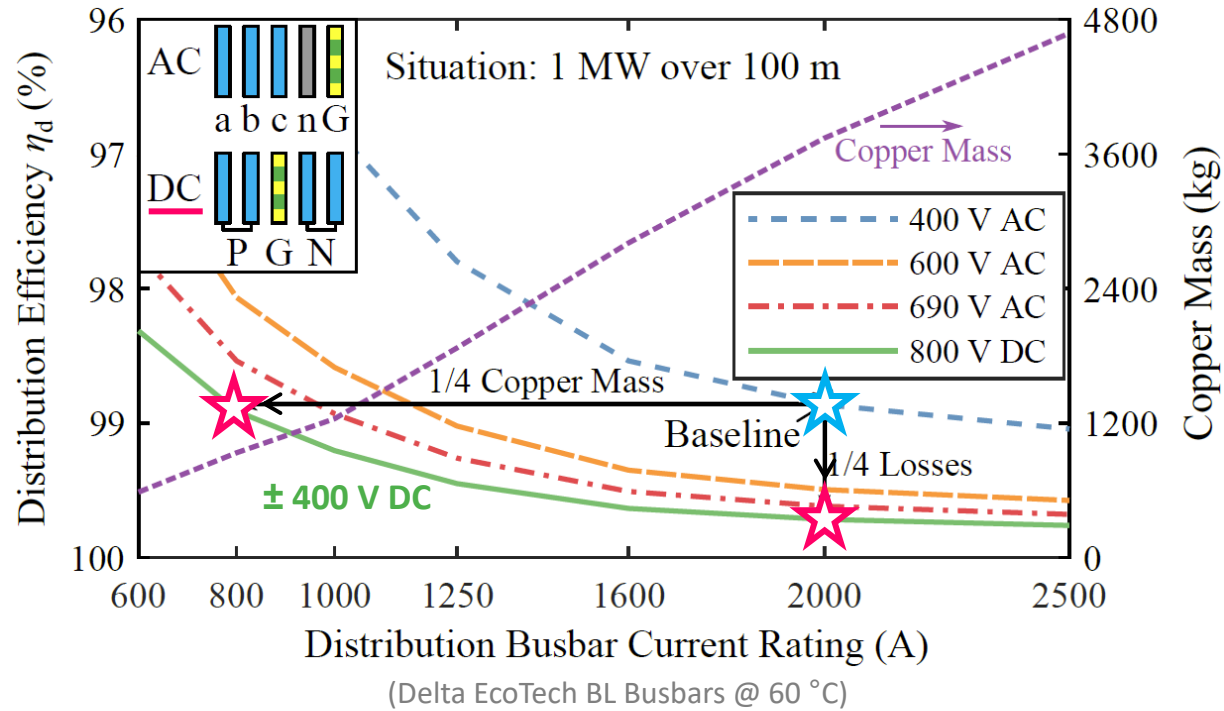


- η_{Σ} : Efficiency from MVAC to Input of Rack-Level 400 V / 48 V DC-DC Conversion
- η_d : Distribution Efficiency for 1 MW Over 100 m with Delta EcoTech BL 2000 A Busbar
- η_{LFT} : Requirement by, e.g., EU Ecodesign Directive 2009/125/EC



Distribution Losses

■ 400 V AC → 690 V AC: Significant Loss Reduction or Lower Copper Usage



■ Same Busbar in AC or DC Configuration: 400 V AC → 800 V DC (± 400 V DC)

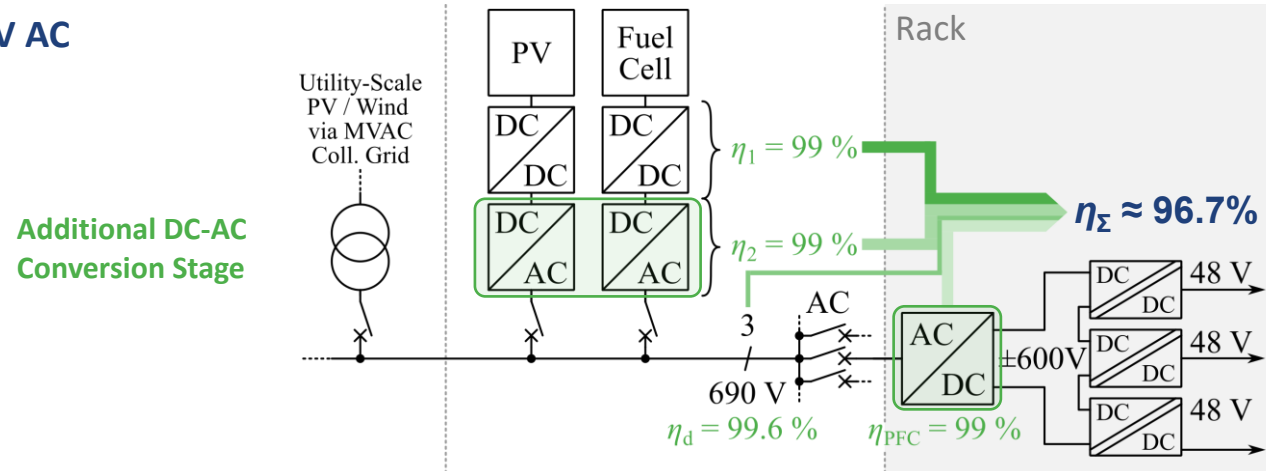
● -75% Distribution Losses (or -75% Copper Mass)

● DC Distribution Challenges: Protection, DC Breakers, DC PSUs, ...

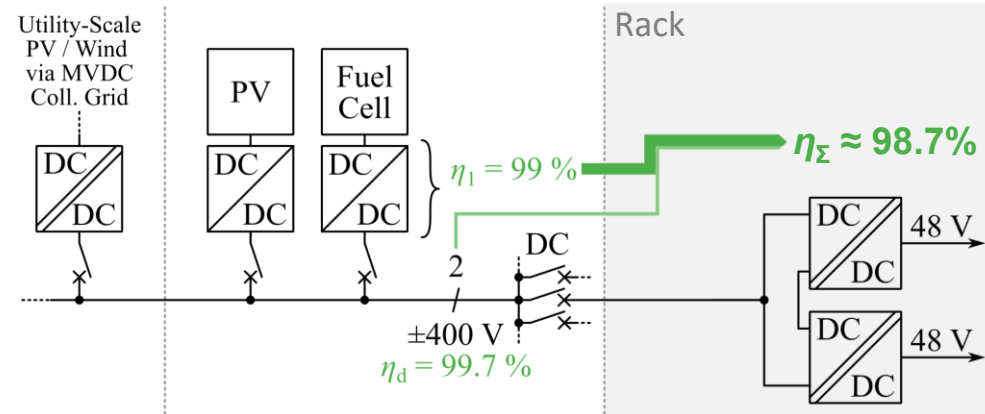


DC Power Distribution (1) – DC Sources

■ 690 V AC



■ ±400 V DC



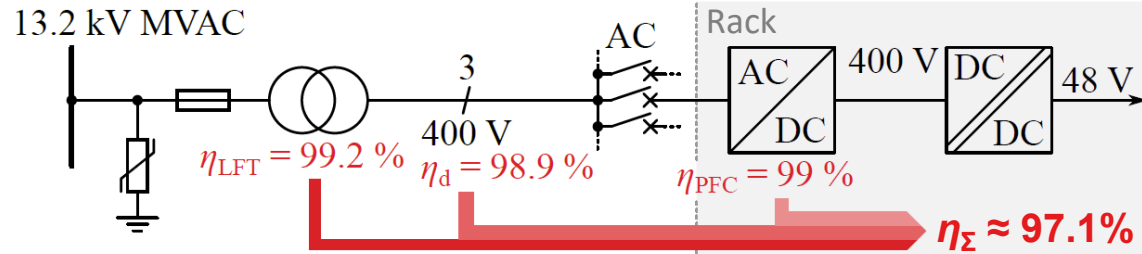
■ DC Distribution Leverages DC Output of Fuel Cells / Batteries / PV

- Note: Utility-Scale Renewable Energy System Requires Higher-Voltage DC Collector Grid

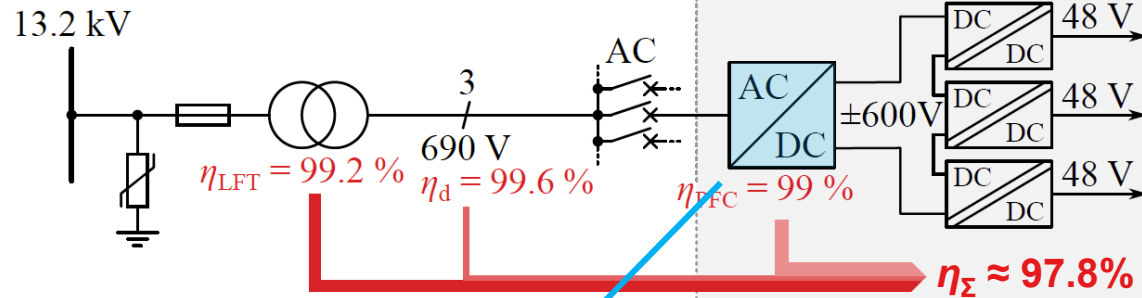


DC Power Distribution (2) – Grid Supply

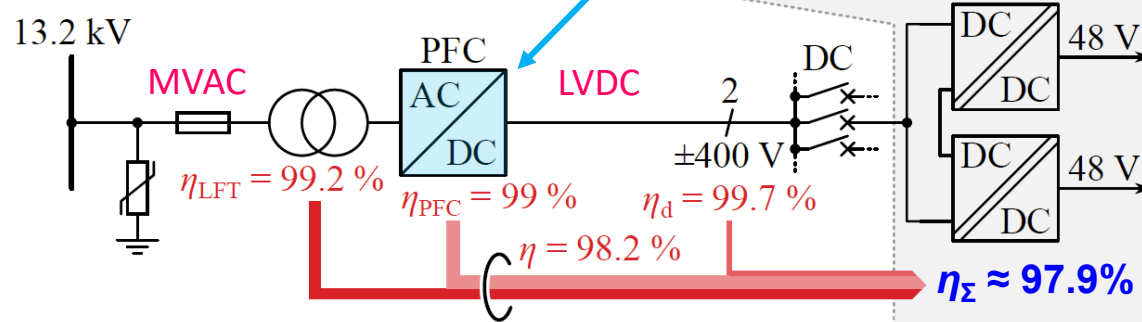
■ 400 V AC



■ 690 V AC



■ ±400 V DC



• Similar η_{Σ} as For 690 V AC Distr.

■ Simply Centralizing the PFC Rectifier Functionality → Only Minor Efficiency Gain!

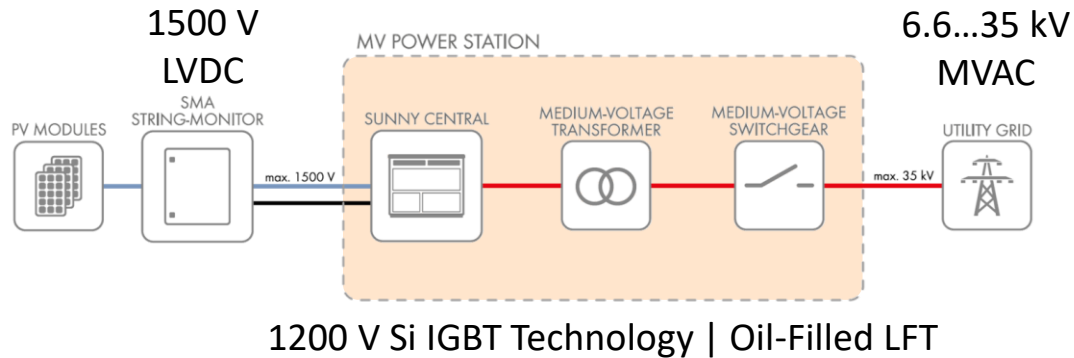


Medium-Voltage AC-DC Interfaces



MV Power Station for Photovoltaics

- State-of-the-Art **3 MVA** Turnkey Solution
- 20 ft Container: PV Inverter, LFT, MV Switchgear, etc.
- 3 MVA | 6.1 m x 2.6 m x 2.4 m | $\approx 0.08 \text{ kW/dm}^3$



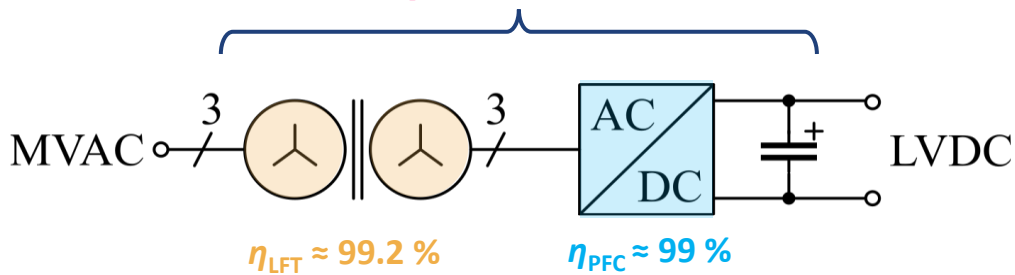
- Inverter Efficiency: 98.5% CEC
- Transformer Efficiency: 99% (EcoDesign, oil-filled)
- Overall Efficiency $\approx 97.5\%$ → Improvements Expected for SiC and Dry-Type LFT → 98+ %



MVAC-LVDC with LFT and Central SiC PFC Rectifier

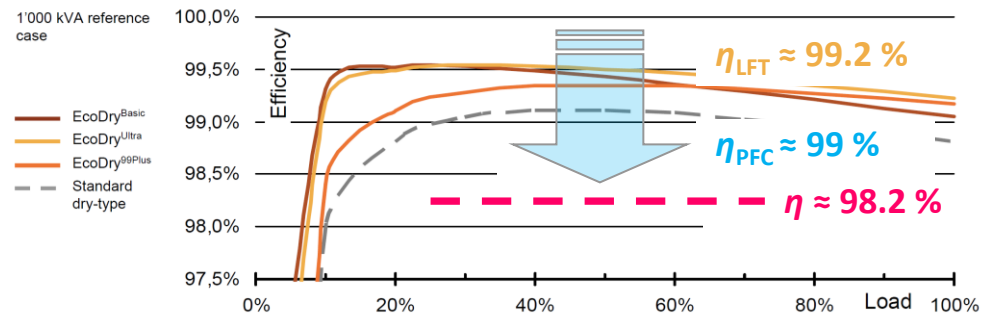
- Centralized PFC Rectifier with **1200 V SiC Technology** & High-Efficiency **Dry-Type/Ecodesign LFT**

MVAC-LVDC: $\eta \approx 98.2\%$, $\rho \approx 0.25 \text{ kW/dm}^3$

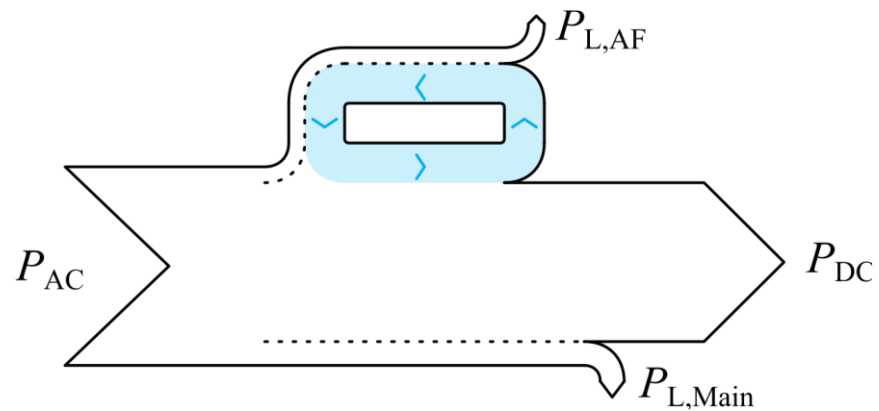


- Full Functionality (Reactive Power, Bidir. Power Flow, ...)
- High Robustness & Low Complexity
- Scalability to Higher MVAC Levels
- Proven LV Converter Design Paradigms | [Parallel-Interleaving \(Modularization, Redundancy\)](#)
- Compatible with Existing MV-side Infrastructure
- No DC fault Current Limiting

Example: ABB EcoDry™ High-Efficiency Transformers
(ABB, 2011 – Today, 99.2% Required by, e.g., EU EcoDesign Directive)

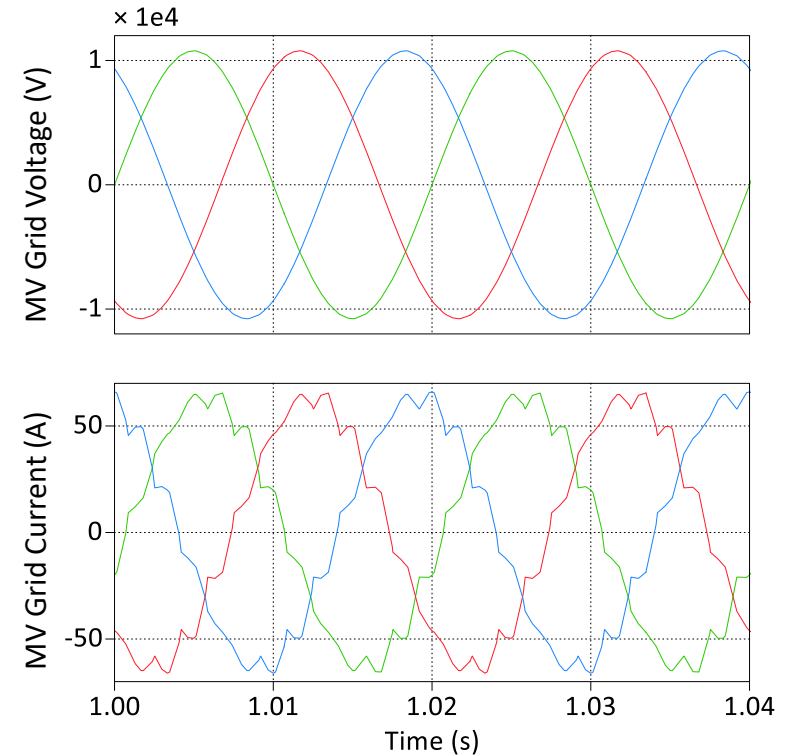
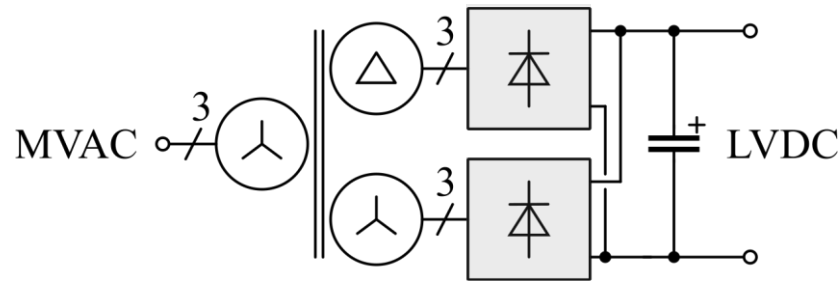


MVAC-LVDC Hybrid Transformers



12-Pulse / Multi-Pulse Rectifiers

- **No Explicit PFC Stage (!)** → Passive Realization of PFC Functionality with Phase-Shifting Transformer
- High Robustness
- Low Complexity
- High Efficiency ($\approx 0.25\%$ Diode Losses)
- No DC-Side Inductors Required (!)
- 18-Pulse or 24-Pulse for Higher Power Levels



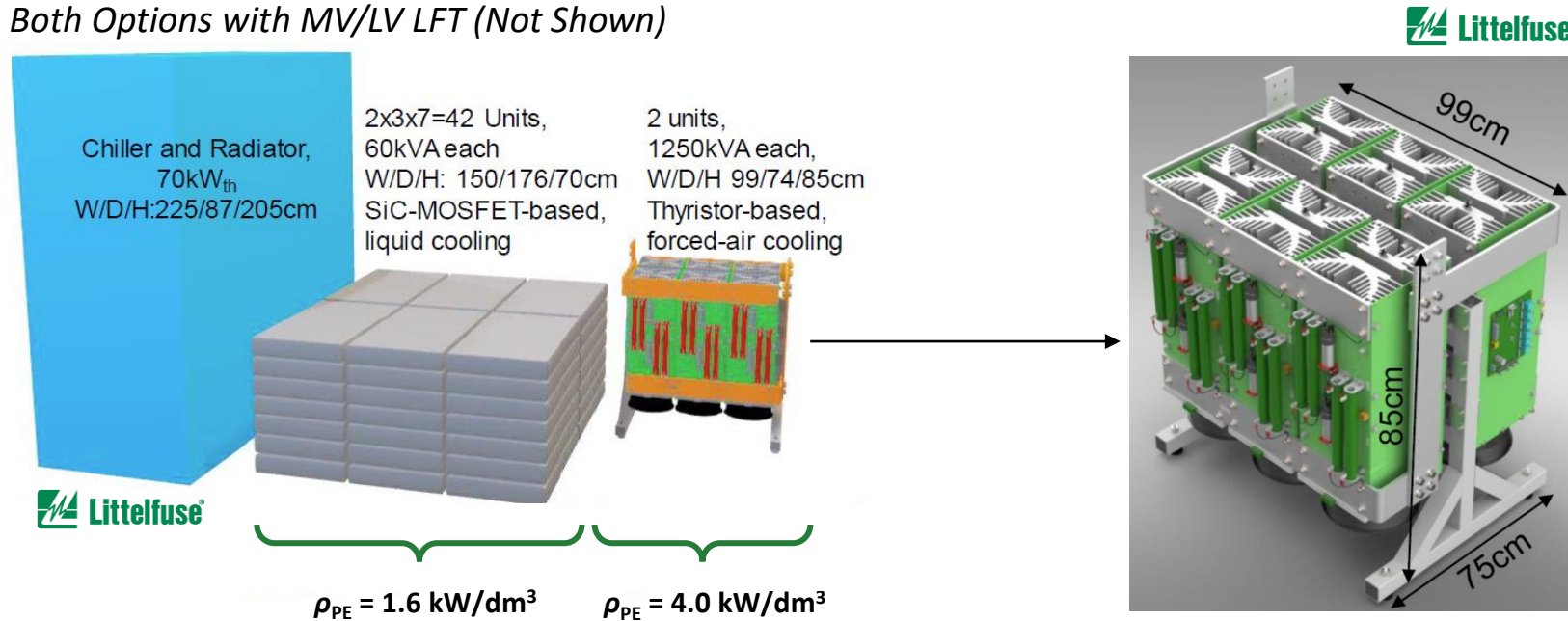
- Unidirectional
- No Active Output Voltage Control (Tap Changer: Wear & Tear, Limited Dynamics / Thyristors: High VAr Consumption)
- Remaining Current Distortions / Reactive Power Consumption



Example: MW-Level Charging of Commercial Vehicles

- Future Charging Power Up to **2.5 MW** / Supply from MV → LFT for Galvanic Separation
- Modular: 2.5 MW = **42 x 60 kW PSU Mod. Parallel** (AC-DC + DC-DC Non-Isol.) / **97% Effi.** / Liquid Cooling
- Monolithic: 2.5 MW **12-Pulse Thyristor Rectifier** / 2 x 1250 kW / **99.7% Efficiency** / **Air Cooling**

Both Options with MV/LV LFT (Not Shown)



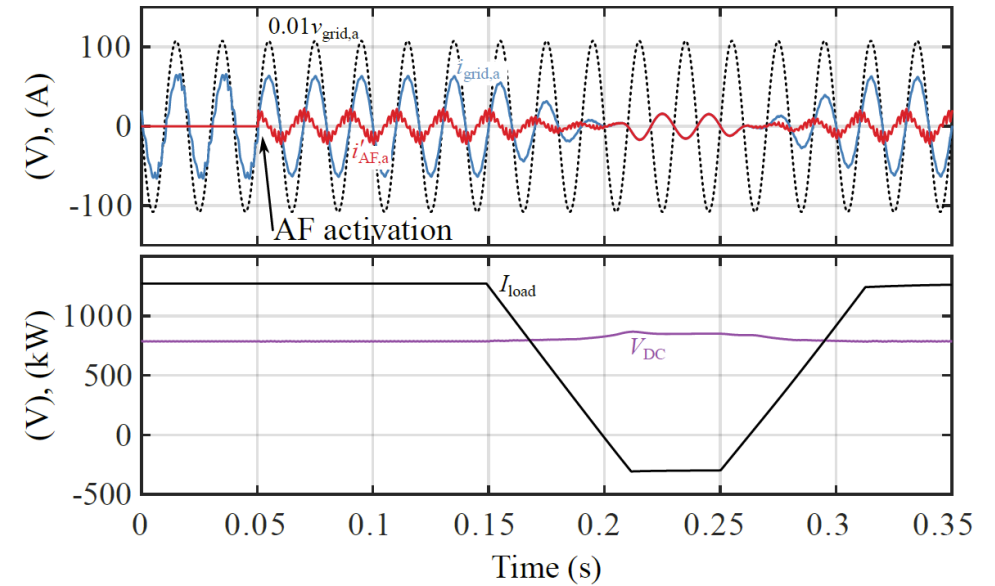
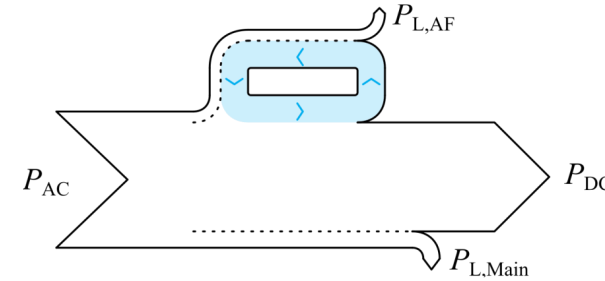
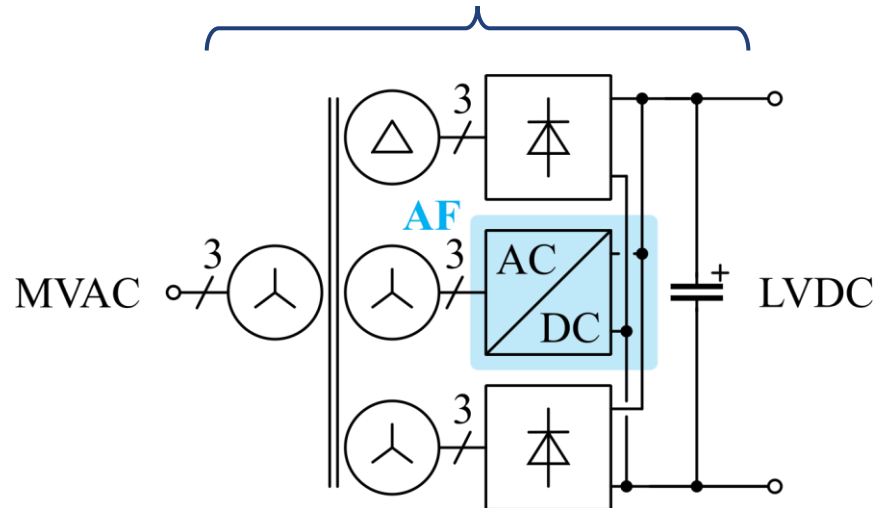
- Longevity of Disk-Type Thyristors / Decades in the Field → Electrolyzers w. Similar DC Volt./Cur. Control Req.



MVAC-LVDC Hybrid Transformer

- **Hybridization:** Partial Switch-Mode Power Processing
- **Active Filter (AF) Modules** with $\approx 25\%$ Power Rating
 → Sinusoidal Grid Currents & Reactive Power Compensation

MVAC-LVDC: $\eta \approx 98.5\%$, $\rho \approx 0.2 \text{ kW/dm}^3$



- Remaining 12-Pulse Operation in Case of AF Failure | Central, Shared FACTs as Complement/Alternative
- Connection of AF to Output DC Bus → Reverse Power Flow Capability
- No Active Output Voltage Control (Tap Changer: Wear & Tear, Limited Dynamics / Thyristors: High VAR Consumption)



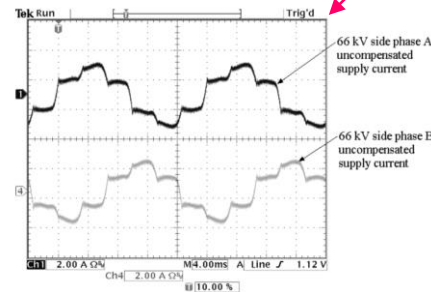
Example: 3 kV DC Traction Substation

- Substation 66 kV AC → 3 kV DC Traction Grid w. Diode Rect. 5+ MW
- 1.5 MW Series-Stacked Converter Enables Active Power Filtering & Regeneration Capability

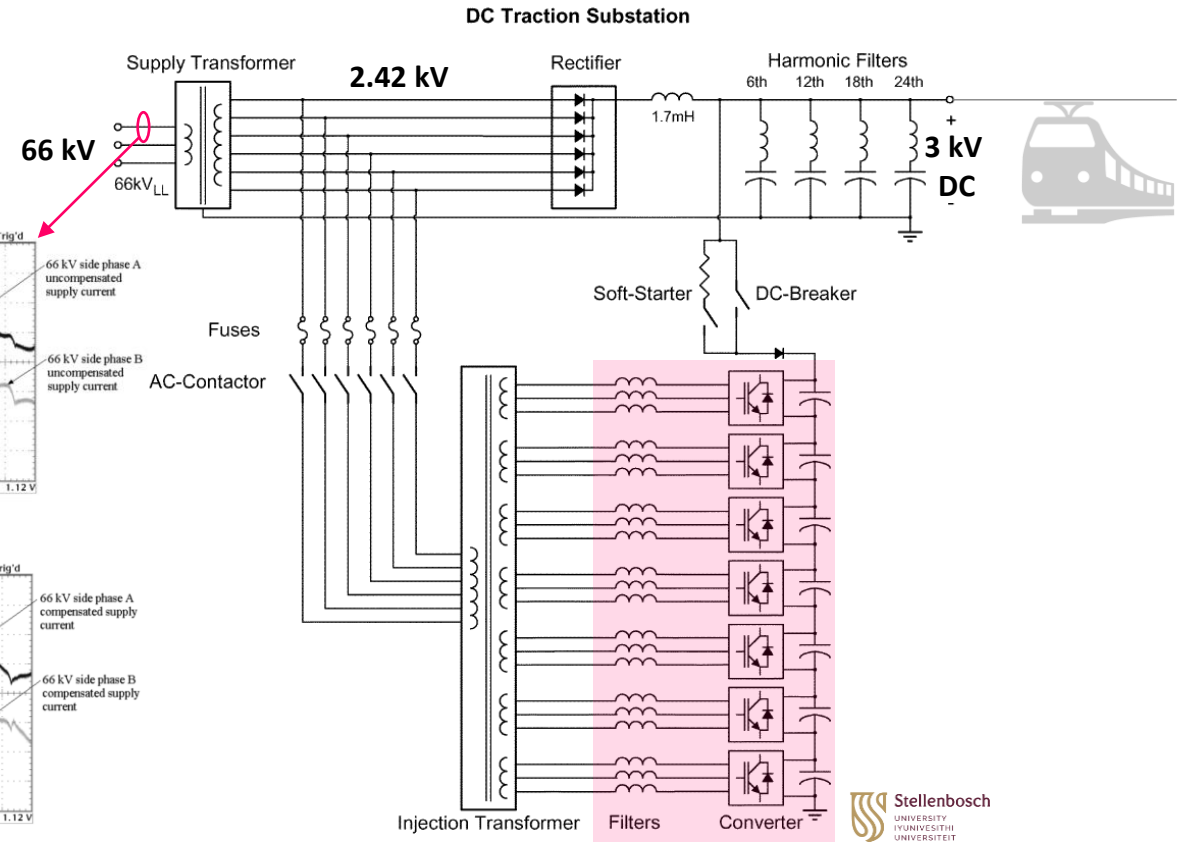
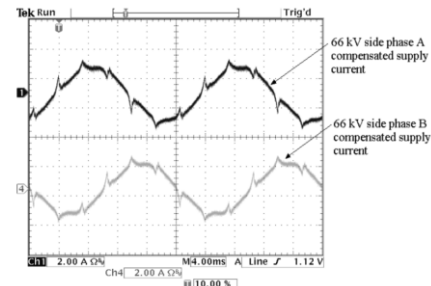
1.5 MW / 7 Stacked 3-Ph. Inv.
 5.4 kV DC (7 x 800 V DC)
 35 kHz Eff. Sw. Freq. (7 x 5 kHz)



W/o Act. Filt.



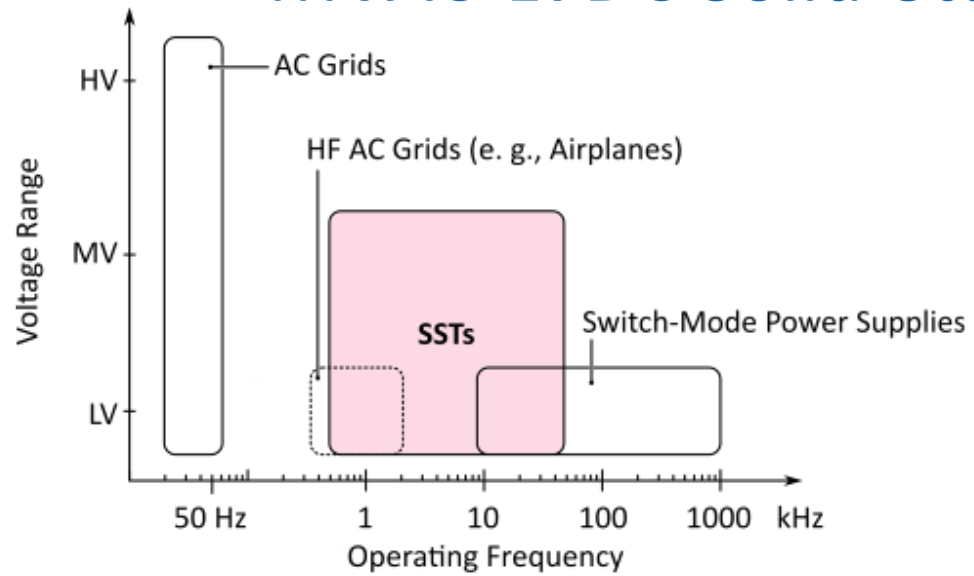
With Act. Filt.



- Full-Scale Tests w. 5 MW Load (Accelerating Trains) and 1.5 MW Regeneration (Braking Trains)



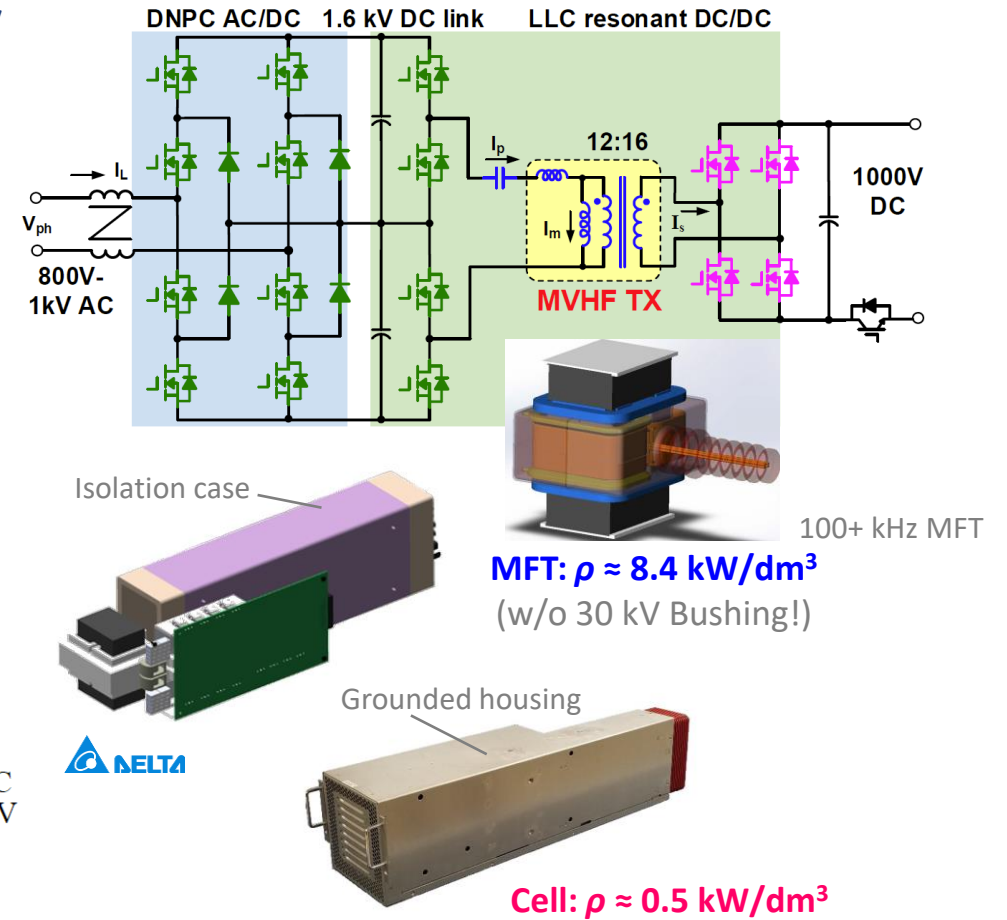
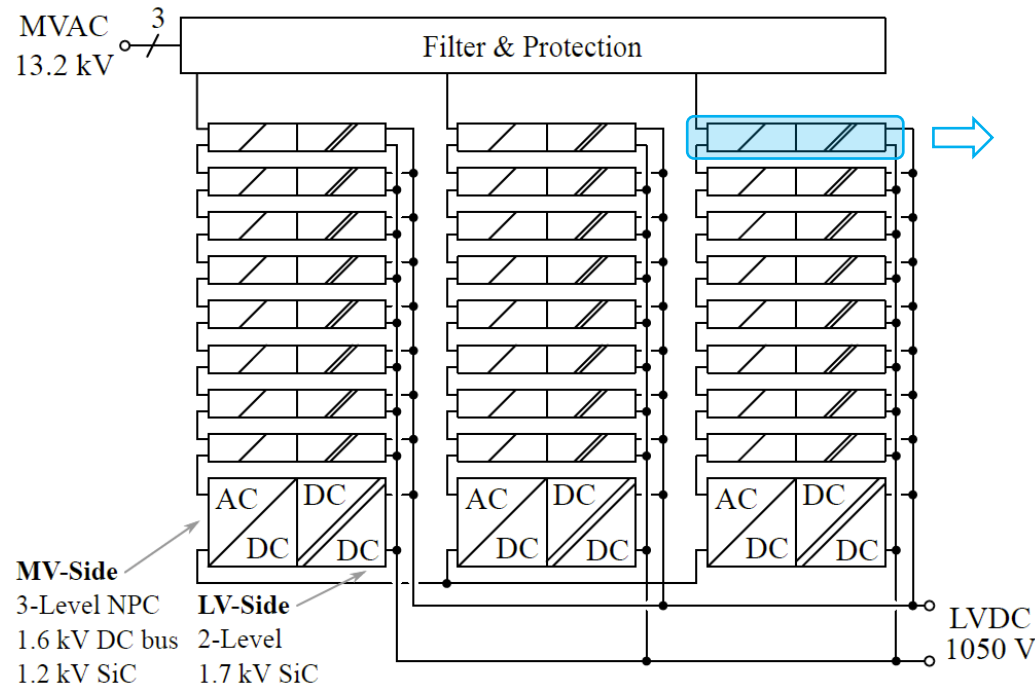
MVAC-LVDC Solid-State Transformers



13.2 kV / 400 kW SST-Based EV Charger (1)

■ **Fully Modular Input-Series-Output-Parallel (ISOP) Topology**

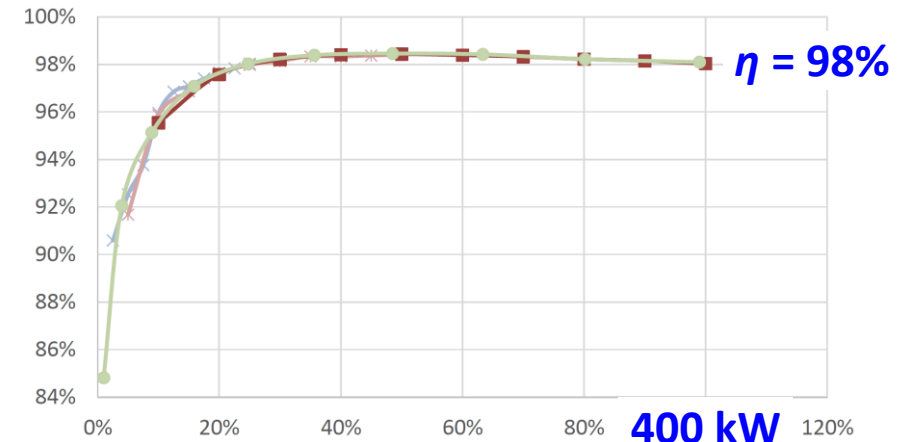
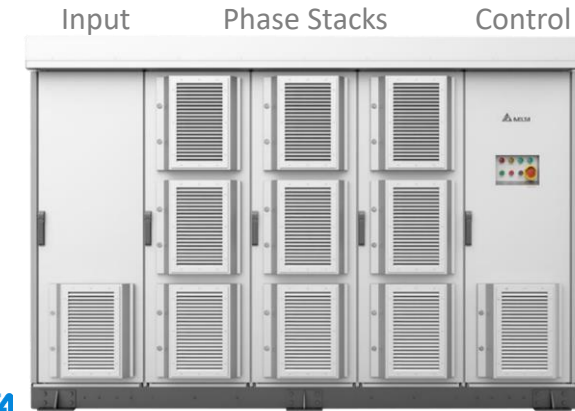
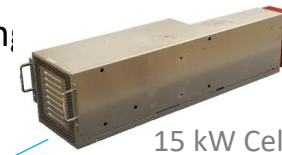
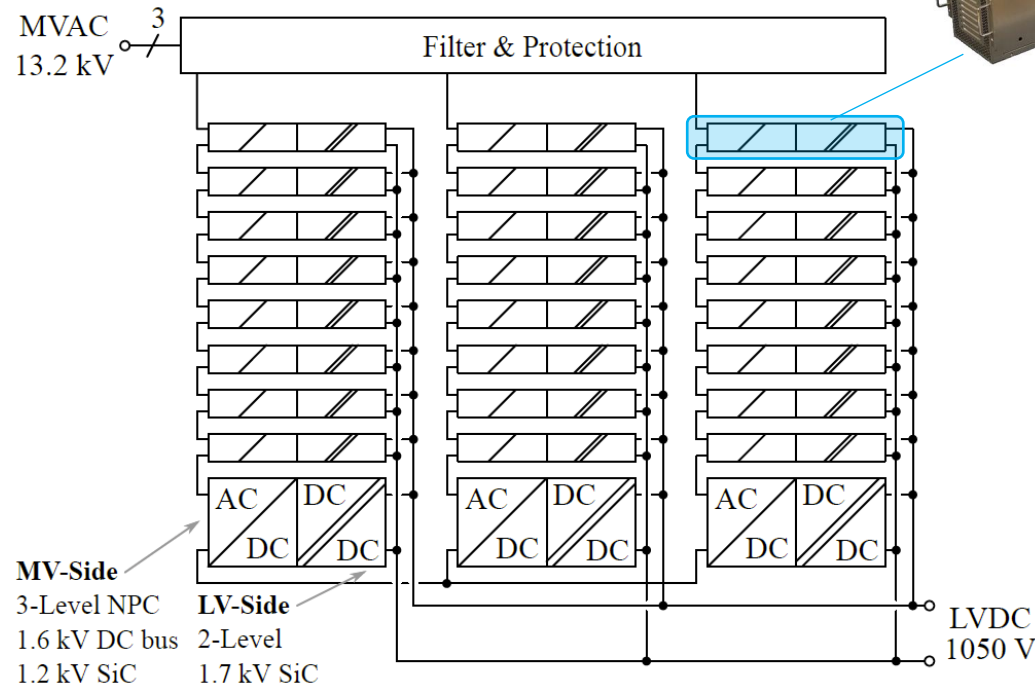
- 3 x 9 = 27 AC-DC/DC-DC Cells | **438 Switches**
- 15 kW per Cell | All-SiC Realization | Forced-Air Cooling



13.2 kV / 400 kW SST-Based EV Charger (2)

■ One of the Most Advanced Industrial MVAC-LVDC SST Prototypes

- 3 x 9 = 27 AC-DC/DC-DC Cells | 438 Switches
- 15 kW per Cell | All-SiC Realization | Forced-Air Cooling



- 3000 kg Weight | 3.1 m x 1.3 m x 2.1 m Outer Dimensions
- Power Density: $\rho \approx 0.05 \text{ kW/dm}^3$ | 0.5 kW/dm^3 (Cells) | 8.4 kW/dm^3 (MFT)

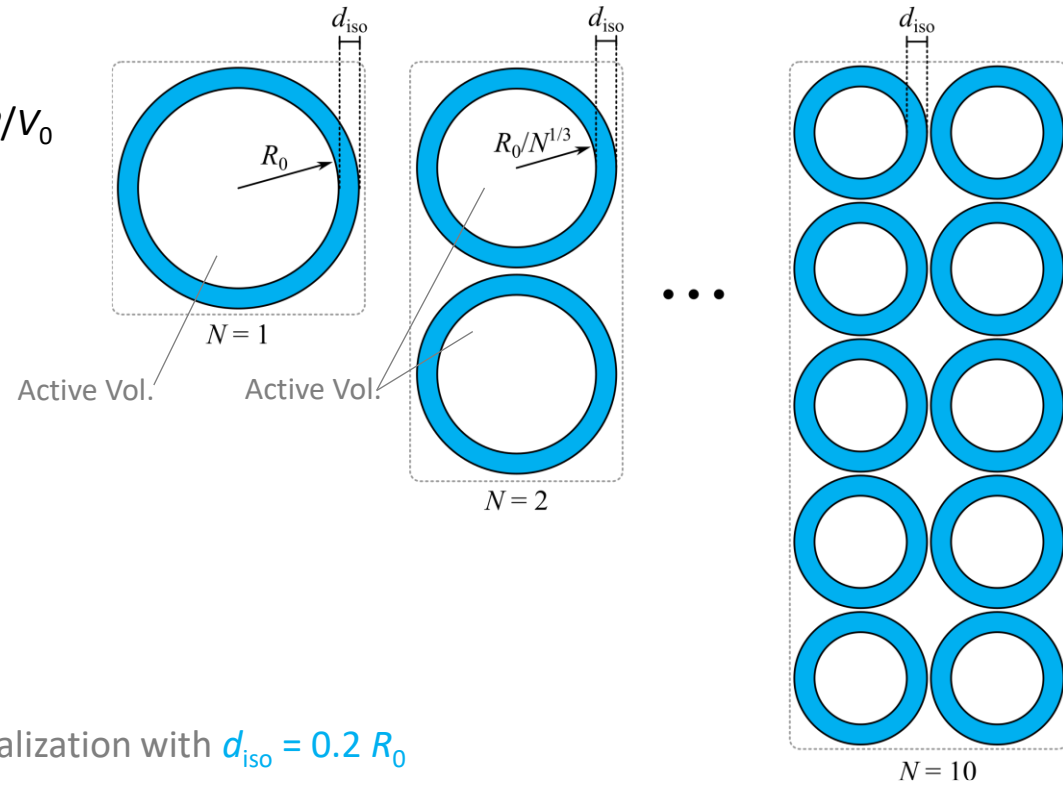
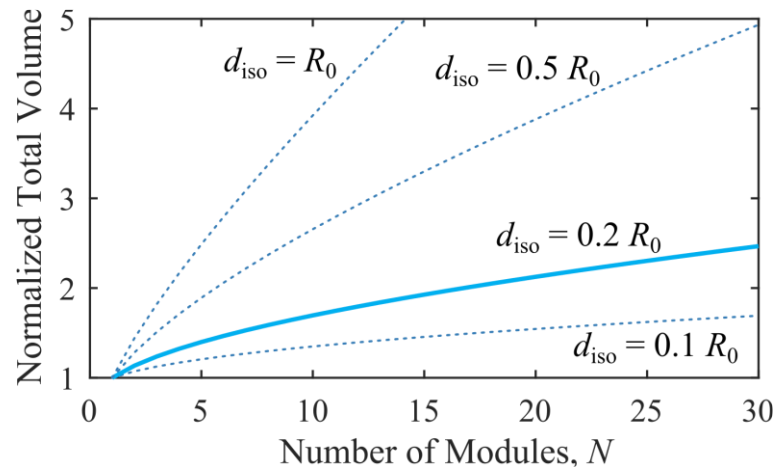


Intuition: Modularization Penalty

■ **Highly (!) Simplified Consideration**

- Power P Processed in Sphere with Radius R_0
- Modularizing Assuming Constant Power Density P/V_0
- Const. Isolation / Overhead Distance d_{iso}

$$V(N) = \frac{4}{3} \pi \left(\frac{R_0}{N^{1/3}} + d_{iso} \right)^3 \cdot N$$



2D Visualization with $d_{iso} = 0.2 R_0$

■ **High Module Count → Massive Reduction of Overall Power Density Expected**

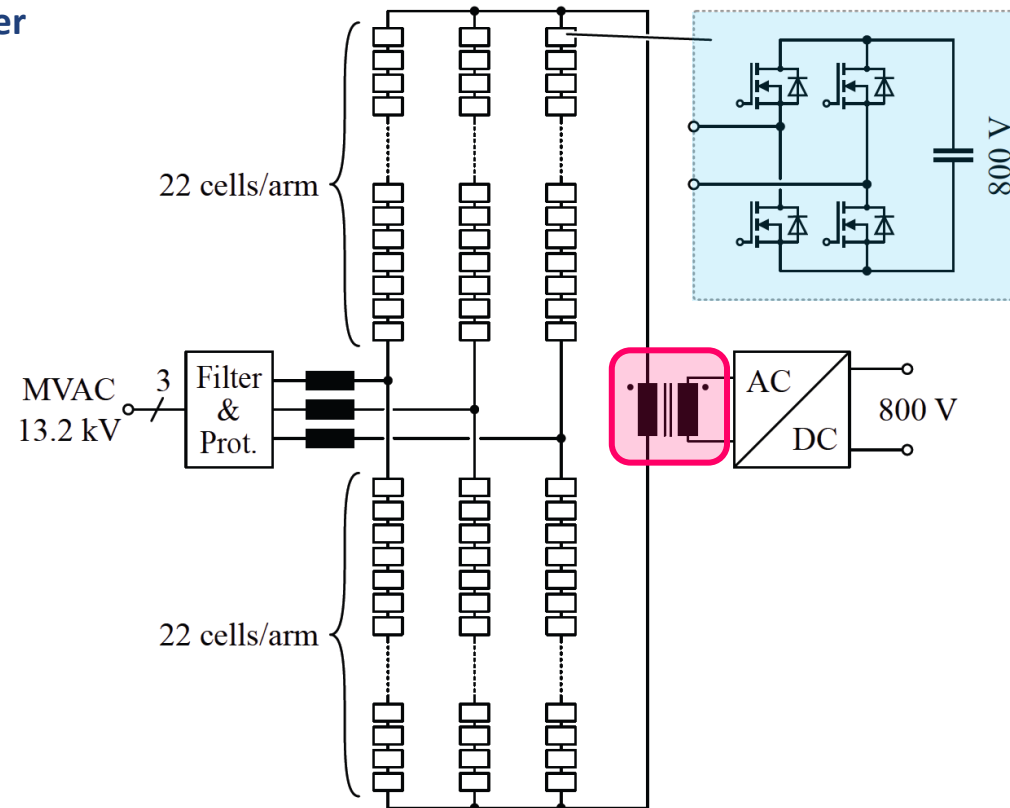
- **Additional Overhead: Input & Output Filters | Protection Equipment | Mech. Assembly | Cabinets etc.**



MMC-Based SST Concepts

■ **Limit Modularity to PE | Single MF Transformer**

- Example for 13.2 kV Grid
- 22 Full-Bridge Cells per MMC Arm | 6 Arms
- 528 Switches (1200 V, MV-Side Only)



■ **Benefits of Modularity → Redundancy | Availability | Economies of Scale | Transportability**

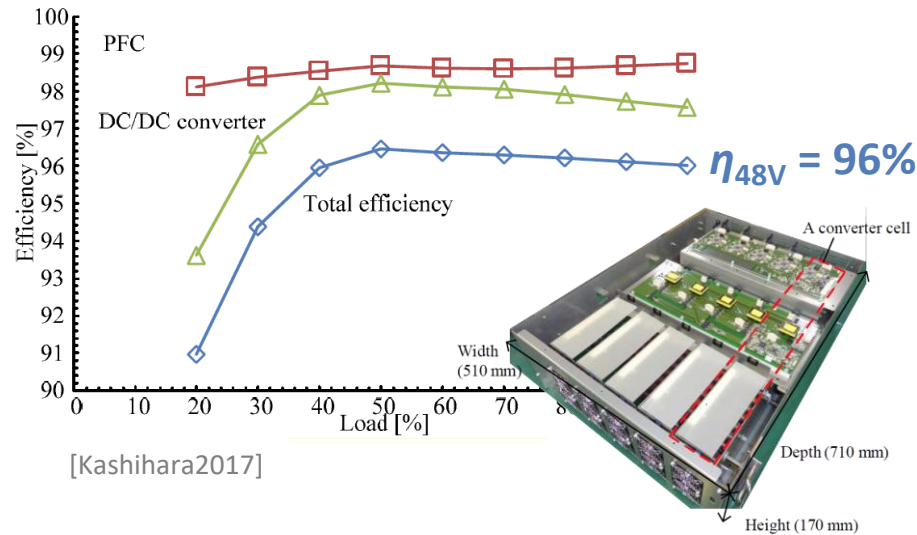


Remark: Datacenter Rack-Level MVAC-LVDC SSTs

MVAC Distribution to the Rack & Small Rack-Level SSTs

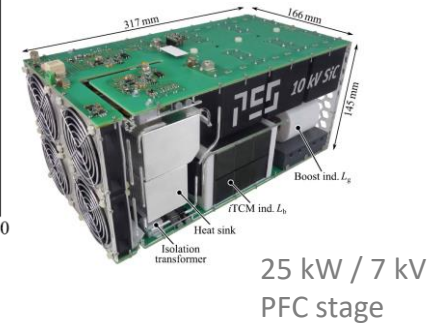
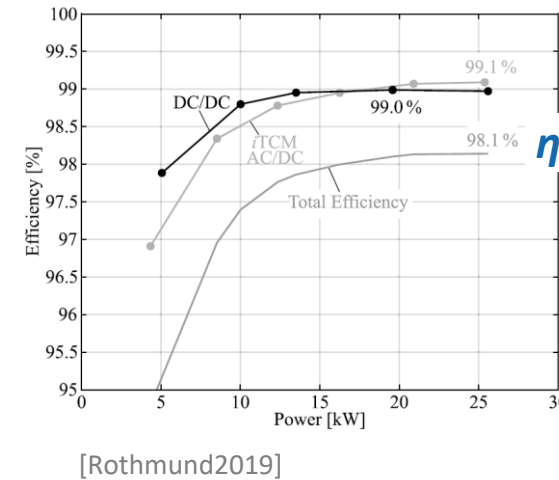
Fuji Electric, 2017

- 2.4 kV rms (l-n) | 25 kW | **48 V DC**
- LV Si Multicell ISOP | **0.4 kW/dm³**



ETH Zürich, 2019

- 3.8 kV (l-n) | 25 kW | **400 V DC**
- **10 kV SiC Single Cell** | **3.5 kW/dm³**



Large Overhead!

- MV Protection Equipment & MV Switchgear (Disconnectors, Grounding Switches, ...)
- Central LFT Needed Unless Incoming MV Level is Distributed (Typ. >> 2.4 kV)

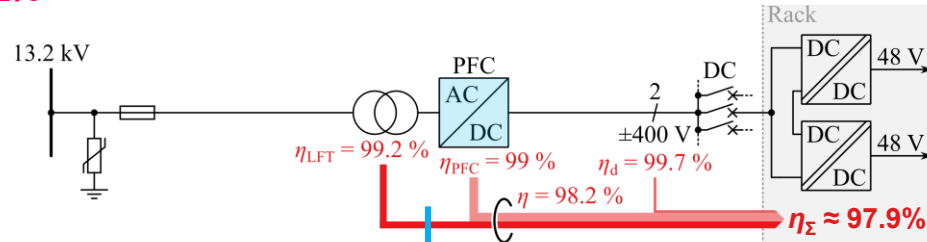


Comparative Evaluation of MVAC-LVDC Interfaces

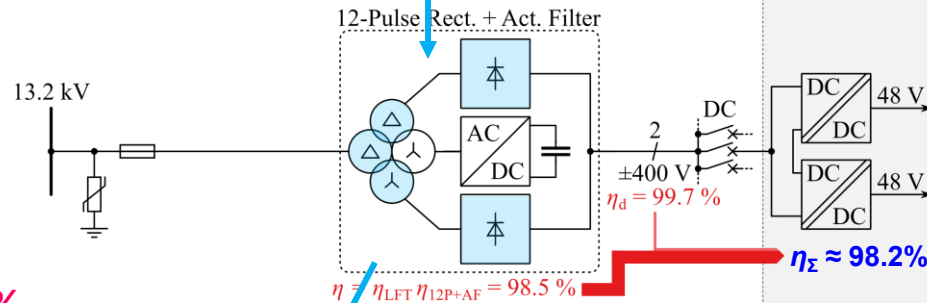


Efficiency

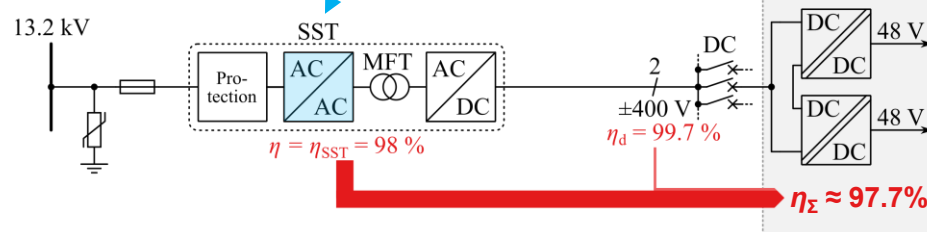
■ LFT + SiC PFC: $\eta \approx 98.2\%$



■ 12-Pulse + AF: $\eta \approx 98.5\%$



■ Industrial SST: $\eta \approx 98\%$



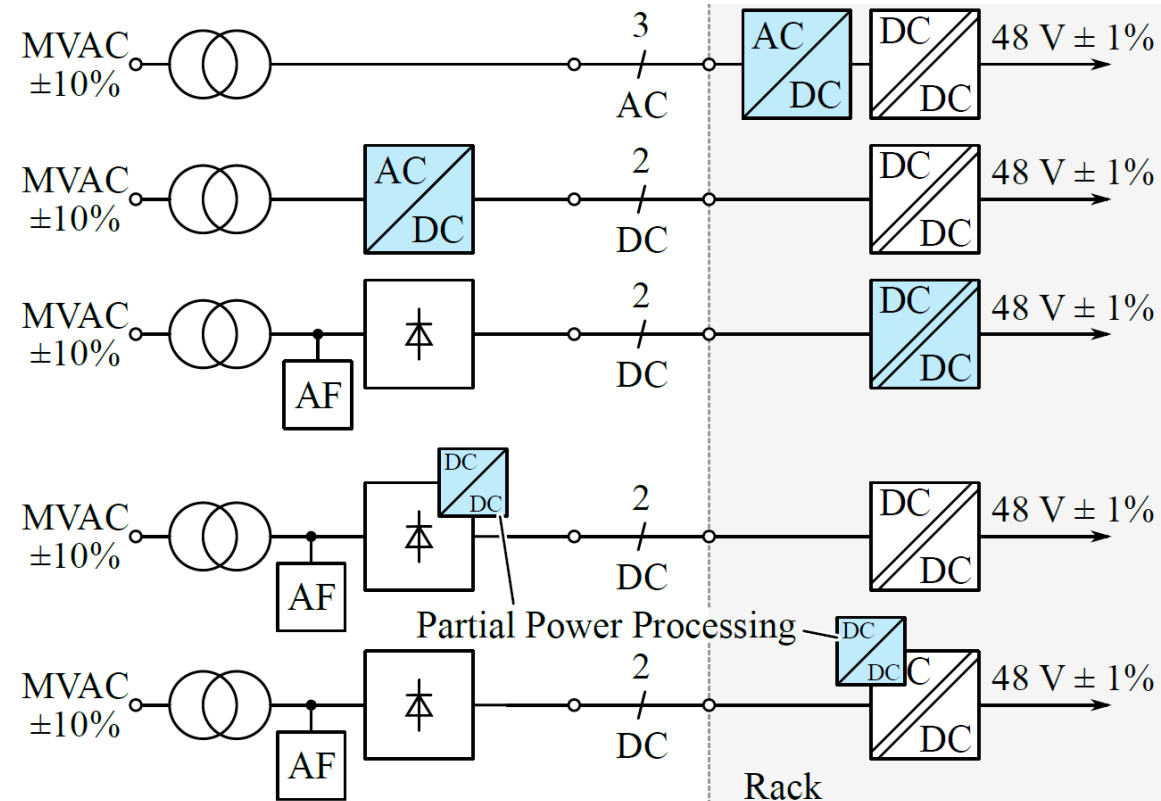
■ 12-Pulse + AF → Highest Efficiency & Robustness vs. Reduced Functionality

- Central PFC on LV-side
- No Switch-Mode PFC
- Active Filter / Partial-Power Proc.
- Central PFC on MV-side



Remark: DC Voltage Control

- Grid Voltage Varies $\pm 10\%$ (EN 50160) | Stable 48 V DC for IT Equipment Needed



- One Converter Stage Must Provide Regulation Capability!

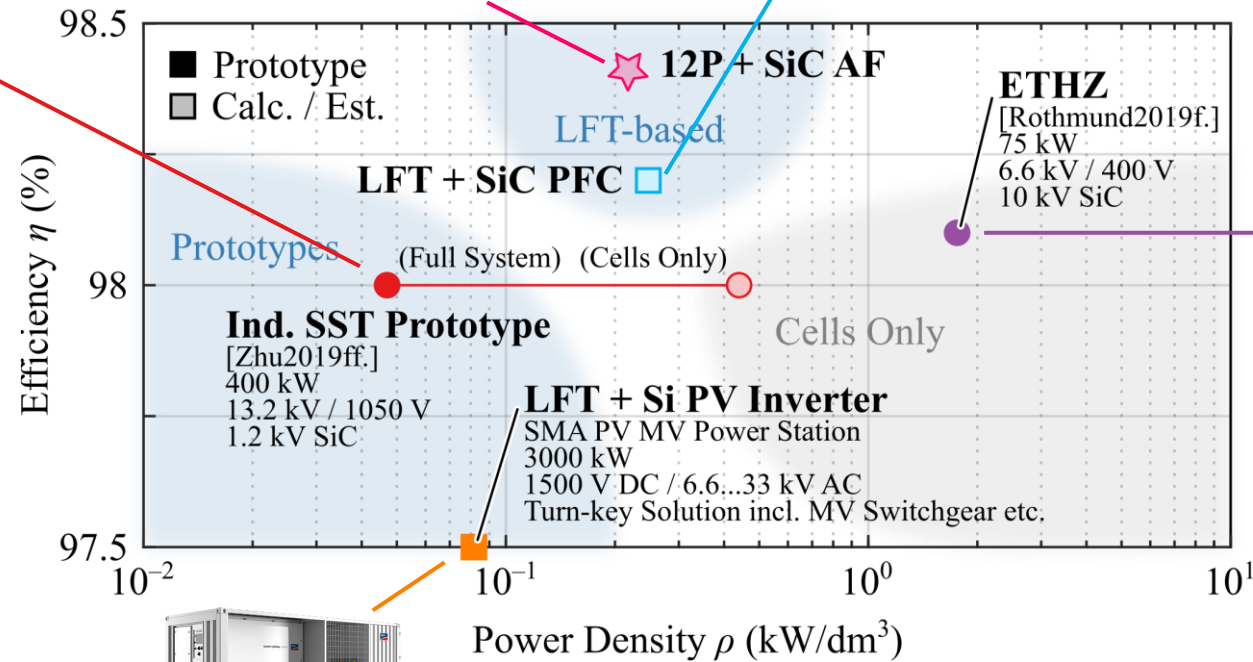


Efficiency & Power Density

- Industrial MVAC-LVDC SSTs → No Volume / Efficiency / Functionality Advantage Over LFT + LV SiC PFC
- LFT-Based Solutions → Robustness & Scalability
- 12-Pulse Rectifier + Act. Filter → Low Complexity | Reduced Functionality



400 kVA LFT
Shown for Comparison



10 kV SiC
(Not Industrialized)



Case Study Summary

690 V AC Competitive with ±400 V DC

- Add. Considerations on Integration of Renewables, Fuel-Cell Backup Power, Grid Services, etc.

LFT + LV SiC PFC

- Full Functionality, Scalability, High Robustness

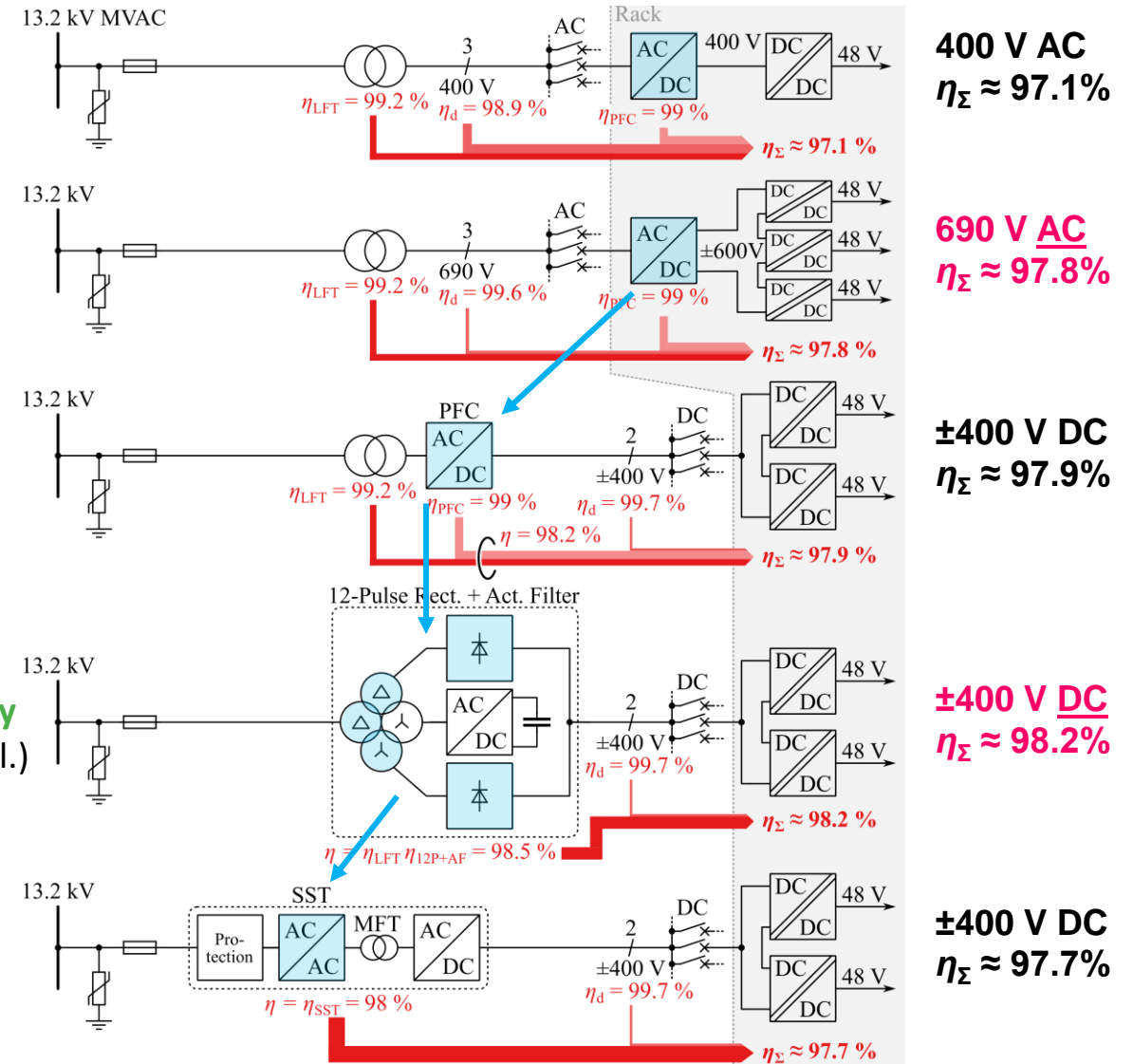
12-Pulse Rectifier & Act. Filter

- Low Complexity, High Efficiency, Scalability
- High Robustness, Long Lifetime, Good Recyclability
- Reduced Functionality (Unidir., No Act. DC Volt. Ctrl.)

Existing SST w/o Clear Advantages

- High Complexity Even for MMC-Based Designs
- Modularity / Economies of Scale / Protection / ...

→ Need for Future Research!

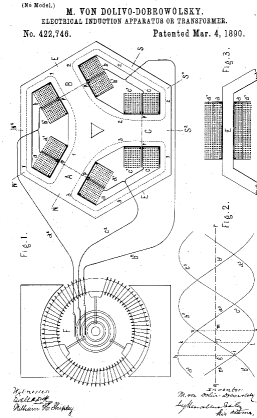


Part V

Summary & Research Vectors

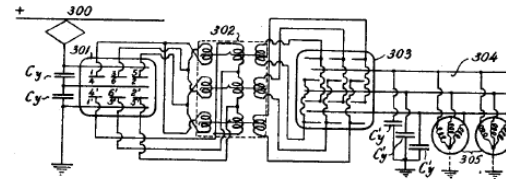


1830 Faraday
Law of Induction

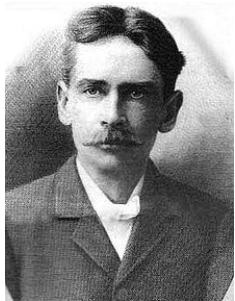
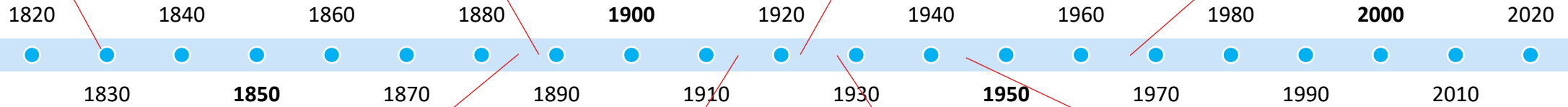
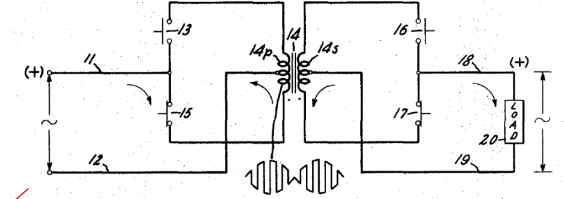


1889 Dobrovolsky
Three-Phase XFRM

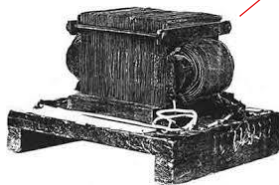
1923 Hazeltine
Electronic XFRM for DC Traction



1968 McMurray
Electronic XFRM with
Solid-State Switches

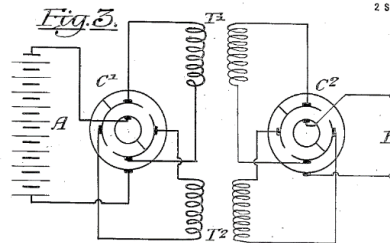


1885 Stanley / Westinghouse
Easily Manufact. XFRM &
First AC Distr. System



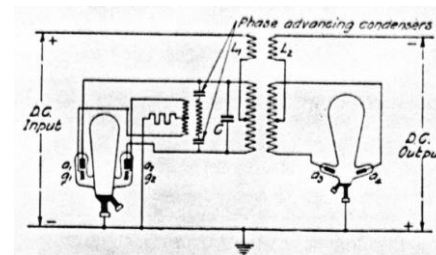
Img. Src.: IEEE NY Monitor

1,206,662.

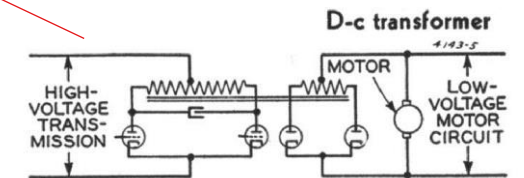


1914 Boucherot
Electronic XFRM w.
Mech. Switches

Patented Nov. 28, 1916.
2 SHEETS-SHEET 2.



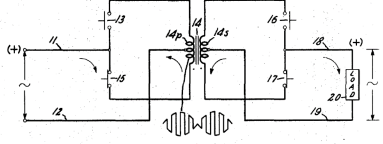
1928 D. C. Prince
Electronic XFRM with
Mercury-Arc Valves



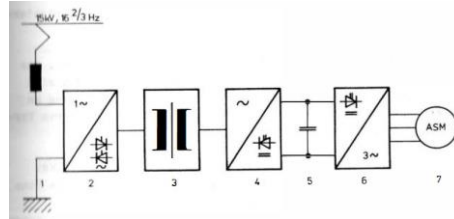
1944 Alexanderson
Electronic XFRM w.
Mercury Arc Valves



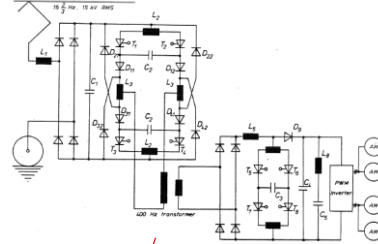
1968 McMurray
Electronic XFRM with
Solid-State Switches



1978 Mennicken / BBC
Medium-Freq. Isol. for Traction



1984 Weiss & Rentmeister
Isolated Front-End for Traction



2011 GE
1 MW AC-AC SST w. 10 kV SiC



2021 Delta
13.2 kV / 400 kW EV Fast Charger

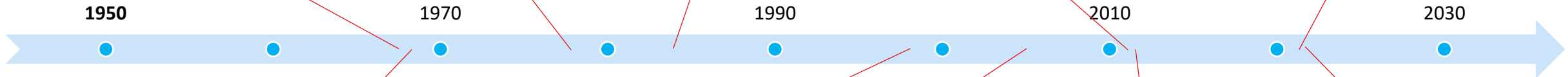
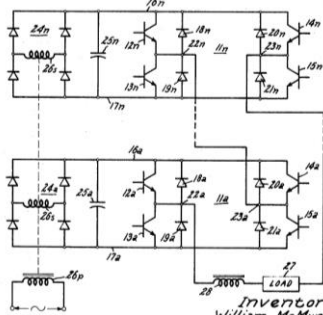


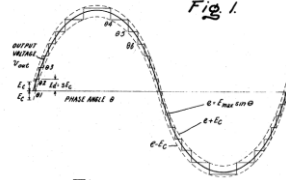
Fig. 2.



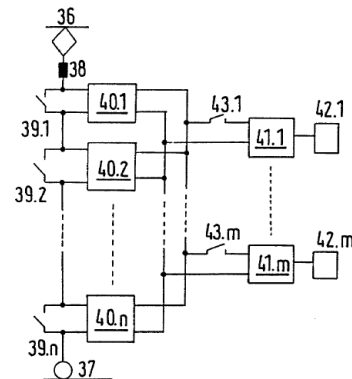
Inventor:
William McMurray
by Robert R. ...
His Attorney.

1969 McMurray
Cascaded H-Bridge (CHB)

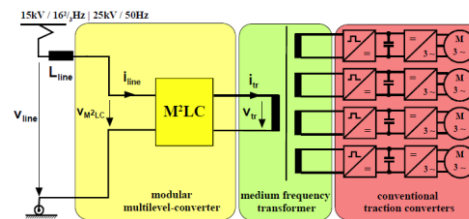
Fig. 1.



1996 Steiner & Reinold
Multi-Cell CHB SST for Traction



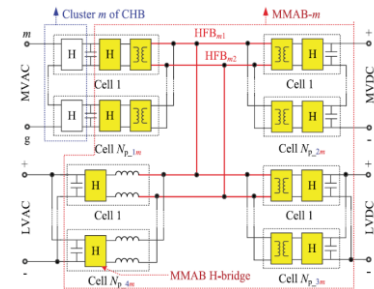
2004 Marquardt & Glinka
Modular Multilevel Conv. (MMC)



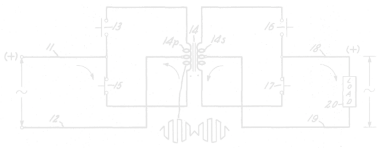
2012 ABB
1.2 MW Traction SST
Field Test



2021 Wen et al.
2 MW HFAC-Bus SST



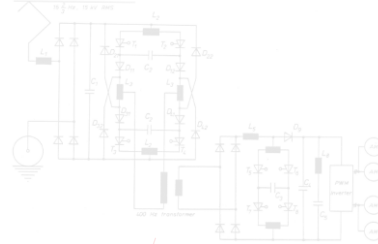
1968 McMurray
Electronic XFRM with
Solid-State Switches



1978 Mennicken / BBC
Medium-Freq. Isol. for Traction



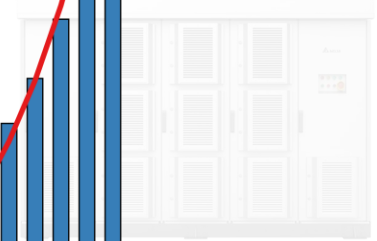
1984 Weiss & Rentmeister
Isolated Front-End for Traction



2011 GE
1 MW AC-AC SST w. 10



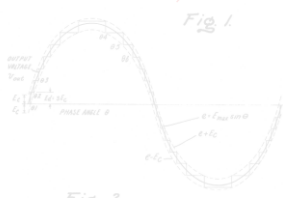
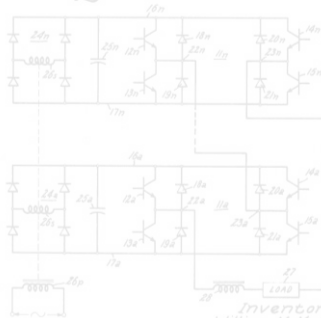
2000 Delta
13.7 kV / 400 kW EV Fast Charger



SST Publications Per Year $\propto e^{ax}$

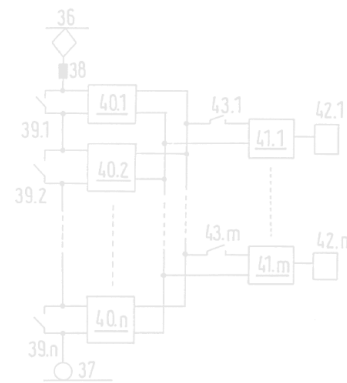


Fig. 2.

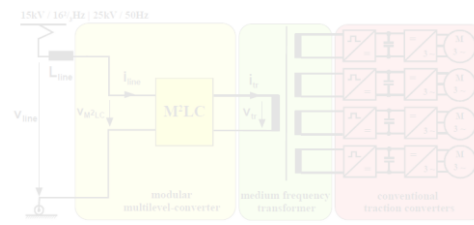


1969 McMurray
Cascaded H-Bridge (CHB)

1996 Steiner & Reinold
Multi-Cell CHB SST for Traction



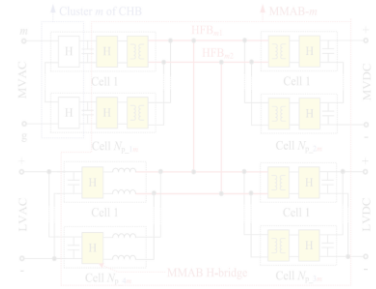
2004 Marquardt & Glinka
Modular Multilevel Conv. (MMC)



2012 ABB
1.2 MW Traction SST
Field Test

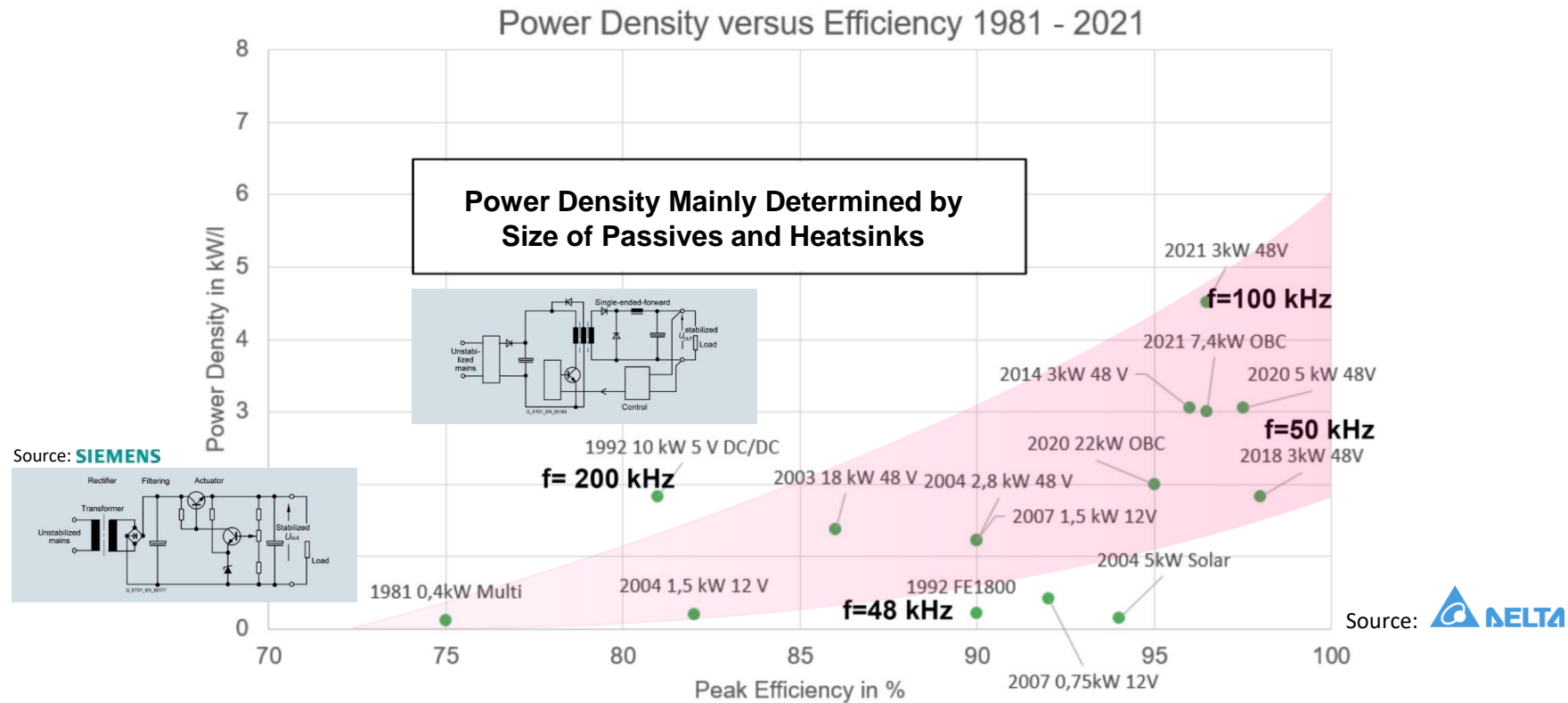


2021 Wen et al.
2 MW HFAC-Bus SST



LV Low-Power SMPS Efficiency / Power Density 1981 – 2021

- 1981 — Large Volume Line-Frequ. Isolation/Voltage Step-Down | Diode Rectifier | Low Eff. Linear Stabilization
- 2021 — PFC Rectifier Front-End | High-Frequency Isol. DC/DC Converter



- Power Density AND Eff. Improvement | Line-Frequ. → High-Frequ. Conv. & Linear → Sw.-Mode Regulation

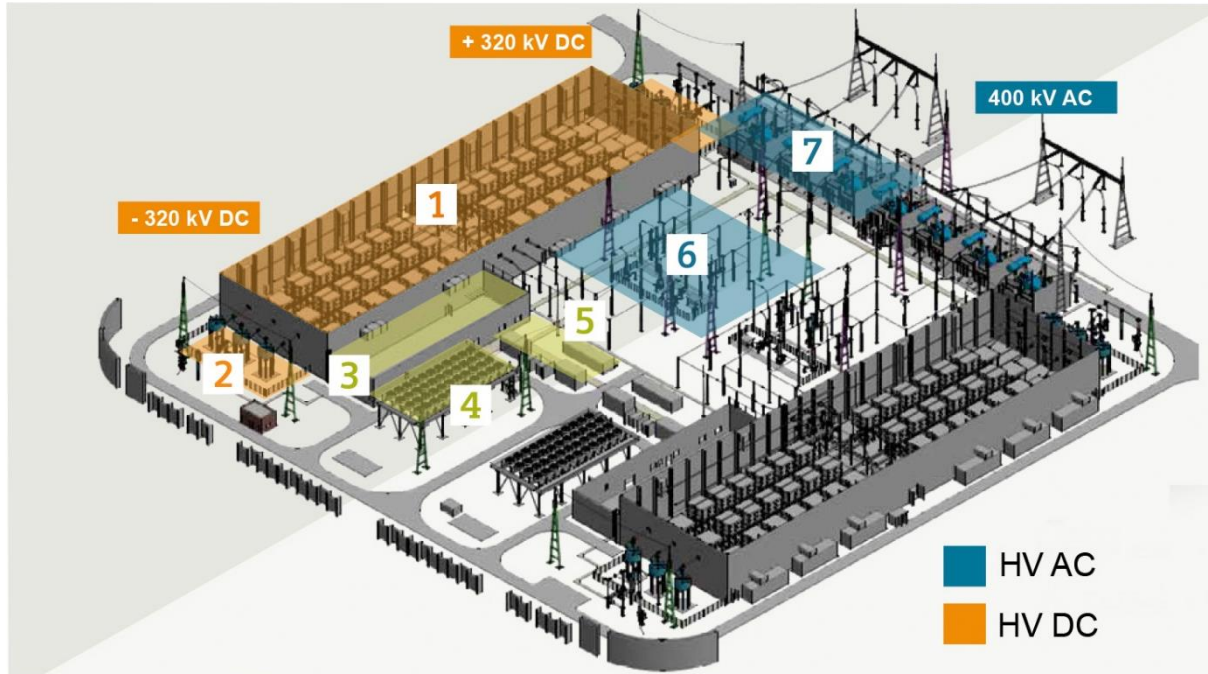
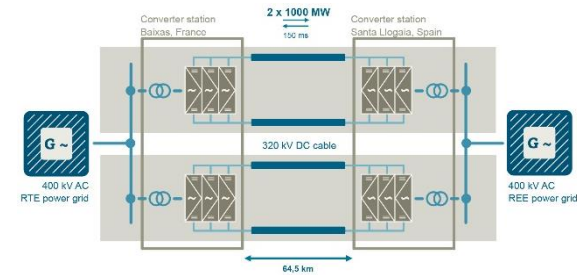


Remark

HVDC Converter Station (1)

■ 2 x 1 GW / ± 320 kV HVDC Transmission Link btw. France & Spain

Source: SIEMENS



- 1 Power modules (IGBT)
- 2 Converter reactors
- 3 Power modules cooling system
- 4 Control and protection room
- 5 Auxiliary power supplies
- 6 Starpoint reactors and insertion reactor
- 7 Power transformers

■ HV AC
■ HV DC

■ Isolation Clearances (!) Largely Determine Space Requirement | Low LFT Volume Contribution (!)



Remark

HVDC Converter Station (2)

- 2 x 1 GW / ± 320 kV HVDC Transmission Link btw. France & Spain



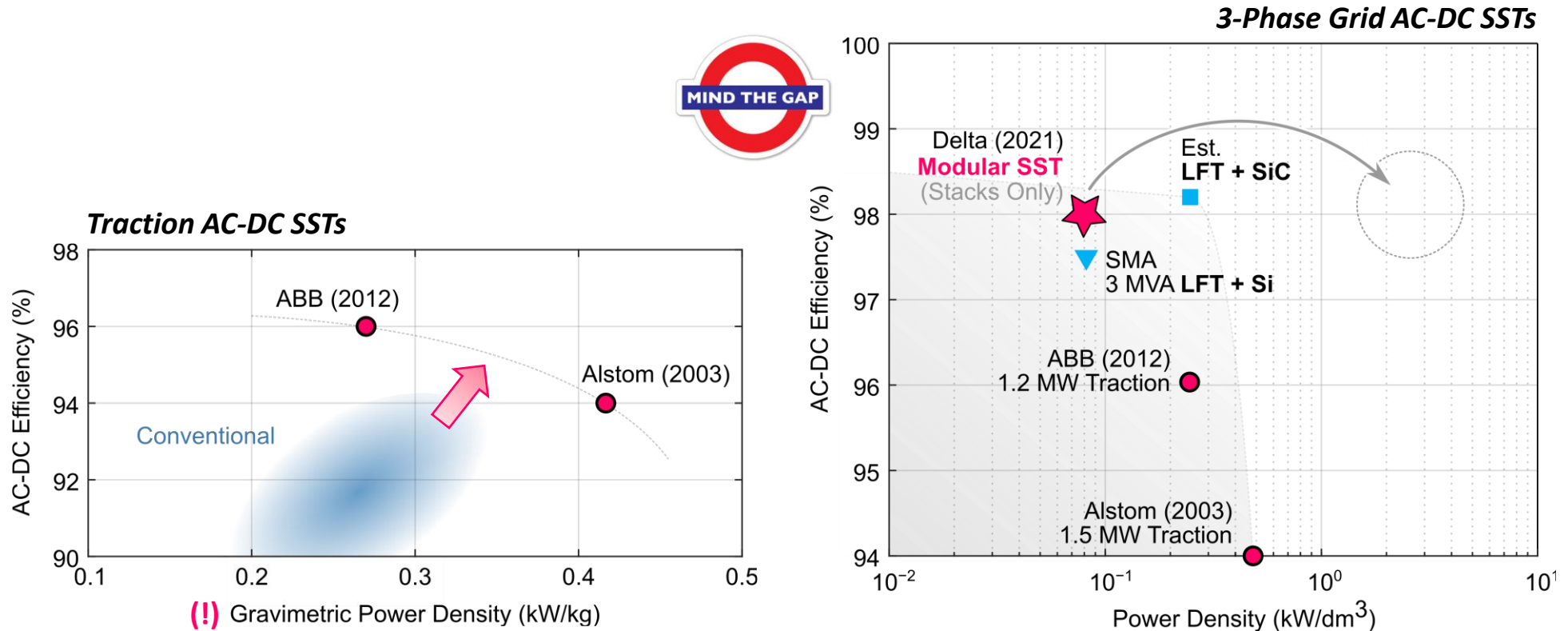
Source: **SIEMENS**

- Isolation Clearances (!) Largely Determine Space Requirement | Low LFT Volume Contribution (!)



Status Quo: Traction & Grid AC-DC SSTs

- Traction: **Clear Improvements in Efficiency / Power Density > 10 Years Ago**
- Grid: **Recently 1st Full Industrial Demonstrator w/o Performance Advantage**

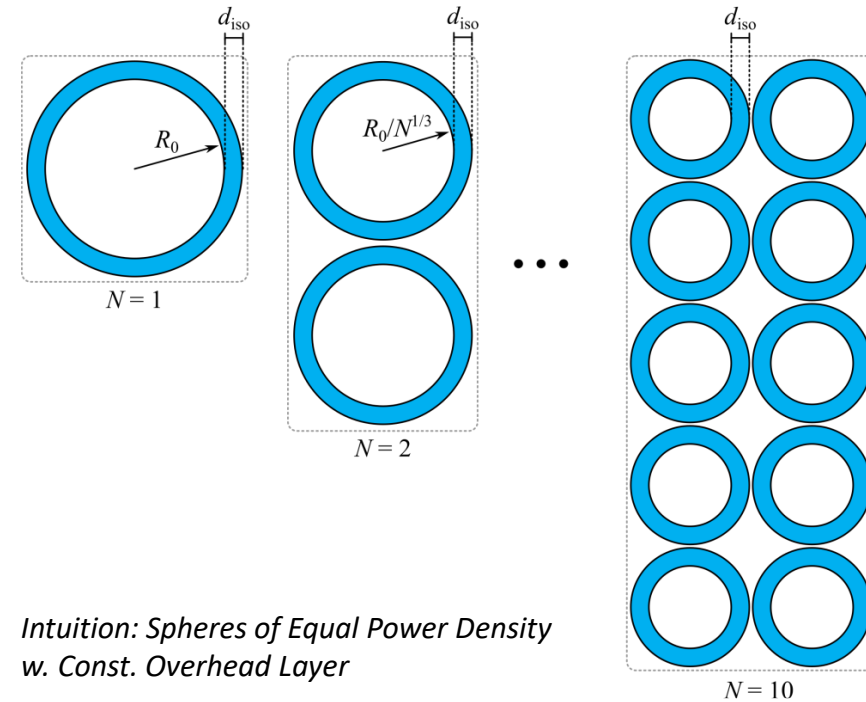
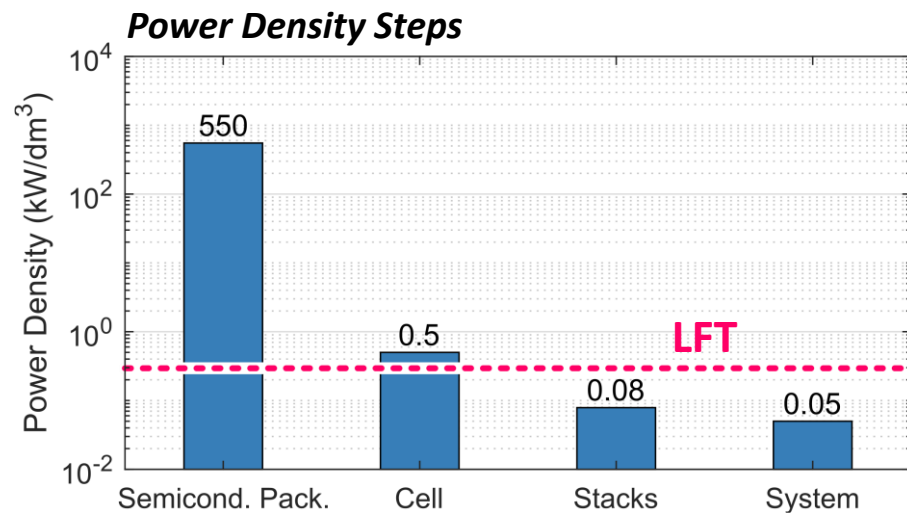


- **Full-Scale Demonstrators Engineered to Standards Needed for Realistic Assessment!**



Grid AC-DC SSTs: Challenges (1)

- Massive Reduction of Power Density from Cell to Full System → Modularity Penalty

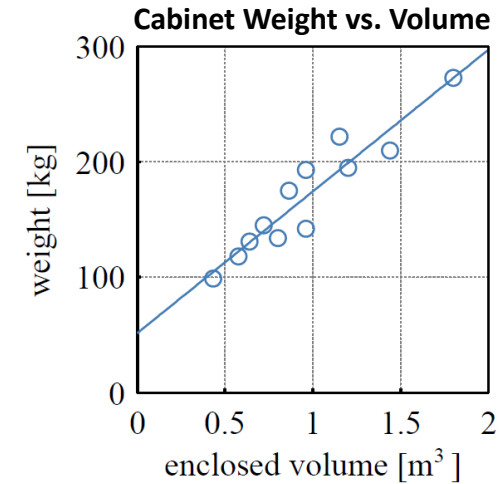
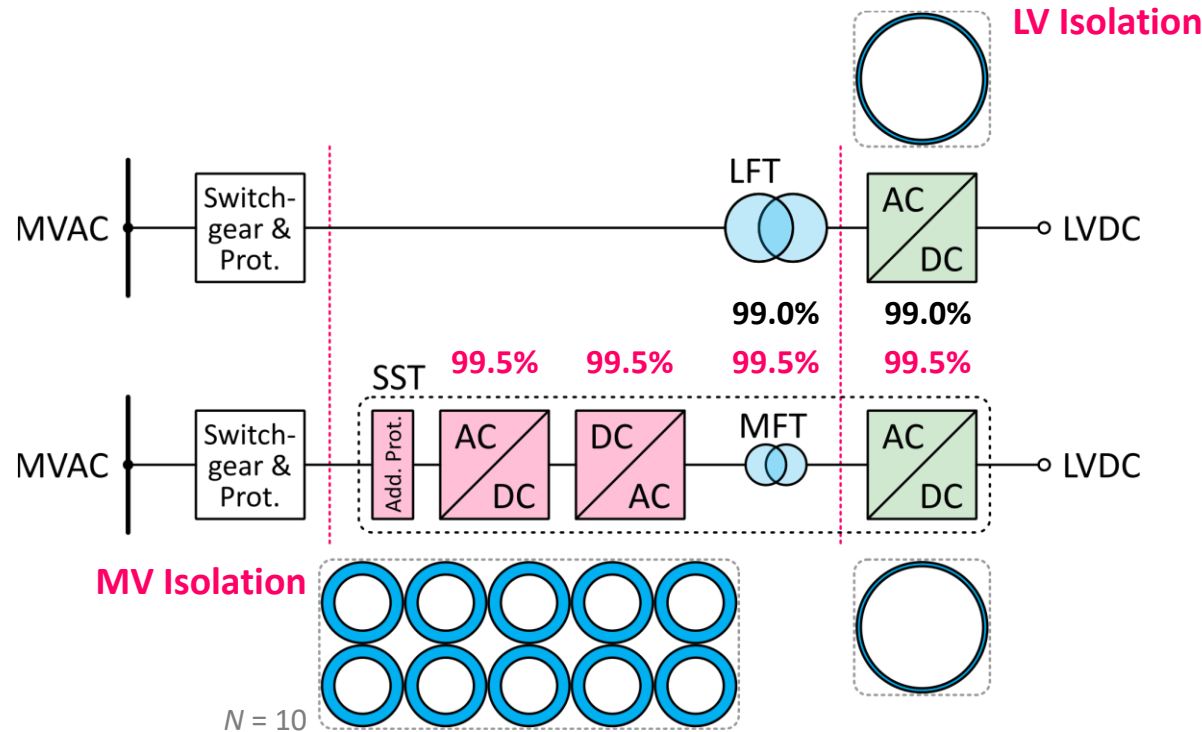


- Future High-Voltage SiC Devices (10+ kV) → Fewer Cells for Given System Voltage



Grid AC-DC SSTs: Challenges (2)

- PFC Functionality on MV Side → Modularity Penalty + Overhead
- Target Efficiency of 98% → 2% Loss Budget for 4 Conversion Stages vs. 2 Conversion Stages

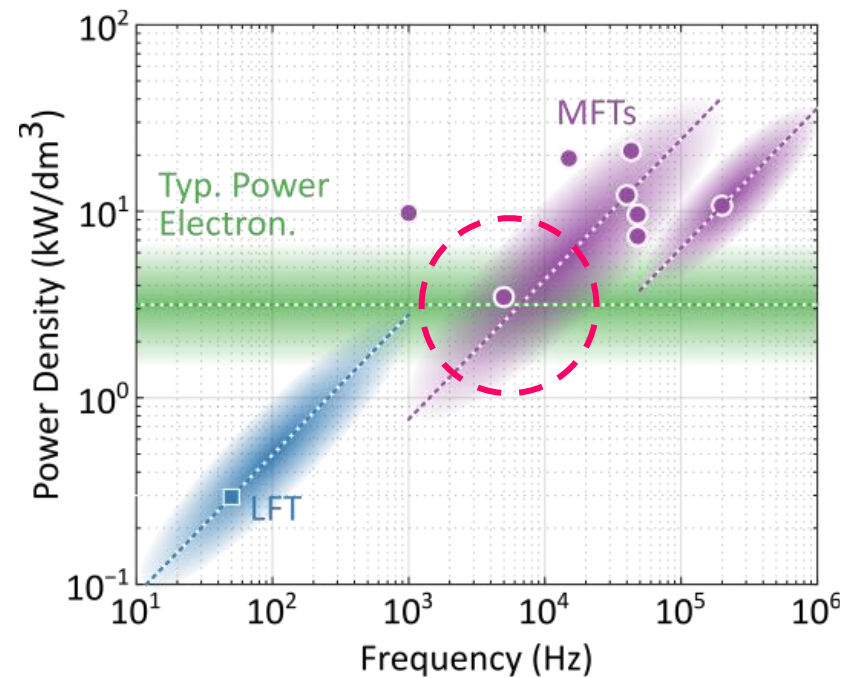


- MV PE Overhead: Protection, Connectors, Access for Maintenance, ...
- Volume (Modularity Penalty + MV PE Overhead) → Larger Cabinets / Heavier Weight



Next-Gen. SSTs: Selection of MFT Operating Frequency

- 5...50 kHz Operating Frequency Sweet Spot ($\rho_{MFT} \approx \rho_{PE}$)

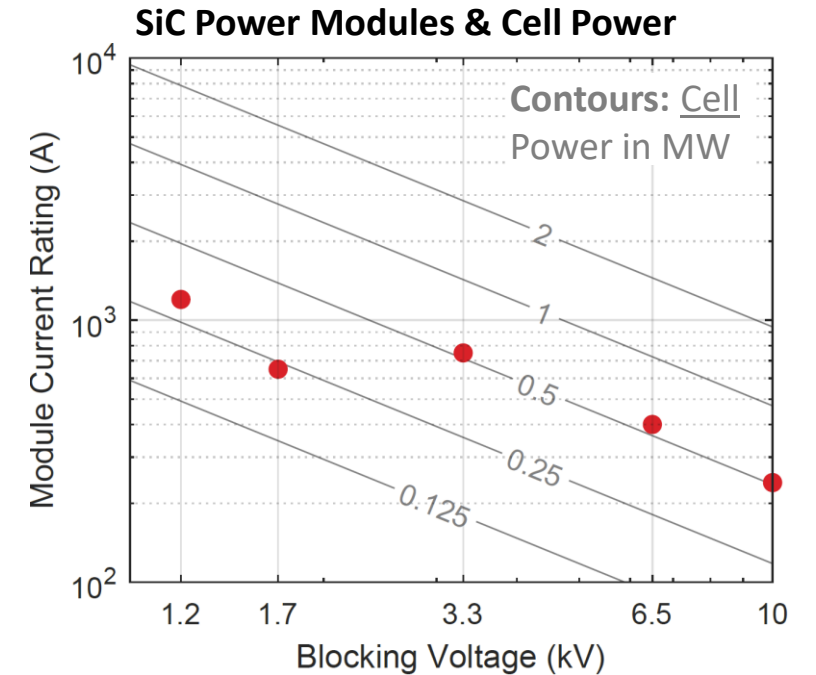
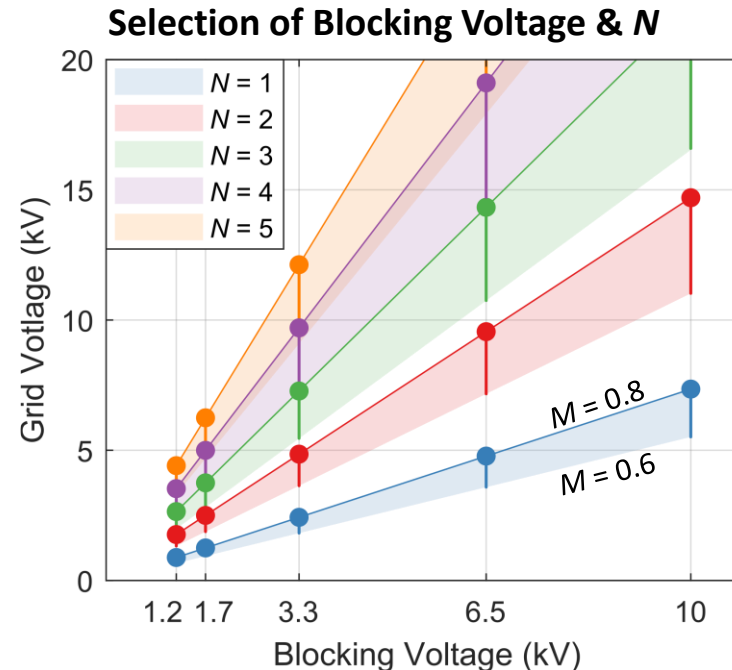
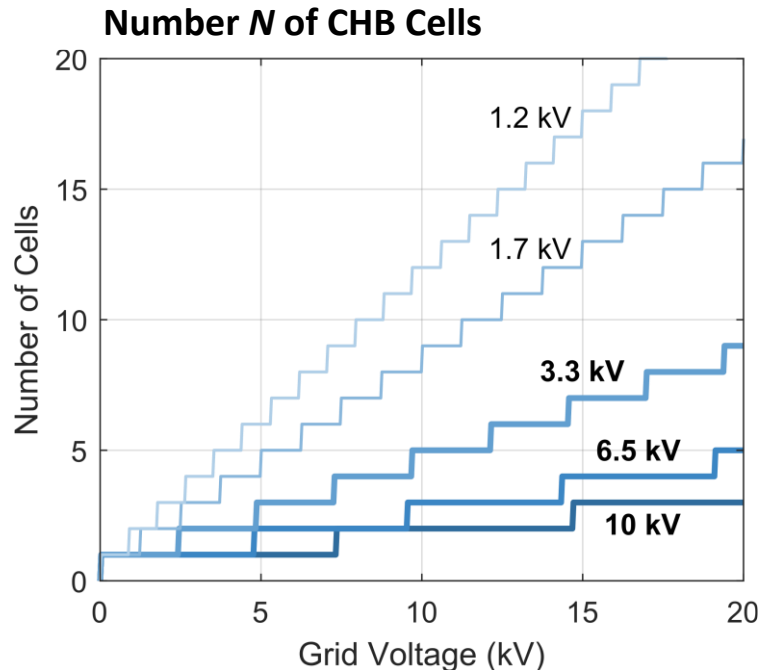


- Isolation Requirements (Clearance & Creepage Distances) Limit Power Density Gain from Higher Frequency



Next-Gen. SSTs: Selection of Number of Cascaded Cells

- Recent 6.5 kV and 10 kV SiC Devices → 13.8 kV Grid Reachable with < 4 Cells
- Today's Available Power Modules → Sensible Cell Power Ratings 250...500 kW w/o Paralleling

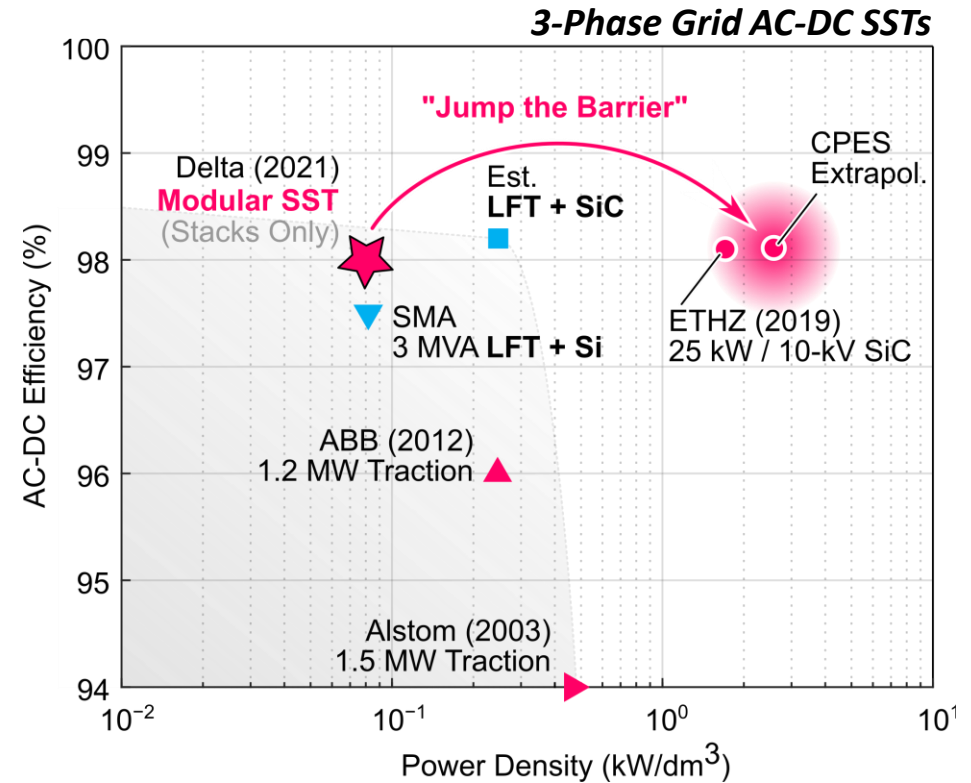
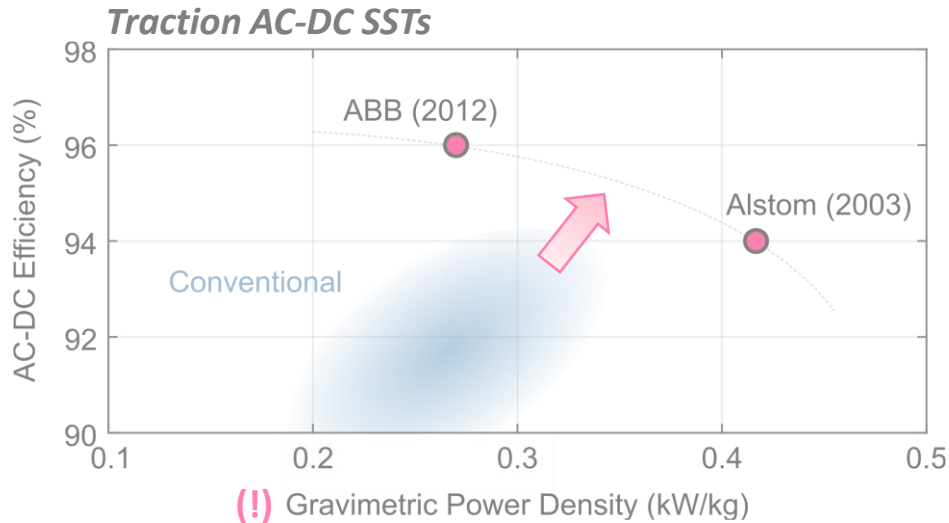


- CHB Topology w. 75% Semicond. Blocking Voltage Utilization and $M = 0.8$ ($M < 0.6$ → Uneconomic Utilization)



Next-Gen. SSTs: Improvement Potential

- 10 kV SiC and/or MMC Topology Might Facilitate the **Jump Over the Power Density Barrier**
- AC-DC Efficiencies >> 98% Remain Difficult to Attain
- Other Dimensions with Clear Improvement Potential Over the State of the Art **Unclear**

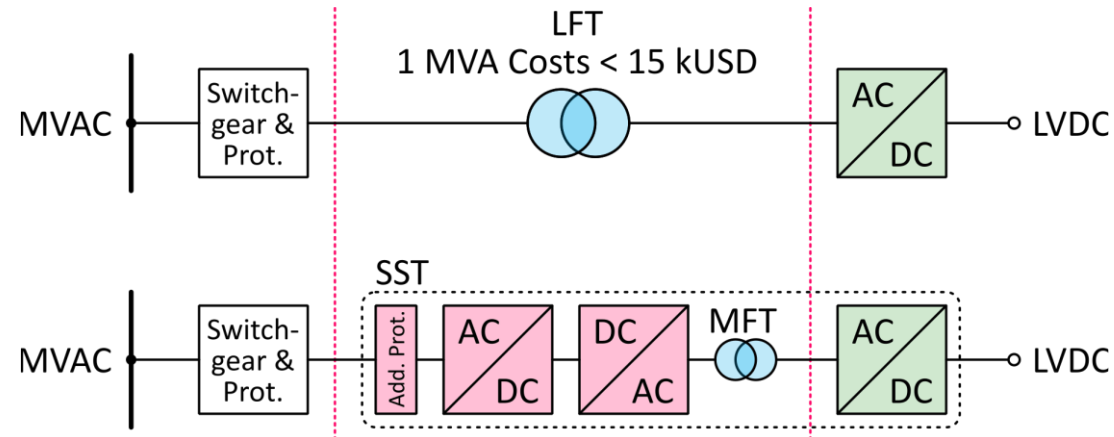


- **Full-Scale Demonstrators** Engineered to Standards Needed for Realistic Assessment!



SST Realization Costs (CAPEX)

- High-Efficiency (Ecodesign) LFTs Cost < 15 kUSD/MVA
- MMC-Based SST: Similar LV-Side Power Electronics → Similar Cost
- MFT Smaller But Likely Higher Specific Cost (e.g., Litz Wire vs. Solid Copper, etc.)



■ Budget for SST’s MV-Side PE Incl. Additional Protection < 15 kUSD/MVA

- State of the Art
 - Automotive LV DC-AC Inv.: 3 USD/kW (U.S. Drive Roadmap R&D Target 2025; Only Transistors, GDs, Sensors)
 - Grid-Connected PV DC-AC Inv.: 30...55 USD/kW (Fraunhofer, 2022; Incl. Sw. Stage, Inductors, EMI Filter)

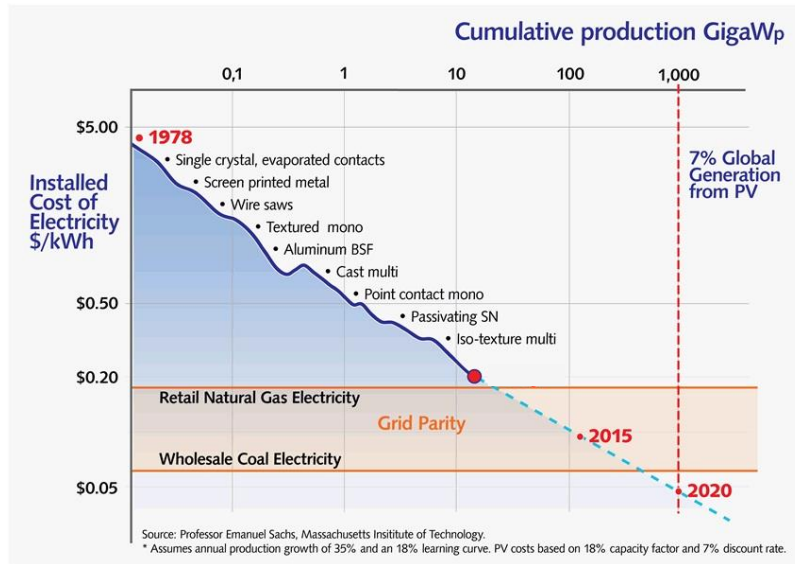
■ SST Cost Drivers: MFT, MV-Level Isolation Coordination, Assembly, Communication Systems, ...



Outlook: Experience Curve of Technologies

- Analysis of the **Performance Improvement as Function of Accumulated Experience**
- **Learning Rate** → Improvement / Cost Reduction for Each Doubling of Cumulative Installed Capacity

Experience Curve of PV Electricity Generation



Experience Curve of SST / SST Module Production?

- Can SSTs Ever Become **Cheaper** than LFT-Based Solutions?
- How Would That Change the Picture?
- Procurement vs. Life-Cycle Cost (Energy Losses)?

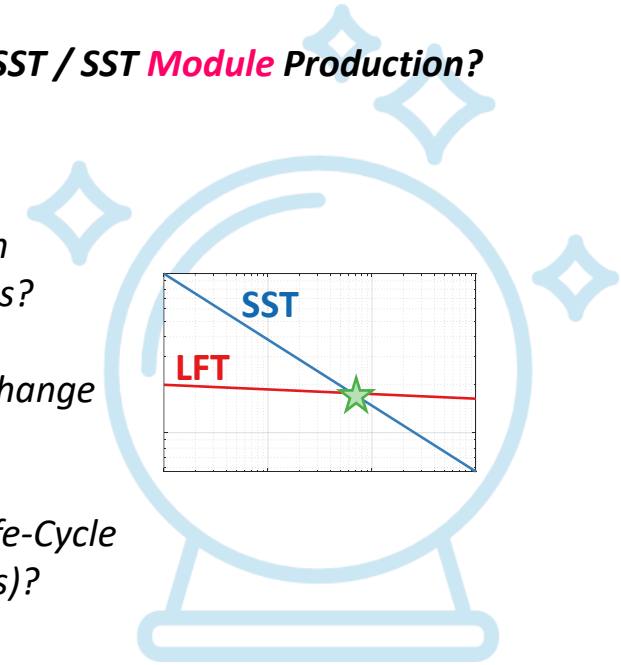


Image: Flaticon.com

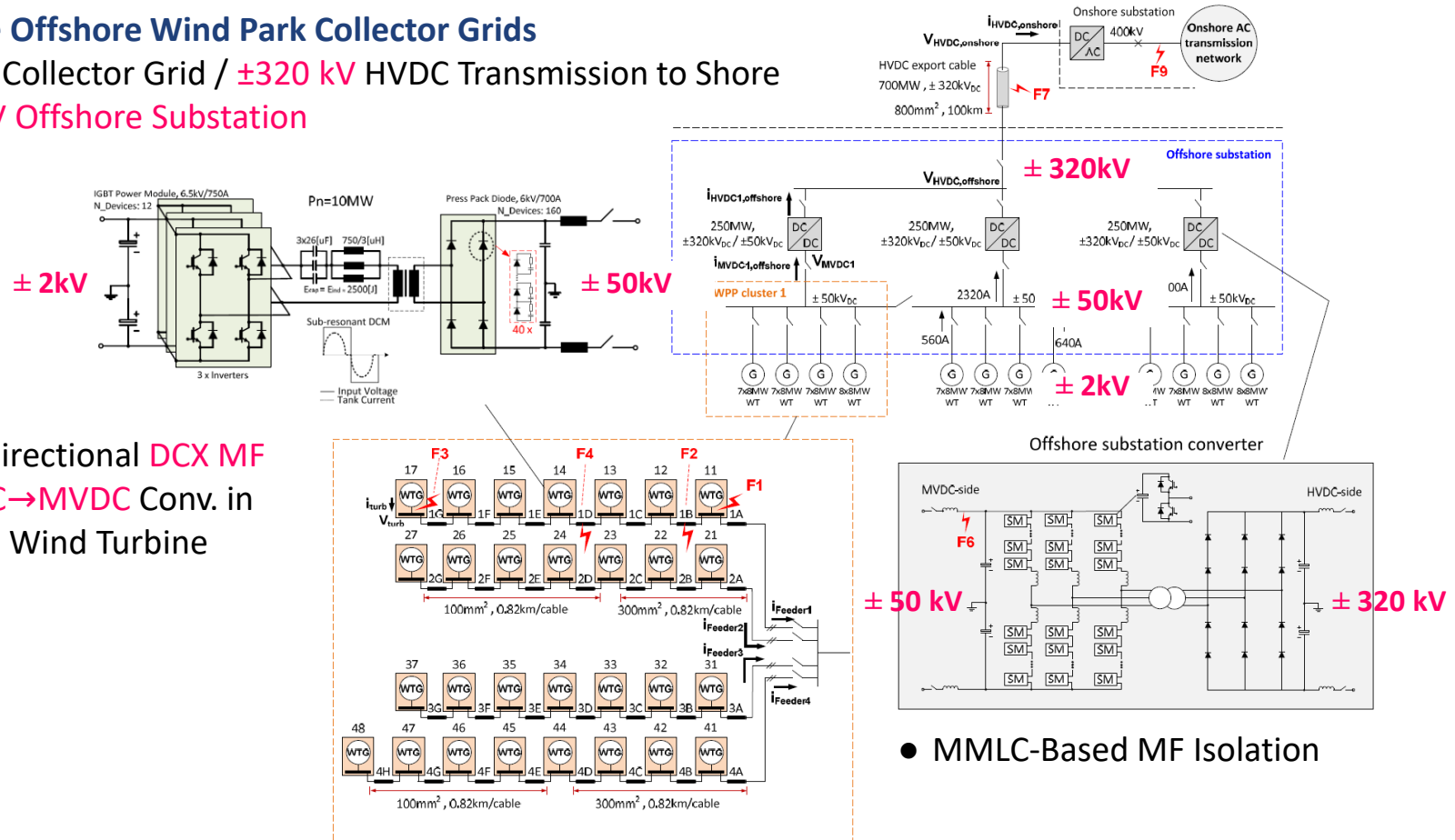
- **Typ. Empirical Learning Rates of 15...25%** → Dramatic Cost Reduction Over Longer Timespan
- Used for Prediction of Future Costs of a Technology (e.g., PV “Grid Parity”) → **Long-Term Strategies**



Outlook: DC Grids / MVDC-LVDC Conversion

Example: Future Offshore Wind Park Collector Grids

- ± 50 kV Offshore Collector Grid / ± 320 kV HVDC Transmission to Shore
- ± 50 kV / ± 320 kV Offshore Substation



- Unidirectional DCX MF LVDC \rightarrow MVDC Conv. in Each Wind Turbine

- MMLC-Based MF Isolation

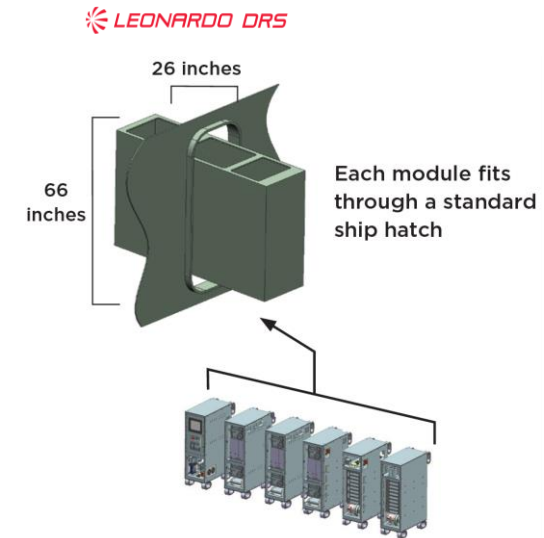
DC Grids Require "AC-Transformer"-Like Functionality \rightarrow DC-DC SSTs w/o Alternative!



Outlook: Future Combat Ships

- **MV Cellular DC Power Distribution** — 6kV DC/DC SST for Size & Weight Reduction

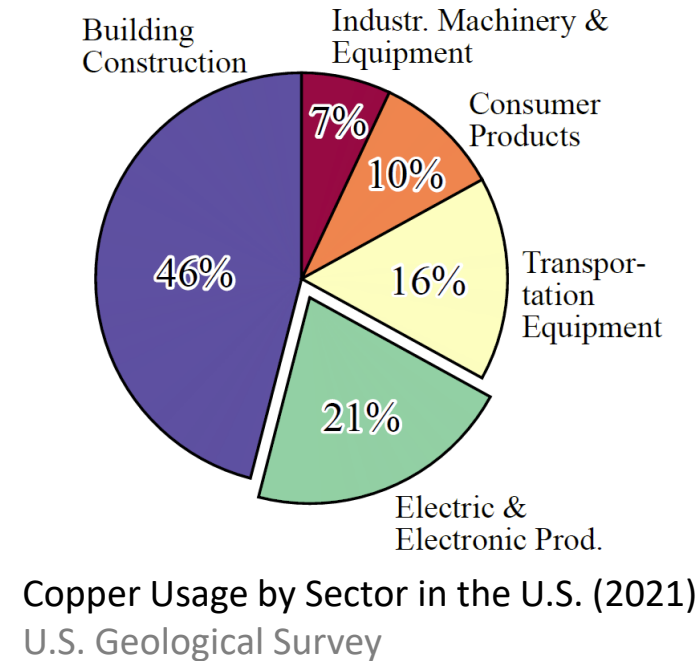
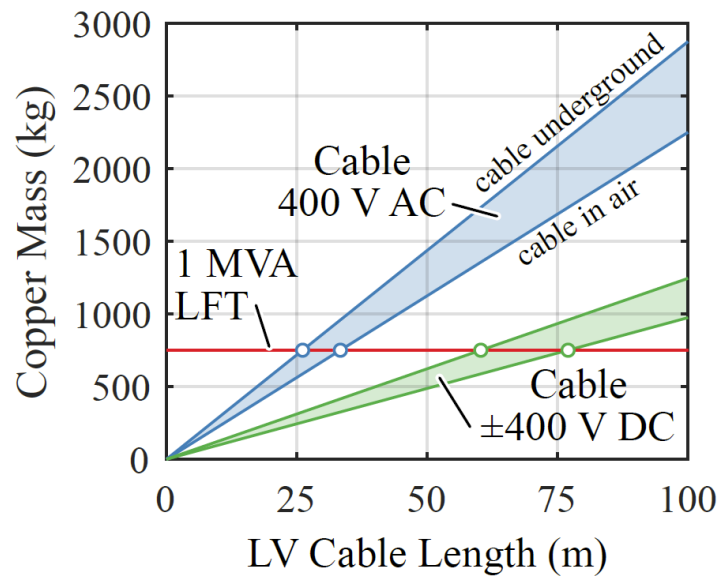
Source: General Dynamics



- “Energy Magazine” as Extension of Electric Power System / Individual Load Power Conditioning
- Bidirectional Power Flow for Advanced Weapon Load Demand
- Extreme Energy and Power Density Requirements

Ecological Aspects / Resource Usage

- LV Distribution Busbars / Cables Dominate the **Installed Copper Mass**
- 40+ vs. 10 Years Typ. **Lifetime of LFTs** vs. Power Electronics/SSTs
- **Recyclability** Advantage of LFTs & High-Power Single Units (Such as Diode/Thyristor Rectifiers)



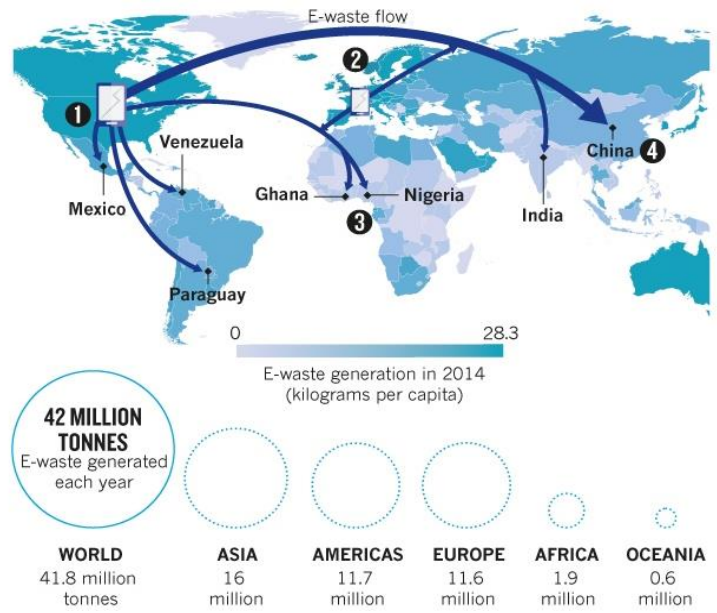
- Global Copper Usage Dominated by Other Sectors
- Life-Cycle Assessments—Cradle-to-Grave / **Cradle-to-Cradle**—Still Missing!



! Remark Increasing E-Waste Problem

- 53'000'000 Tons of Electronic Waste Produced Worldwide in 2019 → 74'000'000 Tons in 2030
- Large Proportion Ends Up in Africa & China → Melting of PCBs & Cables etc. / Hazardous Substances
- Increasingly Complex Constructions → No Repair or Recycling

Source: Green IT Solution



- Growing Global E-Waste Streams → Increasing Attention of the Public / Upcoming Regulations

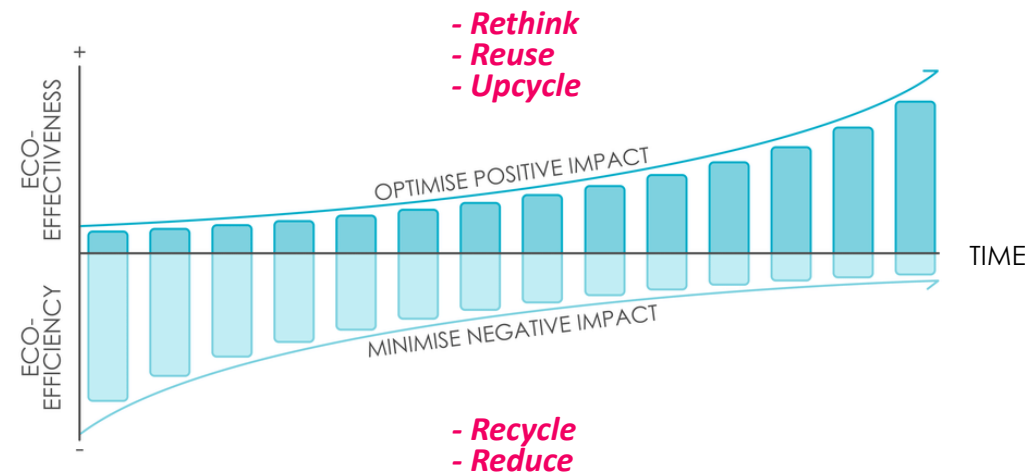
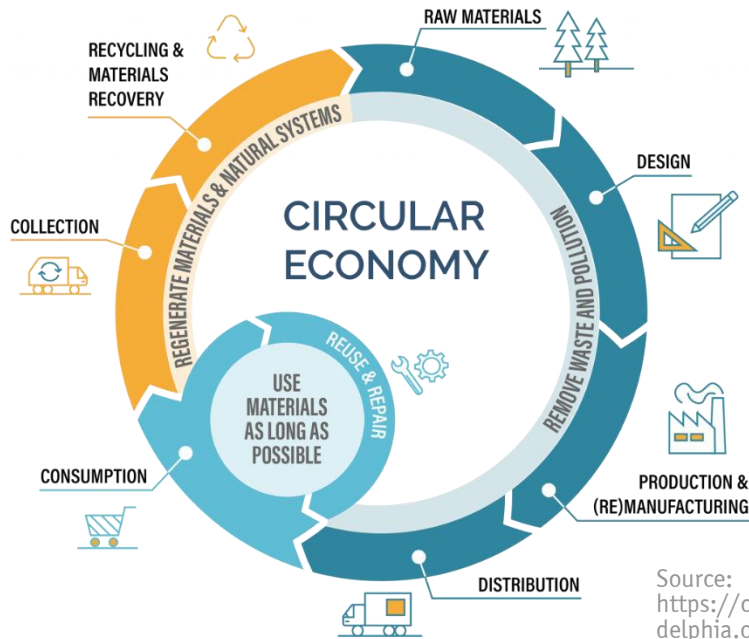


Remark

Cradle-to-Cradle (C2C) Design Concept



- “Linear” Economy / Take–Make–Dispose → “Circular” Economy / Perpetual Flow & Maintained Value of Resources
- Resources Returned Into the Product Cycle at the End of Use / Generation of Waste Minimized
- Maximized Use of Pure and Non-Toxic Reusable Materials

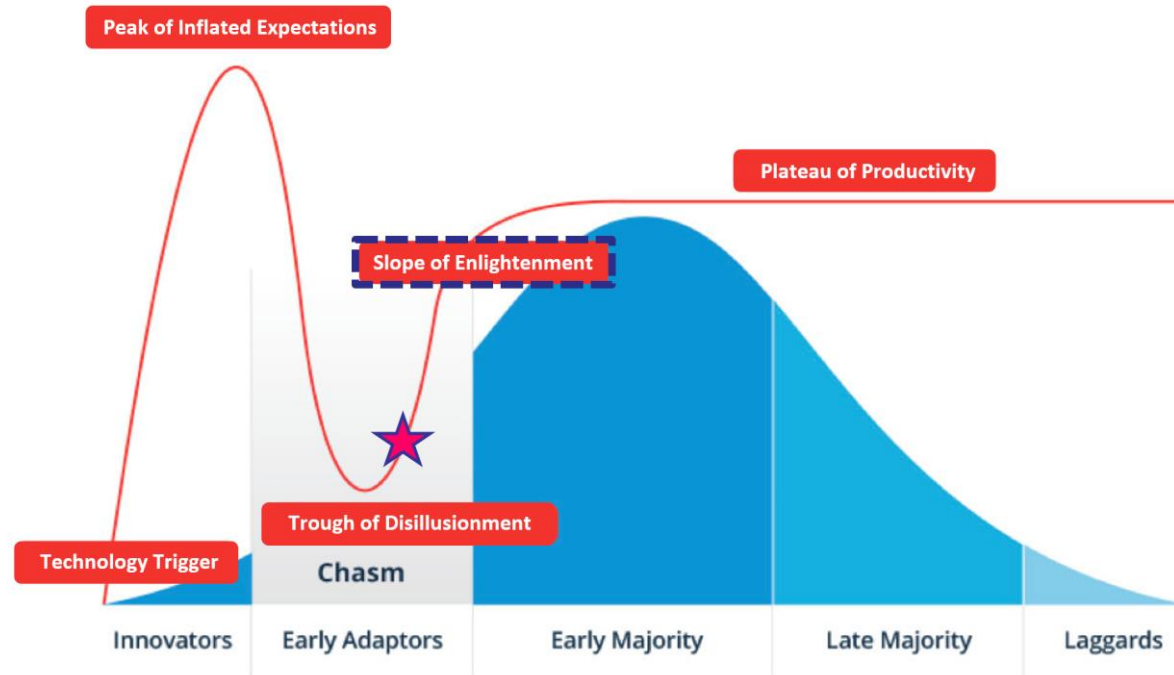


- Decoupling of Economic Growth & Use of Resources
- Measures Covering the Entire Lifecycle → Design | Manufacturing | Consumption | Repair | Reuse | Recycling



SST Technology Hype Cycle

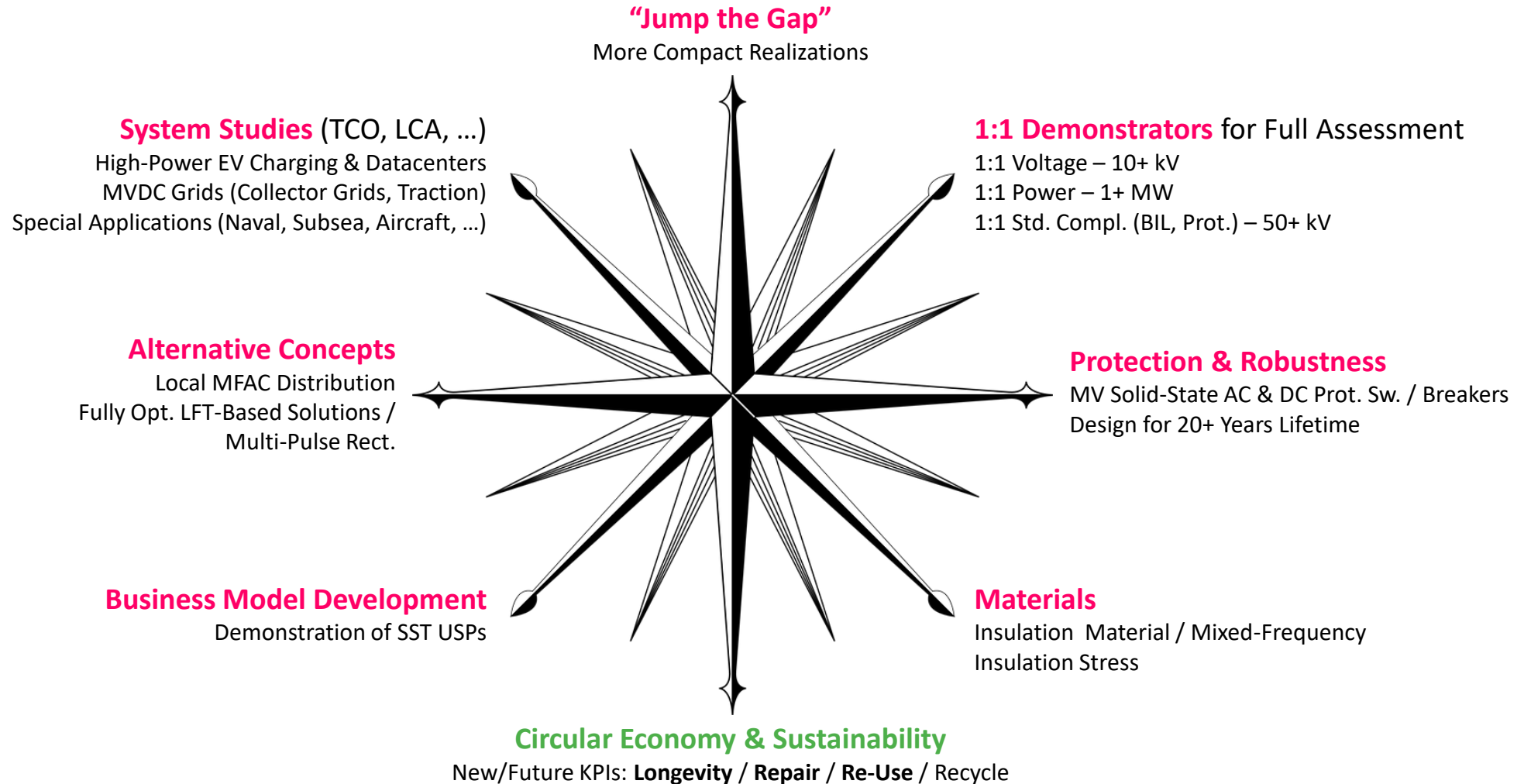
- Graphical Representation of **Technology Perception / Acceptance / Maturity**



- Peak of Inflated Expectations → Early Publicity / Success Stories
- Trough of Disillusionment → Implementations Fail to Deliver
- Slope of Enlightenment → Benefits Start to Crystallize



Research Vectors



Thank You!



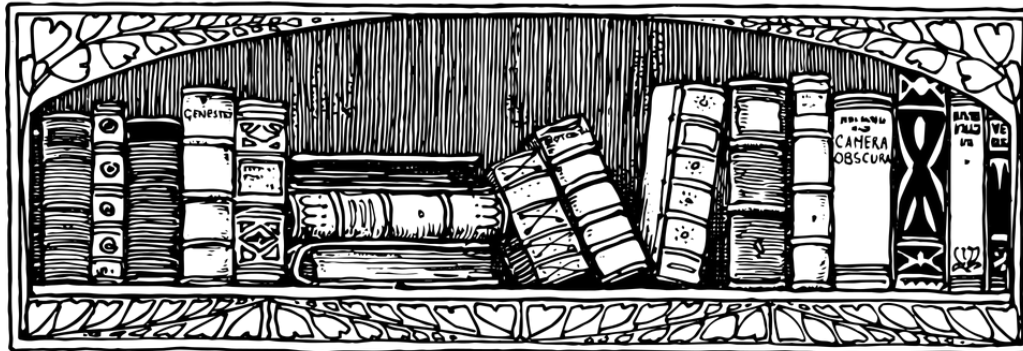
PDF Download



<https://u.ethz.ch/Y6nxX>



References



References (1)

Adam2008 | G. P. Adam, S. J. Finney, A. M. Massoud, and B. W. Williams, “Capacitor balance issues of the diode-clamped multilevel inverter operated in a quasi two-state mode,” *IEEE Trans. Ind. Electron.*, vol. 55, no. 8, pp. 3088–3099, Aug. 2008, doi: <https://doi.org/10.1109/TIE.2008.922607>.

Anurag2022 | A. Anurag, S. Acharya, N. Kolli, S. Bhattacharya, T. R. Weatherford, and A. A. Parker, “A three-phase active-front-end converter system enabled by 10-kV SiC MOSFETs aimed at a solid-state transformer application,” *IEEE Trans. Power Electron.*, vol. 37, no. 5, pp. 5606–5624, May 2022, doi: [10.1109/TPEL.2021.3131262](https://doi.org/10.1109/TPEL.2021.3131262).

Anurag2022a | A. Anurag, S. Acharya, S. Bhattacharya, T. R. Weatherford, and A. A. Parker, “A Gen-3 10-kV SiC MOSFET-based medium-voltage three-phase dual active bridge converter enabling a mobile utility support equipment solid state transformer,” *IEEE Trans. Emerg. Sel. Topics Power Electron.*, vol. 10, no. 2, pp. 1519–1536, Apr. 2022, doi: [10.1109/JESTPE.2021.3069810](https://doi.org/10.1109/JESTPE.2021.3069810).

Baker1974 | R. H. Baker and L. H. Bannister, “Electric power converter,” U.S. Pat. 3 867 643, Feb. 18, 1975, (filed Jan. 14, 1974).

Baker1979 | R. H. Baker, “Bridge converter circuit,” U.S. Pat. 4 270 163, May 26, 1981, (filed Aug. 2, 1979).

Bala2012 | S. Bala, D. Das, E. Aeloiza, A. Maitra, and S. Rajagopalan, “Hybrid distribution transformer: Concept development and field demonstration,” in *Proc. IEEE Energy Conv. Congr. and Expo. (ECCE USA)*, Raleigh, NC, USA, Sep. 2012, pp. 4061–4068. doi: [10.1109/ECCE.2012.6342271](https://doi.org/10.1109/ECCE.2012.6342271).

Baranwal2018 | R. Baranwal, K. V. Iyer, K. Basu, G. F. Castelino, and N. Mohan, “A reduced switch count single-stage three-phase bidirectional rectifier with high-frequency isolation,” *IEEE Trans. Power Electron.*, vol. 33, no. 11, pp. 9520–9541, Nov. 2018, doi: [10.1109/TPEL.2018.2790800](https://doi.org/10.1109/TPEL.2018.2790800).

Beermann2012 | S. Beermann-Curtin, “Next generation technologies for today’s warfighter,” Office of Naval Research Presentation, 2012. [Online]. Available: <http://goo.gl/J9rWLH>.

Biolini1997 | A. Birolini, *Quality and Reliability of Technical Systems*, 2nd ed. Berlin and Heidelberg: Springer, 1997.

Bohn2020 | T. Bohn, “Multi-port, 1+MW charging system for medium- and heavy-duty EVs: What we know and what is on the horizon?,” Jan. 07, 2020. [Online]. Available: <https://tinyurl.com/fcrm6tha>.

Bohn2020a | T. Bohn, “DC as a service testbed and industry collaboration on standards/gaps at MW power level for multiport systems,” Nov. 18, 2020. [Online]. Available: <https://tinyurl.com/4rvhd8z2>.

Bohn2021 | T. Bohn, “DC as a service approach to high power commercial vehicle charging systems,” Oct. 13, 2021. [Online]. Available: <https://tinyurl.com/mwrxmpdv>.

Burgos2020 | R. Burgos, D. Dong, X. Lin, and L. Ravi, “A 16 kV PV Inverter Using Series-Connected 10 kV SiC MOSFET Devices,” in *Proc. 66th IEEE Int. Electron Dev. Meet. (IEDM)*, San Francisco, CA, USA, Dec. 2020.

Burkard2015 | J. Burkard and J. Biela, “Evaluation of topologies and optimal design of a hybrid distribution transformer,” in *Proc. 17th Europ. Power Electron. and Appl. Conf. (EPE)*, Geneva, Switzerland, Sep. 2015. doi: [10.1109/EPE.2015.7309097](https://doi.org/10.1109/EPE.2015.7309097).

Busse2015 | S. Busse, M. Hiller, K. Kahlen, and P. Himmelmann, “MTBF comparison of cutting edge medium voltage drive topologies for oil & gas applications,” in *Proc. Petroleum and Chemical Industry Conf. Europ. (PCIC Europe)*, London, UK, Jun. 2015. doi: [10.1109/PCICEurope.2015.7790028](https://doi.org/10.1109/PCICEurope.2015.7790028).



References (2)

Chen2017 | W. W. Chen, R. Zane, and L. Corradini, “Isolated bidirectional grid-tied three-phase AC–DC power conversion using series-resonant converter modules and a three-phase unfold,” *IEEE Trans. Power Electron.*, vol. 32, no. 12, pp. 9001–9012, Dec. 2017, doi: [10.1109/TPEL.2017.2652477](https://doi.org/10.1109/TPEL.2017.2652477).

Chen2018 | H. Chen and D. Divan, “Soft-switching solid-state transformer (S4T),” *IEEE Trans. Power Electron.*, vol. 33, no. 4, pp. 2933–2947, Apr. 2018, doi: [10.1109/TPEL.2017.2707581](https://doi.org/10.1109/TPEL.2017.2707581).

Chowdhury2016a | S. Chowdhury, C. Hitchcock, R. Dahal, I. B. Bhat, and T. P. Chow, “High voltage 4H-SiC Bi-directional IGBTs,” in Proc. 28th Int. Symp. Power Semiconductor Dev. Ics (ISPSD), Prague, Czech Republic, Jun. 2016, pp. 463–466. doi: <https://doi.org/10.1109/ISPSD.2016.7520878>.

Chowdhury2016b | S. Chowdhury, C. Hitchcock, Z. Stum, R. P. Dahal, I. B. Bhat, and T. P. Chow, “Experimental demonstration of high-voltage 4H-SiC bi-directional IGBTs,” *IEEE Electron Device Lett.*, vol. 37, no. 8, pp. 1033–1036, Aug. 2016, doi: <https://doi.org/10.1109/LED.2016.2581419>.

Collins2020 | W. Collins, K. Gomatam, and M. Simpson, “DCaaS for High Power EV Fast Charging -- Scalable, Interoperable Architecture,” Nov. 18, 2020. [Online]. Available: <https://tinyurl.com/mr2psebx>.

Cottet2015 | D. Cottet et al., “Integration technologies for a fully modular and hot-swappable MV multi-level concept converter,” in Proc. PCIM Europ. Conf., Nuremberg, Germany, May 2015.

Cottet2015a | D. Cottet et al., “Integration technologies for a medium voltage modular multi-level converter with hot swap capability,” in Proc. IEEE Energy Conversion Congr. Expo. (ECCE), Montreal, Canada, Sep. 2015, pp. 4502–4509. doi: [10.1109/ECCE.2015.7310295](https://doi.org/10.1109/ECCE.2015.7310295).

Cremasco2022 | A. Cremasco, D. Rothmund, M. Curti, and E. A. Lomonova, “Voltage distribution in the windings of medium-frequency transformers operated with wide bandgap devices,” *IEEE Trans. Emerg. Sel. Topics Power Electron.*, vol. 10, no. 4, pp. 3587–3602, Aug. 2022, doi: [10.1109/JESTPE.2021.3064702](https://doi.org/10.1109/JESTPE.2021.3064702).

Czyz2022 | P. Czyz et al., “Analysis of the performance limits of 166 kW/7 kV air- and magnetic-core medium-voltage medium-frequency transformers for 1:1-DCX applications,” *IEEE Trans. Emerg. Sel. Topics Power Electron.*, vol. 10, no. 3, pp. 2989–3012, Jun. 2022, doi: [10.1109/JESTPE.2021.3123793](https://doi.org/10.1109/JESTPE.2021.3123793)

Das2011 | M. K. Das et al., “10 kV, 120 A SiC half H-bridge power MOSFET modules suitable for high frequency, medium voltage applications,” in Proc. IEEE Energy Conv. Congr. and Expo. (ECCE USA), Phoenix, AZ, USA, Sep. 2011, pp. 2689–2692. doi: [10.1109/ECCE.2011.6064129](https://doi.org/10.1109/ECCE.2011.6064129).

DeDoncker1989 | R. W. DeDoncker, M. H. Kheraluwala, and D. M. Divan, “Power conversion apparatus for DC/DC conversion using dual active bridges,” U.S. Pat. 5 027 264, Sep. 1989.

DeDoncker1991 | R. W. DeDoncker, D. M. Divan, and M. H. Kheraluwala, “A three-phase soft-switched high-power-density DC/DC converter for high-power applications,” *IEEE Trans. Ind. Appl.*, vol. 27, no. 1, pp. 63–73, Jan. 1991, doi: [10.1109/28.67533](https://doi.org/10.1109/28.67533).

DeDoncker2012 | R. W. DeDoncker, “Can do with Power Electronics and DC Grids within next 15 years!,” presented at the IEEE Future of Electronic Power Proc. Conv. Workshop (FEPPCON), Sep. 2012.

DeDoncker2018 | R. W. DeDoncker, “Energy System Transition and DC Hybrid Power Systems,” presented at the EU Directorate General for Energy Round Table – Hybrid Grids, Brussels, Belgium, Sep. 2012, <https://tinyurl.com/5hsvt8uu>.



References (3)

DeDoncker2020 | R. W. DeDoncker, “Power Electronics - Key Enabling Technology for a CO2 Neutral Energy Supply Linking HVDC and MVDC Grids,” presented at the *EU Horizon 2050 – HVDC Workshop*, Brussels, Belgium, Feb. 2020, <https://tinyurl.com/2z6c7tv9>.

DeDoncker2021 | R. W. DeDoncker, “The future of power electronics in grid-related applications – Power electronics the key enabling technology for the energy transition,” presented at the *ECPE Network Meeting*, Oct. 2021.

Dias2021 | T. Dias, P. Ladoux, S. Sanchez, T. Mielczarski, and P. Aubin, “Wide input voltage range soft switching converter for railway rolling stock auxiliary power supply,” in *Proc. PCIM Europ. Conf.*, Nuremberg, Germany, May 2021.

Dincan2019 | C. G. Dincan et al., “Design of a high-power resonant converter for DC wind turbines,” *IEEE Trans. Power Electron.*, vol. 34, no. 7, pp. 6136–6154, Jul. 2019, doi: [10.1109/TPEL.2018.2876320](https://doi.org/10.1109/TPEL.2018.2876320).

Djekanovic2022 | N. Djekanovic and D. Dujic, “Design optimization of a MW-level medium frequency transformer,” in *Proc. Power Conversion and Intelligent Motion Conf. (PCIM)*, Nuremberg, Germany, May 2022. doi: [10.30420/565822101](https://doi.org/10.30420/565822101).

Dobrowolski1890 | M. von Dolivo-Dobrowolsky, “Electrical induction apparatus or transformer,” U.S. Pat. 422 746, 1890.

Dong2020 | D. Dong, X. Lin, L. Ravi, N. Yan, and R. Burgos, “Advancement of SiC high-frequency power conversion systems for medium-voltage high-power applications,” in *Proc. 9th IEEE Int. Power Electron and Motion Conf. (IPEMC/ECCE Asia)*, Nanjing, China, Nov. 2020, pp. 717–724. doi: [10.1109/IPEMC-ECCEAsia48364.2020.9367948](https://doi.org/10.1109/IPEMC-ECCEAsia48364.2020.9367948).

Drofenik2019 | U. Drofenik, T. Gradinger, and F. Canales, “Current balancing in power semiconductors of a dc/dc converter,” World Pat. Appl. 2021053166A1, Sep. 20, 2019.

Drofenik2019a | U. Drofenik, F. Canales, C. Liu, and F. Brem, “Power module based on normally-on semiconductor switches,” U. S. Pat. 10 797 586 B2, Oct. 06, 2020, (filed Oct. 25, 2019).

Drofenik2020 | U. Drofenik, T. Gradinger, and F. Canales, “Transformer assembly with medium frequency transformers,” U.S. Pat. Appl. 2021/0018554 A1, Jul. 10, 2020.

Drofenik2020a | U. Drofenik, F. Canales, and K.-B. Park, “A charging system for electric vehicles,” EU Pat. Appl. 3 905 480 A1, Nov. 03, 2021.

Engel2003 | B. Engel, M. Victor, G. Bachmann, and A. Falk, “15 kV/16.7 Hz energy supply system with medium frequency transformer and 6.5 kV IGBTs in resonant operation,” in *Proc. 10th Europ. Power Electron. Appl. Conf. (EPE)*, Toulouse, France, Sep. 2003.

Fabre2019 | J. Fabre, J.-M. Blaquière, A. Verdicchio, P. Ladoux, and S. Sanchez, “Characterization in ZVS Mode of SiC MOSFET Modules for MVDC Applications,” in *Proc. Int. Conf. Clean Electr. Power (ICCEP)*, Otranto, Italy, Jul. 2019, pp. 470–477. doi: [10.1109/ICCEP.2019.8890157](https://doi.org/10.1109/ICCEP.2019.8890157).

Fabre2021 | J. Fabre et al., “Characterization and implementation of resonant isolated DC/DC converters for future MVdc railway electrification systems,” *IEEE Trans. Transport. Electrific.*, vol. 7, no. 2, pp. 854–869, Jun. 2021, doi: [10.1109/TTE.2020.3033659](https://doi.org/10.1109/TTE.2020.3033659).

Falcones2010 | S. Falcones, X. Mao, and R. Ayyanar, “Topology comparison for Solid State Transformer implementation,” in *Proc. IEEE PES General Meeting*, Minneapolis, MN, USA, Jul. 2010. doi: [10.1109/PES.2010.5590086](https://doi.org/10.1109/PES.2010.5590086).

Fan2022 | B. Fan et al., “Cell capacitor voltage switching-cycle balancing control for modular multilevel converters,” *IEEE Trans. Power Electron.*, vol. 37, no. 3, pp. 2525–2530, Mar. 2022, doi: [10.1109/TPEL.2021.3116803](https://doi.org/10.1109/TPEL.2021.3116803).



References (4)

Fortes2021 | G. Fortes, P. Ladoux, J. Fabre, and D. Flumian, “Characterization of a 300 kW Isolated DCDC Converter using 3.3 kV SiC-MOSFETs,” in *Proc. Power Conversion Intelligent Motion Conf. (PCIM)*, Nuremberg, Germany, May 2021.

Fuerback2018 | V. B. Fuerback, G. J. M. de Sousa, and M. L. Heldwein, “Hybrid Unidirectional MMC-Based Rectifier,” in *Proc. 4th IEEE Southern Power Electron. Conf (SPEC)*, Singapore, Dec. 2018, doi: [10.1109/SPEC.2018.8636041](https://doi.org/10.1109/SPEC.2018.8636041).

Glinka2005 | M. Glinka and R. Marquardt, “A new AC/AC multilevel converter family,” *IEEE Trans. Ind. Electron.*, vol. 52, no. 3, pp. 662–669, Jun. 2005, doi: [10.1109/TIE.2005.843973](https://doi.org/10.1109/TIE.2005.843973).

Götz2019 | S. Götz, “Charging apparatus with a phase unit having multiple strands,” U.S. Pat. 10 439 407B2, Oct. 08, 2019.

Gowaid2015 | I. A. Gowaid, G. P. Adam, A. M. Massoud, S. Ahmed, D. Holliday, and B. W. Williams, “Quasi two-level operation of modular multilevel converter for use in a high-power DC transformer with DC fault isolation capability,” *IEEE Trans. Power Electron.*, vol. 30, no. 1, pp. 108–123, Jan. 2015, doi: [10.1109/TPEL.2014.2306453](https://doi.org/10.1109/TPEL.2014.2306453).

Gradinger2017 | T. B. Gradinger, U. Drogenik, and S. Alvarez, “Novel insulation concept for an MV dry-cast medium-frequency transformer,” in *Proc. 19th Europ. Conf. Power Electron. Appl. (EPE)*, Warsaw, Poland, Sep. 2017, doi: [10.23919/EPE17ECCEEurope.2017.8099006](https://doi.org/10.23919/EPE17ECCEEurope.2017.8099006).

Gradinger2018 | T. Gradinger and U. Drogenik, “Electrical component, especially transformer or inductor,” EU Pat. 3 648 126 B1, Aug. 25, 2021, (filed Oct. 31, 2018).

Gradinger2018a | T. Gradinger, U. Drogenik, and B. Wunsch, “Medium frequency transformer,” EU Pat. 3 629 349 B1, Apr. 14, 2021, (filed Sept. 25, 2018).

Gradinger2021 | T. B. Gradinger and M. Mogorovic, “Foil-winding design for medium-frequency medium-voltage transformers,” in *Proc. 23rd European Conf. Power Electron. Appl. (EPE)*, Ghent, Belgium, Sep. 2021, doi: [10.23919/EPE21ECCEEurope50061.2021.9570471](https://doi.org/10.23919/EPE21ECCEEurope50061.2021.9570471).

Grinberg2013 | R. Grinberg, G. Riedel, A. Korn, P. Steimer, and E. Bjornstad, “On reliability of medium voltage multilevel converters,” in *Proc. IEEE Energy Conv. Congr. and Expo. (ECCE USA)*, Denver, CO, USA, Sep. 2013, pp. 4047–4052, doi: [10.1109/ECCE.2013.6647238](https://doi.org/10.1109/ECCE.2013.6647238).

Guillod2014 | T. Guillod, J. E. Huber, G. Ortiz, A. De, C. M. Franck, and J. W. Kolar, “Characterization of the voltage and electric field stresses in multi-cell solid-state transformers,” in *Proc. Energy Conversion Congr. and Expo (ECCE USA)*, Pittsburgh, PA, USA, Sep. 2014, pp. 4726–4734, doi: [10.1109/ECCE.2014.6954048](https://doi.org/10.1109/ECCE.2014.6954048).

Guillod2017 | T. Guillod, J. Huber, F. Krismer, and J. W. Kolar, “Litz wire losses: Effects of twisting imperfections,” in *Proc. 18th IEEE 18th Workshop Control Modeling Power Electron. (COMPEL)*, Stanford, CA, USA, Jul. 2017, doi: [10.1109/COMPEL.2017.8013327](https://doi.org/10.1109/COMPEL.2017.8013327).

Guillod2017a | T. Guillod, F. Krismer, and J. W. Kolar, “Protection of MV converters in the grid: the case of MV/LV solid-state transformers,” *IEEE Trans. Emerg. Sel. Topics Power Electron.*, vol. 5, no. 1, pp. 393–408, Mar. 2017, doi: [10.1109/JESTPE.2016.2617620](https://doi.org/10.1109/JESTPE.2016.2617620).

Guillod2020 | T. Guillod, D. Rothmund, and J. W. Kolar, “Active magnetizing current splitting ZVS modulation of a 7 kV/400 V DC transformer,” *IEEE Trans. Power Electron.*, vol. 35, no. 2, pp. 1293–1305, Feb. 2020, doi: [10.1109/TPEL.2019.2918622](https://doi.org/10.1109/TPEL.2019.2918622).



References (5)

Guillod2020a | T. Guillod, R. Faerber, D. Rothmund, F. Krismer, C. M. Franck, and J. W. Kolar, “Dielectric losses in dry-type insulation of medium-voltage power electronic converters,” *IEEE Trans. Emerg. Sel. Topics Power Electron.*, vol. 8, no. 3, pp. 2716–2732, Sep. 2020, doi: [10.1109/JESTPE.2019.2914997](https://doi.org/10.1109/JESTPE.2019.2914997).

Gupta2009 | R. K. Gupta, K. K. Mohapatra, and N. Mohan, “A novel three-phase switched multi-winding power electronic transformer,” in *Proc. IEEE Energy Conv. Congr. and Expo. (ECCE)*, San Jose, CA, USA, Sep. 2009, pp. 2696–2703. doi: [10.1109/ECCE.2009.5316288](https://doi.org/10.1109/ECCE.2009.5316288).

Gupta2010 | R. K. Gupta, K. K. Mohapatra, N. Mohan, G. Castelino, K. Basu, and N. Weise, “Soft switching power electronic transformer,” U.S. Pat. 8 446 743 B2, May 21, 2013 (filed Jul. 12, 2010).

Hafez2014 | B. Hafez, H. S. Krishnamoorthy, P. Enjeti, S. Ahmed, and I. J. Pitel, “Medium voltage power distribution architecture with medium frequency isolation transformer for data centers,” in *Proc. 29th Annu. IEEE Appl. Power Electron. Conf. and Expo. (APEC)*, Fort Worth, TX, USA, Mar. 2014, pp. 3485–3489. doi: [10.1109/APEC.2014.6803810](https://doi.org/10.1109/APEC.2014.6803810).

Han2014 | B. M. Han, N. S. Choi, and J. Y. Lee, “New bidirectional intelligent semiconductor transformer for smart grid application,” *IEEE Trans. Power Electron.*, vol. 29, no. 8, pp. 4058–4066, Aug. 2014, doi: [10.1109/TPEL.2013.2284009](https://doi.org/10.1109/TPEL.2013.2284009).

Hartmann2014 | M. Hartmann, “Gleichrichterschaltung (in German),” Austrian Patent AT 516 643B1, Feb. 15, 2018 (filed Dec. 18, 2014).

Heinemann2001 | L. Heinemann and G. Mauthe, “The universal power electronics based distribution transformer, an unified approach,” in *Proc. 32nd Annu. IEEE Power Electron. Specialists Conf. (PESC)*, Vancouver, Canada, Aug. 2001, pp. 504–509. doi: [10.1109/PESC.2001.954164](https://doi.org/10.1109/PESC.2001.954164).

Heinemann2002 | L. Heinemann, “An actively cooled high power, high frequency transformer with high insulation capability,” in *Proc. 17th Annu. IEEE Appl. Power Electron. Conf. and Expo. (APEC)*, Dallas, TX, USA, Mar. 2002, pp. 352–357. doi: [10.1109/APEC.2002.989270](https://doi.org/10.1109/APEC.2002.989270).

Heinig2022 | S. Heinig et al., “Experimental insights into the MW range dual active bridge with silicon carbide devices,” in *Proc. Int. Power Electron. Conf. (IPEC/ECCE Asia)*, Himeji, Japan, May 2022, pp. 1601–1606. doi: [10.23919/IPEC-Himeji2022-ECCE53331.2022.9806987](https://doi.org/10.23919/IPEC-Himeji2022-ECCE53331.2022.9806987).

Henning2008 | P. H. Henning, H. D. Fuchs, A. D. le Roux, and H. du T. Mouton, “A 1.5-MW seven-cell series-stacked converter as an active power filter and regeneration converter for a DC traction substation,” *IEEE Trans. Power Electron.*, vol. 23, no. 5, pp. 2230–2236, Sep. 2008, doi: [10.1109/TPEL.2008.2001882](https://doi.org/10.1109/TPEL.2008.2001882).

Hoffmann2011 | H. Hoffmann and B. Piepenbreier, “Medium frequency transformer for rail application using new materials,” in *Proc. 1st Int. Electric Drives Production Conf.*, Nuremberg, Germany, Sep. 2011, pp. 192–197. doi: [10.1109/EDPC.2011.6085569](https://doi.org/10.1109/EDPC.2011.6085569).

Huber2018 | J. E. Huber, J. Miniböck, and J. W. Kolar, “Generic derivation of dynamic model for half-cycle DCM series resonant converters,” *IEEE Trans. Power Electron.*, vol. 33, no. 1, pp. 4–7, Jan. 2018, doi: [10.1109/TPEL.2017.2703300](https://doi.org/10.1109/TPEL.2017.2703300).

Huang2009 | A. Q. Huang and J. Baliga, “FREEDM system: tole of power electronics and power semiconductors in developing an energy internet,” in *Proc. 21st Int. Symp. Power Semiconductor Devices & ICs (ISPSD)*, Barcelona, Spain, Jun. 2009, pp. 9–12. doi: [10.1109/ISPSD.2009.5157988](https://doi.org/10.1109/ISPSD.2009.5157988).



References (6)

Huang2011 | A. Q. Huang, M. L. Crow, G. T. Heydt, J. P. Zheng, and S. J. Dale, “The future renewable electric energy delivery and management (FREEDM) system: The energy internet,” *Proc. IEEE*, vol. 99, no. 1, pp. 133–148, Jan. 2011, doi: [10.1109/JPROC.2010.2081330](https://doi.org/10.1109/JPROC.2010.2081330).

Huber2016 | J. E. Huber, D. Rothmund, and J. W. Kolar, “Comparative evaluation of isolated front end and isolated back end multi-cell SSTs,” in *Proc. 8th Int. Power Electron. and Motion Contr. Conf. (IPEMC/ECCE Asia)*, Hefei, China, May 2016, pp. 3536–3545. doi: [10.1109/IPEMC.2016.7512863](https://doi.org/10.1109/IPEMC.2016.7512863).

Huber2017 | J. E. Huber and J. W. Kolar, “Optimum number of cascaded cells for high-power medium-voltage AC-DC converters,” *IEEE Trans. Emerg. Sel. Topics Power Electron.*, vol. 5, no. 1, pp. 213–232, Sep. 2017, doi: [10.1109/JESTPE.2016.2605702](https://doi.org/10.1109/JESTPE.2016.2605702).

Huber2022 | J. Huber, P. Wallmeier, R. Pieper, F. Schafmeister, and J. W. Kolar, “Comparative evaluation of MVAC-LVDC SST and hybrid transformer concepts for future datacenters,” in *Proc. Int. Power Electron. Conf. (IPEC/ECCE Asia)*, Himeji, Japan, May 2022, pp. 2027–2034. doi: [10.23919/IPEC-Himeji2022-ECCE53331.2022.9807028](https://doi.org/10.23919/IPEC-Himeji2022-ECCE53331.2022.9807028).

Joseph2020 | S. Joseph, A. K. Abraham, P. H. Raj, J. Joseph, and K. R. M. Nair, “An iterative algorithm for optimum design of high frequency transformer in SST application,” in *Proc. 46th Annu. IEEE Ind. Electron. Soc. Conf. (IECON)*, Singapore, Oct. 2020, pp. 1538–1543. doi: [10.1109/IECON43393.2020.9254914](https://doi.org/10.1109/IECON43393.2020.9254914).

Joung1988 | G. B. Joung, C. T. Rim, and G. H. Cho, “Modeling of quantum series resonant converters-controlled by integral cycle mode,” in *Conf. Rec. IEEE Ind. Appl. Soc. Annu. Meet.*, Pittsburgh, PA, USA, Oct. 1988, pp. 821–826. doi: [10.1109/IAS.1988.25156](https://doi.org/10.1109/IAS.1988.25156).

Joung1989 | G. B. Joung, C. T. Rim, and G. H. Cho, “Integral cycle mode control of the series resonant converter,” *IEEE Trans. Power Electron.*, vol. 4, no. 1, pp. 83–91, Jan. 1989, doi: [10.1109/63.21875](https://doi.org/10.1109/63.21875).

Kalvelage2002 | G. Kalvelage and P. Aubin, “Selectable arrangement energy converter,” US6654266B2, Nov. 25, 2003, (filed Feb. 5, 2002).

Kashihara2017 | Y. Kashihara, Y. Nemoto, W. Qichen, S. Fujita, R. Yamada, and Y. Okuma, “An isolated medium-voltage AC/DC power supply based on multil-cell converter topology,” in *Proc. IEEE Appl. Power Electron. Conf. and Expo. (APEC)*, Tampa, FL, USA, Mar. 2017, pp. 2187–2192. doi: [10.1109/APEC.2017.7931002](https://doi.org/10.1109/APEC.2017.7931002).

Kasper2016 | M. Kasper, “Analysis and multi-objective optimization of multi-cell DC/DC and AC/DC converter systems,” Ph.D. Dissertation, ETH Zurich, 2016. doi: [10.3929/ethz-a-010836609](https://doi.org/10.3929/ethz-a-010836609).

Keister2018 | L. T. Keister, J. D. Keister, B. J. Schafer, and A. A. M. Esser, “Power management utilizing a high-frequency low voltage pre-charge and synchronous common coupling,” U.S. Pat. 9 906 155 B2, Feb. 27, 2018.

Keister2020 | L. T. Keister, J. D. Keister, B. J. Schafer, and A. A. M. Esser, “Power management utilizing synchronous common coupling,” U.S. Pat. 10 608 545 B2, Mar. 31, 2020.

Keister2020a | L. T. Keister, J. D. Keister, B. J. Schafer, and A. A. M. Esser, “Power management utilizing synchronous common coupling,” U.S. Pat. 10 811 988 B2, Oct. 20, 2020.

Kjaer2016 | P. C. Kjaer, Y.-H. Chen, and C. G. Dincan, “DC Collection: Wind Power Plant with Medium Voltage DC Power Collection Network,” presented at *ECPE Workshop on Smart Transformers*, Zurich, Switzerland, Feb. 2016.



References (7)

Kokkonda2021 | R. K. Kokkonda, A. Kumar, A. Anurag, N. Kolli, S. Parashar, and S. Bhattacharya, “Medium voltage shore-to-ship connection system enabled by series connected 3.3 kV SiC MOSFETs,” in *Proc. Appl. Power Electron. Conf. and Expo. (APEC)*, Phoenix, AZ, USA, Jun. 2021, pp. 1380–1387. doi: <https://doi.org/10.1109/APEC42165.2021.9487119>.

Kopacz2023 | R. Kopacz, D. Menzi, F. Krismer, J. Rabkowski, J. W. Kolar, and J. Huber, “New single-stage bidirectional three-phase ac-dc solid-state transformer,” in preparation, 2023.

Krismer2012 | F. Krismer and J. W. Kolar, “Closed form solution for minimum conduction loss modulation of DAB converters,” *IEEE Trans. Power Electron.*, vol. 27, no. 1, pp. 174–188, Jan. 2012, doi: [10.1109/TPEL.2011.2157976](https://doi.org/10.1109/TPEL.2011.2157976).

Kucka2022 | J. Kucka and D. Dujic, “IGCT gate unit for zero-voltage-switching resonant DC transformer applications,” *IEEE Trans. Ind. Electron.*, vol. 69, no. 12, pp. 13799–13807, Dec. 2022, doi: [10.1109/TIE.2021.3128923](https://doi.org/10.1109/TIE.2021.3128923).

Leibl2017 | M. Leibl, G. Ortiz, and J. W. Kolar, “Design and experimental analysis of a medium-frequency transformer for solid-state transformer applications,” *IEEE Trans. Emerg. Sel. Topics Power Electron.*, vol. 5, no. 1, pp. 110–123, Mar. 2017, doi: [10.1109/JESTPE.2016.2623679](https://doi.org/10.1109/JESTPE.2016.2623679).

LeMétayer2021 | P. Le Métayer et al., “Break-even distance for MVDC electricity networks according to power loss criteria,” Ghent, Belgium, Sep. 2021. doi: [10.23919/EPE21ECCEurope50061.2021.9570416](https://doi.org/10.23919/EPE21ECCEurope50061.2021.9570416).

Lesnicar2003 | A. Lesnicar and R. Marquardt, “An innovative modular multilevel converter topology suitable for a wide power range,” in *Proc. IEEE Power Tech Conf.*, Bologna, Italien, Jul. 2003, pp. 272–277. doi: [10.1109/PTC.2003.1304403](https://doi.org/10.1109/PTC.2003.1304403).

Li2021 | Z. Li, Y.-H. Hsieh, Q. Li, F. C. Lee, and C. Zhao, “Insulation design on high-frequency transformer for solid-state transformer,” in *Proc. IEEE Energy Conv. Congr. Expo. (ECCE USA)*, Vancouver, Canada, Oct. 2021, pp. 1149–1155. doi: [10.1109/ECCE47101.2021.9595657](https://doi.org/10.1109/ECCE47101.2021.9595657).

Li2022 | H. Li, P. Yao, Z. Gao, and F. Wang, “Medium voltage converter inductor insulation design considering grid requirements,” *IEEE Trans. Emerg. Sel. Topics Power Electron.*, vol. 10, no. 2, pp. 2339–2350, Apr. 2022, doi: [10.1109/JESTPE.2021.3131602](https://doi.org/10.1109/JESTPE.2021.3131602).

Lin2022 | X. Lin, L. Ravi, R. Burgos, and D. Dong, “Hybrid voltage balancing approach for series-connected SiC MOSFETs for DC–AC medium-voltage power conversion applications,” *IEEE Trans. Power Electron.*, vol. 37, no. 7, pp. 8104–8117, Jul. 2022, doi: [10.1109/TPEL.2022.3149146](https://doi.org/10.1109/TPEL.2022.3149146).

Lu2022 | S. Lu, D. Kong, S. Xu, L. Luo, and S. Li, “A high-efficiency 80-kW split planar transformer for medium-voltage modular power conversion,” *IEEE Trans. Power Electron.*, vol. 37, no. 8, pp. 8762–8766, Aug. 2022, doi: [10.1109/TPEL.2022.3151796](https://doi.org/10.1109/TPEL.2022.3151796).

Mainali2015 | K. Mainali et al., “A transformerless intelligent power substation: A three-phase SST enabled by a 15-kV SiC IGBT,” *IEEE Power Electron. Mag.*, vol. 2, no. 3, pp. 31–43, Sep. 2015, doi: [10.1109/MPEL.2015.2449271](https://doi.org/10.1109/MPEL.2015.2449271).

Makoschitz2022 | M. Makoschitz, “Unidirectional medium voltage rectifier utilizing sinusoidal input currents,” *Electron. Lett.*, vol. 58, no. 12, pp. 474–476, 2022, doi: [10.1049/ell2.12495](https://doi.org/10.1049/ell2.12495).

Marca2021 | Y. P. Marca, M. G. L. Roes, J. L. Duarte, and K. G. E. Wijnands, “Isolated MMC-based ac/ac stage for ultrafast chargers,” in *Proc. 30th Int. IEEE Ind. Electron. Symp. (ISIE)*, Kyoto, Japan, Jun. 2021. doi: [10.1109/ISIE45552.2021.9576217](https://doi.org/10.1109/ISIE45552.2021.9576217).



References (8)

Marquardt2002 | R. Marquardt, A. Lesnicar, and J. Hildinger, “Modulares Stromrichterkonzept für Netzkupplungsanwendungen bei hohen Spannungen (in German),” in *Proc. ETG-Fachtagung*, Bad Nauheim, Germany, 2002.

Mauger2020 | M. J. Mauger, P. Kandula, and D. Divan, “Soft-switching current source inverter for next-generation electric vehicle drivetrains,” in *Proc. IEEE Transportation Electrification Conf. Expo (ITEC)*, Chicago, IL, USA, Jun. 2020, pp. 651–658. doi: [10.1109/ITEC48692.2020.9161493](https://doi.org/10.1109/ITEC48692.2020.9161493). **Mauger2021** | M. J. Mauger, V. R. Chowdhury, P. Kandula, and D. Divan, “A multiport DC transformer to enable flexible scalable DC as a service,” in *Proc. Energy Conversion Congr. and Expo (ECCE USA)*, Vancouver, Canada, Nov. 2021, doi: [10.1109/ECCE47101.2021.9595494](https://doi.org/10.1109/ECCE47101.2021.9595494).

McMurray1969 | W. McMurray, “Multipurpose power converter circuits,” U.S. Pat. 3,487,289, Apr. 16, 1969.

McMurray1971 | W. McMurray, “The thyristor electronic transformer: A power converter using a high-frequency link,” *IEEE Trans. Ind. Gen. A.*, vol. IGA-7, no. 4, pp. 451–457, Jul. 1971, doi: [10.1109/TIGA.1971.4181326](https://doi.org/10.1109/TIGA.1971.4181326).

McMurray1971a | W. McMurray, “Fast response stepped-wave switching power converter circuit,” U.S. Pat. 3,581,212, May 25, 1971.

Meintz2021 | A. Meintz, M. Starke, and T. Bohn, “Charging infrastructure technologies: development of a multiport, >1 MW charging system for medium- and heavy-duty electric vehicles,” Jan. 24, 2021. [Online]. Available: <https://www.nrel.gov/docs/fy22osti/79988.pdf>.

Meynard1992 | T. A. Meynard and H. Foch, “Multi-level conversion: high voltage choppers and voltage-source inverters,” in *Conf. Rec. 23rd Annu. IEEE Power Electron. Specialists Conf. (PESC)*, Toledo, Spain, Jun. 1992, pp. 397–403. doi: [10.1109/PESC.1992.254717](https://doi.org/10.1109/PESC.1992.254717).

Menzi2022 | D. Menzi, J. W. Kolar, J. Huber, and J. Everts, “Polyphase Single-Stage High-Frequency Isolated AC/DC and AC/AC Converter,” EU Pat. Appl., filed May 13, 2022.

Menzi2023 | D. Menzi, J. W. Kolar, H. Sarnago, Ó. Lucia, and J. Huber, “New 600 V GaN single-stage isolated bidirectional 400 V input three-phase PFC rectifier,” in *Proc. Energy Convers. Congr. Expo. (ECCE US)*, Nashville, TN, USA, Oct. 2023.

Mocevic2021 | S. Mocevic et al., “Power cell design and assessment methodology based on a high-current 10-kV SiC MOSFET half-bridge module,” *IEEE Trans. Emerg. Sel. Topics Power Electron.*, vol. 9, no. 4, pp. 3916–3935, Aug. 2021, doi: [10.1109/JESTPE.2020.2995386](https://doi.org/10.1109/JESTPE.2020.2995386).

Mocevic2021a | S. Mocevic et al., “Design of a 10 kV SiC MOSFET-based high-density, high-efficiency, modular medium-voltage power converter,” *iEnergy*, vol. 1, no. 1, pp. 1–14, Mar. 2022, doi: [10.23919/IEEN.2022.0001](https://doi.org/10.23919/IEEN.2022.0001).

Nabae1981 | A. Nabae, I. Takahashi, and H. Akagi, “A new neutral-point-clamped PWM inverter,” *IEEE Trans. Ind. Appl.*, vol. IA-17, no. 5, pp. 518–523, Sep. 1981, doi: [10.1109/TIA.1981.4503992](https://doi.org/10.1109/TIA.1981.4503992).

Nakatsu2022 | K. Nakatsu, T. Kumazaki, A. Kanouda, K. Ide, and T. Tsukishima, “Development of smart power management for achieving carbon neutrality by 2050: Energy ecosystems for widespread EV adoption,” *Hitachi Rev.*, vol. 71, no. 1, pp. 51–57, 2022.

Neuner2023 | D. Neuner, M. Hartmann, J. W. Kolar, and J. Huber, “Analysis of a solid-state transformer employing capacitively isolated series-stacked converter cells and a single medium-frequency transformer,” in *Proc. Control Modeling Power Electron. Conf. (COMPEL)*, Ann Arbor, MI, USA, Jun 2023.



References (9)

Ortiz2017 | G. Ortiz, M. Leibl, J. Huber, and J. W. Kolar, “Design and experimental testing of a resonant DC-DC converter for solid-state transformers,” *IEEE Trans. Power Electron.*, vol. 32, no. 10, pp. 7534–7542, Oct. 2017, doi: [10.1109/TPEL.2016.2637827](https://doi.org/10.1109/TPEL.2016.2637827).

Pouresmaeil2022 | K. Pouresmaeil, J. Duarte, K. Wijnands, M. Roes, and N. Baars, “Single-phase bidirectional VZCS AC-DC converter for MV-connected ultra-fast chargers,” in *Proc. Power Conversion and Intelligent Motion Conf. (PCIM)*, Nuremberg, Germany, May 2022.

Raju2008 | R. N. Raju, R. S. Zhang, L. D. Stevanovic, J. N. Slotnick, R. L. Steigerwald, and L. J. Garces, “AC-AC converter with high frequency link,” U.S. Pat. 8 644 037 B2, Feb. 04, 2014, (filed Jul. 15, 2008).

Raju2014 | R. Raju, “Silicon carbide high voltage, high frequency conversion,” presented at the *NIST High Megawatt Variable Speed Drive Technology Workshop*, Apr. 2014. [Online]. Available: <http://goo.gl/cTzaAg>.

Rothmund2018 | D. Rothmund, “10 kV SiC-based medium-voltage solid-state transformer concepts for 400V DC distribution systems,” Ph.D. Dissertation, ETH Zurich, 2018. doi: [10.3929/ethz-b-000331208](https://doi.org/10.3929/ethz-b-000331208).

Rothmund2019 | D. Rothmund, T. Guillod, D. Bortis, and J. W. Kolar, “99% efficient 10 kV SiC-based 7 kV/400 V DC transformer for future data centers,” *IEEE Trans. Emerg. Sel. Topics Power Electron.*, vol. 7, no. 2, pp. 753–767, Jun. 2019, doi: [10.1109/JESTPE.2018.2886139](https://doi.org/10.1109/JESTPE.2018.2886139).

Rothmund2019a | D. Rothmund, T. Guillod, D. Bortis, and J. W. Kolar, “99.1% efficient 10 kV SiC-based medium-voltage ZVS bidirectional single-phase PFC AC/DC stage,” *IEEE Trans. Emerg. Sel. Topics Power Electron.*, vol. 7, no. 2, pp. 779–797, Jun. 2019, doi: [10.1109/JESTPE.2018.2886140](https://doi.org/10.1109/JESTPE.2018.2886140).

Saha2018 | J. Saha, G. N. B. Yadav, and S. K. Panda, “A matrix-based solid-state-transformer for a hybrid nanogrid,” in *Proc. IEEE Int. Conf. Power Electron. Drives Energy Systems (PEDES)*, Chennai, India, Dec. 2018. doi: [10.1109/PEDES.2018.8707623](https://doi.org/10.1109/PEDES.2018.8707623).

Saha2019 | J. Saha, G. N. Brahmendra Yadav, and S. Kumar Panda, “A review on bidirectional matrix-based AC-DC conversion for modular solid-state-transformers,” in *Proc. 4th IEEE Int. Future Energy Electron. Conf. (IFEEC)*, Singapore, Nov. 2019. doi: [10.1109/IFEEC47410.2019.9015013](https://doi.org/10.1109/IFEEC47410.2019.9015013).

Saha2020 | J. Saha, G. N. Brahmendra Yadav, and S. Kumar Panda, “A bidirectional matrix-based AC-DC dual-active bridge for modular solid-state-transformers,” in *Proc. 46th Annu. IEEE Ind. Electron. Soc. Conf. (IECON)*, Singapore, Oct. 2020, pp. 1136–1141. doi: [10.1109/IECON43393.2020.9255301](https://doi.org/10.1109/IECON43393.2020.9255301).

Saha2021 | J. Saha, D. Hazarika, N. B. Y. Gorla, and S. K. Panda, “Machine-learning-aided optimization framework for design of medium-voltage grid-connected solid-state transformers,” *IEEE Trans. Emerg. Sel. Topics Power Electron.*, vol. 9, no. 6, pp. 6886–6900, Dec. 2021, doi: [10.1109/JESTPE.2021.3074408](https://doi.org/10.1109/JESTPE.2021.3074408).

Schulz2022 | M. Schulz, D. Hoffmann, and M. Ketterer, “The resurrection of GTOs and thyristors as core components in MW-charger-application and railway/mining refurbishment,” in *Proc. Power Conversion and Intelligent Motion Conf. (PCIM)*, Nuremberg, Germany, May 2022.

Schwarz1970 | F. C. Schwarz, “A method of resonant current pulse modulation for power converters,” *IEEE Trans. Ind. El. Con. In.*, vol. IECI-17, no. 3, pp. 209–221, May 1970, doi: [10.1109/TIECI.1970.230769](https://doi.org/10.1109/TIECI.1970.230769).



References (10)

Schweizer2017 | M. Schweizer and T. B. Soeiro, “Heatsink-less quasi 3-level flying capacitor inverter based on low voltage SMD MOSFETs,” in *Proc. Europ. Power Electron. Appl. Conf. (EPE)*, Warsaw, Poland, Sep. 2017. doi: [10.23919/EPE17ECCEEurope.2017.8098916](https://doi.org/10.23919/EPE17ECCEEurope.2017.8098916).

Shao2020 | S. Shao et al., “A modular multilevel resonant DC–DC converter,” *IEEE Trans. Power Electron.*, vol. 35, no. 8, pp. 7921–7932, Aug. 2020, doi: [10.1109/TPEL.2019.2962032](https://doi.org/10.1109/TPEL.2019.2962032).

Soltau2014 | N. Soltau, H. Stagge, R. W. De Doncker, and O. Apeldoorn, “Development and demonstration of a medium-voltage high-power DC-DC converter for DC distribution systems,” in *Proc. 5th IEEE Int. Power Electron. for Distributed Generation Syst. Symp. (PEDG)*, Galway, Ireland, Jun. 2014. doi: [10.1109/PEDG.2014.6878696](https://doi.org/10.1109/PEDG.2014.6878696).

Soltau2017 | N.-J. Soltau, “High-power medium-voltage DC-DC converters design, control and demonstration,” Ph.D. Dissertation, RWTH Aachen, 2017.

Stackler2021 | C. Stackler, F. Morel, P. Ladoux, A. Fouineau, and F. Wallart, “Optimal sizing on a mission profile of isolated NPC DC-DC converters using 3.3 kV SiC MOSFETs for power electronic traction transformers,” in *Proc. Power Conversion Intelligent Motion Conf. (PCIM)*, Nuremberg, Germany, May 2021.

Stanley1886 | W. Stanley, “Induction-Coil,” U.S. Pat. 349 611, 1886.

Steiner1996 | M. Steiner and H. Reinold, “Antriebssystem für ein Schienenfahrzeug und Ansteuerverfahren hierzu (in German),” German Pat. Appl. DE 196 30 284 A1, Jul. 26, 1996.

Steiner1998 | M. Steiner and H. Reinold, “Antriebsschaltung für ein Schienenfahrzeug (in German),” German Pat. DE 198 27 872 B4, Apr. 09, 200,9 (filed Jun. 23, 1998).

Steiner2007 | M. Steiner and H. Reinold, “Medium frequency topology in railway applications,” in *Proc. 12th Europ. Power Electron. Appl. Conf. (EPE)*, Aalborg, Denmark, Sep. 2007. doi: [10.1109/EPE.2007.4417570](https://doi.org/10.1109/EPE.2007.4417570).

Stewart2022 | J. Stewart, J. Motwani, J. Yu, I. Cvetkovic, and R. Burgos, “Improved power density of a 6 kV, 1 MW power electronics building block through insulation coordination,” in *Proc. 23rd IEEE Workshop Control Modeling Power Electron. (COMPEL)*, Tel Aviv, Israel, Jun. 2022. doi: [10.1109/COMPEL53829.2022.9829968](https://doi.org/10.1109/COMPEL53829.2022.9829968).

Ulissi2022 | G. Ulissi, U. R. Vemulapati, T. Stiasny, and D. Dujic, “High-frequency operation of series-connected IGBTs for resonant converters,” *IEEE Transactions on Power Electronics*, vol. 37, no. 5, pp. 5664–5674, May 2022, doi: [10.1109/TPEL.2021.3132200](https://doi.org/10.1109/TPEL.2021.3132200).

vanderMerwe2009 | W. van der Merwe and T. Mouton, “Solid-state transformer topology selection,” in *Proc. IEEE Int. Ind. Techn. Conf. (ICIT)*, Gippsland, Australia, Feb. 2009. doi: [10.1109/ICIT.2009.4939592](https://doi.org/10.1109/ICIT.2009.4939592).

Weiss1985 | H. Weiss, “Elimination of the 16 2/3 Hz, 15 kV main transformer on electric traction vehicle,” in *Proc. 1st Europ Power Electron. and Appl. Conf. (EPE)*, Brussels, Belgium, Oct. 1985.

Wen2021 | W. Wen, K. Li, Z. Zhao, L. Yuan, X. Mo, and W. Cai, “Analysis and control of a four-port megawatt-level high-frequency-bus-based power electronic transformer,” *IEEE Trans. Power Electron.*, vol. 36, no. 11, pp. 13080–13095, Nov. 2021, doi: [10.1109/TPEL.2021.3075739](https://doi.org/10.1109/TPEL.2021.3075739).

Xu2022 | Y. Xu et al., “High power density medium-voltage converter integration via electric field management,” *IEEE Trans. Emerg. Sel. Topics Power Electron.*, vol. 10, no. 1, pp. 895–905, Feb. 2022, doi: [10.1109/JESTPE.2021.3107343](https://doi.org/10.1109/JESTPE.2021.3107343).



References (11)

Zhao2014 | C. Zhao et al., “Power electronic traction transformer—medium voltage prototype,” *IEEE Trans. Ind. Electron.*, vol. 61, no. 7, pp. 3257–3268, Jul. 2014, doi: [10.1109/TIE.2013.2278960](https://doi.org/10.1109/TIE.2013.2278960).

Zhang2023 | C. Zhang, R. Wang, Z. Shen, T. Sadilek, A. Anurag, and P. Barbosa, “A single-stage three-phase isolated AC-DC converter for medium voltage solid state transformer applications,” in *Proc. Appl. Power Electron. Conf. (APEC)*, Orlando, FL, USA, Mar. 2023.

Zheng2020 | L. Zheng, R. P. Kandula, and D. Divan, “New single-stage soft-switching solid-state transformer with reduced conduction loss and minimal auxiliary switch,” in *Proc. IEEE Appl. Power Electron. Conf. and Expo. (APEC)*, New Orleans, LA, USA, Mar. 2020, pp. 560–567. doi: [10.1109/APEC39645.2020.9124346](https://doi.org/10.1109/APEC39645.2020.9124346).

Zheng2021 | L. Zheng et al., “SiC-based 5-kV universal modular soft-switching solid-state transformer (M-S4T) for medium-voltage DC microgrids and distribution grids,” *IEEE Trans. Power Electron.*, vol. 36, no. 10, pp. 11326–11343, Oct. 2021, doi: [10.1109/TPEL.2021.3066908](https://doi.org/10.1109/TPEL.2021.3066908)

Zheng2022 | L. Zheng et al., “7.2 kV three-port SiC single-stage current-source solid-state transformer with 90 kV lightning protection,” *IEEE Trans. Power Electron.*, vol. 37, no. 10, pp. 12080–12094, Oct. 2022, doi: [10.1109/TPEL.2022.3172946](https://doi.org/10.1109/TPEL.2022.3172946).

Zheng2022a | L. Zheng, R. P. Kandula, and D. Divan, “Current-source solid-state DC transformer integrating LVDC microgrid, energy storage, and renewable energy into MVDC grid,” *IEEE Trans. Power Electron.*, vol. 37, no. 1, pp. 1044–1058, Jan. 2022, doi: [10.1109/TPEL.2021.3101482](https://doi.org/10.1109/TPEL.2021.3101482).

Zheng2022a | L. Zheng, R. P. Kandula, K. Kandasamy, and D. Divan, “New modulation and impact of transformer leakage inductance on current-source solid-state transformer,” *IEEE Trans. Power Electron.*, vol. 37, no. 1, pp. 562–576, Jan. 2022, doi: [10.1109/TPEL.2021.3101811](https://doi.org/10.1109/TPEL.2021.3101811).

Zhu2019 | C. Zhu, “High-efficiency, medium-voltage input, solid-state, transformer-based 400-kW/1000-V/400-A extreme fast charger for electric vehicles,” Presented at the *DOE Vehicle Techn. Off. Annu. Merit Rev. Electrification*, Jun. 2019, <https://tinyurl.com/2tvyshxi>.

Zhu2020 | C. Zhu, “High-efficiency, medium-voltage input, solid-state, transformer-based 400-kW/1000-V/400-A extreme fast charger for electric vehicles,” Presented at the *DOE Vehicle Techn. Off. Annu. Merit Rev. Electrification*, Jun. 2020, <https://tinyurl.com/2pcxn839>.

Zhu2021 | C. Zhu, “High-efficiency, medium-voltage input, solid-state, transformer-based 400-kW/1000-V/400-A extreme fast charger for electric vehicles,” Presented at the *DOE Vehicle Techn. Off. Annu. Merit Rev. Electrification*, Jun. 2021, <https://tinyurl.com/4nnjbm7u>.

Zumel2014 | P. Zumel, C. Fernandez, A. Lazaro, M. Sanz, and A. Barrado, “Overall analysis of a modular multi active bridge converter,” in *Proc. 15th IEEE Workshop Control Modeling Power Electron. (COMPEL)*, Santander, Spain, Jun. 2014. doi: [10.1109/COMPEL.2014.6877198](https://doi.org/10.1109/COMPEL.2014.6877198).



Authors

Johann W. Kolar (M'89–F'10) is a Fellow of the IEEE, an International Member of the US NAE and a Full Professor and Head of the Power Electronic Systems Laboratory at the Swiss Federal Institute of Technology (ETH) Zurich. He has proposed numerous novel converter concepts incl. the Vienna Rectifier, has spearheaded the development of x-million rpm motors and has pioneered fully automated multi-objective power electronics design procedures. He has graduated 80+ Ph.D. students, has published 900+ research papers, 4 book chapters, and has filed 200+ patents. He has served as IEEE PELS Distinguished Lecturer from 2012 - 2016. He has received 40+ IEEE Transactions and Conference Prize Paper Awards, the 2014 IEEE Power Electronics Society R. David Middlebrook Achievement Award, the 2016 IEEE PEMC Council Award, the 2016 IEEE William E. Newell Power Electronics Award, the 2021 EPE Outstanding Achievement Award and 2 ETH Zurich Golden Owl Awards for excellence in teaching. The focus of his current research is on ultra-compact/efficient WBG PFC rectifier and inverter systems, ultra-high BW switch-mode power amplifiers, multi-port converters, Solid-State Transformers, multi-functional actuators, ultra-high speed / motor-integrated drives, bearingless motors, ANN-based multi-objective design optimization and Life Cycle Assessment of power electronics systems.

Jonas Huber (S'11–M'16–SM'22) received the M.Sc. and Ph.D. degrees from the Swiss Federal Institute of Technology (ETH) Zürich, Switzerland, in 2012 and 2016, respectively. Since 2012, he has been with the Power Electronic Systems Laboratory, ETH Zürich; since 2016 as a Postdoctoral Researcher. Since 2017, he has gained industry experience as a Power Electronics R&D Engineer at ABB Switzerland, working on high-power dc-dc converter systems for traction applications, and as a Business Development Manager with a Swiss utility company. Then, in 2020, he returned to the Power Electronic Systems Laboratory as a Senior Researcher. His research interests include solid-state transformers, motor drives, and all types of WBG-semiconductor-based ultra-compact, ultra-efficient or highly dynamic converter systems, including circularity aspects. He has authored and/or coauthored more than 50 journal and conference papers and a book chapter, has filed more than 10 patents, and has presented more than 10 educational seminars at leading international conferences.

■ Contact Information

Prof. Dr. Johann W. Kolar
 Dr. Jonas Huber

kolar@lem.ee.ethz.ch
huber@lem.ee.ethz.ch

